Targeting the Type 5 Metabotropic Glutamate Receptor in a Mouse Model of Terminal Neurodegeneration

Rebecca Budgett

BSc, MSc (Hons)

Submitted in fulfilment of the requirements for the Degree of

Doctor of Philosophy

School of Molecular Biosciences

College of Medical, Veterinary and Life Science

University of Glasgow

August 2023

Abstract

The type 5 metabotropic glutamate receptor ($mGlu_5$) plays an important role in learning and memory processes and has been identified as a potential drug target for the treatment of neurodegenerative diseases (NDD). Given the limited treatment options available to patients living with NDD, there is a pressing need for novel therapeutic interventions that treat both the symptomatic and progressive components of neurodegeneration. Promisingly, the pharmacological and genetic blockade of $mGlu_5$ has been shown to reduce disease pathology and improve cognition in several preclinical mouse models of neurodegeneration (Budgett et al., 2022). Expressed in both neurons and glia, $mGlu_5$ has been shown to play a role in neuroinflammation and, therefore, represents a potential target for regulating neuroinflammation in disease (Byrnes et al., 2009). Therefore, this thesis aimed to evaluate the role of $mGlu_5$ in the modulation of neuroinflammation and the progression of NDD in a model of terminal neurodegeneration, murine prion disease.

To provide insights into the signalling mechanisms of $mGlu_5$ and the characteristics of novel compounds, *in vitro* functional assays were conducted on cell lines expressing $mGlu_5$. Flp-in cells expressing mouse $mGlu_5$ and mouse primary cortical astrocytes were found to be suitable systems for investigating the signalling properties of $mGlu_5$ ligands. In these systems, VU0424238 was confirmed to be a $mGlu_5$ negative allosteric modulator (NAM) that binds to the main allosteric binding site on $mGlu_5$ (Felts et al., 2017). Furthermore, target engagement and efficacy *in vivo* were established.

Recent studies have shown close correlates between murine prion disease and human NDDs, including hippocampal-based cognitive deficits, neuroinflammation, and terminal neurodegeneration (Bourgognon et al., 2018; Bradley et al., 2016). Here, the model of murine prion disease was investigated using histological and biochemical studies to characterise the neuroinflammatory response throughout disease progression. The astrocytic and microglial markers GFAP, vimentin, Iba-1, and CD68 were confirmed to be upregulated in murine prion disease, in addition to several pro-inflammatory cytokines. This is similar to human NDDs characterised by chronic neuroinflammation.

Subsequently, this thesis aimed to define the impact of $mGlu_5$ blockade, both pharmacologically and genetically, on the progression of murine prion disease. Firstly, $mGlu_5$ was inhibited pharmacologically using the NAM VU0424238. Although chronic VU0424238 treatment significantly reduced the expression of GFAP in the hippocampus of female prion-diseased mice, $mGlu_5$ antagonism did not alter the overall progression of murine prion disease. There were no alterations to the accumulation of misfolded prion protein, symptom onset, survival, or behaviour after chronic VU0424238 treatment. Next, $mGlu_5$-deficient mice were inoculated with prion disease. Although $mGlu_5$ deficiency resulted in the reduced expression of the inflammatory markers Iba-1 and GFAP in early-stage disease, it did not affect overall disease progression.

Overall, these findings suggest that $mGlu_5$ may represent a potential approach by which neuroinflammatory processes in NDDs might be modulated. However, the results also suggest that $mGlu_5$ may not play a significant role in the progression of prion disease and may function differently in prion disease compared to other NDDs.

Table of Contents

List of Tables

List of Figures

List of Publications

Budgett, R.F., Bakker, G., Sergeev, E., Bennett, K.A., & Bradley, S.J. (2022) Targeting the Type 5 Metabotropic Glutamate Receptor: A Potential Therapeutic Strategy for Neurodegenerative Diseases? *Frontiers in pharmacology*, 13, 893422. doi.org/10.3389/fphar.2022.893422

Scarpa, M., Molloy, C., Jenkins, L., Strellis, B., **Budgett, R.F.**, Hesse, S., Dwomoh L., Marsango S., Tejeda G.S., Rossi M., Ahmed Z., Milligan G., Hudson B.D., Tobin A.B., Bradley S.J. (2021) Biased M1 muscarinic receptor mutant mice show accelerated progression of prion neurodegenerative disease. *Proc Natl Acad Sci U S A*; 118(50): e2107389118. doi: 0.1073/pnas.2107389118.

Acknowledgements

Firstly, I would like to extend a huge thank you to my supervisors: Sophie Bradley, Mathis Riehle, Kirstie Bennett, and Andrew Tobin. Sophie, your consistent encouragement and guidance played an invaluable role in my growth and development as a scientist over the past few years. Mathis, thank you for stepping in as my Glasgow supervisor at the last minute. I really appreciated the time we spent discussing my project over coffee at the Gilchrist and for all your help with my thesis. It was so useful to hear a perspective from outside of my field. Kirstie, thank you for your supervision at Sosei Heptares, and for your ongoing support and input throughout my PhD. You helped make my placement at Heptares a really enjoyable time. Andrew, thank you for sharing your knowledge and passion for science. I also want to thank Brian Hudson. Although not an official supervisor of mine, I am so grateful to you for being there for assistance when I needed it and for letting me gate crash your lab meetings.

I would also like to thank all the technicians and postdocs who have helped me throughout my PhD. In particular, I'd like to thank Gonzalo, Aisling, Louis, and Lisa. Thank you for answering all my questions, helping me think critically about my work, and reading thesis chapters for me. Thank you also to Colin and everyone at the animal unit for their help with all my mouse work.

I am so grateful to those in lab 241/441 who provided me with friendship and encouragement throughout different stages of my PhD, especially Sarah, Eloise, Jose, Miriam, and Woroud. In particular, I'd like to thank the ARC crafters, Beth S, Beth D, and Elaine, for providing me with a fun, creative distraction from my PhD. Our craft sessions were a highlight of each month. Thank you also to all my friends back home, whose consistent friendship and support has meant the world to me, especially when separated by a global pandemic.

Thank you to my mum and dad, who have supported me throughout my academic journey. I am so grateful to you for housing and feeding me whilst I wrote up this thesis. A huge thank you to my partner, Alex. I'm not sure what I would have done without your unwavering love and support, especially when I was finding things tough. Thank you for believing in me when I found it hard to believe in myself. An extra special thank you goes to my cat, Brie. You will never

understand how much your company and affection has meant to me throughout my PhD.

A final thank you goes to my grandparents. It was seeing my grandad suffer from Alzheimer's disease that sparked my interest in neuroscience and set me on a journey that ultimately culminated in this PhD. I am grateful for the wonderful grandparents he and Nana were to me, and I know they would both be so proud of the work I have gone on to do. This thesis is dedicated to them.

Author's Declaration

"I declare that, except where explicit reference is made to the contribution of others, this thesis is the result of my own work and has not been submitted for any other degree at the University of Glasgow or any other institution."

August 2023
Rebecca Budgett

Definitions/Abbreviations

2-AG	2-arachidonoylglycerol
Aß	ß-amyloid
Aßo	ß-amyloid oligomers
AD	Alzheimer's disease
AICD	APP intracellular domain
Akt	Protein kinase ß
ALS	Amyotrophic lateral sclerosis
AMPA	α-amino-3-hydroxy-5-methyl-4-isoxazole propionic acid
ANOVA	Analysis of variance
AO	Aldehyde oxidase
APOE	Apolipoprotein E
APP	Amyloid precursor protein
APS	Ammonium persulfate
ARIA	Amyloid-related imaging abnormalities
Asn	Asparagine
ATP	Adenosine triphosphate
BCA	Bicinchoninic acid
BDNF	Brain-derived neurotrophic factor
BRET	Bioluminescence resonance energy transfer
BSA	Bovine serum albumin
CA	Cornu Ammonis
CaMKII	Calmodulin-dependent protein kinase II
cAMP	Cyclic adenosine monophosphate
CaN	Calcineurin
CaSR	Calcium-sensing receptor
CB1	Cannabinoid receptor 1
CD68	Cluster of differentiation 68
CDPPB	3-cyano-N-(1,3-diphenyl-1H-pyrazol-5-yl)benzamide
CHO	Chinese hamster ovary
CJD	Creutzfeldt-Jakob disease
CMV	Cytomegalovirus
CNS	Central nervous system
COCS	Cerebellar organotypic cultured slices

CPPHA	[5-chloro-2-[(-1,3-dioxoisoindolin-2-yl)methyl]phenyl]-2-hydroxybenzamide
CRD	Cysteine-rich domain
CREB	cAMP response element binding protein
cryo-EM	Cryoelectron microscopy
CSF	Cerebral spinal fluid
C_T	Comparative cycle threshold
CTEP	2-chloro-4-((dimethyl-1-(4-(trifluoromethoxy)phenyl)-1H-imidazol-4yl)ethynyl)pyridine
DAG	Diacylglycerol
DAPI	4′,6-diamidino-2-phenylindole
DFB	3,3′-difluorobenzaldazine
DG	Dentate gyrus
DHPG	(S)-3,5-dihydroxyphenyl glycine
DMEM	Dulbecco's Modified Eagle Medium
DMSO	Dimethylsulfoxide
DPBS	Dulbecco's Phosphate Buffered Saline
d.p.i	Days post inoculation
D.P.M.	Disintegrations per minute
EAAT	Excitatory amino-acid transporter
EBSS	Earle's Balanced Salt Solution
ECL	Extracellular loop
EDTA	Ethylenediaminetetraacetic acid
EGF	Epidermal growth factor
EGTA	Egtazic acid
EOAD	Early-onset Alzheimer’s disease
ERK	Extracellular signal-regulated kinase
FBS	Fetal Bovine Serum
FDA	United States Food and Drug Administration
FGF	Fibroblast growth factor
FMRP	Fragile X mental retardation protein
FRET	Fluorescence resonance energy transfer
FRT	Flp Recombination Target
FST	Forced swim test
FUS	Fused in sarcoma

FZD	Frizzled
GABA	γ-aminobutyric acid
GAIN	G protein-coupled receptor autoproteolysis-inducing
GDP	Guanosine diphosphate
GEF	Guanine nucleotide exchange factor
GFAP	Glial fibrillary acidic protein
GKAP	Guanylate kinase-associated protein
GLAST	Glutamate Aspartate Transporter
GLT	Glutamate transporter
GM-CSF	Granulocyte-Macrophage Colony-Stimulating Factor
GPCR	G protein-coupled receptor
GPI	Glycosylphosphatidylinositol
GPT	Glutamate-pyruvate transaminase
GRK	GPCR kinases
GSK3β	Glycogen synthase kinase 3β
GTP	Guanosine triphosphate
GWAS	Genome-wide association studies
HA	Haemagglutinin
HBSS	Hank's Balanced Salt Solution
HD	Huntington’s disease
HEK	Human Embryonic Kidney
HEPES	N-(2-Hydroxyethyl)piperazine-N′-(2-ethanesulfonic acid)
HTRF	Homogeneous Time-Resolved Fluorescence
Htt	Huntingtin protein
i.p.	Intraperitoneal
Iba-1	Ionised Calcium Binding Adaptor Molecule 1
ICC	Immunocytochemistry
ICL	Intracellular loop
IHC	Immunohistochemistry
IL	Interleukin
IP1	Inositol monophosphate
IP2	Inositol diphosphate
IP3	Inositol 1,4,5-triphosphate
IP3R	Inositol 1,4,5-triphosphate receptor

iPSC	Induced pluripotent stem cell
IPTG	Isopropyl ß-D-1-thiogalactopyranoside
kDa	Kilodaltons
KO	Knockout
LOAD	Late-onset Alzheimer's disease
LPS	Lipopolysaccharide
LTD	Long-term depression
LTP	Long-term potentiation
MAPK	Mitogen-activated protein kinase
MAPT	Microtubule-associated protein tau
MCP	Monocyte Chemoattractant Protein
MDD	Major depressive disorder
mGlu	Metabotropic glutamate
mHtt	Mutant huntingtin protein
MPEP	2-methyl-6-(phenylethynyl) pyridine
MSN	Medium spiny neurons
MTEP	3-[(2-methyl-1,3-thiazol-4-yl)ethynyl] pyridine
mTOR	Mammalian target of rapamycin
NAM	Negative allosteric modulator
NBH	Normal brain homogenate
NDD	Neurodegenerative disease
NFT	Neurofibrillary tangles
NF-κB	Nuclear factor κB
NII	Neuronal intranuclear inclusions
NMDA	N-methyl-D-aspartate
NRSF	Neuron restrictive silencer factor
OCD	Obsessive-compulsive disorder
P13K	Phosphoinositide 3-kinase
PAG	Periaqueductal grey matter
PAM	Positive allosteric modulator
PBS	Phosphate Buffered Saline
PD	Parkinson's disease
PDK	Phosphoinositide-dependent kinase
PDL	Poly-D-lysine

PEI	Polyethyleneimine
PET	Positron emission tomography
PFA	Paraformaldehyde
PIKE	Phosphatidylinositol triphosphate
PIP_2	Phosphoinositide
PK	Proteinase K
PKA	Protein kinase A
PKC	Protein kinase C
PLC	Phospholipase C
PrP	Prion protein
PrP_C	Cellular prion protein
PrP_{Sc}	Scrapie prion protein
PSD	Postsynaptic density
PSEN1	Presenilin-1
PSEN2	Presenilin-2
REM	Rapid eye movement
REST	Repressor element 1-silencing transcription factor
RML	Rocky Mountain Laboratories
ROI	Region of interest
RT-qPCR	Real-Time quantitative PCR
SAM	Silent allosteric modulator
SDS	Sodium dodecyl sulphate
S.E.M	Standard error of the mean
Sema4D	Semaphorin 4D
SMO	Smoothened
SOD1	Cu/Zn superoxide dismutase
TARDBP	Transactive response DNA binding protein
TAS2	Taste2
TBS	Tris-buffered saline
TDP-43	TAR DNA-binding protein of 43 kDa
TEMED	N,N,N′,N′-Tetramethyl ethylenediamine
TetR	Tetracycline repressor
TM	Transmembrane
TNF-α	Tumour necrosis factor α

ULK1	Unc-51-like kinase 1
VFT	Venus flytrap
w.p.i.	Weeks post inoculation
WT	Wild-type
xCT	Cysteine-glutamate exchangers
ZBTB	Zinc finger and BTB domain-containing protein

Chapter 1 Introduction

1.1 G Protein-coupled Receptors

The G protein-coupled receptor (GPCR) superfamily comprises over 800 members and is the largest group of cell surface receptors in the human genome (Hauser et al., 2017). Due to highly divergent sequences in the extracellular ligand-binding domain, GPCRs mediate intracellular signalling in response to a wide range of stimuli, including hormones, light, small molecules, and neurotransmitters (Fredriksson et al., 2003). GPCRs are expressed in every organ and play a role in a large variety of functions in both health and disease (Fredriksson et al., 2003). Given their important role in numerous physiological processes, GPCRs have emerged as one of the most successful families of therapeutic targets. Currently, more than 30% of clinically approved drugs target a member of this superfamily (Santos et al., 2017).

GPCRs possess a common structural architecture that plays an important role in transmitting signals across the plasma membrane (Venkatakrishnan et al., 2013). Generally, GPCRs consist of an extracellular *N*-terminus, seven transmembrane (TM) α-helices linked by three intra- (ICL) and three extracellular (ECL) loops, and an intracellular *C*-terminus (Rosenbaum et al., 2009). The seven TM α-helices are made up of hydrophobic residues that facilitate the integration of the GPCR in the hydrophobic plasma membrane (Crasto, 2010). In contrast, the ICLs and ECLs contain hydrophilic residues that enable interactions within the extracellular and cytoplasmic environments (Fredriksson & Schiöth, 2005). Ligands typically bind to either the TM binding pocket or *N*-terminus, activating intracellular signalling cascades that usually involve G proteins or arrestins (Lefkowitz, 2007; Wacker et al., 2017).

1.1.1 GPCR Classification

Several classification systems have been suggested to categorise GPCRs based on characteristics such as amino acid sequence and evolutionary conservation. Here, the GRAFS system is described, which groups human GPCRs into subfamilies based on shared sequences and structural features (Schiöth & Fredriksson, 2005). Following this system, GPCRs can be broadly characterised into five classes: Glutamate (class C), Rhodopsin (class A), Adhesion (Class B2), Frizzled (class F)/taste2 (class T2) and Secretin-like (class B1) (Schiöth &

Fredriksson, 2005). Of the over 800 GPCRs present in mammals, approximately 140 of them are orphan receptors, meaning that they have unknown endogenous ligands that are not yet classified (Tang et al., 2012).

The **glutamate** receptor family (class C) consists of 22 receptors, including metabotropic glutamate (mGlu) receptors, a calcium-sensing receptor (CaSR), γ-aminobutyric acid (GABA) receptors, the sweet and amino acid taste receptors, and several orphan receptors (Fredriksson et al., 2003). These receptors typically exist as dimers (Figure 1-1A) (Pin et al., 2005). Glutamate receptors have a large *N*-terminus made up of 500-600 amino acid residues that form the ligand-binding domain (Pin et al., 2003). The *N*-terminus forms two distinct lobes making up a Venus flytrap (VFT) domain, constituting the orthosteric ligand-binding pocket where the endogenous ligand binds (O'Hara et al., 1993; Fredriksson et al., 2003). Except for $GABA_B$ receptors, most members of the glutamate family have a cysteine-rich domain (CRD) which connects the 7 TM-domain with the VFT domain (Pin et al., 2003). Typically, agonist-binding stabilises the conformation of the VFT domain, leading to a conformational change that triggers the rearrangement of the TM domain through interactions between the second ECL and the CRD (Koehl et al., 2019; Mao et al., 2020).

The **rhodopsin** receptor family (class A) is the biggest GPCR subfamily and contains approximately 720 human receptor proteins (Gloriam et al., 2007; Foster et al., 2019). This subfamily includes receptors for diverse ligands, including light, odorants, neurotransmitters, and hormones (Gether, 2000; Fredriksson et al., 2003). Most receptors in the rhodopsin family share a similar arrangement of their 7 TM domain (Baldwin et al., 1997). Unlike other GPCR subfamilies, most rhodopsin receptor orthosteric ligand-binding sites are within the TM region (Figure 1-1B) (Lagerström & Schiöth, 2008). Given the wide range of physiological functions and ligands, the rhodopsin family contains the most significant number of therapeutically targeted receptors (Tyndall & Sandilya, 2005). Over 500 drugs target this family, with many drugs acting at more than one receptor (Yang et al., 2021).

The **adhesion** receptor family (class B2) used to be classified together with secretin (class B1) receptors, to whom they are phylogenetically related. However, the identification of structural and residual differences has resulted in

their reclassification as two separate families. The adhesion family contains 33 receptors and is the second-largest subfamily of human GPCRs (Alexander et al., 2019). These receptors play a crucial role in cell adhesion and migration (Pal et al., 2012; Bhudia et al., 2020). While adhesion receptors share similarities with secretin receptors in the TM domain, they differ in their long and diverse *N*-termini (Figure 1-1C) (Fredriksson et al., 2003). Moreover, adhesion receptors contain a conserved GPCR autoproteolysis-inducing (GAIN) domain and a proteolysis site that are involved in receptor activation (Prömel et al., 2013).

The **frizzled** (class F)/**taste2** (class T2) receptors are the most recently discovered GPCR subfamily. This family is composed of two distinct groups: the smoothed (SMO) and frizzled (FZD) receptors and the Taste2 (TAS2) receptor (Lagerström & Schiöth, 2008). The SMO and FZD receptors are activated by Hedgehog proteins and Wingless/Int-1 glycoproteins, respectively (Schulte & Wright, 2018) and play a role in cell fate, proliferation, and polarity (Fredriksson et al., 2003). SMO and FZD share a characteristic long *N*-terminus which contains a highly conserved CRD, which is essential for ligand-binding (Figure 1-1D) (Fredriksson et al., 2003). Taste2 receptors are expressed in the palate and tongue epithelium and function as bitter taste receptors (Fredriksson et al., 2003). They have a short *N*- and *C*-terminus, and ligands bind to the TM domain (Figure 1-1D) (Pronin, 2004; Lagerström & Schiöth, 2008; Nordstrom et al., 2008).

The **secretin** receptor family (class B1) contains 15 human members (Hauser et al., 2017). These receptors bind peptides such as glucagon and glucagon-like peptide which have high sequence similarity (Fredriksson et al., 2003). The *N*-terminus of secretin receptors is long and contains conserved cysteine bridges, which play a vital role in ligand-binding (Figure 1-1E) (Fredriksson et al., 2003). Upon peptide binding, the peptide's *C*-terminus interacts with the receptor's extracellular domain, orientating the peptide's *N*-terminus towards the TM domain. This interaction activates the receptor (Karageorgos et al., 2018).

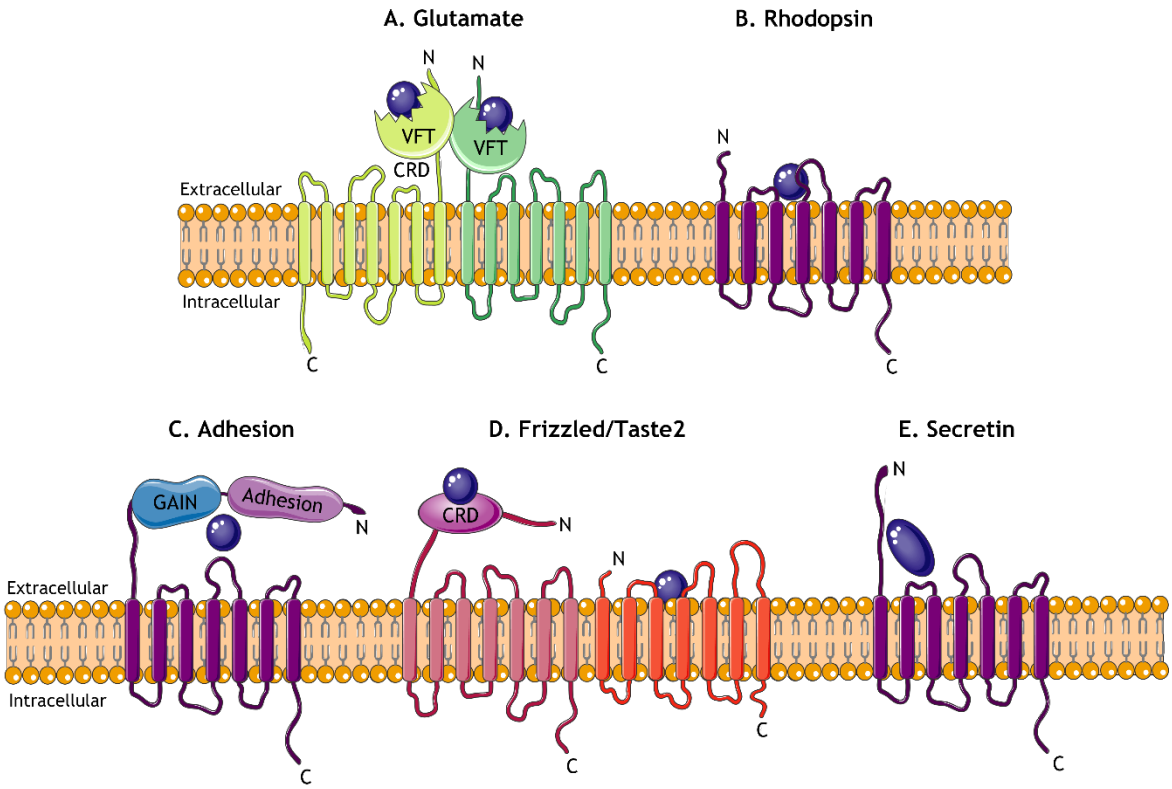

Figure 1-1 GRAFS classification of GPCR subfamilies. The core architecture of GPCRs consists of an extracellular *N*-terminus, seven transmembrane (TM) α-helices linked by alternating intra- and extracellular loops and an intracellular *C*-terminal tail. GPCR subfamilies have exceptionally diverse extracellular regions. (A) Glutamate receptors are typically organised as dimers and have a long *N*-terminal tail structured as a Venus flytrap (VFT) domain. The VFT constitutes the orthosteric binding site and is attached to the 7 TM domain by a cysteine-rich domain (CRD). (B) Ligand binding to rhodopsin receptors occurs in the TM domain, and these receptors have a shorter *N*-terminal tail. (C) Adhesion receptors contain diverse domains within the *N*-terminal tail, including a GPCR autoproteolysis-inducing (GAIN) domain. (D) Frizzled receptors contain a CRD within the *N*-terminal tail that facilitates ligand binding. Taste2 receptors have a short *N*- and *C*-terminal tail, and ligand-binding occurs in the TM domain. (E) Ligand binding occurs in secretin receptors *via* hormone peptide binding domains found within a long *N*-terminal tail. Ligands are shown in dark blue. Figure created using Reactome Icon Library, licensed under CC BY 4.0 (Sidiropoulos et al., 2017).

1.1.2 GPCR Activation

Receptors, including GPCRs, work to transduce signals from the extracellular environment across the plasma membrane to effector proteins in the cytoplasm, thus enabling the cell to respond to cues in their environment. Typically, these receptors are activated by a ligand binding to its orthosteric site, which triggers conformational changes in the receptor's TM and intracellular domains. These changes lead to the recruitment of effector proteins which bind to the intracellular domain of the GPCR (Calebiro et al., 2021).

1.1.2.1 G Protein-dependent Signalling

The GPCR superfamily derives its name from the first cytoplasmic effector to be identified, known as the G protein. Also known as guanine nucleotide-binding proteins, G proteins are the main effectors of GPCRs and a highly studied component of the GPCR signalling cascade (Calebiro et al., 2021). They are composed of an α, ß, and γ subunit, which together form a heterotrimeric G protein complex (Lambright et al., 1996). Lipid modifications on the α and γ subunits attach the G protein complex to the plasma membrane (Vögler et al., 2008). Gα, which contains distinct structural features such as an α-helical domain, signals independently (Kamato et al., 2015). Gß and Gγ subunits function as an obligate heterodimer (Gßγ) with the ß-sheets and an α-helix of Gß forming multiple interactions with the two α-helices of Gγ (Syrovatkina et al., 2016) (Figure 1-2).

G proteins get their name from guanosine triphosphate (GTP), and its inactive form, guanosine diphosphate (GDP), which regulate the activity of G proteins. Under basal conditions, the heterotrimeric G protein complex is in a GDP-bound state, with one molecule of GDP bound to the inactive Gα subunit (Gilman, 1987). Following a stimulus or ligand binding, GPCRs undergo a conformational change which catalyses the exchange of GDP for GTP, with the receptor functioning as a guanine nucleotide exchange factor (GEF) (Dror et al., 2015). This exchange results in a rearrangement of the G protein complex, with dissociation of the GTP-bound Gα subunit and the Gßγ dimer (Hamm, 1998; Cabrera-Vera et al., 2003; Oldham & Hamm, 2008). This dissociation enables the Gα and Gßγ subunits to interact with downstream signalling pathways independently. This signalling is terminated by the intrinsic GTPase activity of the Gα subunit, which hydrolyses GTP to GDP, therefore promoting the reassociation of the heterotrimeric Gαßγ complex and terminating signalling (McCudden et al., 2005). The human genome encodes for 16 Gα, 5 Gß, and 13 Gγ subunits, allowing for the formation of a wide range of G protein complexes which can all initiate different signalling pathways (Gautam et al., 1998; Hermans, 2003; Hewavitharana & Wedegaertner, 2012).

G proteins are categorised into four functional families based on their Gα subunit: $G\alpha_S$, $G\alpha_i$, $G\alpha_{12/13}$, and $G\alpha_{q/11}$ (Simon et al., 1991; Oldham & Hamm,

2006). Each family has a distinct signalling profile, which dictates the downstream cellular effects upon activation (Figure 1-2). $G\alpha_S$ and $G\alpha_i$ stimulate and inhibit adenylyl cyclase enzymes, respectively (Ross & Gilman, 1977; Hsia et al., 1984). Upon stimulation, activated adenylyl cyclase converts adenosine triphosphate (ATP) into cyclic adenosine monophosphate (cAMP). The cellular effects of cAMP are diverse, including hormone release, neuronal activation, and smooth muscle relaxation (Sutherland, 1972; Wettschureck & Offermanns, 2005). Importantly, not all isoforms of adenylyl cyclase are inhibited by $G\alpha_i$, and prolonged $G\alpha_i$ activation can enhance cAMP production (Brust et al., 2015). $G\alpha_{12/13}$ stimulates Rho-specific GEFs which activate the Rho family of small GTPases. These play a role in regulating intracellular actin dynamics (Spiering & Hodgson, 2011). Lastly, $G\alpha_{q/11}$ activates phospholipase C (PLC), leading to the synthesis of diacylglycerol (DAG) and inositol 1,4,5-triphosphate (IP3). DAG activates protein kinase C (PKC), and IP3 mediates the release of Ca^{2+} from intracellular stores (Kamato et al., 2015). These effectors play a role in synaptic transmission, smooth muscle contraction, and cellular hypertrophy (Wettschureck & Offermanns, 2005). Although it was once thought that individual GPCRs primarily coupled to one type of G protein, it is now known that GPCRs can be promiscuous, signalling via multiple G protein subtypes (Wootten et al., 2018).

Initially, Gβγ subunits were considered an accessory component of G protein signalling, thought to facilitate the reassociation and anchoring of the G protein complex with the plasma membrane (Calebiro et al., 2021). However, it is now known that the Gβγ subunit plays a key role in signal transduction (Smrcka & Fisher, 2019). After the dissociation of Gβγ from Gα, multiple Gβγ surfaces become exposed, allowing for interactions with receptors, membrane proteins, and a number of downstream effectors. For example, Gβγ plays a role in regulating Ca^{2+} and K^+ channels (Logothetis et al., 1987; Ikeda, 1996; Waard et al., 1997), mitogen-activated protein kinases (MAPKs) (Luttrell et al., 1997), phosphatidylinositol 3-kinase γ (P13Kγ) (Brock et al., 2003), and PLC-ß (Park et al., 1993; Illenberger et al., 2003) (Figure 1-2).

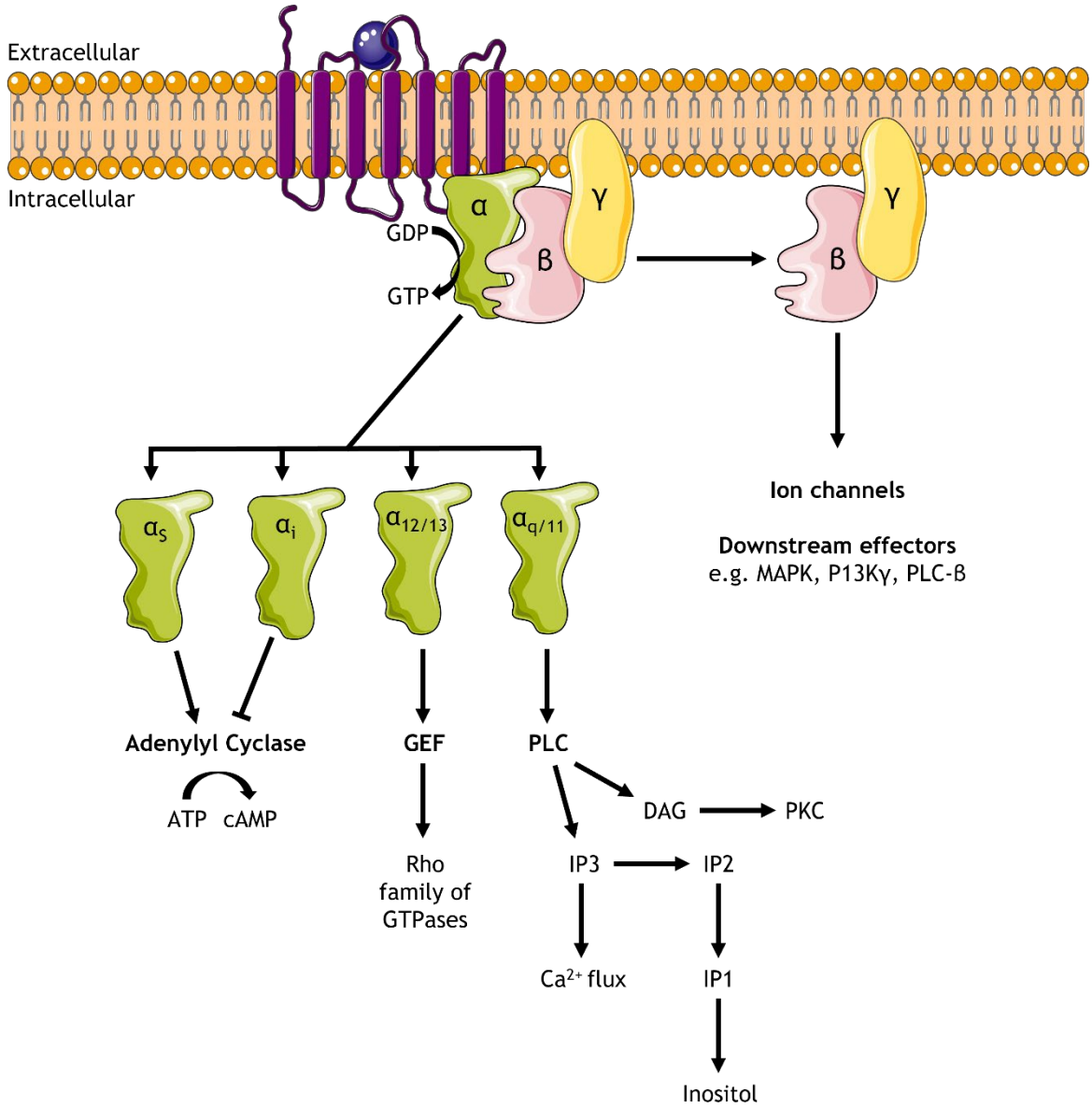

Figure 1-2 G protein-dependent signalling. Following activation of a GPCR, conformational changes induce the exchange of guanosine diphosphate (GDP) for guanosine triphosphate (GTP) on the Gα subunit. This results in dissociation between the Gα and Gβγ subunits. Gα proteins are grouped into four subfamilies: $G\alpha_S$, $G\alpha_i$, $G\alpha_{12/13}$, and $G\alpha_{q/11}$. $G\alpha_S$ and $G\alpha_i$ proteins regulate adenylyl cyclase activity. $G\alpha_{12/13}$ activates the Rho family of GTPase by stimulating Rho-specific guanosine exchange factors (GEF). $G\alpha_{q/11}$ stimulates phospholipase C (PLC), which leads to an increase in intracellular calcium (Ca_{2+}) through IP3 synthesis. PLC also leads to diacylglycerol (DAG) synthesis, which activates protein kinase C (PKC). Dissociated Gβγ subunits activate effectors such as ion channels, mitogen-activated protein kinases (MAPK), phosphatidylinositol 3-kinase γ (P13Kγ), and PLC-β. Figure created using Reactome Icon Library, licensed under CC BY 4.0 (Sidiropoulos et al., 2017).

1.1.2.2 Receptor Desensitisation and G Protein-independent Signalling

The signalling of GPCRs is terminated by receptor phosphorylation at threonine and serine residues located in the *C*-terminus and/or intracellular loops. This is mediated by GPCR kinases (GRKs) when the receptor is in an agonist-bound state

(Tobin, 2008). This phosphorylation increases the receptor's affinity for ß-arrestin binding, which mediates desensitisation by preventing the Gα subunit from binding to the receptor (Carman & Benovic, 1998) (Figure 1-3). This is due to the overlapping of the ß-arrestin and Gα binding interfaces (Szczepek et al., 2014). Thus, G protein-dependent signalling is terminated. This process is important as prolonged GPCR signalling can be toxic to the cell (Rajagopal & Shenoy, 2018). Furthermore, ß-arrestin facilitates clathrin-mediated endocytosis upon association with a GPCR. This results in receptor internalisation and the resulting intracellular vesicles are targeted for either recycling to the cell membrane or degradation (Goodman et al., 1996). Receptor phosphorylation can also occur independently from agonist-binding in a process known as heterologous desensitisation. This is *via* second messenger kinases such as PKC and protein kinase A (PKA) (Pierce & Lefkowitz, 2001; Carmona-Rosas et al., 2019). This process directly uncouples a GPCR and its G proteins, thus halting G protein-dependent signalling.

Apart from the role ß-arrestin plays in GPCR desensitisation, it has recently been recognised as an important mediator of GPCR signalling. ß-arrestins can induce signalling cascades by activating effectors such as MAPK (Eichel et al., 2016) and act as scaffold proteins for cytoplasmic signalling proteins (DeWire et al., 2007). Signalling via ß-arrestin is slower and more sustained compared to G protein-dependent signalling (Shenoy et al., 2006).

Activated receptors display distinct phosphorylation patterns, known as a phosphorylation barcode; therefore, the downstream functional outcomes are diverse (Butcher et al., 2011). The phosphorylation pattern is also dependent on the GRK expression. As kinase expression differs between cell types, this results in cell type-specific signalling (Tobin, 2008).

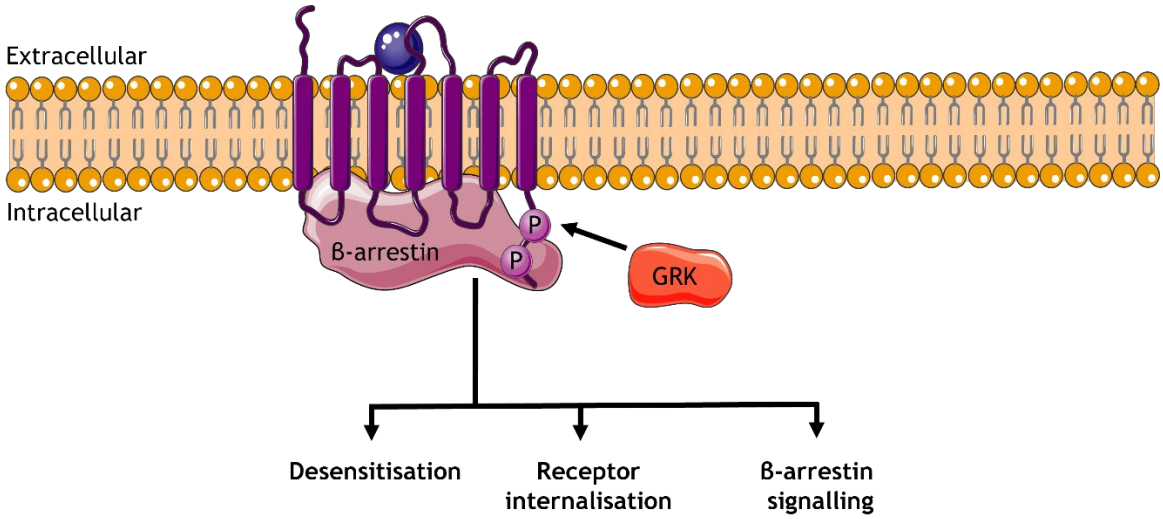

Figure 1-3 G protein-independent signalling. Following agonist-binding and G protein-signalling, GPCR kinases (GRK) phosphorylate threonine and serine residues on the intracellular loops or *C*-terminal tail of the GPCR. This recruits β-arrestin to the receptor, thus preventing G protein binding (receptor desensitisation). The GPCR is then internalised in intracellular vesicles. Moreover, GPCRs are able to signal *via* β-arrestin. Figure created using Reactome Icon Library, licensed under CC BY 4.0 (Sidiropoulos et al., 2017).

1.1.3 GPCR Pharmacology

The activity of a receptor after ligand binding can be described using a number of parameters, such as efficacy, affinity, and potency. Efficacy measures the ability of a ligand to induce a response from the receptor (Kenakin, 2002). Affinity measures the strength of the interaction between the ligand and its receptor (Rosenkilde & Schwartz, 2000). Lastly, the potency of a ligand measures the amount of drug needed for an effect of a given magnitude. Usually, this is quantified as the ligand concentration necessary to evoke 50% of the ligand's maximal response (EC_{50}) (Weatherall, 1966).

The activity of a GPCR can be pharmacologically manipulated using ligands that either bind to the same site as the endogenous ligand, known as the orthosteric site, or by ligands that bind to a site that is topologically distinct from the orthosteric binding site, known as the allosteric site (Wootten et al., 2013). Ligands binding to the receptor's orthosteric site can be categorised as full, partial, or inverse agonists, or neutral antagonists (Figure 1-4A). Endogenous ligands usually maximally activate their GPCR and are thus considered full agonists. Agonists that do not maximally activate their GPCR are defined as partial agonists. By contrast, antagonists block receptor activity. These can

either be inverse agonists, which reduce the constitutive activity of a receptor, or neutral antagonists, which inhibit the effect of an agonist, but do not alter constitutive activity (Wacker et al., 2017).

Allosteric ligands can be characterised based on their effect on the orthosteric ligand: they can affect the efficacy or binding affinity of the orthosteric ligand, or they can exert an effect that is independent of the orthosteric ligand (Langmead & Christopoulos, 2006). The modulation of GPCRs using allosteric ligands is an attractive therapeutic option as they can be developed to have increased spatial and temporal selectivity (Christopoulos et al., 2014). Positive allosteric modulators (PAMs) increase the efficacy/affinity of the orthosteric ligand, negative allosteric modulators (NAMs) decrease the efficacy/affinity of the orthosteric ligand, and silent allosteric modulators (SAMs) have no effect on the efficacy/affinity of the orthosteric ligand, but block PAM or NAM activity by acting as a competitive agonist at the allosteric site (Figure 1-4B).

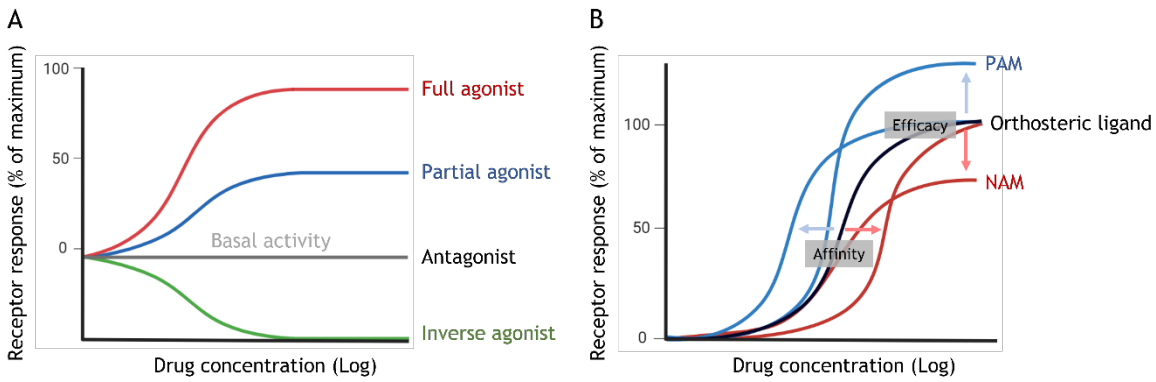

Figure 1-4 The pharmacology of GPCR ligands. Simplified concentration response curves demonstrating the activity of (A) orthosteric and (B) allosteric ligands. (A) Full (red) and partial (blue) orthosteric ligands result in a maximum or partial activation of the receptor, respectively. Orthosteric antagonists (black) elicit no response from the receptor. Inverse agonists (green) reduce the receptor's constitutive activity. (B) The concentration response curve of an orthosteric ligand is shown in black. Allosteric ligands bind to a site that is distinct from the orthosteric site. These can be classified as positive allosteric modulators (PAM), which increase the activity induced by the orthosteric ligand, or negative allosteric modulators (NAM), which inhibit the activity induced by the orthosteric ligand. While PAMs increase the efficacy/affinity of the orthosteric ligand, NAMs reduce the efficacy/affinity of the orthosteric ligand.

Some ligands can engage both the orthosteric and allosteric sites simultaneously. These are known as bitopic ligands and can be agonists or antagonists (Valant et al., 2012). Similar to allosteric ligands, bitopic ligands are therapeutically attractive as they provide an opportunity for increased selectivity.

Ligands targeting GPCRs can exhibit “signalling bias”, which refers to their ability to selectively activate a specific signalling pathway whilst minimising unwanted side effects from the activation of other pathways (Rajagopal et al., 2010; Violin et al., 2014; Hauser et al., 2017). For example, ligands can be developed to favour coupling to either a G protein or ß-arrestin (Maudsley et al., 2012). Several potential therapeutic ligands which show bias towards one of these pathways over the other are currently being investigated in preclinical studies or clinical trials. For example, the ß-arrestin signalling pathway of the M1 muscarinic receptor provides neuroprotective effects and minimises adverse responses in rodent models of neurodegenerative disease (NDD) (Scarpa et al., 2021). A recent FDA-approved drug, oliceridine, which targets the μ-opioid receptor (Lambert & Calo, 2020), is designed to not signal *via* ß-arrestin, a pathway linked to opioid-induced respiratory depression and constipation (Bohn et al., 1999).

1.1.4 GPCRs as Drug Targets for Central Nervous System Disorders

The diversity of GPCR downstream signalling cascades make GPCRs attractive candidates for drug development (Hauser et al., 2017). There are 826 human GPCRs, of which approximately 350 non-olfactory GPCRs are considered “druggable”. “Druggability” is the ability of a receptor to be targeted by a small, potent “drug-like” ligand (Hopkins & Groom, 2002). Of these 350 GPCRs, 165 have been validated as drug targets, accounting for over 30% of all clinically approved drugs (Kunishima et al., 2000; Hauser et al., 2017; Santos et al., 2017).

Around 25% of all approved GPCR-target drugs target diseases of the central nervous system (CNS) (Hauser et al., 2017). Several CNS disorders are NDDs, characterised by the progressive degeneration and loss of neurons. Common NDDs include Alzheimer’s disease (AD), Huntington’s Disease (HD), Amyotrophic lateral sclerosis (ALS), and Parkinson’s disease (PD) (Lamptey et al., 2022). Most current treatments for these diseases focus on alleviating disease symptoms rather than modifying the underlying disease pathology. Therefore, there is an urgent need for the development of novel therapeutics.

GPCRs play a role in the pathogenesis of a number of these diseases. For example, several GPCRs are downregulated in HD, with several GPCR-targeted drugs currently in clinical trials (Hauser et al., 2017). A number of GPCR-targeted drugs are in clinical trials for AD (Hauser et al., 2017), and GPCRs play a role in several neurotransmitter systems that are dysregulated in AD, such as the glutamatergic (Conway, 2020), cholinergic (Ferreira-Vieira et al., 2016), and serotonergic (Chakraborty et al., 2019) pathways. The dysregulation of the glutamatergic system, for example, is discussed in this thesis (see 1.3.2.2).

Despite the large number of GPCR-target drugs, just over 10% of GPCRs have approved drugs targeting them (Sriram & Insel, 2018). However, as new functions are uncovered and orphan receptors are deorphanized, the number of GPCR-targeted drugs is hoped to increase (Laschet et al., 2018).

1.2 Glutamate Receptors

The type 5 metabotropic glutamate receptor ($mGlu_5$) is a GPCR that has been proposed as a potential therapeutic target for the treatment of NDDs and is the focus of this thesis. However, as $mGlu_5$ plays an important role in the modulation of *N*-methyl-D-aspartate (NMDA) receptor signalling, these are also discussed in this introduction.

1.2.1 Classification

Glutamate, the major excitatory neurotransmitter in the CNS, acts on two types of receptors: ionotropic receptors, which mediate fast, excitatory responses, and metabotropic receptors, which mediate slow, long-lasting responses (Conn & Pin, 1997). Ionotropic glutamate receptors are classified by function and molecular homology into three classes: NMDA, α-amino-3-hydroxy-5-methyl-4-isoxazole propionic acid (AMPA), and kainate receptors. Each ionotropic glutamate receptor comprises a tetrameric assembly of multiple subunits exclusive to each receptor class (Rojas & Dingledine, 2013). The mGlu receptors belong to the glutamate (class C) GPCR subfamily (see section 1.1.1). The eight members of the mGlu family are divided into three subgroups based on their pharmacological profile and sequence homology (Table 1-1). Members within each group share around 70% of their sequence homology, while between

groups, sequence homology is reduced to approximately 45% (Conn & Pin, 1997). The $mGlu_5$ receptor belongs to group I, along with the $mGlu_1$ receptor, and predominantly couples to $G\alpha_{q/11}$ proteins, which stimulate PLC, leading to the synthesis of DAG and IP3, which in turn leads to intracellular Ca^{2+} release (see section 1.1.2.1 and 1.2.5).

Table 1-1 Group classification of metabotropic glutamate receptors.

Subgroup	Receptors	G protein	Synaptic localisation*	Function**
Group I	$mGlu_1$ $mGlu_5$	$G\alpha_{q/11}$	Mainly postsynaptic	Stimulation of PLC and adenylyl cyclase, MAPK phosphorylation, increase NMDA receptor activity
Group II	$mGlu_2$ $mGlu_3$	$G\alpha_i$	Mainly presynaptic	Inhibition of adenylyl cyclase, activation of K^+ channels, inhibition of Ca^{2+} channels, decrease NMDA receptor activity
Group III	$mGlu_4$ $mGlu_6$ $mGlu_7$ $mGlu_8$	$G\alpha_i$	Mainly presynaptic	Inhibition of adenylyl cyclase, activation of K^+ channels, inhibition of Ca^{2+} channels, decrease NMDA receptor activity

*(Shigemoto et al., 1993) **(Niswender & Conn, 2010)

1.2.2 Ionotropic Glutamate Receptors

Ionotropic glutamate receptors are ligand-gated ion channels (Traynelis et al., 2010). Among these receptors, NMDA and AMPA receptors are the most extensively studied. AMPA receptors are primarily localised to the postsynaptic membrane of glutamatergic neurons (Patriarchi et al., 2018). They exist as either homo- or hetero-tetramers with four subunits (GluA1-4). The GluA2 subunit determines whether an AMPA receptor is permeable to Ca^{2+}: GluA2-containing AMPA receptors are Ca^{2+}-impermeable and mainly expressed on excitatory projection neurons (Lodge, 2009), whereas GluA2-lacking AMPA receptors are Ca^{2+}-permeable and are mainly expressed on inhibitory interneurons (Mahanty & Sah, 1998). In addition, AMPA receptors are expressed on glial cells, including astrocytes and microglia (Ceprian & Fulton, 2019). Their activation on microglia contributes to the release of pro-inflammatory cytokines (Noda, 2013).

Like $mGlu_5$ receptors (see 1.2.3), NMDA receptors are primarily localised to the postsynaptic membrane of glutamatergic neurons but can also be found on presynaptic membranes. They exist as obligate heterodimers, with two GluN1 subunits and either two GluN2 subunits or a combination of GluN2 and GluN3 subunits (Paoletti, 2011). The activation of NMDA receptors requires the binding of both glutamate and the co-agonist glycine (Johnson & Ascher, 1987), in addition to the removal of a Mg^{2+} block by membrane depolarisation (Mayer et al., 1984). Upon opening, NMDA receptors allow positively charged ions, such as Ca^{2+}, to enter the cell (Furukawa et al., 2005). The signalling of NMDA receptors is slower and more prolonged than AMPA receptor signalling due to the requirement for membrane depolarisation and the slower kinetics of activation and desensitisation (Paoletti, 2011). Like AMPA receptors, NMDA receptors are expressed in astrocytes, although their specific functions in astrocytes are poorly understood (Skowrońska et al., 2019). It has been suggested that NMDA receptors containing a GluN2C subunit may regulate synaptic strength in hippocampal astrocytes (Chipman et al., 2021). As discussed later in this thesis, $mGlu_5$ receptors are physically associated with NMDA receptors and can modulate their signalling (see 1.2.6.1).

1.2.3 Distribution of $mGlu_5$ Receptors

There are two isoforms for the $mGlu_5$ receptor, $mGlu_5a$ and $mGlu_5b$ (Joly et al., 1995; Minakami et al., 2002). These isoforms have a similar structure except for the insertion of a 32 amino acid region in the *C*-terminus of $mGlu_5b$ (Joly et al., 1995). While $mGlu_5$ is expressed in most brain regions, $mGlu_5a$ is the predominant isoform during early postnatal development, and $mGlu_5b$ is the predominant isoform in adulthood (Romano et al., 1996; Minakami et al., 2002). The differential expression of the two isoforms suggests that they may have distinct functions during development.

In situ hybridisation and RNA blot analysis have been used to analyse the expression of $mGlu_5$ mRNA in the CNS (Figure 1-5A). In adults, $mGlu_5$ is found in the hippocampus, cerebral cortex, striatum, olfactory bulb, and basal ganglia (Shigemoto et al., 1993; Wong et al., 2013). The highest expression is found in the hippocampus and basal ganglia and the lowest in the pons/medulla and

cerebellum (Abe et al., 1992; Shigemoto et al., 1993). Moreover, $mGlu_5$ is abundantly expressed in spinal cord neurons (Valerio et al., 1997).

Although also found on the presynaptic membrane, $mGlu_5$ is predominantly expressed on the postsynaptic membrane of glutamatergic neurons (Figure 5-1B) (Luján et al., 1996). Along with $mGlu_1$, it is localised in perisynaptic zones, where synaptic vesicle endocytosis occurs (Brodin & Shupliakov, 2006). A large proportion (50-80%) of $mGlu_5$ receptors are found on intracellular membranes, such as the endoplasmic reticulum and nuclear membrane (Figure 5-1B) (Hubert et al., 2001; Kumar et al., 2008). These intracellular receptors are oriented with the *C*-terminal tail in the cytoplasm and the *N*-terminal tail in the lumen of the organelle, thus allowing access to the same cytoplasmic effectors as $mGlu_5$ that is expressed on the plasma membrane (Jong et al., 2014). However, in order to reach intracellular $mGlu_5$, ligands need to be transported or diffuse across the plasma membrane (Jong et al., 2005). Glutamate stimulates intracellular $mGlu_5$ after being transported into the cell via excitatory amino-acid transporters (EAATs) or cysteine-glutamate exchangers (xCT) (Jong et al., 2005). The activation of intracellular $mGlu_5$ results in distinct downstream signalling pathways and Ca^{2+} responses as compared to $mGlu_5$ receptors on the cell surface (Jong et al., 2009).

In addition to its neuronal expression, $mGlu_5$ is found in glial cells, including microglia and astrocytes (Loane et al., 2012). In rodents, $mGlu_5$ expression has been observed in astrocytes isolated and maintained in culture from the cortex, hippocampus, striatum, and thalamus, but not the spinal cord or cerebellum (Biber et al., 1999; Silva et al., 1999). In cells isolated from rodent tissue and brain slices, the expression of $mGlu_5$ in astrocytes peaks during neurodevelopment. This expression then decreases with age, suggesting that the role of astrocytic $mGlu_5$ decreases with age (Cai et al., 2000).

The expression of $mGlu_5$ in the brain is altered in both ageing humans and those with a NDD. This is discussed in more detail in section 4.1.1.

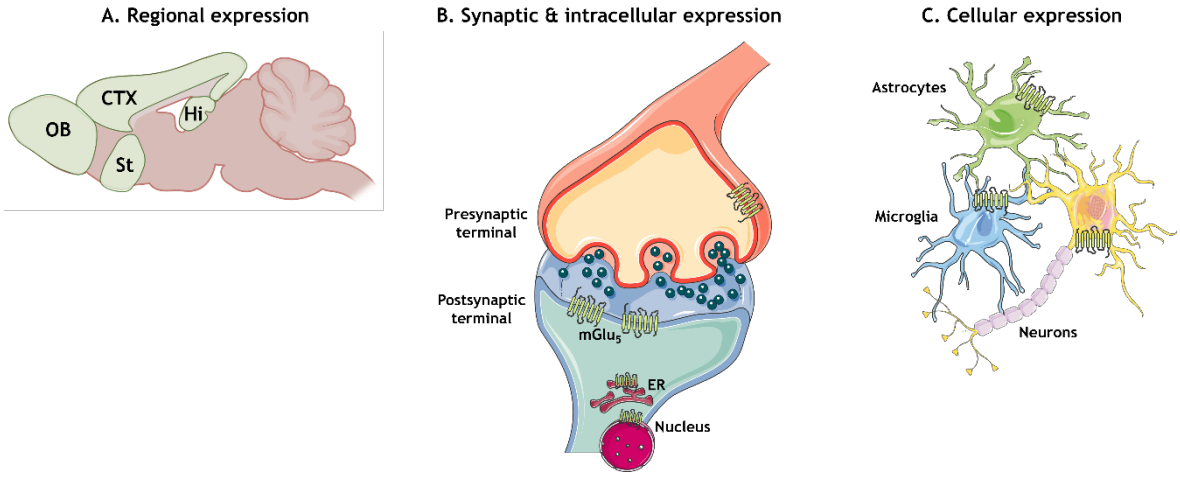

Figure 1-5 Regional, synaptic, intracellular, and cellular expression of $mGlu_5$. (A) Sagittal slice of a mouse brain showing $mGlu_5$ expression in the hippocampus (Hi), cerebral cortex (CTX), striatum (St), and olfactory bulb (OB). (B) Although found on the pre-synaptic membrane, $mGlu_5$ is predominantly expressed in perisynaptic zones on the postsynaptic membrane. In addition, $mGlu_5$ is expressed on intracellular membranes, including the endoplasmic reticulum (ER) and nuclear membranes. (C) In addition to its expression on neurons, $mGlu_5$ is expressed on glial cells, including astrocytes and microglia. Figure created using Reactome Icon Library, licensed under CC BY 4.0 (Sidiropoulos et al., 2017).

1.2.4 Structure of $mGlu_5$ Receptors

As discussed in section 1.1, all GPCRs have a similar core architecture (Venkatakrishnan et al., 2013). Glutamate receptors commonly exist as obligate dimers (McCullock & Kammermeier, 2021) (Figure 1-6). This is true for $mGlu_5$, which is functional as a homodimer (Romano et al., 1996; Pin & Bettler, 2016; Nasrallah et al., 2021). This dimerisation is mediated by an intermolecular disulphide bridge that forms between the extracellular domain of each monomer (Nasrallah et al., 2021). In addition, $mGlu_5$ can form an intra-group heterodimer with $mGlu_1$, but it cannot associate with mGlu receptors in the other groups (Nicoletti et al., 2011).

Glutamate receptors have a large extracellular VFT domain on their *N*-terminal tail. The VFT domain contains two lobes that close around glutamate upon binding, forming the orthosteric binding site (Kunishima et al., 2000). In an inactive state, neighbouring VFT domains have a single interaction interface primarily composed of hydrophobic residues and stabilised by a conserved disulphide bond (Koehl et al., 2019). This disulphide bond is not required for signalling or dimer formation (Ray & Hauschild, 2000). Linking the VFT domain to the 7 TM domain is a semi-rigid CRD which plays an important role in relaying

the conformational changes induced by glutamate in the VFT domain to the 7 TM, thereby facilitating coupling with intracellular effectors (Rondard et al., 2006; Nasrallah et al., 2021).

Cryoelectron microscopy (cryo-EM) structures have revealed how the VFT domain, CRD, and 7 TM domain of $mGlu_5$ reorganise upon receptor activation (Koehl et al., 2019). The binding of an agonist to a VFT lobe stabilises it in a closed state and reorients the VFT dimer into an active state. While closure of one VFT lobe is sufficient for activation of the receptor, closure of both lobes is necessary for full efficacy (Kniazeff et al., 2004). In contrast, the binding of an antagonist to a VFT lobe stabilises it in an open and inactive dimer state (Pin & Bettler, 2016). Following agonist-binding, the $mGlu_5$ dimer compacts and the CRDs of adjacent VFT domains are brought into close proximity to each other (Figure 1-6B) (Kunishima et al., 2000; Koehl et al., 2019). This conformational change is propagated through the CRD to the second ECL (ECL2) of the 7 TM domain. In the resting state, the two 7 TM domains that make up the dimer are completely separated (Figure 1-6A). When activated, the conformational changes bring these into close proximity to each other, and intermolecular interactions occur at the top of the sixth TM (TM6) of each dimer (Koehl et al., 2019) (Figure 1-6B). This TM6-TM6 interaction is a key hallmark of $mGlu_5$ activation, which promotes G protein coupling to the 7 TM domain, in the vicinity of the allosteric binding site (Nasrallah et al., 2021).

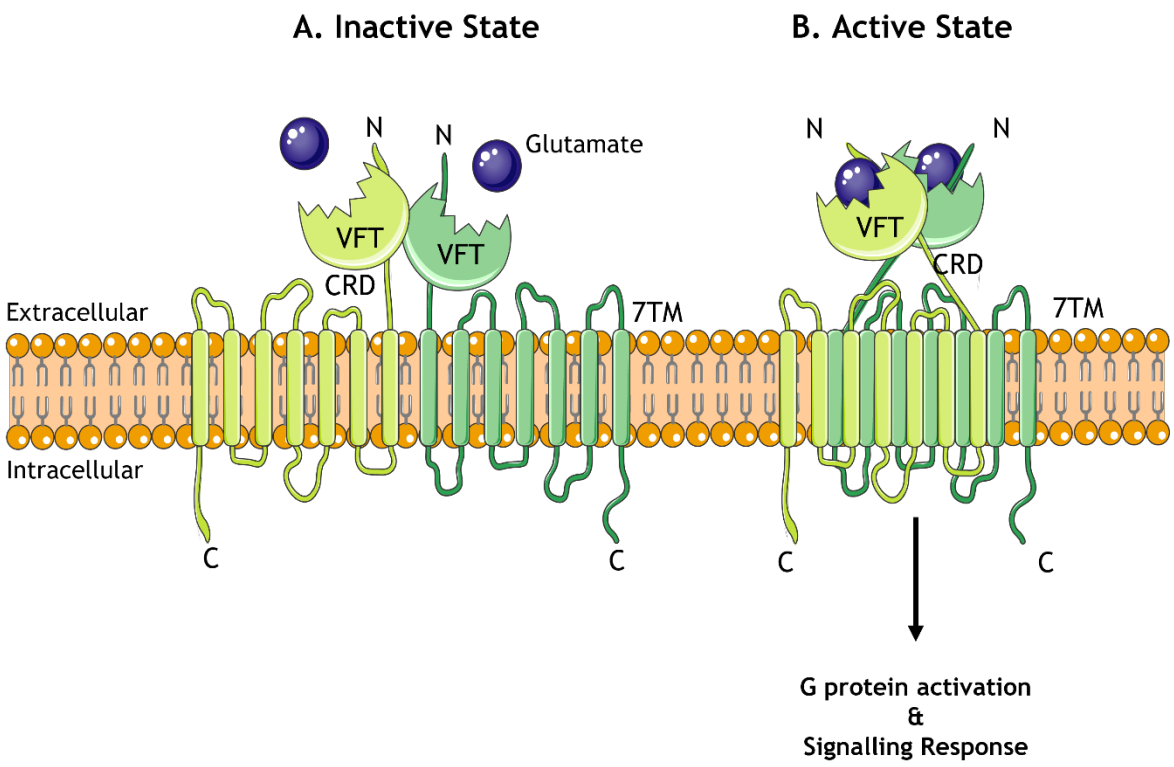

Figure 1-6 Schematic of mGlu$_5$ activation. (A) In an inactive state, the mGlu$_5$ dimers are physically separated, and the Venus flytrap domain (VFT) is stabilised in an inactive position. (B) Upon binding of glutamate (dark blue circle), a conformational change occurs. The VFT domain is stabilised in an active state, and the two 7 transmembrane domains (7 TM) and cysteine-rich domains (CRD) are brought into close proximity with each other. This conformational change promotes G protein coupling to the 7 TM domain and receptor activation. Figure created using Reactome Icon Library, licensed under CC BY 4.0 (Sidiropoulos et al., 2017).

The main allosteric binding site of mGlu receptors is found in the 7 TM domain, situated between TM2, TM3, TM5, TM6, and TM7 (Figure 1-7). Crystal structures have revealed that this site overlaps with the orthosteric binding site in the rhodopsin (class A) receptor family (Doré et al., 2014; Christopher et al., 2015, 2019). To allow for the binding of group I-specific ligands, group I mGlu receptors have three hydrophilic residues at the entrance to their allosteric binding site. Notably, the allosteric binding pocket of mGlu1 has been shown to sit higher in the 7 TM domain than that of mGlu$_5$ (Bennett et al., 2015; Gregory & Conn, 2015).

A second allosteric binding site has been proposed for mGlu$_5$. Several mGlu$_5$ PAMs have shown non-competitive behaviour with a 2-methyl-6-(phenylethynyl) pyridine (MPEP) radioligand, which is known to bind to the well characterised allosteric binding pocket in the 7 TM domain (O'Brien et al., 2004; Noetzel et

al., 2013). Mutagenesis studies have suggested that a phenylalanine residue located in TM1 may contribute to this second allosteric binding pocket (Chen et al., 2008). Mutations in this residue do not affect the binding of ligands to the MPEP allosteric site and *vice versa* (Chen et al., 2008).

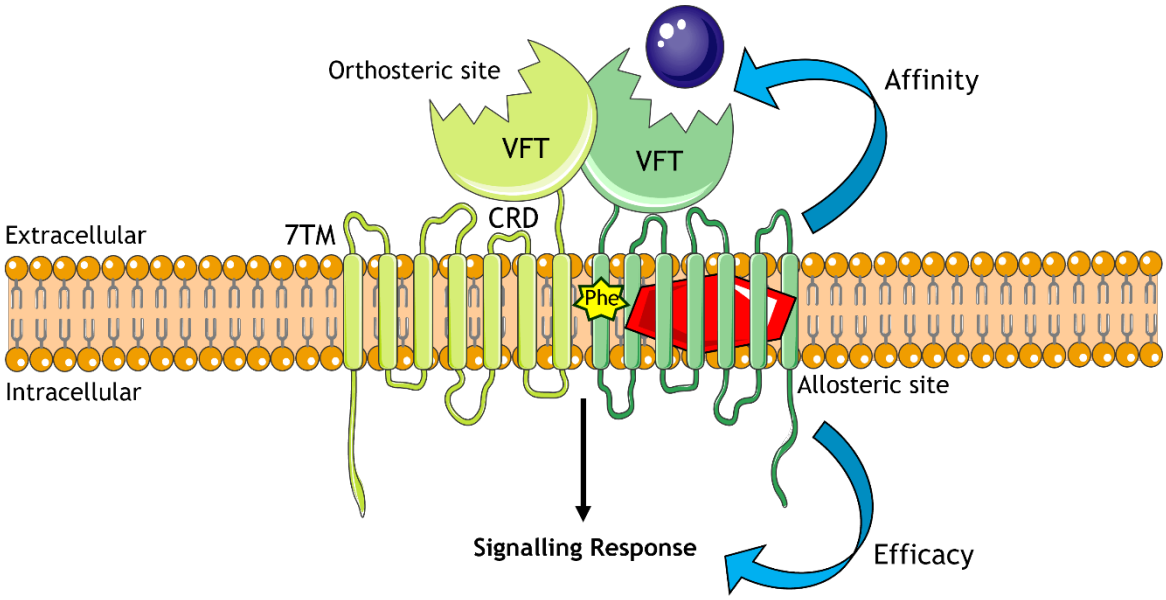

Figure 1-7 Schematic of the allosteric binding sites of mGlu$_5$. Allosteric modulators (red hexagon) bind to a site that is topographically distinct from the orthosteric site, known as the allosteric site, in the 7 transmembrane domain (7TM). The main allosteric site of mGlu$_5$ is situated between TM2 and TM7. A phenylalanine (Phe) residue in TM1 (yellow star) may contribute to a second allosteric binding site. The simultaneous binding of an allosteric modulator and an orthosteric agonist (dark blue circle) affects the efficacy and affinity of the orthosteric agonist. Some allosteric modulators can exert their effect without orthosteric ligand binding. Figure adapted from Budgett et al., 2022 and created using Reactome Icon Library, licensed under CC BY 4.0 (Sidiropoulos et al., 2017).

1.2.5 Signalling of mGlu$_5$ Receptors

As a glutamate (class C) receptor, mGlu$_5$ preferentially couples to G$\alpha_{q/11}$ proteins upon activation. G$\alpha_{q/11}$ activates PLC-β, which hydrolyses membrane-bound phosphoinositides into IP3 and DAG. Subsequently, IP3 binding to its receptors releases Ca^{2+} from intracellular stores (Masu et al., 1991; Abe et al., 1992; Hermans & Challis, 2001). Unlike mGlu$_1$, which induces a single peak of Ca^{2+} release, mGlu$_5$ is able to induce Ca^{2+} oscillations (Kawabata et al., 1996). The generation of Ca^{2+} oscillations is due to the phosphorylation of a threonine residue in mGlu$_5$ by PKC, which is not found in mGlu$_1$ (Kawabata et al., 1996).

Intracellular Ca^{2+}, together with DAG, can modulate the activation of a variety of cellular substrates such as PKC, MAPK, and ion channels, providing diverse downstream signalling effects (Hermans & Challis, 2001; Conn et al., 2009).

In addition to coupling to $G\alpha_{q/11}$, $mGlu_5$ has been shown to interact with $G\alpha_S$ in HEK293 cells (Francesconi & Duvoisin, 1998), leading to increased cAMP formation (Joly et al., 1995). However, cAMP formation is not observed when $mGlu_5$ is expressed in CHO cells or cultured astrocytes (Abe et al., 1992; Balázs et al., 1997), suggesting that the promiscuous activity of $mGlu_5$ is cell-type dependent.

The termination of $mGlu_5$ signalling is initiated by the phosphorylation of threonine and serine residues in the *C*-terminus by GRKs, which initiates desensitisation and the recruitment of ß-arrestin (see section 1.1.2.2). This process uncouples the receptor from its G proteins and initiates receptor internalisation (Ferguson, 2001; Dhami & Ferguson, 2006). GRK2 has been demonstrated to contribute to the phosphorylation of $mGlu_5$, but it is also able to uncouple $mGlu_5$ and $G\alpha_{q/11}$ in a phosphorylation-dependent manner (Sorensen & Conn, 2003; Dhami & Ferguson, 2006; Ribeiro et al., 2009). PKC phosphorylation can also desensitise group I mGlu receptors (Alaluf et al., 1995; Gereau & Heinemann, 1998). In addition to the role of ß-arrestin in receptor desensitisation, $mGlu_5$ is able to signal via ß-arrestin (Stoppel et al., 2017). Although there is currently no evidence for the coupling of ß-arrestin directly to $mGlu_5$, they have been shown to co-immunoprecipitate (Eng et al., 2016). Moreover, ß-arrestin is required for some signalling pathways downstream of $mGlu_5$ (Stoppel et al., 2017).

Several proteins, other than G proteins, interact with $mGlu_5$ at the plasma membrane. For example, Homer proteins bind to the *C*-terminal tail of $mGlu_5$ (Brakeman et al., 1997), linking $mGlu_5$ with a number of signalling effectors such as PLC, P13K and the IP3 receptor (Tu et al., 1998; Xiao et al., 1998; Rong et al., 2003). Moreover, Homer proteins enable $mGlu_5$ to form physical connections with membrane proteins, including NMDA receptors, *via* connections with other scaffolding proteins such as postsynaptic density 95 (PSD95), guanylate kinase-associated protein (GKAP) and SHANK (Tu et al., 1999).

A number of effectors downstream of $mGlu_5$ have been identified, including MAPK, mammalian target of rapamycin (mTOR), cAMP response element binding protein (CREB), and extracellular signal-regulated kinase 1/2 (ERK1/2). These are shown in Figure 1-8 and discussed in more detail in section 1.2.6.

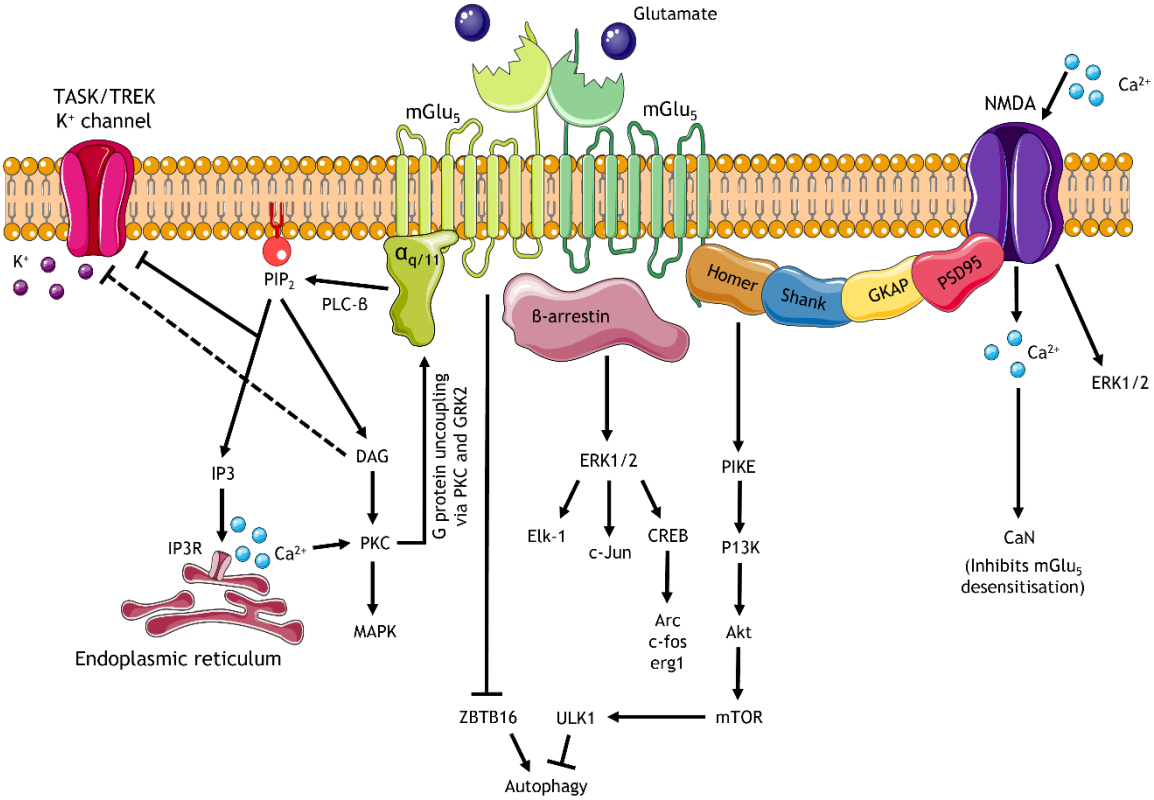

Figure 1-8 Schematic of $mGlu_5$ signalling pathways. Upon glutamate binding, $mGlu_5$ predominantly couples to $G\alpha_{q/11}$ proteins, which activate phospholipase C-β (PLC-β), which mediates the hydrolysis of phosphoinositide (PIP_2) into inositol-1,4,5-triphosphate (IP3) and diacylglycerol (DAG). IP3 binds to IP3 receptors (IP3R) on the endoplasmic reticulum, resulting in the release of calcium (Ca^{2+}). Ca^{2+} and DAG activate protein kinase C (PKC). PKC activates a number of effectors including mitogen-activated protein kinases (MAPK). PKC and GRK2 are able to terminate $mGlu_5$ signalling by uncoupling the G protein. $mGlu_5$ inhibits TASK and TREK K^+ channels via the depletion of PIP_2 and the activation of DAG. Autophagy is regulated by $mGlu_5$ via alterations in the Unc-51-like kinase 1 (ULK1) and zinc finger and BTB domain-containing protein (ZBTB16) pathways. Additionally, $mGlu_5$ recruits β-arrestin, which mediates the activation of other signalling pathways, including ERK1/2 recruitment. ERK1/2 phosphorylation activates transcription factors such as Elk-1, c-Jun, and cAMP response element binding protein (CREB). CREB modulates the transcription of learning and memory-related genes such as Arc, c-fos, and erg-1. Homer proteins bind to the *C*-terminal tail of $mGlu_5$ and allow the formation of protein complexes which bridge $mGlu_5$ to ligand-gated receptors, such as NMDA. This protein bridge includes SHANK, guanylate kinase-associated protein (GKAP), and postsynaptic density 95 (PSD95). NMDA is activated by $mGlu_5$, and the subsequent influx of Ca^{2+} into the cell activates calcineurin (CaN), which reduces $mGlu_5$ desensitisation. NMDA and $mGlu_5$ also interact to regulate ERK1/2 phosphorylation. In addition, the association of Homer proteins with $mGlu_5$ results in an increase in phosphatidylinositol 3-kinase (P13K) activity, which is mediated by phosphatidylinositol triphosphate (PIKE). Subsequently, this results in protein kinase B (Akt) phosphorylation and the activation of mammalian target of rapamycin (mTOR). mTOR is able to modulate autophagy via interactions with ULK-1. Figure adapted from (Abd-Elrahman & Ferguson, 2022) and created using Reactome Icon Library, licensed under CC BY 4.0 (Sidiropoulos et al., 2017).

1.2.6 The Function of $mGlu_5$ Receptors in the CNS

1.2.6.1 Modulation of Other Receptors

Electrophysiological studies have shown that $mGlu_5$ receptors expressed on the postsynaptic membrane can modulate the activity of ligand- and voltage-gated ion channels in the CNS. In particular, group I mGlu receptors, including $mGlu_5$, can contribute to cellular excitability by inhibiting background K^+ channels, thus affecting membrane potential. Background K^+ channels, which control the resting potential of a cell, are made up of four transmembrane segments and have two pore domains (K_{2P}) in their primary sequence (Lesage & Lazdunski, 2000; Patel & Honoré, 2001). Of the K_{2P} family of K^+ channels, TREK and TASK channels are highly expressed in the CNS (Duprat, 1997; Fink, 1998; Lesage & Lazdunski, 2000; Lauritzen et al., 2005). Glutamate inhibits TASK and TREK channels *via* $G\alpha_{q/11}$-coupled mGlu receptors, including $mGlu_5$. This occurs through two distinct pathways. Firstly, *via* the depletion of PIP_2 and the synthesis of IP3 following the activation of PLC. And secondly, the channels are directly blocked by DAG (Chemin, 2003). Inhibition of background K^+ channels induces membrane depolarisation and the subsequent firing of an action potential (Patel et al., 1999).

In addition, $mGlu_5$ is able to modulate currents conducted by ligand-gated ion channels, including NMDA receptors. NMDA receptors are physically associated with $mGlu_5$ *via* the interaction of Homer proteins with SHANK, GKAP, and PSD95 (Tu et al., 1999). NMDA receptors play an important role in synaptic function and plasticity (Salter, 1998), and their physical association with $mGlu_5$ has been shown to be crucial for long-term potentiation (Awad et al., 2000). The activation of $mGlu_5$ results in NMDA receptor activation and the entry of Ca^{2+} into the cytoplasm (Salter, 1998; Awad et al., 2000; Huang & van den Pol, 2007). This positive modulation of NMDA receptors *via* $mGlu_5$ has been observed after the addition of a $mGlu_5$ agonist to rat hippocampal slices (Doherty et al., 1997), mouse striatal medium spiny neurons (Pisani et al., 2001), and rat subthalamic nucleus slices (Awad et al., 2000). The influx of Ca^{2+} into the cell activates calcineurin (CaN), which subsequently reduces the desensitisation of $mGlu_5$.

Furthermore, $mGlu_5$ has been found to have functional interactions with dopaminergic neurons (Vezina & Kim, 1999). Although $mGlu_5$ is not located on dopaminergic neurons (Testa et al., 1994), $mGlu_5$ activation has been observed to reduce K^+-stimulated dopamine release. For example, activating $mGlu_5$ reduced dopamine in the nucleus accumbens (Liu et al., 2008). Conversely, the $mGlu_5$ NAM MPEP has been found to enhance dopamine release in the prefrontal cortex (Homayoun et al., 2004). It is thought that $mGlu_5$ may modulate the activity of dopaminergic neurons either directly or indirectly through interaction with other neurotransmitter systems, such as the GABAergic (Smolders et al., 1995) and cholinergic (Tallaksen-Greene et al., 1998) systems.

In addition, $mGlu_5$ plays a role in the activation of the endocannabinoid system. Endocannabinoids, including anandamide and 2-arachidonoylglyercol (2-AG), are endogenous lipids with similar properties to cannabinoids (Chanda et al., 2019). They are typically synthesised in postsynaptic neurons and exert their effects *via* cannabinoid receptors located at presynaptic terminals. The primary cannabinoid receptor in the CNS is cannabinoid receptor 1 (CB1), which is a $G\alpha_{i/o}$-coupled receptor. In the CNS, CB1 is predominantly expressed in the hippocampus, cerebral cortex, cerebellum, and basal ganglia (Katona et al., 2006). The activation of $mGlu_5$ by glutamate stimulates endocannabinoid formation through both Ca^{2+}-dependent (Cadas et al., 1996) and Ca^{2+}-independent (Ohno-Shosaku et al., 2002) mechanisms. In addition, $mGlu_5$-dependent endocannabinoid synthesis occurs following the interaction of homer proteins with PLCß and diacylglycerol lipase-α (Jung et al., 2007, 2012). Following synthesis, endocannabinoids activate CB1 receptors on nearby presynaptic terminals. This activation subsequently inhibits neurotransmitter release, including GABA and glutamate (Shen et al., 1996; Ohno-Shosaku et al., 2001; Wilson et al., 2001; Marsicano et al., 2003; Kano et al., 2009). Together, $mGlu_5$ and CB1 have been shown to promote neuronal survival and activate neuroprotective pathways, such as ERK1 (Batista et al., 2016).

1.2.6.2 Role in Cellular Processes

Recent studies have demonstrated that $mGlu_5$ plays a role in regulating autophagy, a cellular process responsible for the clearance of organelles and protein aggregates (Menzies et al., 2017). One mechanism by which $mGlu_5$

regulates autophagy is through the zinc finger and BTB domain-containing protein (ZBTB16)-dependent pathway (Abd-Elrahman et al., 2017, 2018). In AD mouse models, aberrant $mGlu_5$ signalling inhibits autophagy (Zhang et al., 2015; Abd-Elrahman et al., 2017). Following the genetic deletion or pharmacological blockade of $mGlu_5$ in AD mice, autophagy is restored *via* alterations in the Unc-51-like kinase 1 (ULK1)-dependent and ZBTB16 pathways (Abd-Elrahman et al., 2018). Similarly, targeting $mGlu_5$ in a mouse model of HD reduced the activation of ULK1-dependent autophagy *via* the activation of mTOR (Abd-Elrahman et al., 2017). In addition, $mGlu_5$ has been shown to regulate autophagy in a rat model of chronic migraine through mTOR signalling (Niu et al., 2021).

The role of $mGlu_5$ in apoptosis, the process of programmed cell death (Elmore, 2007), is complex, with studies showing both pro- and anti-apoptotic effects. In mouse primary cortical astrocytes, the upregulation of $mGlu_5$ expression after oxygen-glucose deprivation was found to contribute to the apoptosis of astrocytes, suggesting that astrocytic $mGlu_5$ plays a pro-apoptotic role (Paquet et al., 2013). This pro-apoptotic effect was reduced in astrocytes cultured from $mGlu_5$ knockout mice. Similarly, in a mouse model of HD, chronic antagonism of $mGlu_5$ using the NAM 2-chloro-4-((dimethyl-1-(4-(trifluoromethoxy)phenyl)-1H-imidazol-4yl)ethynyl)pyridine (CTEP) led to a decrease in neuronal apoptosis and a related increase in cell survival (Abd-Elrahman et al., 2017). On the other hand, in primary neuronal cultures, the activation of $mGlu_5$ was observed to reduce caspase-dependent neuronal apoptosis (Movsesyan et al., 2004). It is likely that the role of $mGlu_5$ in apoptosis is cell-type and context-dependent.

1.2.6.3 Modulation of Synaptic Plasticity

One of the most studied roles of $mGlu_5$ in the CNS is in synaptic plasticity, specifically long-term potentiation (LTP) and long-term depression (LTD). LTP is the strengthening of synapses, whereas LTD is a long-lasting decrease in synaptic strength. As memories are encoded by synapse modification, synaptic plasticity is thought to be a major cellular mechanism underlying learning and memory processes (Magee & Grienberger, 2020). Two brain regions are particularly important for learning and memory: the hippocampus plays an important role in short-term cognition and working memory, and the cortices store this

information (Frankland & Bontempi, 2005). These brain regions have abundant $mGlu_5$ expression (Romano et al., 1996). In rodent studies, the knockout of $mGlu_5$ has highlighted the role of $mGlu_5$ in learning and memory processes, with knockout animals exhibiting impaired spatial learning in the Morris water maze, with a reduction in learning acquisition, and they show decreased contextual fear conditioning (Lu et al., 1997; Xu et al., 2009). Moreover, these knockout animals display a decrease in LTP in the CA1 region of the hippocampus (Lu et al., 1997). Similarly, the chronic administration of the $mGlu_5$ NAM MPEP in rats impairs spatial, working, and reference memory, in addition to LTP (Manahan-Vaughan & Braunewell, 2005; Bikbaev et al., 2008).

Several signalling pathways downstream of $mGlu_5$ activation have been implicated in the contribution of $mGlu_5$ to learning and memory processes. One such pathway involves the functional interaction of $mGlu_5$ and NMDA receptors, as discussed in section 1.2.6.1 (Tu et al., 1999). The stimulation of NMDA receptors results in an influx of Ca^{2+} into cells which activates a number of signalling pathways and contributes to synaptic plasticity (Morris et al., 1986; Kullmann & Lamsa, 2007; Lee & Silva, 2009). The activation of NMDA receptors has been shown to be crucial for the induction of LTP in the CA1 region of the hippocampus (Tsien et al., 1996). Importantly, changes in Ca^{2+} homeostasis is associated with memory impairments that develop in ageing (Burke & Barnes, 2010).

NMDA and $mGlu_5$ receptors interact synergistically to regulate the phosphorylation of ERK1/2 (Yang et al., 2004), an important signalling pathway for cell proliferation, differentiation, and survival (Thandi et al., 2002). ERK1/2 is also recruited to $mGlu_5$ *via* the scaffolding role of ß-arrestin, which recruits cytoplasmic effectors to $mGlu_5$ (Ferguson, 2001; Stoppel et al., 2017). The $mGlu_5$-dependent activation of ERK1/2, and subsequently synaptic protein synthesis and LTP, is abolished in ß-arrestin2 knockout mice (Thandi et al., 2002; Eng et al., 2016; Stoppel et al., 2017). The stimulation of ERK1/2 signalling following $mGlu_5$ activation is independent of PKC and Ca^{2+} release and is required for mGlu receptor-dependent LTD in the hippocampus (Gallagher et al., 2004). Moreover, ERK1/2 inhibition prevents long-term spatial memory formation (Blum et al., 1999). The activation of a number of transcription factors lies

downstream of $mGlu_5$-mediated ERK1/2 phosphorylation, including Elk-1, c-Jun, and CREB (Choe & Wang, 2001; Gallagher et al., 2004; Kumar et al., 2012). These proteins play a key role in mediating LTP (Rush et al., 2002; Gallagher et al., 2004; Wang et al., 2007).

The activation of $mGlu_5$ leads to increased activity of mTOR, an important kinase for multiple signalling pathways (Hou & Klann, 2004; Page et al., 2006; Hoeffer & Klann, 2010; Huber et al., 2015). Agonist binding to $mGlu_5$ increases P13K activity through the association of Homer proteins and phosphatidylinositol triphosphate (PIKE) (Rong et al., 2003). P13K converts PIP_2 on the plasma membrane into PIP_3, which activates mTOR *via* the phosphorylation of protein kinase B (Akt) by phosphoinositide-dependent kinase 1/2 (PDK1/2) (Dhami & Ferguson, 2006; Niswender & Conn, 2010; Abd-Elrahman & Ferguson, 2019). Downstream effectors of mTOR include several proteins that support mRNA translation (L. Hou & Klann, 2004; Ronesi & Huber, 2008). The inhibition of mTOR has been shown to prevent LTD (Hou & Klann, 2004) and impair the formation of long-term fear memory (Parsons et al., 2006). Disruption of the $mGlu_5$-Homer-PIKE complex impairs mTOR activation and the subsequent protein synthesis that enhances synaptic plasticity (Ronesi & Huber, 2008).

Through the regulation of three key transcription factors, CREB, c-Jun, and nuclear factor κB (NF-κB), $mGlu_5$ is able to regulate synaptic protein expression and regulate gene transcription that supports synaptic function (Wang & Zhuo, 2012; De Souza et al., 2020). CREB plays in important role in synaptic plasticity and memory formation (Kandel, 2012). The expression of CREB is reduced in aged memory-impaired rats (Brightwell, 2004), and it is dysregulated after fear conditioning experiments in the hippocampus of aged rats (Monti et al., 2005). CREB modulates the transcription of a number of important learning and memory-related genes, including Arc, c-fos, and erg1 (Finkbeiner et al., 1997; Bramham & Messaoudi, 2005; Shepherd & Bear, 2011; Kandel, 2012; Wang & Zhuo, 2012). A reduced expression of Arc has been shown to correlate with age-related cognitive deficits (Monti et al., 2005; Ménard & Quirion, 2012). Moreover, the translation of Arc-encoding mRNA in dendrites is thought to underlie the induction and maintenance of LTP and LTD (Bramham et al., 2008; Shepherd & Bear, 2011). The transcription factor c-fos regulates a number of

genes, such as brain-derived neurotrophic factor (BDNF), which promotes synaptic processes underlying learning and memory (Finkbeiner et al., 1997; Bramham & Messaoudi, 2005). Erg1 is important for the consolidation of long-term memory (Jones et al., 2001). The activation of $mGlu_5$ increases CREB phosphorylation, resulting in elevated expression of these genes (Kandel, 2012; Kumar et al., 2012; Wang & Zhuo, 2012). The phosphorylation of c-Jun plays a role in the gene expression underlying synaptic plasticity (Costello & Herron, 2004; Yang et al., 2006). Similarly, NF-κB, whose expression is increased in the cell nucleus following the activation of $mGlu_5$ (O'Riordan et al., 2006; Sitcheran et al., 2008), regulates the expression of genes crucial for LTP (Mincheva-Tasheva & Soler, 2013).

1.2.6.4 Regulation of Behaviour

Aside from its role in learning and memory processes, $mGlu_5$ has been shown to play a role in a number of other behaviours. The role of $mGlu_5$ in locomotor activity is well established. Knockout $mGlu_5$ mice, in addition to mice treated with the $mGlu_5$ NAMs MPEP or 3-[(2-methyl-1,3-thiazol-4-yl)ethynyl] pyridine (MTEP), have been shown to have increased locomotor behaviour (Gray et al., 2009; Olsen et al., 2010; Ribeiro et al., 2014; Xu et al., 2021). Further experiments using microinfusion of MPEP into distinct brain regions of mice highlighted that $mGlu_5$ in specific regions (specifically the hippocampus, motor cortices, and limbic structures) regulated locomotor activity, with different locomotor outcomes observed depending on the brain region injected (Guimaraes et al., 2015).

In the spinal cord and periaqueductal grey matter (PAG), $mGlu_5$ has been shown to play a key role in mediating pain (Dogrul et al., 2000; Fisher et al., 2002; Vincent et al., 2016). Under physiological conditions, $mGlu_5$ expressed in the PAG is persistently active and helps to maintain normal sensory perception. However, in cases of neuropathic pain, this persistent $mGlu_5$ activation is disrupted, leading to chronic pain (Chung et al., 2020). Moreover, the acute pharmacological blockade of $mGlu_5$ in the PAG matter results in chronic pain, even without nerve injury (Chung et al., 2020).

Evidence suggests that $mGlu_5$ and its downstream signalling pathways play an important role in regulating sleep. The dysregulation of $mGlu_5$ signalling can lead to sleep/wake abnormalities, with downregulation promoting sleep and upregulation promoting wakefulness (Ahnaou et al., 2015; Holst et al., 2017). Furthermore, knockout $mGlu_5$ mice exhibit more fragmented sleep and struggle to adjust to novel tasks following sleep deprivation (Holst et al., 2017; Aguilar et al., 2020). In *drosophila*, a small molecule screening approach found that the $mGlu_5$ NAM 3,3′-difluorobenzaldazine (DFB) promoted longer and more consolidated sleep in older flies which usually have reduced and fragmented sleep (Hou et al., 2023).

Research suggests that $mGlu_5$ plays a role in regulating social behaviour and mood disorders. The treatment of rodent autism spectrum disorders models with $mGlu_5$ NAMs has been shown to normalise social deficits and increase social investigation (Silverman et al., 2010; Burket et al., 2011; Chung et al., 2015; Liao et al., 2018). Moreover, MPEP and MTEP have been shown to decrease aggressive behaviour in mice (Navarro et al., 2006; Newman et al., 2012). Knockout $mGlu_5$ mice and mice treated with a $mGlu_5$ NAM have been shown to have reduced levels of anxiety behaviour (Varty et al., 2005; Olsen et al., 2010; Xu et al., 2021). Similarly, the knockout or blockade of $mGlu_5$ has had antidepressant-like effects on behavioural despair tests such as the forced swim test (Domin et al., 2014; Felts et al., 2017; Pałucha et al., 2005; Shin et al., 2015). The utility of basimglurant, a $mGlu_5$ NAM, was examined in a phase II clinical trial for depression and had some anti-depressant efficacy in some secondary endpoints (Quiroz et al., 2016). However, another $mGlu_5$ NAM, AZD20666, was found to not be efficacious in a phase II clinical trial for patients with mild depressive disorder (clincaltrials.gov; NCT01145755).

1.2.7 Pharmacology of $mGlu_5$ Receptors

A diverse repertoire of ligands targeting $mGlu_5$ is available, including orthosteric and allosteric ligands. However, the highly conserved orthosteric binding pocket between mGlu receptors is a limitation for developing ligands that are selective for $mGlu_5$ (Sengmany & Gregory, 2016). Orthosteric ligands, such as (*S*)-3,5-dihydroxyphenyl glycine (DHPG) and quisqualate, block the binding of glutamate to $mGlu_5$ in a competitive manner. DHPG was the first orthosteric

agonist to be developed that was selective for group I mGlu receptors. It is equally potent at both $mGlu_1$ and $mGlu_5$ (Wiśniewski & Car, 2006). Quisqualate is another group I receptor agonist, with higher potency than DHPG but less selectivity (Pin & Duvoisin, 1995).

Allosteric modulators are a promising class of compounds for targeting $mGlu_5$, offering a number of advantages over orthosteric ligands. As they are binding to the allosteric site, which is less conserved than the orthosteric site between mGlu receptor subtypes, they allow for greater selectivity. In addition, as most allosteric modulators exert their effects following binding of the orthosteric agonist, they allow for the fine-tuning of receptor responses in proportion to normal receptor physiology (Sengmany & Gregory, 2016). This maintains the spatial and temporal pattern of endogenous glutamate signalling (Trinh et al., 2018) and is in contrast to the complete inhibition or activation of $mGlu_5$ using orthosteric ligands, which may lead to adverse or undesirable effects (Christopoulos, 2002; Leach et al., 2007).

The first $mGlu_5$ NAMs to be reported were SIB-1893 and SIB-1757 (Varney et al., 1998). Since then, $mGlu_5$ NAMs have been developed to show both increased potency and selectivity, including MPEP (Gasparini et al., 1999), MTEP (Cosford et al., 2003), and CTEP (Lindemann et al., 2011). CTEP is the most potent and selective of these (Lindemann et al., 2011). Several $mGlu_5$ NAMs have demonstrated promising results in preclinical trials for neurodegenerative diseases (NDDs) and disorders, such as mood disorders, that are characterised by impaired brain immune function. Some have progressed to phase II clinical trials for NDDs but have failed to show efficacy (Budgett et al., 2022). One $mGlu_5$ NAM, dipraglurant, showed efficacy in a phase II trial in NDD (clinicaltrials.gov: NCT01336088) and has recently progressed to phase III (clinicaltrials.gov: NCT04857359). However, $mGlu_5$ NAMs have been associated with psychomimetic effects in humans, such as insomnia and hallucinations (Friedmann et al., 1980; Porter et al., 2005; Abou Farha et al., 2014). These side effects may be due to the interaction between $mGlu_5$ and NMDA receptors. The inhibition of NMDA receptors caused psychomimetic effects in both rodents and humans, and the inhibition of $mGlu_5$ may enhance NMDA inhibition (Marino & Conn, 2002).

The first $mGlu_5$ PAM to be identified was DFB (O'Brien et al., 2003). Subsequently, [5-chloro-2-[(-1,3-dioxoisoindolin-2-yl)methyl]phenyl]-2-hydroxybenzamide (CPPHA) was developed and demonstrated increased potency (O'Brien et al., 2004). 3-cyano-N-(1,3-diphenyl-1H-pyrazol-5-yl)benzamide (CDPPB) was the first $mGlu_5$ PAM to be developed with sufficient solubility for *in vivo* studies (O'Brien et al., 2003, 2004). PAMs for $mGlu_5$ have shown promising efficacy in preclinical models of neurodegeneration, psychosis, and drug addiction (Kinney et al., 2005; Rodriguez et al., 2010; Reichel et al., 2011; Gregory et al., 2013; LaCrosse et al., 2015). However, they have also been linked to adverse side effects in the CNS. For example, $mGlu_5$ PAMs have caused seizures, convulsions, and excitability in wild-type rats (Rook et al., 2013; Parmentier-Batteur et al., 2014).

SAMs for $mGlu_5$ allow for the targeting of $mGlu_5$ without an alteration in glutamate-mediated signalling (Haas et al., 2017). The $mGlu_5$ SAM BMS-984923 has shown therapeutic benefit in a mouse model of AD by uncoupling $mGlu_5$ from neurotoxic pathways (see 1.3.4.1) (Haas et al., 2017). Recently, a phase I clinical trial was conducted to assess its tolerability and safety in human patients (Huang et al., 2016; clinicaltrials.gov: NCT04805983).

Biased agonists have been developed for $mGlu_5$, such as VU29 and CDPPB, two PAMs which have higher efficacy for ERK1/2 signalling relative to Ca^{2+} mobilisation (Gregory et al., 2012). Biased agonism is therapeutically attractive, as it allows for fine-tuning $mGlu_5$ signalling towards beneficial pathways while avoiding those associated with adverse effects (Trinh et al., 2018). The novel $mGlu_5$ PAM, VU0409551, potentiates the coupling of $mGlu_5$ to $G\alpha_{q/11}$-mediated Ca^{2+} mobilisation but does not result in NMDA activation (Rook et al., 2015). This enables VU0409551 to show efficacy in preclinical models whilst avoiding adverse side-effects such as seizures (Balu et al., 2016).

1.3 The $mGlu_5$ Receptor as a Therapeutic Target for Neurodegenerative Disease

1.3.1 Introduction to NDDs

The $mGlu_5$ receptor has been highlighted as a potential therapeutic target for a number of NDDs (Budgett et al., 2022). Here, the focus is on its potential in AD, HD, and ALS, three common NDDs.

1.3.1.1 Alzheimer's Disease

AD is a progressive NDD and the most prevalent form of dementia, affecting an estimated 32 million people worldwide. Including those with prodromal and preclinical AD, this figure increases to a global estimate of 416 million people (Gustavsson et al., 2023). AD patients typically have short-term memory difficulties and can also present with impairment in visuospatial processing, executive function, language, and attention (Knopman et al., 2021).

Early-onset AD (EOAD) is a rare and familial form of AD, caused by genetic mutations that account for 5% of AD patients (Bateman et al., 2010). Typically, EOAD is caused by mutations in *amyloid protein precursor* (*APP*), *presenilin-1* (*PSEN1*), and *presenilin-2* (*PSEN2*) (Lanoiselée et al., 2017). This dominantly inherited form of AD has an age of onset that is approximately 40 years earlier than the majority of cases, which are sporadic. Sporadic AD typically develops over the age of 65 and is termed late-onset AD (LOAD) (Knopman et al., 2021).

AD is a multifactorial disorder that results from a complex interplay of environmental and genetic risk factors. Age represents that greatest risk factor for AD (Knopman et al., 2021). Environmental factors, such as education and physical exercise, have been linked to a reduced risk of developing AD. In contrast, factors such as diabetes, hearing loss, and stress have been associated with increased risk (Livingston et al., 2020). Around 20 new genes have been identified as risk factors for LOAD using genome-wide association studies (GWAS) (Karch & Goate, 2015). This included genes linked to inflammation, immune responses, and lipid metabolism. The *Apolipoprotein E* (*ApoE*) gene, particularly the ApoE ε4 allele was the first gene to be associated with LOAD (Verghese et al., 2011). Inheriting the *ApoE ε4* allele increases a person's risk of developing

dementia by 3-4 times in heterozygous carriers and 2-15 times in homozygous carriers (van der Lee et al., 2018). However, taken together, genetic risk factors play a modest role in the development of AD (Thambisetty et al., 2013).

1.3.1.2 Huntington's Disease

HD is an autosomal dominant NDD characterised by motor deterioration, cognitive decline, and psychiatric symptoms (McColgan & Tabrizi, 2018). The main feature of human HD is chorea, which causes abnormal, dance-like movements. However, in late-stage disease, bradykinesia and rigidity become the prominent motor symptoms (Heemskerk & Roos, 2011). The primary pathological characteristic of HD is the loss of striatal medium spiny neurons (MSNs) (Vonsattel et al., 1985; Waldvogel et al., 2014).

HD is an inherited disease caused by a trinucleotide CAG repeat expansion in the gene that codes for the huntingtin protein (Htt) on chromosome 4. CAG encodes the amino acid glutamine, and mutant Htt (mHtt) has an abnormally long polyglutamine repeat (Macdonald, 1993). Repeats of 36 or more CAG units is pathogenic (Bates et al., 2015), with the repeat length determining the onset age. Longer repeats result in earlier disease onset. Typically, HD develops in mid-life and leads to the death of HD patients within 15-20 years of disease onset. In European communities, the prevalence of HD is approximately 12 in every 100,000 individuals (Evans et al., 2013).

1.3.1.3 Amyotrophic Lateral Sclerosis

ALS is a NDD characterised by motor neuron degeneration in the motor cortex, spinal cord, and brainstem, leading to progressive muscle atrophy and weakness (Mejzini et al., 2019). The median survival for ALS patients is approximately three years after disease onset, with death most commonly attributed to respiratory failure (Masrori & Van Damme, 2020).

ALS is estimated to affect 1.75-3 in every 100,000 people annually (Marin et al., 2016). While the majority of ALS cases are sporadic, approximately 10% of ALS patients have familial ALS, which follows an autosomal dominant inheritance pattern (Kirby et al., 2016). Over 20 genes have been associated with ALS, the most common being hexanucleotide expansions in *C9orf72* and mutations in

superoxide dismutase 1 (*SOD1*), *transactive response DNA binding protein* (*TARDBP*), and *fused in sarcoma* (*FUS*) (Hardiman et al., 2017; van Es et al., 2017). In addition to genetic factors, a number of environmental factors play a role in the development of ALS. Risk factors such as smoking, exposure to metals and pesticides, viral infection, and head injury have been linked to the disease (Al-Chalabi & Hardiman, 2013; Fang et al., 2015; Pupillo et al., 2018). The most significant risk factors are age and male sex.

1.3.2 Common Hallmarks of NDDs

1.3.2.1 The Accumulation of Misfolded Proteins

Most NDDs are characterised by the misfolding and aggregation of a specific protein, which varies between diseases (although there is a large overlap). Typically, these misfolded proteins have a similar intermolecular ß-sheet-rich structure in both large fibrillar aggregates and smaller oligomeric forms (Soto et al., 2006).

In the case of AD, there are two types of protein aggregate: ß-amyloid (Aß) plaques and neurofibrillary tangles (NFTs). Aß plaques, formed of extracellular deposits of misfolded Aß, are distributed throughout the cerebral cortex (Montine et al., 2012). The production of pathogenic Aß peptides results from the cleavage of amyloid precursor protein (APP) (Chen et al., 2017). APP can be cleaved *via* two main pathways: the non-amyloidogenic and amyloidogenic pathways (Chen et al., 2017). In the non-amyloidogenic pathway, APP is cleaved by α-secretase at the plasma membrane or trans-golgi network. This results in the production of a membrane-bound C83 fragment, APP intracellular domain (AICD) fragments, and an extracellularly-released, soluble APPα peptide (Chen et al., 2017). As α-secretase cuts within the Aß peptide sequence, Aß production is blocked. The amyloidogenic pathway, on the other hand, promotes pathogenic Aß production. In this pathway, APP is sequentially cleaved by ß-secretase and γ-secretase, at the N- and C-terminals of Aß, respectively. Further processing of the C-terminal fragment results in the production of AICD fragments, soluble APPß peptides, and pathogenic Aß peptides (Chen et al., 2017). Aß peptides are released into the extracellular space, where they form Aß plaques. The

42-amino acid form of Aß, AB_{42}, is the most pathogenic Aß peptide and has a high propensity to aggregate (Hampel et al., 2021).

Recent evidence suggests that Aß oligomers (Aßos), rather than Aß plaques, are the primary cause of neurotoxicity in the AD brain (Kayed & Lasagna-Reeves, 2013). Aßos are toxic and are able to interact with receptors, including $mGlu_5$ and NMDA receptors (Spires-Jones & Hyman, 2014; Benarroch, 2018). Mutations that lead to EOAD typically affect APP processing and result in an increase in Aß production (TCW & Goate, 2017). This finding forms the basis of the amyloid hypothesis, which proposes that Aß accumulation in the brain of an AD patient is the primary driver of AD pathology (Selkoe & Hardy, 2016). NFTs are intracellular inclusions forms of hyperphosphorylated tau. Tau is a microtubule-associated protein that plays a role in several processes including microtubule stabilisation and axonal transport (Pooler et al., 2014; Eftekharzadeh et al., 2018). Post-translational modifications can result in the hyperphosphorylation and aggregation of tau in cell bodies and dendrites. Initially, NFTs occur in the medial temporal lobe, followed by spreading to the isocortical regions of the frontal, temporal, and parietal lobes (Arnold et al., 1991; Montine et al., 2012). Compared to Aß plaques, NFT pathology exhibits a more robust correlation with neuronal loss and cognitive impairments (Bennett et al., 2004; Serrano-Pozo et al., 2011). Despite this, misfolded Aß and tau are thought to work together to cause the pathogenesis of AD (Guo et al., 2006; Sherman et al., 2016).

In HD, the polyglutamine region of mHtt results in mHtt misfolding and aggregation. This region can be cleaved, with the resulting *N*-terminal fragments forming neuronal intranuclear inclusions (NIIs) or cytoplasmic aggregates (Hoffner et al., 2005). These aggregates have been observed in the striatum and cortex of both human HD patients and animal models (Sieradzan et al., 1999; Gray et al., 2008). The formation of these aggregates correlates with striatal neurodegeneration and disease progression (Miller et al., 2010). Initially, it was thought that mHtt aggregates were the main drivers of HD pathology (Davies et al., 1999; Ross et al., 1997). However, neuronal death can occur without the presence of aggregates and *vice versa* (Saudou et al., 1998; Kuemmerle et al., 1999). Recent evidence suggests that, similar to toxic Aßos in AD, it is mHtt

oligomers that are toxic in HD (Lajoie & Snapp, 2010; J. Miller et al., 2011; Nucifora et al., 2012; Pieri et al., 2012; Sahl et al., 2012). Studies in animal models of HD have shown that the formation of mHtt oligomers occurs before symptom onset, and their levels increase in line with disease progression (Ast et al., 2018).

ALS is characterised by the aggregation of multiple proteins, including transactive response (TAR) DNA-binding protein of 43 kDa (TDP-43) (Arai et al., 2006; Neumann et al., 2006), Cu/Zn superoxide dismutase (SOD1) (Bruijn et al., 1998), and fused in sarcoma (FUS) (Kwiatkowski et al., 2009; Vance et al., 2009). TDP-43 is a DNA/RNA binding protein that plays a role in RNA metabolism and gene transcription (Lagier-Tourenne et al., 2010). In ALS patients, TDP-43 is cleaved into *C*-terminal fragments, becomes hyperphosphorylated, and translocates from the nucleus to the cytoplasm, where it forms aggregates (Arai et al., 2006; Lagier-Tourenne et al., 2010; Mackenzie et al., 2007; Neumann et al., 2006). Aggregated TDP-43 is present in approximately 97% of sporadic ALS cases (Neumann et al., 2006). Initially, TDP-43 aggregates are found in the spinal motor neurons, agranular neocortex, and bulbar somatomotor neurons, and subsequently, pathology spreads throughout the CNS *via* axonal connections (Braak et al., 2013). SOD1 is an enzyme that protects cells from oxidative damage (McCord & Fridovich, 1969). Mutations in the gene encoding SOD1 were the first to be genetically linked to ALS (Rosen et al., 1993). ALS-associated mutations in SOD1 result in highly variable patient survival (Wang et al., 2008), and the extent of aggregation in cultured cells depends on the specific SOD1 mutation (McAlary et al., 2016). It is not yet clear if SOD1 aggregates or soluble SOD1 oligomers are the cause of cellular toxicity in the brain (McAlary et al., 2016; Sangwan et al., 2017; Weisberg et al., 2012; Zhu et al., 2018). Like TDP-43, FUS is a DNA/RNA binding protein (Lagier-Tourenne et al., 2010) that is translocated from the nucleus to the cytoplasm in ALS patients (Kwiatkowski et al., 2009; Vance et al., 2009). In the cytoplasm, it is thought to disrupt nucleocytoplasmic transport (Dormann et al., 2010). SOD1 mutations account for ~20% and FUS mutations for ~4-5% of all familial ALS cases (Taylor et al., 2016). Misfolded TDP-43, SOD1, and FUS proteins have a number of downstream effects, including mitochondrial dysfunction (Nakaya & Maragkakis, 2018; Tafuri

et al., 2015), disruption of the proteostasis network (Medinas et al., 2017), and impaired mRNA metabolism (Woerner et al., 2016).

1.3.2.2 Altered Excitatory Neurotransmission

Excitotoxicity, a pathological process characterised by excessive neuronal excitation, primarily by glutamate, has been implicated in a number of NDDs. The regulation of glutamate in the brain is primarily through the glutamate/glutamine cycle, where excess glutamate is taken up by astrocytes (Figure 1-9) (Conway & Hutson, 2016). This rapid removal of glutamate from the extracellular space prevents overexcitation. Once astrocytes have taken up glutamate *via* glutamate-specific transporters (such as GLAST/EAAT1 and GLT1/EAAT2), glutamate is converted to glutamine by glutamine synthetase and released back into the extracellular space for reuptake by presynaptic neurons (Conway, 2020). Dysregulation of this system can result in excessive neuronal excitation, leading to synaptic dysfunction and neuronal cell death (Connolly & Prehn, 2015).

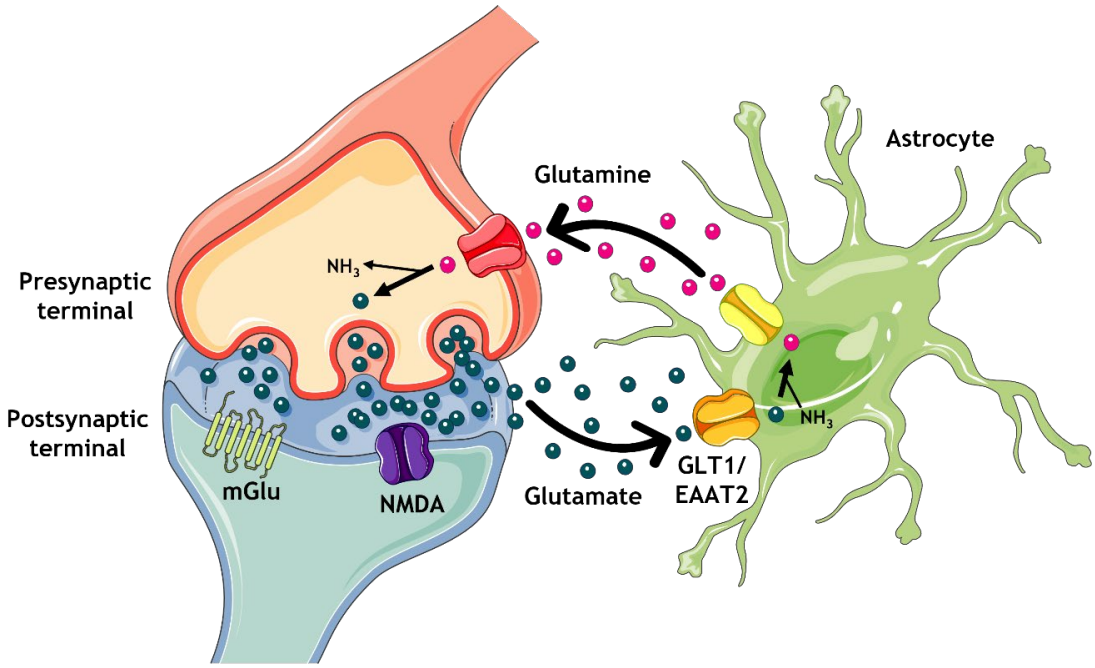

Figure 1-9 Schematic of the glutamate-glutamine cycle. Presynaptic glutamatergic neurons release glutamate (blue) during synaptic transmission. Glutamate then interacts with glutamatergic receptors on the postsynaptic terminal, such as metabotropic glutamate (mGlu) or *N*-methyl-D-aspartate (NMDA) receptors. Excess glutamate can lead to excitotoxicity and neuronal death. Astrocytes help to prevent overexcitation by removing excess glutamate from the synaptic cleft *via* glutamate transporters such as GLT1/EAAT2. Glutamate is converted to glutamine (pink) by glutamine synthetase. Glutamine is released by the astrocytes and is taken up by neurons where it is used to synthesis glutamate. Figure created using Reactome Icon Library, licensed under CC BY 4.0 (Sidiropoulos et al., 2017). NH_3, ammonia.

The excitotoxicity hypothesis of HD proposes that the neurodegeneration observed in the striatum of HD patients is driven by an excess of excitatory neurotransmitters, particularly glutamate, and/or the overactivation of glutamate receptors. The basis for this hypothesis stems from studies demonstrating that the direct injection of glutamate receptor agonists into the striatum of rats induces symptoms and pathology resembling HD (Beal et al., 1986; Coyle & Schwarz, 1976; McGeer & McGeer, 1976). Similarly, altered excitatory neurotransmission is implicated in the progression of ALS. Both human ALS patients and ALS mouse models have elevated levels of extracellular glutamate in their cerebral spinal fluid (CSF) and spinal cord plasma (Alexander et al., 2002; Shaw et al., 1995; Wuolikainen et al., 2011), suggesting that excitotoxicity plays an key role in the degeneration of motor neurons. In the AD brain, there is evidence of damage to glutamatergic neurons in the cortex, specifically in layers III and IV of the neocortex (Albin & Greenamyre, 1992). This suggests that disruptions in glutamatergic signalling may also play a role in AD pathogenesis.

The altered expression of glutamatergic transporters has been reported in several NDDs (Jacob et al., 2007). For example, the expression level of GLT1/EEAT2 is reduced in ALS patients (Ferrarese 2001, Rothstein 1992), and its function impaired in AD (Scott et al., 2011). Furthermore, a reduction in GLT1/EEAT2 mRNA and a subsequent decrease in glutamate uptake has been observed in HD human post-mortem brains (Arzberger et al., 1997) and HD model mice (Liévens et al., 2001). The accumulation of glutamate that results from impaired glutamate transport is neurotoxic, leading to the overstimulation of postsynaptic neurons and an excess of Ca^{2+} entry which occurs predominantly through NMDA receptors (Choi, 1987; Sattler & Tymianski, 2000; Mattson, 2007). Interestingly, in *drosophila* AD models, glutamate toxicity has been associated with tau-mediated neuronal death (Kilian et al., 2017).

In AD, there is evidence to suggest that Aß oligomers promote dysregulation in glutamatergic signalling by binding directly to NMDA receptors and inducing inward Ca^{2+} currents (De Felice et al., 2007; Alberdi et al., 2010; Bieschke et al., 2011). Similarly, NMDA-mediated excitotoxicity plays a critical role in the pathogenesis of HD with the polyglutamine expansion in mHtt resulting in

increased concentrations of intracellular Ca^{2+} *via* the hyperactivation of NMDA receptors and their stabilisation to the postsynaptic membrane (Song et al., 2003). Chronic and mild NMDA activation has been shown to result in neurodegeneration (Greenamyre & Young, 1989; Butterfield & Pocernich, 2003; Mattson, 2007). *In vitro*, striatal and cortical neurons cultured from HD mutant mouse models are more susceptible to NMDA-induced cell death than control mice (Levine et al., 1999). Moreover, mHtt interacts with IP3 receptors, leading to increased release of Ca^{2+} from intracellular stores (Kaltenbach et al., 2007; Tang et al., 2003, 2005).

As Ca^{2+} regulates several signalling pathways, its excess has a number of downstream effects, including an increase in reactive oxygen species, membrane degradation, and the activation of protein kinases which contribute to the hyperphosphorylation of proteins such as tau (Conway, 2020). In addition, elevated Ca^{2+} levels are associated with increased activation of Ca^{2+}-dependent proteases, such as calpain, overactivation of which can impair long-term synaptic potentiation (Jerónimo-Santos et al., 2015; Wu & Lynch, 2006).

1.3.2.3 A Chronic Neuroinflammatory Response

Another pathological hallmark of NDDs is a chronic neuroinflammatory response which involves the upregulation and activation of astrocytes and microglia, termed astro- and microgliosis (Ransohoff, 2016). Under physiological conditions, astrocytes play a key role in homeostasis, regulating the extracellular ionic environment, maintaining the blood brain barrier, and supporting neurons structurally (Wang & Bordey, 2008). Moreover, they prevent glutamate excitotoxicity by taking up excess glutamate and they release antioxidants to protect neurons from oxidative stress (Chen et al., 2001; Shih et al., 2003; Vargas et al., 2008; Chen et al., 2009). Although the activation of astrocytes has neuroprotective features, toxic astrogliosis can be found in NDD, for example surrounding Aß plaques in both humans and animal models, where it leads to neuronal damage (Kumar et al., 2023). In NDD, astrocytes undergo a transformation from a resting to reactive state (Escartin et al., 2021), characterised by their star-like processes stretching towards sites of disease pathology (Schiweck et al., 2018) and the upregulation of inflammatory markers such as glial fibrillary acidic protein (GFAP), vimentin, and nestin (Yamada et

al., 1992; Moreels et al., 2008; Hol & Pekny, 2015). In NDDs, activated astrocytes secrete cytokines such as interleukin-1 (IL-1) and tumour necrosis factor α (TNF-α) (Björkqvist et al., 2008; Heneka et al., 2010). Moreover, in AD, astrocytes internalise misfolded tau, contributing to abnormal tau accumulation and propagation (Ikeda et al., 1995; Chiarini et al., 2017; Martini-Stoica et al., 2018).

In the CNS, physiological microglia act as phagocytes, maintaining CNS tissue, pruning unwanted synapses, and responding to injury and infection (Schafer et al., 2012; Nayak et al., 2014; Colonna & Butovsky, 2017;). However, like astrocytes, microglia also take on a reactive phenotype in NDDs, losing their role in homeostasis. In NDDs, microglia release pro-inflammatory cytokines in response to high levels of misfolded proteins, including TNF-α, IL-6, and interleukin-1 β (IL-1β) (Wang et al., 2015). In turn, this results in the recruitment and activation of astrocytes (Liddelow & Barres, 2017). Since a neuroinflammatory response is a hallmark of not just AD, but a broad spectrum of NDDs, including HD, PD, and ALS (Anneser et al., 2004), drugs that target inflammatory cells may be of benefit across multiple diseases.

1.3.3 The Need for Novel Therapeutic Interventions for NDDs

In 2021, the World Health Organisation estimated that approximately 55 million people were living with dementia worldwide, a number that continues to increase with 10 million new cases each year (World Health Organisation, 2021). This rising prevalence places a considerable demand on health and social care services.

Current treatments for dementia-related diseases, including AD, HD, and ALS, focus on providing symptomatic relief rather than modifying disease progression. For example, the Food and Drug Administration (FDA) in the United States has approved two drugs for the treatment of ALS: riluzole, a glutamate antagonist, and edaravone, a free radical scavenger. Both these drugs offer modest clinical benefits but do not target underlying disease mechanisms (Oskarsson et al., 2018). In the case of HD, current therapies aim to manage specific symptoms, for example, neuroleptics and benzodiazepines aim to treat chorea, and antidepressants and antipsychotics aim to treat behavioural changes (Ferguson

et al., 2022). Since HD is associated with glutamate excitotoxicity, efforts have been made to develop drugs that normalise these alterations. NMDA receptor antagonists, for example, have been shown to improve chorea in clinical trials. However, the adverse side effects of these drugs have resulted in their failure (Ferguson et al., 2022).

The FDA has approved six drugs for the treatment of AD, four of which aim to temporarily alleviate AD symptoms (Alzheimer's Association, 2023; Yiannopoulou & Papageorgiou, 2013). These treatments are based on either the glutamatergic (memantine) or cholinesterase (galantamine, rivastigmine and donepezil) systems (Conway, 2020). Memantine, an NMDA antagonist, works by inhibiting the prolonged influx of Ca^{2+} into cells, thereby reducing excitotoxicity. It has been shown to have a modest effect on cognition, mood, and behaviour in moderate-to-severe AD (McShane et al., 2019; van Dyck et al., 2007), but does not benefit those with mild AD (Schneider, 2011). Unfortunately, due to the non-specific nature of these drugs they are accompanied by side-effects such as headaches and nausea.

While current treatments for NDD offer some symptomatic relief, there remains a need for more effective therapies that target the underlying mechanisms of disease. Recently, two new drugs were approved by the FDA with the promise that they would not only treat the symptoms of AD but also modify disease progression. In 2021, the FDA approved aducanumab (marketed as Aduhelm by Biogen), a human monoclonal antibody that targets Aß aggregates (Arndt et al., 2018). Aducanumab was the first FDA-approved drug for AD since 2003. Although it was shown to reduce Aß levels in the brain (Sevigny et al., 2016; Budd Haeberlein et al., 2022), the effect on cognition was modest, and the effect on disease progression and patient lifespan is unknown. Moreover, there are concerns surrounding its significant side effects, such as seizures, headaches, dizziness, confusion, and amyloid-related imaging abnormalities (ARIA), including haemorrhages and oedema (Sevigny et al., 2016; Behl et al., 2022; Budd Haeberlein et al., 2022). Due to these concerns, aducanumab was rejected by the European Medicines Agency and requires a post-approval clinical trial to confirm any therapeutic benefit (U.S. Food and Drug Administration, 2021; Walsh

et al., 2021). The results of this study will be available in 2030 (Walsh et al., 2021).

In early 2023, a second Aß targeting antibody, lecanemab (marketed as Leqembi by Biogen & Eisai), received accelerated approval from the FDA. Like aducanumab, lecanemab reduced Aß plaques in the brain and slowed the progression of cognitive decline (Satlin et al., 2016; Wang et al., 2016; Swanson et al., 2021). Aducanumab and lecanemab have different mechanisms of action, with the former working to remove Aß from the brain and the latter targeting a form of Aß called N3pG, which plays a key role in the formation of Aß plaques. Although it is unclear whether either of these drugs will effectively halt AD progression, their approval marks a milestone in dementia research. Further research is needed to determine their long-term safety and efficacy.

Several other antibody-based therapies targeting Aß peptides are in different stages of development, including gantenerumab, crenezumab, and donanemab. Recently, Eli Lily published positive results from a phase III clinical trial for donanemab, which was found to slow AD progression by 35% in patients treated with the drug compared to placebo over an 18-month period (Sims et al., 2023). PET imaging showed significant reductions in Aß plaque levels after six months of donanemab treatment. Moreover, donanemab reduced the decline in patients' ability to perform daily tasks by 40%. Similar to aducanumab, a number of patients on donanemab experienced ARIA, with three ARIA-related deaths reported. Based on these results, Lilly plan to apply for FDA drug approval for donanemab by summer 2023 (Eli Lilly and Company, 2023). These breakthroughs in AD research suggest that disease-modifying treatments for NDDs are possible. Nevertheless, further research is necessary to ensure efficacious and safe treatments for all individuals living with NDDs.

1.3.4 Targeting $mGlu_5$ in Neurodegeneration

Recently, the $mGlu_5$ receptor has emerged as a potential target for the treatment of NDDs. As previously discussed (see 1.2.2), $mGlu_5$ is highly expressed in brain regions that are important for learning and memory processes, such as the hippocampus and cortex. Moreover, $mGlu_5$ has been shown to play a key role in cognition, locomotion, and synaptic plasticity (see 1.2.6.3 and 1.2.6.4).

1.3.4.1 The Role of $mGlu_5$ in NDD Pathology

Several studies have shown that $mGlu_5$ plays a direct role in AD pathology. As previously discussed (see 1.3.1), AD is characterised by the accumulation of misfolded Aß peptides into extracellular plaques. Aß also exists in the brain as Aßos (Kayed & Lasagna-Reeves, 2013). Aßos accumulate and create clusters at excitatory synapses (Renner et al., 2010). These clusters recruit $mGlu_5$ to the synapse and act as an extracellular scaffold, thereby reducing the mobility of $mGlu_5$ and preventing its lateral diffusion (Figure 1-10). Therefore, $mGlu_5$ receptors are more readily available for glutamate and further Aßos activation, resulting in increased Ca^{2+} levels and subsequent excitotoxicity. Importantly, in cultured neurons, this increase in Ca^{2+} is blocked by the addition of a $mGlu_5$ antagonist, which suggests that the interaction between Aßo and $mGlu_5$ is essential for mediating Aßo toxicity (Renner et al., 2010). Moreover, these oligomers have been shown to bind to cellular prion protein (PrP_C) with high affinity, forming a complex that requires $mGlu_5$ as a co-receptor (Laurén et al., 2009; Um et al., 2013). PrP_C is a cell surface protein that plays a key role in the pathogenesis of prion disease, as discussed in section 1.5.1. Aßos have been shown to cause a $mGlu_5$- and PrP_C-dependent increase in intracellular Ca^{2+} *via* the activation of PLC and IP3 receptors (Um et al., 2013), with the subsequent excitotoxicity contributing to synapse loss (Renner et al., 2010). This has been observed after the addition of Aßo to hippocampal neurons (Lacor et al., 2007) and in AD mouse models (Koffie et al., 2009).

In addition, Aßos have been shown to modulate the association of $mGlu_5$ with a number of signalling cascades, including Fyn kinase, Pyk2, and calmodulin-dependent protein kinase II (CaMKII) (Figure 1-10) (Haas et al., 2016; Haas & Strittmatter, 2016). These cascades play an important role in AD pathology. Fyn kinase has been shown to associate with tau physically and plays a role in its phosphorylation that is dependent on the formation of the Aßo-PrP_C complex (Lee et al., 2004; Larson et al., 2012). Similarly, Pyk2 phosphorylates glycogen synthase kinase 3ß (GSK3ß), a kinase that plays a role in tau hyperphosphorylation (Hartigan et al., 2001; Sayas et al., 2006). Pyk2 is phosphorylated and activated by a physical interaction with Fyn (Park et al., 2004; Collins et al., 2009). Exposure to Aßos activates these signalling cascades in a PrP_C- and $mGlu_5$-dependent manner (Haas et al., 2016; Um et al., 2013).

Moreover, Aß-mediated Fyn kinase activation increases the surface expression of NMDA receptors (Um et al., 2012, 2013). In addition, Aßos enhance the association between PrP_C and CaMKII. This is mediated through $mGlu_5$ and highlights a mechanism *via* which Aßo aberrantly disrupts normal glutamatergic signalling (Haas et al., 2016; Haas & Strittmatter, 2016). Since Aßo levels are elevated in the brain throughout AD and increase in line with disease severity, this disruption of normal $mGlu_5$ signalling would occur throughout disease progression.

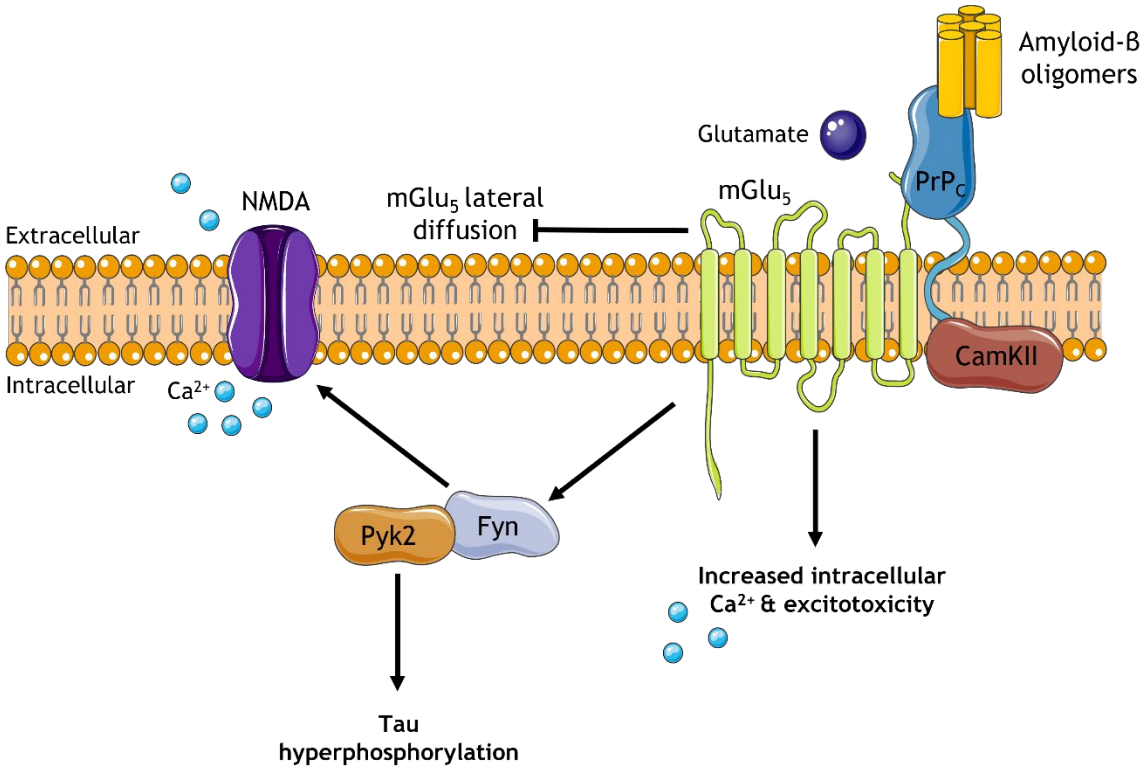

Figure 1-10 Schematic of the Aβo-PrP_C-$mGlu_5$ protein complex and its downstream signalling effects. The binding of amyloid-β oligomers (Aβo) to $mGlu_5$ requires cellular prion protein (PrP_C) as a co-receptor. Clusters of Aβo recruit $mGlu_5$ to the plasma membrane and prevents its lateral diffusion. This makes mGlu5 more accessible for activation by glutamate and Aβos, leading to an increase in intracellular calcium (Ca^{2+}). Aβos activate $mGlu_5$ to stimulate Fyn kinase, which physically associates with and phosphorylates Pyk2, which plays a role in tau hyperphosphorylation. Moreover, Fyn kinase increases the cell surface expression of *N*-methyl-D-aspartate (NMDA) receptors. Finally, Aβos enhance the association of Ca^{2+}/calmodulin-dependent kinase II (CamKII) and PrP_C *via* $mGlu_5$. Figure created using Reactome Icon Library, licensed under CC BY 4.0 (Sidiropoulos et al., 2017).

The $mGlu_5$ SAM, BMS-984923, has been demonstrated to block the Aßo-induced interaction between PrP_C and $mGlu_5$ and, therefore, pathological Aß intracellular signalling without altering physiological glutamate signalling (Haas et al., 2017). In aged APP/PS1 AD mice, treatment with BMS-984923 reversed memory and

learning deficits and alleviated synaptic loss (Haas et al., 2017). Astro- and microgliosis, in addition to the accumulation of Aß plaques, were unaltered with SAM treatment. This suggests that BMS-984923 rescued behaviour by blocking the downstream signalling of Aßo-$mGlu_5$-mediated events rather than altering the upstream Aß accumulation. This highlights the potential of targeting $mGlu_5$ as a therapeutic option for treating AD. Treatment with a $mGlu_5$ SAM, although unable to reverse existing symptoms such as Aß accumulation, may slow or halt further disease progression by preventing neuronal loss. BMS-984923 binds to the main allosteric binding site on $mGlu_5$ (see Figure 1-7), and it is hypothesised that it may block the interaction between Aßos, PrP_C, and $mGlu_5$ by stabilising the receptor in a conformation that allows for glutamate binding, but prevents any conformational change triggered by Aßos binding to PrP_C. It would be interesting to uncover whether other allosteric modulators that bind to this allosteric site also block signalling *via* the Aßo-PrP_C-$mGlu_5$ complex. As excitotoxicity plays a critical role in neuronal damage in NDDs (see 1.3.2.2), it may be important to dampen the excess in glutamate signalling alongside blocking the binding of Aßos to $mGlu_5$.

In HD, there is evidence of a direct interaction between $mGlu_5$ and both Htt and mHtt. This interaction disrupts $mGlu_5$ signalling, resulting in an increase in intracellular Ca^{2+} levels and subsequent excitotoxicity (Anborgh et al., 2005; Tang et al., 2003). Studies have shown that $mGlu_5$ signalling is altered in a HD mouse model, with the uncoupling of $mGlu_5$ from $G\alpha_{q/11}$-mediated inositol phosphate formation due to increased PKC-mediated desensitisation of $mGlu_5$ (Ribeiro et al., 2010).

Autoradiography studies have shown that the expression of $mGlu_5$ is elevated in the frontal, motor, and temporal cortices, and basal ganglia of human ALS patients as compared to controls (Müller Herde et al., 2019). Similarly, $mGlu_5$ expression is elevated in ALS mice, particularly in the hippocampus, cortex, striatum, and spinal cord (Bonifacino et al., 2019; Brownell et al., 2015; Giribaldi et al., 2013). This elevation increases as the disease progresses in the cortex, hippocampus, and spinal cord. Group I mGlu receptors, including $mGlu_5$, have been shown to produce abnormal glutamate release in the spinal cord of both pre-symptomatic and late-stage ALS mice (Bonifacino et al., 2019; Giribaldi

et al., 2013). This glutamate release was excitotoxic in nature and triggered by an increase in intracellular Ca^{2+} released from intracellular stores.

The abnormal activity of $mGlu_5$ in AD, HD, and ALS and its direct role in excitotoxicity supports the rationale for the therapeutic exploitation of reducing $mGlu_5$ signalling.

1.3.4.2 Inhibition of $mGlu_5$ Signalling

Both the genetic knockout of $mGlu_5$ and the pharmacological blockade of $mGlu_5$ signalling have shown that reducing $mGlu_5$ activity is neuroprotective in a number of models of NDD (Um et al., 2013; Hamilton et al., 2014, 2016; Abd-Elrahman et al., 2017, 2018, 2020). Blocking $mGlu_5$ activity reduced spatial, episodic, and recognition memory deficits in AD mice (Um et al., 2013; Hamilton et al., 2014, 2016; Abd-Elrahman et al., 2018, 2020). In HD mice, blocking $mGlu_5$ activity improved motor coordination (Abd-Elrahman et al., 2017; Li et al., 2022; Ribeiro et al., 2014; Schiefer et al., 2004). Similarly, $mGlu_5$ blockade delayed disease onset in ALS mice (Bonifacino et al., 2017, 2019). Importantly, these studies found that $mGlu_5$ blockade reduced the presence of disease pathology, including the accumulation of misfolded proteins, synaptic and neuronal loss, and astro- and microgliosis (Abd-Elrahman et al., 2017; Bonifacino et al., 2017; Hamilton et al., 2014, 2016; Um et al., 2013).

Moreover, $mGlu_5$ blockade was paralleled by the modulation of the autophagy and apoptosis pathways discussed in 1.2.6.2 (Abd-Elrahman et al., 2017, 2018, 2019). In addition, $mGlu_5$ blockade reduced $mGlu_5$-regulated aberrant repressor element 1-silencing transcription factor/neuron restrictive silencer factor (REST-NRSF) signalling (De Souza et al., 2020). These pathways are discussed in more detail in Chapter 5 (see 5.1.2).

Due to the neuroprotective effects of $mGlu_5$ NAMs in preclinical models, a number of $mGlu_5$ NAMs have reached clinical trials. However, many have failed to show efficacy in phase II clinical trials for NDDs (Budgett et al., 2022). Several $mGlu_5$ NAMs have progressed into clinical trials for addiction disorders. These trials are relevant to NDD, as neuropsychiatric symptoms can overlap with symptoms of NDD (Husain, 2017). In a phase II trial for cocaine use disorder,

mavoglurant was found to significantly reduce cocaine use and neuropsychiatric symptoms of addiction and has therefore moved into phase III (clinicaltrials.gov: NCT03242928). As $mGlu_5$ NAMs have shown efficacy in addiction disorders, there is still potential for their success as a treatment for NDDs.

1.3.4.3 Activation of $mGlu_5$ Signalling

Perhaps surprisingly, evidence suggests that the activation of $mGlu_5$ through treatment with a $mGlu_5$ PAM is also neuroprotective in NDD. In transgenic AD mice and mice injected with Aß, the $mGlu_5$ PAM CDPPB reduced AD pathology, including neuronal loss, cytokine release, and gliosis (Bellozi et al., 2019). In the Aß injection model, CDPPB treatment restored contextual and aversive memory. However, there was no alleviation of cognitive impairment in transgenic AD mice. This may be due to the timing of CDPPB treatment, which was administered when the mice already showed severe AD pathology and cognitive decline. Similarly, CDPPB improved cognition and motor function, in addition to reducing toxic protein aggregates and preventing neuronal cell death in a HD mouse model (Doria et al., 2015). It has been suggested that the mechanism by which activation of $mGlu_5$ is neuroprotective is through the enhancement of signalling *via* neuroprotective pathways. The behavioural improvements observed in PAM-treated HD mice were paralleled by an increase in the activation of neuroprotective pathways, such as Akt, ERK1/2, BNDF, and c-Fos (Ribeiro et al., 2010).

As previously mentioned, Aßos result in the clustering of $mGlu_5$ at the plasma membrane, where it becomes accessible for activation. The activation of $mGlu_5$ in NDD has been implicated in the exacerbation of excitotoxicity, as it promoted the release of Ca^{2+} from intracellular stores and the entry of Ca^{2+} into the cell *via* NMDA receptors (see 1.3.2.2). Therefore, it is reasonable to hypothesise that treating mouse or human NDD patients with a $mGlu_5$ PAM may be neurotoxic in the long term. In preclinical models, $mGlu_5$ PAMs have been associated with severe adverse side effects such as seizures and neurotoxicity (Bridges et al., 2013; Parmentier-Batteur et al., 2014; Rook et al., 2013). For example, the administration of the $mGlu_5$ PAM 5PAM523 to wild-type rats has been observed to induce convulsions and excitability (Parmentier-Batteur et al., 2014). Despite preclinical evidence for the use of $mGlu_5$ PAMs as a treatment for NDDs, as well

as other disorders such as schizophrenia (Nicoletti et al., 2019), they have not yet progressed to clinical trial due to issues concerning their lack of oral bioavailability and solubility (Newell, 2013). Consequently, their potential neurotoxic effect in humans is unknown.

Further thought is needed to understand why both reducing and enhancing $mGlu_5$ signalling using NAMs and PAMs, respectively, have been shown to be neuroprotective in rodent models of NDD. It may be that $mGlu_5$ NAMs and PAMs are neuroprotective at different stages of disease progression. Research in an APPswe model of AD has suggested that the contribution of $mGlu_5$ to AD pathology is dependent on disease stage, with the authors suggesting that the contribution of $mGlu_5$ to AD pathology is reduced at advanced disease stages (Abd-Elrahman et al., 2020b).

1.4 Targeting $mGlu_5$ in Neuroinflammation

As discussed in section 1.3.1, a chronic neuroinflammatory response is a key hallmark of NDDs. As $mGlu_5$ is expressed on glial cells (section 1.2.2), it represents a potential target for modulating neuroinflammatory processes in NDDs. This may have a therapeutic benefit across a range of NDDs.

1.4.1 The Function of $mGlu_5$ in Glial Cells

Signalling *via* $mGlu_5$ has been shown to regulate interactions between astrocytes and neurons. Astrocytic $mGlu_5$ signalling plays a key role in regulating structural and functional interactions between these two cell types during development. For example, $mGlu_5$-dependent Ca^{2+} signalling promotes the proliferation and migration of astrocytes towards developing glutamatergic synapses (Bernardinelli et al., 2014). This process facilitates the development of tripartite synapses between the fine processes of astrocytes and the presynaptic and postsynaptic elements of neurons. After early development, the expression of $mGlu_5$ on astrocytes decreases (Cai et al., 2000).

In astrocytes, $mGlu_5$ activation induces Ca^{2+} oscillations (Bradley et al., 2011). Moreover, astrocytic $mGlu_5$ activation leads to the release of glutamate from astrocytes, which triggers a slow, inward current in neurons mediated by

extra-synaptic NMDA receptors (Loane et al., 2012). This promotes the synchronised activation of neighbouring neurons (Pasti et al., 1997), allowing astrocytes to regulate neuronal excitability (Angulo et al., 2004; Fellin et al., 2004). In addition, the activation of astrocytic $mGlu_5$ results in the release of neurotrophic factors, such as BNDF, which impact neuronal function (Jean et al., 2008).

In addition to modulating glutamate release, $mGlu_5$ signalling regulates the expression and function of astrocyte glutamate transporters (see 1.3.2.2). This plays an important role in the regulation of excitatory signalling in the hippocampus. For example, $mGlu_5$ activation increases GLT1 activity in astrocytes, leading to rapid glutamate uptake via PLC- and PKC-mediated mechanisms (Vermeiren et al., 2005). These findings suggest that astrocytic $mGlu_5$ may have neuroprotective potential in the brains of individuals with NDD.

Regarding microglial $mGlu_5$, its activation leads to phosphoinositide hydrolysis and activation of the $G\alpha_{q/11}$ signalling pathway (Byrnes et al., 2009; Loane et al., 2009). However, little is known about the physiological role of microglial $mGlu_5$.

1.4.2 Targeting $mGlu_5$ on Glial Cells

In both AD and ALS, pathological conditions lead to the overexpression of $mGlu_5$ in reactive astrocytes. This has been observed in AD mice and cultured astrocytes after exposure to Aβos (Casley et al., 2009; Lim et al., 2013; Shrivastava et al., 2013). When Aβos bind to cultured astrocytes, it results in the clustering of $mGlu_5$ at the astrocyte cell surface. This leads to a $mGlu_5$-mediated increase in ATP release, which amplifies aberrant Aβo-induced signalling (Shrivastava et al., 2013). Similarly, in diseased astrocytes cultured from ALS rodents, $mGlu_5$ is upregulated as compared to controls (Vermeiren et al., 2006). This impairs glutamate transport (Vermeiren et al., 2006) and increases the vulnerability of astrocytes to glutamate, resulting in their subsequent degeneration (Rossi et al., 2008).

Treatment with a $mGlu_5$ NAM, or the genetic knockout of $mGlu_5$, has been shown to reduce the increased expression of astrocytic and microglial markers in mouse models of AD, ALS, and HD (Abd-Elrahman et al., 2017; Bonifacino et al., 2017;

Hamilton et al., 2014, 2016). In addition, $mGlu_5$ NAMs prevent the release of inflammatory cytokines from cultured astrocytes (Shah et al., 2012). These observations suggest that reducing $mGlu_5$ signalling may contribute to the disease-modifying effects observed in AD models after treatment with an $mGlu_5$ NAM. By reducing the neurotoxic inflammatory response, $mGlu_5$ inhibition may potentially mitigate disease progression.

As reactive microglia secrete proinflammatory cytokines (Wang et al., 2015), it could be assumed that a reduction in microgliosis following $mGlu_5$ NAM treatment would be neuroprotective. However, $mGlu_5$ inhibition using MPEP has been shown to drive cultured microglia towards a pro-inflammatory state, characterised by an increase in the production of reactive oxygen species, IL-6, and mitochondrial superoxide (Chantong et al., 2014). Similarly, the blockade of microglial $mGlu_5$ signalling using MTEP in a PD microglia cell culture model led to enhanced inflammatory signalling pathways (Zhang et al., 2021).

There is evidence to suggest that the activation of microglia $mGlu_5$ is neuroprotective. The addition of a $mGlu_5$ agonist or PAM reduces microglial activation and the subsequent inflammatory response in primary glial cultures and cell lines challenged with Aß (Byrnes et al., 2009; Farso et al., 2009; Piers et al., 2011; Loane et al., 2009, 2012, 2013, 2014). *In vivo,* treatment with an $mGlu_5$ PAM significantly reduced neurodegeneration and improved motor function after traumatic brain injury in mice (Loane et al., 2014). Furthermore, the activation of microglial $mGlu_5$ has been shown to reduce the accumulation of reactive oxygen species, decrease apoptosis, and increase BDNF production in microglial cell lines (Ye et al., 2017). Therefore, while astrocytic $mGlu_5$ activation is neurotoxic, microglial $mGlu_5$ activation appears to be neuroprotective.

Of note, activated microglia have been demonstrated to induce the conversion of astrocytes into a reactive phenotype (Liddelow & Barres, 2017). Therefore, the benefits of microglia activation in neurodegeneration may be compromised by the subsequent neurotoxic response from astrocytes. Conversely, a $mGlu_5$ NAM may reduce astrocyte neurotoxicity in NDDs while subsequently driving a proinflammatory microglial response. Therefore, a better understanding of the

specific contribution of each cell type to NDD pathology is crucial for selecting the most effective ligands to treat disease.

1.5 Modelling Neurodegeneration

A significant challenge in developing novel therapeutics for NDDs is the successful translation of findings from preclinical animal models to clinical trials. This is due, in part, to the lack of available animal models that accurately recapitulate the processes observed in human disease. Extensive efforts have been dedicated to the development of NDD animal models that best reflect human pathology. These models have served as invaluable tools for understanding the underlying mechanisms of neurodegeneration and allow for the development and validation of potential disease-modifying treatments (Selkoe, 2011). However, no single animal model has been developed that fully reproduces the mechanisms and phenotypes of any human NDD. Until more effective animals are available, there will always be limitations in understanding the mechanisms underlying NDDs and identifying novel therapeutic interventions.

Several animal species, including dogs, cats, sheep, and some non-human primates, naturally develop pathology similar to human AD as they age (Van Dam & De Deyn, 2011). Among these species, non-human primates represent an ideal animal model since they show the greatest similarity to humans. However, the use of these spontaneous models in research is limited due to their lack of availability, ethical concerns, and the financial challenges associated with their long lifespans (Van Dam & De Deyn, 2011). There are few natural models of ALS or HD in the animal kingdom. Consequently, researchers have developed induced and transgenic animal models as viable alternatives to overcome these limitations.

Induced models of NDD involve the injection of chemical or pharmacological compounds, as well as physical lesions, to induce disease pathology (Van Dam & De Deyn, 2011). For example, AD-like pathology in rodents can be induced by the injection of pathogenic Aß into the brain (Harkany et al., 1998, 2000; Yamada et al., 2005). The specific pathology and phenotypes in these models vary depending on the administration method and the Aß strain used but

typically include neuroinflammation, oxidative stress, neuronal loss, and AD-like cognitive deficits (Harkany et al., 1998; Yamada et al., 2005; Sipos et al., 2007). However, induced models of AD often exhibit localised Aß pathology that differs from the distribution of Aß plaques in human disease, and they do not develop progressive neurodegeneration. Induced models of HD involve the introduction of selective neurotoxins such as kainic or quinolinic acid, which produce striatal lesions similar to those observed in human HD patients (Beal et al., 1986; Coyle & Schwarz, 1976). While these models replicate some of the histopathology of HD, similar to induced AD models, they do not exhibit progressive disease.

Transgenic models are extensively used in NDD research. While mice are the most common transgenic models, other organisms such as rats, fruit flies, nematodes, and zebrafish are also available (Prüßing et al., 2013; Saleem & Kannan, 2018; Tambini et al., 2020; Giunti et al., 2021). On Alzforum (Alzforum, 2023), over 200 transgenic mouse models are listed for AD, demonstrating the wide range of available models (Alzforum, 2023). Initially, AD transgenic models were developed based on the amyloid hypothesis, involving mutations in genes such as *APP* and *PSEN* (Games et al., 1995; Hsiao et al., 1996; Sturchler-Pierrat et al., 1997; Van Dam & De Deyn, 2011). These mice exhibit AD pathologies such as neuroinflammation, synaptic loss, hippocampal atrophy, and AD-like cognitive impairments. To investigate tau pathology, transgenic mice with mutations in the *MAPT* gene have been produced (Zhang et al., 2022). Many therapies are tested only in an Aß or tau model, but not both, representing a significant limitation. To address this issue, double transgenic mice expressing mutant APP and tau have been produced, however, these mice do not exhibit the colocalization of Aß and NFTs in brain regions typically associated with AD pathology (Götz et al., 2004; Ribé et al., 2005). Triple mutant mice, containing mutations in *PS1, APP,* and *MAPT*, exhibit Aß plaques and NFTs in a temporal and spatial pattern similar to human AD. These mice also display neuroinflammation, synaptic loss, and cognitive deficits (Oddo et al., 2003). It is important to note that the mutations used to develop transgenic AD models are primarily derived from mutations associated with EOAD, which is a rare form of AD. Research has highlighted the differences in AD pathology between LOAD and EOAD, including variations in the patterns of Aß and tau accumulation as well as cognitive

symptoms (Castellano et al., 2011; Drummond & Wisniewski, 2017; Condello et al., 2018).

Since a single gene mutation causes HD, it is possible to develop animal models that closely recapitulate HD pathology. Transgenic models of HD have been created using various approaches. For example, researchers have introduced the full-length human polyglutamine-expanded mHtt protein (e.g., BACHD mice) or the amino-terminal end of mHtt (e.g., R6/2 mice) (Gray et al., 2008; Li et al., 2005). Another strategy involves inserting an expanded CAG repeat into the endogenous HTT gene, known as a 'knock-in' strategy (e.g., $Hdh^{Q111/Q111}$ mice) (Menalled, 2005). However, these animals are slow to develop the motor deficits that characterise HD and, in many cases, the deficits observed are mild. Importantly, a key limitation of genetic HD rodent models is that they do not generally exhibit chorea-like movements, which are characteristic of HD (Pouladi et al., 2013).

The first transgenic mouse model of ALS was developed by overexpressing a mutation in the SOD1 gene, in which alanine was substituted for glycine in position 93 ($SOD1^{G93A}$) (Gurney et al., 1994). Since then, several other transgenic ALS models have been developed based on different SOD1 mutations (Bruijn et al., 1997; Ripps et al., 1995; Wong et al., 1995). While these models may differ in disease onset and presentation, they generally reproduce the major pathological mechanisms observed in human ALS, including significant motor neuron loss, protein aggregation, and progressive paralysis (Philips & Rothstein, 2015). For example, $SOD1^{G93A}$ mice exhibit the rapid degeneration of motor neurons, leading to motor deficits and subsequent paralysis and death within 4-5 months (Gurney et al., 1994). However, a key limitation of this model is that the copy number of the mutation spontaneously and progressively diminishes across generations, directly impacting disease severity. Therefore, each generation requires rigorous monitoring (Lutz, 2018). Moreover, SOD1 mutant mice do not exhibit the TDP-43 pathology which is present in most ALS patients; therefore, this model represents a small proportion of patients. ALS models have been developed that overexpress mutant TDP-43, but the development of these models is challenging as mutant TDP-43 is not well tolerated. Overexpression of TDP-43 is lethal (Philips & Rothstein, 2015; Picher-Martel et al., 2016), and

silencing of TDP-43 can lead to neurodegeneration and non-specific toxicity issues. Furthermore, TDP-43 mutants have diet-related effects on phenotype (De Giorgio et al., 2019; Lutz, 2018; Philips & Rothstein, 2015). Mouse models for FUS have also been developed (Nolan et al., 2016), however FUS loss of function mutations do not result in ALS-like phenotypes (Kino et al., 2015) and its overexpression is toxic in rodents, leading to reduced survival (Nolan et al., 2016). FUS mutant knock-in mice exhibit progressive degeneration of their motor neurons but the disease does not result in paralysis or death (Devoy et al., 2017; Scekic-Zahirovic et al., 2017).

As transgenic models often rely on the forced overexpression of mutant human genes, this can lead to non-disease-associated side effects (Saito et al., 2016). These side effects may be amplified by crossbreeding between transgenic lines (Saito et al., 2014). Moreover, many transgenic models lack some aspects of disease pathology, such as the presence of Aß plaques or NFTs in AD models.

Given that no single model fully replicates the entirety of human AD pathology, researchers must carefully consider which model best suits their specific experimental objectives. In this thesis, the chosen model was murine prion disease, which offers valuable insights into the role of $mGlu_5$ in the advancement of end-stage NDD. By employing this particular model, this study aims to shed light on the contribution of $mGlu_5$ to the progression of terminal NDD.

1.5.1 Prion Disease

In addition to the NDDs described above, there are a number of other NDDs, such as Parkinson's disease, frontotemporal dementia, multiple sclerosis, and prion disease (Wilson et al., 2023). Despite the diversity of clinical symptoms observed in these NDDs, these disorders share several common hallmarks (Bertram, 2005; Bourdenx et al., 2017). One key feature is the presence of misfolded proteins that aggregate within specific regions of the brain, eventually leading to neuronal loss and death (Halliday & Mallucci, 2015). A number of these proteins, including Aß and tau, are capable of spreading templated conformational change in both cell culture and mouse models (Petkova et al., 2005; Clavaguera et al., 2009; Desplats et al., 2009; Frost et al., 2009; Jucker & Walker, 2011; Luk et al.,

2012). This seeding and propagating behaviour has been termed “prion-like”, as this mechanism was first described for prion disease (Prusiner, 1998).

Although the first human cases of prion disease were described in the 1920s (Creutzfeldt, 1989; Jakob, 1989), the term “prion” was not used until 1997 when Stanley Prusiner isolated the infectious agent and confirmed that it was a misfolded protein (Prusiner, 1998). In humans, prion disease can manifest as sporadic, inherited, or acquired forms, and its incidence is very rare (Jankovska et al., 2021). One of the most notable outbreaks of human prion disease occurred in the 1990s in the United Kingdom in the form of variant Creutzfeldt-Jakob disease (CJD), colloquially known as “mad cow disease” (Will et al., 1996; Hill et al., 1997). Other human prion diseases include Gerstmann-Sträussler-Scheinker syndrome, kuru, and fatal familial insomnia. These are all progressive and fatal NDDs (Jankovska et al., 2021).

1.5.1.1 Prion Protein Structure and Function

PrP_C is highly expressed throughout the animal kingdom and has been identified in all mammals, birds, and fish (Strumbo et al., 2001; Rivera-Milla et al., 2003). It is ubiquitously expressed and particularly abundant in neurons (Manson et al., 1992; Kistner et al., 1996), where it is primarily localised to the synapse (Vey et al., 1996).

PrP_C is a membrane-bound glycoprotein attached to the cell membrane with a glycosylphosphatidylinositol (GPI) anchor (Stahl et al., 1987). As determined by NMR spectroscopy, PrP_C has a high α-helical (45%) and low ß-pleated sheet (3%) structure (Riek et al., 1996). PrP_C has a structured C-terminal domain and an unstructured, flexible N-terminal domain. The C-terminal domain consists of three α-helices flanked by two short, antiparallel ß-strands (Riek et al., 1996, 1997). Moreover, the C-terminal domain contains two *N*-linked glycosylation sites at asparagine (Asn) residues: Asn181 and Asn197 in humans, and Asn180 and Asn196 in mice. These sites are variably glycosylated, resulting in di-, mono-, and un-glycosylated forms of PrP_C (DeArmond et al., 1997). The N-terminal domain has a random-coil sequence, a series of octapeptide repeat units, and a positively charged cluster (Riek et al., 1996, 1997).

The specific function of PrP_C remains unclear. PrP_C knockout mice show no overt phenotypes in regard to behaviour and development (Büeler et al., 1992; Manson et al., 1994). Since the initial PrP_C knockout experiments, subtle abnormalities have been observed in PrP_C knockout mice which may shed light on the potential role of PrP_C. For example, hippocampal slices from PrP_C-deficient mice have displayed weakened inhibitory GABA signalling (Collinge et al., 1994). Overall, the predominant discovery from PrP_C knockout mice is that PrP_C knockout results in resistance to prion neurodegeneration (Büeler et al., 1992).

1.5.1.2 Prion Toxicity

Prion diseases involve the conversion of normal PrP_C into a misfolded, toxic form known as scrapie prion (PrP_{Sc}) (Figure 1-11). As previously discussed, PrP_C has a high α-helical and low ß-pleated sheet structure, whereas PrP_{Sc} has a high ß-sheet content (Pan et al., 1993; Riek et al., 1996). The conversion of PrP_C into PrP_{Sc} occurs when the misfolded PrP_{Sc} comes into contact with PrP_C, acting as a template for the conversion process (Figure 1-11A-B). Once converted, the misfolded proteins can either interact with more PrP_C, leading to progressive amplification (Figure 1-11C), or form aggregates (Figure 1-11D). As PrP_C is depleted in neurons, further PrP_C is synthesised, providing additional material for conversion to the misfolded form. PrP_{Sc} can spread between neurons and thus gradually propagate throughout the brain. In addition, PrP_{Sc} is able to spread between organisms if infected material is ingested or transmitted through iatrogenic exposure.

As this self-propagation mechanism has been found to be a common hallmark of numerous NDDs, the study of prion disease has provided valuable insights into their pathology, as well as leading to the development of animal models of prion disease, which allow a unique opportunity to study terminal neurodegeneration. The study of prion disease offers valuable insights into the broader field of NDDs, paving the way for improved therapeutic approaches.

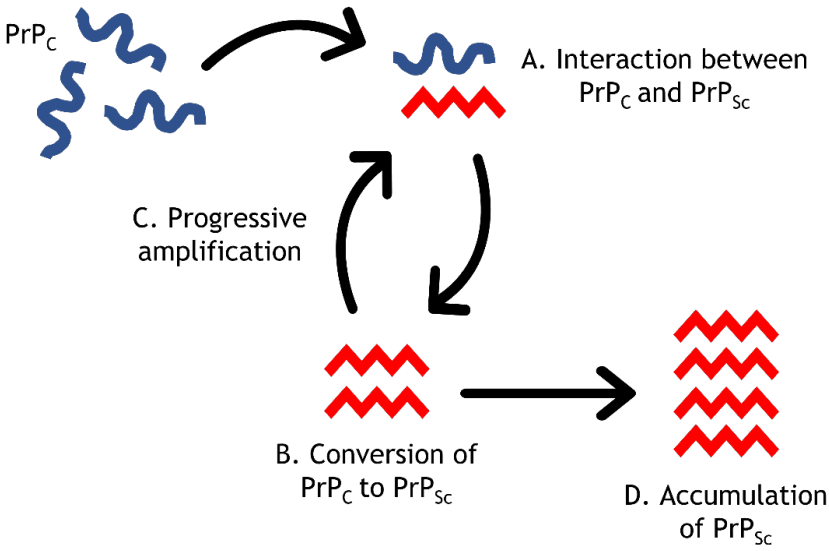

Figure 1-11 Schematic of the prion-misfolding mechanism. In prion disease, endogenous prion protein (PrP_C, blue) can become misfolded, thereby forming PrP_{Sc}. This misfolding can be induced by rare genetic mutations of environmental factors (such as ingestion of PrP_{Sc}). (A) Misfolded PrP_{Sc} then interacts with PrP_C, changing its conformation and converting them to PrP_{Sc} (B). PrP_{Sc} can then either (C) interact with further PrP_C or (D) accumulate into aggregates.

1.5.2 Murine Prion Disease as a Model of Neurodegeneration

Most animal models of neurodegeneration are engineered to express human genes carrying disease-associated mutations (see 1.5). By contrast, the inoculation of misfolded prion protein into the brains of mice induces a natural model of neurodegeneration. As NDDs share a number of key hallmarks, these insights are relevant not just to prion disease but to a broader spectrum of NDD.

The mouse model of prion disease used in this thesis involves inoculating hemizygous Tg37 mice with prion disease. The Tg37 mouse line expresses PrP_C at approximately three times the levels found in wild-type mice (Mallucci et al., 2002). At 3-4 weeks of age, Tg37 mice receive an intracerebral inoculation of rocky mountain laboratory (RML) scrapie-infected brain homogenate prepared from the brains of terminally sick prion-diseased mice. This initiates the propagation of misfolded protein around the brains of these mice. Control mice are inoculated with brain homogenate prepared from the brains of healthy animals. From 8 weeks post inoculation with prion homogenate (w.p.i.), prion-diseased Tg37 mice show disease pathology in their brains, including neuroinflammation, spongiosis, and neuronal loss in the hippocampus, and PrP_{Sc}

deposition in the cortex and hippocampus (Mallucci et al., 2002, 2003; Bradley et al., 2016). This is followed by the onset of disease symptoms at 10 w.p.i., and a terminal disease endpoint at around 12 w.p.i. (Mallucci et al., 2002, 2003; Bradley et al., 2016).

Prion-diseased mice display a progressive decline in behaviour that is typical of mice, such as burrowing and novel object recognition, as well as deficits in learning and memory (Mallucci, 2009; Bradley et al., 2016). These behavioural deficits can be assessed using simple, non-invasive tests, which provide useful paradigms for preclinical studies which aim to investigate any modification in the early stages of disease. These observed deficits correlate with early stages of disease pathology, such as synapse loss in the dorsal hippocampus (Mallucci, 2009). This correlation is similar to the earliest behavioural symptoms of human AD, which correlate with the loss of synapses, dendrites, and spines, before the deposition of Aß plaques (Näslund, 2000). The behavioural deficits observed in prion-diseased mice, in addition to synaptic dysfunction, can be ameliorated with neuronal PrP_C depletion, demonstrating that neuronal function in these mice can be recovered (Mallucci et al., 2003, 2007).

Murine prion disease shares a number of key disease hallmarks with other NDDs. Recent unbiased global proteomic and transcriptomic analyses of murine prion disease demonstrated that murine prion disease is associated with several pathology-associated markers also observed in human NDDs (Dwomoh et al., 2022). This included markers of neuroinflammation such as astro- and microgliosis, mitochondrial dysfunction, and oxidative stress. Notably, the upregulation of protein markers associated with misfolded protein clearance demonstrates that murine prion disease and human NDD share common disease-related changes. Similar to the activation of microglia surrounding Aß plaques in AD (Salter & Stevens, 2017), microglial activation is found in response to PrP_{Sc} accumulation and surrounding PrP_{Sc} deposits (Williams et al., 1997; Bate et al., 2002; Giese et al., 2006; Kercher et al., 2007; Gómez-Nicola et al., 2014; Sandberg et al., 2014; Vincenti et al., 2016). Importantly, prion-diseased mice display neuronal loss, which enables investigation into the mechanisms linking protein misfolding and neuronal death (Mallucci, 2009). Moreover, this

characteristic allows for the evaluation of novel compounds and their potential to modify disease progression and improve survival rates.

As both murine prion disease and other NDDs display prion-like mechanisms of seeding and propagation, they likely share other common pathogenic mechanisms (Halliday & Mallucci, 2015; Condello et al., 2018). An improved understanding of murine prion disease will hopefully lead to the discovery of novel therapeutic interventions for the treatment of NDDs.

1.6 General Aims of the Thesis

As discussed, there are currently limited disease-modifying treatments available for NDDs. The $mGlu_5$ receptor has been proposed as a therapeutic target, with the potential to have both a symptomatic and disease-modifying effect in NDD. Expressed on glial cells, ligands that target $mGlu_5$ provide an opportunity to target the neuroinflammatory processes that occur in NDDs. This thesis builds upon the previous work of my supervisors using murine prion disease as a model of progressive terminal neurodegeneration (Bradley et al., 2016; Bourgognon et al., 2018; Scarpa et al., 2021; Dwomoh et al., 2022). By employing novel pharmacological ligands, together with mouse models of neurodegeneration, this thesis aims to evaluate the role of $mGlu_5$ in the modulation of neuroinflammation and the progression of NDD. The primary hypothesis was that $mGlu_5$ inhibition would be neuroprotective in murine prion disease.

The three general aims of this thesis were to:

1. Characterise two novel $mGlu_5$ allosteric modulators, VU0409551 (a PAM) and VU0424238 (a NAM), in an immortal cell line and mouse primary cortical astrocytes (Chapter 3).

2. Investigate the effect of chronic treatment of prion-diseased mice with VU0424238 (Chapter 4).

3. Investigate the effect of $mGlu_5$ deficiency on the progression of murine prion disease (Chapter 5).

Chapter 2 Materials and Methods

2.1 Materials

The key materials used in this thesis are listed with the corresponding supplier and catalogue number.

2.1.1 Pharmacological Compounds

The $mGlu_5$ agonist Glutamate (D-(+)-Glucose) was purchased from Sigma-Aldrich (G5767), and DHPG ((S)-3,5-DHPG) was purchased from Tocris Bioscience (0805). The $mGlu_5$ NAM, VU0424238, and PAM, VU0409551, were kindly provided by Dr Jerri M. Rook at Vanderbilt University (Warren Center for Neuroscience Drug Discovery, Nashville).

For the *in vitro* and mouse *ex vivo* occupancy studies, [^{3}H]M-MPEP (2-[3-methoxyphenyl]ethynyl)-6-methylpyridine) was custom synthesised by Tritec (Specific activity 65.9 Ci/mmol). HTL0011867/mavoglurant [(3aR,4S,7aR)-4-hydroxy-4(3-methylphenyl)ethynyl-octahydro-indole-1-carboxylic acid methyl ester] was synthesised by Sosei Heptares.

2.1.2 General Materials and Reagents

4–15% Mini-PROTEAN TGX Precast Protein Gels, 15-well, 15 µl (Bio-Rad, 4561086)

384-well MicroAmp Optical PCR plates (Applied Biosystems, 4309849)

384-well Optiplate (PerkinElmer, 6007290)

Acrylamide Bis-Acrylamide Stock Solution, 30% Acrylamide (w/v) Ratio 37.5:1 (Severn Biotech Ltd, 20-2100-10)

Amersham Protran Nitrocellulose western blotting membranes (GE Healthcare, GE10600002)

Ammonium Persulfate (APS) (Sigma-Aldrich, 7727-54-0)

Amphotericin B (Gibco, 15290018)

Beta-mercaptoethanol (ß-mercaptoethanol) (Sigma-Aldrich, M3148)

Bis-Acrylamide 2% solution (Bio-Rad, 1610142)

Blasticidin S HCl (10 mg/ml) (Thermo Fisher, A1113903)

Bovine Serum Albumin (BSA) (Sigma-Aldrich, A9418)

Bradford protein assay reagent (Sigma-Aldrich, B6916-500ml)

Brilliant III Ultra-Fast SYBR Green (Agilent, 600882)

Calcium chloride solution (Sigma, 21115)

cOmplete, Mini, EDTA-free Protease Inhibitor Cocktail (Sigma-Aldrich, 11836170001)

Coverslips, round, 30 mm diameter, thickness no. 1 (VWR, 631-0174)

Dialysed Fetal Bovine Serum (Sigma-Aldrich, F0392)

Dimethyl Sulphoxide (DMSO) (Thermo Fisher, D/4120/PB08)

DNase 1 (Type IV, 15KU) (Sigma-Aldrich, D5025)

Doxycycline hydrochloride (Thermo Fisher, J60422-06)

Dulbecco's Modified Eagle Medium (DMEM), high glucose (Gibco, 1196592)

DMEM, high glucose, GlutaMAX™ Supplement, pyruvate (Gibco, 10569010)

Dulbecco's Phosphate Buffered Saline (DPBS) (Gibco, 14190-094)

Earle's Balanced Salt Solution (EBSS) (Gibco, 14155063)

0.5M EDTA, pH 8.0 (Invitrogen, 15575-038)

0.5M EGTA, pH8.0 (Bioworld, 405200081)

Fast SYBER™ Green Master Mix (Thermo Fisher, 4385612)

Fetal Bovine Serum (FBS) (Sigma-Aldrich, F9665)

Fura-2 AM (Abcam, ab120873)

G5 Supplement (Thermo Fisher, 17503012)

Gentamycin (Gibco, 15750078)

Goat serum (Sigma-Aldrich, G6767)

Glutamate-pyruvate transaminase (GPT) (Sigma-Aldrich, G9880)

Glycine (Sigma-Aldrich, G7126)

Hank's Balanced Salt Solution (HBSS), no calcium, no magnesium, no phenol red (Gibco, 14175129)

Hanks' Balanced Salt Solution (HBSS; 10X), calcium, magnesium, no phenol red (Gibco, 14065049)

N-(2-Hydroxyethyl)piperazine-N′-(2-ethanesulfonic acid) (HEPES; VWR Chemicals, 441485H)

Hygromycin B Solution (Santa Cruz Biotechnologies, sc-29067)

ImmEdge Hydrophobic Barrier PAP Pen (Vector Laboratories, H-4000)

Isoflurane (Zoetis, ISOFLO)

L-Glutamine 200 mM (Thermo Fisher Scientific, 25030081)

Lipopolysaccharides from Escherichia Coli O111:B4 (LPS) (Sigma-Aldrich, L2630-50MG)

Magnesium Sulphate ($MgSO_4$) (Sigma-Aldrich, M2643)

N,N,N′,N′-Tetramethyl ethylenediamine (TEMED) (Merck, 1107320100)

Paraformaldehyde (PFA) powder, 95% (Sigma-Aldrich, 158127)

Penicillin-Streptomycin (Pen-Strep) (10,000U/mL) (Gibco, 15140122)

Phosphatase Inhibitor Cocktail tablets, 20 tablets (PhosSTO EASTpack) (Sigma-Aldrich, 04906837001)

Poly-D-lysine (Thermo Fisher Scientific, A3890401)

Precision Plus Protein All Blue Prestained Protein Standards (Bio-Rad, 1610373)

Proteinase K from Engyodontium album (Sigma, P2308)

Restore Plus Stripping Buffer (Thermo Fisher Scientific, 46430)

RNase*Zap* RNase Decontamination Solution (Invitrogen, AM9780)

ScintLogic U (LabLogic, SG-BXX-14)

Sodium Azide (Sigma-Aldrich, S2002)

Sodium Chloride (NaCl) (Sigma-Aldrich, 7653)

Sodium Dodecyl Sulphate (Sigma-Aldrich, L3771)

Sodium Deoxycholate (Sigma-Aldrich, D6750)

Sodium Pyruvate (Thermo Fisher, 11360070)

TagMan™ Fast Advanced Master Mix (Applied Biosystems™, 444556)

Tris Glycine SDS 10x solution (Severn Biotech Ltd, 20-6400-50)

Tris Hydrochloride (Tris-HCl), 0.5M, pH6.8 (Sigma-Aldrich, T3253)

Tris-HCl, 1.5M, pH8.8 (Sigma-Aldrich, B2237)

Triton X-100 (Sigma-Aldrich, T9284)

Tris Base (Sigma-Aldrich, T1503)

Trypan Blue Solution (0.4%) (Sigma-Aldrich, T8154)

TrypLE Select Enzyme (10X), no phenol red (Gibco, A1217701)

Trypsin (Bovine Pancreas) (Sigma-Aldrich, T9201)

Trypsin-EDTA (0.25%), phenol red (Gibco, 25200056)

Trypsin Inhibitor (Type 1-S) (Sigma-Aldrich, T9003)

Tween-20 (Sigma-Aldrich, P7949)

Tween-80 (Sigma-Aldrich, P1754)

VECTASHIELD Hardset Antifade Mounting Medium with DAPI (Vector Laboratories, H-1500)

Whatman Grade 3MM Chr Cellulose Chromatography Paper (Cytiva, 3030-917)

Whatman GF/C Microfilter Paper (Brandel, FP-200)

2.1.3 Assay Kits

High-Capacity cDNA Reverse Transcription Kit (Applied Biosystems™, 4368813)

IP-One – Gαq kit HTRF® assay (CisBio, 62IPAPEC)

LEGENDplex™ Mouse Inflammation Panel (13-plex) with V-bottom Plate (BioLegend, 740446)

Pierce™ BCA Protein Assay Kit (Thermo Fisher, 23227)

RNeasy Plus Mini Kit (Qiagen, 74134)

TaqMan™ Gene Expression Cells-to-CT™ Kit (Thermo Fisher, AM1728)

2.1.4 Specialised Equipment

24-well Brandel Cell Harvester (Alpha Biotech)

CLARIOstar Microplate Reader (BMG LABTECH)

Eppendorf BioPhotometer™ (Eppendorf)

EVOS™ FL Auto 2 Imaging System (Thermo Scientific, Invitrogen)

FACS Canto™ II Flow Cytometer (BD Biosciences)

FLEXstation II Plate Reader (Molecular Devices)

FLUOstar OPTIMA plate reader (BMG LABTECH)

Hidex 300 SL liquid scintillation counter (Hidex)

Immunoblotting apparatus from the Bio-Rad Mini-PROTEAN range (Bio-Rad Laboratories Ltd.)

IncuCyte® Live-Cell Analysis Incubator (Sartorius)

LI-COR Odyssey Sa Infrared Imaging System (LI-COR Biosciences)

Mr. Frosty™ Freezing Container (Thermo Fisher, 5100-0001)

PHEROstar Microplate Reader (BMG LABTECH)

QuantStudio™ 5 Real-Time PCR System (Thermo Fisher Scientific)

Zeiss LSM 880 Confocal Laser Scanning Microscope (Zeiss)

2.2 Cell Culture

2.2.1 Flp-In $mGlu_5$ Cell Lines

Human Embryonic Kidney (HEK293) cells expressing either human or mouse $mGlu_5$ were previously generated in the laboratory using the Flp-In™ T-Rex™ system. In this thesis, these are referred to as Flp-In $mGlu_5$ cells.

The generation of a Flp-In™ T-Rex™ parental cell line which is able to express a protein of interest requires the integration of two plasmids: pFRT/lacZeo, which contains a Flp Recombination Target (FRT) site; and pcDNA6/TR, which constitutively expresses the tetracycline repressor (TetR) under the control of a human cytomegalovirus (CMV) promotor. These plasmids are made resistant to the antibiotics zeocin and Blasticidin, respectively, to ensure their expression in the genome (Craig, 1988; Sauer, 1994). This parental cell line is then co-transfected with two additional plasmids: pcDNA5/FRT/TO, which contains the gene of interest under the control of a tetracycline-regulated human CMV promotor as well as a hygromycin resistance gene with a FRT site; and pOG44 which expresses Flp recombinase under the control of the human CMV promotor. Upon co-transfection, the Flp recombinase expressed by pOG44 catalyses a homologous recombination event between the FRT site in the host cell genome and the FRT site on pcDNA5/FRT/TO. This results in the insertion of pcDNA5/FRT/TO, and consequently the gene of interest, into the genome (O'Gorman et al., 1991). Once this insertion has occurred, the expression of the protein of interest can be induced by the addition of tetracycline or its derivate doxycycline. Tetracycline (or doxycycline) binds to the tetracycline repressor, causing it to dissociate from the tetracycline operator and allowing for transcription of the protein of interest (Yao et al., 1998).

A haemagglutinin (HA) epitope tag was attached to the *C*-terminal tail of $mGlu_5$ to facilitate the detection of the receptors.

Immunoblot analysis was carried out on both human and mouse Flp-In $mGlu_5$ cells. The results showed $mGlu_5$ receptor expression in the mouse Flp-In $mGlu_5$ cells, while no expression was detected in the human Flp-In $mGlu_5$ cells (Figure 2-1A). In addition, the human Flp-In $mGlu_5$ cells showed a minimal

response in an inositol monophosphate (IP1) accumulation assay (see section 2.9.1) as compared to the mouse Flp-In $mGlu_5$ cells (Figure 2-1B). Based on these findings, it was decided that experiments in this thesis would be conducted solely in the mouse Flp-In $mGlu_5$ cells.

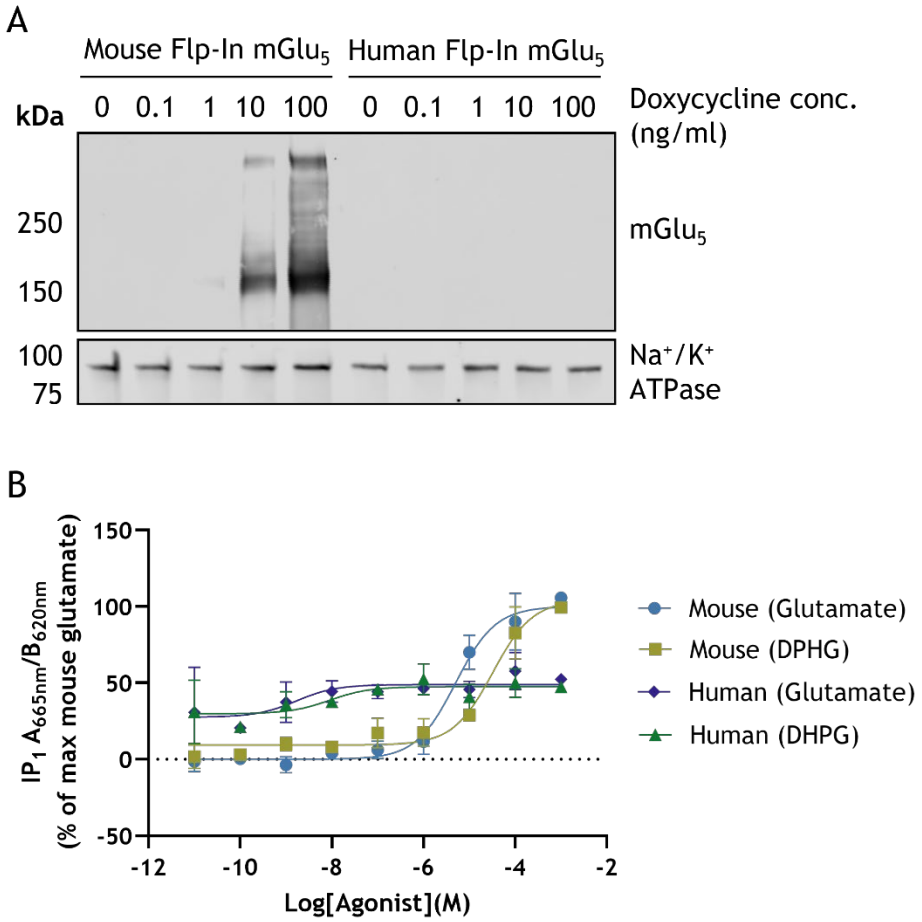

Figure 2-1 Comparison of Flp-In™ T-Rex™ 293 cells expressing human or mouse $mGlu_5$. (A) Detection of $mGlu_5$ expression in membrane samples from Flp-In™ T-Rex™ 293 cells expressing either mouse or human $mGlu_5$ induced with different concentrations of doxycycline overnight (ng/ml). Blot was probed with an anti-$mGlu_5$ antibody. Na^+/K^+ ATPase was used as a loading control. A representative blot is shown (n=2). (B) Concentration response curve showing IP1 accumulation in Flp-In™ T-Rex™ 293 cells expressing- either mouse or human $mGlu_5$ after 1 hour stimulation with increasing concentrations of glutamate or DHPG (n=2). Data were analysed using a log(agonist) vs response (three parameters) analysis of non-linear regression using GraphPad Prism 7 and are shown as means ± S.E.M. for independent experiments performed in duplicate.

2.2.1.1 Maintenance

Flp-In $mGlu_5$ cells were maintained at 37°C, 5% carbon dioxide (CO_2) in a humidified atmosphere and grown until confluent in Dulbecco's minimum essential medium (DMEM) high glucose supplemented with 10% fetal bovine

serum (FBS), 1% Penicillin-Streptomycin, 100 µg/ml Hygromycin, and 5 µg/ml Blasticidin. Parental Flp-In cells were maintained in the same environment but without adding Hygromycin to the medium.

Cells were passaged once confluent. Flasks of Flp-In $mGlu_5$ cells were washed with phosphate-buffered saline (PBS), followed by incubation with TrypLE for 5-10 min at 37°C, 5% CO_2 to detach the cells from the bottom of the flask. To neutralise the TrypLE, culture media was added to the cells, and the cell suspension was subsequently centrifuged (200 xg, 5 min). Cell pellets were resuspended in fresh culture medium and transferred to a sterile culture flask. An appropriate volume of fresh culture medium was added to achieve a 1:10 dilution. The cells were subsequently incubated at 37°C, 5% CO_2 in a humidified atmosphere until confluent.

For experiments, cells were diluted to the desired concentration and seeded onto plates coated with poly-D-lysine (PDL) as described in section 2.2.3). Cells were seeded in DMEM high glucose supplemented with 10% dialysed FBS, and 1% Penicillin-Streptomycin (assay medium). After 3-4 hours, the assay medium was replaced with fresh assay medium containing doxycycline at a concentration of 2 ng/ml unless otherwise specified.

2.2.1.2 Cryopreservation

For long-term storage, cell lines were cryopreserved in liquid nitrogen or a -80°C freezer. Confluent cells were pelleted as described in Section 2.2.1.1. Cell pellets were resuspended in 10% (v/v) DMSO in FBS (1 ml per T75 flask). Aliquots of 1 ml were frozen at -80°C in a Mr. Frosty™ Freezing Container to allow for a cooling rate of approximately -1°C per min, which is optimal for cell preservation. Cryopreserved cells were revived by rapid thawing in a 37°C water bath. Thawed cells were transferred to a flask containing 10 ml of pre-warmed culture medium and passaged as above (Section 2.2.1.1) after 16-24 hours.

2.2.2 Mouse Primary Cortical Astrocyte Culture

2.2.2.1 Preparation and Maintenance

Mouse primary cortical astrocytes were prepared according to a modified protocol described by Zhang *et al*. (2005). The protocol was appropriate for 8 mouse pups and was adjusted depending on the size of the litter. The solutions used for the preparation are summarised in Table 2-1. C57BL/6J mice (postnatal day 1-4) were decapitated, and the cortices removed. The cortices were kept in ice-cold EBSS+ during the dissection. Following this, the cortices were cut into small pieces and incubated in 10 ml of solution 1 at 37°C for 15 min. The tissue was agitated by shaking every 5 min during this period. Next, 10 ml of solution 2 was added to the tissue suspension and allowed to stand for 5 min. The supernatant was then removed and 2.5 ml of solution 3 was added. Tissue was dissociated into a single-cell suspension by triturating using a fire-polished glass pipette. The resulting solution was transferred to a fresh falcon tube and the titration was repeated. Following this, 2.5 ml of solution 4 was added, and the suspension was centrifuged (200 xg 8 min). The supernatant was discarded, and the pellet was resuspended in DMEM high glucose with GlutaMAX™ and pyruvate supplemented with 15% heat-inactivated FBS, 10 mg/ml gentamycin and 250 mg/ml amphotericin B.

Table 2-1 Composition of solutions for mouse primary cortical astrocyte preparation.

EBSS+	100 ml EBSS (Ca^{2+}/Mg^{2+}-free), 1 ml MgSO4 (stock 3.82 g/100 mL), 0.3 g BSA, 0.25 g D-(+)-glucose
Solution 1	2.5 mg trypsin, 10 ml EBSS+
Solution 2	1.6 ml solution 3, 8.4 ml EBSS+
Solution 3	100 µl DNase I (stock 4 mg/ml), 12 mg trypsin inhibitor, 100 µl $MgSO_4$ (stock 3.82 g/100 ml), 10 ml EBSS+
Solution 4	0.4 g BSA, 80 µl $MgSO_4$ (stock 3.82 g/100 ml), 10 ml EBSS+

Cells were grown in PDL-coated T175 cell culture flasks and incubated at 37°C, 5% CO_2 for 7 days, with the medium being refreshed on day 4. On day 7, the medium was replaced with DMEM high glucose with GlutaMAX™ and pyruvate supplemented with 10% heat-inactivated FBS, 10 mg/ml gentamycin and 250 mg/ml amphotericin B, and the flask was transferred to a shaking incubator

overnight (37°C, 320 rpm). Shaking removes oligodendrocytes and microglia, which remain in the supernatant. The cells that remain adhered to the shaken flask are predominantly astrocytes. These were washed twice with PBS and harvested with 0.05% trypsin-EDTA. Flasks were bashed by hand to ensure the detachment of all cells. The astrocytes were centrifuged (200 xg 5 min) and resuspended in fresh culture medium.

Cells were seeded onto PDL-coated plates (Section 2.2.3) at a density of 400,000 cells/ml in a 96-well plate for cell-based assays and IncuCyte® imaging, 400,000 cells/ml in a 6-well plate for immunoblotting, or 200,000 cells/ml in a 6-well plate for immunocytochemistry (ICC). The density chosen for cell-based assays ensured that the cells were confluent in the wells of a 96-well plate, and a lower density was chosen for plating in a 6-well plate for ICC in order for cell morphology to be observed (Figure 2-2). The next day, the medium on the astrocytes was replaced with DMEM high glucose with GlutaMAX™ and pyruvate supplemented with 10 mg/ml gentamycin, 250 mg/ml amphotericin B and G5 supplement. Cells were used for experiments 3-4 days later when visibly differentiated.

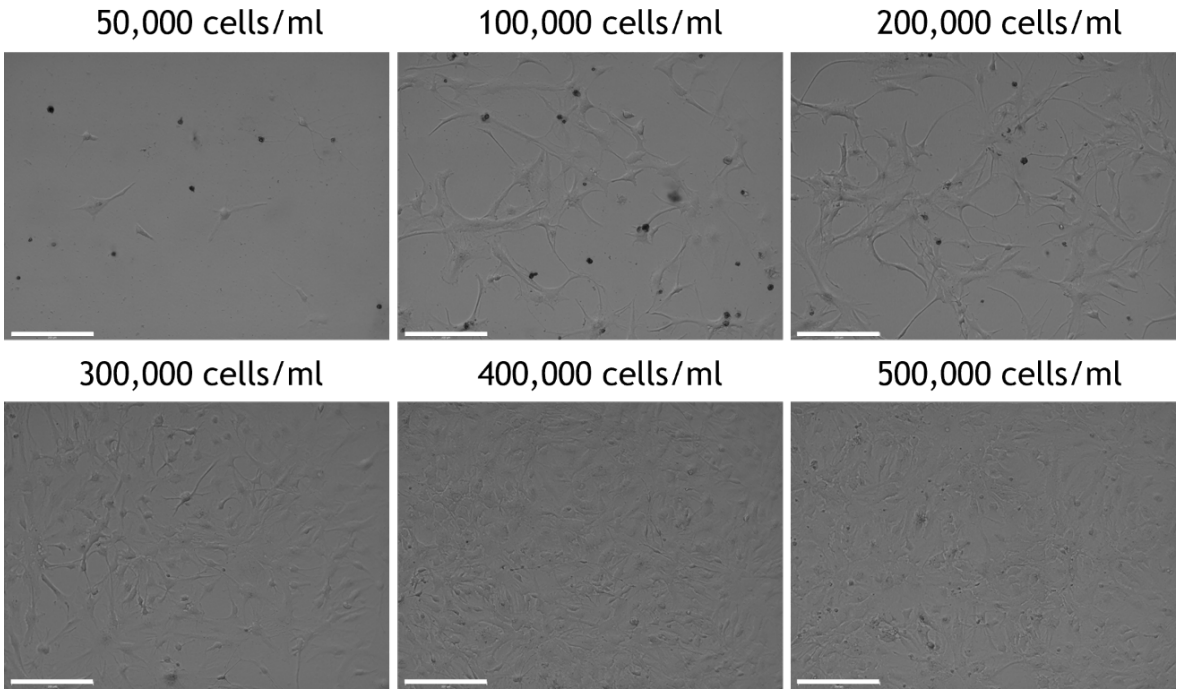

Figure 2-2 Optimisation of mouse primary cortical astrocyte plating density. Phase contrast images taken on an EVOS FL Auto 2 imaging system at 20x magnification showing mouse primary cortical astrocytes plated at six different densities (50-500,000 cells/ml). Cells were grown in the presence of G5 supplement for 4 days before imaging. Scale bar = 200 µm.

2.2.3 Preparation of Experimental Plates

PDL was added to the required plates at a concentration of 0.1 mg/ml in enough volume to cover the plate surface. Plates were incubated at 37°C for 1-24 hours before being washed three times with sterile PBS. Plates were left to dry in a sterile hood under UV light before storage at 4°C until use.

2.2.4 Counting of Cells

Cell counting for Flp-In $mGlu_5$ cells and mouse primary cortical astrocytes was carried out using trypan blue staining. Cell suspensions were gently mixed, and 100 µl added to 0.4% trypan blue at a 1:1 ratio. This dye penetrates the plasma membrane of dead cells, staining them blue. Through manual haemocytometer counting, the total number of viable cells per ml was estimated.

2.3 Experimental Animals

2.3.1 Mouse Maintenance

All procedures were carried out in accordance with the Animals (Scientific Procedures) Act 1986 under personal licence I40161082, held by the undersigned, and project licences PP0894775 and PP7704105, held by Prof Andrew B. Tobin (University of Glasgow). Animals care followed the national guidelines for animal experimentation. Mice were group-housed in groups of 2 or more in individually ventilated cages (GM500 for mice, floor area 501 cm^2; Techniplast). Cages were lined with corn cob bedding which was replaced every two weeks or when wet. In addition, cages contained a cardboard or plastic house, a cardboard tube, and shredded brown paper as nesting material. Animals were fed ad libitum with standard mouse chow and water and were maintained in a controlled environment (18-23°C, 40-60% humidity, 12-hour light/dark cycle).

In Chapter 4, the mice used were Tg37 hemizygous mice that overexpress mouse prion protein, described previously (Mallucci et al., 2003). In Chapter 5, the mice used were $mGlu_5$ wild-type ($mGlu5^{+/+}$), hemizygous ($mGlu5^{+/-}$) or heterozygous ($mGlu5^{-/-}$) knockout on a C57/BL6 background.

2.3.2 Generation of Knockout Animals

Mutant mGlu5$^{+/+}$, mGlu5$^{+/-}$ and mGlu5$^{-/-}$ mice were kindly provided by Stephen Ferguson at the University of Ottawa (Ribeiro et al., 2014). At the University of Glasgow, mouse colonies were generated using heterozygous-heterozygous breeding, with offspring genotyped by PCR analysis. All experiments carried out on mGlu5$^{+/+}$, mGlu5$^{+/-}$ and mGlu5$^{-/-}$ mice in this thesis were carried out blind. Experimental groups were assigned by a different person to the experimenter. During experimentation and statistical analysis, the experimenter was unaware of an animal's genotype. Sample sizes were based on previous publications and studies in the laboratory.

2.3.3 Prion Infection of Mice

Mice were inoculated intracerebrally into the right parietal lobe with 20 µl 1% Rocky Mountain Laboratories (RML) prion-infected brain homogenate or 20 µl 1% normal brain homogenate (NBH) (control) at approximately 3 weeks of age as previously described (Mallucci et al., 2003). Inoculations were carried out free hand by the same animal technician. Sample sizes were based on previous publications and studies in the laboratory.

2.3.4 VU0424238 Dosing Study

Cohorts of male and female control and prion-infected mice were given daily intraperitoneal (i.p.) injections from 4 w.p.i. of either vehicle (10% Tween-80) or VU0424238 (10 mg/kg). Injections were given at the same time each day to ensure consistency. Sample sizes were based on previous studies and publications.

2.3.5 Tissue Harvesting

Mice were sacrificed by cervical dislocation (followed by confirmation of death by exsanguination) and their brain tissue (cortex and hippocampus) collected for biochemical analysis. Harvested tissue was snap-frozen on dry ice and stored at -80˚C until use. For histology protocols, brains were fixed in 4% paraformaldehyde (PFA) by an animal technician using a perfusion-fixation

technique. Anaesthesia was initiated using 5% isoflurane and maintained using 2.5-3.5% isoflurane in 100% oxygen at 2 l/min.

2.3.6 Behavioural Observations

2.3.6.1 Symptom Scoring and Survival Studies

Prion-diseased mice were scored daily based on the appearance of early indicators and confirmatory signs of prion disease. Early indicators include a rigid tail, sustained erect ears, piloerection, erect penis, clasping of hind legs when lifted by the tail, un-sustained hunched posture, mild loss of coordination, and being subdued. Confirmatory signs included ataxia, impairment of the righting reflex, sustained hunched posture, dragging of limbs, and abnormal breathing. Symptom onset was established with the appearance of at least 2 early indicator signs of disease. A clinical disease diagnosis was defined as the presence of 2 early indicator signs and 1 confirmatory sign, or 2 confirmatory signs alone. Animals were culled when they developed clinical signs of prion disease.

2.3.6.2 Burrowing

The assessment of burrowing behaviour was carried out weekly on female control and prion-diseased mice from either 7 w.p.i. (Chapter 4; Tg37 animals) or 12 w.p.i. (Chapter 5; mGlu5$^{+/+}$, mGlu5$^{+/-}$, and mGlu5$^{-/-}$ animals). The mice were acclimatised to the burrowing cages the day before testing began ("training"). On the day of testing, mice were placed into individual cages with a plastic cylinder containing 140 g food pellets. After 2 hours, the pellets remaining in the cylinders were weighed and the percentage of the pellets displaced ("burrowed") was calculated.

2.3.6.3 Open Field

The assessment of locomotor and anxiety-like behaviour using an open field test was carried out on male and female mGlu5$^{+/+}$, mGlu5$^{+/-}$, and mGlu5$^{-/-}$ mice. Animals were habituated to the behavioural testing suite overnight prior to testing, and the light cycle was set to 12 hours dark, 12 hours light. Mice were placed in the centre of a clear Perspex box (50 x 50 cm), and their activity was

tracked for 10 min using ANY-maze software (Stoelting). Before testing and between animals, the testing area was cleaned with 70% ethanol and allowed to dry. Data were analysed using ANY-maze software.

2.4 Human Tissue

Human brain tissue was provided by the London Neurodegenerative Diseases Brain Bank (Brains for Dementia Research). Samples were stored at -80˚C until use. The samples are listed in Table 2-2 below.

Table 2-2 List and description of human brain tissue provided by the London Neurodegenerative Diseases Brain Bank (Brains for Dementia Research). Samples received included 250 mg of the hippocampus and cortex. AD = Alzheimer's Disease, M = male, F = female.

Sample	Pathology	Age	Sex	MRC ID
Control	Normal brain consistent with patient age	81	F	BBN002.32844
Control	Age-related changes and very mild Alzheimer's disease pathology (modified Braak/BNE stage II)	86	F	BBN002.30171
Control	AD-modified Braak (BNE) stage 2 with moderate amyloid angiopathy	98	F	BBN002.30069
Control	Moderate to severe amyloid angiopathy	87	M	BBN002.29416
Control	Normal brain consistent with patient age	80	M	BBN002.28858
AD	Alzheimer's Disease (modified Braak (BNE) stage VI	90	F	BBN002.26094
AD	Alzheimer's disease (modified Braak (BNE) stage VI) with moderate amyloid angiopathy	89	F	BBN002.28697
AD	Alzheimer's disease (modified Braak (BNE) stage VI) with moderate amyloid angiopathy	70	M	BBN002.29053
AD	Alzheimer's disease (modified Braak/BNE stage VI) with mild amyloid angiopathy	80	M	BBN002.29411

AD	Alzheimer's disease (modifed Braak (BNE) stage VI) Thal phase V	95	F	BBN002.30132

2.5 Immunoblotting

2.5.1 Preparation of Lysates from Cultured Cells

Flp-In $mGlu_5$ cells and primary cortical astrocytes were plated in a cell culture dish or 6-well plate as previously described (Sections 2.2.1.1 and 2.2.2) and grown to confluence. The medium was removed, and cells were washed twice with ice-cold PBS. The cells were left to incubate on ice with 1 ml PBS from a stock of 10 ml PBS containing 1 phosphatase inhibitor cocktail tablet and 1 protease inhibitor tablet. Cells were scraped from the bottom of each cell culture dish into an Eppendorf tube and centrifuged (16000 xg, 10 min, 4°C). The pellet was resuspended via sonification and centrifuged again (16000 xg, 30 min, 4°C). The supernatant was discarded, and the cells were resuspended in 200 µl ice-cold RIPA buffer (50 nM Tris/HCl pH 7.5, 1 mM EDTA pH 8, 1 mM EGTA pH8, 1% Triton-X-100, 0.1% ß-mercaptoethanol) from a stock of 10 ml RIPA buffer containing 1 phosphatase inhibitor cocktail tablet and 1 protease inhibitor tablet. The suspension was rotated for 30 min at 4°C, centrifuged (16000 xg, 30 min, 4°C), and the supernatant was collected and kept at -80°C until needed.

2.5.2 Preparation of Membranes from Brain Tissue

Frozen brain tissue (section 2.3.5) was homogenised using a handheld homogeniser in 500 µl T/E buffer (10 mM Tris, 1 mM EDTA, pH 8.0) containing phosphatase and protease inhibitors. Samples were then centrifuged at 100 xg for 10 min at 4°C. The supernatant was further centrifuged at 21000 xg for 1 hour at 4°C. After discarding the supernatant, the pellet was resuspended in 300 µl RIPA buffer (50 nM Tris/HCl pH 7.5, 1 mM EDTA pH 8, 1mM EGTA pH 8, 1% Triton-X-100, 0.1% ß-mercaptoethanol) containing phosphatase and protease inhibitors using a sonicator at amplitude 3-5 Hz. Samples were then rotated for 2 hours or overnight at 4°C and centrifuged at 21000 xg for 10 min at 4°C. The supernatant was transferred into a clean Eppendorf and stored at -80°C.

2.5.3 Determination of Membrane Protein Concentration

A Bicinchoninic acid (BCA) or Bradford assay was used to determine protein concentration in cell lysates.

For a BCA assay, BSA standards or protein standards (20 µl) were mixed with the manufacturer's BCA working reagent (200 µl) for 30 sec on a plate shaker, then incubated at 37°C for 30 min. The plate was cooled to room temperature, and then absorbance at 562 nm was measured using an Optima microplate reader. The data were analysed using Prism. The BSA standard curve ranged from 0 to 2000 µg/ml and was used as a reference for determining the protein concentration of each sample.

For a Bradford assay, a volume of 1 µl of each protein sample and a RIPA control were diluted in 499 µl of distilled H_2O. 500 µl of Bradford protein assay reagent was subsequently added to each sample. Protein concentrations were measured on an Eppendorf BioPhotometer using the pre-calibrated Bradford settings.

Protein concentrations were normalised to the sample with the lowest protein concentration by the addition of RIPA buffer.

2.5.4 Running of Gels

Gels were either manually cast using Bio-Rad Mini-PROTEAN III equipment or 4-15% Mini-PROTEAN® TGX™ precast protein gels were used. For manually cast gels, the percentage of the resolving gel was determined by the size of the protein of interest, typically 12% for proteins smaller than 60 kDa and 8% for proteins larger than 60 kDa. Resolving gels also contained 275 mM Tris (pH 8.8), 0.1% SDS (v/v), 0.1% APS (w/v) and 200 nM TEMED in distilled H_2O. Once the resolving gel was set, the stacking gel was cast on top and contained 4% acrylamide, 125 mM Tris (pH 6.8), 0.1% SDS (v/v), 0.05% APS, 200 nM TEMED in distilled H_2O. Gels were typically 1.5 mm in thickness.

On ice, 2X loading buffer (250 mM 0.5 M Tris/HCl pH 6.8, 10% SDS, 40% glycerol, 5% ß-mercaptoethanol, 0.01% bromophenol blue) was added to each sample to give a 1X final concentration. Samples were denatured by heating at 65°C for 5 min and spun down on a mini centrifuge. Samples were run at 60-120V for

approximately 2 hours in 1X Tris Glycine SDS running buffer (25 mM Tris-Cl, 192 mM glycine, and 0.1% SDS).

2.5.5 Probing and Detection

Nitrocellulose membranes and filter paper were equilibrated in transfer buffer (25 mM tris base, 192 mM glycine, 20% Et-OH) before assembly in a blot sandwich. To assemble a transfer cassette, the gel was placed in direct contact with the nitrocellulose membrane within a sandwich of transfer sponges and 1 mm Whatmann chromatography paper. The cassette was placed in a transfer tank containing transfer buffer, and the transfer from the gel to the membrane was performed for 2 hours at 60 V. The membrane was then incubated in 5% non-fat milk powder in TBS-T buffer (20 mM tris base, 137 mM NaCl, 0.1% Tween-20) for 1 hour at room temperature to block non-specific binding sites. Membranes were then incubated with a primary antibody (Table 2-3) diluted 1:1000 in 5% milk overnight at 4°C. After washing with TBS-T (3x 5 min), membranes were incubated with the relevant secondary antibody (Table 2-4) in the dark for 1 hour at room temperature. The membrane was then washed with TBS-T (3x 5 min) and developed using the LI-COR Odyssey Sa Infrared Imaging System. When re-probing was required, the primary and secondary antibodies were removed by incubating the membrane with Restore Plus stripping buffer for 15 min. The membrane was then washed with TBS-T, blocked with 5% milk in TBS-T for 1 hour and incubated with the desired antibodies for a different protein of interest as outlined above. Quantification of band intensities was carried out as outlined in section 2.5.5.

Table 2-3 List of primary antibodies for immunoblotting. Primary antibodies are listed according to their antigen, and details include the host species, supplier, and catalogue number (Cat#). All antibodies were diluted 1:1000 in 5% milk in TBS-T.

Antibody	Host Organism	Supplier (Cat#)
α-tubulin	Mouse	Abcam (ab7291)
Glial Fibrillary Acidic Protein (GFAP)	Mouse	Sigma-Aldrich (G3893)
Ionised Calcium Binding Adaptor Molecule 1 (Iba-1)	Rabbit	Thermo Fisher (PA5-27436)
Type 5 Metabotropic Glutamate Receptor ($mGlu_5$)	Rabbit	Merck Millipore (MABN139)
Postsynaptic Density Protein 95 (PSD95)	Rabbit	Abcam (ab18258)
Prion Protein (PrP)	Mouse	Abcam (ab61409)
Sodium Potassium ATPase (Na^+/K^+ ATPase)	Rabbit	Abcam (ab76020)
Vimentin	Mouse	R&D Systems (MAB21052)

Table 2-4 List of secondary antibodies for immunoblotting. Secondary antibodies are listed according to their antigen, and details include the host species, supplier, and catalogue number (Cat#). All antibodies were diluted 3:10,000 in 5% milk in TBS-T.

Antibody	Supplier (Cat#)
IRDye® 800CW donkey anti-mouse	LI-COR Biosciences (926-32212)
IRDye® 680LT donkey anti-mouse	LI-COR Biosciences (926-68022)
IRDye® 800CW donkey anti-rabbit	LI-COR Biosciences (926-32213)
IRDye® 680LT donkey anti-rabbit	LI-COR Biosciences (926-68023)

2.5.6 Proteinase K Digestion

To assess levels of scrapie prion protein, brain tissue was prepared as above (Section 2.5.2) and digested with proteinase K before western blotting. Lysates were incubated with 0.01 mg/ml of proteinase K for 10 min at 37°C prior to the addition of sample buffer. Control samples (for probing for total prion protein) were incubated with the equivalent volume of water before the addition of sample buffer. Western blotting was then carried out as described in sections 2.5.4 and 2.5.5.

2.5.7 Densitometry

Band intensities for the protein of interest or a housekeeping protein were quantified using Image Studio Lite (Version 5.2; LI-COR Biosciences) by measuring the median pixel intensity (arbitrary units) of each band. The software automatically corrected for background. Band intensities for the protein of interest were normalised to the band intensity for the corresponding housekeeping band. Housekeeping proteins were probed for on the same blot as the protein of interest following incubation of the membrane with Restore Plus stripping buffer (see section 2.5.5.).

2.6 Histology

2.6.1 Tissue Harvest

Mice were transcardially perfused with 20 ml of ice-cold DPBS followed by 20 ml of freshly prepared ice-cold 4% PFA (in DPBS). Following perfusion, brains were removed immediately and further fixed in 4% PFA for 24-48 hours. Brains were stored in 0.2% sodium azide in DPBS at 4°C until processing.

2.6.2 Tissue Processing

Brains were processed by the University of Glasgow Histology Research Service (Vet Diagnostic Services) as follows:

1. Ethanol 1 hour (4x)
2. Ethanol 1.5 hours
3. Ethanol 2 hours
4. Xylene 2 hours (2x)
5. Xylene 1.5 hours
6. Paraffin wax 2 hours (3x)

The whole process took 17 hours and was carried out overnight. The paraffin-embedded samples were cut coronally into 5 µm sections using a Thermo Shando HM340 rotary microtome by the University of Glasgow Histology Research Service. The sections were then baked overnight in a 37°C oven.

2.6.3 Deparaffinisation and Rehydration

Deparaffinisation and rehydration of brain samples were carried out by the University of Glasgow Histology Research Service (Vet Diagnostic services) as follows:

1. Histoclear (to de-wax) 5 min
2. 100% ethanol 5 min
3. 70% ethanol 5 min
4. Water 5 min

2.6.4 Heat-induced Epitope Retrieval

After deparaffinisation and rehydration of the brain sections, antigen retrieval was carried out on the sections by the University of Glasgow Histology Research Service (Vet Diagnostic Services). This was done using a Menarini Access Retrieval Unit with Sodium Citrate Buffer (pH 6) for 1 min 40 sec at 125°C at full pressure.

2.6.5 Immunohistochemistry

Following antigen retrieval, slices were washed for 1 hour with washing buffer (0.1% Triton-X-100 in TBS). Slides were dried around the edges, and a hydrophobic pen was used to draw around the brain slices in order to reduce the amount of antibody required for staining. Non-specific binding was blocked by incubation with 200 µl blocking buffer (5% BSA, 10% goat serum, 0.1% Titron-X-100) for 24 hours at 4°C. Subsequently, incubation with primary antibodies (Table 2-5) in blocking buffer was conducted for 2 hours at room temperature or overnight at 4°C. After three washes in washing buffer, slides were incubated with the appropriate Alexa Fluor™ antibody (Table 2-6) in blocking buffer for 2 hours at room temperature. Slides were washed a further three times, then mounted on glass slides using VECTASHIELD® Hardset™ Antifade Mounting Medium with DAPI. Samples were left to dry overnight at 4°C and sealed with nail polish the following day.

Table 2-5 List of primary antibodies for immunohistochemistry and immunocytochemistry. Primary antibodies are listed according to their antigen, and details include the host species, working dilution, supplier and catalogue number (Cat#). All antibodies were diluted in the relevant blocking buffer.

Antibody	Host Organism	Working Dilution	Supplier (Cat#)
GFAP	Mouse	1:1000	Sigma-Aldrich (G3893)
Human Influenza Haemagglutinin (HA)	Rat	1:500	Roche (12158167001)
Iba-1	Rabbit	1:500	Thermo Fisher (PA5-27436)
$mGlu_5$	Rabbit	1:1000	Merck Millipore (MABN139)
Vimentin	Mouse	1:400	R&D Systems (MAB21052)

Table 2-6 List of secondary antibodies for immunohistochemistry and immunocytochemistry. Secondary antibodies are listed according to their antigen, and details include the supplier and catalogue number (Cat#). All antibodies were diluted 1:400 in the relevant blocking buffer.

Antibody	Supplier (Cat#)
Alexa Fluor™ 488 goat anti-mouse	Invitrogen (A11001)
Alexa Fluor™ 594 goat anti-mouse	Invitrogen (A11005)
Alexa Fluor™ 488 goat anti-rabbit	Invitrogen (A11008)
Alexa Fluor™ 594 goat anti-rabbit	Invitrogen (A11037)
Alexa Fluor™ 488 goat anti-rat	Invitrogen (A11006)

2.6.6 Fluorescence Microscopy

Samples were imaged either using a confocal microscope (Zeiss LSM 880) or a NanoZoomer S60 digital slide scanner with the fluorescence imaging module (Hamamatsu) using 10x, 20x, 40x (oil-based), or 63x (oil-based) objective. The microscope used is indicated in the appropriate figures. Imaging on the NanoZoomer was conducted at the Glasgow Tissue Research Facility at the Queen Elizabeth University Hospital. Within each experiment, the same microscope settings were used.

2.6.7 Quantification of Fluorescent Staining

Images were analysed using ImageJ to determine the % area stained by each antibody. As shown in Figure 2-3A, appropriate regions of interest (ROI) were selected for the imaging of brain samples analysed in Chapter 4. ROIs included the cortex and three hippocampus regions (CA1, CA3 and dentate gyrus). In Chapter 5, whole brain slices were imaged, and ROIs were selected from a larger image, as shown in Figure 2-3B. Using Zen 3.4 (blue edition) software, images were split and saved as individual channels (i.e., DAPI, red, green) (Figure 2-3C). Using ImageJ, the required colour channel was converted to 16-bit greyscale (Figure 2-3D). Once in greyscale, the images were manually adjusted to a threshold to highlight any area covered by staining and ensure that no background noise was included in the analysis (Figure 2-3D). ImageJ software was then used to calculate the area covered by the stain and gave a figure for the % of the total area for each antibody and ROI analysed.

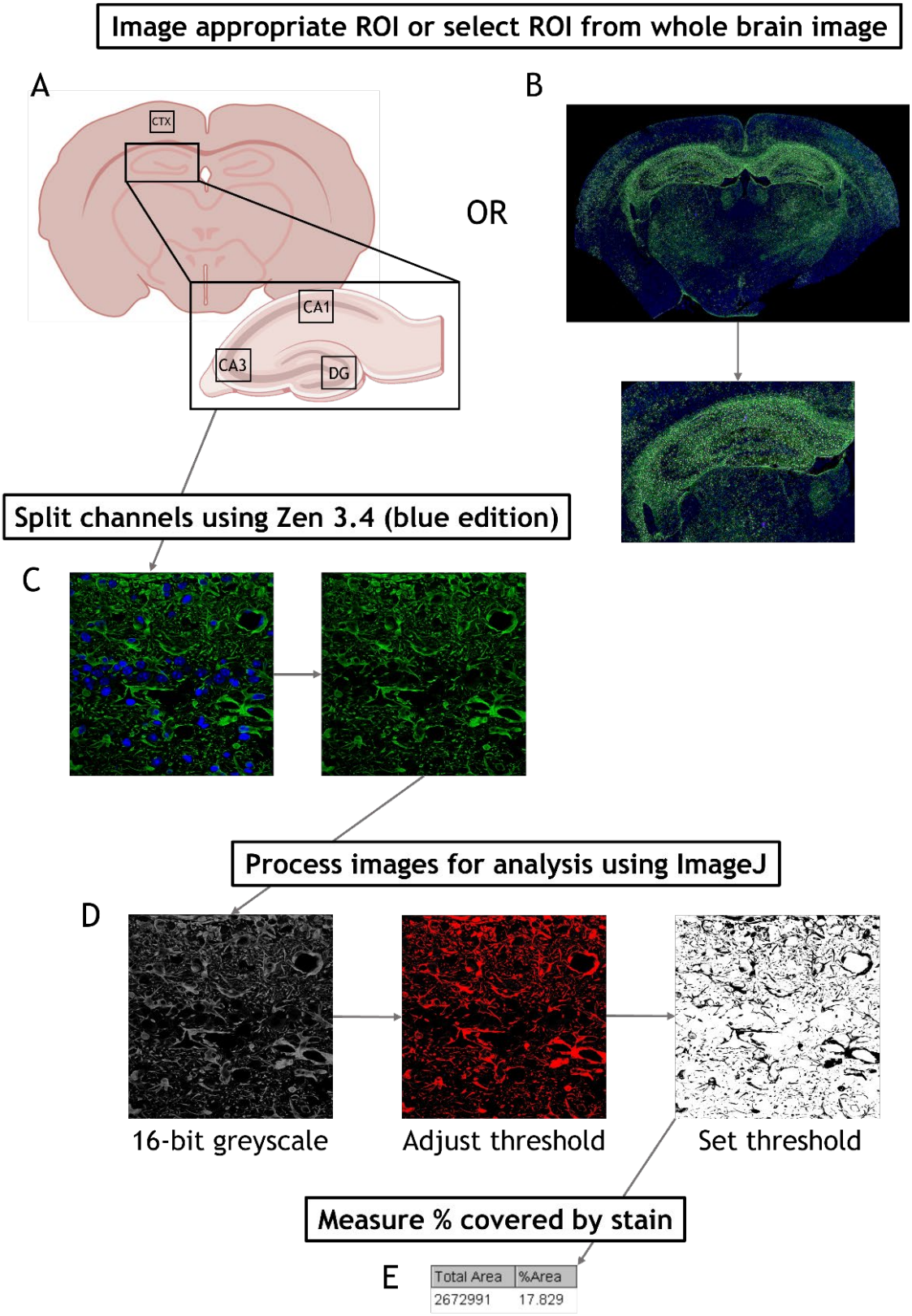

Figure 2-3 Schematic of quantification of immunohistochemistry. (A and B) Appropriate images were selected, focusing on specific regions of interest (ROI). (C) Channels were split and saved as individual images. (D) Images were converted to greyscale, and the threshold was adjusted and set. (E) Images were analysed, and data were expressed as a % of the total area covered by the stain. CA = cornu ammonis, CTX = cortex, DG = dentate gyrus.

2.7 Immunocytochemistry

2.7.1 Immunofluorescence

Flp-In $mGlu_5$ cells and mouse primary cortical astrocytes were seeded onto 25 mm glass coverslips in 6-well plates as previously described (Sections 2.2.1.1 and 2.2.2). The medium was removed and cells were washed with PBS. The cells were then fixed with 4% PFA (10 min, room temperature). After washing three times with PBS, non-specific binding was blocked by incubation with 1 ml blocking buffer (1% BSA, 0.1% Titron-X-100 in PBS) for 1 hour at room temperature. Incubation with primary antibodies (Table 2-5) was carried out at 4°C overnight. After three washes with PBS, the samples were incubated with the appropriate secondary antibodies (Table 2-6) for 2 hours in the dark at room temperature. The samples were then washed three times again and mounted using VECTASHIELD® Hardset™ Antifade Mounting Medium with DAPI. Samples were left to dry overnight at 4°C and sealed with nail polish the following day. Samples were imaged using a Zeiss 880 confocal microscope using 10x, 20x, 40x (oil-based), or 63x (oil-based) objectives as indicated in the appropriate figures. Within each experiment, the same microscope settings were used.

2.7.2 Phase Contrast Imaging

At Sosei Heptares, mouse primary cortical astrocytes were plated in a clear 96-well plate as described in section 2.2.2. Phase contrast imaging was carried out in an IncuCyte® incubator using their Live-Cell Analysis software. Images were taken every 4 hours for a total of 100 hours.

At the University of Glasgow, mouse primary cortical astrocytes were plated in a clear 6-well plate as described in section 2.2.2. Phase contrast imaging was carried out using an EVOS FL Auto 2 imaging system at 20x magnification.

2.8 Radioligand Binding

2.8.1 Preparation of Membranes from Cultured Cells

Flp-In $mGlu_5$ cells were grown in five T175 flasks as previously described (Section 2.2.1.1). The medium was removed, and cells were washed with ice-cold PBS.

Following this, cells were scraped from the bottom of each flask and combined into an Eppendorf tube, centrifuged (300 xg, 5 min, room temperature) and stored at -80°C. Cells were resuspended in 10 ml homogenisation buffer (10 mM HEPES, 0.9% (w/v) NaCl, 0.2% (w/v) EDTA, pH 7.4) using a Polytron homogeniser (20500 rpm, 20 sec). Samples were then centrifuged (300 xg, 5 min, 4°C) and the supernatant was collected into a clean falcon tube. The pellet was homogenised and centrifuged a further 2 times, with the collection of the supernatant into a fresh tube each time. The total supernatant (3 x 10 ml) was centrifuged at 40000 xg for 1 hour at 4°C. This time, the supernatant was discarded, and the pellet was resuspended in storage buffer (20 nM HEPES, 0.1 mM EDTA, pH 7.4) using a needle and syringe. Samples were stored at -80°C until required.

2.8.2 Preparation of Membranes from Brain Tissue

Frozen brain tissue (section 2.3.5) was homogenised on ice in homogenisation buffer (10 mM HEPES, 0.9% (w/v) NaCl, 0.2% (w/v) EDTA, pH 7.4) using a handheld glass homogeniser. Samples were further homogenised using a Polytron homogeniser (15,000 rpm) and subsequently centrifuged (40,000 xg, 1 hour, 4°C). The supernatant was discarded, and the pellet was resuspended in storage buffer (20 nM HEPES, 0.1 mM EDTA, pH 7.4) using a needle and syringe. Samples were stored at -80°C until required.

2.8.3 Radioligand Binding Assays

a. **Saturation binding assays** were performed in triplicate with 25 µl of increasing concentrations of [^{3}H]M-MPEP (~0.015-40 nM) added to each well containing 122 µl binding buffer and 100 µl brain tissue or cell membranes.

b. **Competition binding assays** were performed in triplicate. [^{3}H]M-MPEP at K_d value and increasing concentrations of an unlabelled ligand of choice were added to membrane protein (5 µg cell membranes and 30 µg brain tissue membranes).

In saturation and competition binding assays, non-specific binding of [^{3}H]M-MPEP was determined by the addition of 1 µM of HTL0011867/ mavoglurant in DMSO. In addition, 2.5 µl of 100% DMSO was added to the total

binding wells. The total volume in each well was 250 µl.

Reactions were incubated at room temperature on a shaker (900 rpm) for 90 min. Bound and unbound radioligand were separated by rapid filtration using a 24-well Brandel cell harvester onto GF/C filter paper pre-soaked for 30 min in 0.5% polyethyleneimine (PEI). Filters were dried for a minimum of 30 min at room temperature, then transferred into scintillation vials containing 3 ml of ScintLogic U. Data were read using a Hidex Liquid Scintillation Counter and analysed using GraphPad Prism 7 to obtain non-linear regression curves.

2.8.4 *Ex Vivo* Receptor Occupancy Assay

NBH-infected Tg37 mice (section 2.3.3) were given i.p. injections of 10 mg/kg VU0424238 or vehicle (10% Tween-80). The animals were culled by cervical dislocation 30 min later. The cortex and hippocampus were dissected out, snap-frozen, and stored at -80°C until use. The receptor occupancy assay was carried out using crude brain homogenate. Tissue was weighed and homogenised in binding buffer (50 nM HEPES, 150 nM NaCl, pH 7.5) using a polytron homogeniser (7000 rpm, 20 sec). The volume of binding buffer was 4X the weight of the tissue. Reactions were performed in sextuplicate, with 100 µl of crude brain homogenate added to wells containing 25 µl [^{3}H]M-MPEP and 125 µl binding buffer. Total binding wells contained 2.5 µl 100% DMSO and non-specific binding wells contained 2.5 µl 10 µM MPEP for a total well volume of 250 µl. The brain homogenates were incubated at 4°C on a shaker (900 rpm) for 10 min. This short incubation time is to avoid dissociation of the dosed compound. Bound and unbound radioligand were separated by rapid filtration using a 24-well Brandel cell harvester onto GF/C filter paper pre-soaked for 30 min in 0.5% PEI. Filters were dried for a minimum of 30 min at room temperature, then transferred into scintillation vials containing 3 ml of ScintLogic U. Data were read using a Hidex Liquid Scintillation Counter.

2.9 Cell Signalling Assays

2.9.1 IP1 Accumulation Assay

Gq protein signalling *via* $mGlu_5$ was determined by measuring the inositide signalling pathway. This was conducted by detecting the by-product inositol monophosphate (IP1) using an IP-One Gq kit HTRF® (CisBio). IP1 accumulation assays were carried out on cells seeded in 96-well plates at a density of 40,000 cells/well. For the assay, cells were washed and incubated in pre-warmed stimulation buffer (20 mM HEPES, 1.2 mM $CaCl_2$, 20 mM LiCl, HBSS without phenol red, pH 7.4) supplemented with 1-10U/ml glutamate-pyruvate transaminase (GPT) and 6 mM sodium pyruvate at 37°C, 5% CO2 for 1 hour prior to experimentation. Compound dilutions were prepared at a 10X concentration in supplemented stimulation buffer. Cells were pre-treated with the antagonist for 10 min at room temperature. The agonist was added, and the cells were incubated at 37°C for 1 hour. The reactions were stopped by removing the compounds and adding lysis buffer (IP-One Gq kit, Cisbio). The cells were shaken (600 rpm, 10 min), and the lysates (7 µl/well) were added to a 384-well white optiplate. Serial dilutions of the IP1 standards (IP-One Gq kit, Cisbio) were prepared in stimulation buffer and added to the optiplate for the standard curve. IP1-d2 and IP1-cryptate antibodies were diluted in lysis buffer (both 1:20) and 3 µl added to the lysates and standards in the optiplate. The plate was briefly spun and incubated for 1 hour at 37°C. Fluorescence emissions at 665 and 620 nm wavelengths were measured using a CLARIOstar microplate reader, and results were calculated as a 665/620 nm ratio. Unless otherwise stated, data were normalised by setting the 665/620 nm ratio from the highest ligand concentration as 100% and the 665/620 nm ratio from the lowest ligand concentration as 0%. To estimate ligand potency (EC_{50}), stimulation non-linear regression models in GraphPad Prism were used.

2.9.2 Ca^{2+} Mobilisation Assay

Ca^{2+} mobilisation assays were carried out on cells seeded in black, clear-bottomed 96-well plates at a density of 40,000 cells/well. For the assay, cells were pre-labelled with the Ca^{2+}sensitive dye Fura-2-AM in HBSS supplemented with 10 mM HEPES, 1-10 U/ml GPT and 6 mM sodium pyruvate at

37°C, 5% CO_2 for 45 min. Compound dilutions were prepared in HBSS supplemented with 10 mM HEPES (HBSS-H) in a clean 96-well plate. Cells were then washed and maintained in HBSS-H for 15 min at 37°C, 5% CO_2. An antagonist was added at this point if being used. Fura-2 fluorescent emission at 510 nm resulting from 340 or 380 nm of excitation was then monitored using a Flexstation II plate reader. Unless otherwise stated, data were normalised by setting the Fura-2 ratio from the highest ligand concentration as 100% and the Fura-2 ratio from the lowest ligand concentration as 0%. To estimate ligand potency (EC_{50}), stimulation non-linear regression models in GraphPad Prism were used.

2.10 Gene Expression Analysis

2.10.1 RNA Extraction from Brain Tissue

RNA extraction from human and mouse brain tissue was performed from frozen brain samples using a Qiagen RNeasy Plus Mini Kit. Briefly, tissue was homogenised using a handheld homogeniser in RLT buffer containing 10% ß-mercaptoethanol. The homogenate was centrifuged for 3 min at maximum speed and the supernatant was subsequently centrifuged at 10,000 xg for 30 sec in a gDNA eliminator column. The flow-through was collected and mixed 1:1 with 70% ethanol and added to an RNeasy spin column. This was then centrifuged for 15 sec at 8000 xg, and the flow through was discarded. The column was washed with guanidine containing stringent wash buffer, centrifuged for 15 sec at 10,000 xg, washed with a mild wash buffer, and then centrifuged again for 2 min at 10,000 xg. The columns were placed into a clean collection tube and centrifuged for a further 2 min at maximum speed to remove residual ethanol. Next, a volume of 30 µl nuclease-free water was added to the RNeasy Mini spin column which was subsequently centrifuged for 1 min at 10,000 xg to elute the RNA.

2.10.2 Determination of RNA Concentration

The RNA concentration was determined using a PHERAstar microplate reader by measuring absorbance at 260 nm. RNA purity was assessed using absorbance

ratios of 230/260 nm and 260/280 nm, with ratios of 2-2.2 considered pure. RNA was stored at –80°C until required.

2.10.3 Reverse Transcription

For cDNA synthesis, reverse transcription was carried out using a High-Capacity cDNA Reverse Transcription Kit with RNase inhibitor. Reactions were carried out in PCR tubes with a total volume of 20 µl as follows: 1 µg RNA in 10 µl RNAse-free water and 10 µl reaction mix containing 1X RT buffer, 4 mM dNTP mix, 1X RT random primers, 50 units MultiScribe Reverse Transcriptase and RNAse-free water.

Reaction mixtures were incubated in a thermal cycler using the following conditions:

Step 1	25°C	10 min	Annealing
Step 2	27°C	120 min	RT inactivation
Step 3	85°C	5 min	Inactivation
Step 3	4°C	∞	Storage

cDNA samples were stored at -20°C until needed.

2.10.4 Real-Time Quantitative PCR

Quantitative RT-PCR (RT-qPCR) was conducted using Fast SYBR Green Master Mix. The primers used are listed in Table 2-7. cDNA was diluted 10x before use. Each reaction was performed in duplicate or triplicate in 384-well MicroAmp® Optical PCR plates at a total volume of 10 µl as follows:

5 µl	Fast SYBER Green Master Mix
0.8 µl	primers (10 µM stock)
2.6 µl	Nuclease-free water
1.6 µl	cDNA

Plates were read on a QuantStudio™ 5 Real-Time PCR System using the fluorescence channel for SYBR green. The following conditions were used for the amplification cycles:

Step 1	95°C	3 min	Preheating
Step 2	95°C	5 sec	Denaturing
Step 3	60°C	12 sec	Annealing
Step 4	Repeat steps 2-3 (x40)		

A melt curve was produced using the following conditions:

Step 1	95°C	1 sec	Heating
Step 2	60°C	20 sec	Annealing
Step 3	95°C	1 sec	Heating

Table 2-7 List of primers used for RT-qPCR. All primers were acquired from Qiagen.

Primer Template	Species	Primary Assay Name (Cat#)
α-tubulin	Mouse	Mm_Tuba1b_1_SG (QT00198877)
$mGlu_5$	Mouse	Mm_Grm5_1_SG (QT00288596)
Cluster of Differentiation 68 (CD68)	Mouse	Mm_Cd68_1_SG (QT00254051)
GFAP	Mouse	Mm_Gfap_1_SG (QT00101143)
Tumour Necrosis Factor-alpha (TNF-α)	Mouse	Mm_Tnf_1_SG (QT00104006)
Interleukin-1alpha (IL-1α)	Mouse	Mm_Il1a_1_SG (QT00113505)
Interleukin-1beta (IL-1β)	Mouse	Mm_Il1b_2_SG (QT01048355)
Interleukin-6 (IL-6)	Mouse	Mm_Il6_1_SG (QT00098875)
Interleukin-10 (IL-10)	Mouse	Mm_Il10_1_SG (QT00106169)
Monocyte Chemoattractant Protein-1 (MCP-1)	Mouse	Mm_Ccl2_1_SG (QT00167832)
Granulocyte-Macrophage Colony-Stimulating Factor (GM-CSF)	Mouse	Mm_Csf2_1_SG (QT00251286)

2.10.5 RT-qPCR Data Analysis

Comparative cycle threshold (C_T) values were acquired using QuantStudio™ Design and Analysis software (Thermo Fisher Scientific). Quantification of the qPCR results was carried out using a comparative C_T method. C_T values for the gene of interest were normalised by comparison with a suitable housekeeping

gene which has been run in parallel as an internal control (typically α-tubulin), to calculate ΔC_T values (ΔC_T = C_T of internal control – C_T of gene of interest). ΔC_T values of control conditions were averaged, and $\Delta\Delta C_T$ values were calculated ($\Delta\Delta C_T$ = ΔC_T of gene of interest – averaged control ΔC_T of gene of interest). Data were expressed as $2^{-\Delta\Delta C_T}$ to show the fold change in expression.

2.11 Statistical Analysis

Unless otherwise specified, statistical analyses were carried out using GraphPad Prism (version 9.3.0) software. Statistical tests used are indicated in the relevant figure legends.

Generally, for statistical analysis of differences between groups of measures, a parametric test was used as data were assumed to be normally distributed. For data comparing fewer than two groups, an unpaired t-test was used. A two-way Analysis of Variance (ANOVA) was used to compare more than two groups. Post hoc analysis of multiple comparisons was used following a two-way ANOVA. Tukey's multiple comparisons were used when the mean of every data set was compared with the mean of every other data set. Dunnett's multiple comparisons were used the mean of every data set was compared to one reference mean.

For the analysis of burrowing experiments, a mixed effects model (for analysis of repeated measures) was used as the number of data-points differed between groups. For these experiments, Fisher’s least significant difference test was used to compare the mean of every data set with the mean of every other data set.

For statistical analysis of survival curves, a Gehan-Breslow-Wilcoxon test was applied.

Chapter 3 Characterisation of $mGlu_5$ Receptor Expression and Signalling in Flp-In $mGlu_5$ Cells and Mouse Primary Cortical Astrocytes

3.1 Introduction

The $mGlu_5$ receptor has been identified as a potential therapeutic target for the treatment of neurodegenerative diseases, including AD, HD, and ALS (Kumar et al., 2015; Ribeiro et al., 2014; Zhang et al., 2019). A number of compounds which modulate the activity of $mGlu_5$ have been developed, several of which have progressed into clinical trials for neurodegenerative disorders (Budgett et al., 2022). Once a compound has been identified, it must be characterised in order to understand its pharmacological profile and potential as a drug target. An essential part of the drug discovery process is to understand the properties that drive the efficacy and potency of potential drug candidates. *In vitro*, cell-based assays with defined outcome measures are an important part of this process as they are generally fast, simple, and cost-effective (Michelini et al., 2010). Immortal cell lines are commonly used for screening and evaluating drug candidates using these assays. However, since these cell lines do not capture the physiological state of the target cell, the use of primary cells, which are isolated from tissue, is also important. This chapter investigates $mGlu_5$ receptor expression and signalling using a mouse Flp-In™ T-REx™ 293 cell line and mouse primary cortical astrocytes. Subsequently, these cell types were used to characterise two $mGlu_5$ allosteric modulators, VU0409551 (Conde-Ceide et al., 2015) and VU0424238 (Felts et al., 2017).

3.1.1 The Flp-In™ T-REx™ System

The stable transfection of receptors, such as GPCRs, into cells, followed by clonal cell line selection, is a useful tool for understanding receptor signalling. In this chapter, the Flp-In™ T-REx™ system was used to stably express $mGlu_5$ in a HEK293 cell background (for more details, see 2.2.1). There are several other advantages to the Flp-In™ T-REx™ system as compared to both transient transfection and the generation of traditional stable cell lines (Ward et al., 2011). Unlike traditional methods of generating stable cell lines, this system offers the advantage of inducible receptor expression through the addition of a small molecule inducer, doxycycline. In the context of studying $mGlu_5$ receptors *in vitro*, there is a specific challenge when using traditional stable cell lines constitutively expressing the receptor. In these cell lines, endogenous glutamate is released from the cells into the medium, which can constantly activate and

desensitise $mGlu_5$, posing a potential complication (Desai et al., 1995). The Flp-In™ T-REx™ system allows cells to be grown without the expression of $mGlu_5$ until its expression is required. When expression is required, it can be regulated by varying the concentration of doxycycline added.

Moreover, this method of transfection enables the direct integration of the gene of interest into a well-defined site in the genome of the host cell, while the subsequent clonal selection ensures the generation of an isogenic cell line. This means that protein expression will be consistent across a population of cells and that all the Flp-In cells derived from the same parental cells have the same genetic background (Szczesny et al., 2018). This is advantageous over short-term transient transfection, which results in a heterogeneous cell population, with cells expressing varying levels of the protein of interest across a population (Ward et al., 2011). Overall, this is a reliable way to generate a cell line that is easy to maintain and allows a degree of control over the level and time of onset of $mGlu_5$ expression.

3.1.2 Mouse Primary Cortical Astrocytes

Astrocytes are the most prevalent non-neuronal cell in the CNS, accounting for 20-50% of total CNS cell number (Hasel & Liddelow, 2021). Their distinct morphological properties and spatial distribution mean they play a key role in maintaining neuronal homeostasis *via* functions that include mediating synapse function, providing trophic support to neurons, and regulating neurotransmitter uptake (Hasel & Liddelow, 2021). A key hallmark of NDDs is a chronic inflammatory response involving astrocyte upregulation and activation. This phenomenon, which contributes significantly to the pathogenesis of NDDs, is discussed in detail in 1.3.2.3.

Communication between neurons and astrocytes is achieved, in part, due to the expression of receptors on their cell surfaces (Kofuji & Araque, 2021). Astrocytes express both ionotropic and metabotropic glutamate receptors, but the majority of their glutamatergic signalling is mediated by the latter, specifically $mGlu_1$, $mGlu_3$, and $mGlu_5$ receptors (Loane et al., 2012). Under pathophysiological conditions, the expression of astrocytic $mGlu_5$ is elevated, and its signalling becomes dysregulated (see 1.4.2) (Vermeiren et al., 2006; Casley et al., 2009;

Lim et al., 2013; Shrivastava et al., 2013). Misfolded proteins, such as Aß, which are characteristic of neurodegenerative diseases, can bind to and activate $mGlu_5$ receptors on astrocytes, resulting in excitotoxicity (Vermeiren et al., 2006; Price et al., 2010; Spampinato et al., 2018; Vergouts et al., 2018). This disruption of $mGlu_5$ signalling may play a key role in the pathology of neurodegenerative diseases.

Traditionally, drug development programmes for neurodegenerative diseases have focussed on targeting neurons. However, it is now understood that astrocytes play a pivotal role in maintaining brain health and can both induce and rescue neurons from disease states (Ransohoff, 2016). Therefore, drugs that target astrocytes may offer a novel approach for the treatment of neurodegeneration (Michelini et al., 2010). Due to the expression of $mGlu_5$ receptors in astrocytes and the emerging importance of astrocytes in neurodegeneration, this chapter uses cultured mouse primary cortical astrocytes as a physiologically relevant model in which to investigate $mGlu_5$ signalling and its modulation by allosteric modulators.

In vitro, astrocyte cell cultures are a powerful tool for studying the biological properties of these cells in isolation. Moreover, they enable the investigation of the actions of novel drugs in a more physiologically relevant model. The method of isolating mouse primary cortical astrocytes used in this thesis is based on an astrocyte culture preparation from neonatal rat brains (Zhang et al., 2005). This protocol has three main steps. Firstly, the death of neurons in the culture over the first week due to the composition of the growth medium. Secondly, the rapid proliferation of astrocytes, microglia, and oligodendrocytes. And thirdly, the selective detachment of microglia and oligodendrocytes by shaking. This protocol yields a dense monolayer of pure primary astrocytes. These cells are grown in a culture medium containing G5 growth factor supplement (biotin, epidermal growth factor (EGF), basic fibroblast growth factor (FGF), human transferrin and insulin), a widely used culture additive which is designed to support the growth of primary glial cells (Michler-Stuke et al., 1984; Vermeiren et al., 2005). This protocol is fast and highly reproducible. However, it should be kept in mind that these astrocytes are cultured *in vitro*, and therefore while they reflect many characteristics of *in vivo* astrocytes, they also display

differences. Notably, the astrocytes are grown in serum-containing media, and serum components are usually absent from the CNS (Foo et al., 2011).

3.1.3 Choice of Assay to Investigate $mGlu_5$ Signalling

Selecting an appropriate assay system to investigate receptor signalling and test potential ligands is an important part of the drug discovery process. Using cell-based assays, it is possible to define the action of a ligand as a full or partial agonist, inverse agonist, or antagonist. These assays provide detailed information about a ligand's efficacy in the particular assay (described as the maximal effect of the drug, or E_{Max}) and potency (the concentration required to produce 50% of the maximal effect of the drug, or EC_{50}). A variety of cell-based assays are used to screen compounds that target GPCRs, and often these assays measure signals downstream of activations of specific Gα subtypes activated by the receptor. As discussed in section 1.2.5, $mGlu_5$ predominantly couples to $G\alpha_{q/11}$ G proteins. $G\alpha_{q/11}$ proteins activate phospholipase C, which leads to an increase in the secondary messengers DAG and IP3, resulting in the release of Ca^{2+} from intracellular stores and the activation of PKC (Dhami & Ferguson, 2006).

Given the importance of Ca^{2+} signalling in biological systems, several techniques have been developed to measure Ca^{2+} levels. In this chapter, a Ca^{2+} mobilisation assay is used. This assay uses a calcium-sensitive fluorescent dye to measure the transient increase in intracellular Ca^{2+} associated with the activation of a $G\alpha_{q/11}$-coupled receptor. This method of determining the function of $G\alpha_{q/11}$-coupled GPCRs is robust and amenable to high-throughput screening (Garbison et al., 2012). However, as changes in intracellular Ca^{2+} are typically rapid and transient, this method does not allow for the detection of constitutive activity (Garbison et al., 2012). Therefore, Ca^{2+} assays do not typically enable the characterisation of inverse agonist compounds that inhibit constitutive GPCR signalling (Khilnani & Khilnani, 2011).

Alternatively, an IP1 assay is used, which measures the levels of IP1, a product of IP3 degradation. This method takes advantage of the ability of lithium chloride to prevent the degradation of IP1 and uses an IP1 antibody to quantify the amount of IP1 that accumulates in cells over a period of time as a surrogate

measure of IP3 production (Garbison et al., 2012). Unlike the transient responses measured in Ca^{2+} assays, because IP1 assays measure accumulation over a longer period of time, this assay can measure the constitutive activity of $G\alpha_{q/11}$-coupled GPCRs (Garbison et al., 2012) and, therefore, can determine if a ligand acts as an inverse agonist.

Although they give no functional information about a ligand, ligand binding assays can be used to determine the binding affinity of a ligand to a particular GPCR, either directly (saturation binding) or indirectly (displacement binding). Competition binding assays are used in this chapter to determine the selectivity of VU0409551 and VU0424238 for $mGlu_5$ and to confirm their reported binding sites. By using [^{3}H]M-MPEP, a radioligand known to bind to the main allosteric binding pocket on $mGlu_5$, competition binding assays can assess the ability of an unlabelled ligand to displace the labelled radioligand from the binding pocket, thus confirming that they bind to the same binding pocket on the receptor.

3.1.4 *Ex Vivo* Receptor Occupancy Assay

Receptor occupancy studies are used during drug development to confirm target engagement in the tissue of interest. Receptor occupancy for $mGlu_5$ NAMs has been determined *in vivo* in rodents by measuring direct binding to radioligands or by indirectly measuring the displacement of radiolabelled ligands (Anderson et al., 2002; Gasparini et al., 2002). This involves dosing the animal with the test compound, followed by intravenous administration of a suitable radiotracer for the receptor of interest. The animal is then sacrificed, and the percentage reduction in radiotracer binding to the receptor of interest due to competition with the test compound is measured. Positron emission tomography (PET) imaging has been used in primates and humans, with the development of several $mGlu_5$ PET ligands which allow for the measurement of receptor expression and distribution as well as the receptor occupancy of $mGlu_5$ ligands after drug administration (Hamill et al., 2005; Kågedal et al., 2013; Sullivan et al., 2013; Wong et al., 2013; Xu & Li, 2019). Although PET ligands have been used extensively to investigate $mGlu_5$ expression and distribution, understanding of receptor occupancy in relation to drug exposure is still limited (Bennett et al., 2021). *Ex vivo* tissue homogenate filtration-based assays are an accessible, alternative approach to measuring receptor occupancy (Bennett et al., 2021).

This method involves dosing the animal with the test compound shortly before the animal is sacrificed. The receptor of interest is then labelled with a radioligand, and the reduction in specific binding resulting from receptor occupancy by the test compound is measured. The *ex vivo* receptor occupancy method enables an in-depth investigation of the relationship between drug exposure and receptor occupancy, as well as how receptor occupancy may vary between species. This method was used in this thesis to look at the receptor occupancy of VU0424238 in mice.

3.1.5 VU0409551, an $mGlu_5$ PAM

[6,7-Dihydro-2-(phenoxymethyl)oxazolo[5,4-c]pyridin-5(4H)-yl](fluorophenyl)methanone, or VU0409551 (structure in Figure 3-1), was first discovered in 2015 as part of a collaboration between Janssen Research and Development and the Vanderbilt Centre for Neuroscience Drug Discovery (Conde-Ceide et al., 2015). The collaboration aimed to develop a PAM for $mGlu_5$ that had robust antipsychotic efficacy without directly potentiating NMDA receptors which can lead to neurotoxicity (Conde-Ceide et al., 2015). VU0409551 is a highly selective and potent $mGlu_5$ PAM. Since its discovery, VU0409551 has been shown to rescue cognitive deficits and improve disease pathology in a mouse model of Huntingtin's disease (Doria et al., 2018) and a rat model of schizophrenia (Brown et al., 2022).

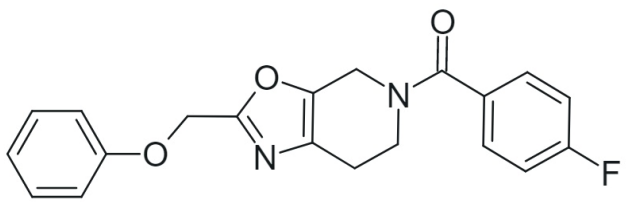

Figure 3-1 Chemical structure of VU0409551. [6,7-Dihydro-2-(phenoxymethyl)oxazolo[5,4-*c*]pyridin-5(4*H*)-yl](fluorophenyl)methanone (VU0409551) is a selective positive allosteric modulator of $mGlu_5$. The structure was drawn using molview.org (based on Conde-Ceide et al., 2015).

3.1.6 VU0424238, an $mGlu_5$ NAM

N-(5-Fluoropyridin-2-yl)-6-methyl-4-(pyrimidin-5-yloxy)picolinamide, or VU0424238 (structure in Figure 3-2), was discovered in 2018 (Felts et al., 2017).

This compound was found to be a highly potent and selective $mGlu_5$ NAM. Initial *in vivo* studies found VU0424238 to be efficacious in rodent models of anxiety and depression (Felts et al., 2017), and a primate model of alcohol self-administration (Salling et al., 2021).

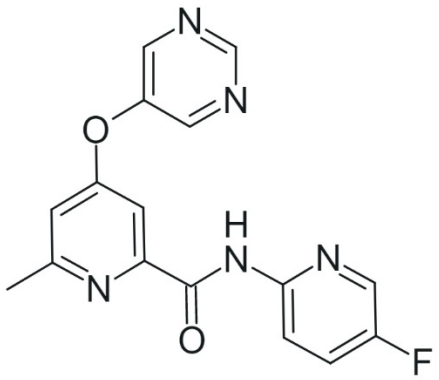

Figure 3-2 Chemical structure of VU0424238. N-(5-Fluoropyridin-2-yl)-6-methyl-4-(pyrimidin-5-yloxy)picolinamide (VU0424238) is a selective negative allosteric modulator of $mGlu_5$. The structure was drawn using molview.org (based on Felts et al., 2017).

3.1.7 Aims

The aims of this chapter were to:

- Examine the expression and signalling of $mGlu_5$ receptors in Flp-In $mGlu_5$ cells.

- Establish a mouse primary cortical astrocyte culture and investigate $mGlu_5$ receptor expression and signalling in these cells, in addition to the effects of growth factor pre-treatment on $mGlu_5$ receptor expression and signalling.

- Characterise two $mGlu_5$ allosteric modulators, VU0409551 (a PAM) and VU0424238 (a NAM), in Flp-In $mGlu_5$ cells and mouse primary cortical astrocytes, and look at their $mGlu_5$ binding sites and VU0424238 receptor occupancy in *ex vivo* mouse tissue.

3.2 Results

3.2.1 Analysis of $mGlu_5$ Receptor Expression in Flp-In $mGlu_5$ Cells

Flp-In™ T-REx™ 293 cells were generated expressing mouse $mGlu_5$ (Flp-In $mGlu_5$ cells). The ability of doxycycline to induce $mGlu_5$ receptor expression in these cells was initially confirmed using immunoblot analysis (Figure 3-3A). Parental Flp-in and Flp-In $mGlu_5$ cells were incubated with 100 ng/ml doxycycline to induce receptor expression. Cell membranes were then prepared and run on an SDS-PAGE gel alongside membranes prepared from wild-type and $mGlu_5$ knockout mouse brain as controls. Using an anti-$mGlu_5$ antibody confirmed the ability of doxycycline to induce $mGlu_5$ receptor expression in this cell line. Two bands were observed, one at ~150 kD and the other at ~300 kD, with the former corresponding to the predicted molecular weight of a $mGlu_5$ receptor monomer and the latter to the predicted weight of a $mGlu_5$ receptor dimer. No bands were observed in Flp-In parental cells or $mGlu_5$ knockout brain. ICC confirmed $mGlu_5$ expression after doxycycline addition at the cellular level, using an antibody for the HA epitope tag on the *C*-terminus of $mGlu_5$ (Figure 3-3B).

A key feature of the Flp-In™ system is that the protein expression level can be regulated by varying the concentration of doxycycline added. Treatment of Flp-In $mGlu_5$ cells with increasing concentrations of doxycycline overnight confirmed that the expression of $mGlu_5$ increased with increasing doxycycline (Figure 3-4). The expression of $mGlu_5$ was observed at all concentrations of doxycycline, with maximal expression levels at 100 ng/ml doxycycline (380-fold increase, $p<0.0001$).

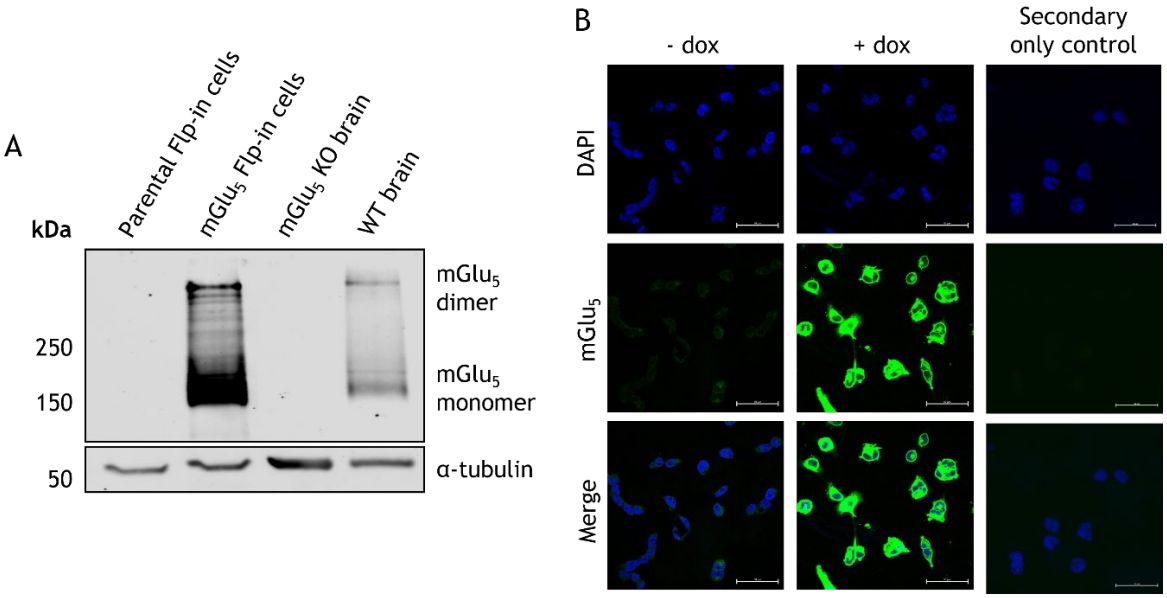

Figure 3-3 Confirmation of mGlu$_5$ expression in Flp-In mGlu$_5$ cells. (A) Western blot analysis of mGlu$_5$ expression in Flp-In mGlu$_5$ cells. Flp-In parental cells are not transfected with mGlu$_5$ and were used as a control alongside membrane samples from the cortex of knockout (KO) and wild-type (WT) mice. Flp-In parental and mGlu$_5$ cells were induced with 100 ng/ml doxycycline the night before the preparation of membrane samples. 10 µg membrane protein was loaded for each sample. Protein expression was detected using a mGlu$_5$-specific antibody. The loading control was α-tubulin. The blot shown is a representative blot from 3 separate experiments. (B) Detection of mGlu$_5$ expression (green) in PFA-fixed Flp-In mGlu$_5$ cells after incubation with either 0 (- dox) or 100 (+ dox) ng/ml of doxycycline overnight. An anti-HA antibody was used to detect HA-tagged mGlu$_5$. The nuclei were stained with DAPI (blue). Representative images of n=3 are shown. Secondary (antibody) only control was included to control for antibody specificity (n=1). Images were taken on a Zeiss 880 confocal microscope with a 40x objective, scale bar is 50 µM.

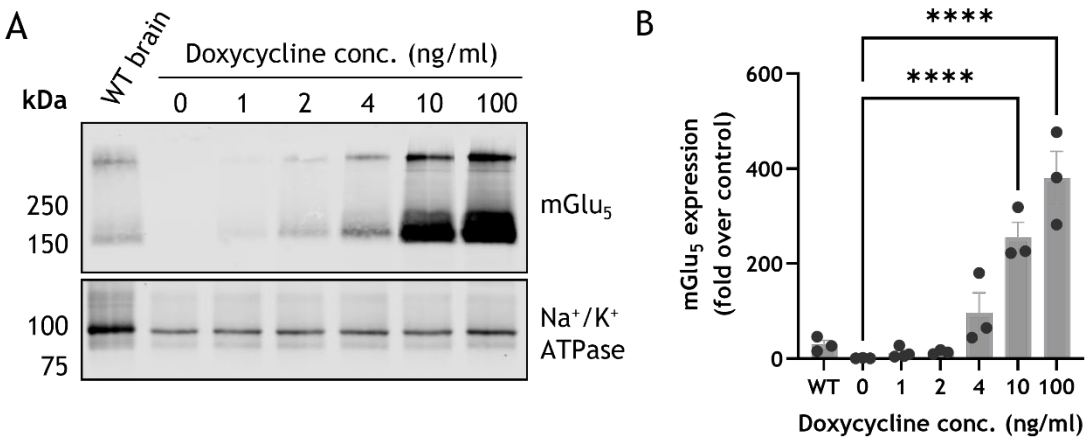

Figure 3-4 Inducibility of mGlu$_5$ expression in Flp-In mGlu$_5$ cells. (A) Detection of mGlu$_5$ expression in membrane samples from Flp-In mGlu$_5$ cells induced with increasing concentrations of doxycycline overnight (0-100 ng/ml). Wild-type (WT) cortex was used as a positive control. 10 µg membrane protein was loaded for each sample. Protein expression was detected using a mGlu-specific antibody. Na^+/K^+ ATPase was used as a loading control. The blot shown is a representative blot from 3 separate experiments. (B) Band analysis (on both mGlu$_5$ bands) for each blot was performed using Image Studio Lite Version 5.2. Protein levels were normalised to the loading control, and data are shown as fold over control (0 ng/ml doxycycline). Data shown are means ± S.E.M., with points representing individual experiments (n=3). Statistical analysis performed was a one-way ANOVA, with comparison to 0 ng/ml doxycycline, where **** P≤0.0001.

To further confirm $mGlu_5$ expression in Flp-In $mGlu_5$ cells, [^{3}H]M-MPEP binding in membrane samples was assessed (Figure 3-5). M-MPEP is a prototypical negative allosteric modulator of $mGlu_5$, which is known to bind to the main allosteric binding pocket of the receptor (see Figure 1-6). Total and non-specific binding was carried out in the presence of the $mGlu_5$ NAM mavoglurant (Figure 3-5A). Subsequently, B_{max} (maximum receptor density) and K_d (equilibrium dissociation constant) values were calculated from the specific binding curves (Figure 3-5B). This experiment yielded a B_{max} of 85.9 ± 8.1 pmol/mg membrane protein, with a K_d value for [^{3}H]M-MPEP of 3.6 ± 1.0 nM.

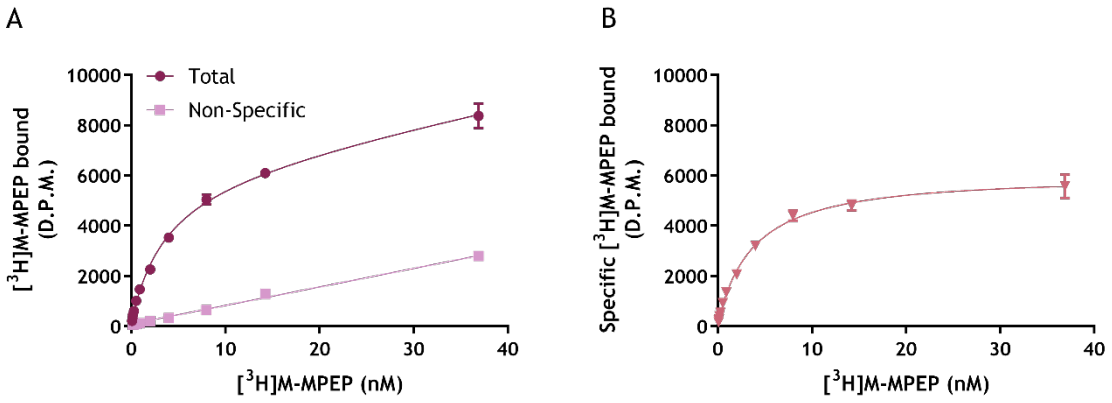

Figure 3-5 Saturation binding experiment in Flp-in $mGlu_5$ cells. (A) Non-linear regression curves of [^{3}H]M-MPEP saturation binding assay on Flp-in $mGlu_5$ cells. The capacity of varying concentrations of [^{3}H]M-MPEP (~0.015-35 nM) to bind to $mGlu_5$ was assessed in the absence (Total) or presence (Non-Specific) of 1 µM HTL0011867/mavoglurant. (B) Specific binding was determined by subtracting non-specific binding from total binding. A single representative experiment is shown, with comparable data being obtained in an additional 2 experiments. Data are displayed as disintegrations per minute (D.P.M.). Data shown are mean ± S.E.M. from single experiments run in triplicate.

3.2.2 Analysis of $mGlu_5$ Receptor Signalling in Flp-In $mGlu_5$ Cells

Concentration response curves for Ca^{2+} mobilisation and IP1 accumulation allow for the assessment of potency (EC_{50}) and efficacy (E_{max}) of compounds at a receptor. Initially, the response of $mGlu_5$ to its endogenous ligand, glutamate, was assessed after Flp-In $mGlu_5$ cells were induced overnight with increasing concentrations of doxycycline. In a Ca^{2+} mobilisation assay, the maximum response of these cells to glutamate was observed with 2 ng/ml of doxycycline, with higher concentrations reducing the signalling window (Figure 3-6A; Table 3-1). The potency of glutamate trended to increase with increasing concentrations of doxycycline, with a significant difference in pEC_{50} at 10 ng/ml doxycycline as compared to 0 ng/ml doxycycline ($P<0.05$) (Table 3-1). In an IP1

accumulation assay, the potency and efficacy of glutamate did not significantly change with higher concentrations of doxycycline (Figure 3-6B; Table 3-2). However, increasing levels of doxycycline resulted in a significant increase in the baseline activity of Flp-In $mGlu_5$ cells (Figure 3-6B-C). This may be due to the constitutive activity of $mGlu_5$: with increasing concentrations of doxycycline, higher $mGlu_5$ expression may lead to higher levels of constitutive activity (Figure 3-6B; Table 3-2). Moreover, at the highest concentrations of doxycycline (10 and 100 ng/ml), the maximum response to glutamate was observed at every concentration of glutamate (Figure 3-6B). This is likely to be due to very high levels of $mGlu_5$ expression at these concentrations. Surprisingly, in both assays, glutamate stimulated a response in cells that had not been induced with doxycycline, suggesting that there might be some leakiness in the Flp-In™ T-REx™ expression system (Figure 3-6A-B).

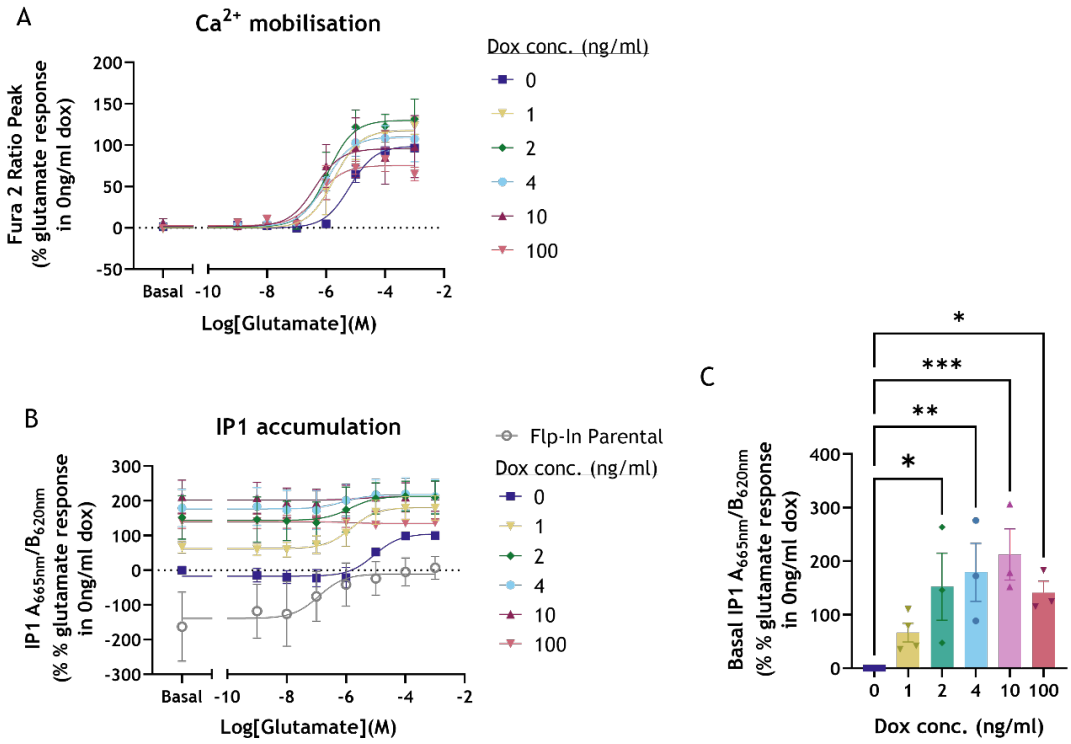

Figure 3-6 G protein-dependent $mGlu_5$ signalling in Flp-In $mGlu_5$ cells treated with varying concentrations of doxycycline. Concentration response curves showing (A) Ca^{2+} mobilisation or (B) IP1 accumulation in Flp-In $mGlu_5$ cells after glutamate treatment (n=3-6). Cells were treated with different doxycycline (dox) concentrations overnight to induce $mGlu_5$ expression. Data were analysed using a log (agonist) vs response (three parameters) analysis of non-linear regression using GraphPad Prism 9.3. Data shown are means ± S.E.M. of at least 3 independent experiments, each implemented in duplicate or triplicate. (C) Bar chart shows basal data from the graph in (B) in order to analyse the change in basal $mGlu_5$ activity with increasing concentrations of doxycycline. Statistical analysis performed was a one-way ANOVA, with comparison to 0 ng/ml doxycycline, where * $P \leq 0.05$, ** $P \leq 0.01$, and *** $P \leq 0.001$.

Table 3-1 Ca^{2+} mobilisation induced by glutamate in Flp-In $mGlu_5$ cells after induction of $mGlu_5$ expression with different concentrations of doxycycline. Potency (pEC_{50}) and efficacy (E_{max}) indicators for each concentration of doxycycline are derived from Figure 3-6A. E_{max} calculated as % of control (0 ng/ml doxycycline). The statistical analysis performed was an ordinary one-way ANOVA (Dunnett's multiple comparisons) with comparison to 0 ng/ml doxycycline, where * P≤0.05.

Ca^{2+} mobilisation

Doxycycline conc. (ng/ml)	pEC_{50} (Log[M]) Mean ± S.E.M.	*P*	E_{max} (%) Mean ± S.E.M.	*P*	*n*
0	5.2 ± 0.1	-	100.0 ± 0.0	-	3
1	5.7 ± 0.3	0.44	128.4 ± 12.4	0.83	3
2	6.0 ± 0.3	0.15	136.1 ± 24.1	0.69	3
4	6.1 ± 0.3	0.08	110.9 ± 27.2	0.99	3
10	6.4 ± 0.0	0.02*	101.2 ± 37.8	>0.99	3
100	6.2 ± 0.3	0.05	67.4 ± 10.00	0.76	3

Table 3-2 IP1 accumulation induced by glutamate in Flp-In $mGlu_5$ cells after induction of $mGlu_5$ expression with different concentrations of doxycycline. Potency (pEC_{50}) and efficacy (E_{max}) indicators for each concentration of doxycycline are derived from Figure 3-6B. E_{max} calculated as % of control (0 ng/ml doxycycline). The statistical analysis performed was a one-way ANOVA (Dunnett's multiple comparisons) with comparison to 0 ng/ml doxycycline.

IP1 accumulation

Doxycycline conc. (ng/ml)	pEC_{50} (Log[M]) Mean ± S.E.M.	*P*	E_{max} (%) Mean ± S.E.M.	*P*	*n*
0	5.1 ± 0.1	-	100.0 ± 0.0	-	6
1	5.9 ± 0.1	0.27	172.1 ± 28.4	0.23	5
2	5.9 ± 0.2	0.39	209.6 ± 47.7	0.07	3
4	6.0 ± 0.1	0.33	212.1 ± 49.6	0.06	3
10	5.2 ± 0.6	0.99	213.5 ± 43.8	0.06	3
100	6.5 ± 0.9	0.05	137.2 ± 11.7	0.90	3

For future experiments, 2 ng/ml doxycycline was used to induce $mGlu_5$ expression in Flp-In $mGlu_5$ cells to avoid over-expression of $mGlu_5$. At 2 ng/ml doxycycline, the $mGlu_5$ receptor agonists, glutamate and DHPG, had pEC_{50} values of 6.2 ± 0.0 and 5.3 ± 0.1 in a Ca^{2+} mobilisation assay and 5.8 ± 0.1 and 5.33 ± 0.0 in an IP1 accumulation assay (Figure 3-7C-D; Table 3-3). The potency of DHPG was significantly lower than glutamate in both assays, with an approximately 8-fold and 3-fold shift to the right in Ca^{2+} mobilisation and IP1

accumulation assays, respectively. Moreover, the efficacy of DHPG was significantly lower than glutamate in an IP1 accumulation assay (Figure 3-7D; Table 3-3).

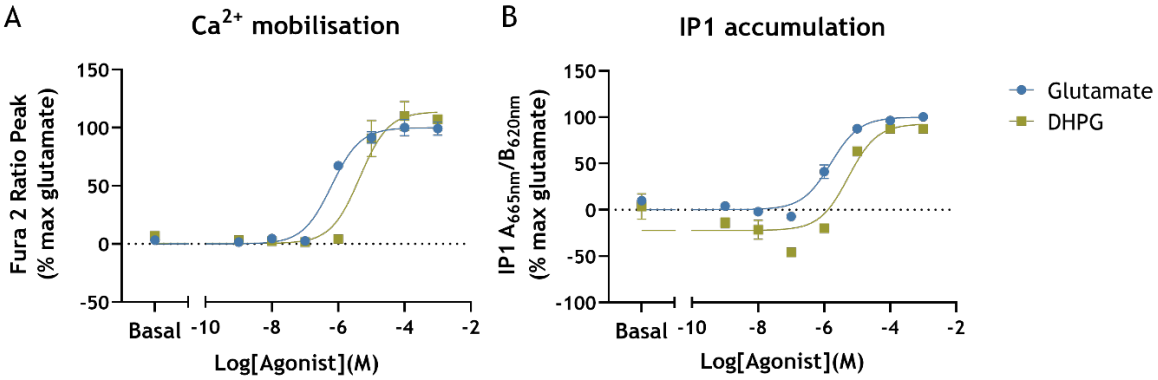

Figure 3-7 G protein-dependent $mGlu_5$ signalling in Flp-In $mGlu_5$ cells treated with 2 ng/ml doxycycline. Concentration response curves showing (A) Ca^{2+} mobilisation or (B) IP1 accumulation in Flp-In $mGlu_5$ cells induced with 2 ng/ml dox overnight with both glutamate and DHPG as agonists (n=3). Data were analysed using a log (agonist) vs response (three parameters) analysis of non-linear regression using GraphPad Prism 9.3. Data shown are means ± S.E.M. of at least 3 independent experiments, each implemented in duplicate or triplicate.

Table 3-3 Ca^{2+} mobilisation and IP1 accumulation induced by $mGlu_5$ agonists glutamate and DHPG in Flp-In $mGlu_5$ cells after induction of $mGlu_5$ expression with 2 ng/ml doxycycline. Potency (pEC_{50}) and efficacy (E_{max}) indicators for each concentration of doxycycline, derived from Figure 3-7C-D. E_{max} is calculated as % of control (glutamate). Statistical analysis performed was an unpaired t-test, where * P≤0.05 and ** P≤0.01.

	Ca^{2+} mobilisation				IP1 accumulation				
Agonist	**pEC_{50} (Log[M]) Mean ± S.E.M.**	***P***	**E_{max} (%) Mean ± S.E.M.**	***P***	**pEC_{50} (Log[M]) Mean ± S.E.M.**	***P***	**E_{max} (%) Mean ± S.E.M.**	***P***	***n***
Glutamate	6.2 ± 0.03	-	100 ± 0	-	5.8 ± 0.1	-	100 ± 0	-	3
DHPG	5.3 ± 0.1	0.001 **	109.0 ± 7.2	0.28	5.3 ± 0.03	0.006 **	85.7 ± 1.0	0.02 *	3

3.2.3 Characterisation of Mouse Primary Cortical Astrocytes

To investigate $mGlu_5$ signalling in a more physiologically relevant context, mouse primary cortical astrocyte cultures were established. Mouse primary cortical astrocytes were grown with and without the addition of G5 supplement (biotin, EGF, FGF, human transferrin, and insulin; see section 3.1.2) for 4 days in an IncuCyte® Live-Cell Analysis System (Figure 3-8A-B). After 4 days of incubation with G5 supplement, the morphology of the cultured astrocytes changed from small, rounded cells to the star-like morphology that characterises astrocytes (i.e., multiple extended processes) (Figure 3-8 A and C). Cells grown without G5 supplement did not adopt this morphology, with most cells remaining rounded with one or two extended processes (Figure 3-8 B and C). Using the IncuCyte® Live-Cell Analysis software, the confluency of these cells was calculated to provide a crude measure of their spread over time. Cells grown both with and without the presence of G5 supplement initially decreased in confluency, with cells grown with G5 supplement increasing in confluency after ~2 days incubation (Figure 3-8D).

ICC analysis confirmed the difference in morphology between cells grown with and without G5 supplement (Figure 3-9). Robust GFAP labelling was observed cells grown with and without G5 supplement; however, there was a stark difference in their morphology that was reflective of what was observed using the IncuCyte® Live-Cell Analysis System in Figure 3-8. Astrocytes were differentiated with G5 supplement for all subsequent experiments.

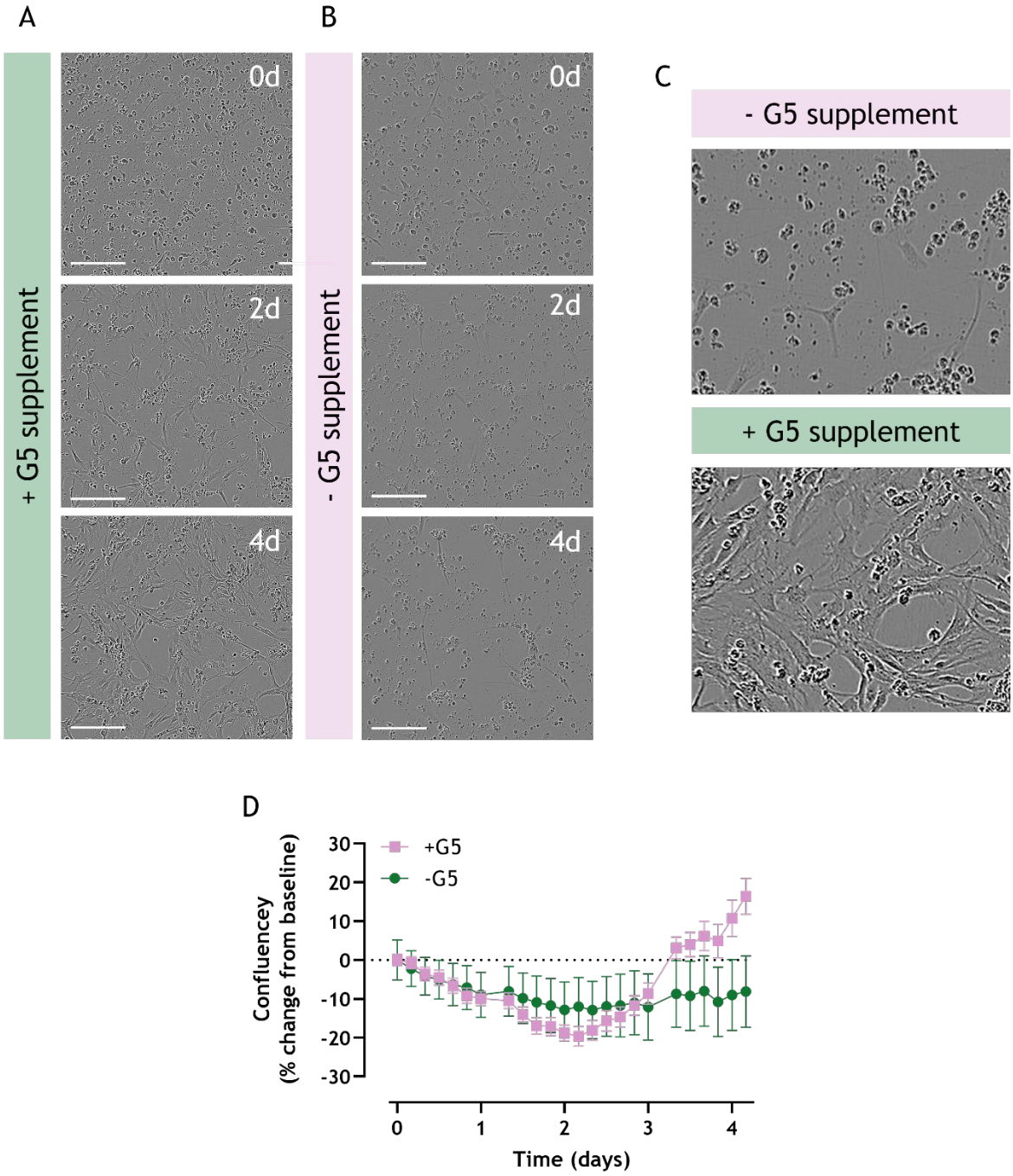

Figure 3-8 Mouse primary cortical astrocytes change morphology and increase in confluence in the presence of G5 supplement. Time-lapse phase contrast images taken using IncuCyte® Live-Cell Analysis system showing the growth of mouse primary cortical astrocytes grown with (A) and without (B) the addition of G5 supplement (n=1; an average of 12-18 biological replicates). Images were taken every hour for 100 hours, with images from 0 hours (0d), 48 hours (2d) and 96 hours (4d) shown. Scale bar is 200 µm. Larger sections of the 4d images in (A) and (B) are shown in (C). Confluency of primary mouse astrocytes grown with (green) and without (purple) the addition of G5 supplement calculated using the IncuCyte® Live-Cell Analysis system. Each point represents 4 hours, from 0-100 hours, and show mean ± S.E.M from 12 (- G5) or 18 (+ G5) wells of the same 96-well plate (n=1).

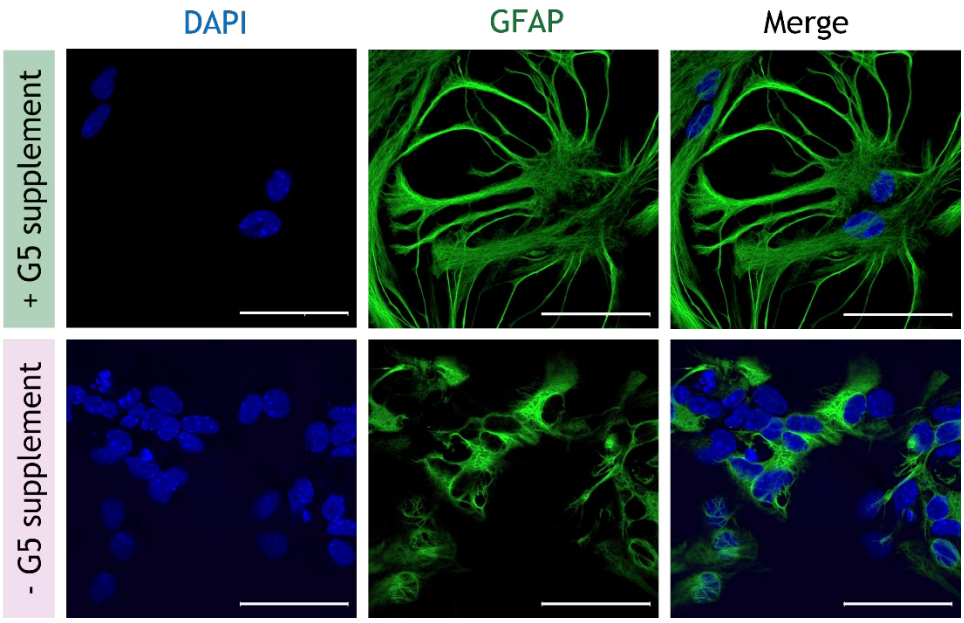

Figure 3-9 Immunocytochemical analysis of mouse primary cortical astrocytes grown with or without G5 supplement. Astrocytes in the top panel were differentiated by the addition of G5 supplement to the media for 4 days prior to fixation. Astrocytes in the bottom panel are non-differentiated i.e., grown in the absence of G5 supplement. Immunostaining was performed using an antibody raised against GFAP (green), and nuclei were stained with DAPI (blue). The images shown are representative of 3 separate experiments (n=3). Images were taken on a Zeiss 880 confocal microscope with a 40x objective, scale bar is 50 µM.

3.2.4 Analysis of $mGlu_5$ Receptor Expression in Mouse Primary Cortical Astrocytes

The expression of $mGlu_5$ in mouse primary cortical astrocytes was initially investigated using ICC, using an antibody specific for $mGlu_5$. This data showed $mGlu_5$ expression in both differentiated and undifferentiated cells (Figure 3-10). Ideally, mouse primary cortical astrocytes cultured from $mGlu_5$ knockout animals would have been used as a control to confirm that this staining was specific. However, $mGlu_5$ homozygous knockout mice are poor breeders, and therefore this experiment was not possible.

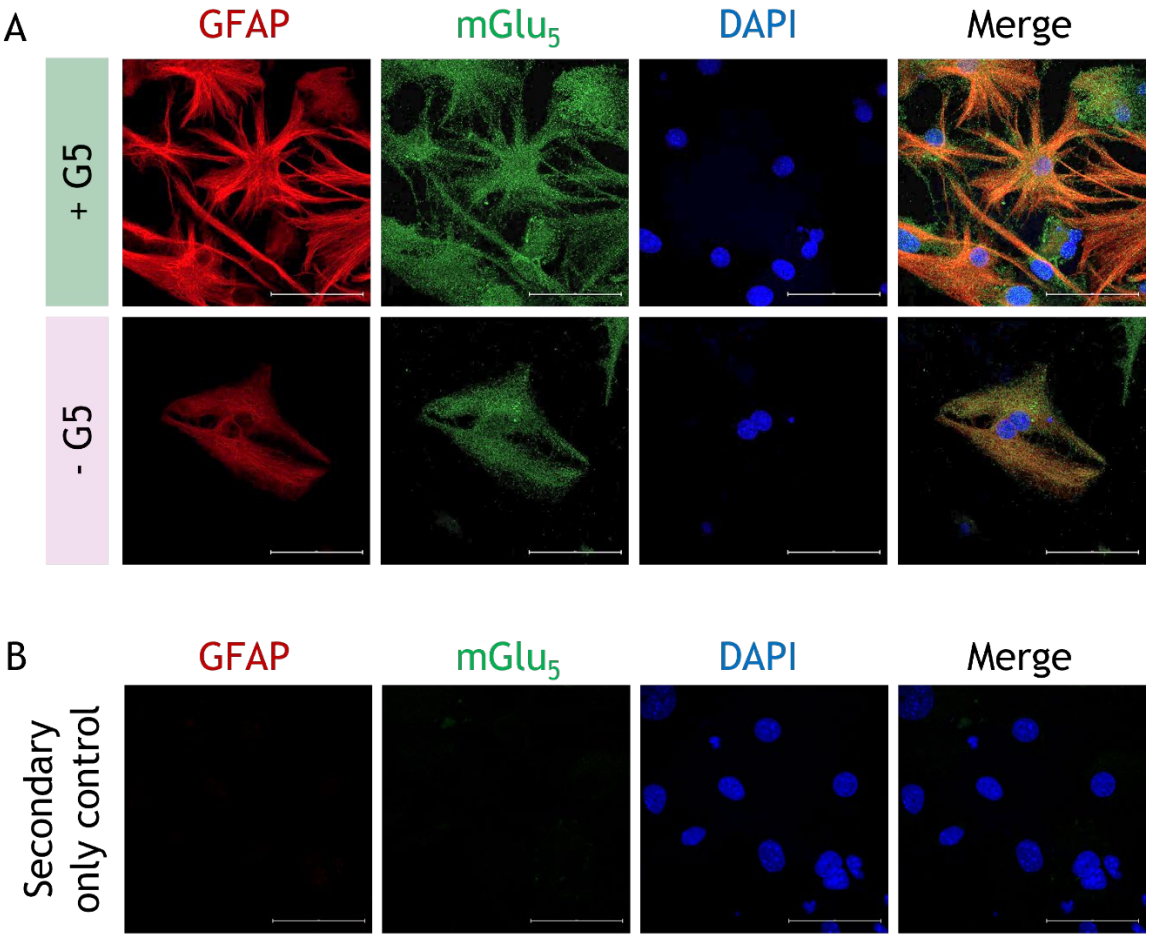

Figure 3-10 Immunocytochemical analysis of $mGlu_5$ expression in mouse primary cortical astrocytes. (A) Images show the detection of $mGlu_5$ expression in differentiated (top panel) and undifferentiated (bottom panel) cultured mouse cortical astrocytes by immunocytochemistry. Cells were incubated with or without G5 supplement for 4 days before being PFA-fixed. Double immunostaining was performed using antibodies raised against $mGlu_5$ (green) and GFAP (red). Nuclei were stained with DAPI (blue). The images shown are representative of 3 separate experiments (n=3). (B) Secondary (antibody) only control was included to control for antibody specificity (n=3). Images were taken on a Zeiss 880 confocal microscope with a 40x objective, scale bar is 50 μM.

Next, Western blot analysis was used to investigate the effect of G5 supplement on $mGlu_5$ expression over time. Cells were grown with and without G5 supplement, and membrane lysates were collected each day for 4 days. There was no increase in $mGlu_5$ expression in the absence of G5 supplement, while in the presence of G5 supplement $mGlu_5$ expression increased with time, particularly 3-4 days after G5 addition (Figure 3-11). Two bands were observed, one at ~150 kD and the other at ~300 kD, which agrees with the data shown for receptor expression in the Flp-In $mGlu_5$ cells and brain cortex in Figure 3-3. Data were analysed using densitometry with $mGlu_5$ bands normalised to Na^+/K^+ ATPase. This showed that $mGlu_5$ receptor expression increased significantly in

cells incubated with G5 at 3 and 4 days after G5 addition (P=0.0087 and 0.0155, respectively) (Figure 3-11B). Therefore, future experiments were carried out after 3-4 days in G5 medium.

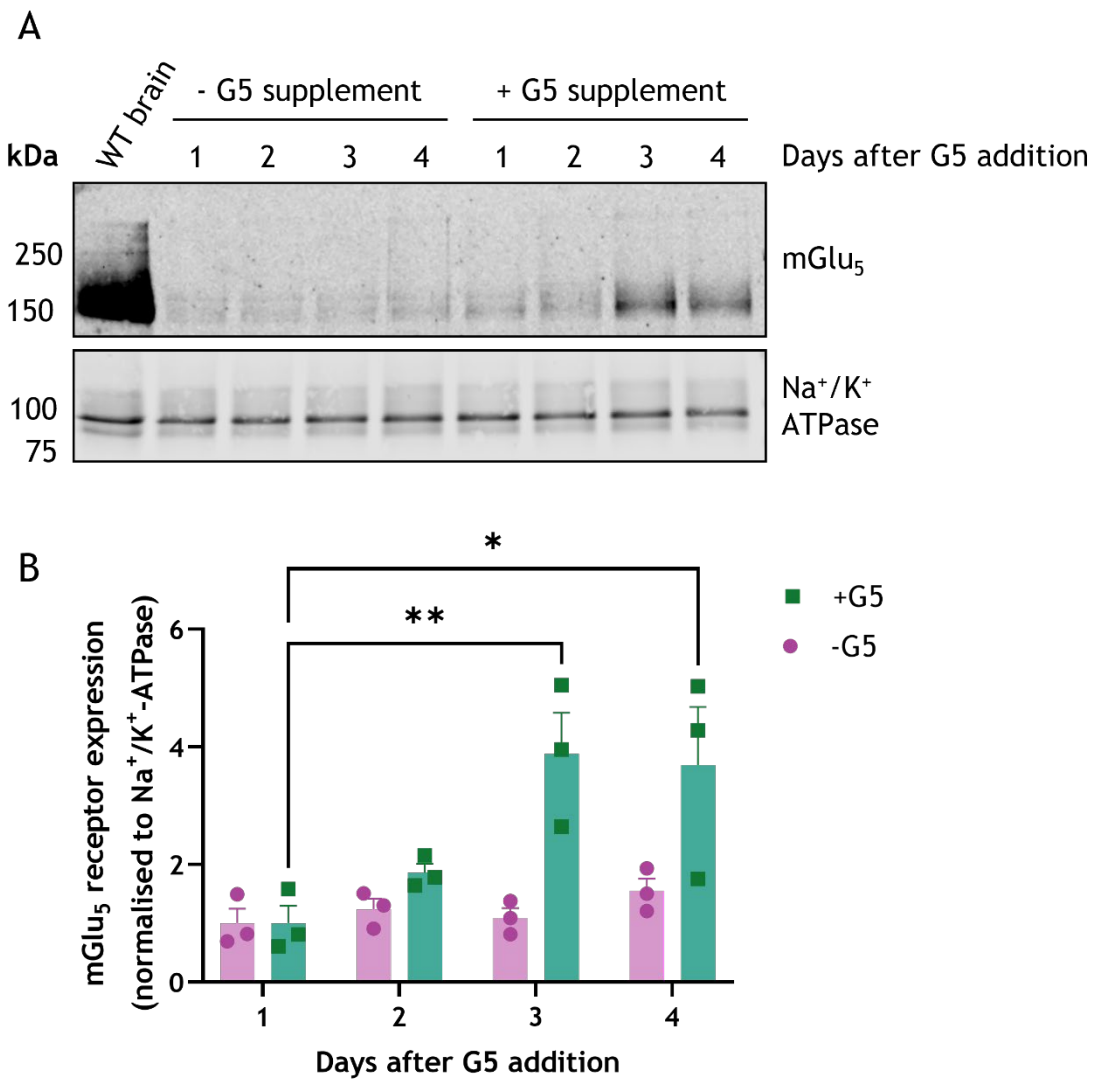

Figure 3-11 Immunoblot analysis of $mGlu_5$ expression in mouse primary cortical astrocytes. (A) Immunoblot analysis of $mGlu_5$ expression in mouse primary cortical astrocytes grown with or without G5 supplement over a 4-day time period. Wild-type (WT) brain was included as a positive control. 3 µg membrane protein was loaded for each sample. Protein expression was detected using a $mGlu_5$-specific antibody. Na^+/K^+ ATPase was used as a loading control. A representative blot from 3 separate experiments is shown. (B) Band analysis (on both $mGlu_5$ bands) for each blot was performed using Image Studio Lite Version 5.2. Protein levels were normalised to the loading control, followed by normalisation to 1 day after G5 addition. Data shown are ± S.E.M. with points representing individual experiments (n=3). Statistical analysis performed was a two-way ANOVA (Tukey's multiple comparisons), where * P≤0.05 and ** P≤0.01.

3.2.5 Analysis of $mGlu_5$ Receptor Signalling in Mouse Primary Cortical Astrocytes

To investigate $mGlu_5$ signalling in astrocytes, initial experiments focussed on evaluating agonist-stimulated changes in Ca^{2+} mobilisation and IP1 accumulation as measures of $mGlu_5$ signalling via $G\alpha_{q/11}$, with and without G5 supplement addition (Figure 3-12). The maximal response of glutamate and DHPG were increased with G5 supplement as compared to glutamate without G5 supplement in both assays, which is likely reflective of increased receptor expression. The E_{max} for glutamate (+G5) was significantly higher than that of glutamate (-G5) in a Ca^{2+} mobilisation assay (P=0.002) (Figure 3-12; Table 3-4). Across both assays, there was no significant difference in potency between conditions (Figure 3-12; Table 3-4).

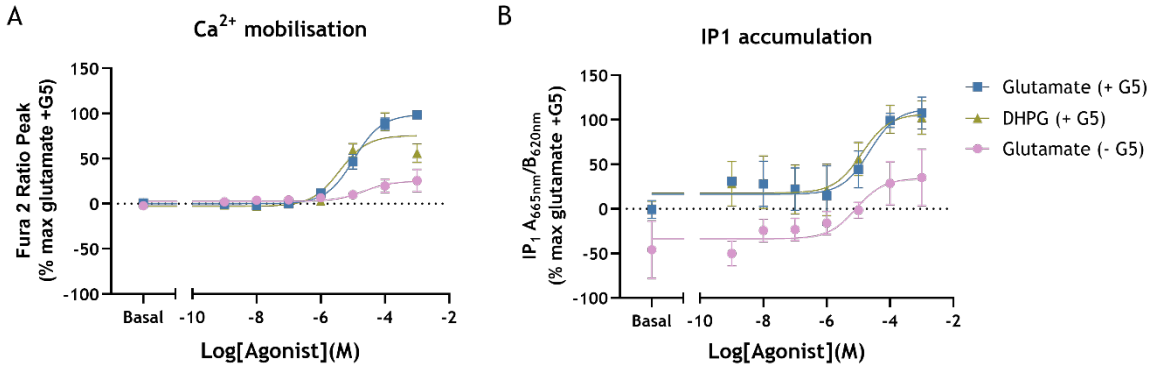

Figure 3-12 G protein-dependent $mGlu_5$ signalling in mouse primary cortical astrocytes in the absence and presence of G5 supplement. Concentration response curve showing (A) Ca^{2+} mobilisation and (B) IP1 accumulation in differentiated (+ G5) or undifferentiated (- G5) mouse primary cortical astrocytes with glutamate and DHPG as the orthosteric agonists. G5 was added for 4 days prior to experimentation. Data were analysed using a log (agonist) vs response (three parameters) analysis of non-linear regression using GraphPad Prism 9.3. Data shown are mean ± S.E.M. for 3 separate experiments, each performed in duplicate or triplicate.

Table 3-4 Ca^{2+} mobilisation and IP1 accumulation induced by $mGlu_5$ agonists in mouse primary cortical astrocytes in the absence and presence of G5 supplement. Potency (pEC_{50}) and efficacy (E_{max}) indicators for each concentration of doxycycline are derived from Figure 3-12. E_{max} calculated as % of control (Glutamate +G5). Statistical analysis performed was an ordinary one-way ANOVA (Dunnett's multiple comparisons) as compared to glutamate (+G5), where ** P≤0.01.

	Ca^{2+} mobilisation				IP1 accumulation				
Agonist (condition)	**pEC_{50} (Log[M]) Mean ± S.E.M.**	***P***	**E_{max} (%) Mean ± S.E.M.**	***P***	**pEC_{50} (Log[M]) Mean ± S.E.M.**	***P***	**E_{max} (%) Mean ± S.E.M.**	***P***	***n***
Glutamate (+G5)	4.9 ± 0.2	-	100.0 ± 0.0	-	5.8 ± 1.2	-	100.0 ± 0.0	-	3
DHPG (+G5)	5.4 ± 0.1	0.75	75.9 ± 8.5	0.17	5.0 ± 0.1	0.64	105.8 ± 16.3	0.97	3
Glutamate (-G5)	6.1 ± 0.9	0.24	24.3 ± 12.8	0.002 **	5.0 ± 0.2	0.64	36.9 ± 29.9	0.11	3

3.2.6 Characterisation of a $mGlu_5$ PAM, VU0409551

Next, VU0409551 was characterised *in vitro*. In an IP1 accumulation assay, the addition of 10 μM VU0409551 to Flp-in $mGlu_5$ cells 10 minutes before the addition of increasing glutamate concentrations induced an approximately 40-fold leftward shift of the glutamate concentration response curve, thus significantly increasing the potency of glutamate in evoking an increase in IP1 (P=0.05) (Figure 3-13A; Table 3-5). In a Ca^{2+} mobilisation assay, pre-incubation with 1 μm VU0409551 induced a significant 10-fold increase in glutamate potency (P=0.03) (Figure 3-13B; Table 3-6). VU0409551 did not significantly increase glutamate efficacy in either assay. Interestingly, VU0409551 increased Ca^{2+} mobilisation in the absence of glutamate at 1 and 10 μM, which suggests that VU0409551 displays agonist activity. This agrees with previously published data (Rook et al., 2015; Sengmany et al., 2017). This data confirmed VU0409551 to be a $mGlu_5$ PAM with agonist activity.

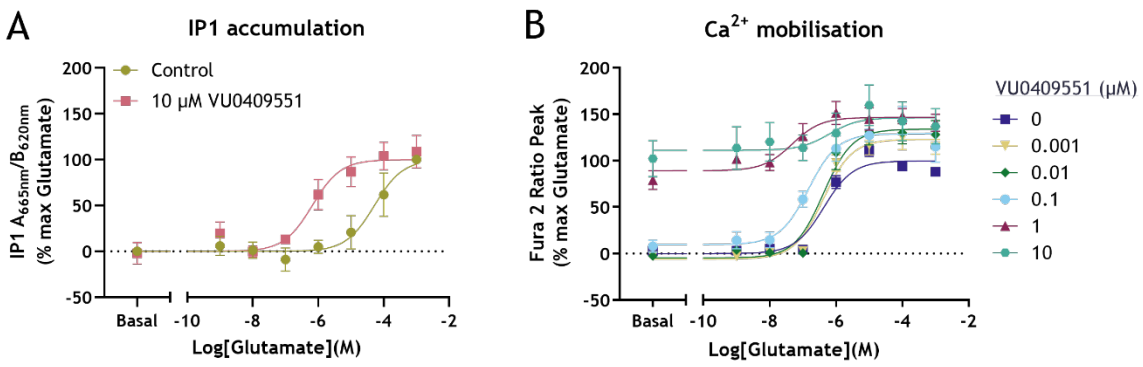

Figure 3-13 Molecular pharmacological profile of VU0409551. (A) Concentration response curve showing IP1 accumulation in Flp-In $mGlu_5$ cells (induced with 2 ng/ml doxycycline overnight) after 1 hour stimulation with increasing concentrations of glutamate. Cells were treated with 10 μM VU0409551 for 10 minutes before the addition of glutamate. Data shown are means ± S.E.M. from 3 separate experiments, each performed in duplicate or triplicate (n=3). (B) Concentration response curve showing Ca^{2+} mobilisation in Flp-In $mGlu_5$ cells (induced with 2 ng/ml doxycycline overnight) after glutamate addition. Cells were pre-treated with increasing concentrations of VU0409551 (0-10 μM) for 10 mins before the addition of a glutamate concentration response curve. Data shown are means ± S.E.M. from 4 separate experiments, each performed in duplicate (n=4). (A and B) IP1 accumulation and Ca^{2+} mobilisation data were analysed using a log (agonist) vs response (three parameters) analysis of non-linear regression using GraphPad Prism 9.3.

Table 3-5 Effect of the $mGlu_5$ PAM VU0409551 on agonist-induced IP1 accumulation in Flp-In $mGlu_5$ cells. Potency (pEC_{50}) and efficacy (E_{max}) indicators for 10 μM VU0409551 as compared to control (0 μM VU0409551), derived from Figure 3-13A. E_{max} was calculated as % of control (0 μM VU0409551). Statistical analysis performed was an unpaired t-test, where * P≤0.05 (10 μM VU0409551 versus control).

IP1 accumulation

VU0409551 conc. (μM)	pEC_{50} (Log[M]) Mean ± S.E.M.	*P*	E_{max} (%) Mean ± S.E.M.	*P*	*n*
Control	4.4 ± 0.4	-	100.0 ± 0.0	-	3
10	6.0 ± 0.4	0.05*	108.7 ± 17.7	0.67	3

Table 3-6 Effect of the $mGlu_5$ PAM VU0409551 on agonist-induced Ca^{2+} mobilisation in Flp-In $mGlu_5$ cells. Potency (pEC_{50}) and efficacy (E_{max}) indicators for increasing concentrations of VU0409551 as compared to control (0 μM VU0409551), derived from Figure 3-13B. E_{max} was calculated as % of control (0 μM VU0409551). Statistical analysis performed was an ordinary one-way ANOVA (Dunnett's multiple comparisons) with comparison to 0 μM VU0409551, where *P≤0.05.

Ca^{2+} mobilisation

VU0409551 conc. (μM)	pEC_{50} (Log[M]) Mean ± S.E.M.	*P*	E_{max} (%) Mean ± S.E.M.	*P*	*n*
0	6.4 ± 0.1	-	100.0 ± 0.0	-	4
0.001	6.4 ± 0.0	>0.99	123.1 ± 10.7	0.58	4
0.01	6.4 ± 0.1	>0.99	134.7 ± 13.5	0.23	4
0.1	6.9 ± 0.1	0.49	129.0 ± 13.8	0.37	4
1	7.4 ± 0.5	0.03*	147.5 ± 9.4	0.06	4
10	6.4 ± 0.4	0.99	147.1 ± 19.7	0.06	4

Previous competition binding assays with VU0409551 showed that VU0409551 binds to the same well-characterised allosteric pocket as the $mGlu_5$ NAM MPEP (Conde-Ceide et al., 2015). To confirm this, a competition binding assay was carried out with the [^{3}H]M-MPEP radioligand in membranes prepared from Flp-In $mGlu_5$ cells and in wild-type mouse brain tissue (Figure 3-14). VU0409551 fully displaced this radioligand, suggesting an interaction with the MPEP binding site. A two-site model fit these data more accurately as the curve of the data was biphasic. This gave a pK_{iHigh} of 11.8 ± 0.2 and a pK_{iLow} of 4.9 ± 0.6 in the Flp-In $mGlu_5$ cells, a pK_{iHigh} of 9.2 ± 0.1 and a pK_{iLow} of 6.1 ± 0.1 in the wild-type mouse cortex, and a pK_{iHigh} of 8.3 ± 0.4 and a pK_{iLow} of 6.4 ± 0.3 in the wild-type mouse hippocampus. This may suggest that VU0409551 binds to an additional site or multiple conformations of $mGlu_5$ (i.e., active vs resting states).

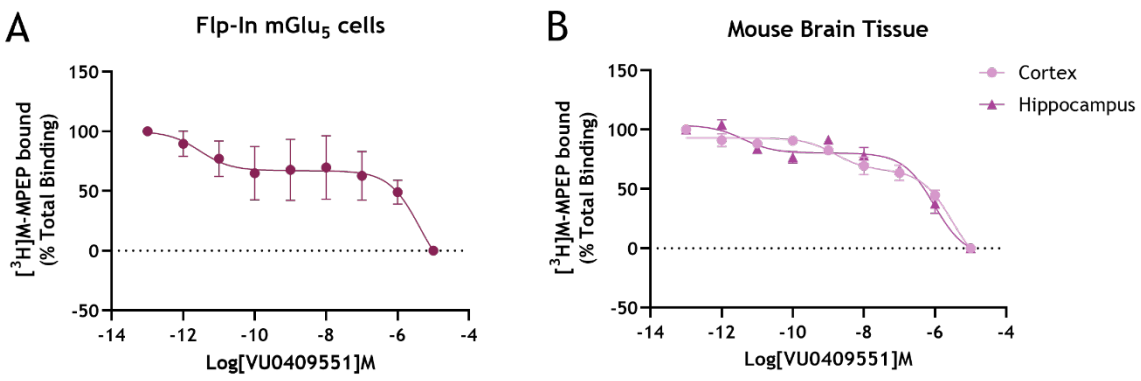

Figure 3-14 Confirmation of VU0409551 mGlu$_5$ binding site. Competition binding curves for VU0409551 in (A) Flp-In mGlu$_5$ cells induced with 100 ng/ml doxycycline and (B) mouse brain tissue (cortex and hippocampus). Membranes (5 µg, Flp-In mGlu$_5$ cells; 30 µg mouse brain tissue) were incubated for 90 mins with 4 nM [^{3}H]M-MPEP and increasing concentrations of VU0409551. Non-specific binding was defined by 1 µM HTL0011867/mavoglurant. Data shown are means ± S.E.M. from 2 (hippocampus) or 3 (Flp-In mGlu$_5$ cells and cortex) separate experiments, each performed in triplicate (n=2-3). Data were normalised to total binding and fit using a two-site model on GraphPad Prism 9.3.

3.2.7 Characterisation of a mGlu$_5$ NAM, VU0424238

To characterise the effect of VU0424238 on mGlu$_5$ signalling *in vitro*, an IP1 assay was initially carried out in Flp-In mGlu$_5$ cells. Increasing concentrations of VU0424238 were added 10 minutes before the addition of the glutamate concentration response curve. With increasing concentrations of VU0424238, a decrease in the maximal response of Flp-In mGlu$_5$ cells to glutamate was observed (Figure 3-15A), becoming significant at 1 and 10 µM VU0424238 (P=0.03 and P=0.001, respectively) (Table 3-7). Interestingly, treatment with VU0424238 was observed to reduce the basal activity of mGlu$_5$ in the absence of an agonist, as shown by a reduction in basal IP1, suggesting that it may function as an inverse agonist.

To study the effect of VU0424238 in a native system, an IP1 assay was conducted in mouse primary cortical astrocytes. As expected from the previously described IP1 accumulation data in Flp-In mGlu$_5$ cells, VU0424238 reduced the maximal response of primary cortical astrocytes to glutamate, similarly becoming significant at 1 and 10 µM VU0424238 (P=0.01 and P=0.0004 respectively) (Figure 3-15B; Table 3-7). Unlike the response in the Flp-In mGlu$_5$ cells, VU0424238 did not reduce the basal IP1 response in mouse cortical astrocytes.

In a Ca^{2+} mobilisation assay, the addition of high concentrations of VU0424238 (0.1, 1 and 10 μM) significantly inhibited the glutamate-induced Ca^{2+} response in Flp-in $mGlu_5$ cells (P = 0.04, P = 0.0007, and P = 0.0007, respectively) (Figure 3-15C; Table 3-8). Lower concentrations of VU0424238 (0.001 and 0.01 μM) did not significantly affect the maximal response of these cells to glutamate. There was no significant change in potency after VU0424238 addition.

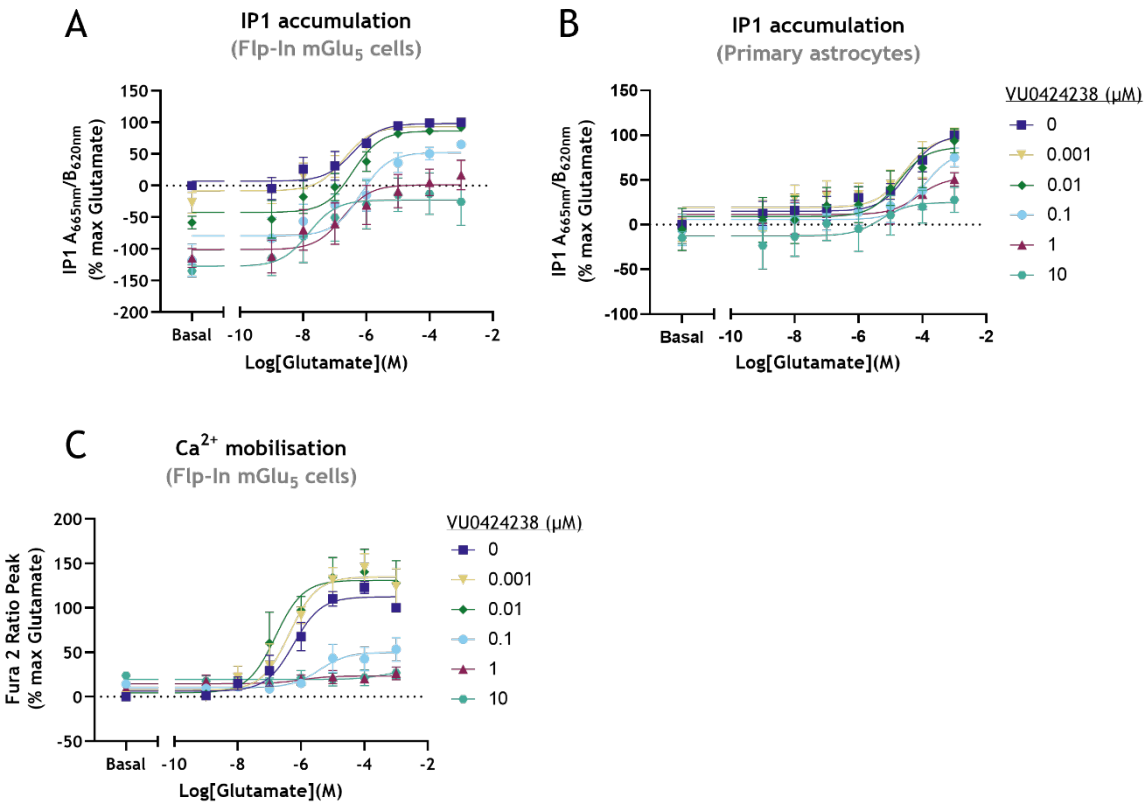

Figure 3-15 Molecular pharmacological profile of VU0424238. (A and B) Concentration response curve showing IP1 accumulation in (A) Flp-In $mGlu_5$ cells (induced with 2 ng/ml doxycycline overnight) and (B) mouse primary cortical astrocytes (4 days after the addition of G5 supplement). Cells had 1 hour of stimulation with increasing concentrations of glutamate. Cells were treated with increasing concentrations of VU0424238 (0-10 μM) for 10 minutes before the addition of glutamate. Data shown are means ± S.E.M. from 3 (Flp-In $mGlu_5$ cells) or 4 (primary astrocytes) separate experiments in duplicate or triplicate. (C) Concentration response curve showing Ca^{2+} mobilisation in Flp-In cells (induced with 2 ng/ml doxycycline overnight) after glutamate addition. Cells were pre-treated with increasing concentrations of VU0424238 (0-10 μM) before the addition of glutamate. Data shown are means ± S.E.M. from 5-7 (Flp-In $mGlu_5$ cells) or 3 (primary astrocytes) separate experiments, each performed in triplicate or duplicate (n=3-7). IP1 accumulation and Ca^{2+} mobilisation data were analysed using a log (agonist) vs response (three parameters) analysis of non-linear regression using GraphPad Prism 9.3.

Table 3-7 Effect of the $mGlu_5$ NAM VU0424238 on agonist-induced IP1 accumulation in Flp-In $mGlu_5$ cells and mouse primary cortical astrocytes. Potency (pEC_{50}) and efficacy (E_{max}) indicators for increasing concentrations of VU0424238 as compared to control (0 μM VU0424238), derived from Figure 3-15A-B. E_{max} was calculated as % of control (0 μM VU0424238). Statistical analysis performed was an ordinary one-way ANOVA (Dunnett's multiple comparisons) with comparison to 0 μM VU0424238, where * P≤0.05, ** P≤0.01, and *** P≤0.001.

	IP1 accumulation									
	Flp-In $mGlu_5$ cells					Primary astrocytes				
VU0424238 conc. (μM)	pEC_{50} (Log[M]) Mean ± S.E.M.	*P*	E_{max} (%) Mean ± S.E.M.	*P*	*n*	pEC_{50} (Log[M]) Mean ± S.E.M.	*P*	E_{max} (%) Mean ± S.E.M.	*P*	*n*
0	7.1 ± 0.6	-	100.0 ± 0.0	-	3	4.4 ± 0.5	-	100.0 ± 0.0	-	4
0.001	7.2 ± 0.7	>0.99	99.7 ± 2.3	>0.99	3	4.5 ± 0.6	>0.99	101.3 ± 13.7	0.99	4
0.01	7.0 ± 0.8	0.99	91.9 ± 5.7	0.99	3	5.0 ± 1.0	0.98	93.6 ± 27.3	0.99	4
0.1	6.6 ± 0.6	0.99	65.1 ± 5.8	0.55	3	5.6 ± 2.2	0.80	75.0 ± 21.2	0.30	4
1	6.8 ± 0.8	0.99	16.5 ± 23.3	0.03 *	3	7.8 ± 2.8	0.66	50.5 ± 15.2	0.01 *	4
10	7.8 ± 0.6	0.92	25.8 ± 37.1	0.001 **	3	7.0 ± 1.6	0.12	27.9 ± 28.1	0.0004 ***	4

Table 3-8 Effect of the $mGlu_5$ NAM VU0424238 on agonist-induced Ca^{2+} mobilisation in Flp-In $mGlu_5$ cells. Potency (pEC_{50}) and efficacy (E_{max}) indicators for increasing concentrations of VU0424238 as compared to control (0 μM VU0424238), derived from Figure 3-15C. E_{max} calculated as % of control (0 μM VU0424238). Statistical analysis performed was an ordinary one-way ANOVA (Dunnett's multiple comparisons) with comparison to 0 μM VU0424238, where *P≤0.05, and *** P≤0.001.

	Ca^{2+} mobilisation				
VU0409551 conc. (μM)	pEC_{50} (Log[M]) Mean ± S.E.M.	*P*	E_{max} (%) Mean ± S.E.M.	*P*	*n*
0	6.4 ± 0.3	-	100.0 ± 0.0	-	7
0.001	6.7 ± 0.3	0.99	124.2 ± 20.0	0.58	5
0.01	6.9 ± 0.4	0.99	127.6 ± 25.5	0.46	5
0.1	4.8 ± 0.4	0.50	53.2 ± 13.2	0.04 *	7
1	7.4 ± 1.5	0.81	26.4 ± 7.1	0.0007 ***	7
10	5.9 ± 0.7	0.99	27.0 ± 6.6	0.0007 ***	7

To confirm whether VU0424238 interacts with the MPEP binding site as reported in the literature (Felts et al., 2017), a competition binding assay was carried out with the [^{3}H]M-MPEP radioligand in membranes prepared from Flp-In mGlu$_5$ cells and wild-type mouse brain tissue (Figure 3-16). The data were fit with a one-site model and confirmed the interaction of VU0424238 with this binding site (pK_i = 9.1 ± 0.5 in the Flp-In mGlu$_5$ cells, 8.9 ± 0.4 in mouse cortex, and 8.8 ± 0.1 in mouse hippocampus).

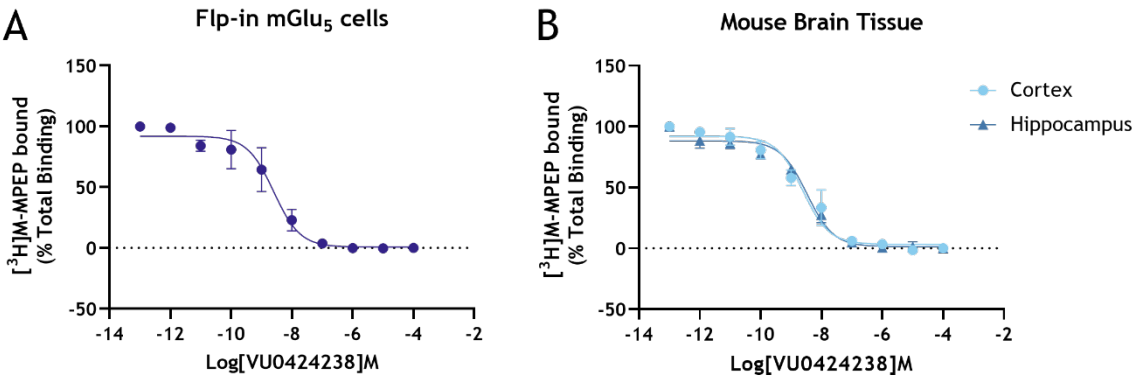

Figure 3-16 Confirmation of VU0424238 mGlu$_5$ binding site. Competition binding curves of VU0424238 in (A) Flp-In mGlu$_5$ cells induced with 100 ng/ml doxycycline and (B) mouse brain tissue (cortex and hippocampus). Membranes (5 µg, Flp-In mGlu$_5$ cells; 30 µg mouse brain tissue) were incubated for 90 mins with 4 nM [^{3}H]M-MPEP and increasing concentrations of VU0424238. Non-specific binding was defined by 1 µM HTL0011867/mavoglurant. Data shown are means ± S.E.M. from 2 (hippocampus) or 3 (Flp-In mGlu$_5$ cells and cortex) separate experiments in triplicate. Data were normalised to total binding and fit using a one-site model on GraphPad Prism 9.3.

It is well known that mice will bury foreign objects, such as marbles, in deep bedding. This behaviour is representative of the repetitive behaviour associated with obsessive-compulsive disorder (Thomas et al., 2009) and can be inhibited by multiple mGlu$_5$ NAMs (Nicolas et al., 2006). A marble burying experiment was used to assess the *in vivo* efficacy of VU0424238, as compared to the mGlu$_5$ NAM MTEP, in reducing anxiety-related behaviour in wild-type mice (experiments performed by SJ Bradley) (Figure 3-17). Mice were given an intraperitoneal dose of either vehicle (10 % tween-80 vehicle) or varying concentrations of VU0424238 30 minutes prior to the experiment. Both MTEP and VU0424238 were found to dose-dependently inhibit marble-burying behaviour in wild-type mice (Figure 3-17A-B), with 10 mg/kg VU0424328 completely inhibiting marble-burying behaviour (Figure 3-17C). Locomotion was controlled for, and VU0424238 was found to have no effect on locomotor activity (data not shown).

Therefore, 10 mg/kg VU0424238 was used for subsequent experiments, including the *in vivo* dosing experiments in Chapter 4.

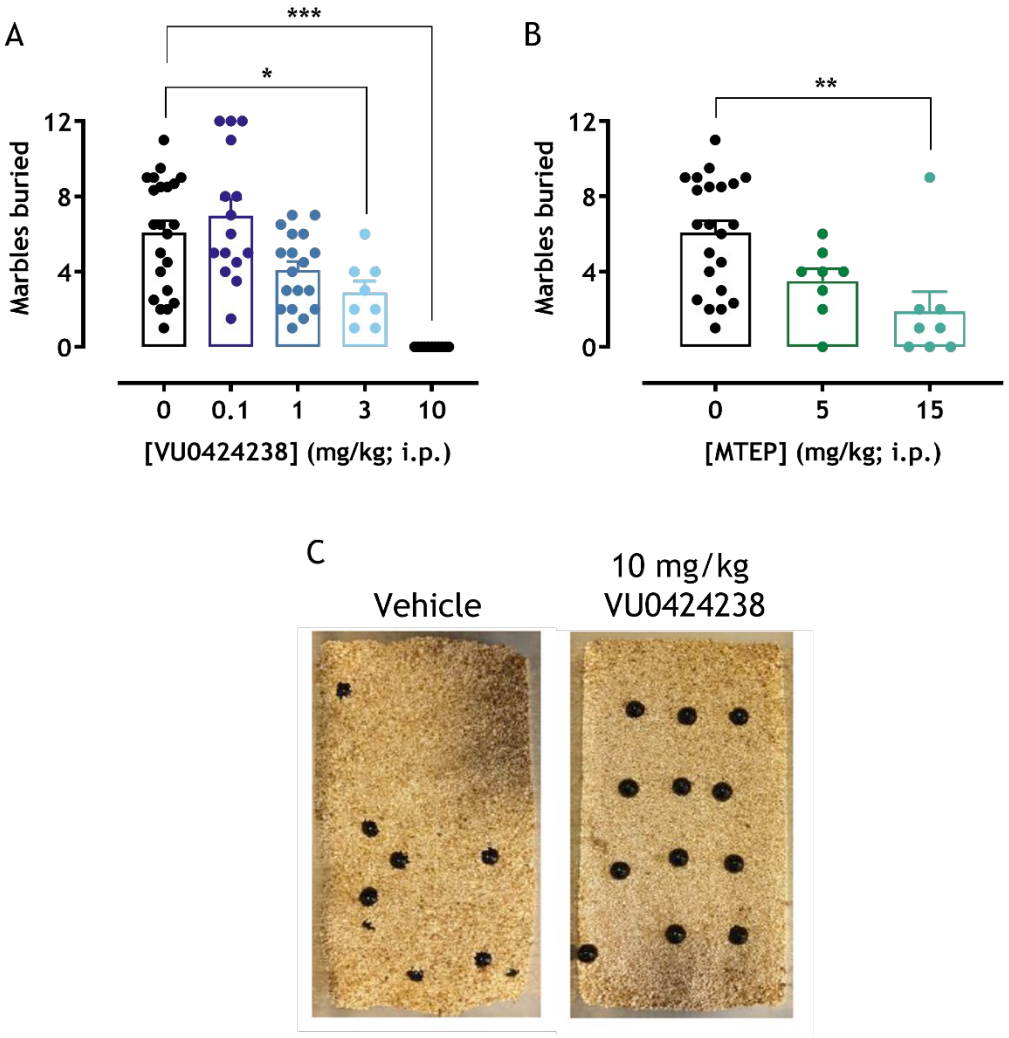

Figure 3-17 VU0424238 dose-dependently inhibits marble-burying behaviour in wild-type mice. Mice were given an intraperitoneal injection of vehicle (10% tween-80) or either MTEP or VU0424238 (increasing concentrations) 30 minutes prior to the marble burying experiment. Both VU0424238 (A) and MTEP (B) dose-dependently decreased marble-burying behaviour. Data are shown as means ± S.E.M., with points representing individual mice (n=8-22). Statistical analysis performed was an ordinary one-way ANOVA (Dunnett's multiple comparisons) with comparison to vehicle-treated mice, where * P≤0.05, ** * P≤0.01, and *** P≤0.001. (C) Glass marbles were placed in a regular pattern on the surface of 5-10 cm deep cage bedding. Animals were placed in the cage for 1 hour, and the number of marbles buried counted. VU0424238 completely inhibited marble-burying behaviour at a concentration of 10 mg/kg. The experiments were carried out by SJ Bradley and used with permission.

A tissue homogenate filtration-based receptor occupancy assay was used to confirm the target engagement of VU0424238 in the cortex and hippocampus of mice. This method relies on labelling the receptor with a radioligand, in this case [^{3}H]M-MPEP, and measuring the reduction in specific binding that results from the receptor occupancy by the dosed compound. Mice were dosed intraperitoneally with vehicle (10% Tween-80) or 10 mg/kg VU0424238 30 minutes prior to sacrifice. By comparing the levels of specific [^{3}H]M-MPEP binding, receptor occupancy was found to be 80 ± 15% in the cortex and 67 ± 15% in the hippocampus (Figure 3-18). This result is comparable to the maximum VU0424238 receptor occupancy observed using PET imaging in rats, which was 80% at 10mg/kg (Felts et al., 2017).

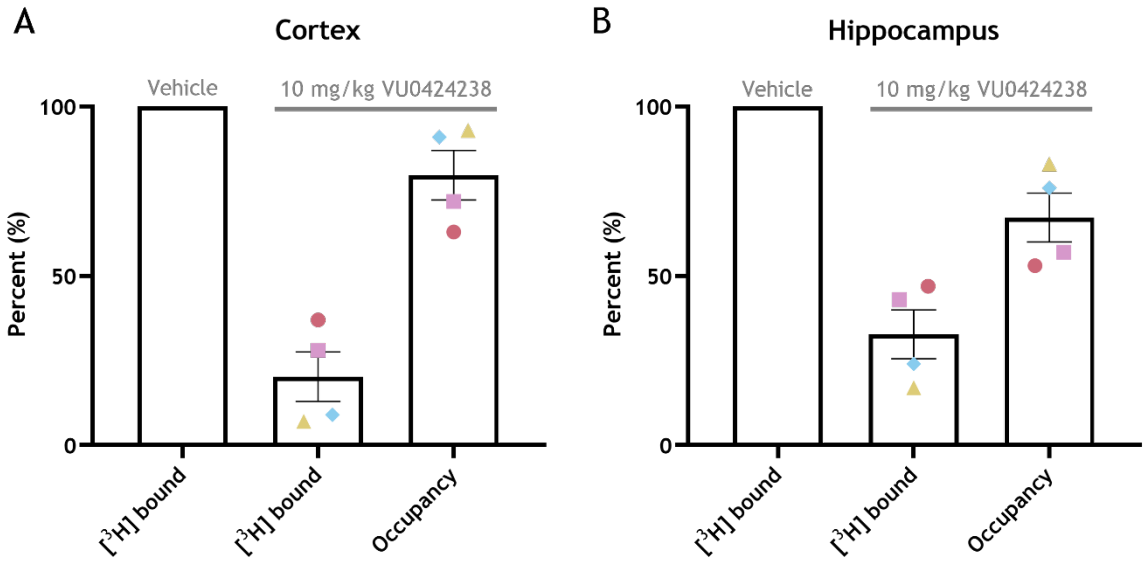

Figure 3-18 *Ex vivo* receptor occupancy assay for VU0424238. mGlu$_5$ receptor occupancy in the (A) cortex and (B) hippocampus of mice injected intraperitoneally with 10 mg/kg VU0424238 30 mins prior to sacrifice, as compared to mice injected intraperitoneally with vehicle (10% Tween-80) 30 mins prior to sacrifice (n=4, each animal is a different colour/shape, the box represents mean, bars represent S.E.M.). Crude brain homogenate (~200-400 µg) was incubated for 10 mins at 4˚C with 66 nM [^{3}H]M-MPEP. Non-specific binding was defined using 10 µM MPEP. Data were read using a Hidex Liquid Scintillation Counter on a standard tritium binding protocol. Receptor occupancy was calculated by subtracting the [^{3}H]M-MPEP bound after VU0424238 dosing from [^{3}H]M-MPEP bound after vehicle dosing.

3.3 Discussion

Initially, this chapter described the characterisation of a stable cell line with inducible expression of $mGlu_5$, which was found to be an appropriate model for measuring acute functional responses to $mGlu_5$ ligands. Maintaining $mGlu_5$ receptors stably expressed in a cell line can be problematic. This is due, in part, to the breakdown of glutamine to glutamate in tissue culture media as well as the secretion of glutamate from cells into the medium, which persistently activates mGlu receptors (Desai et al., 1995). In order to reduce receptor desensitisation, it is possible to remove glutamate in the media by co-expressing a glutamate transporter in the cells (Desai et al., 1995). Others have used a *lac*-repression system to circumvent receptor desensitisation, which uses isopropyl ß-D-1-thiogalactopyranoside (IPTG) to induce receptor expression (Hermans et al., 2002). An ecdysone-inducible expression system has also been used to express mGlu receptors in an inducible manner (Downey et al., 2005); however, ecdysone homologs have been found to alter protein activity in cell culture experiments, including activation of the P13K/Akt pathway (Constantino et al., 2001; Oehme et al., 2006). In this chapter, the stable and inducible expression of $mGlu_5$ was obtained in HEK293 cells using the Flp-In™ T-REx™ system. Immunoblot analysis showed that the administration of doxycycline to the cell medium resulted in $mGlu_5$ receptor expression. By varying the concentration of doxycycline added, the level of receptor expression was able to be controlled, with higher concentrations of doxycycline leading to higher $mGlu_5$ expression. The ability to maintain $mGlu_5$ expression at very low levels during growth and then induce receptor expression at the desired level with the addition of doxycycline prevents prolonged activation of the receptor by endogenous glutamate. In addition to using an inducible cell line, excess glutamate was removed from the medium during experiments with the addition of glutamate pyruvate transaminase (GPT) and sodium pyruvate to the assay media. GPT is a highly active glutamate-degrading enzyme that requires pyruvate as a co-substrate (Matthews et al., 2002). The reversible reaction that GPT catalyses produces α-ketoglutarate and alanine. Elevated alanine levels increase steady-state glutamate levels by raising the equilibrium concentration of the GPT reaction. Therefore, sodium pyruvate is added to compensate for this by increasing pyruvate concentrations (Matthews et al., 2002).

Although using the Flp-In™ T-REx™ system provides many benefits in the study of $mGlu_5$ receptor expression, it is not without disadvantages. Functional IP1 accumulation and Ca^{2+} mobilisation assays showed a response of Flp-in $mGlu_5$ cells to glutamate in cells that had not been induced with doxycycline. This problem has also been reported in other tetracycline-controlled systems (Meyer-Ficca et al., 2004; Mizuguchi & Hayakawa, 2001) and may be due to factors such as intrinsic promotor activity (Johansen et al., 2002). Moreover, an IP1 accumulation assay with Flp-In parental cells showed that these cells also responded to glutamate. This response was variable and less efficacious than the response of $mGlu_5$-expressing cells. Microarray analysis of mRNA levels in HEK293 cells has shown that they do not endogenously express glutamate receptors at a significant level, although mRNA was detectable for $mGlu_2$, $mGlu_4$, $mGlu_6$, $mGlu_7$, and $mGlu_8$ receptors (Atwood et al., 2011). A similar experiment would have confirmed whether these receptors were endogenously expressed in the cells used in this thesis. Although mRNA expression levels do not necessarily mean that the specific functional protein is produced in the cell, it should be kept in mind that the potential low expression of other mGlu receptors in these cells may affect the interpretation of the results of the studies discussed here.

Despite these limitations, Flp-in $mGlu_5$ cells were shown to have robust $mGlu_5$ expression and signalling after the addition of doxycycline to the media. This suggests that the Flp-In™ T-REx™ system is suitable for functional $mGlu_5$ receptor expression and characterisation and, thus, a reasonable tool for studying the signalling properties of $mGlu_5$ ligands.

This chapter also aimed to establish a mouse primary cortical astrocyte culture in the laboratory in order to provide a more physiologically relevant model in which to characterise $mGlu_5$ ligands. Initially, the mouse primary cortical astrocyte protocol was optimised in order to ensure astrocyte growth and $mGlu_5$ expression. Firstly, the effect of pre-treatment with a growth factor supplement, G5, on the growth and morphology of mouse primary cortical astrocytes was investigated. G5 is commonly added to cell cultures to promote the growth of primary astrocytes (Michler-Stuke et al., 1984). Of its components, FGF, EGF and insulin are known to act as growth and differentiation stimulants in astrocytes (Spina Purrello et al., 2002; Zelenaia et al., 2000). After the

removal of unwanted cells by overnight shaking, the addition of G5 supplement supported the growth of primary astrocytes into a branched, star-like morphology, while astrocytes grown without G5 supplement remained small and undefined. In addition to changes in morphology, G5 supplement was shown to increase $mGlu_5$ expression in a time-dependent manner. The expression of $mGlu_5$ in these cells confirmed previous reports of $mGlu_5$ expression on astrocytes. In astrocytes cultured from rodent tissue, $mGlu_5$ has been observed in cells isolated from the cortex, hippocampus, tegmentum, thalamus, and striatum (Biber et al., 1999; Silva et al., 1999). In addition, previous reports show the upregulation of $mGlu_5$ in rat primary cortical astrocytes after the addition of growth factors to the medium (Nakahara et al., 1997).

In NDDs, astrocytes transition from a resting state to a reactive state (Escartin et al., 2021). Reactive astrocytes have an altered morphology, with their processes thickening and stretching towards sites of injury or pathology (Schiweck et al., 2018). It has been suggested that astrocytes cultured using the protocol in this thesis are more similar to reactive astrocytes than normal, resting astrocytes (Foo et al., 2011). This protocol involves maintaining cells in media containing fetal bovine serum (FBS). Serum components are typically excluded from the CNS due to the blood brain barrier, and, therefore, the culture of astrocytes in serum-containing media could be considered non-physiological (Foo et al., 2011). Exposure of astrocytes to serum alters astrocyte morphology in a way that's similar to activated astrocytes. Moreover, growth factors have been shown to mediate the morphological changes observed in reactive astrocytes (Kang et al., 2014). The gene profile of astrocytes cultured in serum-containing medium differs from the genes profile of resting astrocytes *in vivo* (Cahoy et al., 2008; Foo et al., 2011) and instead represent a mixture of developing and reactive astrocyte gene profiles (Foo et al., 2011; Zamanian et al., 2012).

In addition, reactive astrocytes have been shown to have upregulated $mGlu_5$ expression, similar to the astrocytes in this chapter after treatment with growth factors. In primary astrocytes treated with amyloid-ß oligomers, $mGlu_5$ was found to be upregulated at both the mRNA and protein level (Lim et al., 2013; Shrivastava et al., 2013). Immunohistochemistry performed on brain slices from a mouse AD model showed strong $mGlu_5$ immunoreactivity in the astrocytes

surrounding amyloid-β plaques (Shrivastava et al., 2013). Similar results have been observed in models of ALS (Anneser et al., 2004; Vermeiren et al., 2006) and multiple sclerosis (Fulmer et al., 2014). The analysis of post-mortem tissue from human patients has supported these findings, showing an increase in astrocytic $mGlu_5$ in and around areas of disease pathology (Anneser et al., 2004; Aronica et al., 2001; Casley et al., 2009; Lim et al., 2013; Newcombe et al., 2008).

The results shown in this chapter confirmed that $mGlu_5$ was able to signal via $G\alpha_{q/11}$ in mouse primary cortical astrocytes in both Ca^{2+} mobilisation and IP1 accumulation assays. Both agonists, glutamate and DHPG, produced Ca^{2+} mobilisation and IP1 accumulation in astrocytes in a concentration-dependent manner. This signalling was reduced in astrocytes grown without G5 supplement, significantly in the Ca^{2+} mobilisation assays. The data in this chapter showed a very similar response to both DHPG and glutamate in primary astrocytes. Glutamate is a ligand for multiple glutamate receptors, and DHPG is a non-selective group I mGlu agonist that can activate $G\alpha_{q/11}$ signalling *via* both $mGlu_1$ and $mGlu_5$. It is well established that primary astrocytes express $mGlu_1$, $mGlu_3$, and $mGlu_5$, with $mGlu_5$ being the predominant mGlu receptor (Loane et al., 2012). Thus, it is likely that the signalling observed in primary astrocytes after the addition of glutamate or DHPG is not due to $mGlu_5$ signalling alone and most likely also includes some level of $mGlu_1$ signalling.

The final aim of this chapter was to characterise a negative and positive allosteric modulator of $mGlu_5$ in the two cell types discussed. The first compound characterised was VU0409551. The data presented in this chapter found VU0409551 to be a positive allosteric modulator, with data from Ca^{2+} mobilisation assays suggesting that this compound can act as a PAM-agonist (i.e., a PAM with agonist activity). In an IP1 assay, the addition of 10 μM VU0409551 caused an approximately 40-fold shift of the glutamate concentration response curve. Similar responses have been observed previously in HEK293 cells expressing either human or rat $mGlu_5$ (Conde-Ceide et al., 2015; Rook et al., 2015). In a Ca^{2+} mobilisation assay, the effect of VU0409551 on glutamate potency was similar to what has been reported in the literature (6.4 ± 0.4 here compared to 6.6 ± 0.0 at both human and rat $mGlu_5$ at a concentration of 10 μM)

(Conde-Ceide et al., 2015; Rook et al., 2015). A key difference between the Ca^{2+} mobilisation data shown here as compared to the literature is the increase in the basal response at the highest concentrations of VU0409551 tested, which suggests that VU0409551 has agonist activity. Rook et al. (2015) found that VU0409551 had no intrinsic agonist activity in a Ca^{2+} mobilisation assay and instead found it to display pure PAM activity. They argued that if agonist activity was observed in a Ca^{2+} mobilisation assay, this might play a key role in contributing to the adverse effects of $mGlu_5$ PAMs observed *in vivo*. Therefore, they proposed that the lack of agonist activity observed in their data set for VU0409551 may be one of the reasons VU0409551 is a potentially successful therapeutic candidate. The experiments in this thesis were carried out in Flp-In cells expressing mouse $mGlu_5$, whereas the comparative studies in the literature were carried out in HEK293 cells expressing human (Conde-Ceide et al., 2015) or rat (Rook et al., 2015) $mGlu_5$. It is important to note that there can be species differences in the PAM-induced activation of pathways downstream of $mGlu_5$ (Conn et al., 2014), which may be a reason for the differences observed in this thesis chapter and the published literature. This highlights the importance of characterising ligands in multiple assays and in multiple species.

The data presented in this chapter confirmed that VU0424238 acts as a NAM in IP1 accumulation assays in both Flp-In $mGlu_5$ cells and mouse primary cortical astrocytes, where it was observed to significantly reduce the maximum effect of glutamate. In addition, VU0424238 acted as a NAM in a Ca^{2+} mobilisation assay in Flp-In $mGlu_5$ cells, significantly reducing the maximum response of the cells to glutamate at the three highest concentrations tested. By contrast to previously published data on this compound (Felts et al., 2017), the data presented here found VU0424238 to display inverse agonist activity in Flp-In $mGlu_5$ cells, reducing basal receptor activity in the IP1 accumulation assay. MPEP and fenobam, two other $mGlu_5$ NAMs, have previously been shown to act as inverse agonists (Pagano et al., 2000; Porter et al., 2005), but this observation has not been seen previously for VU0424238 (Felts et al., 2017).

In the literature, VU0424238 has been shown to bind to the MPEP allosteric binding site in membranes prepared from HEK293 cells expressing rat $mGlu_5$ (Felts et al., 2017), which was confirmed here in membranes prepared from

Flp-In cells expressing mouse $mGlu_5$ and wild-type mouse brain. Using an *ex vivo* receptor occupancy assay in mice dosed intraperitoneally with 10 mg/kg VU0424238, receptor occupancy was found to be ~80% in the cortex and ~67% in the hippocampus. This result is similar to the maximum receptor occupancy of 80% at 10 mg/kg in the brains of rats orally dosed with VU0424238 for 30 minutes prior to intravenous dosing of a radioligand and 1 hour of PET imaging (Felts et al., 2017). This receptor occupancy data highlights occupancy 30 minutes after intraperitoneal injection of VU0424238. Previous pharmacokinetic studies have shown that at a concentration of 10 mg/kg, clearance of VU0424238 occurred at a rate of 19.3 ml/min/kg when given as an intravenous injection to rats (Felts et al., 2017). In Chapter 4, mice were given injections of VU0424238 daily in order to maintain a receptor occupancy as close to maximum occupancy as possible. Data from the Bradley lab found complete inhibition of marble-burying behaviour in wild-type mice at 10 mg/kg VU0424238, suggesting that this concentration is highly efficacious *in vivo*. The efficacy of VU0424238 in other rodent models is discussed in more depth in Chapter 4 (see 4.1.3).

3.4 Conclusion

In conclusion, the data presented in this chapter characterised $mGlu_5$ receptor expression and signalling in Flp-In $mGlu_5$ cells and mouse primary cortical astrocytes. Moreover, it characterised two $mGlu_5$ allosteric modulators in these cell lines. VU0409551 was observed to be a positive allosteric modulator that binds to the MPEP binding site and exerts agonist activity. VU0424238 was observed to be a NAM, that binds to the same MPEP binding site, and displays inverse agonist activity. Moreover, VU0424238 was found to occupy $mGlu_5$ receptors in the brain at high levels. As the pharmacological blockade of $mGlu_5$ with NAMs has been shown to be neuroprotective in rodent models of neurodegenerative disease, improving cognition and reducing disease pathology (Budgett et al., 2022), the next chapter of this thesis will set out to investigate the effect of chronic VU0424238 treatment on the progression of biochemical and behavioural changes associated with neurodegenerative disease as well as the survival of terminally sick mice.

Chapter 4 Defining the Impact of Targeting $mGlu_5$ in a Model of Neurodegenerative Disease

4.1 Introduction

The challenge of translating the results from preclinical studies in animals into human clinical trials is a major obstacle in the development of effective treatments for human NDDs (see section 1.5). No one animal disease model fully replicates human neurodegeneration; therefore, it is important to test potential drug candidates across various preclinical models of disease to fully validate any disease-modifying effects (LaFerla & Green, 2012; Selkoe, 2011). A model of murine prion disease has been used as a reliable model to test the effect of novel ligands on terminal neurodegeneration (see 1.5.2) (Bradley et al., 2016; Dwomoh et al., 2022). Initially, this chapter aims to validate the neuroinflammatory response observed in this model. As discussed in section 1.3, $mGlu_5$ has been proposed as a potential therapeutic target for treating several NDDs. Therefore, this chapter also characterises the expression profile of $mGlu_5$ in murine prion disease and investigates the impact of the pharmacological inhibition of $mGlu_5$ on inflammatory processes and disease progression.

4.1.1 Expression of $mGlu_5$ in NDDs

As highlighted in section 1.2.3, $mGlu_5$ is predominantly localised on the postsynaptic membrane of glutamatergic neurons found in the cerebral cortex, olfactory bulb, striatum, hippocampus, basal ganglia, and spinal cord (Shigemoto et al., 1993, 1997; Luján et al., 1996; Valerio et al., 1997; Wong et al., 2013). It is also expressed in glial cells, including astrocytes and microglia (Loane et al., 2012). PET imaging studies have shown that the expression of $mGlu_5$ in the human brain declines with age, although this is largely due to grey matter atrophy (Mecca et al., 2021). In rodents, PET imaging found $mGlu_5$ expression to be consistent throughout ageing in mice, whereas immunoblotting suggested that $mGlu_5$ expression decreases with age (Fang et al., 2017). Similarly, the expression of $mGlu_5$ was found to be significantly reduced in the medial prefrontal cortex of aged rats (22 months) as compared to young rats (4 months) at both the protein and mRNA levels (Hernandez et al., 2018). Interestingly, in a study where rats were categorised as either memory-impaired or memory-unimpaired based on Morris water maze data, old rats (24 months) with impaired memory had a significant reduction in $mGlu_5$ expression in the CA1 hippocampal region as compared to both old rats with unimpaired memory and

young rats (6 months) (Ménard & Quirion, 2012). This suggests a complex relationship between $mGlu_5$ expression, age, and memory.

Studies investigating $mGlu_5$ expression in human NDD have found its expression to be altered in diseased individuals compared with healthy controls. For example, PET imaging in human AD patients showed that $mGlu_5$ expression is significantly reduced in the hippocampus and amygdala of patients with mild AD (Mecca et al., 2020; Treyer et al., 2020). This is in agreement with PET imaging in the 5xFAD AD mouse model mice which found $mGlu_5$ expression to be reduced in the striatum and hippocampus of diseased mice compared to wild-type mice (Lee et al., 2018). In contrast, however, human post-mortem data found increased $mGlu_5$ expression in the hippocampus and frontal cortex of patients with severe AD (Müller Herde et al., 2019). It is possible that there may be a variation in $mGlu_5$ expression at different stages of AD in humans, with $mGlu_5$ upregulation occurring later in disease. Further longitudinal studies are needed to understand how $mGlu_5$ expression may change throughout the course of human AD.

An increase in $mGlu_5$ present at the cell surface, without an increase in total $mGlu_5$ expression levels, has been found in several rodent AD models (Abd-Elrahman et al., 2018; Hamilton et al., 2014; Um et al., 2013). This may be due to the Aβo-mediated clustering of $mGlu_5$ (see 1.3.4.1). For example, in APPswe mice, $mGlu_5$ was increased 4.4-fold on the cell surface as compared to control mice, without an alteration in total $mGlu_5$ level (Hamilton et al., 2014). However, another group found that at the same time point in the same model, the expression of $mGlu_5$ on the cell surface was significantly reduced in particular hippocampal cell types, including granule cells in the dentate gyrus and pyramidal cells in the CA1 region (Martín-Belmonte et al., 2021).

Post-mortem studies in human HD tissue have found decreased $mGlu_5$ expression in the putamen and striatum. However, as there were also significant reductions in neuronal density, this observation may be due to neuronal loss (Gulyás et al., 2015). In HD model mice, longitudinal PET imaging studies found reduced $mGlu_5$ expression in the striatum and cortex (Bertoglio et al., 2018). As neuronal density was unaltered in these mice, the observed reduction in $mGlu_5$ expression in diseased mice was assumed to be independent of any neuronal loss.

In ALS, human post-mortem studies found $mGlu_5$ to be upregulated in the frontal, motor, and temporal cortices, and basal ganglia of diseased brains compared to controls (Müller Herde et al., 2019). Similarly, PET imaging, immunoblotting, and IHC found that $mGlu_5$ expression increased in line with disease progression in the hippocampus, striatum, cortex, and spinal cord of ALS model mice (Brownell et al., 2015; Giribaldi et al., 2013).

Astrocytic $mGlu_5$ has been found to be upregulated in and around disease-related lesions in human post-mortem tissue (Aronica et al., 2001; Anneser et al., 2004; Newcombe et al., 2008; Casley et al., 2009; Lim et al., 2013). Similarly, the upregulation of astrocytic $mGlu_5$ has been observed in animal models of several NDDs, including AD (Lim et al., 2013; Shrivastava et al., 2013), ALS (Anneser et al., 2004; Vermeiren et al., 2006), and multiple sclerosis (Fulmer et al., 2014). *In* vitro, $mGlu_5$ is upregulated in cultured primary astrocytes after the addition of AßOs (Casley et al., 2009) and in astrocytes cultured from ALS model rodents (Vermeiren et al., 2006). Furthermore, $mGlu_5$ is upregulated on the activated microglia found surrounding lesions after brain or spinal cord injury in rodents (Byrnes et al., 2009; Drouin-Ouellet et al., 2011).

Previously published immunoblotting data has shown that $mGlu_5$ expression is decreased in the brains of prion-diseased mice and hamsters at the terminal disease endpoint (Hu et al., 2022). There are currently no published longitudinal data investigating $mGlu_5$ expression throughout the progression of murine prion disease; therefore, this chapter aims to investigate $mGlu_5$ expression levels at several time points of disease. Understanding the expression levels of $mGlu_5$ in the context of disease progression is important for gaining insight into the potential function of $mGlu_5$ in murine prion disease and its availability for pharmacological manipulation.

4.1.2 The $mGlu_5$ Receptor and Murine Prion Disease

In this thesis, murine prion disease is used as a model to study terminal neurodegeneration. Two previous studies have examined the potential of $mGlu_5$ antagonism to modulate the progression of murine prion disease. The first study investigated whether $mGlu_5$ knockout mice are susceptible to infection with RML prions (Beraldo et al., 2016). They found that $mGlu_5$ knockout mice did develop

murine prion disease and that the knockout of $mGlu_5$ significantly delayed the onset of symptoms in prion-diseased mice but did not affect their overall survival. In addition, they found that $mGlu_5$ knockout did not alter the levels of total PrP_C or misfolded PrP_{Sc} at the point of death. Missing from their dataset is the level of PrP_{Sc} at the point of symptom onset, which would be valuable data given $mGlu_5$ knockout delayed symptom onset. Moreover, they did not look at any other markers of disease, such as neuroinflammation, in the brains of these mice.

The second study examined the effect of targeting $mGlu_5$ in prion disease both *in vitro* and *in vivo* (Goniotaki et al., 2017). These experiments showed a dose-dependent reduction in neurotoxicity in prion-infected cerebellar organotypic cultured slices (COCS) after treatment with the $mGlu_5$ NAMs MPEP and mavoglurant. Similarly, COCS prepared from homo- or heterozygous $mGlu_5$ knockout mice were protected against prion-induced toxicity. *In vivo,* the oral administration of MPEP to prion-diseased mice significantly delayed the onset of motor deficits on a rotarod test as compared to mice fed a control diet. Moreover, MPEP-treated mice exhibited a small but statistically significant extension in their lifespan as compared to controls. Despite these observations, MPEP treatment did not alter PrP_{Sc} accumulation in the brains of these mice at the point of death. However, vacuole size was reduced across the brain, and astrogliosis was reduced in the hippocampus of MPEP-treated prion-diseased mice as compared to controls. From this data set, the authors concluded that $mGlu_5$ antagonism reduces the toxicity of prions without affecting the total prion load.

Overall, these studies have contributed to our understanding of the role of $mGlu_5$ antagonism in modulating the progression of terminal neurodegeneration and suggest that targeting $mGlu_5$ may be neuroprotective in the context of murine prion disease. This thesis builds on this work by investigating the effect of $mGlu_5$ antagonism using a highly potent $mGlu_5$ NAM, VU0424238, on key disease hallmarks, including PrP_{Sc} accumulation and neuroinflammation, throughout disease progression in both sexes of prion-diseased mice.

4.1.3 Preclinical Studies with the $mGlu_5$ NAM, VU0424238

There are no published data investigating the effect of the $mGlu_5$ NAM VU0424238, characterised in Chapter 3, in models of neurodegeneration. However, this compound has shown efficacy in models of anxiety, depression, and alcohol self-administration (Felts et al., 2017; Holter et al., 2021; Salling et al., 2021). As discussed below, these studies focused on behavioural outcomes and showed improvements in disorder-related behaviour.

An innate species-specific behaviour of mice is that they bury foreign objects, such as glass marbles, in deep bedding. Some researchers use this behaviour as a model for anxiety, although it has been argued that this behaviour may model the repetitive behaviour associated with OCD (Thomas et al., 2009). VU0424238 has been shown to dose-dependently decrease this repetitive behaviour, with complete inhibition at a dose of 30 mg/kg (Felts et al., 2017). As discussed in Chapter 3, our lab found VU0424238 to inhibit this behaviour at a lower dose of 10 mg/kg.

The forced swim test (FST) is an animal model of depression that measures the activity of a rat suspended in a tank of water from which they cannot escape (Slattery & Cryan, 2012). "Depressed" rats are more immobile in the FST, whereas rats treated with antidepressants are more active. VU0424238 dose-dependently reduced the duration of immobility of rats in this test, thus suggesting it may have antidepressant properties (Felts et al., 2017). The antidepressant-like properties of VU0424238 were also investigated with regard to sleep disturbances related to major depressive disorder (MDD) (Holter et al., 2021). MDD patients have a reduction in rapid eye movement (REM) sleep latency and increased REM duration (Armitage, 2007; Steiger & Pawlowski, 2019). VU0424238 was found to increase REM sleep latency and reduce REM duration in rats (Holter et al., 2021), similar to several clinically prescribed antidepressants (Steiger & Pawlowski, 2019).

Finally, the administration of VU0424238 to baboons decreased the trained behaviour of alcohol self-administration in a dose-dependent manner (Salling et al., 2021). Baboons provide a well-established model for drug

self-administration, and the self-administration of alcohol is used as a model of alcohol use disorder (Kaminski et al., 2012).

As VU0424238 is highly selective for $mGlu_5$, highly potent, and orally bioavailable, initial literature suggested that it was an ideal candidate for pharmaceutical development (Felts et al., 2017). Based on those data, methods were developed for its production on a large scale (David et al., 2017). However, the compound failed toxicology studies during preclinical development due to the accumulation of a non-human primate species-specific aldehyde oxidase (AO) metabolite that resulted in anaemia (Crouch et al., 2017). Species differences in the expression of AO present a challenge in translating preclinical animal studies to human clinical trials, and several drug candidates that AO metabolises have previously failed at clinical trial (Crouch et al., 2017). VU0424238 was further optimised to remove the contribution of AO to metabolism, but this resulted in reduced potency (Felts et al., 2019). Although these findings may preclude VU0424238 from being an ideal clinical candidate, it was used as a reliable tool compound in this thesis to investigate the effect of the pharmacological inhibition of $mGlu_5$ on the progression of a terminal neurodegenerative disease.

4.1.4 Sex-specific Differences in the Contribution of $mGlu_5$ to Disease Pathology

The majority of research into the effects of $mGlu_5$ antagonism in mouse models of NDD have used only male mice in their studies. This bias towards the male sex exists across preclinical research (Gogos et al., 2019; Karp & Reavey, 2019). Surprisingly, male bias exists even when the disease of interest is more prevalent in females (Yoon et al., 2014). It is thought that resistance to including female animals in studies is due, in part, to the widely accepted belief that female animals are more variable due to their oestrous cycle (McCarthy, 2015). As individuals belonging to the male or female sex respond differently to disease progression (Yoon et al., 2014) and drug treatment (Anderson, 2005), it is crucial that drugs are tested in both sexes to improve the value of women's health care.

Recent studies have suggested that $mGlu_5$ may not contribute to disease pathology in female AD mice (Abd-Elrahman et al., 2020a). Both male and female APPswe mice display similar levels of Aβos, neuroinflammation, and cognitive decline. However, chronic treatment with the $mGlu_5$ NAM CTEP only reduced disease pathology and improved cognition in male mice. As discussed in section 1.3.4.1, Aβos promote the clustering of $mGlu_5$ receptors at the synapse surface. This increased $mGlu_5$ cell surface expression was observed in male APPswe mice but not in females. Moreover, the Aβ-PrP_C-$mGlu_5$ complex was found to form in the brains of male, and not female, mice. Using radioligand binding assays, the same finding was observed in human brain tissue (Abd-Elrahman et al., 2020a).

Similarly, a recent study investigated the effect of CTEP in male and female *zQ175* HD mice (Li et al., 2022). This study found that chronic CTEP administration improved motor performance at an earlier time point in male mice as compared to females (4 and 12 weeks, respectively). Moreover, male, but not female, mice exhibited improved cognition in a novel object recognition task. Despite differences in behaviour, chronic CTEP administration reduced disease pathology in both sexes, including the aggregation of mHtt and neuronal death.

Differences in the response of male and female mice to $mGlu_5$ treatment have also been observed in the SOD^{G93A} ALS model (Bonifacino et al., 2019; Milanese et al., 2021). The complete knockout of $mGlu_5$ in the SOD^{G93A} model delayed the onset of motor deficits and death in both sexes of ALS mice. Heterozygous knockout of $mGlu_5$ in these mice improved motor symptoms in male mice only (Bonifacino et al., 2019). Surprisingly, when the same group treated SOD^{G93A} mice with CTEP, they found that low doses (2 mg/kg) improved motor skills and survival in female mice only. Increasing the dose of CTEP (4 mg/kg) led to improvements for both sexes, with a more pronounced improvement in female mice (Milanese et al., 2021). Why genetic blockade and pharmacological inhibition of $mGlu_5$ showed sex-specific differences in the responses remains an open question.

In summary, these studies suggest that the contribution of $mGlu_5$ receptors to disease pathology may differ between sexes as well as disease models. This must

be considered when investigating the potential of $mGlu_5$ as a drug target for neurodegenerative diseases. Therefore, the studies in this chapter, as well as Chapter 5, were conducted in both male and female mice where possible.

4.1.5 Aims

The aims of this chapter are to:

1. Confirm the upregulation of neuroinflammatory markers in murine prion disease, thus validating this model for investigating the effects of novel ligands on inflammation.

2. Evaluate the expression profile of $mGlu_5$ throughout the progression of murine prion disease.

3. Define the impact of pharmacologically targeting $mGlu_5$ in murine prion disease, with a focus on neuroinflammation.

4.2 Results

4.2.1 Characterisation of Neuropathological Markers in Murine Prion Disease

A chronic neuroinflammatory response, including astrogliosis, microgliosis, and the release of inflammatory chemokines and cytokines, is a hallmark of many NDDs (see 1.3.2.3) (Liddelow & Barres, 2017). Recent global transcriptomic and proteomic work in our group has found several neuroinflammatory markers, particularly indicators of astrocyte and microglia activation, to be upregulated in murine prion disease (Dwomoh et al., 2022). Here, the expression of the astrocyte markers GFAP and vimentin, the microglia markers CD68 and Iba-1, and several chemokine/cytokine markers were examined in the cortex and hippocampus of prion-diseased mice over the course of disease.

GFAP is an astrocyte-specific intermediate filament protein, and its differential expression is the most commonly used marker for reactive astrocytes (Hol & Pekny, 2015; Escartin et al., 2021). *Gfap* transcript levels were found to be significantly increased at 10 w.p.i. in both the cortex ($P \leq 0.0001$) and hippocampus ($P=0.0004$) of prion-diseased mice (Figure 4-1A). There was no difference in expression level between the cortex and hippocampus. This increase in astrogliosis markers was confirmed using immunohistochemistry (Figure 4-1B), which showed an increase in staining for GFAP and vimentin, another astrocytic intermediate filament (Yamada et al., 1992), in both the cortex and hippocampus at 10 w.p.i.

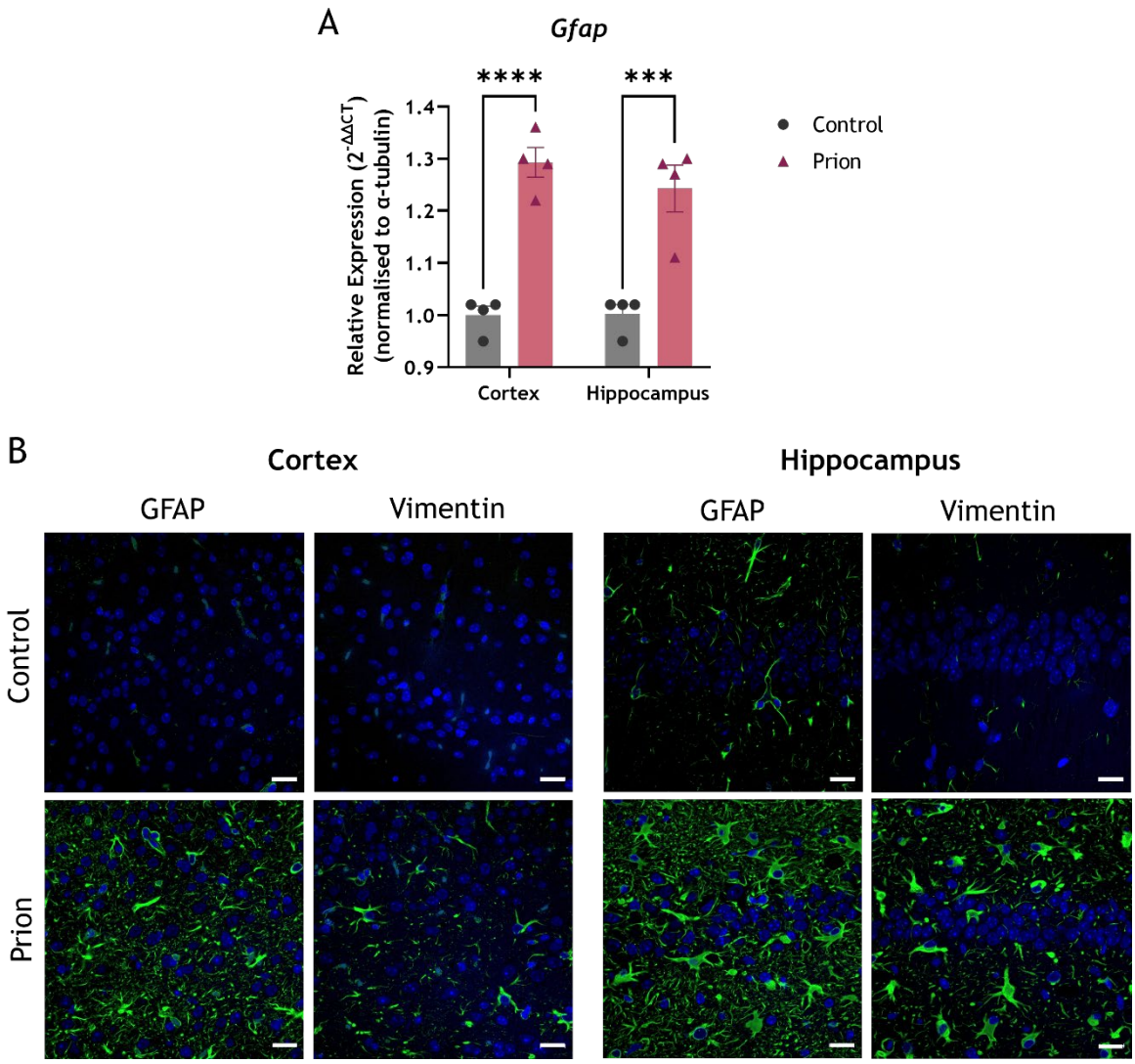

Figure 4-1 A significant increase in astrogliosis is evident in prion-diseased mice at 10 w.p.i. (A) RT-qPCR showing the expression of *Gfap* in the cortex and hippocampus of control or prion-diseased mice at 10 w.p.i. Data are expressed as a ratio of α-tubulin RNA and are shown as means ± S.E.M. and data points represent individual mice. Statistical analysis performed was two-way ANOVA (Tukey's multiple comparisons), where *** P≤0.001 and **** P≤0.0001 (n=4). (B) Immunohistochemical staining for GFAP and vimentin (both green) in the cortex and hippocampus of control and diseased mice. Nuclei were stained with DAPI (blue). Staining was performed on 5 µm thick coronal sections taken from mice at 10 w.p.i. Images shown are representative images from the cortex and CA1 region of the hippocampus (n=3). Images were taken on a Zeiss 880 confocal microscope with 40x objective, scale bar = 20 µM.

In order to investigate changes in astrogliosis throughout disease progression, immunoblotting was carried out on cortical and hippocampal lysates prepared from control and prion-diseased mice at 4 different timepoints (Figure 4-2A). Protein levels of GFAP showed an increasing trend from 10 w.p.i. in the cortex and 8 w.p.i. in the hippocampus as compared to protein levels in control mice (Figure 4-2B). Significant upregulation of GFAP was observed at 11 w.p.i. in both the cortex (6.8-fold, P=0.05) and hippocampus (7.9-fold, P=0.03). Similarly, levels of vimentin showed an increasing trend in the cortex and hippocampus from 8 w.p.i., reaching statistical significance earlier than GFAP expression at 10 w.p.i. in both brain regions (Figure 4-2B). At 10 w.p.i., vimentin was increased 11.8-fold in the cortex (P=0.02) and 11.2-fold in the hippocampus (P=0.02). At 11 w.p.i., vimentin was increased 10.5-fold in the cortex (P=0.02) and 14.3-fold in the hippocampus (P=0.002).

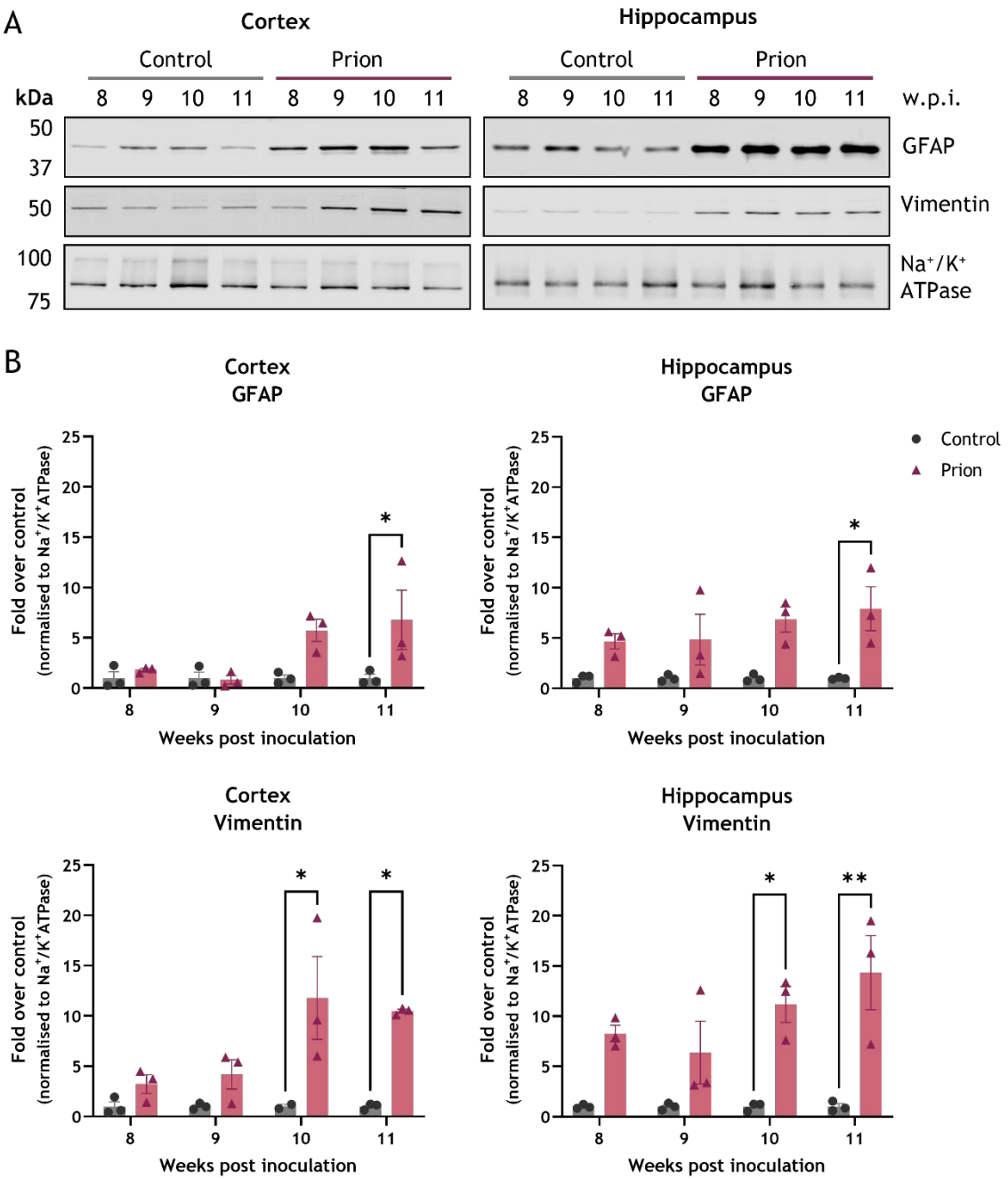

Figure 4-2 The expression of GFAP and vimentin increases in line with the progression of murine prion disease. (A) Astrogliosis was assessed using Western blot analysis on lysates prepared from the cortex or hippocampus of control- or prion-infected mice at 8, 9, 10 and 11 w.p.i. Lysates were probed with antibodies raised against the astrocytic markers GFAP and vimentin. Na^+/K^+ ATPase was used as a loading control. Representative blots are shown (n=3). (B) Protein levels were normalised to the loading control and data is expressed as fold over control. Data shown are means ± S.E.M. with data points representing individual mice (n=3). Statistical analysis was performed using a two-way ANOVA (Tukey's multiple comparisons), where * $P \leq 0.05$ and ** $P \leq 0.01$.

The activation of microglia was initially detected by looking at the transcript levels of *Cd68*, a common marker for activated phagocytic microglia (Walker & Lue, 2015). *Cd68* transcript levels were found to be significantly increased at 10 w.p.i. in both the cortex (P=0.006) and hippocampus (P=0.04) (Figure 4-3A). There was no difference in expression level between the cortex and hippocampus. Immunohistochemical staining using Iba-1, a cytoplasmic microglial protein (Imai et al., 1996), confirmed this increase in microglia in both the cortex and hippocampus of prion-diseased mice (Figure 4-3B).

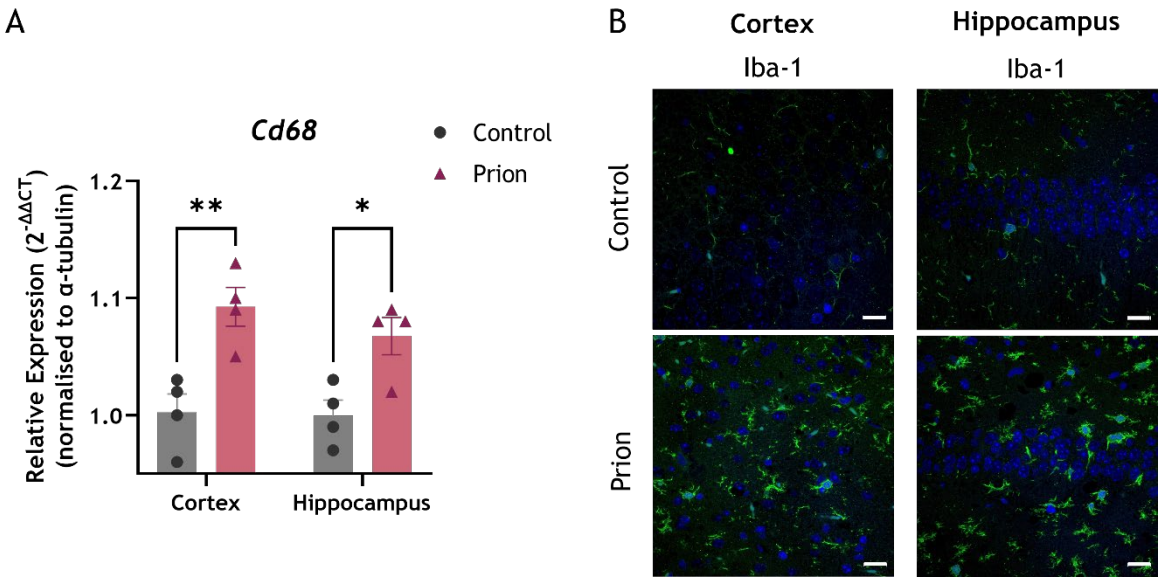

Figure 4-3 A significant increase in microgliosis is evident in prion-diseased mice at 10 w.p.i. (A) RT-qPCR showing the gene expression of *Cd68* in the cortex and hippocampus of control or prion-diseased mice at 10 w.p.i. Data are expressed as a ratio of α-tubulin RNA and are shown as means ± S.E.M. and data points represent individual mice (n=4). Statistical analysis performed was two-way ANOVA (Tukey's multiple comparisons), where * P≤0.05 and ** P≤0.01. (B) Immunohistochemical staining for Iba-1 (green) in the cortex and hippocampus of control and diseased mice, with DAPI staining for nuclei (blue). Staining was performed on 5 µm thick coronal sections at 10 w.p.i. Images shown are representative images from the cortex and CA1 region of the hippocampus (n=3). Images were taken on a Zeiss 880 confocal microscope with 40x objective, scale bar = 20 µM.

In order to investigate if the level of microgliosis changed during disease progression, immunoblotting was carried out on lysates prepared from control- and prion-diseased cortex and hippocampus at 4 different timepoints (Figure 4-4A). Similar to the astrocytic markers discussed previously, protein levels of Iba-1 increased in line with disease expression, with significant upregulation at 11 w.p.i. in the cortex (3.6-fold, P=0.03) and 10 and 11 w.p.i. in the hippocampus (4.1-fold, P=0.003 and 4.8-fold, P=0.0003 respectively) (Figure 4-4B).

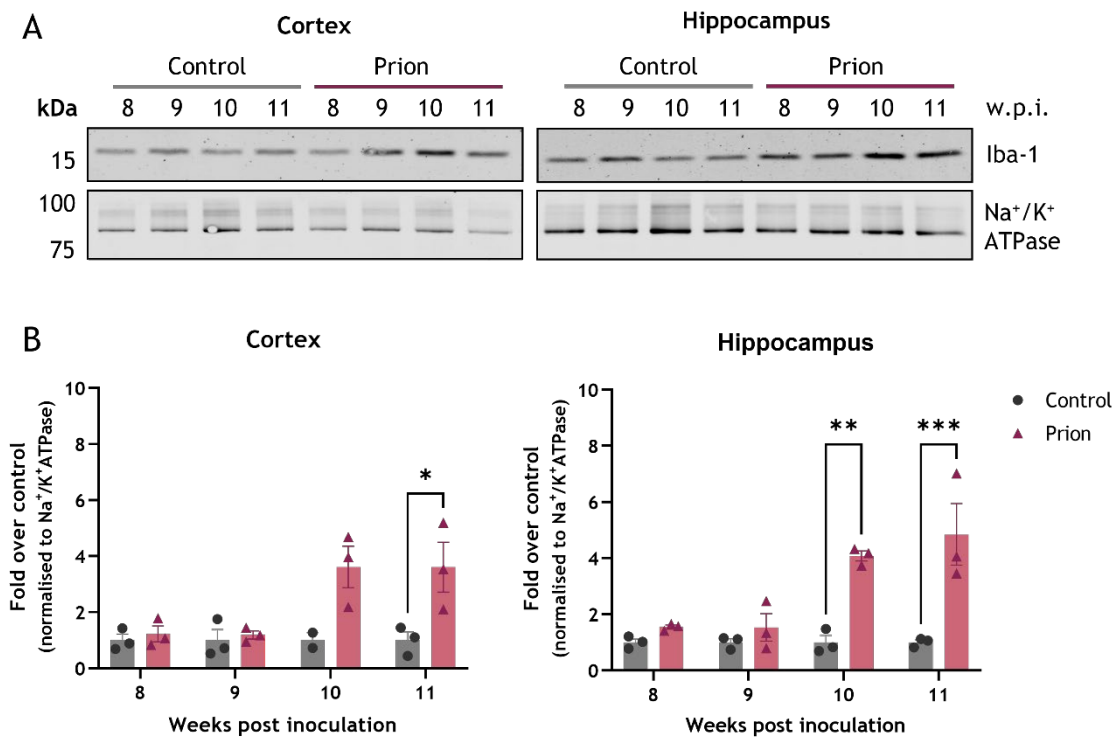

Figure 4-4 The expression of Iba-1 increases in line with the progression of murine prion disease. (A) Microgliosis was assessed using Western blot analysis on lysates prepared from the cortex or hippocampus of control- or prion-infected mice at 8, 9, 10 and 11 w.p.i. Lysates were probed with an antibody raised against the microglial marker Iba-1. Na^+/K^+ ATPase was used as a loading control. Representative blots are shown (n=3). (B) Protein levels were normalised to the loading control and data is expressed as fold over control. Data shown are means ± S.E.M. with data points representing individual mice (n=3). Statistical analysis was performed using a two-way ANOVA (Tukey's multiple comparisons), where * P≤0.05, ** P≤0.01, and *** P≤0.001.

Although reports on cytokine levels in AD patients vary, there is a trend for both pro-inflammatory (e.g., interleukin-1α [IL-1α], interleukin-1β [IL-1β], interleukin-6 [IL-6], and tumour necrosis factor α [TNF-α]) and anti-inflammatory cytokines (e.g., interleukin-10 [IL-10]) to be elevated in the cerebral spinal fluid and plasma of AD patients (Brosseron et al., 2014). These proteins are typically released by activated astrocytes and microglia during neuroinflammation (Li et al., 2011; Smith et al., 2012). The gene expression of the cytokines mentioned above, along with the gene expression of monocyte chemoattractant protein-1 (MCP-1; gene: *Ccl2*), a pro-inflammatory chemokine, and granulocyte-macrophage colony-stimulating factor (GM-CSF; gene: *Csf2*), an adaptive immunity cytokine, were investigated in the cortex and hippocampus of prion-diseased mice at 10 w.p.i. using RT-qPCR (Figure 4-5A). No difference in the transcript level of *Il10* was observed in the cortex or hippocampus of prion-diseased mice as compared to controls (Figure 4-5A). *Il1a*, *Il1β*, *Il6*, *Tnf*, *Ccl2* and *Csf2* transcripts showed an overall upregulation in the cortex and hippocampus (Figure 4-5B-G). *Il1a*, *Il1β*, and *Ccl2* were significantly increased in the cortex (*Il1a* P=0.001; *Il1β* P=0.02; *Ccl2* P=0.04) and hippocampus (*Il1a* P=0.01; *Il1β* P=0.04; *Ccl2* P=0.05) as compared to control mice (Figure 4-5B, C and F). *Il6*, *Tnf*, and *Csf2* transcripts were significantly upregulated in the cortex (*Il6* P=0.004; *Tnf* P=0.0165; *Csf2* P=0.005) but not hippocampus of prion-diseased mice as compared to controls (Figure 4-5D, E and G).

Overall, these data suggest that prion-diseased mice exhibit a robust inflammatory response in the cortex and hippocampus from 10 w.p.i., which is characterised by astro- and microgliosis and the elevation of pro-inflammatory cytokines/chemokines.

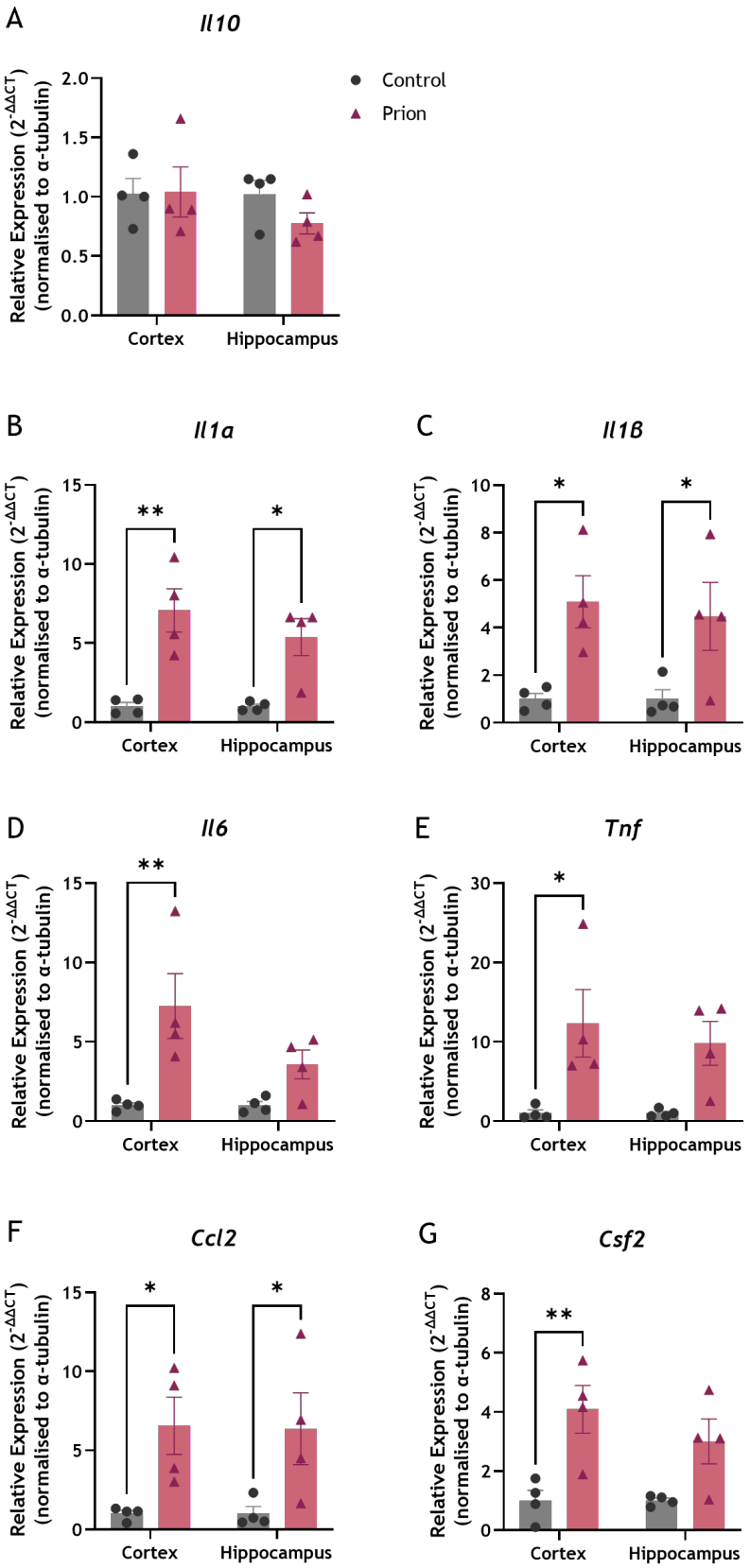

Figure 4-5 Changes in cytokine expression in murine prion disease. RT-qPCR showing the expression of the anti-inflammatory cytokine IL-10- (*Il10*) (A), pro-inflammatory cytokines IL-1α (*Il1α*) (B), IL-1β (*Il1β*) (C), IL-6 (*Il6*) (D), and TNF-α (*Tnf*) (E), the pro-inflammatory chemokine MCP-1 (*Ccl2*) (F) and adaptive immunity cytokine GM-CSF (*Csf2*) (G) in the cortex and hippocampus of control or prion-diseased mice at 10 weeks post inoculation. Data are expressed as a ratio of α-tubulin RNA and are shown as means ± S.E.M. with data points representing individual mice (n=4). Statistical analysis performed was two-way ANOVA (Tukey's multiple comparisons), where * P≤0.05 and ** P≤0.01.

Alterations in the expression of the postsynaptic marker postsynaptic density protein 95 (PSD95) has been previously associated with NDD and memory impairments (Coley & Gao, 2019; Savioz et al., 2014). In AD, for example, the expression of PSD95 is reduced in AD mouse models (Shao et al., 2011) and human AD tissue (Gylys et al., 2004; Shao et al., 2011). Here, immunoblot analysis on lysates prepared from control- and prion-diseased cortex and hippocampus at 4 different timepoints showed no difference in the expression of PSD95 in either the cortex or hippocampus of prion-diseased mice as compared to controls (Figure 4-6).

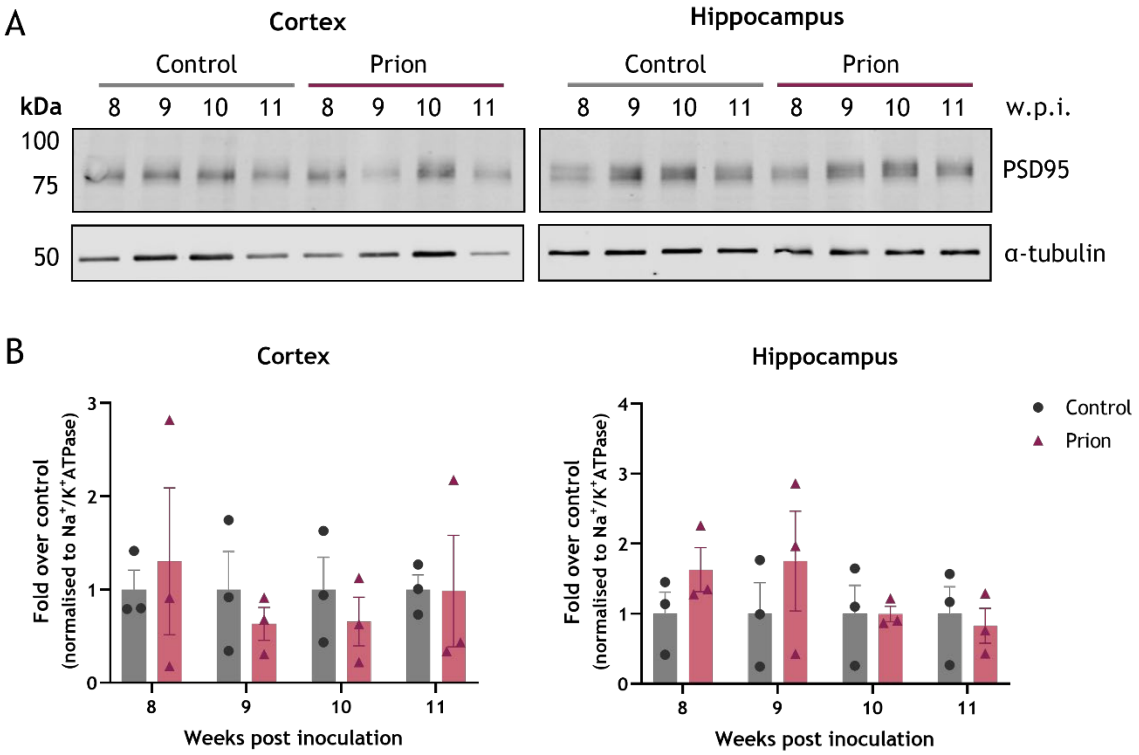

Figure 4-6 PSD95 expression is unaltered in murine prion disease. (A) Western blot analysis on lysates prepared from the cortex or hippocampus of control- or prion-infected mice at 8, 9, 10, and 11 w.p.i. Lysates were probed with an antibody raised against PSD95. α-tubulin was used as a loading control. Representative blots are shown (n=3). (B) Protein levels were normalised to the loading control and data is expressed as fold over control at each time point. Data shown are means ± S.E.M. with data points representing individual mice (n=3). Statistical analysis was performed using a two-way ANOVA (Tukey's multiple comparisons).

4.2.2 Examining the Expression of $mGlu_5$ in Diseased Mouse and Human Brain Tissue

Since the expression of $mGlu_5$ has been observed to be altered in other rodent models of neurodegeneration (Price et al., 2010; Giribaldi et al., 2013; Lee et al., 2018), $mGlu_5$ expression was assessed using immunoblot analysis in control and prion-diseased mice (Figure 4-7A). A time course study using tissue collected at 4 different time points from the cortex and hippocampus showed that the expression of $mGlu_5$ was not altered in the prion-diseased brains as compared to control brains (Figure 4-7B). This finding was found to be consistent in an RT-qPCR time course study, which showed no change in $mGlu_5$ gene (*Grm5*) expression at any timepoint investigated (Figure 4-7C).

To investigate whether $mGlu_5$ expression was altered in human AD patients as compared to controls, RT-qPCR was carried out in cortical and hippocampal brain samples from AD patients and age- and sex-matched controls (Figure 4-8). The study sample consisted of 10 individuals: 5 with AD (aged 70-95), and 5 controls with either brain pathology consistent with normal ageing or mild AD pathology (aged 80-98). All AD patients had pathology consistent with Braak stage VI. This is a late stage of AD, with AD pathology found in most brain regions, including the neocortex (which makes up most of the cerebral cortex) (Braak et al., 2006). Of the 5 control patients, 2 patients had very mild AD pathology consistent with Braak stage II, defined by neurofibrillary tangles confined mainly to the transentorhinal region of the cerebral cortex (Braak et al., 2006). The other 3 control patients had normal brains consistent with patient age. RT-qPCR analysis showed no significant difference in *Grm5* expression between AD patients and controls in either the cortex or hippocampus.

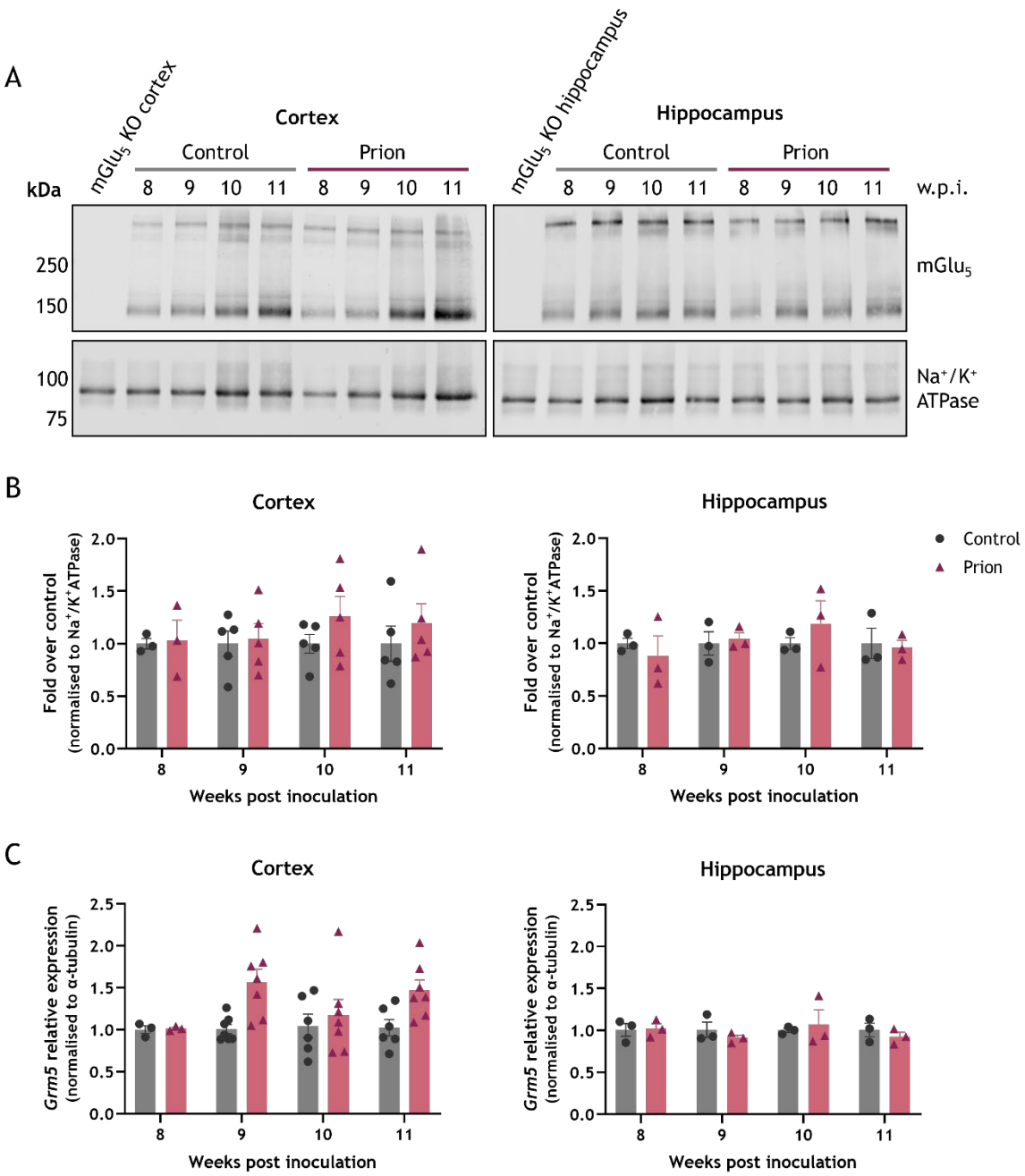

Figure 4-7 The expression of $mGlu_5$ is unaltered in murine prion disease. (A) The expression of $mGlu_5$ was assessed using Western blot analysis on lysates prepared from the cortex and hippocampus of control- or prion-infected mice at 8, 9, 10, and 11 w.p.i. An antibody against $mGlu_5$ was used to probe for $mGlu_5$ expression. Lysates from $mGlu_5$ knockout (KO) cortex or hippocampus were used as a negative control. Na^+/K^+ ATPase was used as a loading control. Representative blots are shown (n=3-5). (B) Protein levels were normalised to the loading control and data is expressed as fold over control at each time point. (C) RT-qPCR showing the expression of *Grm5* in the cortex and hippocampus of control- or prion-infected mice at 8, 9, 10, and 11 w.p.i. Data are expressed as a ratio of α-tubulin RNA. (B and C) Data are shown as mean ± S.E.M. with data points representing individual animals (n=3-7). Statistical analysis was performed using a two-way ANOVA (Dunnett's multiple comparisons).

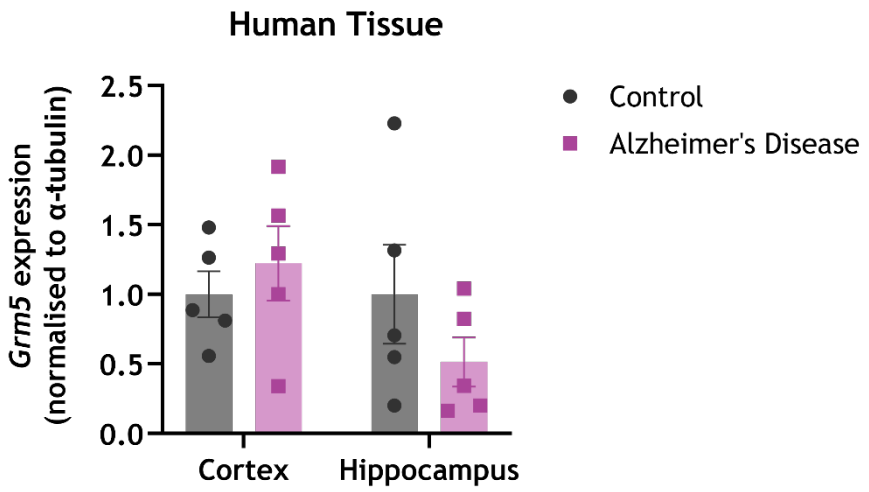

Figure 4-8 The expression of mGlu$_5$ is unaltered in human Alzheimer's disease tissue. RT-qPCR showing the expression of mGlu$_5$ (*Grm5*) in the cortex and hippocampus of human individuals with Alzheimer's disease and healthy/early-stage disease age- and sex-matched controls. Data are expressed as a ratio of α-tubulin RNA and are shown as means ± S.E.M. with data points representing individual patients (n=5). Statistical analysis was performed using an unpaired t-test.

4.2.3 Effect of Chronic VU0424238 Treatment on the Progression of Murine Prion Disease

The next section of this chapter investigates the effect of pharmacological mGlu$_5$ blockade on the progression of biochemical and behavioural changes associated with neurodegenerative disease as well as the survival of terminally sick mice. In this study, control- and prion-diseased mice were given daily intraperitoneal injections of either vehicle (10% tween-80 in PBS) or VU0424238 (10 mg/kg), the selective mGlu$_5$ NAM characterised in chapter 3 (Figure 4-9). A concentration of 10 mg/kg of VU0424238 was chosen based on its effect on marble burying, as discussed in Chapter 3. Briefly, VU0424238 dose-dependently inhibited marble-burying behaviour in wild-type mice, with complete inhibition at 10 mg/kg, thus providing evidence for target engagement at this concentration *in vivo*. The mice were dosed with VU0424238 from 4 w.p.i., a timepoint at which the animals did not yet display indicators of disease. This enables any preventative effect of mGlu$_5$ inhibition to be examined. Importantly, as recent studies have found differences in the response of diseased male and female rodents to mGlu$_5$ inhibition (Abd-Elrahman et al., 2020a; Milanese et al., 2021; Li et al., 2022), this study was carried out in both male and female mice in order to identify any sex-specific differences.

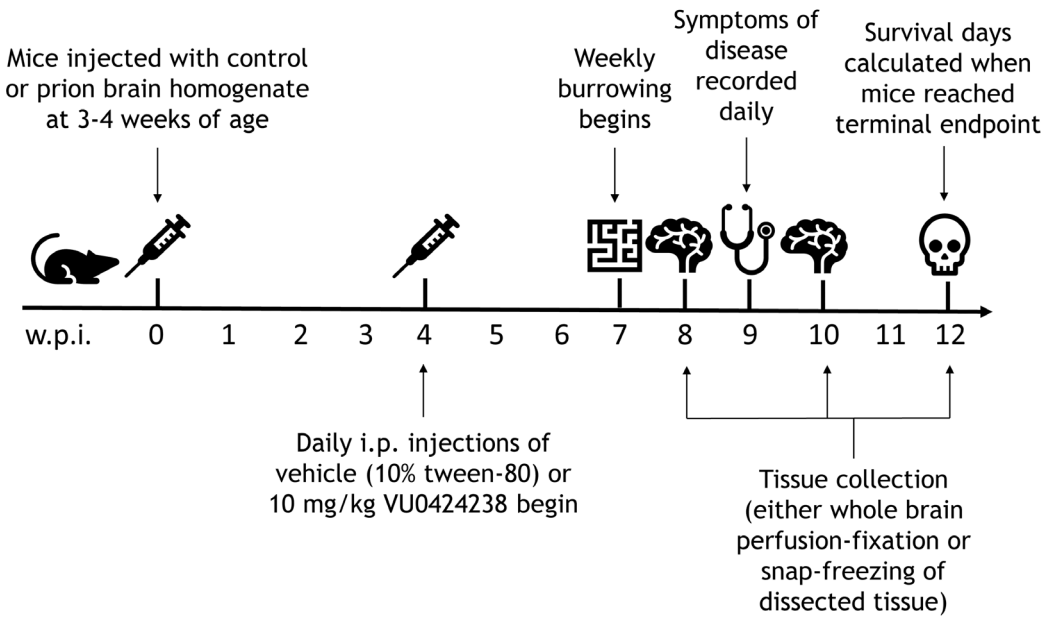

Figure 4-9 Timeline of the VU0424238 dosing study in the murine prion disease model. Mice were inoculated with control or prion-diseased brain homogenate at approx. 3-4 weeks of age (0 w.p.i.). Control- and prion-infected mice were administered vehicle (10% tween-80) or VU0424238 (10 mg/kg) intraperitoneally (i.p.) daily from 4 w.p.i. until survival. The burrowing response of female mice was assessed weekly following training at 7 w.p.i. Mice were sacrificed at 3 time points, 8 and 10 w.p.i., and at survival. The tissue was either perfusion-fixed for immunohistochemical analysis, or the hippocampus and cortex were dissected and snap-frozen for immunoblotting and RT-qPCR. Mice were checked daily for the onset of symptoms of murine prion disease. Once mice started showing symptoms at around 9 w.p.i., their symptoms were recorded daily to monitor disease progression. Mice reached a terminal disease endpoint at around 11-12 w.p.i., and their survival days were calculated.

Initially, the ability of VU0424238 to modify the progression of murine prion disease was investigated. The progression of murine prion disease is characterised by behavioural abnormalities linked to a deterioration in hippocampal function. Burrowing behaviour in mice reflects innate hippocampal function, independent of memory processes, and is a sensitive assay for monitoring the development of murine prion disease (Deacon, 2006). In the burrowing task, mice actively remove pellets from a container, called "burrowing". Burrowing experiments began at 7 w.p.i., before the animals developed any disease symptoms, and were repeated weekly (Figure 4-10). The day before the burrowing task began, a training experiment was conducted to acclimate the animals to their cages. Only female mice were used in this study because removing male mice from their home cage for experimental tasks can result in aggressive behaviour and fighting upon return. At 7 w.p.i., all mice burrowed actively, displacing, on average, 80-82% of the pellets from the

containers. Vehicle- and VU0424238- treated prion-diseased mice showed a progressive decline in burrowing behaviour from 8 w.p.i., which became significant at 9 w.p.i., which is consistent with the literature (Bradley et al., 2016; Mallucci et al., 2007). Specifically, burrowing behaviour was significantly reduced in prion-diseased mice by approximately 29-35% at 9 w.p.i., and 35-37% at 10 w.p.i. There was no difference in burrowing behaviour between vehicle- and VU0424238-treated mice in either the control or prion cohorts. Overall, this shows that chronic VU0424238 treatment from 4 w.p.i. does not affect the burrowing behaviour of mice.

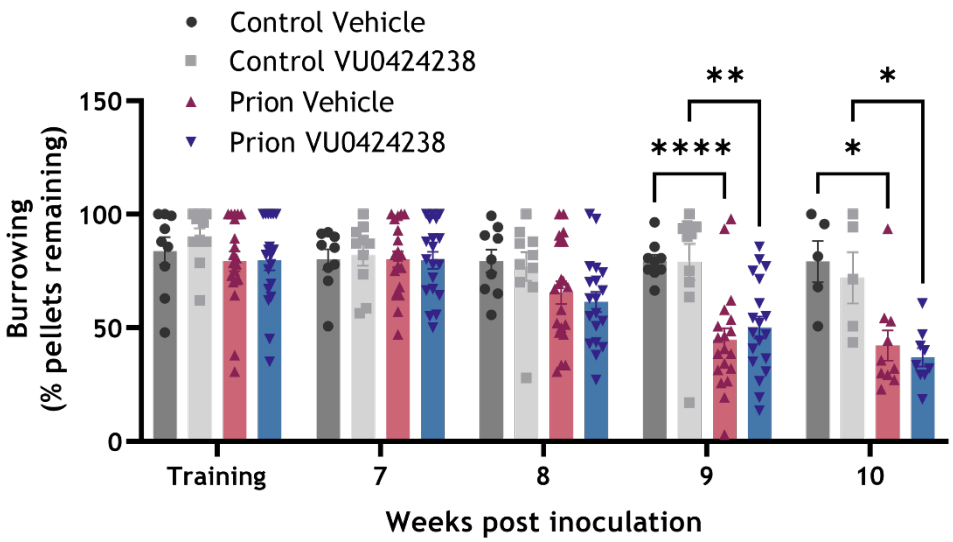

Figure 4-10 Prion-diseased mice show a decline in burrowing ability which is unchanged after chronic dosing with VU0424238. Burrowing response of female control- and prion-infected mice treated with vehicle (10% tween-80) or VU0424238 (10 mg/kg) daily from 4 w.p.i. Burrowing was assessed weekly following training from 7 w.p.i. Data shown are mean ± S.E.M., with each point representing an individual mouse (n=9-19). Statistical analysis was a two-way ANOVA or mixed-effects model with uncorrected Fisher's least significant difference test, where * P<0.5, ** P≤0.01, and **** P≤0.0001.

The onset of prion disease symptoms and the survival of prion-diseased mice were determined by the daily monitoring of early and confirmatory signs of disease (see 2.3.6.1). Mice were recorded to be "symptomatic" when they displayed at least two early indicators (Mallucci et al., 2003). There was no difference in symptom onset between vehicle- and VU0424238-treated prion disease mice, with a median onset of symptoms at 69 days post inoculation with prion infection (d.p.i.) for vehicle-treated animals, and 73 d.p.i. for VU0424238-treated animals (Figure 4-11A).

Murine prion disease is a terminal model of neurodegeneration, and the animals are considered to have reached a disease endpoint when they exhibit two early indicator signs in addition to one confirmatory sign, or the appearance of two confirmatory signs. Confirmatory signs included ataxia, impairment of the righting reflex, and a sustained hunched posture (see 2.3.6.1). When mice reach a disease endpoint, they are culled, thus defining their survival. Initial analysis of survival data grouped data from both male and female cohorts together and found no difference in survival between vehicle- and VU0424238-treated prion disease mice, with a median survival of 83 d.p.i. for vehicle-treated animals and 80 d.p.i. for VU0424238-treated animals (Figure 4-11B).

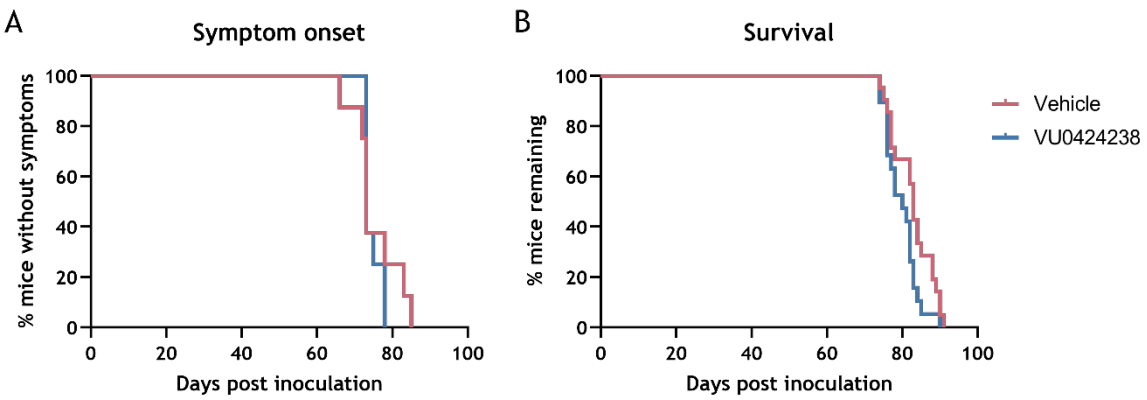

Figure 4-11 Chronic treatment with VU0424238 did not affect the symptom onset or survival of prion-diseased mice. Kaplan-Meier survival plot showing the onset of at least two early indicators of prion-disease (A) or survival (B) for male and female prion-diseased mice treated with vehicle (red) or VU0424238 (blue) daily from 4 w.p.i. (A, n=8; B, n=18-22). Curves were analysed with a Gehan-Breslow-Wilcoxon test.

When the data were analysed for male and female mice separately, no difference was found between VU0424238-treated mice and their vehicle-treated controls for either sex (Figure 4-12). However, the median time of onset for vehicle-treated male mice as compared to vehicle-treated female mice was found to be significantly different, with median disease onset of 85 and 76 d.p.i. respectively (P=0.008; Gehan-Breslow-Wilcoxon Test) (Appendix Figure 1). There was no difference in survival between VU0424238-treated male mice as compared to VU0424238-treated female mice, both with a median survival of 82 d.p.i. Taken together, these results indicate that $mGlu_5$ inhibition by VU0424238 does not overtly influence the progression of murine prion disease.

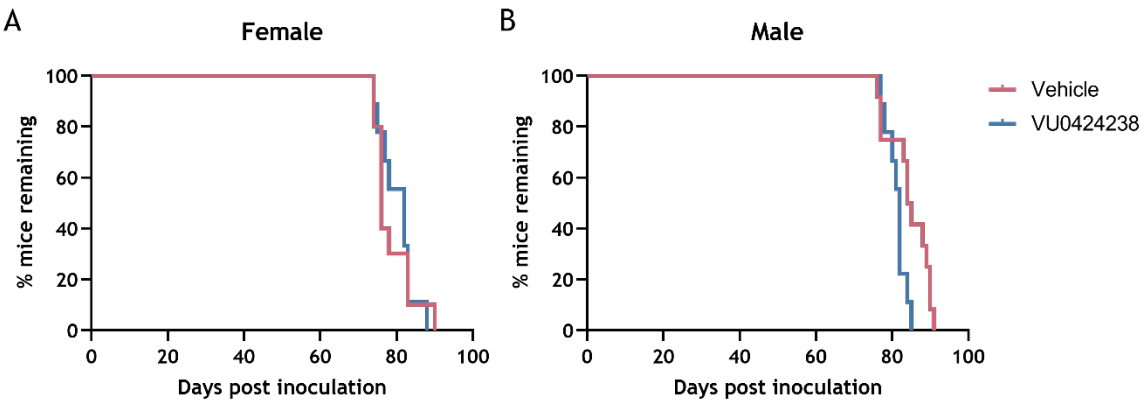

Figure 4-12 Comparison of the survival of male and female vehicle- and VU0424238-treated prion-diseased mice. Kaplan-Meier survival plots for female (A) and male (A) prion-diseased mice treated with vehicle (red) or VU0424238 (blue) daily from 4 w.p.i. Female vehicle n=10, female VU0424238 n=9, male vehicle n=12, male VU0424238 n=9. Curves were analysed with a Gehan-Breslow-Wilcoxon test.

As discussed in section 1.5.1, prion disease is characterised by the conversion of PrP_C into a misfolded, toxic form, PrP_{Sc}. These misfolded proteins act as infectious agents that self-propagate, accumulate, and form aggregates partially resistant to protease digestion (Prusiner, 1982). This process is a common feature of most NDDs, with specific proteins, such as Aß in AD and mHtt in HD, misfolding and spreading in a prion-like manner (see 1.3.2.1). It is well documented that PrP_{Sc} accumulates in the brains of mice with murine prion disease (Mallucci et al., 2003), and that this can be reduced by treatment with ligands for other GPCRs, such as the M1 muscarinic receptor (Dwomoh et al., 2022).

Tissue collected from the terminally sick mice used in the survival studies above, in addition to tissue collected from mice culled at two earlier timepoints, 8 and 10 w.p.i., were probed for the presence of PrP_{Sc} (Figure 4-13). When Western blotting for prion protein, multiple bands are expected due to the differential glycosylation of PrP_C (Collinge et al., 1996; Rudd et al., 1999; Stimson et al., 1999). As expected, no PrP_{Sc} was detected in the brains of control mice at either 8 w.p.i. (Figure 4-13A), 10 w.p.i. (Figure 4-13C), or at survival (Figure 4-13E). PrP_{Sc} was evident in prion-diseased mice from 8 w.p.i. (Figure 4-13A-B) but was highly variable at each time point (Figure 4-13B, D, and F). There was no significant difference in PrP_{Sc} levels between vehicle- and VU0424238-treated prion-diseased mice (Figure 4-13B, D, and F). The prion antibody recognising all

forms of prion protein showed no differences in the total prion protein (PrP_{tot}), which is both PrP_c and PrP_{Sc}, between control and prion-diseased animals at any time point or brain region (Figure 4-13B, D, and F). However, a significant reduction in PrP_{tot} in the hippocampus was observed between vehicle- and VU0424238-treated prion-diseased mice at 10 w.p.i. (P=0.046) (Figure 4-13D).

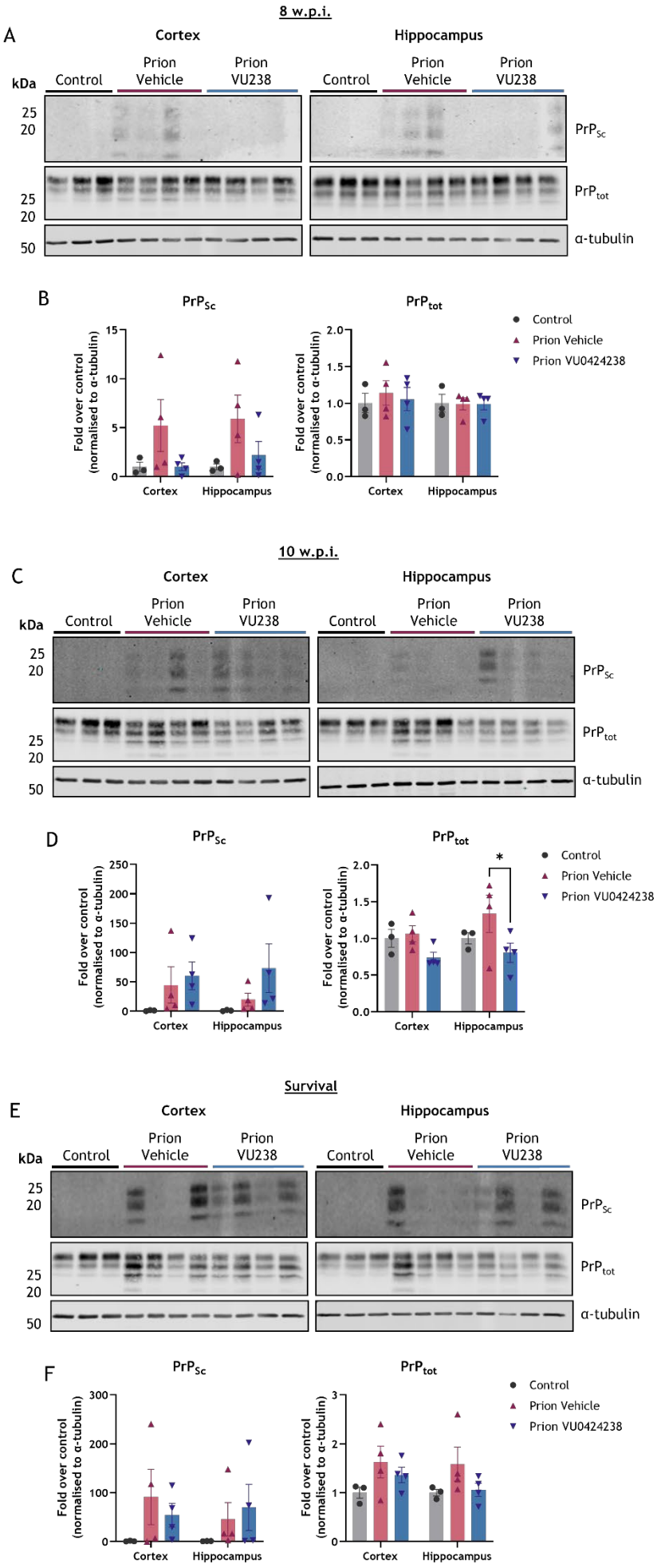
8 w.p.i.
A
Cortex
Hippocampus
kDa
Control
Prion Vehicle
Prion VU238
25
20
50
PrPSc
PrPtot
α-tubulin
B
PrPSc
PrPtot
Fold over control (normalised to α-tubulin)
Cortex
Hippocampus
Control
Prion Vehicle
Prion VU0424238
10 w.p.i.
C
D
*
Survival
E
F

Figure 4-13 Effect of VU0424238 on PrP_{Sc} and PrP_{tot} expression. Western blot analysis of lysates from the cortex and hippocampus of control, prion vehicle, and prion VU0424238-treated mice at 8 w.p.i. (A), 10 w.p.i. (C), and survival (E). Lysates were incubated with water (PrP_{tot}) or proteinase K prior to immunoblotting using anti-PrP to detect PrP_{tot}/PrP_{Sc}, respectively. Each lane represents a different mouse. α-tubulin was used as a loading control. Membranes were stripped and re-probed for multiple antibodies (Figure 4-13 and Figure 4-26). (B, D, F) Protein levels were normalised to the loading control, followed by normalisation to the average protein level of the control bands expressed as fold change. Data shown are means ± S.E.M. with each data point representing an individual mouse (n=3 for control, n=4 for prion vehicle and prion VU0424238). Statistical analysis was performed using a two-way ANOVA (Tukey's multiple comparisons), where * P≤0.05.

As established in section 4.2.2, the expression of $mGlu_5$ is unaltered in murine prion disease. Here, the expression of $mGlu_5$ in prion-diseased mice chronically treated with either vehicle- or VU0424238 was examined (Figure 4-14). Immunoblot analysis of lysates prepared from the cortex and hippocampus of prion-diseased mice at three timepoints, 8 w.p.i., 10 w.p.i., and survival, showed no difference in $mGlu_5$ expression between vehicle- and VU0424238-treated mice.

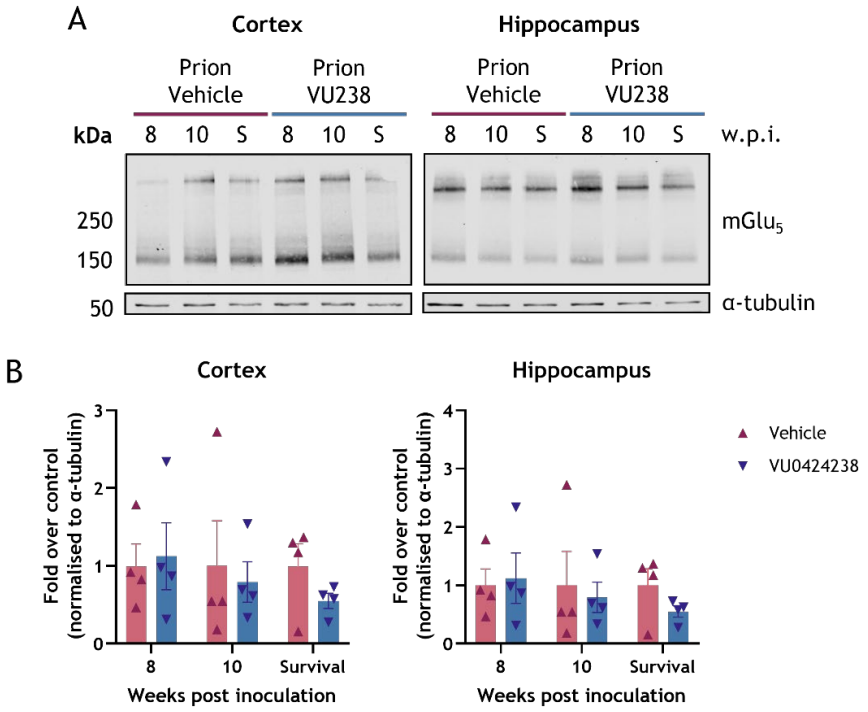

Figure 4-14 The expression of $mGlu_5$ is unaltered in prion-diseased mice after chronic treatment with VU0424238. (A) The expression of $mGlu_5$ was assessed using Western blot analysis on lysates prepared from the cortex and hippocampus of prion-infected mice treated with either vehicle or VU0424238. Tissue was taken at 8 w.p.i., 10 w.p.i., and at survival (S). The blots were probed using an anti-$mGlu_5$ antibody. α-tubulin was used as a loading control. Membranes were stripped and re-probed for multiple antibodies (Figure 4-14, Figure 4-15, and Figure 4-16). Representative blots are shown (n=4). (B) Protein levels were normalised to the loading control. Data shown are means ± S.E.M., with each data point representing an individual mouse (n=4). Statistical analysis was performed using a two-way ANOVA (Dunnett's multiple comparisons).

4.2.4 Effect of Chronic VU0424238 Treatment on Prion-induced Neuroinflammation

As established in section 4.2.1, the upregulation of neuroinflammatory markers, including GFAP, vimentin, CD68, and Iba-1, is a pathological feature of murine prion disease. The pharmacological inhibition of $mGlu_5$ has been shown to reduce the expression of several neuroinflammatory markers in a number of rodent models of neurodegeneration (Hamilton et al., 2016; Bonifacino et al., 2017; Abd-Elrahman et al., 2017, 2020; Milanese et al., 2021). Here, the effect of chronic VU0424238 treatment on neuroinflammation was initially investigated using immunoblotting and RT-qPCR (Figure 4-15 and Figure 4-16).

Immunoblot analysis was carried out on lysates prepared from the cortex and hippocampus of prion-diseased mice at three timepoints, 8 w.p.i., 10 w.p.i., and survival (Figure 4-16A), and RT-qPCR was carried out on samples collected at 10 w.p.i. (Figure 4-16C). Neither analysis identified any difference in the expression of the astrocytic markers GFAP/*Gfap* and vimentin (Figure 4-15) or the microglial markers Iba-1 and *Cd68* (Figure 4-16) with VU0424238 treatment as compared to vehicle treatment. These data were pooled from male and female mice.

Similarly, no effect of VU0424238 treatment was observed when the sexes were analysed separately (Figure 4-17, Figure 4-18, Figure 4-19, Figure 4-20).

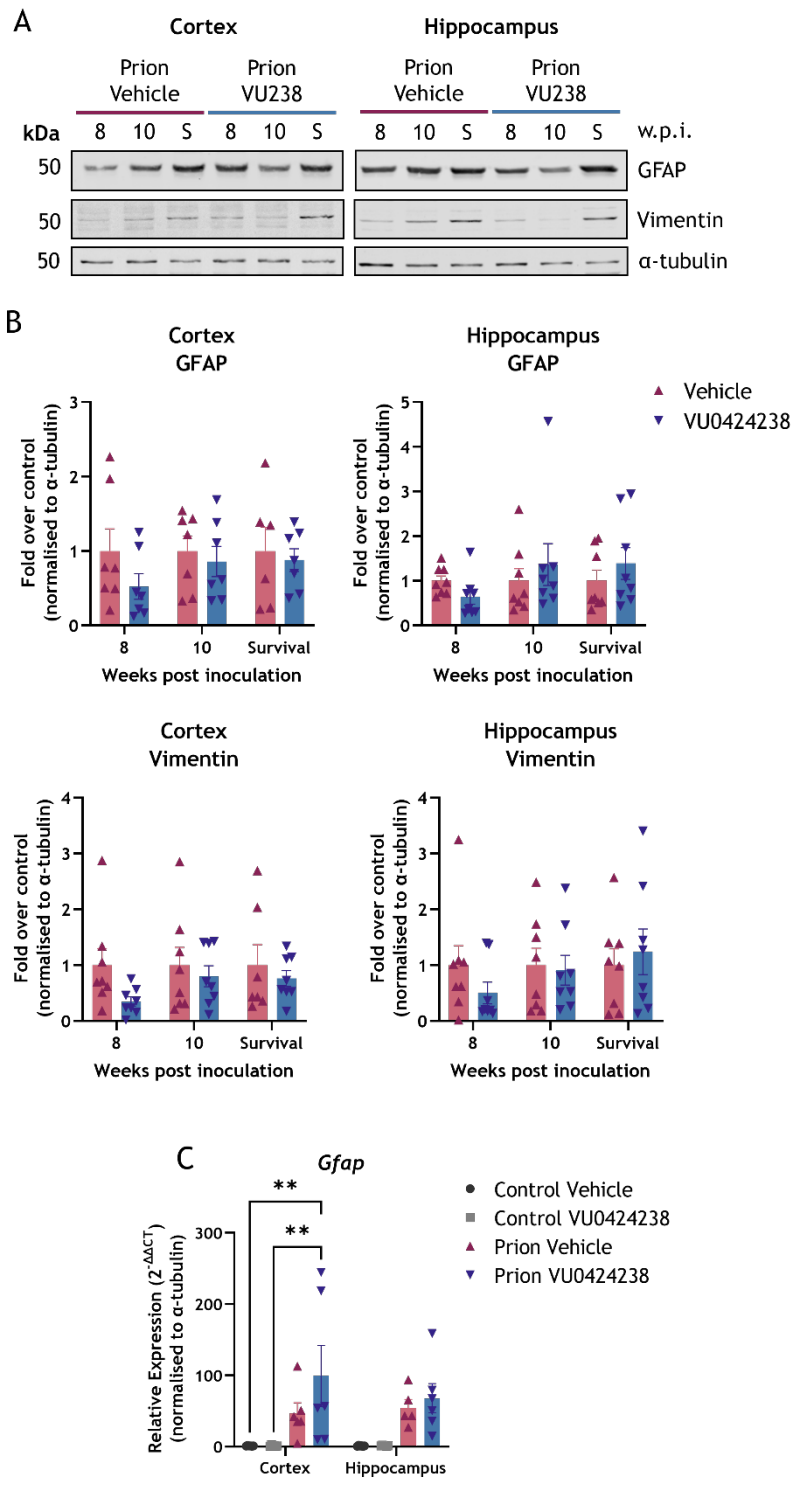

Figure 4-15 Biochemical analysis shows no effect of VU0424238 on astrogliosis in the cortex and hippocampus of prion-diseased mice. (A) Astrogliosis in the cortex and hippocampus was assessed using Western blot analysis in lysates prepared from prion-diseased mice treated with either vehicle or VU0424238. Tissue was taken at 8 and 10 w.p.i., and at survival (S). Lysates were probed for the astrocytic markers GFAP and vimentin. α-tubulin was used as a loading control. Representative blots are shown (n=7-8). Membranes were stripped and re-probed for multiple antibodies (Figure 4-14, Figure 4-15, and Figure 4-16). (B) Protein levels were normalised to the loading control followed by normalisation to vehicle-treated mice shown as fold over control. Data shown are means ± S.E.M., with each data point representing an individual mouse (n=7-8). (C) RT-qPCR showing the expression of *Gfap* in the cortex and hippocampus of control- or prion-infected mice at 10 weeks post inoculation. Data are expressed as a ratio of α-tubulin RNA and are shown as means ± S.E.M. (n=6). Statistical analysis was performed using a two-way ANOVA (Dunnett's multiple comparisons), where **P≤0.01.

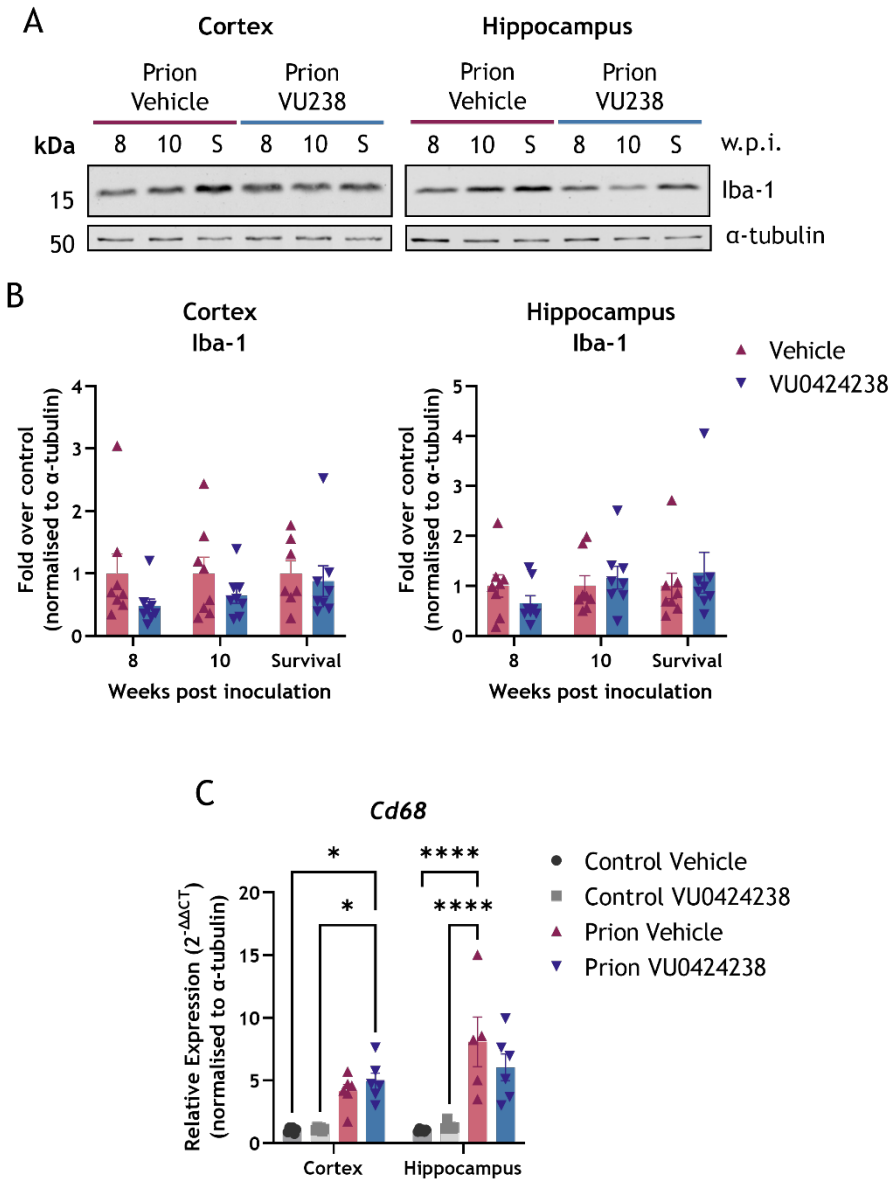

Figure 4-16 Biochemical analysis shows no effect of VU0424238 on microgliosis in the cortex and hippocampus of prion-diseased mice. (A) Microgliosis in the cortex and hippocampus were assessed using Western blot analysis on lysates prepared from prion-diseased mice treated with either vehicle or VU0424238. Tissue was taken at 8 and 10 w.p.i., and at survival (S). Lysates were probed for the microglia marker Iba-1. α-tubulin was used as a loading control. Representative blots are shown (n=7-8). Membranes were stripped and re-probed for multiple antibodies (Figure 4-14, Figure 4-15, and Figure 4-16). (B) Band analysis for each blot was performed using Image Studio Lite Version 5.2. Protein levels were normalised to the loading control followed by normalisation to vehicle-treated mice shown as fold over control. Data shown are means ± S.E.M., with each data point representing an individual mouse (n=7-8). (C) RT-qPCR showing the expression of *Cd68* in the cortex and hippocampus of control- or prion-infected mice at 10 weeks post inoculation. Data are expressed as a ratio of α-tubulin RNA and are shown as means ± S.E.M. (n=6). Statistical analysis was performed using a two-way ANOVA (Dunnett's multiple comparisons), where * P≤0.05 and *** P≤0.0001.

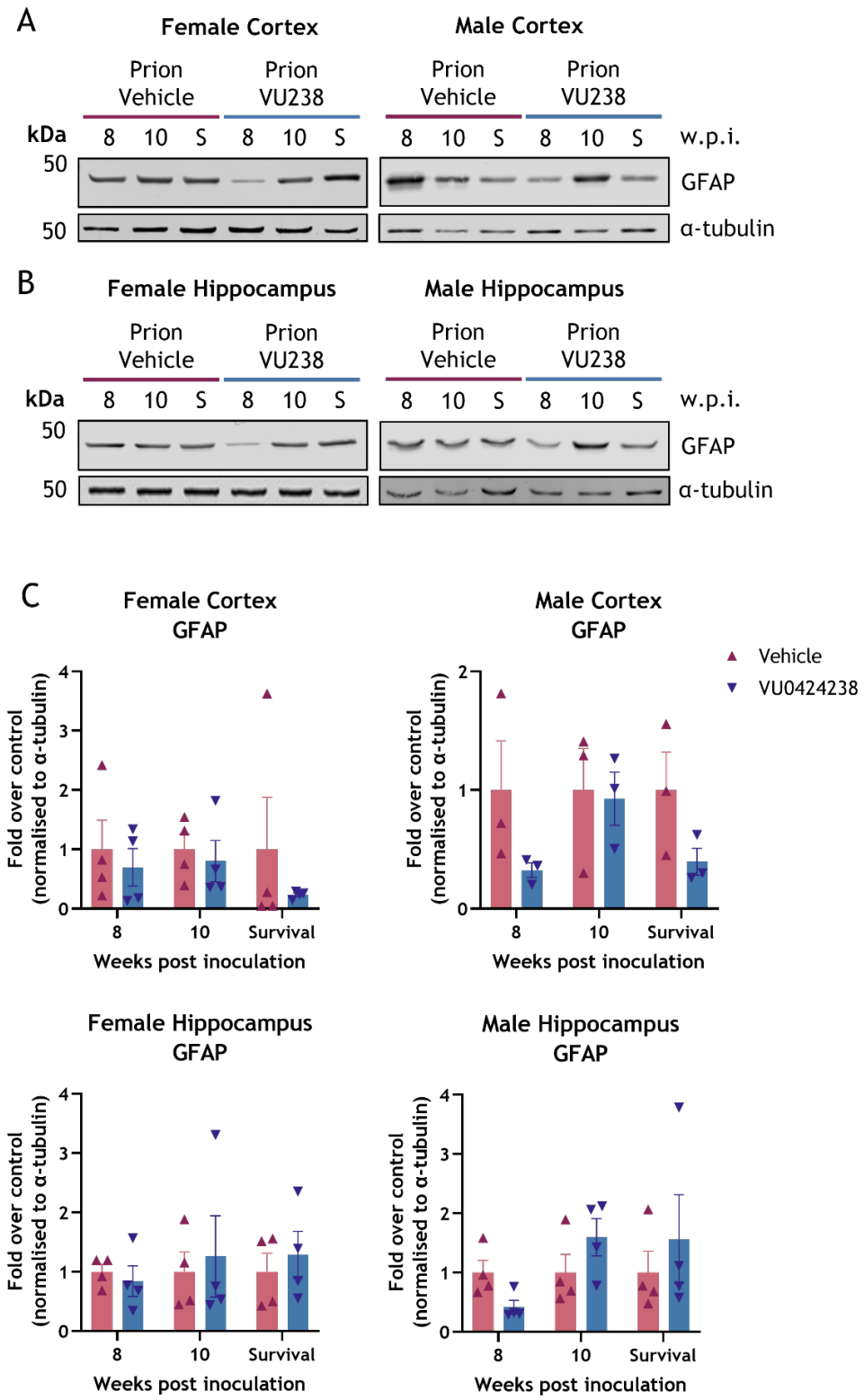

Figure 4-17 Comparison of GFAP expression in male and female prion-diseased mice treated with either vehicle or VU0424238. Astrogliosis in the (A) cortex and (B) hippocampus of female and male prion-diseased mice treated with either vehicle or VU0424238 was assessed using Western blot analysis. Tissue was taken at 8 and 10 w.p.i., and at survival (S). α-tubulin was used as a loading control. Representative blots are shown (n=3-4). Membranes were stripped and re-probed for multiple antibodies (Figure 4-17, Figure 4-18, and Figure 4-19). (C) Protein levels were normalised to the loading control followed by normalisation to vehicle-treated mice, expressed as fold over control. Data shown are means ± S.E.M., with each data point representing an individual mouse (n=3-4). Statistical analysis was performed using a two-way ANOVA (Dunnett's multiple comparisons).

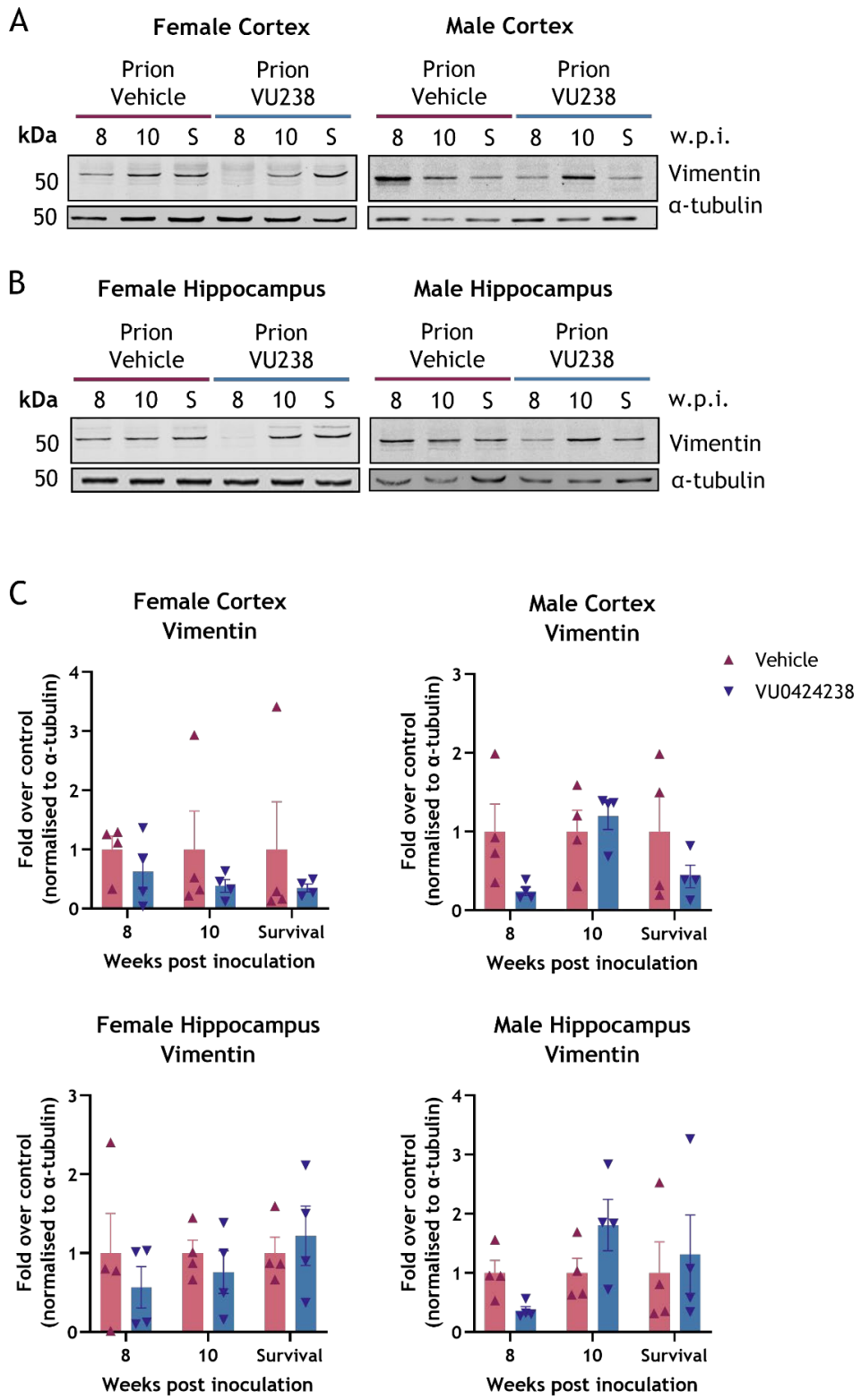

Figure 4-18 Comparison of vimentin expression in male and female prion-diseased mice treated with either vehicle or VU0424238. Astrogliosis in the (A) cortex and (B) hippocampus of female and male prion-diseased mice treated with either vehicle or VU0424238 was assessed using Western blot analysis. Tissue was taken at 8 and 10 w.p.i., and at survival (S). α-tubulin was used as a loading control. Representative blots are shown (n=3-4). Membranes were stripped and re-probed for multiple antibodies (Figure 4-17, Figure 4-18, and Figure 4-19). (C) Protein levels were normalised to the loading control followed by normalisation to vehicle-treated mice, expressed as fold over control. Data shown are means ± S.E.M., with each data point representing an individual mouse (n=3-4). Statistical analysis was performed using a two-way ANOVA (Dunnett's multiple comparisons).

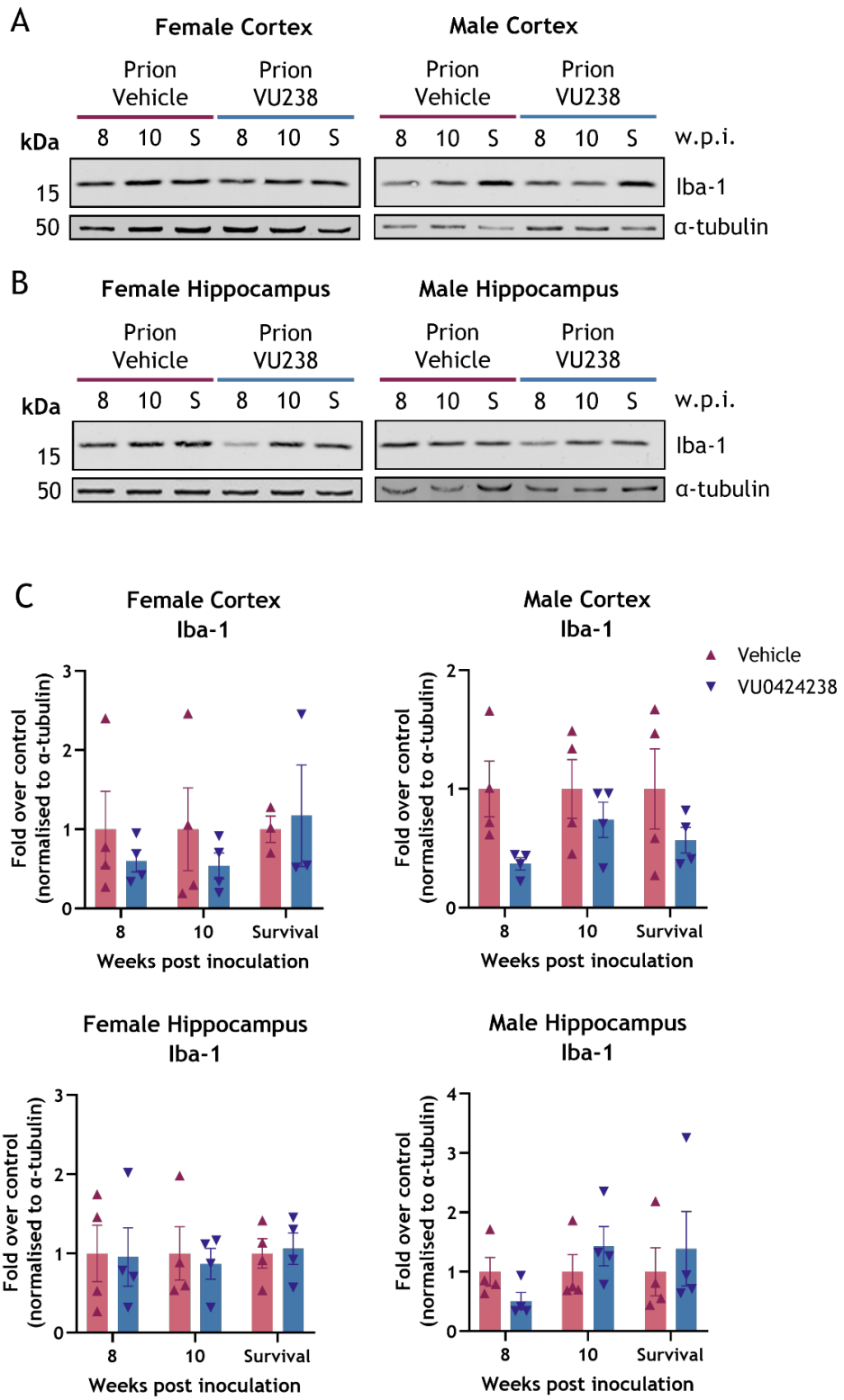

Figure 4-19 Comparison of Iba-1 expression in male and female prion-diseased mice treated with either vehicle or VU0424238. Microgliosis in the (A) cortex and (B) hippocampus of female and male prion-diseased mice treated with either vehicle or VU0424238 was assessed using Western blot analysis. Tissue was taken at 8 and 10 w.p.i., and at survival (S). α-tubulin was used as a loading control. Representative blots are shown (n=3-4). Membranes were stripped and re-probed for multiple antibodies (Figure 4-17, Figure 4-18, and Figure 4-19). (C) Protein levels were normalised to the loading control followed by normalisation to vehicle-treated mice, expressed as fold over control. Data shown are means ± S.E.M., with each data point representing an individual mouse (n=3-4). Statistical analysis was performed using a two-way ANOVA (Dunnett's multiple comparisons).

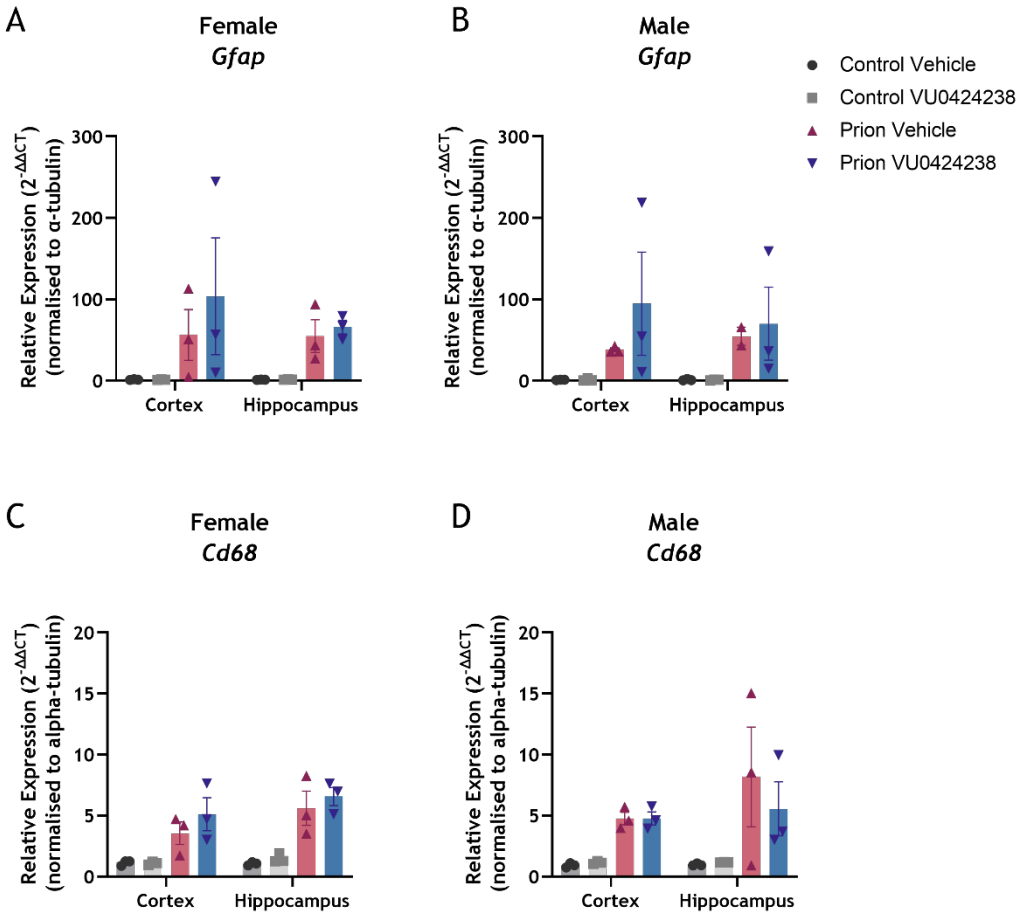

Figure 4-20 Comparison of *Gfap* and *Cd68* transcript levels in male and female control and prion-diseased mice treated with either vehicle or VU0424238. RT-qPCR showing the expression of *Gfap* (A and B) and *Cd68* (C and D) in the cortex and hippocampus of female (A and C) and male (B and D) control- or prion-infected mice at 10 w.p.i. Data are expressed as a ratio of α-tubulin RNA and are shown as means ± S.E.M. (n=2-3 for each sex). Statistical analysis was performed using a two-way ANOVA (Dunnett's multiple comparisons).

In the immunoblot and RT-qPCR analysis, the hippocampus was analysed as a whole, whereas IHC allows for a more in-depth look at the different hippocampal regions. In order to look more closely at the effect of chronic VU0424238 treatment on inflammation, IHC analysis was performed in 5 µm coronal brain slices from the same cohorts of mice (Figure 4-21, Figure 4-22, Figure 4-23). Samples were analysed from tissue collected at the same three timepoints as the immunoblot analysis, 8 w.p.i., 10 w.p.i., and survival, and protein levels were assessed in the cortex as well as the CA1, CA3, and dentate gyrus regions of the hippocampus. GFAP and vimentin were used as markers of astrogliosis (Figure 4-21, Figure 4-22), and Iba-1 as a marker of microgliosis (Figure 4-23).

Initially, analysis was conducted on data pooled from both male and female mice. As expected from the data discussed in section 4.2.1, all three markers were upregulated in the cortex and hippocampus in prion-diseased mice as compared to controls. Quantification of the immunohistochemical images showed significant upregulation at an earlier timepoint than the immunoblots in section 4.2.1, with significant upregulation from 8 w.p.i. of GFAP in the cortex and CA3 region of the hippocampus (Figure 4-21A), vimentin in the CA1 region of the hippocampus (Figure 4-22B), and Iba-1 in the cortex (Figure 4-23B). Conversely, Iba-1 in the cortex of prion-diseased mice was not upregulated at 10 w.p.i. and survival, but this may have been due to high variability between control samples (Figure 4-23D and F). Although these data confirmed that neuroinflammation is increased in the brains of prion-diseased mice, there was no observable difference in protein expression levels between vehicle- and VU0424238-treated prion-diseased mice. This agrees with the immunoblot and RT-qPCR data shown in Figure 4-15 and Figure 4-16 and together suggests that the pharmacological blockade of $mGlu_5$ does not significantly affect prion-induced astro- or microgliosis.

However, when the sexes were separated for analysis, only in female prion-diseased mice was a significant reduction in GFAP expression levels after VU0424238 treatment as compared to vehicle treatment observed in the CA1 (P=0.02) and CA3 (P=0.0003) regions at 10 w.p.i. (Figure 4-24). No significant difference was seen between vehicle- and VU0424238-treated male mice or in the female mice at any other timepoint or marker (Appendix Figure 2, Appendix Figure 3, and Appendix Figure 4).

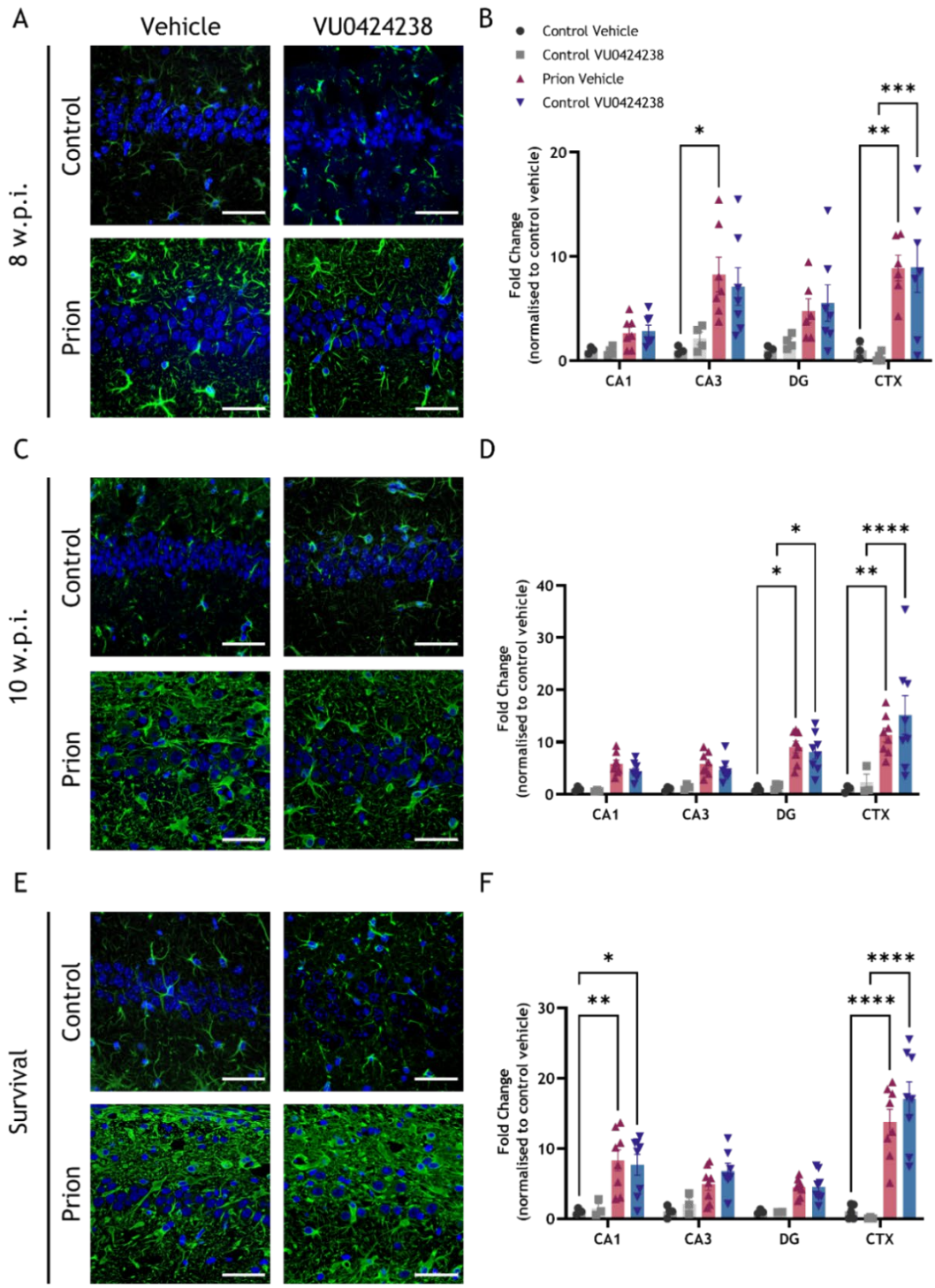

Figure 4-21 Immunohistochemical analysis of chronic VU0424238 treatment on the expression of GFAP in the hippocampus and cortex of both sexes of prion-diseased mice. Representative images of immunohistochemical staining of 5 µm thick coronal sections through the brains of vehicle- and VU0424238-treated control- and prion-infected mice at 8 w.p.i. (A), 10 w.p.i. (C), and survival (E). Images shown are from the CA1 region of the hippocampus with staining for GFAP (green) and DNA (blue). Images shown are representative of n=3-8 mice per group. Images were taken on a Zeiss 880 confocal microscope with 40x objective, scale bar = 50 µm. Quantification is shown at 8 w.p.i. (B), 10 w.p.i. (D), and survival (F), and was carried out in three areas of the hippocampus (CA1 region, CA3 region, and dentate gyrus (DG)) and in the cortex (CTX). Representative images for the other brain regions analysed but not shown here are in Appendix Figure 5 and 6. Data were normalised to control vehicle and are shown as the mean ± S.E.M. with data points representing individual mice (n=3-8). Statistical analysis was a two-way ANOVA (Tukey's multiple comparisons), where * $P \leq 0.05$, ** $P \leq 0.01$, *** $P \leq 0.001$, and **** $P \leq 0.0001$.

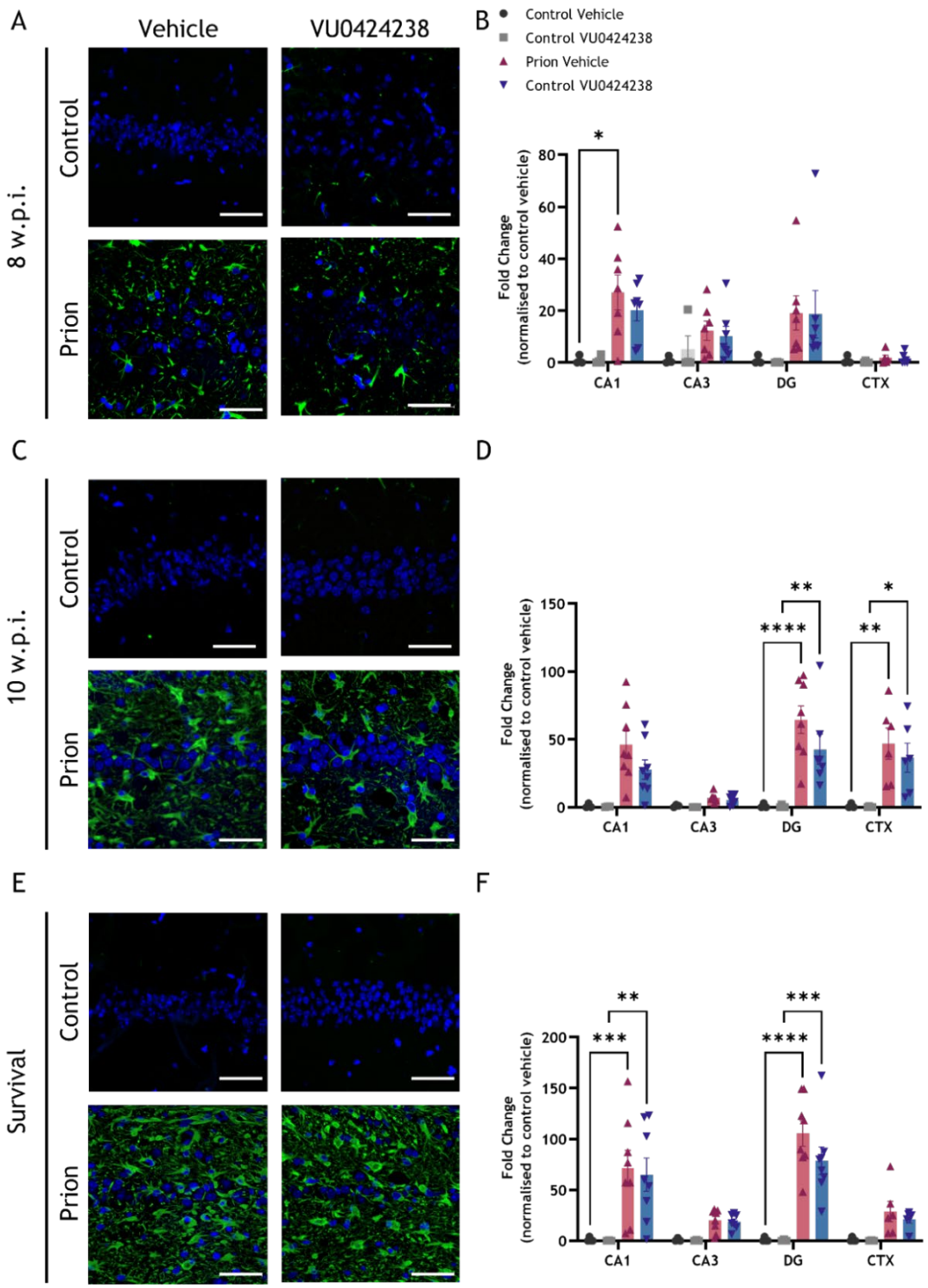

Figure 4-22 Immunohistochemical analysis of chronic VU0424238 treatment on the expression of vimentin in the hippocampus and cortex of both sexes of prion-diseased mice. Representative images of immunohistochemical staining of 5 µm thick coronal sections through the brains of vehicle- and VU0424238-treated control- and prion-infected mice at 8 w.p.i. (A), 10 w.p.i. (C), and survival (E). Images shown are from the CA1 region of the hippocampus with staining for vimentin (green) and DAPI (blue). Images shown are representative of n=3-8 mice per group. Images were taken on a Zeiss 880 confocal microscope with 40x objective, scale bar = 50 µm. Quantification is shown at 8 w.p.i. (B), 10 w.p.i. (D), and survival (F), and was carried out in three areas of the hippocampus (CA1 region, CA3 region, and dentate gyrus (DG)) and in the cortex (CTX). Representative images for brain regions not shown here are shown in Appendix Figure 7 and 8. Data were normalised to control vehicle and are shown as the mean ± S.E.M. with data points representing individual mice (n=3-8). Statistical analysis was a two-way ANOVA (Tukey's multiple comparisons), where * P ≤ 0.05, ** P ≤ 0.01, *** P ≤ 0.001, and **** P ≤ 0.0001.

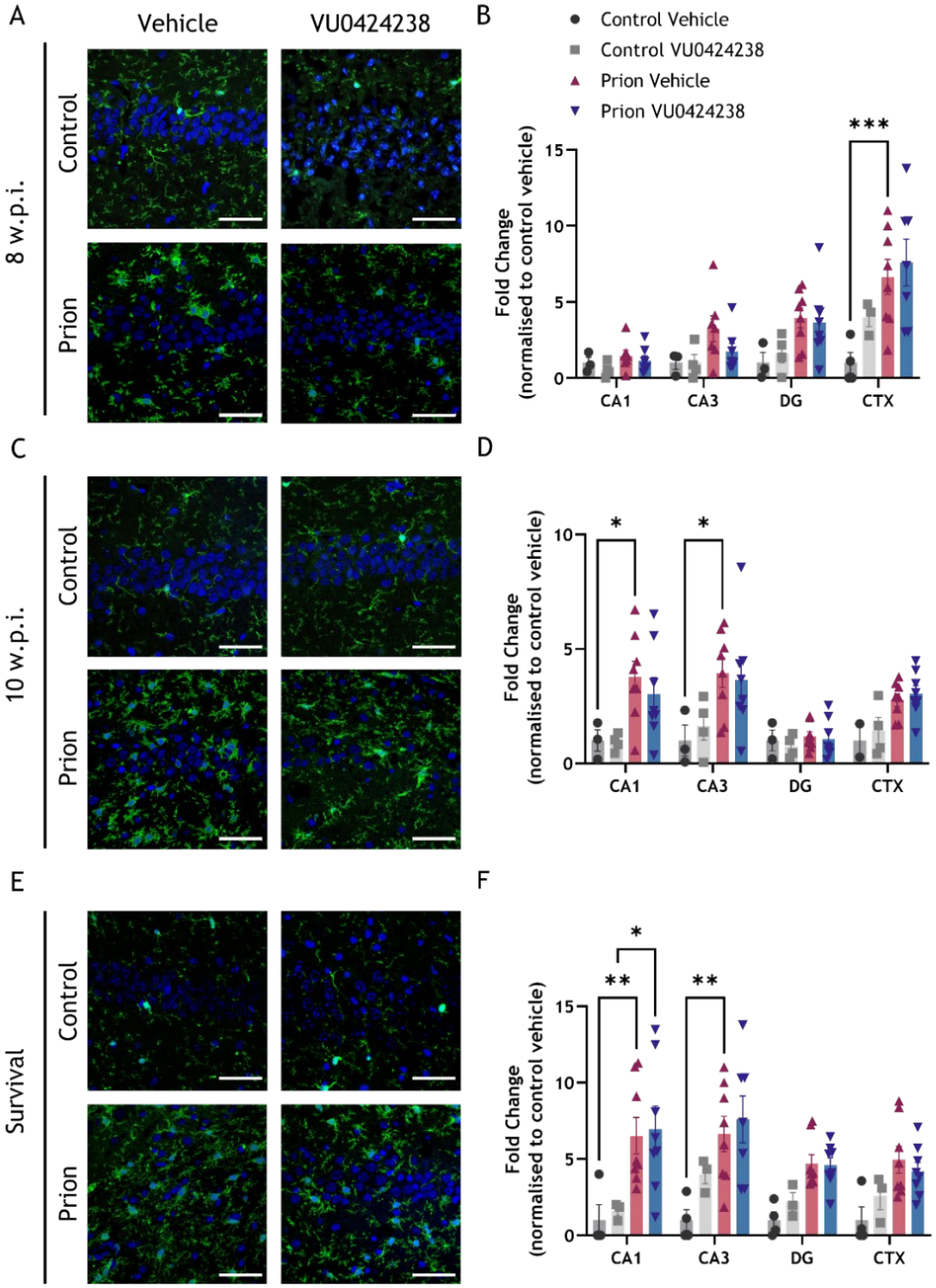

Figure 4-23 Immunohistochemical analysis of chronic VU0424238 treatment on the expression of Iba-1 in the hippocampus and cortex of both sexes of prion-diseased mice. Representative images of immunohistochemical staining of 5 µm thick coronal sections through the brains of vehicle- and VU0424238-treated control- and prion-infected mice at 8 w.p.i. (A), 10 w.p.i. (C), and survival (E). Images shown are from the CA1 region of the hippocampus with staining for Iba-1 (green) and DAPI (blue). Images shown are representative of n=3-8 mice per group. Images were taken on a Zeiss 880 confocal microscope with 40x objective, scale bar = 50 µm. Quantification is shown at 8 w.p.i. (B), 10 w.p.i. (D), and survival (F), and was carried out in three areas of the hippocampus (CA1 region, CA3 region, and dentate gyrus (DG)) and in the cortex (CTX). Representative images for brain regions not shown here are shown in Appendix Figure 9 and 10. Data were normalised to control vehicle and are shown as the mean ± S.E.M. with data points representing individual mice (n=3-8). Statistical analysis was a two-way ANOVA (Tukey's multiple comparisons), where * $P \leq 0.05$, ** $P \leq 0.01$, and *** $P \leq 0.001$.

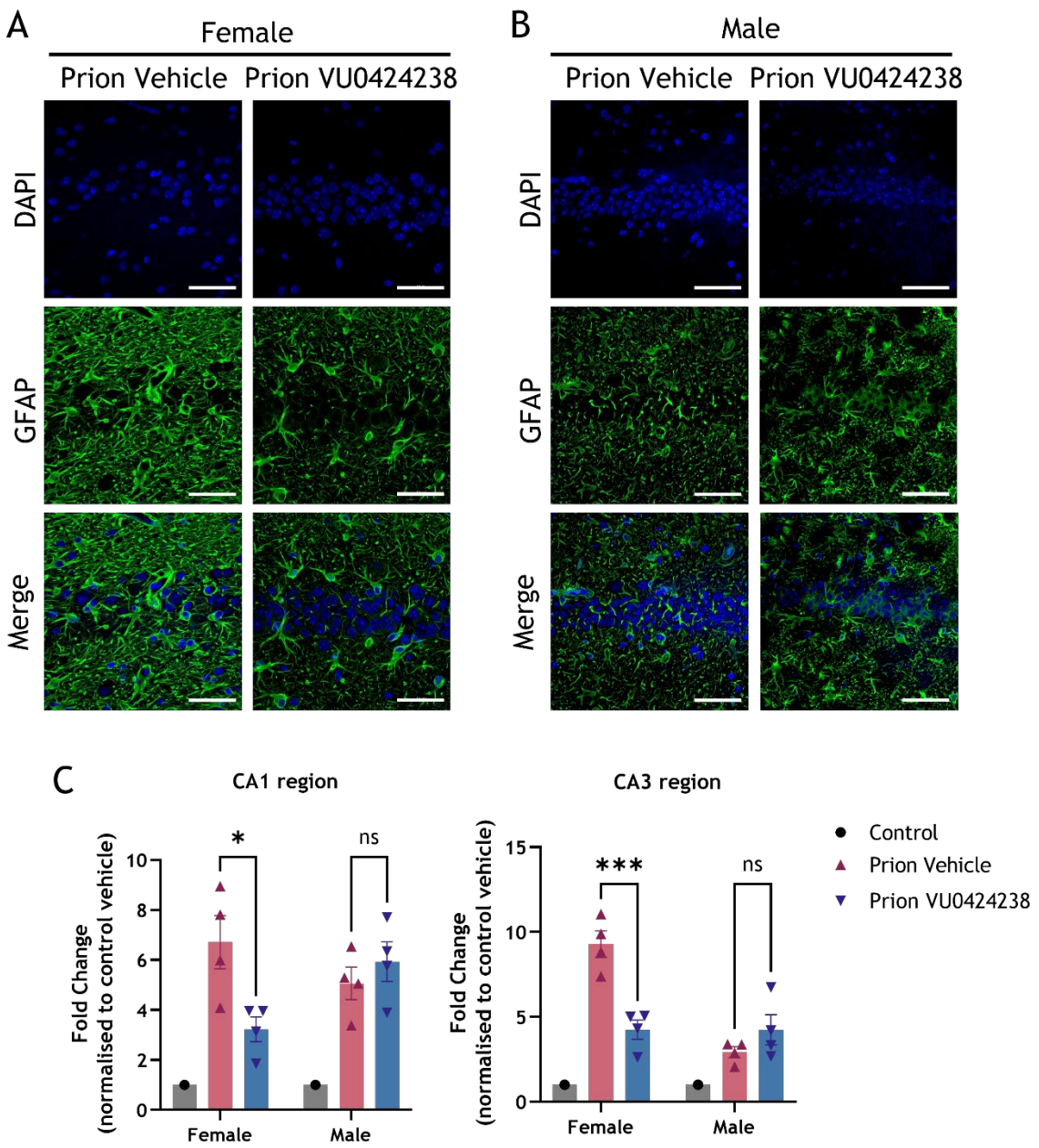

Figure 4-24 VU0424238 reduces GFAP staining in the CA1 and CA3 hippocampal regions of female prion-diseased mice. Representative images of immunohistochemical staining of 5µm thick coronal sections through the hippocampus of female (A) and male (B) prion-diseased mice treated with either vehicle or VU0424238. Images shown were taken at 10 w.p.i. in the CA1 region after staining for GFAP (green). Nuclei have been stained with DAPI (blue). Scale bar = 50µm. (B) Quantification of staining for GFAP using ImageJ in the CA1 and CA3 regions of male and female mice (n=4). Data were normalised to control vehicle (n=3) and are shown as the mean ± S.E.M. with data points representing individual mice. Statistical analysis was a two-way ANOVA (Tukey's multiple comparisons), where * $P \leq 0.05$, *** $P \leq 0.001$.

Next, the effect of chronic VU0424238 treatment on the elevated cytokine levels observed in prion-diseased mice (Figure 4-5) was investigated using RT-qPCR (Figure 4-25). This analysis was carried out in tissue collected at 10 w.p.i. and failed to detect any differences in cytokine expression levels between vehicle- and VU0424238-treated mice of either sex (Figure 4-25; sexes separated in Appendix Figure 11), suggesting that $mGlu_5$ pharmacological blockade does not alter the cytokine profile of prion-diseased mouse brains.

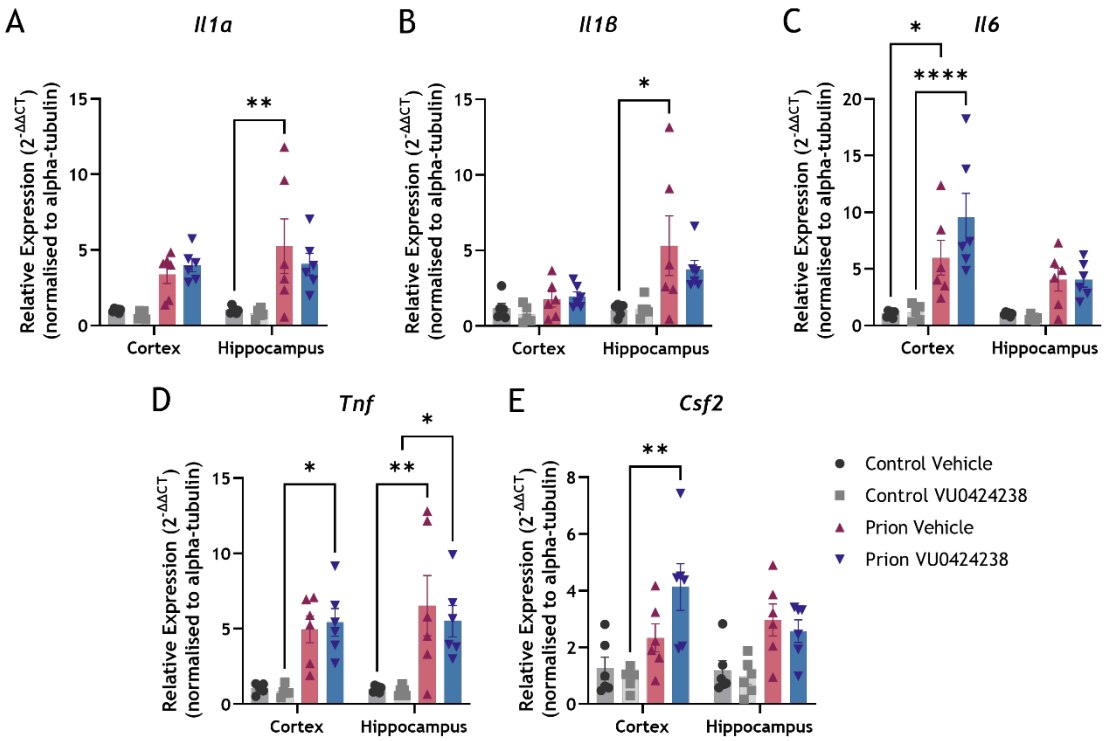

Figure 4-25 Levels of pro-inflammatory cytokines, IL-1α, IL-1β, IL-6, and TNF-α, as well as the adaptive immunity cytokine GM-CSF in murine prion disease after chronic dosing with VU0424238. RT-qPCR showing the expression of pro-inflammatory cytokines (A-D) and an adaptive immunity cytokine (E) in the cortex and hippocampus of control or prion-diseased mice treated with either vehicle or VU0424238 at 10 w.p.i. Data are expressed as a ratio of α-tubulin RNA. Statistical analysis was performed using a two-way ANOVA (Dunnett's multiple comparisons), where* P≤0.05, ** P≤0.01, and **** P≤0.0001 (n=6).

Overall, these results suggest that $mGlu_5$ inhibition using VU0424238 does not significantly affect the progression of murine prion disease or prion-induced neuroinflammation.

4.2.5 The Effect of Chronic VU0424238 Treatment on PSD95 Expression

Although the levels of PSD95 were previously found to be unaltered in murine prion disease (Figure 4-6), as $mGlu_5$ is an important regulator of signalling on the postsynaptic membrane (Luján et al., 1996), its expression in control and vehicle- or VU0424238-treated prion-diseased animals was investigated using immunoblotting (Figure 4-26). These data confirmed no alteration in PSD95 protein levels in prion-diseased animals compared to controls. At all timepoints examined, there was no difference in PSD95 expression between vehicle- and VU0424238-treated animals in either the hippocampus or cortex.

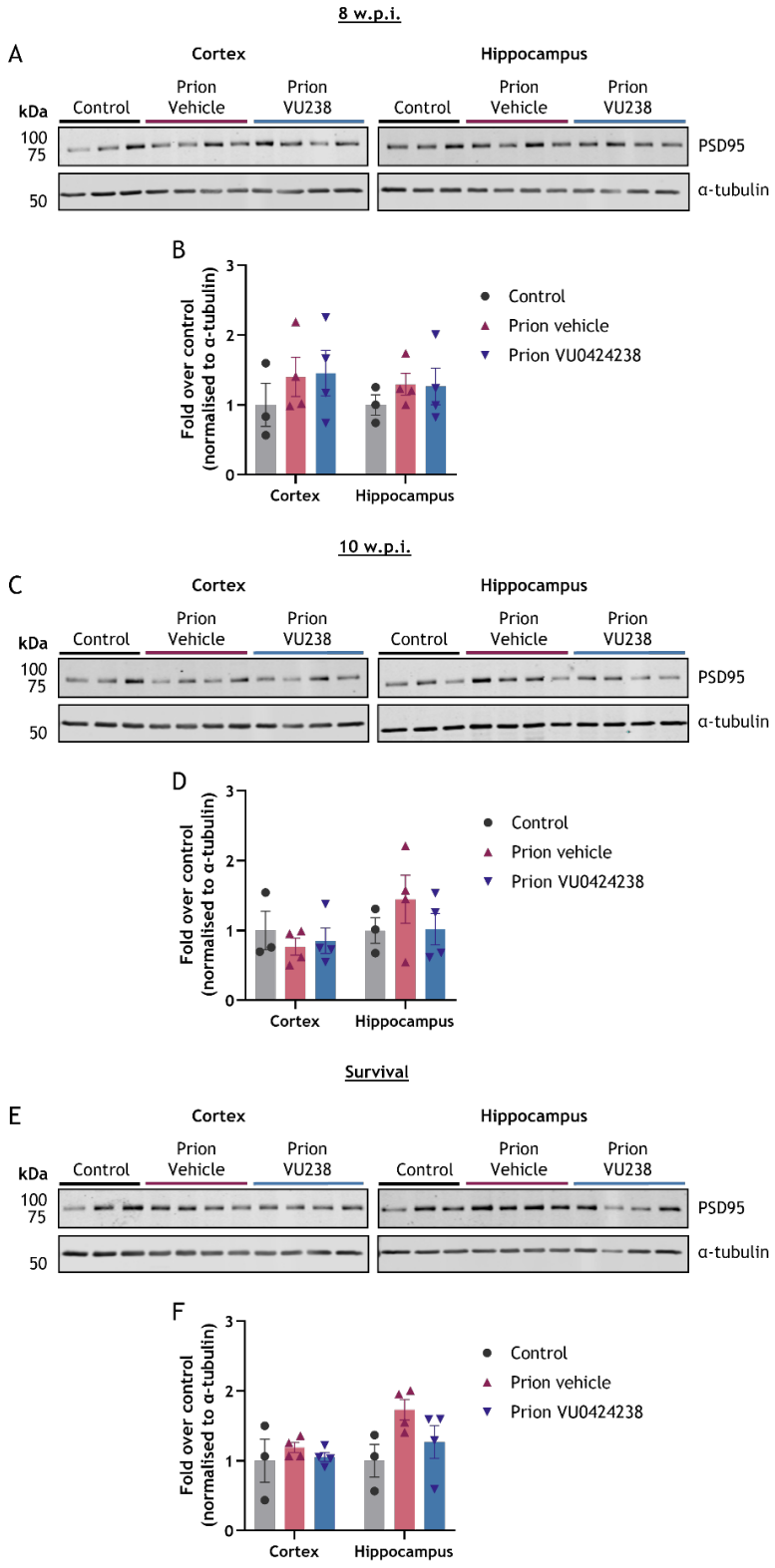

Figure 4-26 Effect of VU0424238 on PSD95 expression over time. Western blot analysis of lysates from the cortex and hippocampus of control, prion vehicle, and prion VU0424238-treated mice at 8 w.p.i. (A), 10 w.p.i. (C), and survival (E). Each lane represents a different mouse. Blots were probed with an anti-PSD95 antibody. α-tubulin was used as a loading control. Membranes were stripped and re-probed for multiple antibodies (Figure 4-13 and Figure 4-26). (B, D, F) Protein levels were normalised to the loading control, followed by normalisation to the average protein level of the control bands expressed as fold change. Data shown are means ± S.E.M. with each data point representing an individual mouse (n=3 for control, n=4 for prion vehicle and prion VU0424238). Statistical analysis was performed using a two-way ANOVA (Tukey's multiple comparisons).

4.3 Discussion

Recent preclinical evidence has suggested that targeting $mGlu_5$ may be a promising approach for treating NDDs (Budgett et al., 2022), diseases for which there are currently limited therapeutic options available to patients. Specifically, previous research has indicated that the antagonism of $mGlu_5$ is neuroprotective in rodent models of NDD (see 1.3.4.2). In this study, the therapeutic effects of $mGlu_5$ antagonism were investigated in a well-characterised model of murine prion disease, which develops as a fast and progressive AD-like disease driven by the accumulation of misfolded prion protein. Understanding the pathogenesis of murine prion disease may shed light on the mechanisms underlying the progression of human NDDs that spread in a prion-like manner and provide insights for the development of improved therapeutics for human patients.

Initially, this study aimed to validate the suitability of the murine prion disease model for investigating the effect of $mGlu_5$-targeting compounds on neuroinflammatory responses. The results confirmed elevated levels of several neuroinflammatory markers in this model (Bradley et al., 2016; Dwomoh et al., 2022). Secondly, since altered expression of $mGlu_5$ has been observed in human NDD and rodent NDD models (see section 4.1.1), this chapter aimed to examine $mGlu_5$ expression in both murine prion disease and human AD tissue. Immunoblot and RT-qPCR data revealed no significant difference between healthy and diseased tissue in either disease. Finally, this study investigated the effects of chronic antagonism of $mGlu_5$ using a $mGlu_5$ NAM, VU0424238, on the progression of murine prion disease. These data showed that VU0424238 had no significant impact on disease onset, progression, or survival of prion-diseased mice.

4.3.1 Neuroinflammation is Elevated in Murine Prion Disease

A key pathological hallmark of NDDs is a chronic neuroinflammatory response that includes the activation of glial cells, such as astrocytes and microglia (see section 1.3.2.3) (Ransohoff, 2016). Previous reports on murine prion disease have shown that prion-diseased mice display elevated markers of neuroinflammation that are seen across human NDDs, including markers of astro- and microgliosis such as GFAP, vimentin, and Iba-1 (Dwomoh et al., 2022;

Ransohoff, 2016). Unlike rodent models of other NDDs, which rely primarily on genetic modification, prion-diseased animals exhibit genuine prion disease (Makarava et al., 2011, 2015), thus providing a unique opportunity to examine glial responses in a genuine NDD. The data presented in this chapter confirmed that the murine prion disease model displays these elevated markers of neuroinflammation.

Initially, both RT-qPCR and IHC on tissue collected at 10 w.p.i showed an increase in the astrocytic markers GFAP and vimentin in prion-diseased mouse brains. Time course immunoblotting analysis showed that astrogliosis was significantly increased in the cortex and hippocampus of prion disease mice from 10 w.p.i., with a significant upregulation of the same two markers. This agrees with published data that show pronounced and widespread astrogliosis in murine prion disease (Mallucci et al., 2003; Bradley et al., 2016; Dwomoh et al., 2022). In human prion disease, astrogliosis has been reported in multiple forms of disease, including vCJD and fatal familial insomnia (Fraser et al., 2003; Frau-Méndez et al., 2017).

Under physiological conditions, astrocytes display several phenotypic profiles with distinct distribution patterns (Zeisel et al., 2018), known as astrocyte heterogeneity. Similarly, in disease conditions, reactive astrocytes can adopt multiple states depending on the context (Escartin et al., 2021). While accumulating evidence suggests that neurodegeneration can occur, at least in part, due to neuroinflammation (Ransohoff, 2016), whether these reactive astrocyte states are neuroprotective or neurotoxic remains unclear (Ferrer, 2017; Hartmann et al., 2019; Scheckel et al., 2020).

In this chapter, two astrocytic markers were used, GFAP and vimentin. These are both major constituents of astrocyte intermediate filaments and therefore share functional properties (Middeldorp & Hol, 2011; Danielsson et al., 2018). However, vimentin is thought to play a more regulatory role in astrocytes because its expression, unlike GFAP, is required for the translation of other astrocytic intermediate filaments such as nestin (Jing et al., 2007; Pekny, 2001). Although GFAP is commonly used as a marker of astrocyte reactivity (Eng et al., 1971), recent findings suggest that the expression of GFAP alone is insufficient to identify an astrocyte as reactive (Escartin et al., 2021). The upregulation of

GFAP mRNA and/or protein is a common feature of many reactive astrocytes, including those present in various NDDs (Ben Haim et al., 2015). However, GFAP expression in rodents can also be altered by physiological stimuli such as physical activity and an enriched environment (Rodríguez et al., 2013), and it has been found to change with circadian rhythms (Gerics et al., 2006). Therefore, GFAP and vimentin were used as astrocyte markers in this thesis.

The data presented in this chapter support the concept of astrocyte heterogeneity, with differences observed in GFAP and vimentin expression. Immunoblotting data showed that the expression of vimentin was significantly increased in prion-diseased mice from 10 w.p.i., whereas GFAP expression was significantly increased later at 11 w.p.i. This difference in expression is consistent with previous studies investigating the heterogeneity of astrocytes in NDD, which demonstrated some, but not full, colocalisation of GFAP and vimentin (Habib et al., 2020; Makarava et al., 2021). A study in healthy human post-mortem brain tissue found that approximately 70% of GFAP-expressing astrocytes also express vimentin (O'Leary et al., 2020). Morphologically, vimentin-expressing astrocytes differed from those expressing GFAP alone, with vimentin staining astrocytes with exceptionally long, thin processes and astrocytes with two cell bodies. Additionally, the distribution of vimentin-expressing astrocytes varied throughout the brain, unlike GFAP-expressing astrocytes which were more uniform. For example, there were approximately 5 times more vimentin-expressing astrocytes in the prefrontal cortex than the primary visual cortex (O'Leary et al., 2020). Previous work in our lab (unpublished) has found vimentin to be particularly upregulated in areas with high levels of microgliosis and spongiosis. Further work must be done to understand whether the heterogeneity in vimentin expression represents different subpopulations of reactive astrocytes, different degrees of activation, or something else altogether (Makarava et al., 2021). Previous studies have found vimentin-labelled astrocytes to be upregulated in human post-mortem tissue collected from patients with AD, ALS, multiple sclerosis, Pick's disease, and cerebral infarction (Yamada et al., 1992). In AD, these vimentin-labelled astrocytes were almost exclusively associated with Aß plaques (Yamada et al., 1992).

Although GFAP and vimentin were significantly upregulated in both the hippocampus and cortex at later disease timepoints, both markers were increased in the hippocampus at all time points examined. Interestingly, previous studies have shown region-dependent astrogliosis in prion disease. In mice infected with 22L prions, GFAP expression was increased in the hippocampus in line with PrP_{Sc} accumulation, whereas GFAP expression in the thalamus was less pronounced, despite increased PrP_{Sc} deposition (Makarava et al., 2019). This region-specific pattern was lost with disease progression and replaced with uniform GFAP expression across brain regions (Makarava et al., 2020). The work presented in this chapter supports the data described in the literature, in that astrogliosis occurred in the hippocampus at earlier timepoints than in the cortex, but became significantly upregulated in both brain regions at late-stage disease.

It is well-established that astrocytes play a role in prion propagation. PrP_{Sc} is deposited in astrocytes in both rodent prion disease models and human prion disease patients (Diedrich et al., 1991; Lasmezas et al., 1996; Na et al., 2007). PrP_C knockout mice are not susceptible to prion infection, but the astrocyte-specific expression of PrP_C can restore this susceptibility (Raeber, 1997). A number of astrocytic cell culture systems, including primary astrocytes and human induced pluripotent stem cell (iPSC)-derived astrocytes, have been able to replicate and propagate misfolded prion in culture (Cronier et al., 2004; Krejciova et al., 2017; Tahir et al., 2020). Despite the role astrocytes play in prion pathogenesis, the mechanism by which prions trigger astrogliosis is unknown.

Similarly, the data in this chapter showed an increase in the expression of microglial markers in prion-diseased mice. Immunoblotting data showed that the expression of Iba-1 was significantly increased from 10 w.p.i. in the hippocampus and 11 w.p.i. in the cortex. Microglia were first observed to be upregulated in human prion disease surrounding PrP_{Sc} deposits in Creutzfeldt-Jakob disease, Gerstmann-Sträussler-Scheinker syndrome, and kuru patients (Miyazono et al., 1991; Sasaki et al., 1993; Barcikowska et al., 1993; Guiroy et al., 1994). Similar observations have been made in prion-diseased mice, with microglia activation occurring around PrP_{Sc} deposits and in response

to PrP_{Sc} accumulation (Williams et al., 1994, 1997; Bate et al., 2002; Van Everbroeck et al., 2004; Kercher et al., 2007; Sandberg et al., 2014; Vincenti et al., 2016; Greenlee et al., 2016).

Like astrocytes, microglia take on various activated states in disease, which can be either neuroprotective or neurotoxic (Hanisch & Kettenmann, 2007). Neuroprotective microglia mediate their effects by releasing anti-inflammatory factors (Cherry et al., 2014), whereas neurotoxic microglia release pro-inflammatory factors (Block et al., 2007). In prion disease, research has shown that microglia can take on both of these phenotypes (Gómez-Nicola et al., 2013; Grizenkova et al., 2014; Sorce et al., 2014; Zhu et al., 2016; Muth et al., 2017; Carroll et al., 2018). Notably, microglia activation occurs at the early stages of prion disease, before neuronal loss and the onset of clinical symptoms (Betmouni et al., 1996; Williams et al., 1997; Baker & Manuelidis, 2003; Gómez-Nicola et al., 2013; Sandberg et al., 2014), suggesting that microgliosis is a cause, rather than a consequence, of neurodegeneration. In line with this, the chemical ablation of microglia using an inhibitor of CSF-1R, a tyrosine kinase receptor, in prion-diseased mice resulted in a significant delay in disease progression and the onset of behavioural symptoms as well as an increase in survival (Gómez-Nicola et al., 2013). On the other hand, several studies have demonstrated that microglial depletion enhances the accumulation and neurotoxicity of PrP_{Sc} in *ex vivo* models (Falsig et al., 2008; Kranich et al., 2010; Zhu et al., 2016). Using a different CSF-1R inhibitor, another group showed that microglial ablation significantly accelerated the progression of prion disease in RML, ME7, and 22L strains of prion (Carroll et al., 2018). Similarly, injecting prions into mice with fewer microglia resulted in accelerated prion disease progression (Zhu et al., 2016).

Importantly, microglia can phagocytose aggregated PrP_{Sc} *in vitro* (Aguzzi & Zhu, 2017). One emerging hypothesis is that in the early stages of prion disease, microglia are neuroprotective, phagocytosing and clearing PrP_{Sc} aggregates and secreting anti-inflammatory factors (Baker et al., 1999; Cunningham et al., 2002). However, as the disease progresses, the clearance of PrP_{Sc} becomes inefficient, resulting in sustained PrP_{Sc} accumulation and subsequent neuronal damage (Hughes et al., 2010). Moreover, chronic microglia activation shifts them

towards a pro-inflammatory state, which is likely to be detrimental to brain health (Peggion et al., 2020). This hypothesis has therapeutic relevance as it may be important to inhibit the pro-inflammatory properties of microglia at the late stages of prion disease while preserving their initial anti-inflammatory properties.

As previously mentioned, activated microglia can produce pro-inflammatory factors, such as TNF-α, IL-1ß, and IL-6, as well as anti-inflammatory factors, such as IL-10 (Ishijima & Nakajima, 2021; Smith et al., 2012). In this thesis, the anti-inflammatory cytokine IL-10 was not increased in the brains of prion-diseased mice, whereas the pro-inflammatory cytokines IL-1α, IL-1ß, IL-6, and TNF-α were found to be elevated. The expression of pro-inflammatory cytokines has been found to be significantly increased in the brains of prion-diseased mice and human CJD patients (Williams et al., 1994; Campbell et al., 1994; Kordek et al., 1996; Sharief et al., 1999; Baker & Manuelidis, 2003; Stoeck et al., 2005). The release of pro-inflammatory cytokines correlates with the onset of prion pathology and clinical symptoms (Campbell et al., 1994) and occurs predominantly in brain regions that show neuronal loss and spongiosis (Williams et al., 1994). Anti-inflammatory cytokines are also increased in human CJD patients (Stoeck et al., 2005). In mouse models of prion disease, the release of cytokines depends on the prion strain and mouse background used. For example, no IL-1ß upregulation was observed in C57BL/6J mice after inoculation with ME7 prions (Walsh et al., 2001), whereas IL-1ß is overexpressed in C57BL/6JxVM/Dk mice inoculated with ME7 prions (Brown et al., 2003).

The role of cytokines in prion pathogenesis has been investigated by infecting mouse models in which specific cytokines have been either knocked down or overexpressed. Knockout of the receptor for IL-1α and IL-1ß significantly reduced disease progression (Schultz et al., 2004; Tamgüney et al., 2008), suggesting that these cytokines may play a harmful role in prion disease. Conversely, knockout of IL-10 in prion-diseased mice (129Sv background) accelerated prion disease progression (Thackray et al., 2004), suggesting a neuroprotective role in prion disease. This benefit is dependent on the mouse genetic background as knockout of IL-10 in prion-diseased C57Bl/6 mice slowed the progression of prion disease (Tamgüney et al., 2008). These findings

highlight a complex, content-dependent role of cytokines in prion disease, which must be considered when developing novel therapeutics for NDDs.

Two other inflammatory markers were investigated in this chapter, MCP-1 and GM-CSF. Expression of the pro-inflammatory chemokine MCP-1 is upregulated in line with disease progression in mice infected with ME7 prions (Felton et al., 2005) and was observed to be upregulated in this thesis. However, deficiency in MCP-1 or its receptor, CCR2, does not alter prion disease progression (Felton et al., 2005; Gómez-Nicola et al., 2014; O'Shea et al., 2008; Tamgüney et al., 2008). GM-CSF is a monomeric glycoprotein that has been shown to improve cognition and reduce amyloid-related pathology in an AD mouse model (Boyd et al., 2010; Kiyota et al., 2018). These findings are surprising, considering GM-CSF is usually defined as a pro-inflammatory cytokine as it upregulates several other pro-inflammatory cytokines, such as IL-6 and TNF-α (Bhattacharya et al., 2015). In this chapter, GM-CSF was upregulated in the brains of prion-diseased mice, a finding which has been reported previously (Tribouillard-Tanvier et al., 2009).

Overall, these findings validate these markers of neuroinflammation as neuropathological markers for both neurodegeneration and inflammation in the subsequent dosing study with the $mGlu_5$ NAM VU0424238.

4.3.2 The Expression of the Synaptic Marker PSD95 is Unaltered in Murine Prion Disease

Neuronal loss, and the loss of synapses, are common hallmarks of neurodegenerative diseases such as AD (Scheff et al., 1990, 2006). Similarly, neuronal loss is observed in prion-diseased mice (Bradley et al., 2016) and human prion-diseased patients (Budka, 2003). In addition to neuronal loss, neuronal dysfunction in NDD can also be due to synaptic loss or dysfunction (Gorman, 2008). The postsynaptic density (PSD) on the postsynaptic membrane of excitatory synapses is an important region for synaptic plasticity (Sheng & Kim, 2011). This region is enriched in scaffolding proteins such as PSD95, which binds to a number of membrane proteins, including ionotropic glutamate receptors and voltage-gated potassium channels (Fukata et al., 2021), and plays a crucial role in the regulation of excitatory signalling and plasticity (Béïque & Andrade, 2003). In human AD patients, studies into PSD95 expression have given

contradictory results, with some showing increased expression (Gong et al., 2009; Leuba et al., 2008), some showing decreased expression (Gylys et al., 2004; Love et al., 2006; Proctor et al., 2010), and some showing no change in expression (Dracheva et al., 2001). In AD rodent models, the expression of PSD95 is consistently reduced during disease progression (Savioz et al., 2014). In prion-diseased animals, a reduction in PSD95 expression has been observed from 9 w.p.i. in RML-infected Tg37 mice (Moreno et al., 2012) and at the terminal disease stage in RML-infected CD1 mice (Boese et al., 2016). In RML-infected Tg37 mice, this reduction in PSD95 was associated with deficits in hippocampal synaptic transmission and burrowing behaviour (Moreno et al., 2012). Conversely, C57BL/6J mice injected with 22L prions found PSD95 to be upregulated at an early disease stage (Ojeda-Juárez et al., 2022). However, this study provided no longitudinal data on the expression of PSD95. Consistent with unpublished work from a previous PhD student in our lab, no change in PSD95 expression was observed in prion-diseased mice in this thesis. Similar observations have been made in sporadic CJD patients, with immunoblot analysis showing no change in PSD95 expression in the occipital cortex of diseased patients as compared to controls (Ojeda-Juárez et al., 2022). In the data presented in this thesis, PSD95 showed high variability in the expression level in prion-diseased mice, particularly in the cortex, and therefore larger sample sizes would be required in the future for statistically powered analysis. Moreover, additional neuronal and synaptic markers could be used to examine whether the unaltered PSD95 levels were separate from overall synaptic loss.

4.3.3 The Expression of $mGlu_5$ is Unaltered in Murine Prion Disease

There is high expression of $mGlu_5$ in brain regions most affected by AD, such as the cortex and hippocampus (Shigemoto et al., 1993). Furthermore, it has been suggested that alterations in $mGlu_5$ expression could be involved in AD pathogenesis (Hamilton et al., 2014; Overk et al., 2014). In this chapter, time course immunoblotting and RT-qPCR experiments showed no difference in the expression of $mGlu_5$ in the hippocampus or cortex throughout prion disease progression. This finding contrasts with previous research which reported a reduction in $mGlu_5$ expression in prion-diseased mice and hamsters at the disease endpoint (Hu et al., 2022). It may be that $mGlu_5$ expression depends on

the prion strain and mouse genetic background used considering Hu and colleagues (2022) inoculated C57Bl/6J mice with 139A and ME7 prion strains, whereas this study inoculated Tg37 mice with RML prions. Of note, in Chapter 5, no change in $mGlu_5$ expression was observed at the terminal disease endpoint in C57Bl/6J mice inoculated with RML prions, confirming the data presented in this chapter. As a number of studies in other neurodegenerative disease models have found alterations in $mGlu_5$ expression on the surface of cells without a change in total $mGlu_5$ expression (Abd-Elrahman et al., 2018; Hamilton et al., 2014; Martín-Belmonte et al., 2021; Um et al., 2013), future work would include investigating this same phenomenon in murine prion disease.

As discussed in section 4.1.1, the expression of $mGlu_5$ in human neurodegenerative disease varies depending on the disease and timepoint investigated. For AD, PET imaging showed a significant reduction in $mGlu_5$ expression in the hippocampus of mild AD patients with a non-significant reduction in the cortex (Mecca et al., 2020), whereas *in vitro* autoradiography on post-mortem slices from patients with severe AD showed an increase in $mGlu_5$ expression in the hippocampus and cortex (Müller Herde et al., 2019). As these studies were carried out in early- and late-stage disease, respectively, their results are not necessarily contradictory, as it may be that $mGlu_5$ expression changes throughout disease progression. In this chapter, RT-qPCR was performed on samples collected from 5 AD and 5 control patients at post-mortem and found no significant differences in $mGlu_5$ expression between disease and control tissue. It is difficult to compare the results of this post-mortem study with the previously mentioned *in vitro* autoradiography study as the authors provided no demographic information on their patient samples (Müller Herde et al., 2019). Moreover, *in vitro* autoradiography measures protein levels, whereas RT-qPCR measures mRNA levels. Gene expression levels do not directly correlate with protein expression levels; therefore, the data cannot be directly compared (Murgaš et al., 2022). A recent study compared *in vitro* autoradiography data on the density of 15 different receptors, including AMPA and NMDA receptors, to mRNA expression data from the Allen Human Brain Atlas and found that the correlation between protein density and mRNA expression varied greatly depending on the receptor, with most receptors having a weak correlation (Murgaš et al., 2022). Following this study, another group investigated the

relationship between protein density and mRNA expression levels of 14 neurotransmitter receptors in the human hippocampus, including $mGlu_2$ and $mGlu_3$ receptors (Zhao et al., 2023). A key advantage of this study was that samples for autoradiography and RNA quantification were obtained from the same hippocampus samples. The results showed a weak correlation between protein densities and RNA expression across most receptors investigated in the hippocampus, including $mGlu_2$ and $mGlu_3$ receptors. Although $mGlu_5$ was not investigated in the correlation study, this may partially explain the differences in the $mGlu_5$ mRNA levels reported in this thesis and the protein expression level reported in the literature (Müller Herde et al., 2019). This poor correlation may be due to factors such as post-translational modifications, protein folding and trafficking, and different mRNA and protein degradation rates (Stephenson et al., 2008; Buccitelli & Selbach, 2020; Levitz et al., 2016; Payne, 2015; Schwappach, 2008).

4.3.4 Chronic VU0424238 Treatment Does Not Alter the Progression of Murine Prion Disease

Next, this study investigated the ability of VU0424238, a $mGlu_5$ NAM, to modulate the progression of murine prion disease. Firstly, the effect of VU0424238 on the burrowing behaviour of female control and prion-diseased mice was examined. The burrowing paradigm is commonly used to monitor the progression of murine prion disease (Deacon, 2006; Mallucci et al., 2007, 2009), and treatment with other GPCR-targeting ligands, such as PAMs targeting the M1 muscarinic receptor, have been shown to reverse deficits in burrowing behaviour (Bradley et al., 2016; Dwomoh et al., 2022). In this study, prion-diseased mice exhibited a significant decline in their burrowing ability from 9 w.p.i., consistent with what has previously been reported in the literature (Bradley et al., 2016; Dwomoh et al., 2022; Mallucci et al., 2003, 2007). However, no difference was seen in the burrowing behaviour of vehicle- and VU0424238-treated prion-diseased mice in this study, demonstrating that chronic VU0424238 treatment from 4 w.p.i. does not affect the burrowing behaviour of prion-diseased mice. Moreover, chronic VU0424238 treatment did not alter the time of symptom onset or the survival of prion-diseased mice.

PrP_{Sc} aggregation is a major pathological feature of murine prion disease (Bradley et al., 2016; Dwomoh et al., 2022), and targeting prion protein misfolding and accumulation will likely be important for developing effective disease-modifying therapeutics. The misfolding and prion-like spread of specific proteins is a key hallmark of most NDDs (Halliday & Mallucci, 2015). Previously, the antagonism of $mGlu_5$ has been shown to reduce the accumulation of misfolded proteins in rodent models of AD, HD, and ALS (Um et al., 2013; Hamilton et al., 2014, 2016; Abd-Elrahman et al., 2017, 2018, 2020). However, in this study, PrP_{Sc} levels were not affected by VU0424238 treatment, indicating that VU0424238 did not alter prion clearance. Taken together, these results show that chronic VU0424238 treatment did not alter the progression of murine prion disease.

As previously discussed (section 4.2.1), the astrocytic markers GFAP and vimentin, and the microglia marker Iba-1 are increased in the cortex and hippocampus of prion-diseased mice, significantly in late-stage disease. Western blot and RT-qPCR analysis of cortical and hippocampal tissue from both male and female prion-diseased mice found that VU0424238 did not alter these elevated levels, indicating continued neuroinflammation. While protein and gene expression analysis are good methods to investigate functional diversity, these methods lack the ability to focus on changes in smaller defined regions of interest. Instead, they provide insight into expression levels across a population of cells in a larger brain region, for example, the whole hippocampus. IHC, on the other hand, allows for the analysis of particular areas of interest, revealing more detailed patterns of neuroinflammation. Closer analysis of the brains of male and female prion-diseased mice revealed that VU0424238 significantly reduced GFAP expression in the CA1 and CA3 hippocampal regions of female, but not male, prion-diseased mice. As previously discussed, it is documented in the literature that male and female rodent models of neurodegeneration respond differently to $mGlu_5$ modulation (Abd-Elrahman et al., 2020a; Bonifacino et al., 2019; Milanese et al., 2021) so this finding, although novel, is not surprising. However, despite a reduction in inflammation in the brains of female prion-diseased mice, VU0424238 did not alter the progression of murine prion disease as neither sex of mouse showed an extension in their lifespan or a

reduction in prion load, nor did female mice have any improvement in behavioural deficits.

In contrast to the work presented here, the oral administration of MPEP to prion-diseased mice has been shown to significantly improve locomotor abilities, prolong survival, and decrease hippocampal GFAP staining in male prion-diseased mice (Goniotaki et al., 2017). However, PrP_{Sc} accumulation was not reduced, similar to the data shown in this thesis. There are a few possible explanations for the differences in the results of these studies. In both studies, mice began treatment before the onset of pathology, however, MPEP treatment began earlier than VU0424238 treatment: mice were given MPEP in their food from the same date as prion inoculation, whereas in this study, VU0424238 treatment began 4 weeks after prion inoculation. It may be that earlier treatment with VU0424238 would have had some benefit. A further key difference between the two studies is the mouse genetic background. In this study, Tg37 mice were used, which overexpress PrP_C to a level three times above wild-type (Mallucci et al., 2003). Once inoculated with RML prions, these mice survive for 11-12 weeks. Conversely, the MPEP study used C57BL/6J wild-type mice which once inoculated with RML prions survive for 22-25 weeks. It may not be possible to identify the subtle positive effects observed in previous studies in the more aggressive, short-term disease model used in this thesis.

There are several limitations to the VU0424238 dosing study. Prion inoculation experiments were performed with an appropriate number of animals (n=18-22 per group for survival studies and n=10-16 for timepoint experiments). At each timepoint (8 and 10 w.p.i. and survival), animals were randomly divided into subgroups for either biochemical analysis (n=6-8) or histology (n=4-8). However, analysis of the sexes separately resulted in relatively small n numbers (n=3-5 mice per group). Another limitation is that the behavioural analysis was carried out on female mice only. Male prion-diseased mice tend to exhibit aggressive behaviour when returned from experimental cages (1 mouse per cage) to their home cages (4-5 mice per cage), resulting in injuries and stress-related behavioural changes (Weber et al., 2022). Therefore, only female mice were used in the burrowing paradigm in this study, and behaviour in VU0424238-treated male mice remains unexamined. A third limitation is the

time at which treatment with VU0424238 began. In this study, VU0424238 treatment began at 4 w.p.i., before any pathology or symptoms were evident to investigate if VU0424238 could prevent the progression of murine prion disease. Evidence suggests that involvement of $mGlu_5$ in AD is disease stage-dependent. In APPswe mice, when CTEP was administered from the age of 6 months for 24 weeks, CTEP significantly reduced AD pathology and reversed memory deficits. However, extending CTEP treatment to 36 weeks proved ineffective at reversing AD pathology or memory deficits (Abd-Elrahman et al., 2020b). The authors proposed that the contribution of $mGlu_5$ to AD-related pathology is reduced at advanced disease stages. A similar phenomenon may be at play in murine prion disease, and the specific timing of drug treatment may be important. Notably, drug treatment before symptom onset, as seen in this study, does not represent what would happen in a clinical situation where treatment is likely to begin after the onset of symptoms when pathology is more severe. To better predict the usefulness of $mGlu_5$ inhibition in a clinical context, treating mice after the onset of symptoms would have been more informative. Moreover, as prions exist in many strains (Collinge et al., 1996), it cannot be excluded that $mGlu_5$ modulation using VU0424238 may have altered prion disease progression in the context of a different prion strain.

4.4 Conclusion

Overall, the results presented in this chapter suggest that the antagonism of $mGlu_5$ using the $mGlu_5$ NAM VU0424238 does not alter the progression of murine prion disease. Since data presented in Chapter 3 demonstrated that VU0424238 was able to sufficiently occupy $mGlu_5$ receptors at a concentration of 10 mg/kg and that this concentration was effective at altering behaviour in a marble burying assay, we can be confident that this compound is efficacious *in vivo*. However, chronic treatment with VU0424238 did not significantly alter any of the disease markers examined in this model of NDD. It cannot be excluded that this compound may have been beneficial in a different model of NDD.

To further explore the potential of $mGlu_5$ as a therapeutic target for the treatment of NDDs, Chapter 5 investigates whether the progression of murine prion disease is altered in $mGlu_5$ homo- and heterozygous knockout mice as compared to wild-type controls.

Chapter 5 Characterising the Impact of $mGlu_5$ Knockout on the Progression of Neurodegenerative Disease

5.1 Introduction

Previous studies have highlighted the potential of $mGlu_5$ as a drug target for treating NDDs (Budgett et al., 2022). There is an immediate need to identify and validate novel targets that are able to modify the progression of these diseases. Chapter 4 investigated the effects of chronic treatment with a $mGlu_5$ NAM on the progression of murine prion disease. These results showed that the $mGlu_5$ NAM, VU0424238, did not alter disease onset, progression, or the survival of diseased mice. The study detailed in this chapter aimed to understand the effect of $mGlu_5$ depletion on the progression of neurodegenerative disease by inoculating $mGlu_5$ homo- and heterozygous knockout mice, as well as wild-type controls, with prion disease. The knockout of $mGlu_5$ in mouse models of AD, HD, and ALS has previously been shown to be neuroprotective (Hamilton et al., 2014; Ribeiro et al., 2014; Bonifacino et al., 2017, 2019), suggesting that $mGlu_5$ plays a key role in disease pathology across a spectrum of NDD.

5.1.1 The Use of Knockout Models in Target Validation

Taking a drug to market is a long and expensive process, with as little as 10% of tested compounds gaining approval from regulatory bodies (Sun et al., 2022). It is estimated that ~75% of research and development budgets are spent on developing compounds that are never approved due to reasons such as poor efficacy and adverse side effects at clinical trial (Zuberi and Lutz, 2016). Effective target validation at early stages of the drug development process could vastly reduce the failure of clinical trials (Paul et al., 2010). The primary goal of target validation is to understand gene function *in vivo* in both normal physiology and disease (Hughes et al., 2011). Knockout animal models are an invaluable tool in this process. By deleting a target gene, researchers can provide a rationale for drug development by showing that mutations lead to a specific phenotype or disease state. With the correct design, these studies can assess the safety of potential drugs by highlighting any toxic effects of mutating the target gene. Successful animal studies can greatly improve confidence in a potential drug target and hopefully lead to breakthrough therapeutics.

However, it is important to note that there are limitations to the use of knockout animals in target validation. For example, the relevance of knockout

animal models for common human diseases has been brought into question by the failure to translate findings of preclinical animal studies into successful human clinical trials (Pound and Ritskes-Hoitinga, 2018). Although mice and humans share approximately 99% of the same genes (Capecchi, 2005), it cannot be assumed that the function of a gene in one is translatable to the other. Some knockout animals do not display a unique phenotype, which can be due to redundancy (i.e., two genes having similar or identical functions) (Barbaric et al., 2007). This can make it challenging to identify the function of the gene of interest. The most severe phenotypic consequence of genetic knockout is lethality, and approximately 25% of genetic knockouts in mice are developmentally lethal (Du, 2020; Wu et al., 2019). In some cases, loss of gene expression during development can have a knock-on effect on adult phenotypes, particularly if the gene is involved in numerous developmental processes (Cardoso-Moreira et al., 2019). In order to overcome these limitations, conditional knockout animals can be used, which allow for the targeting of a gene at a specific timepoint or in a specific tissue (Friedel et al., 2011; Kos, 2004).

5.1.2 The Effect of $mGlu_5$ Knockout in Preclinical Models of Neurodegeneration

As discussed in section 1.2.6, $mGlu_5$ plays a role in normal cognitive function, specifically in regulating synaptic plasticity and long-term potentiation (Rodrigues et al., 2002), motor coordination (Kinney et al., 2003; Jew et al., 2013), social behaviour (Zoicas and Kornhuber, 2019), anxiety, and depression (Esterlis et al., 2018). These functions are altered in NDDs (Gale et al., 2018).

Several studies have shown that the specific knockout of $mGlu_5$ in rodent models of neurodegeneration results in disease-modifying effects and cognitive improvements. The knockout of $mGlu_5$ has been shown to reverse memory deficits in the Morris water maze in an AD mouse model (Hamilton et al., 2014) and improve motor coordination in HD and ALS mouse models (Ribeiro et al., 2014; Bonifacino et al., 2019). Importantly, evidence suggests that $mGlu_5$ knockout reduces levels of the specific misfolded proteins that are considered to be classical hallmarks of each NDD. For example, in an APPswe/PS1 AD model crossed with a $mGlu_5$ knockout mouse line, a significant decrease in Aß

aggregates and plaque number was observed (Hamilton et al., 2014). Similarly, in a *Hdh*$^{Q111/Q111}$ HD model crossed with a mGlu$_5$ knockout mouse line, the size of mHTT aggregates was reduced (Ribeiro et al., 2014). In both these models, as well as *SOD*^{G93A} ALS mice, the knockout of mGlu$_5$ led to a significant reduction in neuroinflammation, specifically astrocyte and microglia activation (Hamilton et al., 2014; Ribeiro et al., 2014; Bonifacino et al., 2017, 2019). These knockout studies not only suggest that mGlu$_5$ could be a potential target for the treatment of NDDs, but they also highlight a possible role for mGlu$_5$ in disease pathology, as discussed below.

In a mouse model of AD, the most common NDD (Gustavsson et al., 2023), the activation of mGlu$_5$ has been shown to modulate the activity and expression of fragile X mental retardation protein (FMRP). FMRP is an RNA-binding protein that plays a role in APP processing (Westmark and Malter, 2012). As discussed in section 1.3.2.1, APP is a key protein in AD, with its cleavage resulting in the Aß peptides that aggregate into plaques (Zhang et al., 2011). The genetic deletion of mGlu$_5$ significantly reduced FMRP expression in APPswe/PS1 mice, subsequently reducing Aß formation (Hamilton et al., 2014).

In both AD and HD, mGlu$_5$ plays a role in disease pathology *via* the modulation of autophagy, a process by which protein aggregates are cleared (Nixon, 2013). The reduction in disease pathology observed in AD and HD mice following the genetic deletion of mGlu$_5$ (see 1.3.4.2) is accompanied by an increase in autophagy in the brain. This increase in autophagy is specifically attributed to increased ULK-1 signalling and reduced ZBTB16 expression (see 1.2.6.2), which subsequently rescued the function of specific autophagy factors such as autophagy-related proteins 13 and 14 (ATG13 and ATG14) and the autophagy marker p62 (Abd-Elrahman et al., 2017, 2018). The activation of autophagy correlated with the clearance of neurotoxic aggregates and thus highlights a key role of mGlu$_5$ in NDD.

In HD, the knockout of mGlu$_5$ from BACHD mice has been shown to decrease CREB signalling in the hippocampus (de Souza et al., 2022). CREB is a transcription factor that modulates memory formation (Silva et al., 1998). Downstream of CREB signalling is BDNF, a key modulator of synaptic loss and cognitive decline in ageing (Molinari et al., 2020). BACHD mGlu$_5$ knockout mice

have reduced levels of BDNF mRNA as compared to wild-type mice (de Souza et al., 2020). As these genes are relevant to memory formation in the hippocampus (Silva et al., 1998; Molinari et al., 2020), their reduction in $mGlu_5$ knockout mice highlights the important role that $mGlu_5$ plays in the modulation of essential memory-related proteins.

In addition, the genetic ablation of $mGlu_5$ in BACHD mice has highlighted the role $mGlu_5$ plays in the modulation of REST/NRSF expression (de Souza et al., 2020). In HD, REST/NRSF expression reduces the transcription of several neuronal genes (including BDNF) in the nucleus of diseased cells. BACHD $mGlu_5$ knockout mice have reduced REST/NSRF expression at both the protein and mRNA levels (de Souza et al., 2020), suggesting that $mGlu_5$ is a regulator of REST/NSRF signalling in HD.

Moreover, as previously discussed in section 1.3.4.1, the toxic, misfolded proteins that are a hallmark of NDDs bind to and activate $mGlu_5$, including Aß oligomers in AD (Um et al., 2013), mHTT in HD (Anborgh et al., 2005), and α-synuclein in PD (Ferreira et al., 2017). This has been suggested as a mechanism *via* which these misfolded proteins cause excitotoxicity in a diseased brain (Tang et al., 2003; Renner et al., 2010; Um et al., 2013; Ferreira et al., 2017). Therefore, it could be hypothesised that the knockout of $mGlu_5$ could slow the progression of disease pathology by disrupting this signalling mechanism and subsequent excitotoxicity.

Importantly, these studies demonstrate that $mGlu_5$ contributes directly to disease pathology across a number of NDDs and is implicated in a range of mechanisms found across these diseases. The neuroprotective effects of knocking out $mGlu_5$ highlight this receptor as a promising therapeutic target for treating NDD.

5.1.3 Aims

The aims of this chapter are to:

1. Characterise the biochemical properties and behaviour of $mGlu_5$ wild-type ($mGlu5^{+/+}$), heterozygous knockout ($mGlu5^{+/-}$), and homozygous knockout ($mGlu5^{-/-}$) C57 mice.

2. Define the impact of $mGlu_5$ deficiency on the progression of murine prion disease.

5.2 Results

5.2.1 Characterisation of $mGlu_5$ Deficient Mice

To investigate the effects of $mGlu_5$ knockout on the progression of murine prion disease, a pre-existing $mGlu_5$ knockout C57 mouse line was used (kindly provided by S Ferguson). Receptor expression in $mGlu5^{+/+}$, $mGlu5^{+/-}$, and $mGlu5^{-/-}$ mice was confirmed using immunoblot analysis which showed a complete loss of $mGlu_5$ receptor expression in $mGlu5^{-/-}$ mice (Figure 5-1A). As expected, the density of $mGlu_5$ expression was lower in $mGlu5^{+/-}$ mice compared to $mGlu5^{+/+}$ mice (Figure 5-1B).

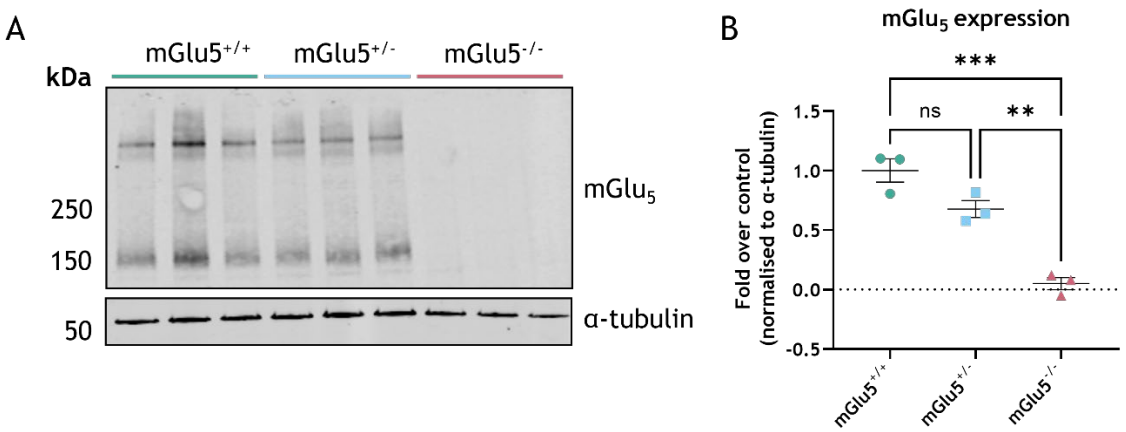

Figure 5-1 Confirmation of $mGlu_5$ receptor expression in $mGlu_5$ wild-type, hetero-, and homozygous knockout C57 mice. (A) Immunoblot analysis of membrane lysates prepared from the cortex of $mGlu_5$ wild-type ($mGlu5^{+/+}$), heterozygous knockout ($mGlu5^{+/-}$), and homozygous knockout ($mGlu5^{-/-}$) C57 mice. An antibody against $mGlu_5$ was used to probe for $mGlu_5$ expression. The loading control used was α-tubulin. Each lane is a sample from an individual mouse (n=3). The quantification of (A) is shown in (B). Protein levels were normalised to the loading control, and data are expressed as fold over control ($mGlu5^{+/+}$). Data are shown as mean ± S.E.M. with points representing an individual mouse (n=3). Statistical analysis performed was an ordinary one-way ANOVA (Tukey's multiple comparisons), where ** P≤0.01 and *** P≤0.001. ns = non-significant.

As previous studies have found that $mGlu_1$ expression is elevated in $mGlu_5$ knockout mice (Goniotaki et al., 2017), $mGlu_1$ expression was investigated in the cortex and hippocampus of the $mGlu5^{+/+}$, $mGlu5^{+/-}$, and $mGlu5^{-/-}$ mice used in this study. Using an anti-$mGlu_1$ antibody, immunoblot analysis showed that $mGlu_5$ deficiency did not alter the protein levels of $mGlu_1$ in these mice (Figure 5-2). However, a limitation of this experiment is that there are extra bands visible in the $mGlu5^{-/-}$ samples. There was no $mGlu_1$ knockout tissue available to be used as a control to confirm the specificity of the $mGlu_1$ antibody. As

immunoblot analysis is semi-quantitative, RT-qPCR could have been carried out to improve this dataset and confirm that there is no difference in $mGlu_1$ expression between the samples.

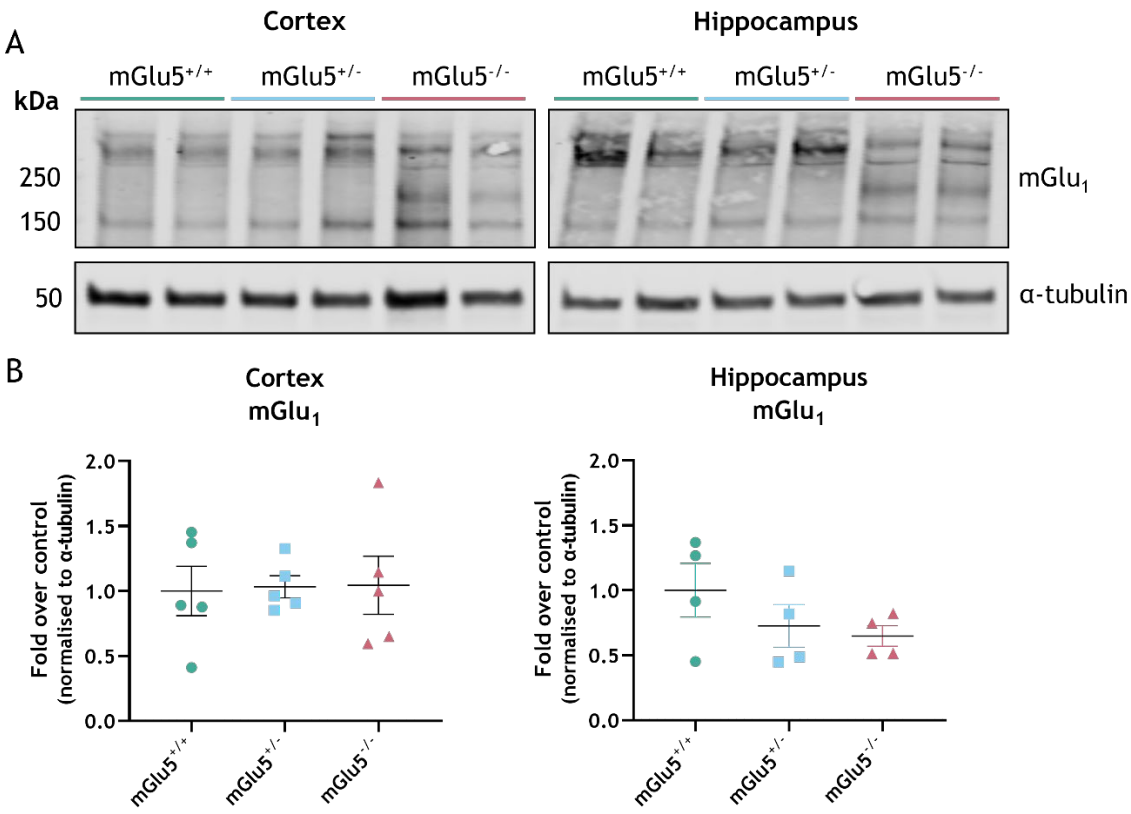

Figure 5-2 The expression of $mGlu_1$ is unaltered in $mGlu_5$ wild-type, hetero-, and homozygous knockout C57 mice. (A) Immunoblot analysis of membrane lysates prepared from the cortex or hippocampus of $mGlu_5$ wild-type ($mGlu5^{+/+}$), heterozygous knockout ($mGlu5^{+/-}$), and homozygous knockout ($mGlu5^{-/-}$) C57 mice. Representative blots are shown, with each lane containing a sample from an individual mouse. An antibody against $mGlu_1$ was used to probe for $mGlu_1$ expression. The loading control used was α-tubulin. The quantification of (A) is shown in (B). Protein levels were normalised to the loading control, and data are expressed as fold over control ($mGlu5^{+/+}$). Data are shown as mean ± S.E.M. with points representing an individual mouse (n=4-5; cortex, n=2 female, n=3 male; hippocampus, n=2 female, n=2 male).

To assess whether $mGlu_5$ deficiency in C57 mice influenced the expression of PrP_C, immunoblot analysis was performed on tissue collected from $mGlu5^{+/+}$, $mGlu5^{+/-}$, and $mGlu5^{-/-}$ mice using an anti-PrP antibody. The expression level of PrP_C is a major determining factor for susceptibility to prion disease and the rate of disease progression (Büeler et al., 1994; Mallucci et al., 2003), and therefore any regulation of PrP_C by $mGlu_5$ could confound the interpretation of any potential results The results showed that $mGlu_5$ deficiency did not alter PrP_C protein levels in the cortex or hippocampus of these mice (Figure 5-3).

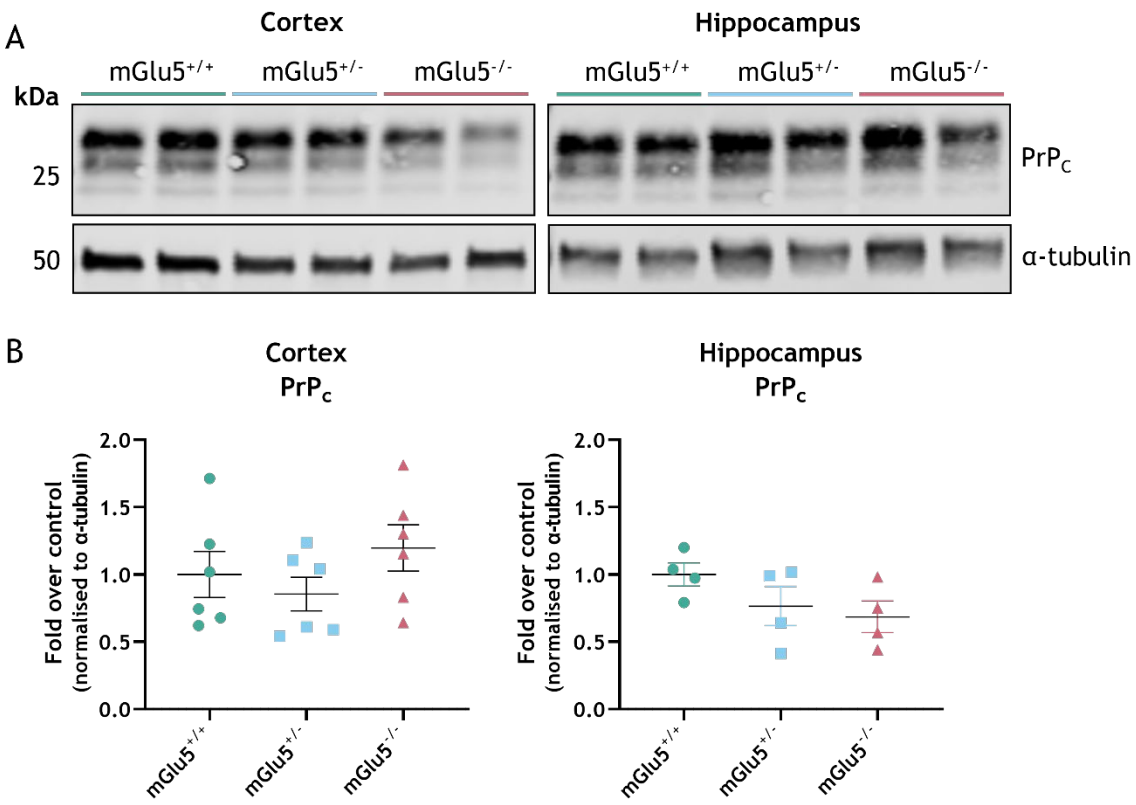

Figure 5-3 The expression of PrP_C is unaltered in $mGlu_5$ wild-type, hetero-, and homozygous knockout C57 mice. (A) Immunoblot analysis of membrane lysates prepared from the cortex and hippocampus of $mGlu_5$ wild-type ($mGlu5^{+/+}$), heterozygous knockout ($mGlu5^{+/-}$), and homozygous knockout ($mGlu5^{-/-}$) C57 mice. Representative blots are shown here, with each lane containing a sample from an individual mouse. An antibody against PrP was used to probe for PrP_C expression. The loading control used was α-tubulin. The quantification of (A) is shown in (B). Protein levels were normalised to the loading control, and data are expressed as fold over control ($mGlu5^{+/+}$). Data are shown as mean ± S.E.M. with points representing individual mice (n=4-6; cortex, n=3 female, n=3 male; hippocampus, n=2 female, n=2 male).

Next, the effect of $mGlu_5$ deficiency on *in vivo* behavioural phenotypes was investigated using an open field test (Figure 5-4A). It has been suggested that $mGlu_5$ plays a role in locomotor (Gray et al., 2009; Hamilton et al., 2014; Ribeiro et al., 2014) and anxiety behaviour (Tatarczyńska et al., 2001; Belozertseva et al., 2007; Inta et al., 2013). Several parameters can be measured using an open field test, including locomotor activity, exploration, and emotional behaviour (Võikar and Stanford, 2023). Locomotor activity is commonly measured as the total distance travelled around the test arena. Avoidance of the centre zone is indicative of anxiety-like behaviour, with “anxious” animals spending more time exploring the walls of the test arena (Lipkind et al., 2004). Here, no difference was found in the locomotor activity of $mGlu5^{+/+}$, $mGlu5^{+/-}$, and $mGlu5^{-/-}$ mice, with all genotypes travelling a similar distance in the test arena (Figure 5-4B).

Two measurements of anxiety-like behaviour were measured: time spent and distance travelled in the centre zone. There was no difference in either parameter and, therefore, anxiety-like behaviour between genotypes (Figure 5-4C-D). The results indicated that $mGlu_5$ deficiency did not alter the locomotor and anxiety-like behaviour of mice in a novel environment. The open field test is a relatively simple and quick test of anxiety-like behaviours, and further experiments in other anxiety tests (e.g., elevated plus maze) would be needed to confirm the effect of $mGlu_5$ deficiency on this behaviour.

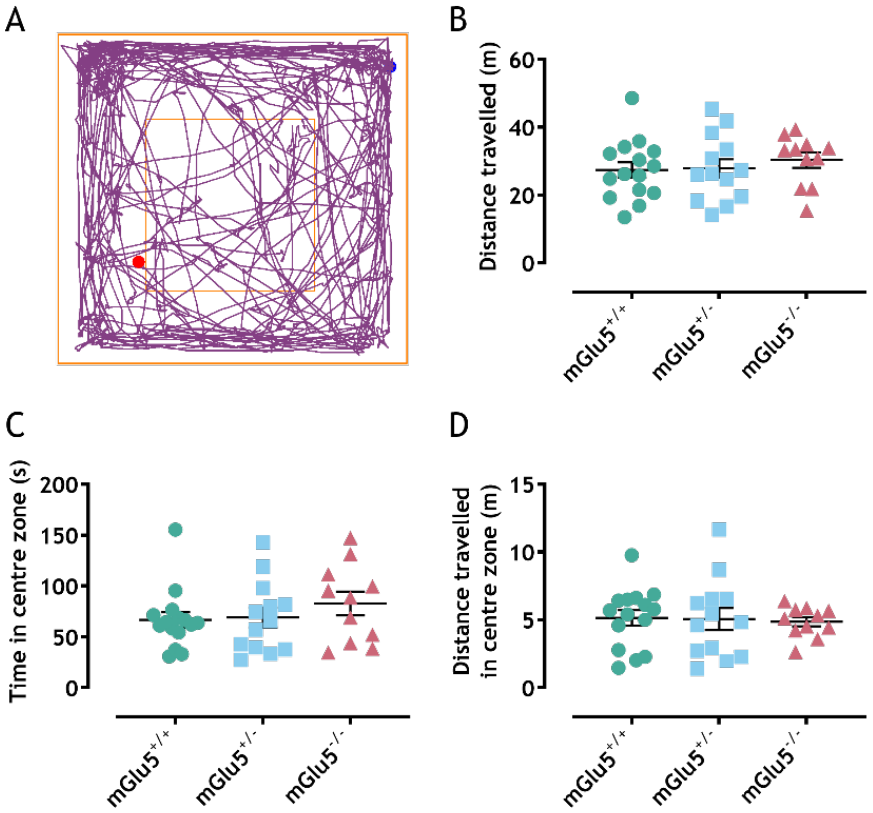

Figure 5-4 Assessment of the behaviour of $mGlu_5$ wild-type, hetero-, and homozygous knockout mice in an open field test. (A) A representative image of the typical pattern of activity of a mouse in the open field test, measured using ANY-maze software. The red dot represents the location of the mouse's head, and the purple line represents its movement. Using ANY-maze software, the locomotor activity (B) and anxiety levels (C) and (D) of $mGlu_5$ wild-type ($mGlu5^{+/+}$) (n=15), heterozygous knockout ($mGlu5^{+/-}$) (n=13), and homozygous knockout ($mGlu5^{-/-}$) (n=11) C57 mice in the open field test was calculated, as measured by total distance travelled (B), time spent in the centre zone (C), and distance travelled in the centre zone (D). Data are shown as means ± S.E.M, with points representing individual mice.

5.2.2 Characterisation of $mGlu_5$ Deficient Mice Inoculated with Murine Prion Disease

As discussed in section 4.1.1, the expression of $mGlu_5$ can be altered by various forms of neurodegeneration (Anneser et al., 2004; Vermeiren et al., 2006; Lim et al., 2013; Shrivastava et al., 2013; Fulmer et al., 2014). In Chapter 4, the expression of $mGlu_5$ was found to be unaltered in prion-diseased Tg37 mice. To test whether prion disease alters $mGlu_5$ expression in C57 mice, the brains of prion-diseased C57 $mGlu5^{+/+}$ mice were collected when they reached a terminal disease endpoint. C57 $mGlu5^{+/+}$ mice inoculated with normal brain homogenate and collected at the same time point were used as controls. The expression of $mGlu_5$ was initially assessed using immunoblot analysis on cortical and hippocampal tissue from control and prion-diseased mice, which showed no significant difference in $mGlu_5$ expression (Figure 5-5A-B).

Subsequently, RT-qPCR was carried out using cortical and hippocampal tissue collected at survival and at 8 w.p.i., to investigate whether $mGlu_5$ expression changes with disease progression. There was no difference in $mGlu_5$ gene expression (*Grm5*) between control and prion-diseased mice at either 8 w.p.i., or at survival in either brain region (Figure 5-5C-D). These results show that $mGlu_5$ protein and gene expression is unaltered in murine prion disease as compared to control, which agrees with the data in Chapter 4.

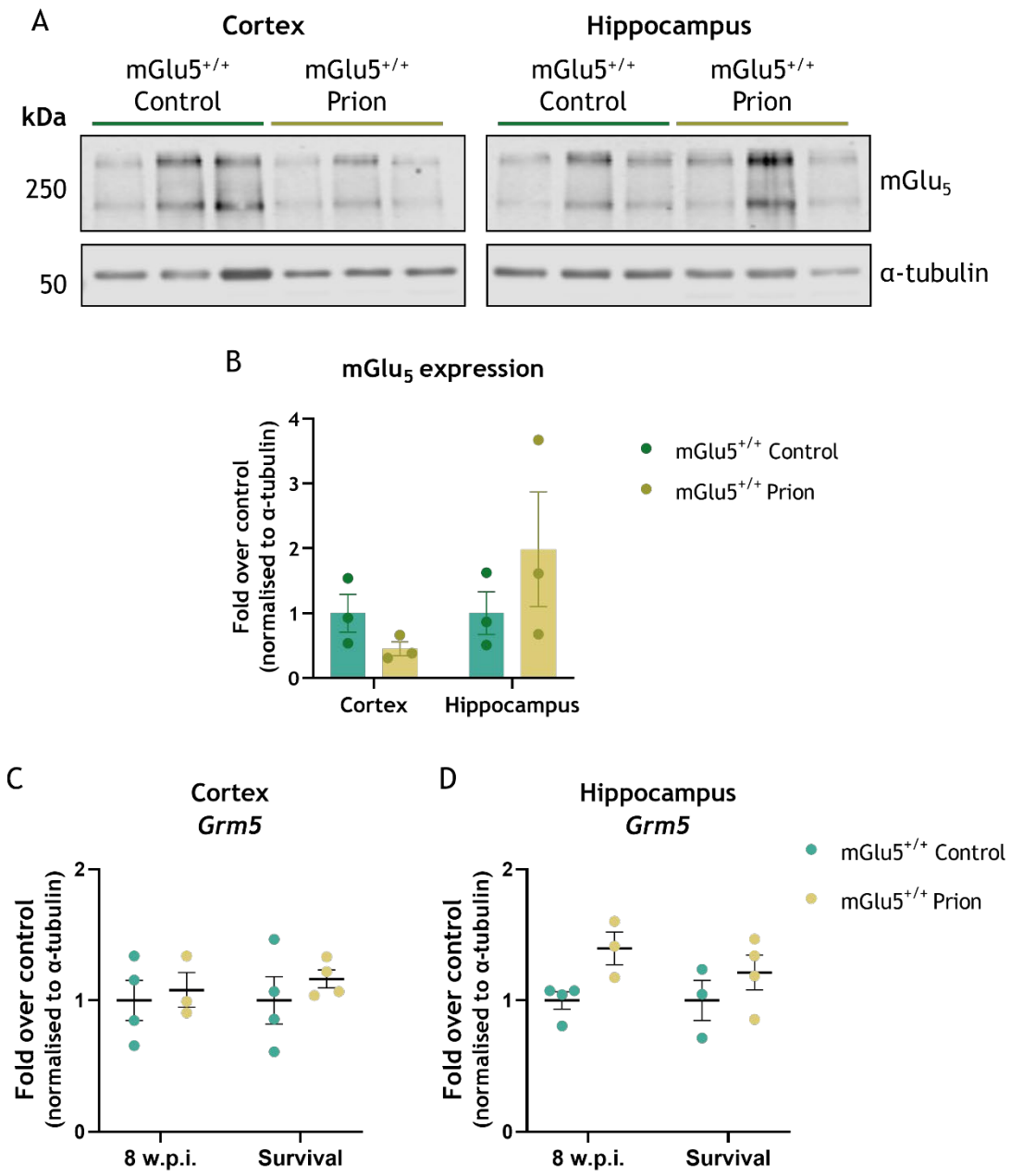

Figure 5-5 The expression of $mGlu_5$ is unaltered in murine prion disease (C57 background). (A) The expression of $mGlu_5$ was assessed using Western blot analysis on lysates prepared from the cortex or hippocampus of control- or prion-infected mice at the terminal disease endpoint. An antibody against $mGlu_5$ was used to probe for $mGlu_5$ expression. The loading control used was α-tubulin. Each lane represents an individual mouse (n=3). Membranes were stripped and re-probed for multiple antibodies (Figure 5-5 and Figure 5-6). Quantification of (A) is shown in (B). Protein levels were normalised to the loading control, and data are expressed as fold over control. Data are shown as mean ± S.E.M., with each point representing an individual mouse (n=3). (C and D) RT-qPCR showing the expression of *Grm5* in the cortex (C) and hippocampus (D) of control- or prion-infected mice at 8 w.p.i. and survival. To assess relative expression levels, data were analysed using the ΔΔCT method, normalising first to α-tubulin and then to the mean of the control value for the gene of interest, *Grm5*. Data shown are mean ± S.E.M., and data points represent individual animals (n=3-4). Statistical analysis was performed using two-way ANOVA (Tukey's multiple comparisons).

As previously established, $mGlu_1$ expression is unchanged between $mGlu5^{+/+}$, $mGlu5^{+/-}$, and $mGlu5^{-/-}$ mice (Figure 5-2). Moreover, western blot analysis of cortical and hippocampal tissue from $mGlu5^{+/+}$ mice inoculated with either control or prion brain homogenate showed that $mGlu_1$ expression is unaltered with murine prion disease (Figure 5-6).

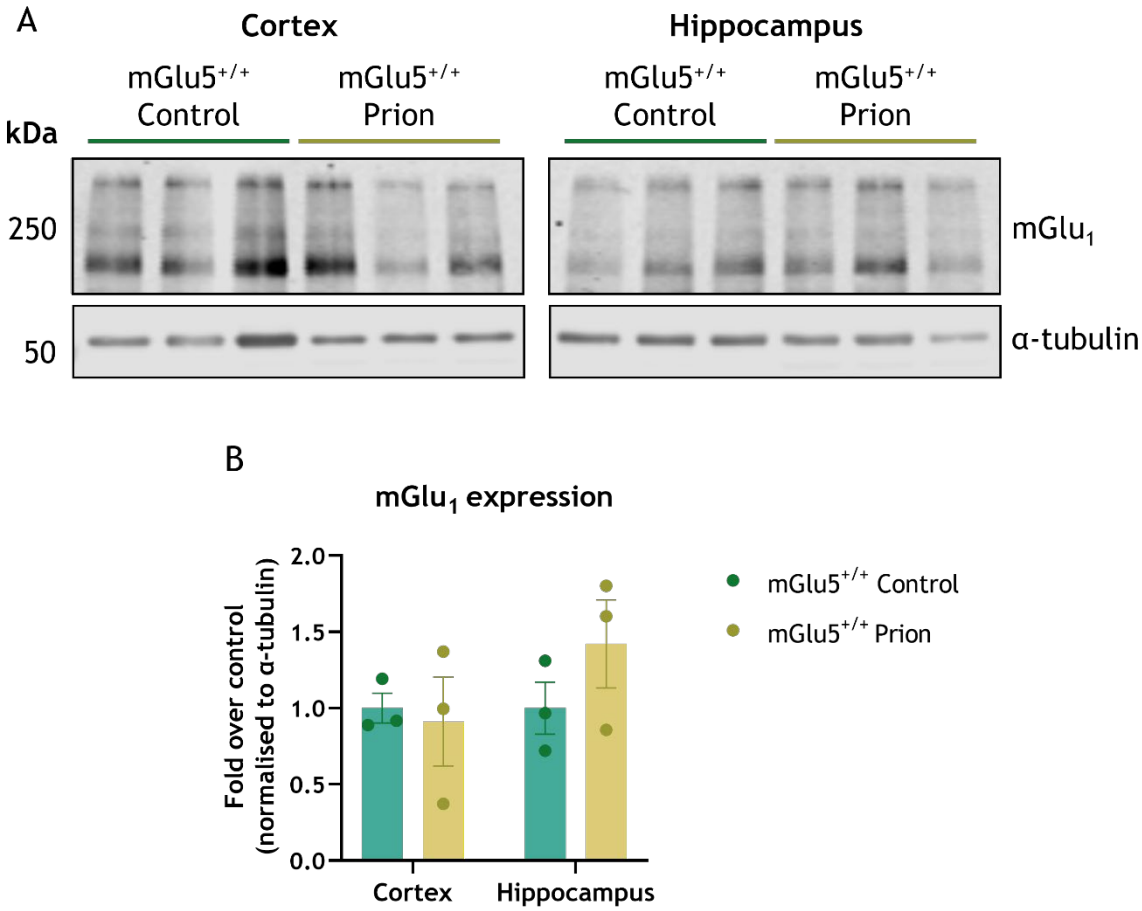

Figure 5-6 The expression of $mGlu_1$ is unaltered in murine prion disease (C57 background). (A) The expression of $mGlu_1$ was assessed using western blot analysis on lysates prepared from the cortex or hippocampus of control- or prion-infected mice at the terminal disease endpoint. An antibody against $mGlu_1$ was used to probe for $mGlu_1$ expression. The loading control used was α-tubulin. Membranes were stripped and re-probed for multiple antibodies (Figure 5-5 and Figure 5-6). Each lane contains a sample from an individual mouse (n=3). Quantification of (A) is shown in (B). Protein levels were normalised to the loading control, and data are expressed as fold over control. Data are shown as mean ± S.E.M., with each point representing an individual mouse (n=3).

5.2.3 The Effect of $mGlu_5$ Deficiency on the Progression of Murine Prion Disease

The next section of this chapter investigates the effect of $mGlu_5$ deficiency on the progression of behavioural and biochemical changes associated with NDD as well as the survival of terminally sick mice.

Firstly, the effect of $mGlu_5$ deficiency on the progression of murine prion disease was investigated. As discussed in Chapter 4, the burrowing paradigm is a sensitive assay for monitoring the progression of murine prion disease (Deacon, 2006). In this assay, mice actively "burrow" pellets out of a container, which is reflective of innate hippocampal function that is independent of memory processing. In this study, burrowing experiments began at 12 w.p.i., before the animals had developed any disease symptoms, and were repeated weekly. At late disease time points, mice were beginning to show signs of a terminal disease endpoint and were culled when they reached a terminal endpoint (see 2.3.6.1). Therefore, the number of mice included in the burrowing experiment declined at the later timepoints since fewer mice remained for testing. Although this experiment is a well-established readout for the progression of prion disease, here the genotype of the animals influenced the measurements and made the results difficult to interpret (Figure 5-8, Figure 5-9, and Figure 5-10). The data is initially presented in one graph for the entire study (Figure 5-7), and then separated to make data visualisation simpler.

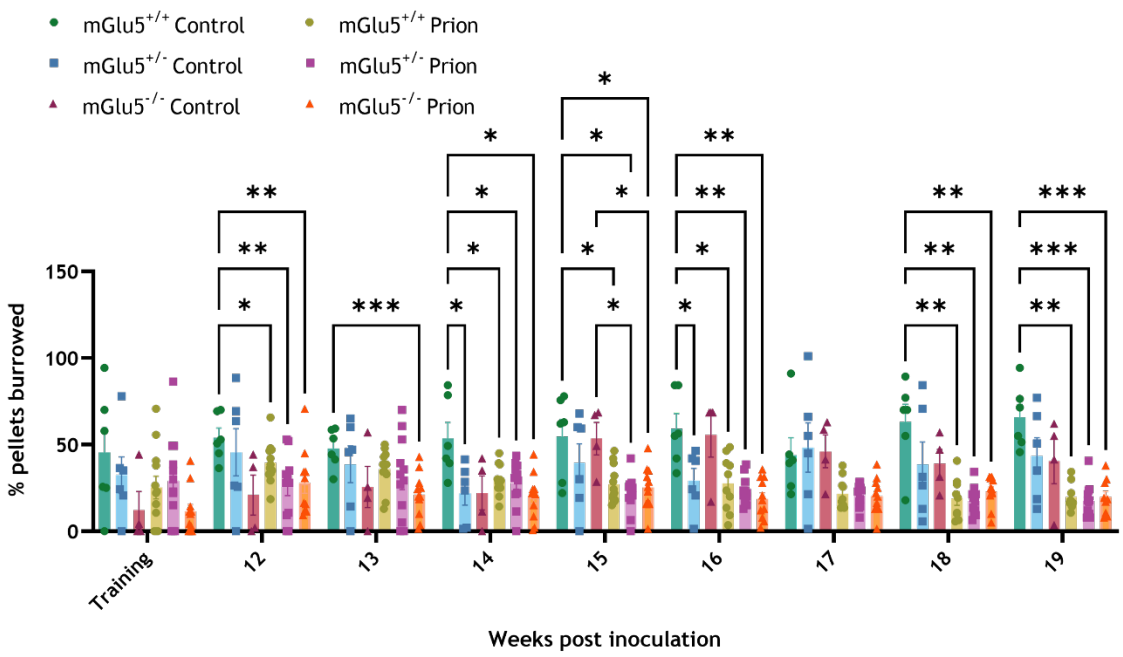

Figure 5-7 Burrowing behaviour in mGlu$_5$ deficient control and prion-diseased mice. The graph shows the burrowing response of female control mGlu5$^{+/+}$ (green), mGlu5$^{+/-}$ (blue), and mGlu5$^{-/-}$ (red) compared to prion mGlu5$^{+/+}$ (yellow), mGlu5$^{+/-}$ (purple), and mGlu5$^{-/-}$ (orange) over time. Burrowing was assessed weekly following training from 12 w.p.i. Data shown are mean ± S.E.M., with each point representing an individual mouse (n=4-12). Statistical analysis was performed using a two-way ANOVA or mixed-effects model with uncorrected Fisher's least significant difference test, where * P≤0.05, ** P≤0.01, and *** P≤0.001.

Initially, the behaviour of mGlu5$^{+/+}$, mGlu5$^{+/-}$, and mGlu5$^{-/-}$ prion-diseased mice were compared to that of mGlu5$^{+/+}$ control mice (Figure 5-8). From 12 w.p.i., the burrowing behaviour of prion-diseased mice was significantly reduced as compared to controls. The burrowing behaviour of mGlu5$^{+/+}$, mGlu5$^{+/-}$, and mGlu5$^{-/-}$ prion-diseased mice was equivalent, suggesting that mGlu$_5$ deficiency did not alter the progression of murine prion disease (Figure 5-8).

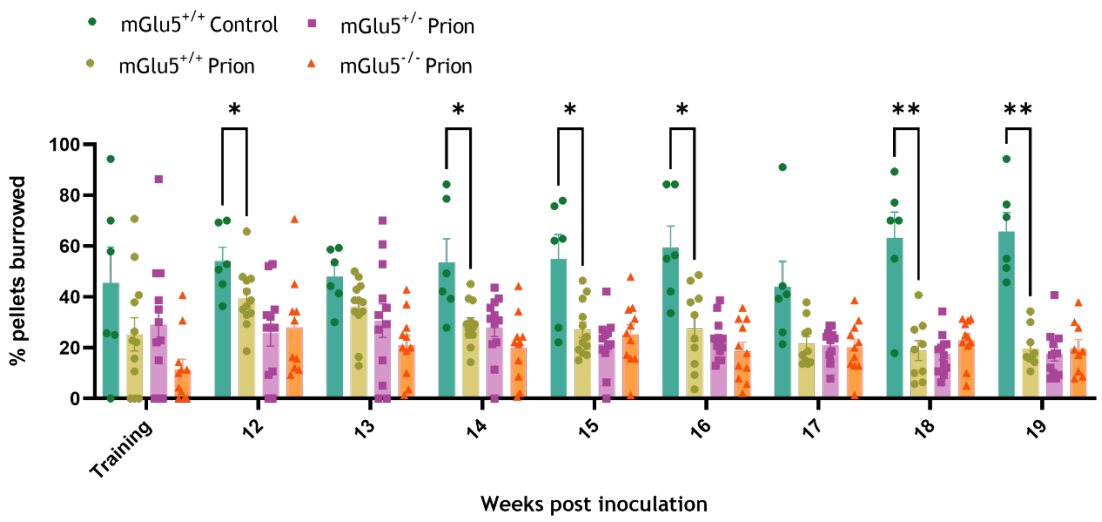

Figure 5-8 Prion-diseased mice show a decline in burrowing behaviour which is unchanged with mGlu$_5$ deficiency. The graph shows the burrowing response of female control (green) and mGlu$_5$ wild-type (mGlu5$^{+/+}$, yellow), heterozygous knockout (mGlu5$^{+/-}$, purple), and homozygous knockout (mGlu5$^{-/-}$, orange) prion-diseased mice over time. Burrowing was assessed weekly following training from 12 w.p.i. Data shown are mean ± S.E.M., with each point representing an individual mouse (n=6-12). Statistical analysis was performed using a two-way ANOVA or mixed-effects model with uncorrected Fisher's least significant difference test, where * P≤0.05, and ** P≤0.01.

However, mGlu5$^{+/+}$, mGlu5$^{+/-}$, and mGlu5$^{-/-}$ control mice were found to have varying levels of burrowing activity, with mGlu5$^{+/-}$ mice burrowing significantly fewer pellets than mGlu5$^{+/+}$ mice at 14 and 16 w.p.i. (P=0.0220 and P=0.0230 respectively) (Figure 5-9).

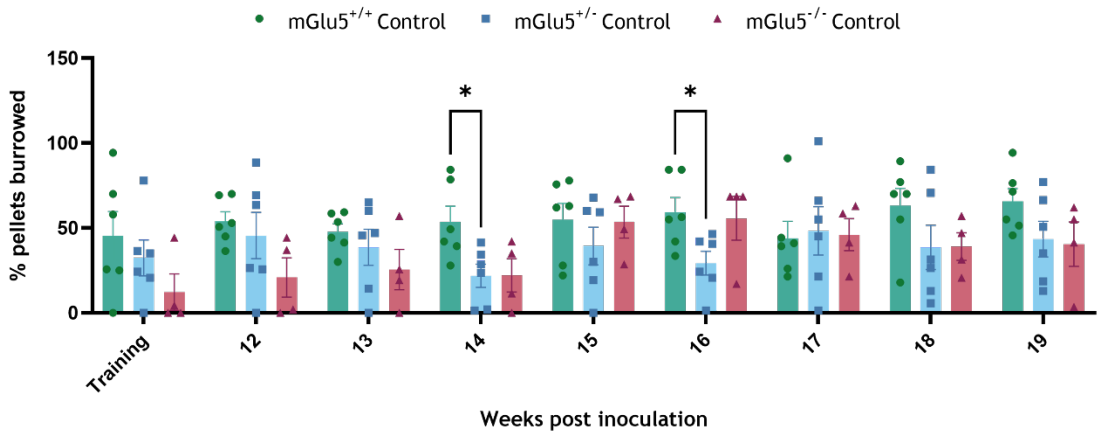

Figure 5-9 Control mice show alterations in burrowing behaviour with mGlu$_5$ deficiency. The graph shows the burrowing response of female control mGlu$_5$ wild-type (mGlu5$^{+/+}$, green), heterozygous knockout (mGlu5$^{+/-}$, blue), and homozygous knockout (mGlu5$^{-/-}$, red) mice over time. Data shown are mean ± S.E.M., with each point representing an individual mouse (n=4-6). Statistical analysis was performed using a two-way ANOVA or mixed-effects model with uncorrected Fisher's least significant difference test , where * P≤0.05.

Comparison of the behaviour of control and prion-diseased mice within genotypes confirmed that the burrowing assay may not be appropriate for drawing conclusions surrounding the effect of $mGlu_5$ deficiency on prion disease progression (Figure 5-10). Importantly, $mGlu5^{-/-}$ control and prion-diseased mice both performed poorly in the burrowing experiment at training and from 12 to 14 w.p.i. (Figure 5-10C). Prion-diseased $mGlu5^{-/-}$ mice continued to perform poorly throughout disease progression, whereas control $mGlu5^{-/-}$ mice showed some improvement in their burrowing behaviour from 15 w.p.i. (Figure 5-10C). As $mGlu_5$ deficiency altered the burrowing behaviour of the control mice used here, this assay may not be a suitable experiment to examine whether $mGlu_5$ deficiency has any effect on the burrowing behaviour of prion-diseased mice as compared to controls. In order to better understand the effect of $mGlu_5$ deficiency on burrowing behaviour, these experiments should have been carried out on non-infected mice prior to carrying them out on control- and prion-infected mice.

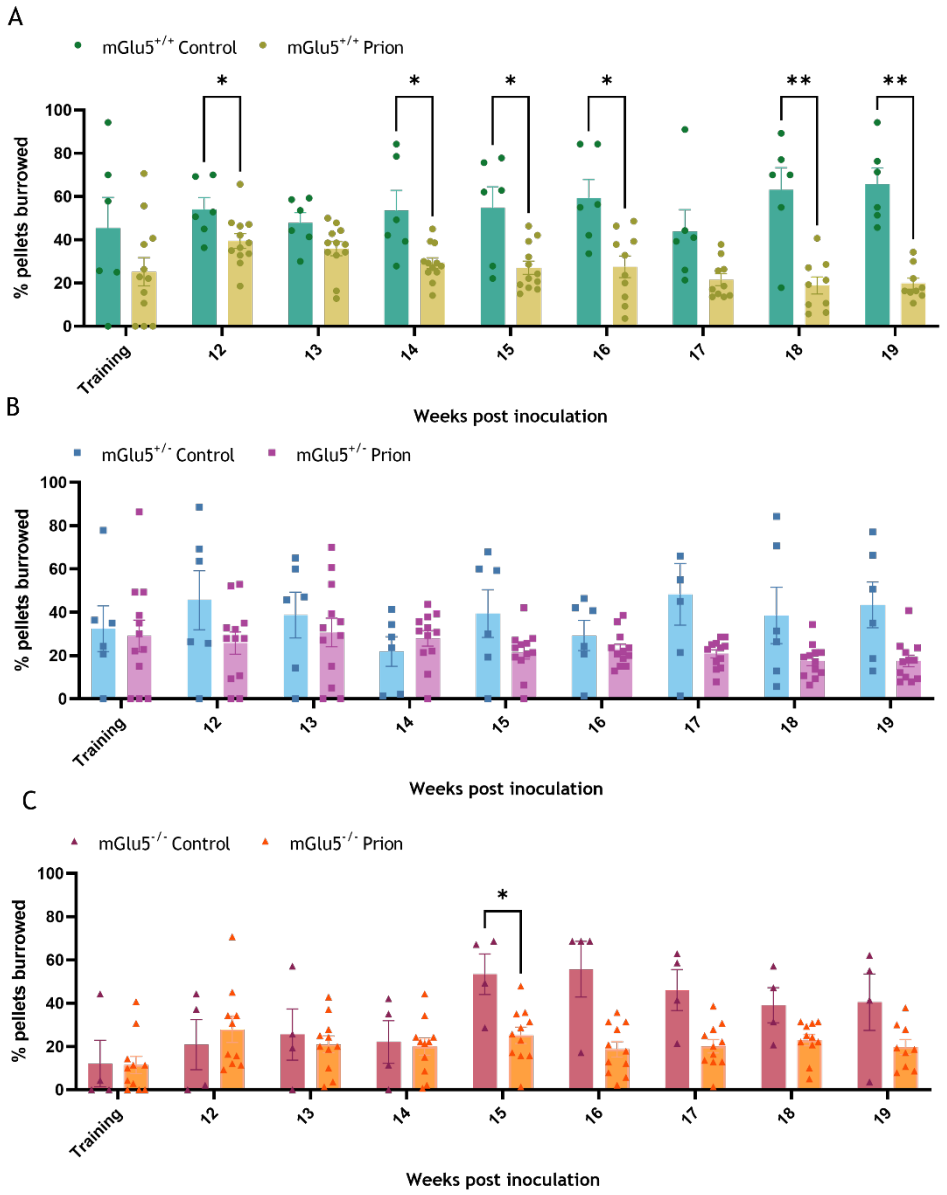

Figure 5-10 Burrowing behaviour of control and prion-disease mice split by $mGlu_5$ genotype. Graphs show the burrowing response of female control and prion-diseased (A) $mGlu_5$ wild-type ($mGlu5^{+/+}$) (control n=5, prion n=12), (B) heterozygous knockout ($mGlu5^{+/-}$) (control n=6, prion n=12), and (C) homozygous knockout ($mGlu5^{-/-}$) (control n=4, prion n=11) mice over time. Data shown are mean ± S.E.M., with each point representing an individual mouse. Statistical analysis was performed using a two-way ANOVA or mixed-effects model with uncorrected Fisher's least significant difference test, where * P≤0.05, and ** P≤0.01.

Symptom onset and survival were determined by the daily observation of early and confirmatory signs of disease (see 2.3.6.1). Mice were considered "symptomatic" when they displayed at least two early indicators of prion disease (Mallucci et al., 2003). The disease course seen here differs from that observed in Chapter 4 as Tg37 mice overexpress PrP_C to three times normal levels (Mallucci et al., 2003). There was no significant difference in symptom onset between genotypes, regardless of sex (Figure 5-11). The median time of symptom onset was 125 days post inoculation (d.p.i.) for $mGlu5^{+/+}$ mice, 120 d.p.i. for $mGlu5^{+/-}$ mice, and 125 d.p.i. for $mGlu5^{-/-}$ mice (Figure 5-11C). Individual early indicators of disease had a similar onset across the three genotypes, suggesting that none of the early indicators are associated with $mGlu_5$ deficiency (Figure 5-12).

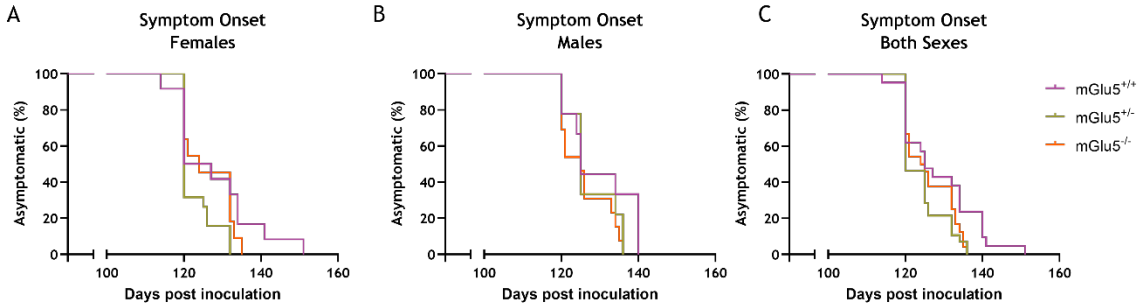

Figure 5-11 Knockout of $mGlu_5$ does not alter symptom onset in murine prion disease. Kaplan-Meier plot showing the onset of at least two early indicators of prion disease in (A) female, (B) male, or (C) both sexes of $mGlu_5$ wild-type ($mGlu5^{+/+}$), heterozygous knockout ($mGlu5^{+/-}$), and homozygous knockout ($mGlu5^{-/-}$) prion-diseased mice (female $mGlu5^{+/+}$ n=11, female $mGlu5^{+/-}$ n=16, female $mGlu5^{-/-}$ n=10; male $mGlu5^{+/+}$ n=9, male $mGlu5^{+/-}$ n=9, male $mGlu5^{-/-}$ n=13). Curves were analysed with a Gehan-Breslow-Wilcoxon test.

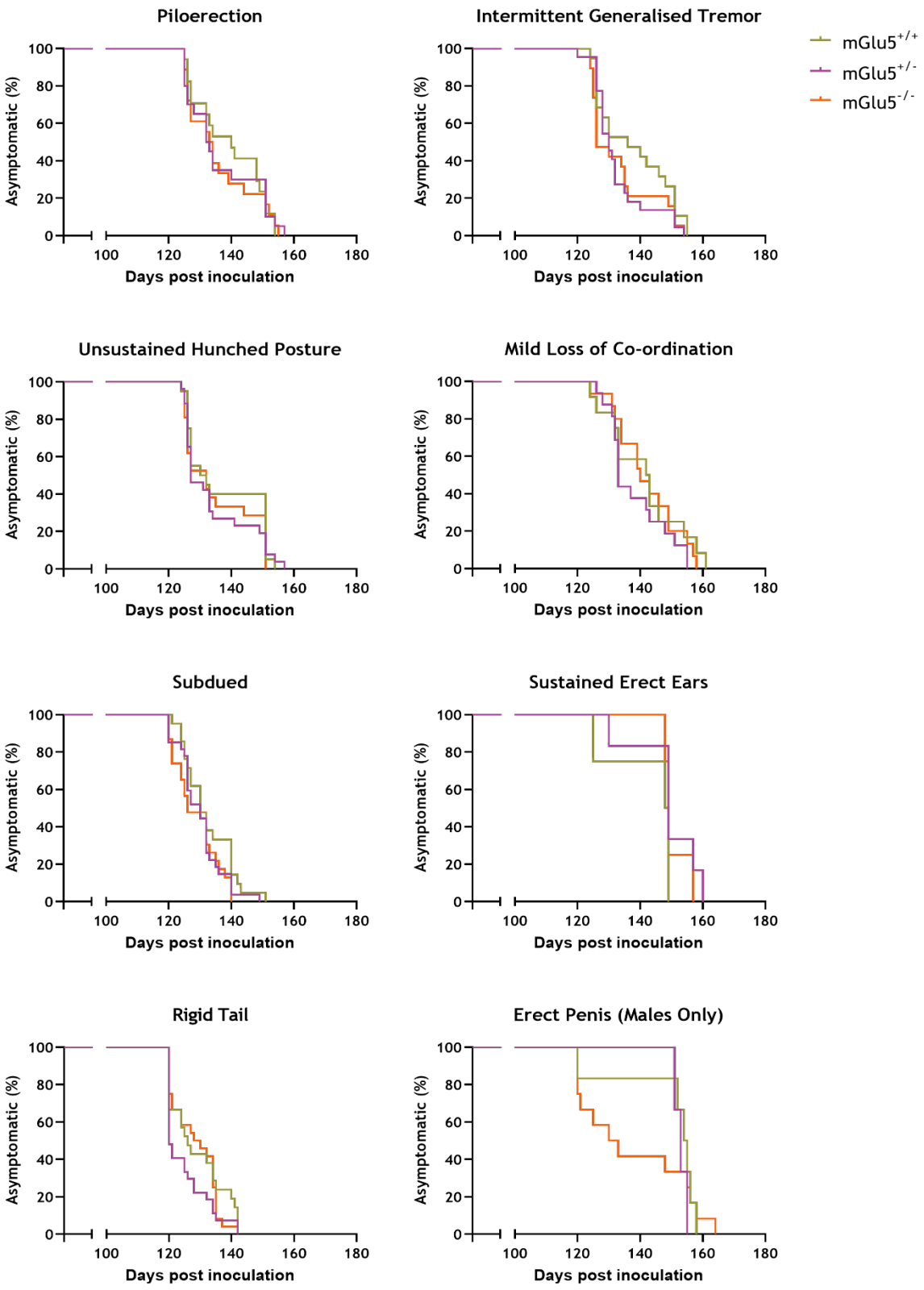

Figure 5-12 Knockout of mGlu$_5$ does not alter the onset of individual symptoms in murine prion disease. Kaplan-Meier curves for the onset of individual symptoms (n=20-25). Curves were analysed with a Gehan-Breslow-Wilcoxon test.

In addition to a similar median onset, most of the early indicators were observed at equivalent levels across the three genotypes (Figure 5-13). Although there was no significant difference in the Kaplan-Meier survival curve for an erect penis (Figure 5-12), this early indicator differed in the percentage of each genotype in which it was observed. Specifically, an erect penis was observed in 66% of mGlu5$^{+/+}$ mice, 33% of mGlu5$^{+/-}$ mice, and 92% of mGlu5$^{-/-}$ mice (Figure 5-13). The difference in frequency between mGlu5$^{+/-}$ and mGlu5$^{-/-}$ mice was significant according to a two-sided Fisher's exact test (P=0.007). Erectile dysfunction is a symptom of human prion diseases, including CJD and fatal familial insomnia (Cali et al., 2015; Rare Disease Database, 2018). It is worth nothing that in humans, mGlu$_5$ is expressed in the male reproductive system (Storto et al., 2001), however further investigation is needed to understand why the frequency of an erect penis in prion-diseased mice was significantly higher in mGlu5$^{-/-}$ mice as compared to mGlu5$^{+/-}$ mice. It could be a phenotype of the genotype that has not yet been fully investigated.

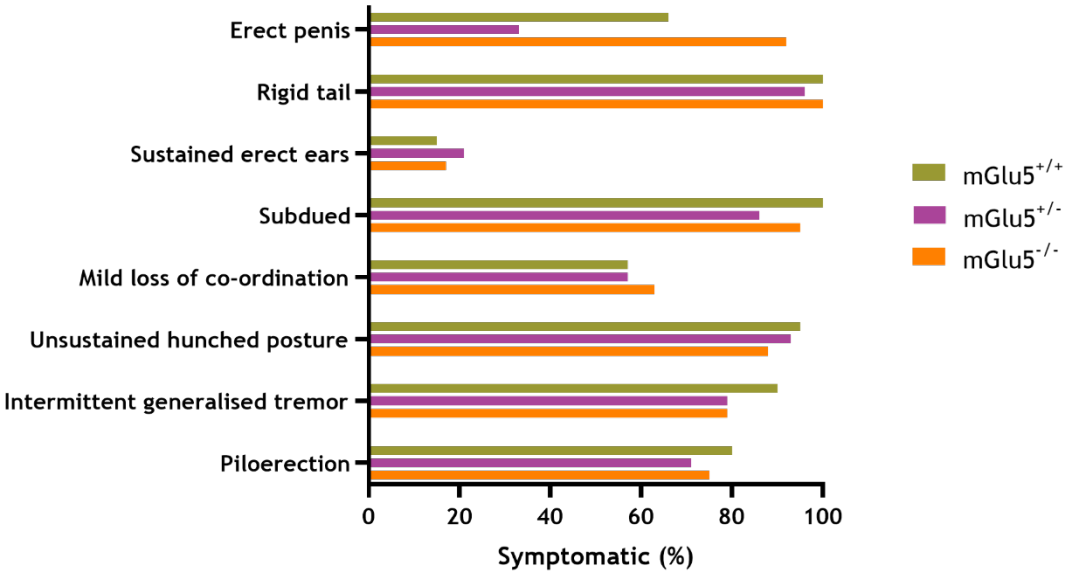

Figure 5-13 Frequency of individual prion disease symptoms across mGlu$_5$ genotypes. Bar lengths correspond to the percentage prevalence in the respective cohort, mGlu$_5$ wild-type (mGlu5$^{+/+}$), heterozygous knockout (mGlu5$^{+/-}$), and homozygous knockout (mGlu5$^{-/-}$) prion-diseased mice (n=20-25).

Prion-diseased mice were considered to have reached a terminal disease endpoint after the appearance of two early indicator signs in addition to one confirmatory sign, or the appearance of two confirmatory signs. When mice reach a terminal endpoint, they are culled, thus defining their survival. There was no significant difference in the survival of prion-diseased mice between genotypes, regardless of sex (Figure 5-14). The median survival was 156 d.p.i. for mGlu5$^{+/+}$ mice, 153 d.p.i. for mGlu5$^{+/-}$ mice, and 150 d.p.i. for mGlu5$^{-/-}$ mice (Figure 5-14C).

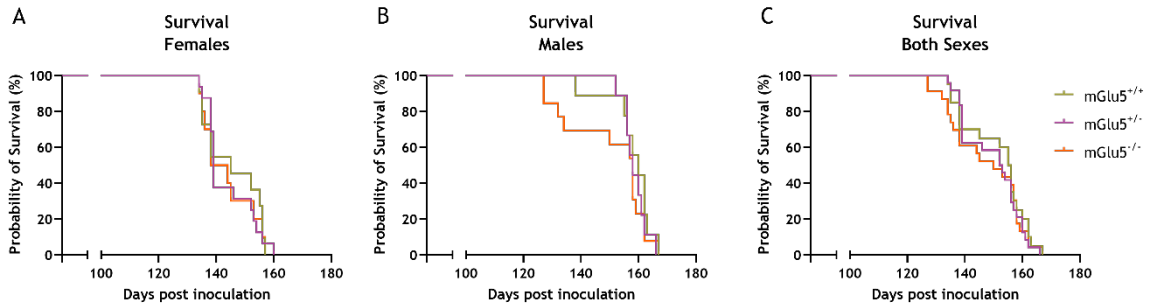

Figure 5-14 Knockout of mGlu$_5$ does not alter the survival of prion diseased mice. Kaplan-Meier plot showing the survival of (A) female, (B) male, or (C) both sexes of mGlu$_5$ wild-type (mGlu5$^{+/+}$), heterozygous knockout (mGlu5$^{+/-}$), and homozygous knockout (mGlu5$^{-/-}$) prion-diseased mice (female mGlu5$^{+/+}$ n=11, female mGlu5$^{+/-}$ n=16, female mGlu5$^{-/-}$ n=10; male mGlu5$^{+/+}$ n=9, male mGlu5$^{+/-}$ n=9, male mGlu5$^{-/-}$ n=13). Curves were analysed with a Gehan-Breslow-Wilcoxon test.

Prion disease is characterised by the propagation and accumulation of misfolded, toxic PrP$_{Sc}$ which is partially resistant to protease digestion (Prusiner, 1998). To investigate whether mGlu$_5$ knockout affects the accumulation of PrP$_{Sc}$ in murine prion disease, tissue collected from the terminally sick mice used in the survival study in Figure 5-14, as well as tissue collected from mice culled at 8 w.p.i. were probed for the expression of PrP$_{Sc}$ (Figure 5-15). As expected, no PrP$_{Sc}$ was observed in the brains of control mice at either 8 w.p.i. or survival (Figure 5-15 A and C).

At 8 w.p.i., no PrP$_{Sc}$ was observed in the brains of prion-diseased mice (Figure 5-15A). An undigested sample was run alongside the PK-digested samples at 8 w.p.i. to ensure that the blank blot was due to a lack of PrP$_{Sc}$ in the samples

rather than an error in experimentation. PrP_{Sc} was evident in prion-diseased mice at survival (Figure 5-15C-D). In the survival samples, there was a similar level of PrP_{Sc} accumulation in $mGlu5^{+/+}$, $mGlu5^{+/-}$, and $mGlu5^{-/-}$ mouse brains (Figure 5-15D). This suggests that $mGlu_5$ does not affect PrP_{Sc} accumulation in mouse brains. The expression of PrP_{Sc} was variable, and further data points would strengthen this finding.

Together with the symptom onset and survival data, this suggests that $mGlu_5$ knockout does not alter the progression of murine prion disease.

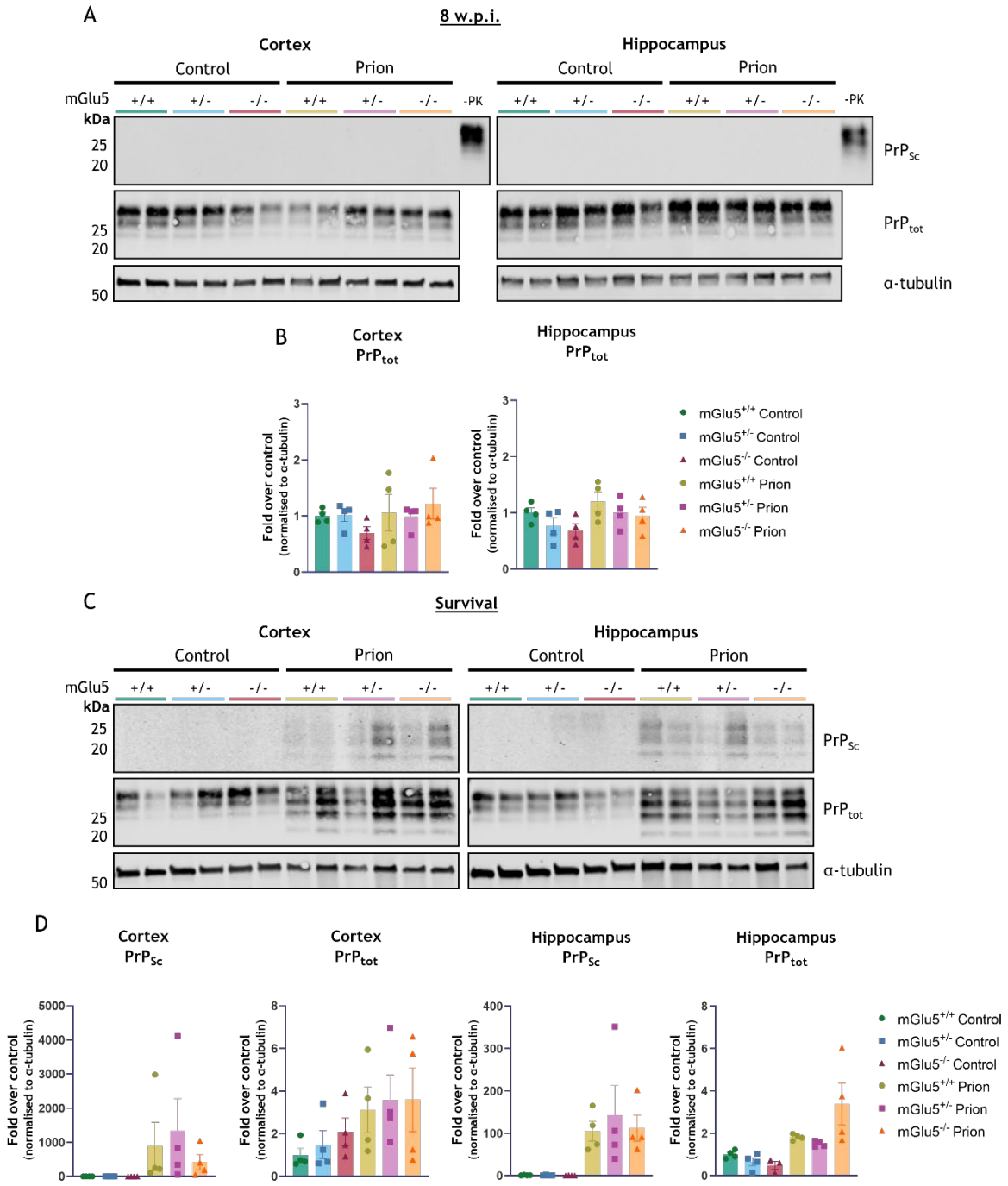

Figure 5-15 The accumulation of PrP_{Sc} in prion-diseased mice is unaltered with $mGlu_5$ deficiency. Western blot analysis of lysates from the cortex and hippocampus of control and prion-diseased $mGlu_5$ wild-type ($mGlu5^{+/+}$), heterozygous knockout ($mGlu5^{+/-}$), and homozygous knockout ($mGlu5^{-/-}$) mice at 8 w.p.i. (A-B) and survival (C-D). Lysates were incubated with proteinase K prior to immunoblotting using an anti-PrP to detect PrP_{Sc}. Incubation with water was used to detect PrP_{tot}. In (A), a control brain sample incubated with water (-PK) was run in the last lane as a positive control. α-tubulin was used as a loading control. Each lane represents a different mouse, and a representative blot is shown. PrP_{tot} membranes were stripped and re-probed for multiple antibodies (Figure 5-15, Figure 5-16, Figure 5-20, and Figure 5-27). (B and D) Protein levels were normalised to the loading control, followed by normalisation to the average protein level of the $mGlu5^{+/+}$ control samples expressed as fold change. Data shown are means ± S.E.M., with each data point representing an individual mouse (n=4).

5.2.4 The Effect of $mGlu_5$ Deficiency on Prion-induced Neuroinflammation

A common pathological hallmark found across NDDs is a chronic neuroinflammatory response, characterised by the upregulation of neuroinflammatory cell markers such as GFAP and Iba-1 (Liddelow and Barres, 2017; Bachiller et al., 2018). The $mGlu_5$ receptor is expressed on glial cells, including astrocytes and microglia, and targeting $mGlu_5$ may be a way in which inflammatory processes can be modulated. Several studies have found that the genetic knockout of $mGlu_5$ reduces the upregulation of astrocyte and microglial markers in animal models of AD, HD, and ALS (Hamilton et al., 2014, 2016; Bonifacino et al., 2017; Abd-Elrahman et al., 2020). By contrast, two recent studies found that the genetic deletion of $mGlu_5$ resulted in accelerated neurodegeneration in wild-type mice, with increased astrogliosis and microglial activation observed in $mGlu_5$ knockout mice as compared to wild-type controls (Carvalho et al., 2019; de Souza et al., 2022).

In this study, the expression of GFAP in both control and prion-diseased $mGlu5^{+/+}$, $mGlu5^{+/-}$, and $mGlu5^{-/-}$ mice was examined, initially using immunoblotting on 2 male and 2 female samples (Figure 5-16). Cortical and hippocampal tissue were collected at 8 w.p.i. and at survival to look at any changes in GFAP expression over time. In control mice, there was no significant difference in GFAP expression between genotypes at either time point (Figure 5-16 B and D). At survival, prion-diseased mice had an increase in GFAP expression as compared to control mice, but there was no difference in GFAP expression between genotypes (Figure 5-16D).

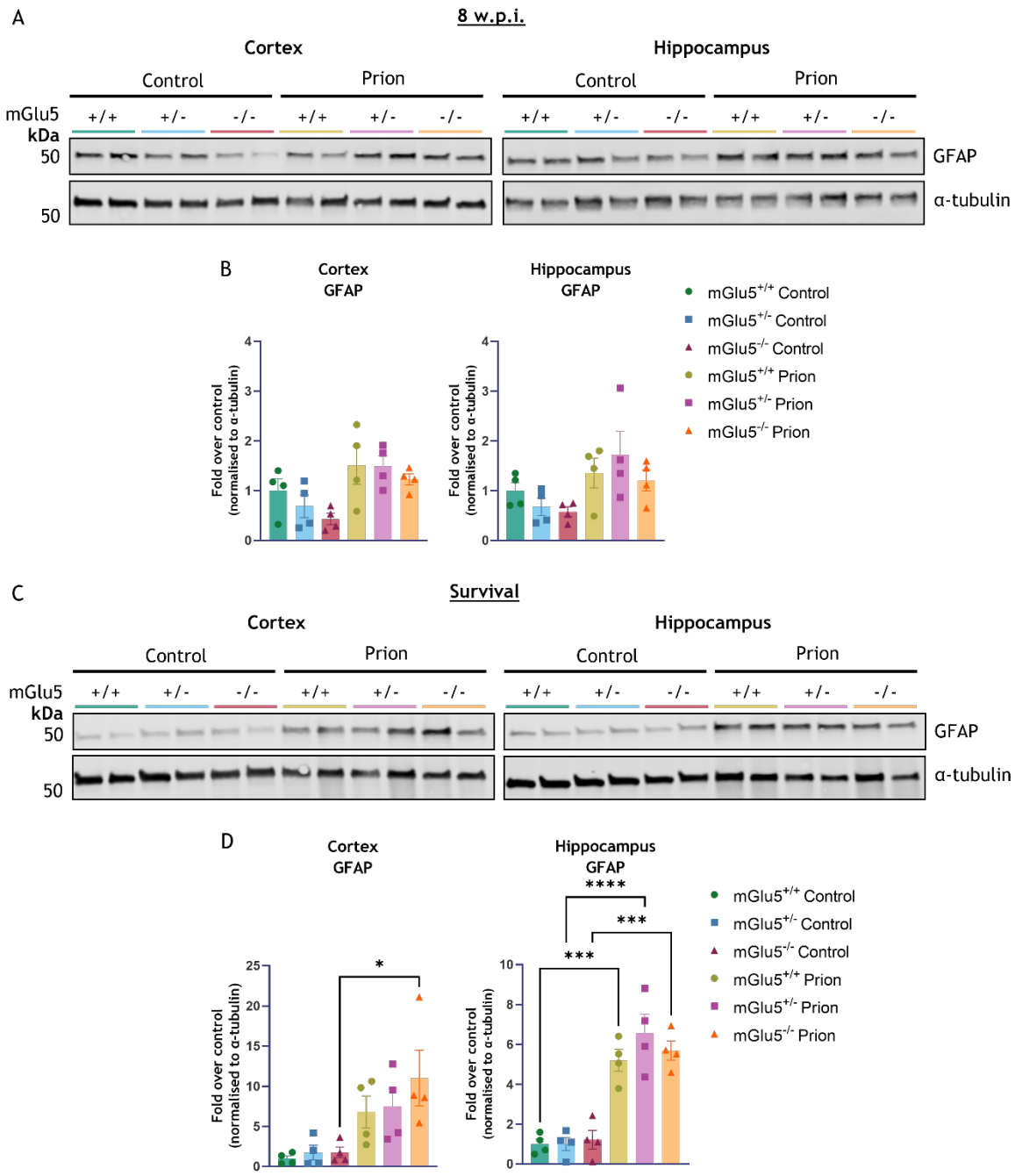

Figure 5-16 Immunoblot analysis of the effect of mGlu$_5$ deficiency on astrogliosis in control and prion-diseased mice. Astrogliosis in the cortex and hippocampus was assessed using western blot analysis on lysates prepared from control- or prion-infected mGlu$_5$ wild-type (mGlu5$^{+/+}$), heterozygous knockout (mGlu5$^{+/-}$), and homozygous knockout (mGlu5$^{-/-}$) mice at 8 w.p.i. (A-B) and survival (C-D). Lysates were probed for GFAP, and α-tubulin was used as a loading control. Each lane represents a sample from an individual mouse, and representative blots are shown. Membranes were stripped and re-probed for multiple antibodies (Figure 5-15, Figure 5-16, Figure 5-20, and Figure 5-27). (B and D) Expression levels were normalised to the loading control, followed by normalisation to the average protein level of the mGlu5$^{+/+}$ control samples expressed as fold change. Data shown are means ± S.E.M., with each data point representing an individual mouse (n=4; 2 male, 2 female). Statistical analysis was performed using a two-way ANOVA (Tukey's multiple comparisons), where * P≤0.05, *** P≤0.001, and **** P≤0.0001.

Next, RT-qPCR was performed to analyse the gene expression levels of *Gfap* in the brains of control and prion-diseased mGlu5$^{+/+}$, mGlu5$^{+/-}$, and mGlu5$^{-/-}$ mice (Figure 5-17). In agreement with the immunoblot data, this experiment did not detect any significant differences in *Gfap* expression levels between the three genotypes at either time point. As expected, there was an increase in *Gfap* expression in prion-diseased mice as compared to controls at the terminal disease timepoint (Figure 5-17B).

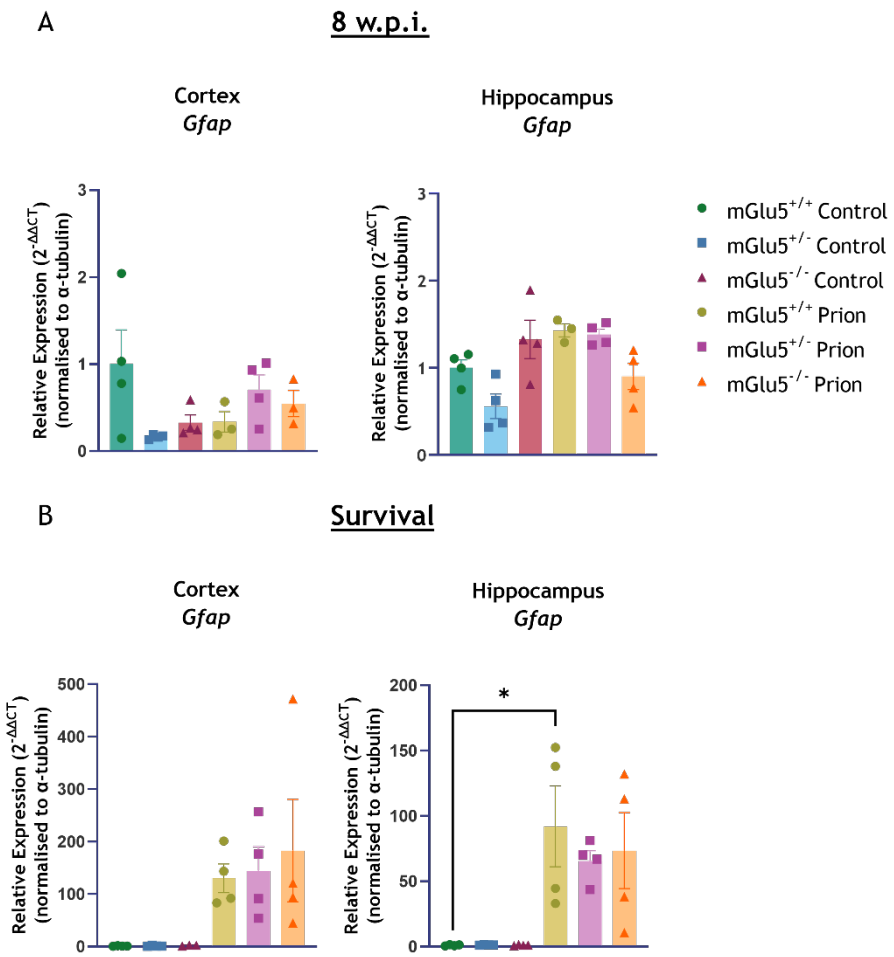

Figure 5-17 RT-qPCR analysis of the effect of mGlu$_5$ deficiency on astrogliosis in control and prion-diseased mice. RT-qPCR showing the gene expression of *Gfap* in the cortex and hippocampus of control- or prion-infected mGlu$_5$ wild-type (mGlu5$^{+/+}$), heterozygous knockout (mGlu5$^{+/-}$), and homozygous knockout (mGlu5$^{-/-}$) mice at 8 w.p.i. (A) and survival (B). To assess relative expression levels, data were analysed using the ΔΔCT method, normalising first to α-tubulin and then to the mean of the control value for the gene of interest, *Gfap*. Data shown are means ± S.E.M. (n=3-4). Statistical analysis was performed using a two-way ANOVA (Tukey's multiple comparisons), where * P≤0.05.

To look more closely at the effect of $mGlu_5$ deficiency on astrogliosis, immunohistochemistry was performed on 5 µm coronal slices taken through the brains of male and female control and prion-diseased $mGlu_5$ genotype littermates. For each mouse, the % area covered by GFAP staining was calculated for 3 consecutive slices and averaged to give n=1. Analysis was carried out on brains collected at 8 w.p.i. (Figure 5-18) and at survival (Figure 5-19). Protein levels were investigated in the cortex, hippocampus, and hippocampal CA1 area. At 8 w.p.i, there was very little staining observed in the cortex of both control and prion-diseased mice (< 6%) (Figure 5-18A) and this was equivalent between genotypes (Figure 5-18B). In the entire hippocampus and CA1 region, there were elevated levels of GFAP staining in $mGlu5^{+/+}$ prion diseased animals as compared to controls (hippocampus P=0.0228; CA1 P=0.0079) which was reduced in $mGlu5^{-/-}$ prion-diseased mice, significantly in the CA1 (P=0.0165). At survival, astrogliosis was elevated in the cortex in all three genotypes of prion-diseased mice as compared to their controls (P<0.0001), but there was no difference between genotypes (Figure 5-19A-B). Similarly, in the entire hippocampus and the CA1 region, GFAP staining was elevated in prion-diseased mice with no difference between genotypes (Figure 5-19C-D). Preliminary analysis found no difference between male and female mice at survival (Appendix Figure 12).

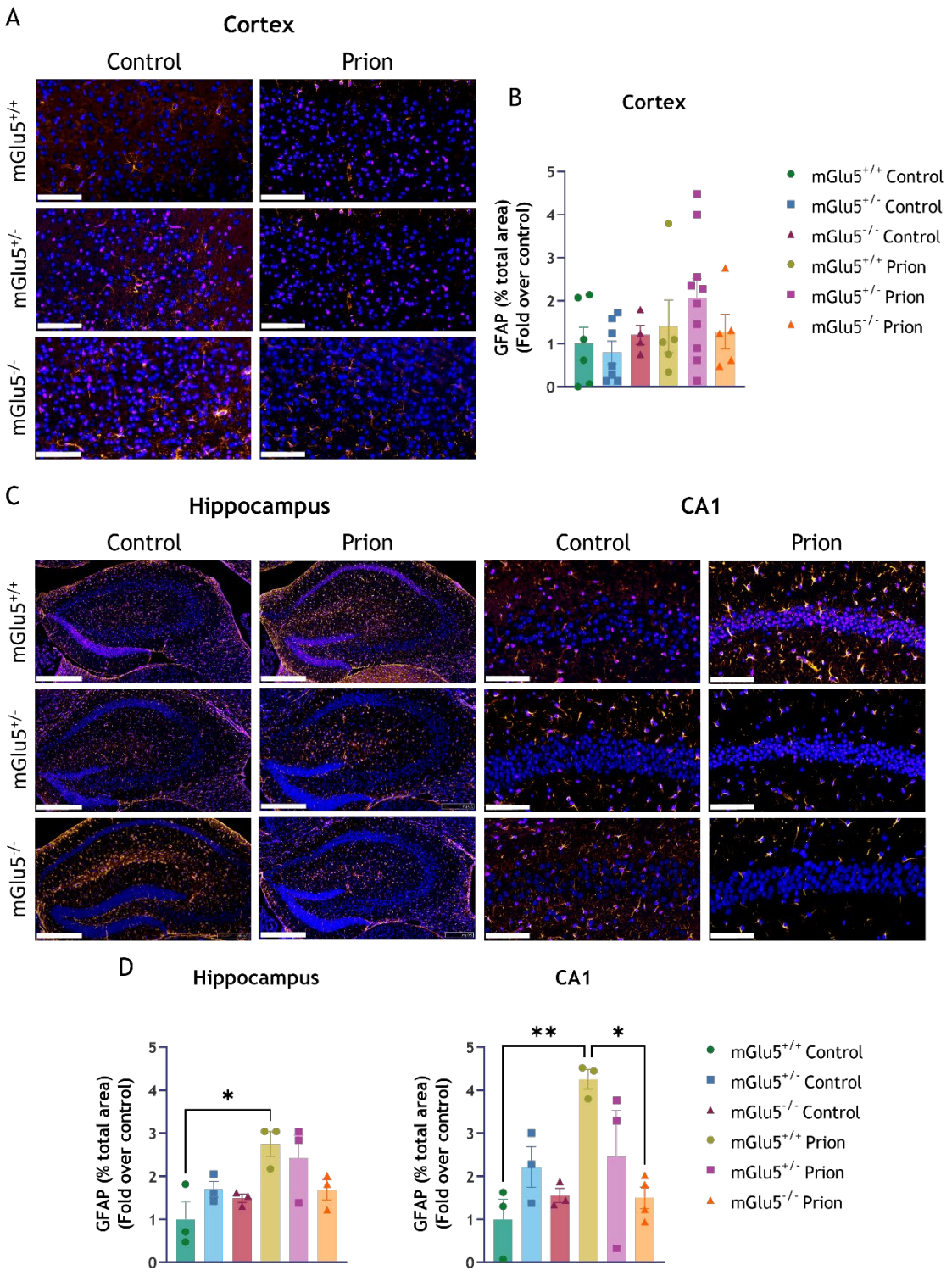

Figure 5-18 Immunohistochemical analysis of the effect of mGlu$_5$ deficiency on astrogliosis in control and prion-diseased mice at 8 w.p.i. Staining for GFAP (red) in the (A-B) cortex, and (C-D) hippocampus and CA of control or prion-diseased mGlu$_5$ wild-type (mGlu5$^{+/+}$), heterozygous knockout (mGlu5$^{+/-}$), and homozygous knockout (mGlu5$^{-/-}$) mice at 8 w.p.i. Representative images are shown in (A) and (C) of n=3-10 mice per group. Staining was performed on 5 µm thick coronal sections (Bregma lateral: ~1.40-1.70 mm) and the images were acquired using a NanoZoomer S60 digital slide scanner at 40x magnification. Nuclei are stained with DAPI (blue). Scale bars represent 100 µm in the cortex, 500 µm in the hippocampus, and 100 µm in the CA1. For the quantification in (B) and (D), data are shown as means ± S.E.M, with each data point representing an individual mouse. For each mouse, the data point represents the average staining across 3 consecutive slices. Data are shown as fold over control (mGlu5$^{+/+}$ control). Statistical analysis was performed using a two-way ANOVA (Tukey's multiple comparisons), where * P≤0.05 and ** P≤0.01.

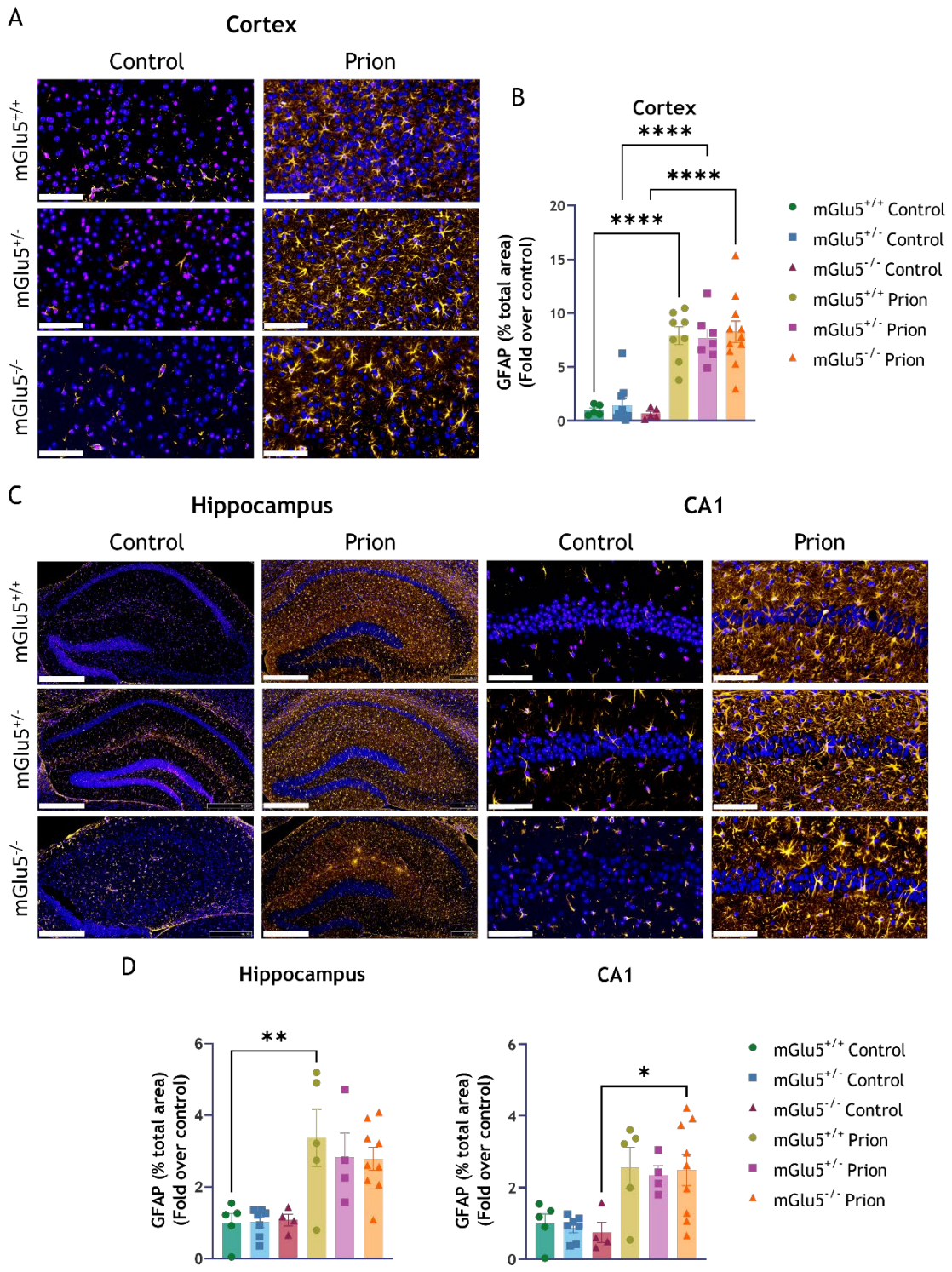

Figure 5-19 Immunohistochemical analysis of the effect of $mGlu_5$ deficiency on astrogliosis in control and prion-diseased mice at survival. Staining for GFAP (red) in the (A-B) cortex, and (C-D) hippocampus and CA of control or prion-diseased $mGlu_5$ wild-type ($mGlu5^{+/+}$), heterozygous knockout ($mGlu5^{+/-}$), and homozygous knockout ($mGlu5^{-/-}$) mice at survival. Representative images are shown in (A) and (C) of n=4-11 mice per group. Staining was performed on 5 µm thick coronal sections (Bregma lateral: ~1.40-1.70 mm) and the images were acquired using a NanoZoomer S60 digital slide scanner at 40x magnification. Nuclei are stained with DAPI (blue). Scale bars represent 100 µm in the cortex, 500 µm in the hippocampus, and 100 µm in the CA1. For the quantification in (B) and (D), data are shown as means ± S.E.M with each data point representing an individual mouse. For each mouse, the data point represents the average staining across 3 consecutive slices. Data are shown as fold over control ($mGlu5^{+/+}$ control). Statistical analysis was performed using a two-way ANOVA (Tukey's multiple comparisons), where * P≤0.05, ** P≤0.01, and **** P≤0.0001.

Next, microgliosis was examined in the cortex and hippocampus of mGlu5$^{+/+}$, mGlu5$^{+/-}$, and mGlu5$^{-/-}$ control and prion-diseased mice. Immunoblotting analysis on 2 male and 2 female samples showed that at 8 w.p.i., there was no difference in Iba-1 expression between control and prion-diseased mice (Figure 5-20A-B). However, Iba-1 expression in mGlu5$^{-/-}$ prion-diseased mice was significantly lower than in mGlu5$^{+/+}$ prion-diseased mice (cortex, P=0.0072; hippocampus, P=0.003) (Figure 5-20B). At survival, there was increased Iba-1 expression in prion-diseased mice but no difference in expression between genotypes (Figure 5-20C-D). Similarly, RT-qPCR data showed that *Cd68* was not upregulated in prion-diseased mice at 8 w.p.i. as compared to control mice (Figure 5-21A) but was upregulated in the cortex and hippocampus of prion-diseased mice at survival (Figure 5-21B). At both time points, there was no difference in *Cd68* gene expression between genotypes in either control or prion-diseased mice (Figure 5-21A-B).

Next, IHC analysis exploring microgliosis was carried out on brains collected at 8 w.p.i. (Figure 5-22) and at survival (Figure 5-23), and protein levels were investigated in the cortex, entire hippocampus, and CA1 region. At 8 w.p.i., microgliosis was evident in the cortex of both control and prion-diseased at equivalent levels, with no difference between genotypes (Figure 5-22A-B). In the hippocampus, Iba-1 staining was elevated in mGlu5$^{+/+}$ prion-diseased mice as compared to mGlu5$^{+/+}$ control mice (P=0.0212) (Figure 5-22D). In the CA1, there was a significant reduction in Iba-1 expression in mGlu5$^{+/-}$ prion-diseased animals as compared to mGlu5$^{+/+}$ prion-diseased mice (P=0.0046) (Figure 5-22D). This data is similar to the immunoblot data which also saw a trend towards decreased microgliosis in mGlu5$^{+/-}$ and mGlu5$^{-/-}$ prion-diseased mice as compared to mGlu5$^{+/+}$ prion-diseased mice at 8 w.p.i. (Figure 5-20B). At survival, microgliosis was elevated in prion-diseased mice as compared to controls, significantly in the cortex and hippocampus (Figure 5-23). However, there was no difference observed between genotypes at survival, with similar levels of microgliosis across all prion-diseased animals (Figure 5-23). Preliminary analysis found no difference between male and female mice at survival (Appendix Figure 13).

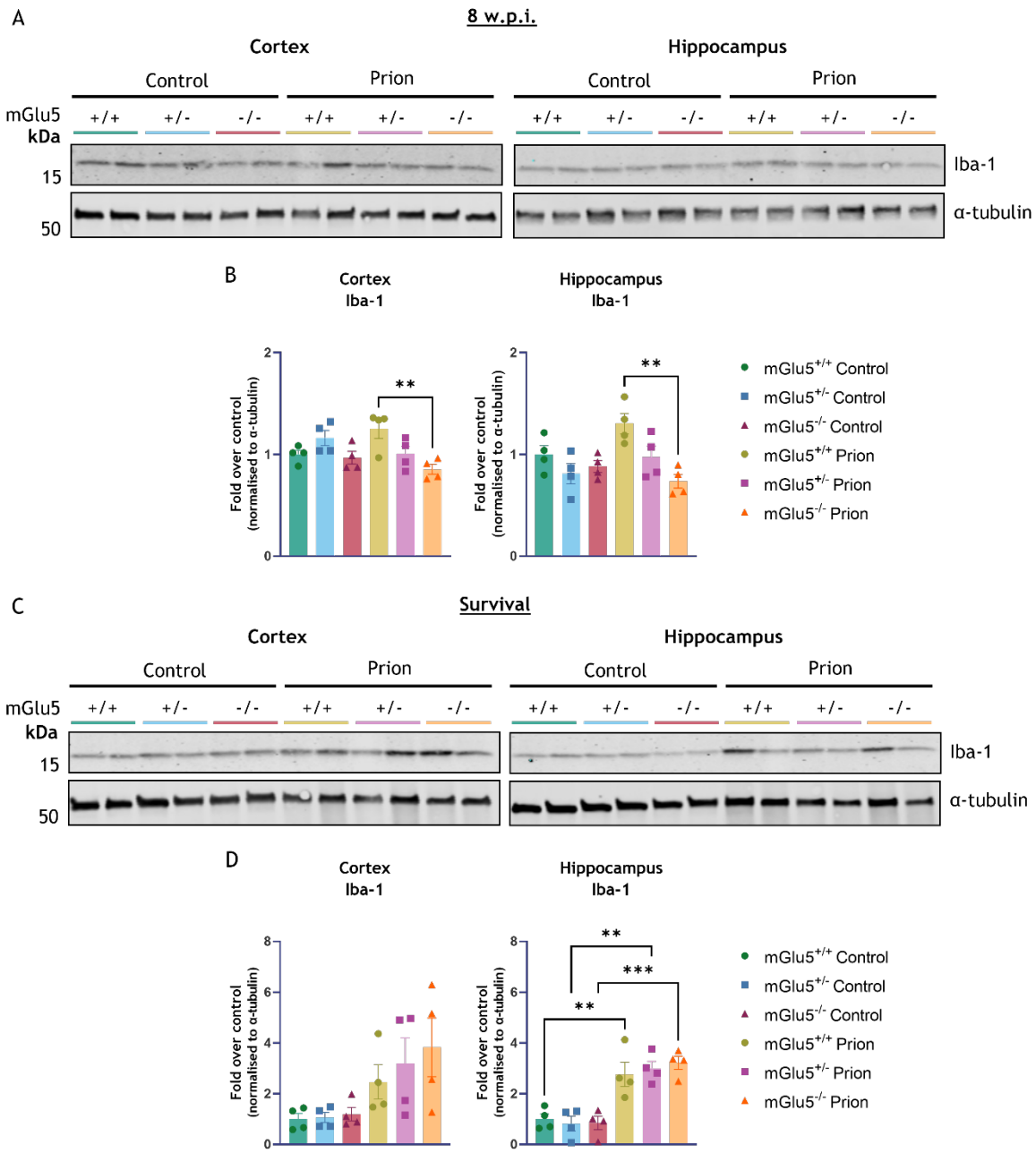

Figure 5-20 Immunoblot analysis of the effect of mGlu$_5$ deficiency on microgliosis in control and prion-diseased mice. Microgliosis in the cortex and hippocampus was assessed using western blot analysis on lysates prepared from control- or prion-infected mGlu$_5$ wild-type (mGlu5$^{+/+}$), heterozygous knockout (mGlu5$^{+/-}$), and homozygous knockout (mGlu5$^{-/-}$) mice at 8 w.p.i. (A-B) and survival (C-D). Lysates were probed for Iba-1, and α-tubulin was used as a loading control. Each lane represents a different mouse, and representative blots are shown. Membranes were stripped and re-probed for multiple antibodies (Figure 5-15, Figure 5-16, Figure 5-20, and Figure 5-27). (B and D) Protein levels were normalised to the loading control, followed by normalisation to the average protein level of the mGlu5$^{+/+}$ control samples expressed as fold change. Data shown are means ± S.E.M., with each data point representing an individual mouse (n=4). Statistical analysis was performed using a two-way ANOVA (Tukey's multiple comparisons), where ** P≤0.01 and *** P≤0.001.

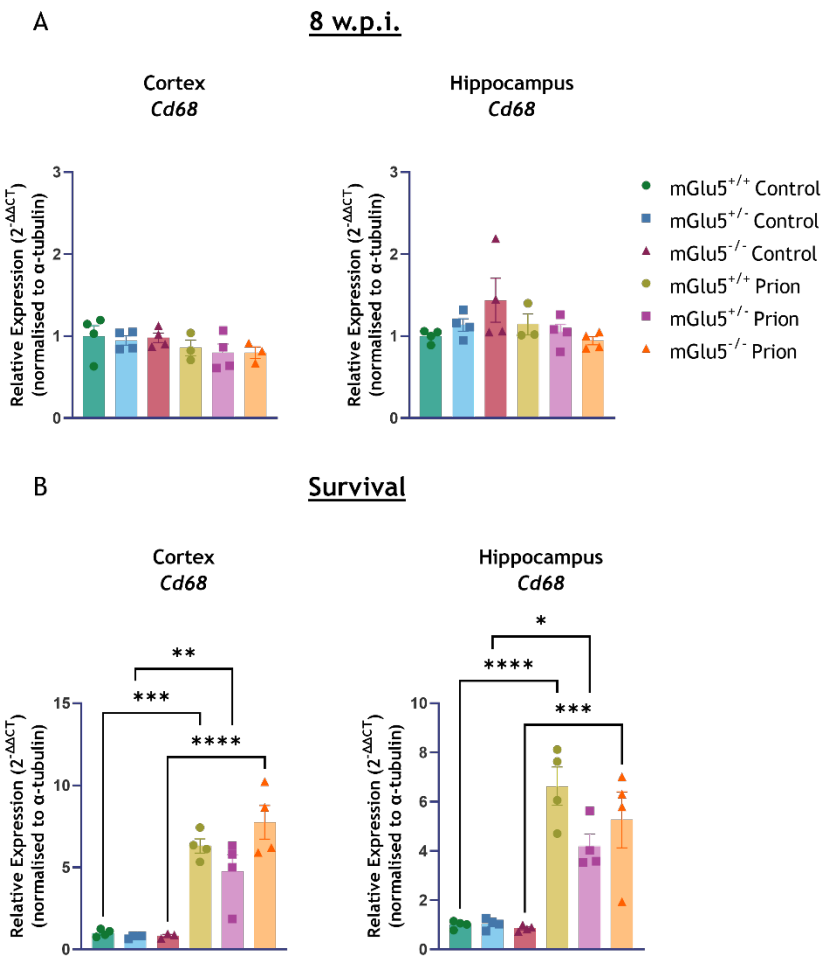

Figure 5-21 RT-qPCR analysis of the effect of mGlu$_5$ deficiency on microgliosis in control and prion-diseased mice. RT-qPCR showing the expression of *Cd68* in the cortex and hippocampus of control- or prion-infected mGlu$_5$ wild-type (mGlu5$^{+/+}$), heterozygous knockout (mGlu5$^{+/-}$), and homozygous knockout (mGlu5$^{-/-}$) mice at 8 w.p.i. (A) and survival (B). To assess relative expression levels, data were analysed using the ΔΔCT method, normalising first to α-tubulin and then to the mean of the control value for the gene of interest, *Cd68*. Data shown are means ± S.E.M. (n=3-4). Statistical analysis was performed using a two-way ANOVA (Tukey's multiple comparisons), where * P≤0.05, **P≤0.01, *** P≤0.001, and **** P≤0.0001.

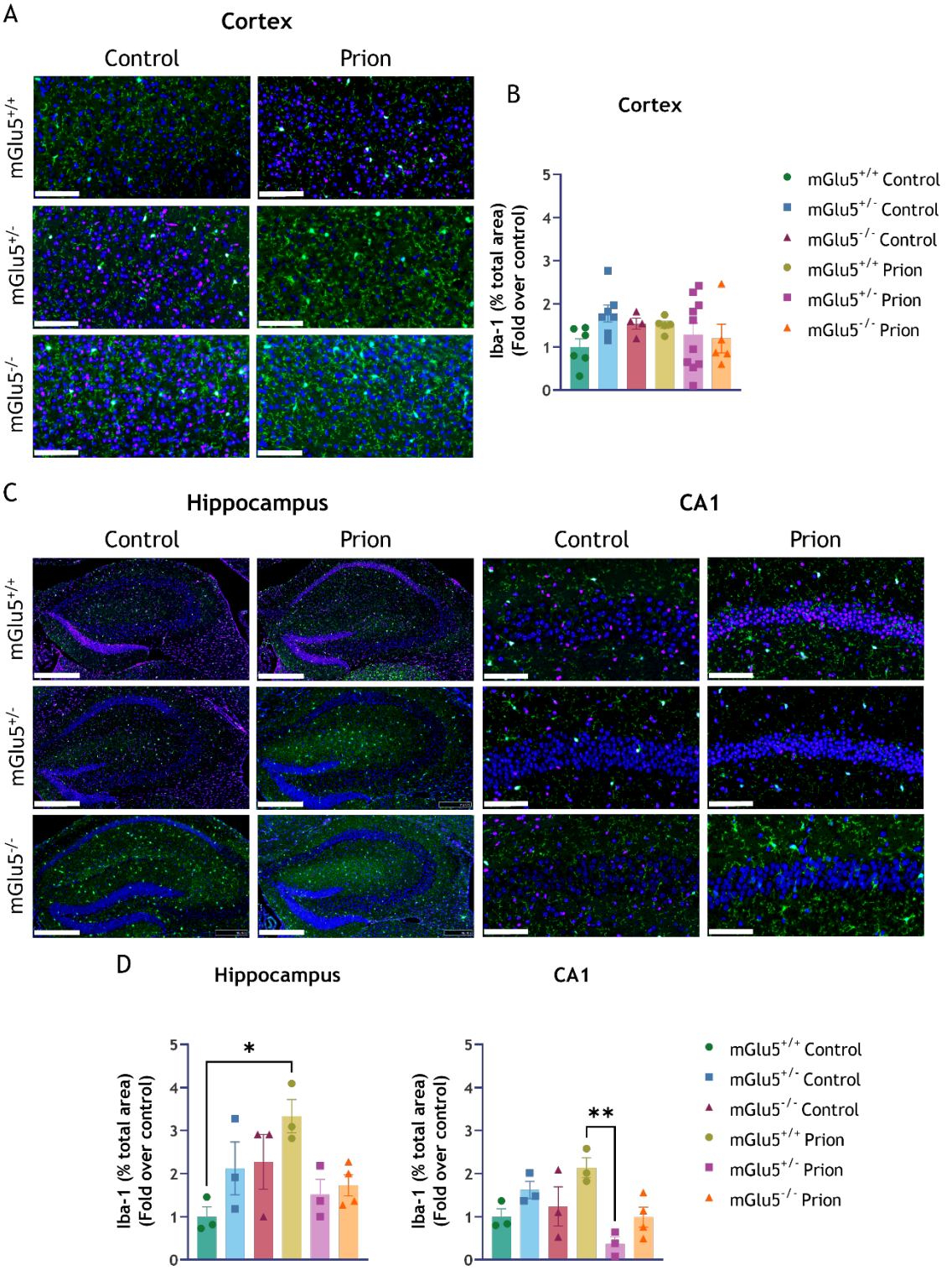

Figure 5-22 Immunohistochemical analysis of the effect of $mGlu_5$ deficiency on microgliosis in control and prion-diseased mice at 8 w.p.i. Staining for Iba-1 (green) in the cortex (A-B), hippocampus, and CA1 (C-D) of control- or prion-infected $mGlu_5$ wild-type ($mGlu5^{+/+}$), heterozygous knockout ($mGlu5^{+/-}$), and homozygous knockout ($mGlu5^{-/-}$) mice at 8 w.p.i. Representative images are shown in (A) and (C) of n=3-10 mice per group. Staining was performed on 5 µm thick coronal sections (Bregma lateral: ~1.40-1.70 mm) and the images were acquired using a NanoZoomer S60 digital slide scanner at 40x magnification. Nuclei are stained with DAPI (blue). Scale bars represent 100 µm in the cortex, 500 µm in the hippocampus, and 100 µm in the CA1. For the quantification in (B) and (D), data are shown as means ± S.E.M, with each data point representing an individual mouse. For each mouse, the data point represents the average staining across 3 consecutive slices. Data are shown as fold over control ($mGlu5^{+/+}$ control). Statistical analysis was performed using a two-way ANOVA (Tukey's multiple comparisons), where * $P \leq 0.05$ and ** $P \leq 0.01$.

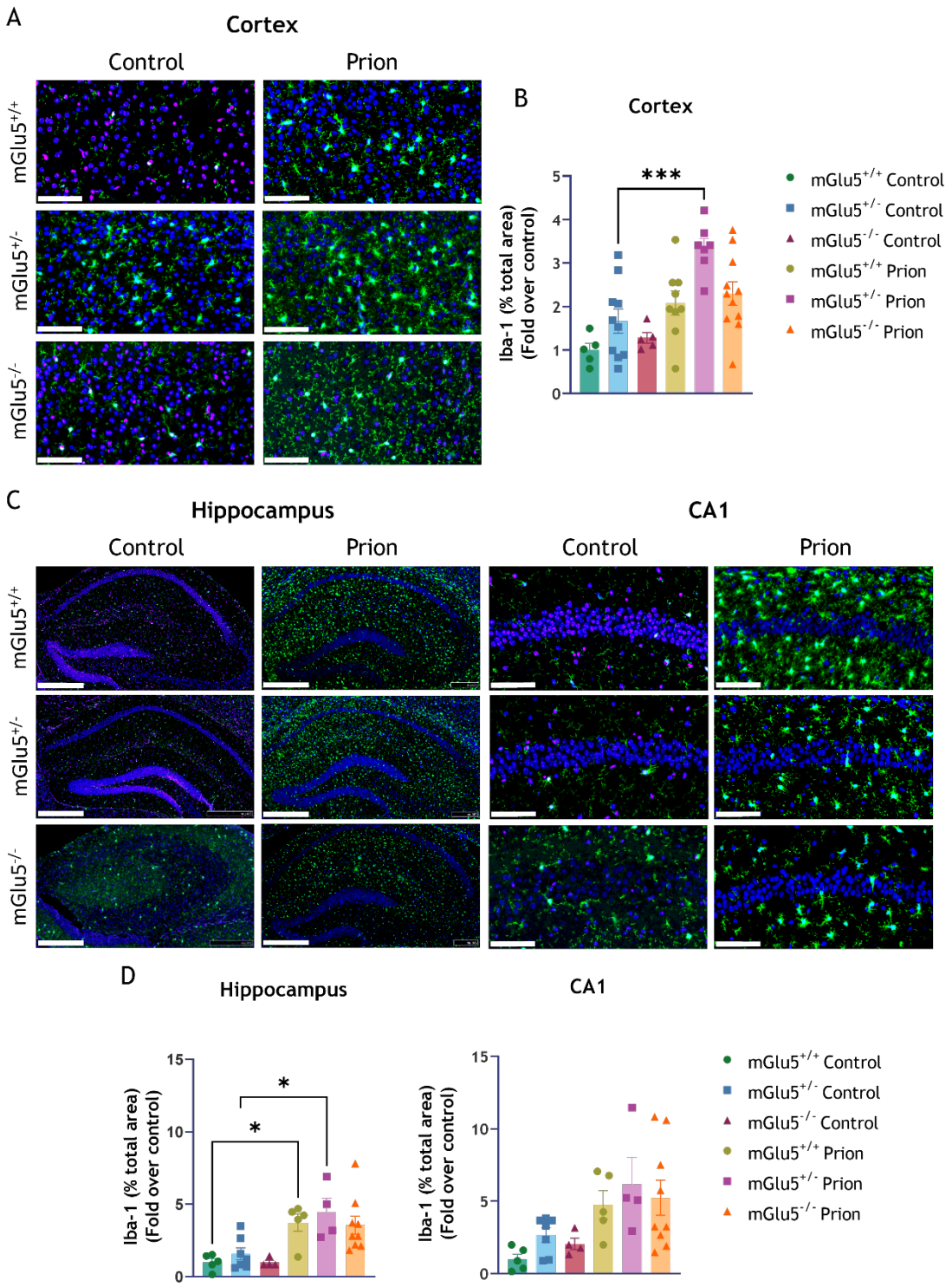

Figure 5-23 Immunohistochemical analysis of the effect of $mGlu_5$ deficiency on microgliosis in control and prion-diseased mice at survival. Staining for Iba-1 (green) in the cortex (A-B), hippocampus, and CA1 (C-D) of control- or prion-infected $mGlu_5$ wild-type ($mGlu5^{+/+}$), heterozygous knockout ($mGlu5^{+/-}$), and homozygous knockout ($mGlu5^{-/-}$) mice at survival. Representative images are shown in (A) and (C) of n=4-11 mice per group. Staining was performed on 5 µm thick coronal sections (Bregma lateral: ~1.40-1.70 mm), and the images were acquired using a NanoZoomer S60 digital slide scanner at 40x magnification. Nuclei are stained with DAPI (blue). Scale bars represent 100 µm in the cortex, 500 µm in the hippocampus, and 100 µm in the CA1. For the quantification in (B) and (D), data are shown as means ± S.E.M, with each data point representing an individual mouse. For each mouse, the data point represents the average staining across 3 consecutive slices. Data are shown as fold over control ($mGlu5^{+/+}$ control). Statistical analysis was performed using a two-way ANOVA (Tukey's multiple comparisons), where * P≤0.05 and *** P≤0.001.

As a recent study found that the genetic deletion of $mGlu_5$ resulted in increased astro- and microgliosis in the cortex of $mGlu_5$ knockout mice as compared to wild-type controls at 6 and 12 months of age (Carvalho et al., 2019), the previously discussed IHC data sets (Figure 5-18, Figure 5-19, Figure 5-22, and Figure 5-23) were used to investigate whether there were any changes in inflammation between control mice taken at 8 w.p.i. and survival (Figure 5-24). At 8 w.p.i, mice were 12 weeks old (3 months) and at survival, mice were 28 weeks old (7 months), allowing for a similar comparison to the published data which compared animals at 2 and 6 months of age (Carvalho et al., 2019). These data cannot be directly compared as here control mice had been inoculated with control brain homogenate at 4 weeks of age. Nevertheless, $mGlu_5$ deficiency did not result in a significant elevation in astro- or microgliosis in these mice at either timepoint (Figure 5-24).

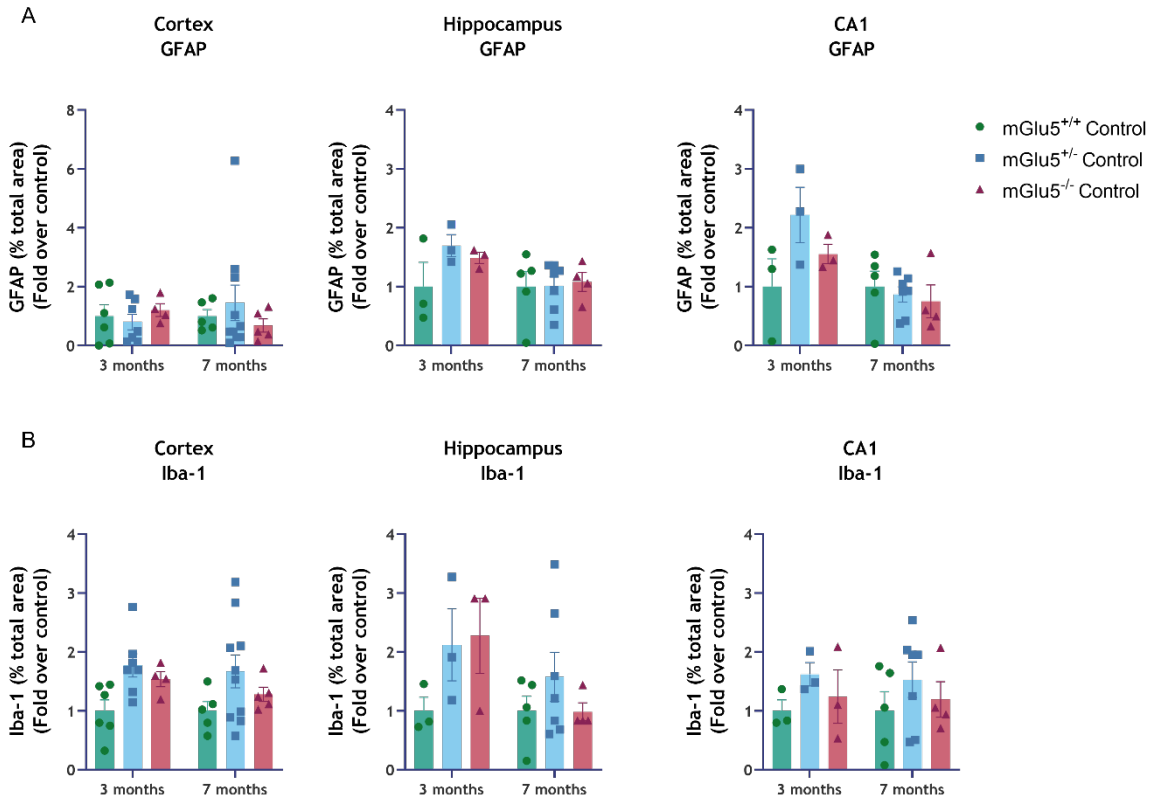

Figure 5-24 Deletion of $mGlu_5$ does not alter levels of astro- and microgliosis in control mice. Graphs show the quantification of GFAP (A) and Iba-1 (B) immunostaining in the cortex, hippocampus, and CA1 in 3- and 7-month-old control mice. This analysis was performed on the data set for which representative images are shown in Figure 5-18, Figure 5-19, Figure 5-22, and Figure 5-23. Data are shown as means ± S.E.M, with each data point representing an individual mouse (n=3-10). For each mouse, the data point represents the average staining across 3 consecutive slices. Data are shown as fold over control ($mGlu5^{+/+}$ control).

Since several cytokines and chemokines are upregulated in human NDD (Brosseron et al., 2014) and have been observed to be increased in murine prion disease (see 4.3.1), their levels were analysed in this study using RT-qPCR. Here, the expression of the pro-inflammatory cytokines, *Il1a*, *Il1β*, *Il6*, and *Tnf*, as well as the expression of the pro-inflammatory chemokine *Csf2*, were investigated in the cortex and hippocampus of control and prion-diseased C57 mice at 8 w.p.i. (Figure 5-25) and survival (Figure 5-26).

At 8 w.p.i., there was no significant difference in the expression of these markers between control and prion-diseased mice in either brain region (Figure 5-25). However, *Il1a* and *Il1β* expression levels were significantly elevated in the hippocampus of mGlu5$^{-/-}$ control mice as compared to mGlu5$^{+/+}$ control mice (P=0.0161 and P=0.0113 respectively) (Figure 5-25 D and E). Interestingly, this upregulation of *Il1a* and *Il1β* in mGlu5$^{-/-}$ control mice was alleviated in mGlu5$^{-/-}$ prion-diseased mice, significantly for *Il1β* (P=0.0318) (Figure 5-25E).

At survival, all three genotypes of prion-diseased mice had elevated gene expression levels of *Il6*, *Tnf*, *Il1a*, and *Il1β* in their cortex and hippocampus as compared to control mice (Figure 5-26). *Csf2* was upregulated in the hippocampus of prion-diseased mice, but not the cortex (Figure 5-26C). This analysis did not detect any differences in expression levels between genotypes in both control and prion-diseased mice, suggesting that mGlu$_5$ ablation does not change the cytokine profiles of prion-diseased mouse brains at end-stage disease.

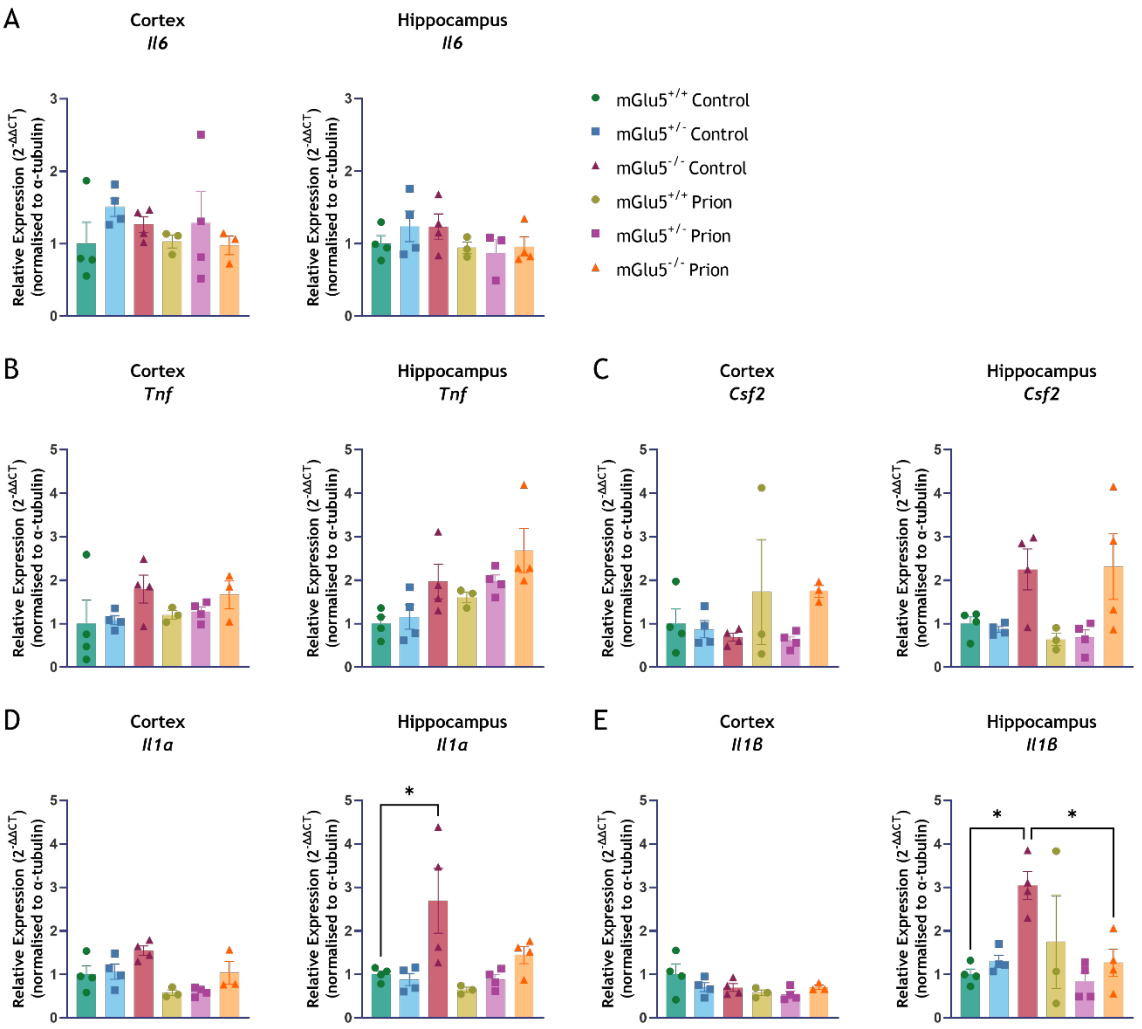

Figure 5-25 RT-qPCR analysis of the effect of mGlu$_5$ deficiency on cytokine and chemokine expression in control and prion-diseased mice at 8 w.p.i. RT-qPCR showing the expression of (A) IL-6 (*Il6*), (B) TNF-α (*Tnf*), (C) GM-CSF (*Csf2*), (D) IL-1α (*Il1α*), and (E) IL-1β (*Il1β*) in the cortex and hippocampus of control- or prion-infected mGlu$_5$ wild-type (mGlu5$^{+/+}$), heterozygous knockout (mGlu5$^{+/-}$), and homozygous knockout (mGlu5$^{-/-}$) mice at 8 w.p.i. To assess relative expression levels, data were analysed using the ΔΔCT method, normalising first to α-tubulin and then to the mean of the control value for the gene of interest. Data shown are means ± S.E.M. (n=4; 2 male, 2 female). Statistical analysis was performed using a two-way ANOVA (Tukey's multiple comparisons), where * P≤0.05.

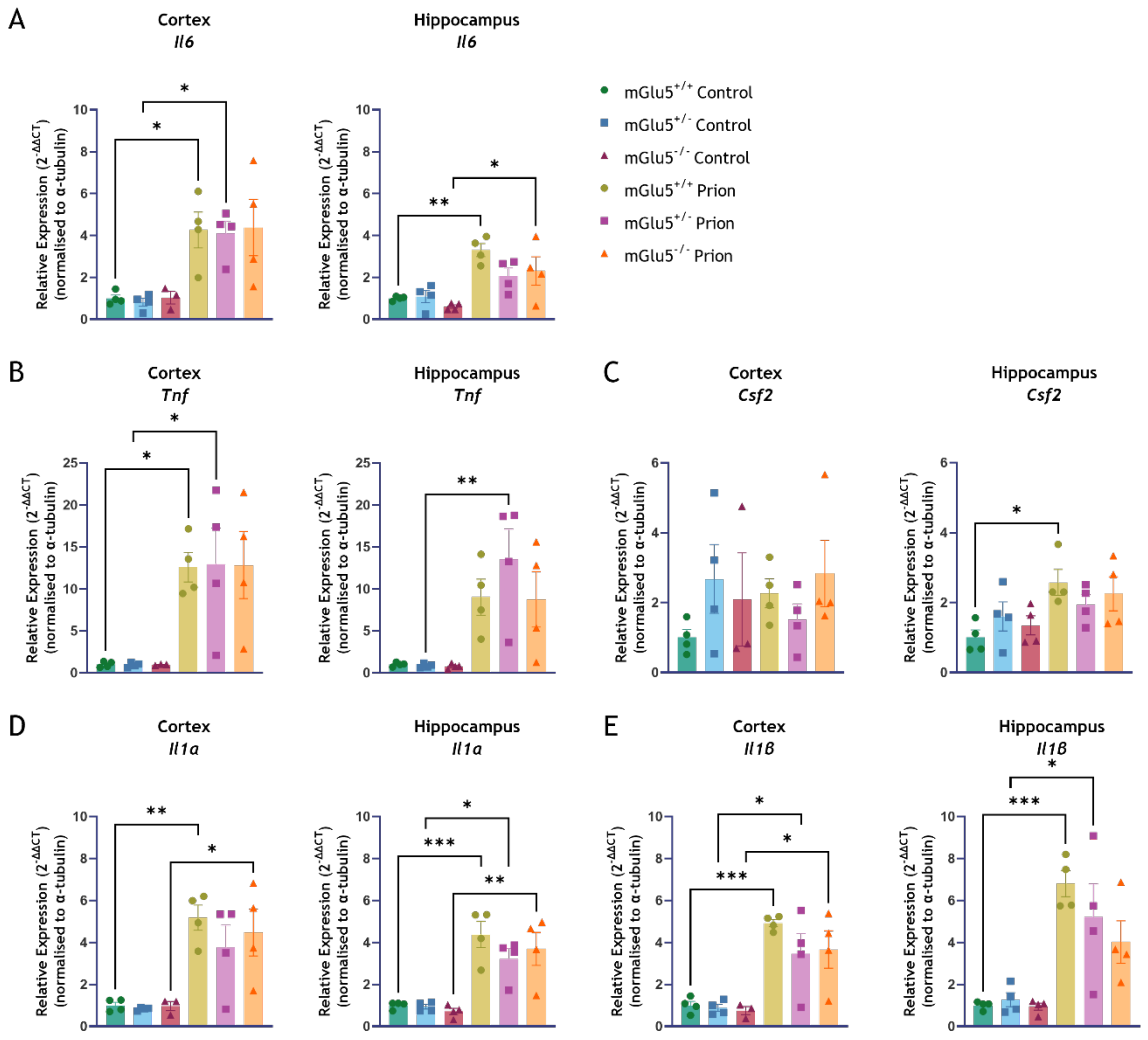

Figure 5-26 RT-qPCR analysis of the effect of mGlu$_5$ deficiency on cytokine and chemokine expression in control and prion-diseased mice at survival. RT-qPCR showing the expression of (A) IL-6 (*Il6*), (B) TNF-α (*Tnf*), (C) GM-CSF (*Csf2*), (D) IL-1α (*Il1α*), and (E) IL-1β (*Il1β*) in the cortex and hippocampus of control- or prion-infected mGlu$_5$ wild-type (mGlu5$^{+/+}$), heterozygous knockout (mGlu5$^{+/-}$), and homozygous knockout (mGlu5$^{-/-}$) mice at survival. To assess relative expression levels, data were analysed using the ΔΔCT method, normalising first to α-tubulin and then to the mean of the control value for the gene of interest. Data shown are means ± S.E.M. (n=4; 2 male, 2 female). Statistical analysis was performed using a two-way ANOVA (Tukey's multiple comparisons), where * P≤0.05, ** P≤0.01, and *** P≤0.001.

Neuronal and synaptic loss are hallmarks of murine prion disease (Mallucci et al., 2003), and a reduction in the expression of PSD95, a post-synaptic marker, has been previously observed in prion-diseased mice (Moreno et al., 2012; Boese et al., 2016). However, in Chapter 4, no change in PSD95 expression was observed in Tg37 prion-diseased mice as compared to controls. Regarding mGlu$_5$, aged mGlu$_5$ knockout mice have been observed to have a reduction in PSD95 levels in the hippocampus, striatum, and cerebral cortex (de Souza et al., 2022). Here, western blot analysis was used to look at protein levels of PSD95 in the cortex

and hippocampus of mGlu5$^{+/+}$, mGlu5$^{+/-}$, and mGlu5$^{-/-}$ control and prion-diseased mice (Figure 5-27). No significant difference was observed in PSD95 expression between control and diseased mice or between genotypes at either timepoint (Figure 5-27 B and D).

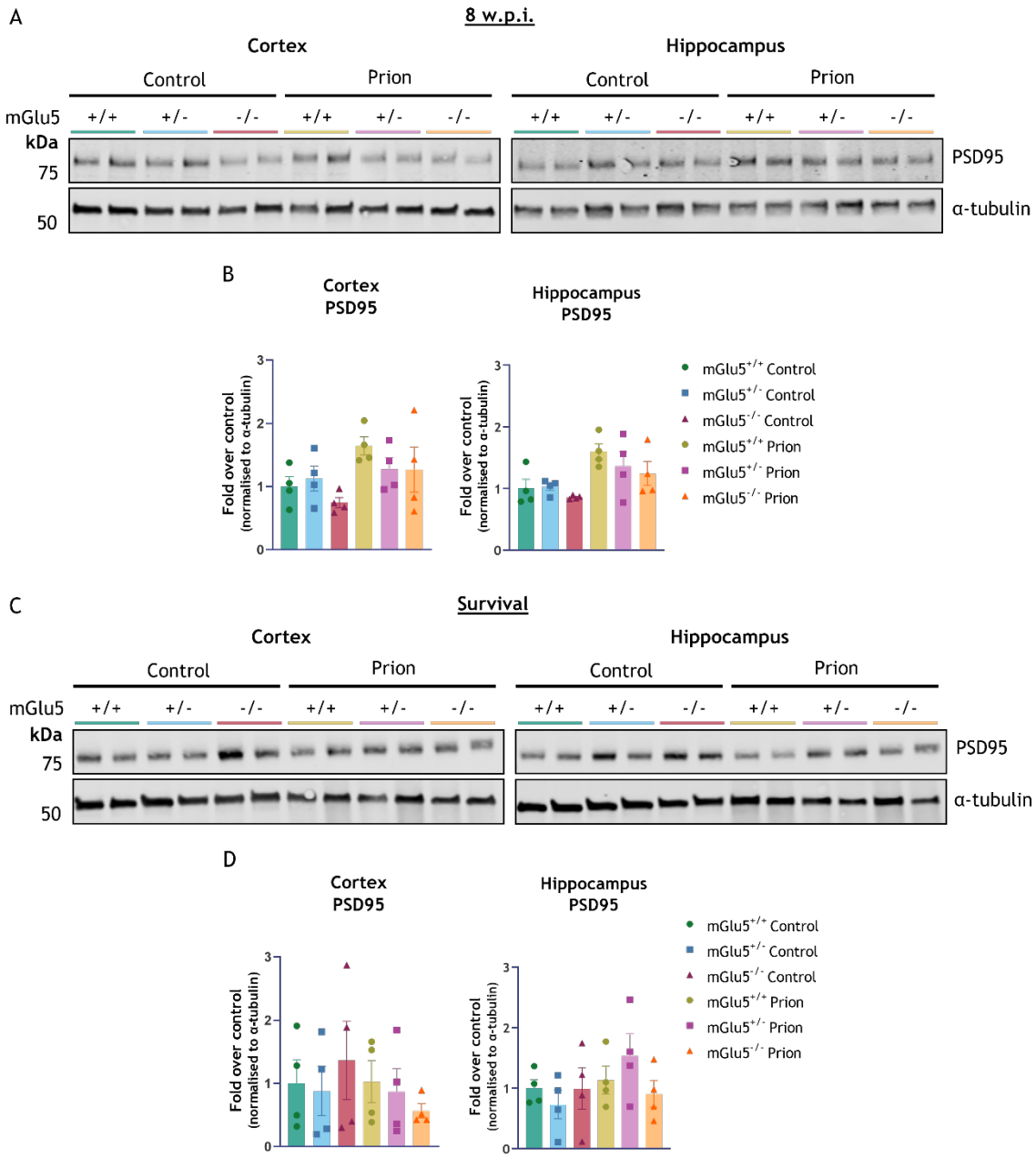

Figure 5-27 Immunoblot analysis of the effect of mGlu$_5$ deficiency on PSD95 expression in control and prion-diseased mice. PSD95 in the cortex and hippocampus was assessed using western blot analysis on lysates prepared from control- or prion-infected mGlu$_5$ wild-type (mGlu5$^{+/+}$), heterozygous knockout (mGlu5$^{+/-}$), and homozygous knockout (mGlu5$^{-/-}$) mice at 8 w.p.i. (A-B) and survival (C-D). Lysates were probed for PSD95, and α-tubulin was used as a loading control. Each lane represents a different mouse, and representative blots are shown. Membranes were stripped and re-probed for multiple antibodies (Figure 5-15, Figure 5-16, Figure 5-20, and Figure 5-27). (B and D) Protein levels were normalised to the loading control, followed by normalisation to the average protein level of the mGlu5$^{+/+}$ control samples expressed as fold change. Data shown are means ± S.E.M., with each data point representing an individual mouse (n=4; 2 male, 2 female).

5.3 Discussion

The $mGlu_5$ receptor has been proposed to play a role in the pathology of a number of NDDs (Budgett et al., 2022). This has highlighted its potential as a therapeutic target that is able to modify disease progression. Murine prion disease, characterised in Chapter 4, is a progressive, terminal NDD which has important similarities with human NDDs. These similarities include the spread of misfolded proteins, elevated neuroinflammation, synaptic dysfunction, and neuronal loss (Bradley et al., 2016; Dwomoh et al., 2022). The inhibition of $mGlu_5$, either pharmacologically or genetically, has been found to be neuroprotective in several rodent models of neurodegeneration. Therefore, it was reasonable to hypothesise that the knockout of $mGlu_5$ would result in a similar neuroprotective role in murine prion disease. However, this study showed that $mGlu_5$ deficiency did not alter the progression of murine prion disease.

5.3.1 The Progression of Murine Prion Disease is Unaltered in $mGlu_5$ Deficient Mice

The focus of this study was to define the impact of $mGlu_5$ knockout on the progression of murine prion disease with the aim of defining a role for $mGlu_5$ in disease progression. Hetero- and homozygous $mGlu_5$ knockout mice were inoculated with prion-infected brain homogenate and the progression of disease evaluated in comparison to wild-type prion-diseased mice. Due to limits on mouse numbers, only two timepoints were investigated: 8 w.p.i. and survival. These timepoints were chosen to compare end-stage disease with an early disease timepoint. The results showed that $mGlu_5$ deficiency did not overtly influence the progression of murine prion disease, with no difference in symptom onset or the survival of $mGlu5^{+/+}$, $mGlu5^{+/-}$, and $mGlu5^{-/-}$ prion-diseased mice.

Two previous papers have investigated the role of $mGlu_5$ in murine prion disease and found that $mGlu_5$ deficiency significantly delayed symptom onset in prion-diseased mice but did not affect mouse survival (Beraldo et al., 2016; Goniotaki et al., 2017). The data presented in this chapter partly agrees with these studies, as $mGlu_5$ knockout did not affect the survival of prion-diseased mice. However, the data differed in that Beraldo et al. (2016) reported a

significant delay in disease onset, which was not observed here. One potential reason for this discrepancy is the differences in scoring protocols. In the previous study, symptom onset was determined by the observation of either clasping of the feet when the mouse was picked up by the tail or a hunched posture. In contrast, this thesis employed a scoring protocol that defined symptom onset as the appearance of two early indicator signs, which included a broad range of symptoms, including a rigid tail, mild loss of coordination, and subdued behaviour, in addition to clasping of the feet and a hunched posture. Two early indicator signs were required for a clinical diagnosis in this thesis as the first symptom to appear was typically subdued behaviour, which is subjective in nature.

Moreover, Goniotaki et al. (2017) found that $mGlu_1$ expression was increased in the brains of $mGlu_5$ knockout mice and suggested that this may have compensated for the lack of $mGlu_5$ and prevented the knockout of $mGlu_5$ from having a neuroprotective effect (Goniotaki et al., 2017). However, in this study, $mGlu_1$ protein expression levels were found to be equivalent in $mGlu5^{+/+}$, $mGlu5^{+/-}$, and $mGlu5^{-/-}$ mice. Therefore, it is unlikely that $mGlu_1$ expression compensated for the lack of $mGlu_5$ in these mice.

Notably, in this study, PrP_{Sc} accumulation was equivalent between the three genotypes of prion-diseased mice, indicating that $mGlu_5$ did not alter the clearance of misfolded prion protein. This agrees with previously published data which similarly found no alteration in PrP_{Sc} accumulation in $mGlu_5$ knockout prion-diseased mice (Beraldo et al., 2016; Goniotaki et al., 2017). However, these results differ from the findings in previous work which knocked out $mGlu_5$ from AD, HD and ALS mouse models and observed a reduction in the presence of misfolded toxic proteins (Hamilton et al., 2014; Ribeiro et al., 2014; Bonifacino et al., 2017, 2019). In AD and HD mouse models, $mGlu_5$ knockout activated autophagy which correlated with the clearance of protein aggregates (Abd-Elrahman et al., 2017, 2018). Further work would reveal whether $mGlu_5$ plays a different role in autophagy in murine prion disease.

5.3.2 Knockout of $mGlu_5$ Reduced Neuroinflammation in Early-Stage Disease

As discussed throughout this thesis, murine prion disease is characterised by the upregulation of neuroinflammatory markers, including the astrocytic marker GFAP and the microglial markers CD68 and Iba-1. Although published data has shown the effect of $mGlu_5$ knockout on symptom onset, survival and PrP_{Sc} accumulation in prion-diseased mice (Beraldo et al., 2016; Goniotaki et al., 2017), there is no published data regarding the effect of $mGlu_5$ knockout on early-stage murine prion disease or prion-induced neuroinflammation.

The data presented in this chapter showed a reduction in astrocytic and microglia markers at 8 w.p.i. in $mGlu_5$-deficient mice. Specifically, IHC staining for GFAP was significantly reduced in $mGlu5^{-/-}$ prion-diseased mice as compared to $mGlu5^{+/+}$ prion-diseased mice in the CA1 region. Moreover, immunoblot analysis showed a significant reduction in Iba-1 expression in both the cortex and hippocampus of $mGlu5^{-/-}$ prion-diseased mice as compared to $mGlu5^{+/+}$ prion-diseased mice, and IHC showed a reduction in Iba-1 staining in the hippocampus and CA1 region of $mGlu5^{+/-}$ and $mGlu5^{-/-}$ prion-diseased mice as compared to $mGlu5^{+/+}$ prion-diseased mice. These differences between genotypes were not observed at the survival time point, with all genotypes of prion-diseased mice exhibiting high levels of inflammation. Therefore, the early dampening of neuroinflammation was not beneficial in the long-term.

There is evidence to suggest that the contribution of $mGlu_5$ to neurodegeneration is disease-stage dependent. The administration of the $mGlu_5$ NAM CTEP to APPswe mice from the age of 6 months for either 24 or 36 weeks was ineffective at ameliorating memory deficits and AD pathology with the longer treatment course (Abd-Elrahman et al., 2020b). In mice treated for 24 weeks, CTEP reversed memory deficits and reduced the levels of Aß plaques and neuroinflammation. The authors suggested that $mGlu_5$ may have a reduced contribution to AD pathology at more advanced stages of disease. These data highlight that targeting $mGlu_5$ may be important in the early stages of AD in order to slow disease progression.

The data discussed in this chapter agrees with the conclusion that $mGlu_5$ may have a reduced contribution to disease pathology at late stages of neurodegeneration (Abd-Elrahman et al., 2020b), with modulation of neuroinflammation observed only in an early disease stage. To gain a more comprehensive understanding of how the modulation of inflammation changed throughout disease progression, it would be important to carry out a longitudinal study that investigates neuroinflammation in $mGlu5^{-/-}$ prion-diseased mice at more time points. However, despite the early reduction in neuroinflammation, $mGlu_5$ deficiency did not alter the progression of prion disease, with no change in PrP_{Sc} accumulation, symptom onset, or survival.

Importantly, as discussed in Chapter 4 (see 4.3.1), microglia are thought to be neuroprotective in early stages of prion disease, clearing PrP_{Sc} aggregates and secreting anti-inflammatory factors (Baker et al., 1999; Cunningham et al., 2002). Therefore, it may be important to enhance the activity of microglia in early-stage disease, rather than reducing their expression as seen here, in order to improve disease progression.

Due to constraints on both time and resources, a limitation of this study is the number of samples used for the biochemical analysis. For example, samples from two male and two female mice were used for most of the biochemical analysis. Given more time and more animals, immunoblotting and RT-qPCR analysis would have been carried out on additional samples from each sex to suitably determine whether there were any sex differences in this study.

Furthermore, IHC analysis was outsourced to the Glasgow Tissue Research Facility, where imaging was carried out on an automatic microscope (NanoZoomer S60 digital slide scanner). Therefore, a slightly larger sample size was achieved, with up to five females and five males. Nonetheless, a key limitation of the IHC data was the low quality of hippocampal sections, with some hippocampal detachment occurring during slicing. Consequently, the available sample numbers for hippocampal and CA1 analysis were lower than initially planned, thus making a comprehensive analysis of male and female samples difficult. Analysis of the cortical samples found no difference between male and female prion-diseased mice.

5.3.3 The Pro-inflammatory Cytokines IL-1α and IL-1β are Increased with $mGlu_5$ Deficiency

In this study, the mRNA expression levels of a number of pro-inflammatory cytokines, as well as the expression of a pro-inflammatory chemokine, were investigated in the cortex and hippocampus of control and prion-diseased mice. Interestingly, gene expression of the pro-inflammatory cytokines *Il1a* and *Il1β* were found to be elevated in the hippocampus of $mGlu5^{-/-}$ control mice as compared to wild-type controls at 8 w.p.i., when the mice were 3 months old. There was no difference in *Il6*, *Tnf*, or *Csf2* expression between genotypes. At survival, all target genes had increased mRNA in the brains of prion-diseased mice as compared to controls, with no difference between genotypes.

IL-1α and IL-1β are two distinct isoforms of the interleukin-1 (IL-1) cytokine family (Allan et al., 2005). Although these isoforms are encoded by distinct genes, they share part of their sequence homology and have similar biological functions (Shaftel et al., 2008). IL-1 plays an important role in local tissue responses to CNS insult and its expression is elevated in a number of CNS diseases, including prion disease (Kordek et al., 1996). A variety of cell types express IL-1, including microglia, astrocytes, oligodendrocytes, endothelial cells, and neurons (Higgins and Olschowka, 1991; Eriksson et al., 1999; Vela, 2002). Importantly, the activation of astrocytes and microglia in neurodegeneration are accompanied by elevated levels of pro-inflammatory cytokines, including IL-1 (Shaftel et al., 2008).

In this study, *Il1a* and *Il1β* were found to be elevated at 8 w.p.i. in the hippocampus of $mGlu5^{-/-}$ control mice. Previous studies investigating the effect of $mGlu_5$ knockout on cytokine expression in mice found expression levels of *Il1β* to be unaltered in the cortex (Carvalho et al., 2019) and prefrontal cortex (Cai et al., 2020). Further work is required to confirm the elevated levels of *Il1a* and *Il1β* in the hippocampus of $mGlu5^{-/-}$ mice seen in this study. Particularly because the $mGlu5^{-/-}$ control animals in this study had been previously inoculated with normal brain homogenate.

5.3.4 PSD95 Expression is Unaltered with $mGlu_5$ Deficiency

In this study, the expression of PSD95 was investigated in control and prion-diseased $mGlu_5$ deficient mice. The results found PSD95 expression to be unaltered both in murine prion disease (confirming the data presented in Chapter 4) and with $mGlu_5$ deficiency. The latter finding is in contrast to published data which reported a reduction in PSD95 expression in $mGlu_5$ knockout mice at 6 and 12 months of age (de Souza et al., 2022). However, in this study, no change was observed in PSD95 expression in $mGlu5^{-/-}$ mice at 3 and 7 months of age. Two key differences between these datasets are: firstly, the mouse background (C57 here, and CD1 previously); and secondly, the experiment used. Here, protein levels were investigated using Western blotting, whereas the previous study examined mRNA levels using RT-qPCR. As previously discussed, mRNA and protein expression levels do not always correlate (Murgaš et al., 2022; see section 4.3.2), and gene expression can vary depending on the mouse strain used (Turk et al., 2004). These differences in protocol may explain the discrepancies between the two sets of findings.

Previously, the authors also observed impaired memory in $mGlu_5$ knockout mice, which they attributed to the loss of PSD95 expression, as well as a reduction in BNDF and Arc/Arg3.1 levels (de Souza et al., 2022). All three of these genes play an important role in memory and synaptic plasticity (Coley and Gao, 2019; Miranda et al., 2019; Plath et al., 2006). Therefore, it would be valuable to conduct further studies on the $mGlu_5$ deficient mice used here, focusing on PSD95 mRNA levels and memory function, similar to the previous work. As the studies described here were carried out on mice inoculated with control and prion brain homogenate, it would be important to conduct these studies in non-inoculated animals.

5.3.5 Burrowing Behaviour is Impaired in $mGlu_5$ Deficient Mice

A common experiment for evaluating the progression of murine prion disease is the burrowing paradigm (Deacon, 2006; Mallucci, 2007, 2009). An innate behaviour of mice is to remove pellets from a container with their feet, termed “burrowing”. As hippocampal lesions result in a significant impairment in burrowing behaviour, this experiment is thought to give an indication of

hippocampal processes (Deacon, 2006). Prion-diseased mice burrow progressively fewer pellets in line with disease progression (Mallucci, 2009; Chapter 4, Figure 4-10). Importantly, this experiment can examine whether treatment with a ligand, or genetic mutations, alters the progression of murine prion disease. For example, treatment of prion-diseased mice with a PAM targeting the M1 muscarinic receptor improved burrowing behaviour in prion-diseased mice (Dwomoh et al., 2022). Conversely, mutations in the M1 receptor to make it phosphorylation-deficient accelerated the decline in burrowing behaviour (Scarpa et al., 2021). In Chapter 4, chronic treatment of prion-diseased mice with a $mGlu_5$ NAM, VU0424238, did not alter the decline in burrowing behaviour observed in prion-diseased mice.

In this chapter, the burrowing paradigm was used in the hope that it would shed light on the effect of $mGlu_5$ deficiency on the progression of murine prion disease. However, $mGlu5^{+/-}$ and $mGlu5^{-/-}$ control mice were found to have a reduction in their burrowing behaviour as compared to $mGlu5^{+/+}$ control mice. In an open field test, this study found $mGlu5^{+/+}$, $mGlu5^{+/-}$, and $mGlu5^{-/-}$ mice to have equivalent locomotor activity, suggesting that the reduction in burrowing behaviour in $mGlu5^{+/-}$ and $mGlu5^{-/-}$ control mice was not due to reduced movement around the cage. Previous work has observed reduced marble-burying in $mGlu_5$ knockout mice (Jew et al., 2013; Xu et al., 2021), a behaviour that is similar to burrowing. Similarly, work in the Bradley lab (Chapter 3, Figure 3-17) has found that $mGlu_5$ NAMs dose-dependently reduce marble-burying behaviour in mice. Other work has found that $mGlu_5$ knockout mice exhibit depression-like behaviour, such as social withdrawal (Shin et al., 2015). Burrowing is a rewarding activity for mice, and as a symptom of depression is withdrawal from rewarding activities (Deacon, 2006), it may be that decreased burrowing in $mGlu_5$ knockout mice is due to an emotional aspect of $mGlu_5$ deficiency.

A key advantage of using the burrowing paradigm is that it is a relatively simple experiment that can be carried out weekly. This enables disease progression to be monitored until end-stage disease. Other behavioural paradigms that enable longitudinal study include motor and balance tests, such as the rotarod, which tests the ability of a mouse to walk on a rotating cylinder. Prion-diseased mice have a progressive decline in rotarod performance (Goniotaki et al., 2017) and

previous studies have found that $mGlu_5$ knockout mice have unaltered motor coordination in this task (Xu et al., 2021). A more thorough characterisation of the $mGlu_5$ deficient mice used in this thesis prior to carrying out the prion-inoculation study would have ensured that a more suitable behavioural paradigm was chosen to examine the potential effects of $mGlu_5$ deficiency on the behaviour of prion-diseased mice.

5.4 Conclusion

Overall, the results presented here suggest that $mGlu_5$ does not play a significant role in the progression of murine prion disease. Neuroinflammation, characterised by astro- and microgliosis, is a hallmark of various NDDs, including prion diseases (Dwomoh et al., 2022; Ransohoff, 2016). Here, $mGlu_5$ deficiency was found to reduce the expression of the inflammatory markers Iba-1 and GFAP at an early stage of murine prion disease. This is a potentially interesting finding and should be investigated more fully. However, the accumulation of PrP_{Sc}, symptom onset, and survival, and therefore, the overall progression of murine prion disease, were unaffected by $mGlu_5$ deficiency.

Taken together with the finding in Chapter 4 that $mGlu_5$ antagonism did not alter the progression of murine prion disease, the results here suggest that $mGlu_5$ is not a major determinant of the progression of murine prion disease. Further work, discussed in Chapter 6, must be done to understand why $mGlu_5$ blockade is neuroprotective in other rodent models of NDD but not murine prion disease. This will have relevance to the treatment of human NDD, as it may be that $mGlu_5$ is a good therapeutic target for some NDDs, but not others.

Chapter 6 Final Discussion

NDDs are a group of neurological disorders characterised by the loss of neurons in the CNS. As neurons are vital for proper brain function, their loss drastically impacts the lives of individuals living with NDDs, leading to impairments in memory, cognition, behaviour, and sometimes motor function (Lamptey et al., 2022). These diseases place a significant burden on the healthcare system as their prevalence rapidly increases due to an ageing population (Qiu, et al., 2009). While recent promising results of AD clinical trials have led to new drug approvals in the United States (see 1.3.3), current treatments for NDDs primarily focus on improving disease symptoms, leaving a significant unmet need for new therapies that can modify disease progression. Due to their involvement in a wide range of physiological processes, around 30% of clinically approved drugs target the GPCR family of receptors (Santos et al., 2017). Among these receptors, $mGlu_5$ has emerged as a potential target for the treatment of NDDs. Previous preclinical studies in rodents have shown that the selective inhibition of $mGlu_5$ using NAMs can modify the underlying disease pathologies associated with several NDDs, such as AD, HD, and ALS. Additionally, these modifications in pathology have been accompanied by improvements in cognitive, behavioural, and motor deficits (for review, see Budgett et al., 2022). Therefore, the primary aim of this thesis was to investigate $mGlu_5$ as a potential therapeutic target for the treatment of NDDs by blocking its activity in a model of murine prion disease using a $mGlu_5$ NAM (Chapter 4) and genetic knockout (Chapter 5). However, in contrast to previous studies indicating neuroprotective effects of $mGlu_5$ NAMs in rodent models of NDDs, the findings presented in this thesis suggest that the blockade of $mGlu_5$ signalling is not beneficial in a preclinical model of murine prion disease.

6.1 Key Findings

Before investigating the therapeutic potential of $mGlu_5$ inhibition in NDD, this thesis characterised a model of murine prion disease. As discussed in section 1.5, numerous animal models are available to study NDDs. However, unlike other NDD models, this murine prion disease model stands out as a bona fide NDD initiated by exposure to brain homogenate containing misfolded PrP_{Sc} (Mallucci, 2009;

Watts & Pruisner, 2014). Mice inoculated with RML prions exhibit several key hallmarks of human NDDs and the disease progression is well-defined (Mallucci, 2009; Watts & Pruisner, 2014). Importantly, this model of neurodegeneration allows for the investigation of the effect of target manipulation on the progression of disease and the lifespan of diseased animals. Moreover, the data presented in Chapter 4 confirmed murine prion disease to be a translatable model of neuroinflammation which can provide valuable insights into the potential of novel ligands to modify the inflammatory response that is a hallmark of NDDs. The characterisation of these mice confirmed previous studies which showed a significant upregulation of several neuroinflammatory markers also observed in human NDD, including GFAP, vimentin, CD68, Iba-1, and several cytokines (Bradley et al., 2016; Mallucci et al., 2003; Dwomoh at al., 2022). This holds particular importance for this study as $mGlu_5$, which is expressed on glial cells, is a potential target for modulating neuroinflammatory processes in NDDs.

However, as part of the characterisation of murine prion disease, this thesis presented two key findings that contrast with the published literature. Firstly, the expression of the postsynaptic marker PSD95 was found to be unaltered in RML-infected Tg37 (Chapter 4) and C57 (Chapter 5) mice. This finding differs from previous research that reported reduced PSD95 expression levels in RML-infected Tg37 (Moreno et al., 2012) and RML-infected CD1 mice (Boese et al., 2016), but was in line with data from human sporadic CJD patients which also found no change in PSD95 expression (Ojeda-Juárez et al., 2022). PSD95 is a key scaffolding protein in the brain, anchoring several proteins to the plasma membrane (Béïque & Andrade, 2003; Fukata et al., 2021). Importantly, PSD95 is one of the scaffolding proteins that enables $mGlu_5$ to form connections with NMDA receptors (Tu et al., 1999). As PSD95 expression was unaltered in the animals used in this thesis, this suggests it may not play a significant role in the pathology of murine prion disease. In CNS disorders where PSD95 does play an important role, the development of PSD95-targeting peptides represents a promising therapeutic strategy as they are able to reduce excitotoxicity and the subsequent neuronal death (Ugalde-Triviño & Díaz-Guerra, 2021). For example, in organotypic hippocampal slices, the overexpression of PSD95 has been shown to protect synapses from the neurotoxic effects of Aß by blocking Aß-induced

conformational changes within the *C*-terminus of NMDA receptors (Dore et al., 2021).

Secondly, the expression of $mGlu_5$ was found to be unaltered with murine prion disease in both Tg37 (Chapter 4) and C57 (Chapter 5) mice at both the protein and mRNA levels, and in human AD patients (Chapter 4) at the mRNA level. This contrasts with previous research that reported reduced $mGlu_5$ expression in prion-diseased mice and hamsters at the disease endpoint (Hu et al., 2022). The previously reported reduction in expression was attributed to neuronal loss, as $mGlu_5$ was significantly co-localised with the neuronal marker NeuN. To better understand the unaltered $mGlu_5$ expression levels reported in this thesis, neuronal loss should be thoroughly investigated in the mice used here. Additionally, it would be interesting to uncover the localisation of $mGlu_5$ to different cell types during murine prion disease by conducting double-staining immunofluorescent co-localisation studies in brain sections. As previous research has found $mGlu_5$ to be upregulated in glial cells surrounding NDD pathology (Casley et al., 2009; Lim et al., 2013; Shrivastava et al., 2013; Vermeiren et al., 2006), and glial cells are themselves upregulated in murine prion disease, it is plausible to hypothesise that an elevation in glial $mGlu_5$ may have hidden any loss of neuronal $mGlu_5$ when $mGlu_5$ expression was probed for in western blot experiments in this thesis. As discussed in section 4.3.3, the data from human AD patients contrasts with *in vitro* autoradiography studies in human post-mortem tissue, which reported increased $mGlu_5$ expression in human AD (Müller Herde et al., 2019). PET imaging studies have shown a reduction in $mGlu_5$ expression in human patients at early stages of AD (Mecca et al., 2020; Treyer et al., 2020). Further studies, preferably longitudinal in nature, are required to fully understand how $mGlu_5$ expression changes throughout the course of human AD. This understanding is important for the development of any future drug strategies that target $mGlu_5$ in neurodegeneration. Although, as discussed below, the results in this thesis may preclude $mGlu_5$ from being an ideal drug target for treating NDDs, it is evident that it does play a role in several disease-related processes. Therefore, there is still a need for basic science to improve understanding of its role throughout the course of NDDs.

Against the initial hypothesis that $mGlu_5$ inhibition would be neuroprotective in murine prion disease, and in contrast to prior findings reported in the literature, the main finding of this thesis is that the inhibition of $mGlu_5$, both pharmacologically (Chapter 4) and genetically (Chapter 5), did **not** significantly alter the progression of murine prion disease. This is based on solid but unexpected data demonstrating that $mGlu_5$ inhibition did not result in significant changes in symptom onset or survival rates of either sex of prion-diseased mice, or the burrowing behaviour of female prion-diseased mice. These findings contrast with previous studies investigating $mGlu_5$ inhibition in murine prion disease, which demonstrated that the pharmacological inhibition of $mGlu_5$ significantly improved behaviour and survival in prion-diseased mice (Goniotaki et al., 2017), and that the genetic inhibition of $mGlu_5$ significantly delayed symptom onset (Beraldo et al., 2016). As discussed in the relevant results chapters, these discrepancies may have been due to factors such as experimental protocols, mouse genetic background, and the compounds administered.

Although $mGlu_5$ inhibition provided no significant neuroprotective effect in murine prion disease, the results in this thesis highlight the potential of $mGlu_5$ inhibition to modulate neuroinflammatory processes in NDD, as discussed subsequently. These results are in line with previous *in vivo* studies that demonstrated that the blockade of $mGlu_5$ signalling, either pharmacologically or genetically, significantly reduced the elevated expression of astrocyte and microglia markers in preclinical models of AD, ALS, and HD (Abd-Elrahman et al., 2017; Bonifacino et al., 2017; Hamilton et al., 2014, 2016). In previous studies in murine prion disease, the expression of GFAP was found to be reduced in prion-diseased mice after the chronic inhibition of $mGlu_5$ using MPEP (Goniotaki et al., 2017). However, the previous study was limited to male mice and lacked specific details surrounding the time point at which GFAP reduction occurred. In contrast, the study in this thesis provides novel insights which indicate that the reduction in neuroinflammation observed here in murine prion disease is dependent on both sex and disease stage.

In Chapter 4 of this thesis, IHC analysis showed that VU0424238 significantly reduced GFAP expression in the CA1 and CA3 hippocampal regions of female, but

not male, prion-diseased mice. In the context of NDDs, and specifically studies involving $mGlu_5$, most animal research has focused solely on male mice (discussed in section 4.1.4). As mentioned above, this is true for the published study investigating MPEP in prion-diseased mice (Goniotaki et al., 2017). The other study investigating $mGlu_5$ and prion disease did not specify the sex of the mice (Beraldo et al., 2016). Therefore, this thesis likely represents the first study examining the effect of $mGlu_5$ inhibition in both male and female prion-diseased mice. Previous work in other rodent models of NDD has found that male and female mice respond differently to $mGlu_5$ inhibition (Abd-Elrahman et al., 2020; Bonifacino et al., 2019; Milanese et al., 2021). However, there are inconsistencies in these previous studies, with some studies showing benefits in males but not females (Abd-Elrahman et al., 2020; Bonifacino et al., 2019; Li et al., 2022), and *vice versa* (Milanese et al., 2021). Further work is required to fully understand the differences in the contribution of $mGlu_5$ to disease pathology between the sexes. The finding that there are differences, however subtle, highlights how important it is to include both sexes of mice in preclinical studies to improve healthcare for women. This is particularly relevant in the field of NDD, where it is well-established that sex affects an individual's susceptibility to and progression of disease, including AD (Deming et al., 2018), HD (Hentosh et al., 2021), and ALS (Trojsi et al., 2020). In human AD, for example, disease pathology, including hippocampal atrophy and Aß and tau accumulation, occurs earlier (Buckley et al., 2019) and progresses more quickly (Canevelli et al., 2017) in women compared with men. Subsequently, cognitive and physical decline occurs faster in women (Zalewska et al., 2022). By taking sex-specific responses into consideration, more targeted and effective treatments for NDD can be developed.

In Chapter 5, the neuroinflammatory markers GFAP and Iba-1 were reduced in $mGlu_5$ knockout mice at 8 w.p.i. but not at the disease endpoint. Previously published work has suggested that the contribution of $mGlu_5$ to the pathology of NDDs is disease stage-dependent, with the efficacy of $mGlu_5$ antagonism diminishing with age in AD model mice (Abd-Elrahman et al., 2020). The data presented in this thesis agree with the conclusion of the previous study, suggesting that $mGlu_5$ inhibition may contribute to a reduction in pathology in early but not late-stage disease. Importantly, as there was no significant

reduction in $mGlu_5$ expression throughout disease progression, these findings are likely due to a decreased contribution of $mGlu_5$ signalling to disease pathology with age, rather than a loss in $mGlu_5$ expression. These findings have therapeutic implications as it is important to consider which targets will maintain efficacy throughout the progression of NDDs. More work is required to understand the contribution of $mGlu_5$ to the pathology of various NDDs throughout disease progression. However, the data presented here and previously (Abd-Elrahman et al., 2020), suggest that alternative treatments may be needed for late-stage NDD. Some current treatments for NDDs also show disease stage-dependent effects. For example, the recently FDA-approved drugs for AD, aducanumab and lecanemab, have been shown to have efficacy in individuals at early, and therefore mild, stages of AD (Budd Haeberlein et al., 2022; Swanson et al., 2021). Both these drugs target the accumulation of Aß, and it is unknown if they will continue to have benefits in the late stages of AD where disease pathology is severe and has spread to the entire cortex. Of the two FDA-approved treatments for ALS, riluzole, a glutamatergic antagonist, has been shown to significantly extend the lifespan of ALS patients (Bensimon et al., 1994; Lacomblez et al., 1996). However, post-hoc analysis of the original clinical studies found that riluzole prolongs the survival of patients at the final stage of the disease rather than prolonging the earlier disease stages or the entire course of the disease (Fang et al., 2018). These findings highlight the importance of understanding the contribution of drug targets to each stage of disease progression to ensure the development and provision of the most optimal therapeutic options for patients.

Targeting common mechanisms shared amongst NDDs, such as the neuroinflammation discussed throughout this thesis, is a promising approach for the treatment of these diseases. While neuroinflammation is typically a neuroprotective mechanism that helps to maintain neuronal health (Wang & Bordey, 2008), in the context of NDDs, chronic neuroinflammation can result in neurotoxicity (Ransohoff, 2016). Microglia and astrocytes are the key mediators of the inflammatory processes that occur in NDD and targeting these cell types represents an exciting avenue for the development of novel therapeutics (Ransohoff, 2016; Si et al., 2023). Importantly, in humans, elevated levels of inflammatory markers occur at an early stage of the progression of several NDDS, including AD (Gispert et al., 2016; Hall et al., 2017) and PD (Zhang et al., 2023).

This may allow for the targeting of these cell types from the earliest stages of disease. Several small molecules and monoclonal antibodies have been developed that target the signalling pathways and receptors involved in neuroinflammatory processes (Zhang et al., 2023). For example, semaphorin 4D (Sema4D) is a protein that regulates the transition of glial cells from a resting to reactive state under chronic stress or injury (Smith et al., 2015). Pepinemab, a monoclonal antibody for Sema4D, has shown promise in preclinical models of NDD where it preserved the normal function of glial cells (Southwell et al., 2015). This novel compound has been investigated in clinical trials for multiple sclerosis (LaGanke et al., 2017) and HD (Feigin et al., 2022) and is currently in a phase I trial for the treatment of mild AD (clinicaltrials.gov; NCT04381468). In addition, several drugs that protect against microglial activation, such as naloxone (Tang et al., 2021), minocycline (Cankaya et al., 2019) and CSF1R inhibitors (Han et al., 2022) are at various stages of development. As microglia and astrocytes also play a neuroprotective role in the brain, it is important to consider the timing of therapies that halt their activation. In the early stages of disease, anti-inflammatory drugs may prove to be detrimental and encouraging the activation of these cell types may be required instead. In mice models of AD, activating microglia prior to plaque formation has been shown to reduce Aß load and, in some cases, improve cognition (Boissonneault et al., 2008; DiCarlo, 2001; Iaccarino et al., 2016). Overall, it is hoped that therapies which target neuroinflammatory processes will provide effective therapeutic interventions for NDD in the future. However, an improved understanding of the contribution of neuroinflammation to neurodegeneration is important for the fine-tuning of these potential therapies.

Regarding $mGlu_5$, its inhibition has been shown to reduce neuroinflammation in several rodent models of NDD, which was paralleled by overall neuroprotection and improved cognition (Abd-Elrahman et al., 2017; Bonifacino et al., 2017; Hamilton et al., 2014, 2016). However, despite the reduction in gliosis observed in female mice in Chapter 4, and at the early disease timepoint in Chapter 5, here the inhibition of $mGlu_5$ did not significantly alter the overall progression of murine prion disease, as previously discussed. It is important to recognise that NDDs are complex, multifaceted diseases characterised by numerous hallmarks. In the case of murine prion disease, these hallmarks include not only

neuroinflammation but also PrP_{Sc} accumulation, neuronal loss, and the loss of cholinergic signalling (Mallucci et al., 2003). Each of these hallmarks is complex in its own right, and targeting one aspect alone may not improve the others or the overall disease pathology. Therefore, a multifaceted approach is likely required for effective NDD treatment.

Understanding the precise involvement of $mGlu_5$ in NDDs is vitally important for the development of future drug strategies. Studies in AD mouse models have shed light on the potential role of $mGlu_5$ in the pathology of NDDs. As discussed in 1.3.4.1, the Aßos that are a key hallmark of AD form a complex with PrP_C and $mGlu_5$. This complex results in the clustering of $mGlu_5$ at the cell surface, where they are more readily available for activation, leading to excitotoxicity (Laurén et al., 2009; Um et al., 2013). Notably, this complex involving a pathogenic misfolded protein and $mGlu_5$ has been observed not only in AD but also in other NDDs such as HD (Anborgh et al., 2005; Tang et al., 2003), dementia with Lewy bodies, and PD (Ferreira et al., 2017). In dementia with Lewy bodies and PD, α-synuclein is the disease-causing misfolded protein. Soluble α-synuclein oligomers form a complex with $mGlu_5$, with PrP_C acting as a co-receptor, similar to what is observed in AD (Ferreira et al., 2017). Interestingly, a $mGlu_5$ SAM, BMS-984923, has shown neuroprotective effects in AD rodent models by blocking neurotoxic Aßo signalling while preserving glutamate signalling *via* $mGlu_5$ (Haas et al., 2017; Spurrier et al., 2022) (see 1.3.4.1). This compound has recently been tested in a phase I clinical trial in healthy human patients to assess its pharmacokinetics and safety (clinicaltrials.gov: NCT04805983). The results of this trial have not yet been made public. These findings highlight the therapeutic benefit of targeting the Aßo-PrP_C-$mGlu_5$ complex in preclinical AD models.

However, in murine prion disease, where PrP_C is converted into PrP_{Sc} upon direct interaction between the two proteins (Resenberger et al., 2011), whether a similar complex forms between PrP_{Sc} and $mGlu_5$ remains unclear. To further the work in this thesis, it would be important to determine whether PrP_{Sc} and $mGlu_5$ directly interact. This could be established by carrying out a co-immunoprecipitation assay. Moreover, it would be interesting to establish whether PrP_{Sc} triggers the same toxic signalling pathways downstream of $mGlu_5$

as Aβo and α-synuclein oligomers. Both Aβos and α-synuclein oligomers result in neurotoxicity *via* the phosphorylation of Fyn Kinase and excessive Ca^{2+} release (Ferreira et al., 2017; Haas & Strittmatter, 2016; Um et al., 2013). Similarly, direct interaction between mHtt and $mGlu_5$ in HD leads to downstream Ca^{2+}-mediated excitotoxicity (Anborgh et al., 2005; Tang et al., 2003). As PrP_C binds directly to $mGlu_5$ (Um et al., 2013), PrP_{Sc} toxicity may impact $mGlu_5$ signalling *via* a different mechanism to other misfolded proteins such as Aβ and α-synuclein. For example, it has been demonstrated that PrP_C which is converted into PrP_{Sc} at the cell surface mediates pro-apoptotic signalling (Resenberger et al., 2011). Differences in the relationship between PrP_{Sc} and $mGlu_5$ compared with other disease-associated misfolded proteins may explain why $mGlu_5$ antagonism is neuroprotective in other rodent models of NDD but not murine prion disease.

In NDDs where $mGlu_5$ is directly involved in disease pathology, it may be that $mGlu_5$ inhibition would be most effective in combination with a protein-clearing therapy. As the accumulation of misfolded, toxic proteins is the most common hallmark of NDDs, many therapeutic strategies focus on clearing these proteins from the brain. These therapies are broad in their mechanism of action and include enhancing protein degradation (Guo et al., 2018), reducing protein production (Menting & Claassen, 2014) and using immunotherapy (Valiukas et al., 2022). In AD and HD mouse models, the inhibition of $mGlu_5$ has been shown to reduce the levels of the disease-associated misfolded proteins (Hamilton et al., 2014; Ribeiro et al., 2014). This has been attributed to mechanisms that include a $mGlu_5$-dependent increase in autophagy (Abd-Elrahman et al., 2017, 2018) and, in AD, a reduction in FMRP expression leading to decreased Aβ formation (Hamilton et al., 2014). Moreover, $mGlu_5$ may play a role in tau accumulation in AD through its association with Fyn kinase. Fyn kinase is activated *via* the formation of the Aβo-PrP_C-$mGlu_5$ complex (Um et al., 2013) and this activation leads to the downstream hyperphosphorylation of tau (Larson et al., 2012). The inhibition of Fyn kinase has been shown to reduce the accumulation of hyperphosphorylated tau and ameliorate cognitive deficits in both a traumatic and transgenic tauopathy mouse model (Tang et al., 2020). The $mGlu_5$ NAM MTEP prevents the Aβo-induced activation of Fyn kinase (Haas & Strittmatter, 2016), and it would be interesting to uncover whether $mGlu_5$

inhibition would reduce both Aß and tau load in an AD mouse model which exhibits both amyloid and tau pathologies.

However, as $mGlu_5$ inhibition did not alter the accumulation of PrP_{Sc} in murine prion disease in this thesis and in the published literature (Beraldo et al., 2016; Goniotaki et al., 2017), it is likely that $mGlu_5$ does not play a protein-clearing role in this particular disease model. Nevertheless, $mGlu_5$ inhibition has been shown to alter several pathways that are downstream from the accumulation of disease-associated misfolded proteins. For example, it reduces excitotoxicity (Lv et al., 2014) and decreases CREB and BDNF signalling (De Souza et al., 2020, 2022). In murine prion disease, $mGlu_5$ inhibition has been shown to reduce the toxicity of prions both *in vitro* and *in vivo* (Goniotaki et al., 2017) and reduce neuroinflammation *in vivo* (here and Goniotaki et al., 2017). Therefore, inhibiting $mGlu_5$ may be an effective therapy for NDDs if combined with a therapy that aims to clear misfolded proteins from the brain. Protein-clearing therapies are currently of huge interest in the field of NDDs, particularly with the recent FDA approval of two anti-amyloid therapies for AD: aducanumab (Arndt et al., 2018; Sevigny et al., 2016) and lecanemab (Swanson et al., 2021). Both these anti-amyloid antibodies have been shown to reduce Aß levels in the brains of patients with mild AD, thus providing evidence that modifying disease in human patients is possible.

Finally, in this thesis, a decision was made to focus on inhibiting $mGlu_5$ based on findings that $mGlu_5$ inhibition has been consistently neuroprotective in other rodent models of NDDs (see 1.3.4.2). However, a small number of previous studies have found $mGlu_5$ PAMs to be neuroprotective in AD and HD (Bellozi et al., 2019; Doria et al., 2015; see 1.3.4.3). Consequently, future work could investigate whether $mGlu_5$ agonism, rather than $mGlu_5$ antagonism, is neuroprotective in murine prion disease. However, a key consideration regarding $mGlu_5$ PAMs compared to $mGlu_5$ NAMs is their neurotoxic side effects in rodent models, which has halted their progress to clinical trial (Bridges et al., 2013; Parmentier-Batteur et al., 2014; Rook et al., 2013).

6.2 Conclusions

In conclusion, the findings presented in this thesis suggest that the inhibition of $mGlu_5$ is not neuroprotective in prion-diseased mice, contrary to what has been reported previously in *in vivo* rodent models of AD, HD, ALS, and PD (Budgett et al., 2022). This finding is of importance as it highlights a key issue faced by researchers in the field of NDDs: the lack of comprehensive models of NDD that fully replicate human neurodegeneration. As demonstrated here, a drug target may show promise in one model but not others. As many studies have reported beneficial outcomes of $mGlu_5$ inhibition in mouse models of NDD (Um et al., 2013; Hamilton et al., 2014, 2016; Abd-Elrahman et al., 2017, 2018, 2020; Bonifacino et al., 2017, 2019; Ribeiro et al., 2014; Schiefer et al., 2004; Li et al., 2022), it was surprising to find that neither the pharmacological inhibition nor the complete knockout of $mGlu_5$ had a significant effect on the progression of murine prion disease. Overall, this suggests that $mGlu_5$ does not play a major role in prion pathogenesis in this model of murine prion disease and highlights that, although there are some common hallmarks between NDDs, $mGlu_5$ may play a different role in these diseases.

Notably, previous studies have demonstrated significant neuroprotection in the specific model of murine prion disease used in this thesis, with compounds such as VU0486846, BQCA, DBM and trazodone showing efficacy (Bradley et al., 2016; Dwomoh et al., 2022; Halliday et al., 2017). This indicates that other mechanisms can be targeted to achieve neuroprotection in this model of murine prion disease, despite its aggressive and rapid progression. Importantly, some of these compounds have also shown efficacy in other models of NDD. For example, VU0486846 has been shown to be neuroprotective in the APPswe model of AD (Abd-Elrahman et al., 2022). Therefore, the lack of neuroprotection observed after $mGlu_5$ inhibition in murine prion disease brings into question the suitability of $mGlu_5$ as a target for the treatment of NDDs.

These findings are important as they highlight that the mechanism of neurodegeneration may impact the neuroprotective potential of a drug and emphasises the need to test novel clinical candidates in a variety of models of NDD. Moreover, the data presented in this thesis highlights the importance of considering sex and disease stage when investigating the impact of $mGlu_5$

inhibition, and likely other novel ligands, on neuroinflammation and other neurodegenerative processes.

Recent significant advancements in the field do provide hope for patients with NDDs. Within the two years preceding this thesis, the FDA approved two novel drugs that have shown promise in altering the underlying pathology of AD: aducanumab (Budd Haeberlein et al., 2022) and lecanemab (Swanson et al., 2021). A third drug, donanemab, is currently being considered for FDA approval (Eli Lilly and Company, 2023). These three drugs target Aß peptides and indicate that disease-modifying treatments for NDD are possible. Similarly, tofersen received accelerated approval from the FDA in April 2023 for the treatment of ALS. This drug is an antisense oligonucleotide which slows the production of SOD1 and aims to reduce SOD1 accumulation in the brains of ALS patients (Biogen, 2023). Other promising strategies targeting biological processes such as neuroinflammation, mitochondrial dysfunction, and vasculature are in various stages of development and provide further hope for disease-modifying therapies in the future (Cummings et al., 2022). Although targeting $mGlu_5$ in this thesis did not demonstrate neuroprotective potential as initially hoped, it may be that combining this approach with protein-clearing therapies would provide more effective therapies for NDD in the future.

Appendices

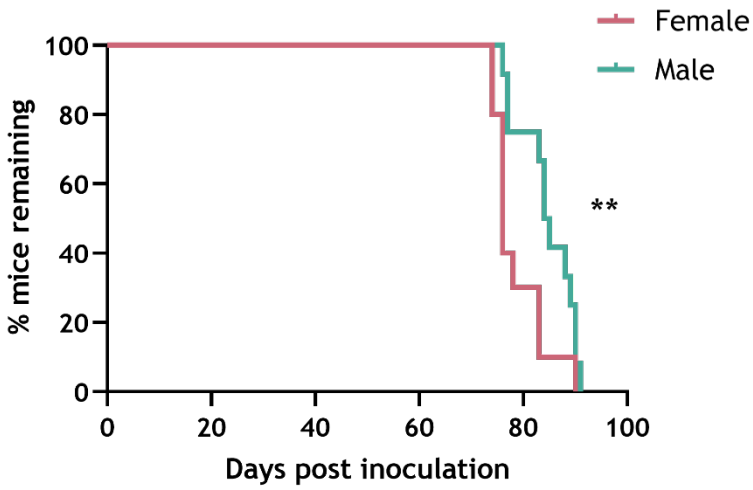

Appendix Figure 1 Comparison of survival between vehicle-treated male and female prion-diseased mice. Kaplan-Meier survival plots for vehicle-treated female (red) and male (green) prion-diseased mice. Data shown form part of Figure 4-12. Curves were analysed with a Gehan-Breslow-Wilcoxon test, where ** P≤0.01 (female vehicle n=10, male vehicle n=12).

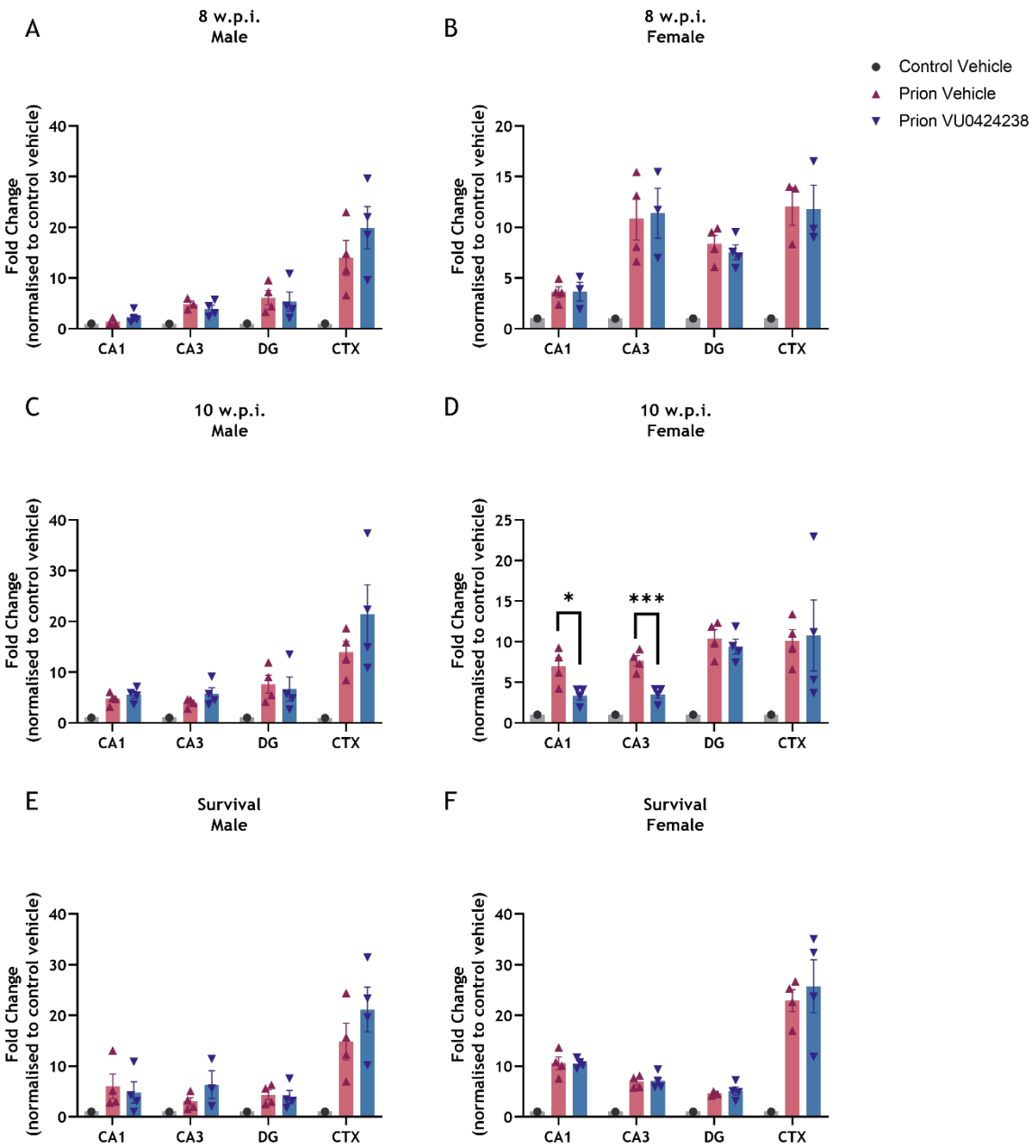

Appendix Figure 2 Comparison of GFAP expression in the cortex and hippocampus of male and female prion-diseased mice treated with either vehicle or VU0424238. Quantification of IHC images from Figure 4-21, Appendix Figure 5, and Appendix Figure 6, showing data from male (A, C and E) and female (B, D, and F) mice at 8 w.p.i. (A-B), 10 w.p.i. (C-D) and survival (E-F). Data were normalised to control vehicle and are shown as mean ± S.E.M. with data points representing individual mice (n=3-4). Statistical analysis was a two-way ANOVA (Tukey's multiple comparisons), where * $P \leq 0.05$, *** $P \leq 0.001$; only differences between prion vehicle and prion VU0424238 are shown.

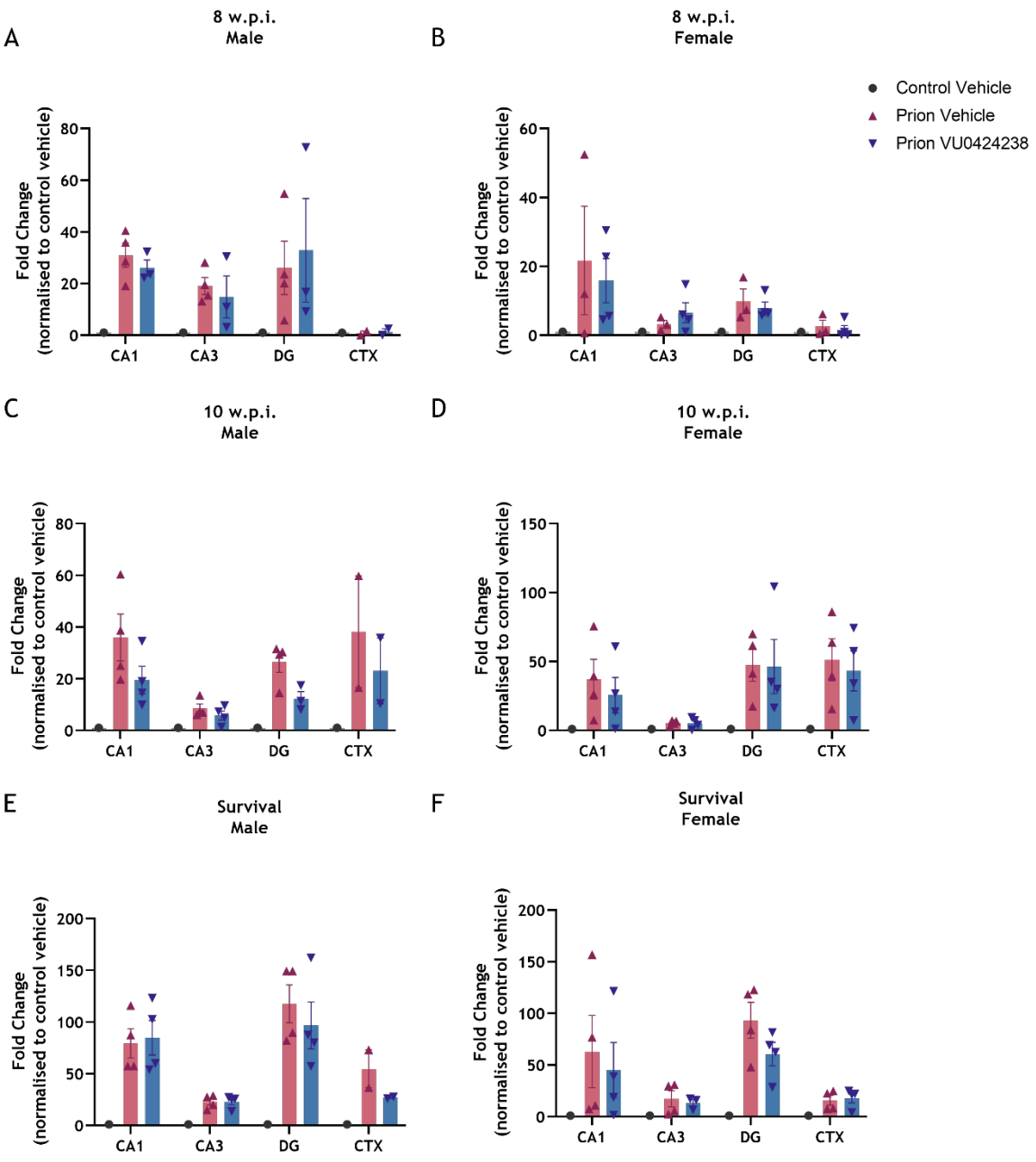

Appendix Figure 3 Comparison of vimentin expression in the cortex and hippocampus of male and female prion-diseased mice treated with either vehicle or VU0424238. Quantification of IHC images from Figure 4-22, Appendix Figure 7, and Appendix Figure 8, showing data from male (A, C and E) and female (B, D, and F) mice at 8 w.p.i. (A-B), 10 w.p.i. (C-D) and survival (E-F). Data were normalised to control vehicle and are shown as mean ± S.E.M. with data points representing individual mice (n=2-4). Statistical analysis was a two-way ANOVA (Tukey's multiple comparisons); only differences between prion vehicle and prion VU0424238 are shown.

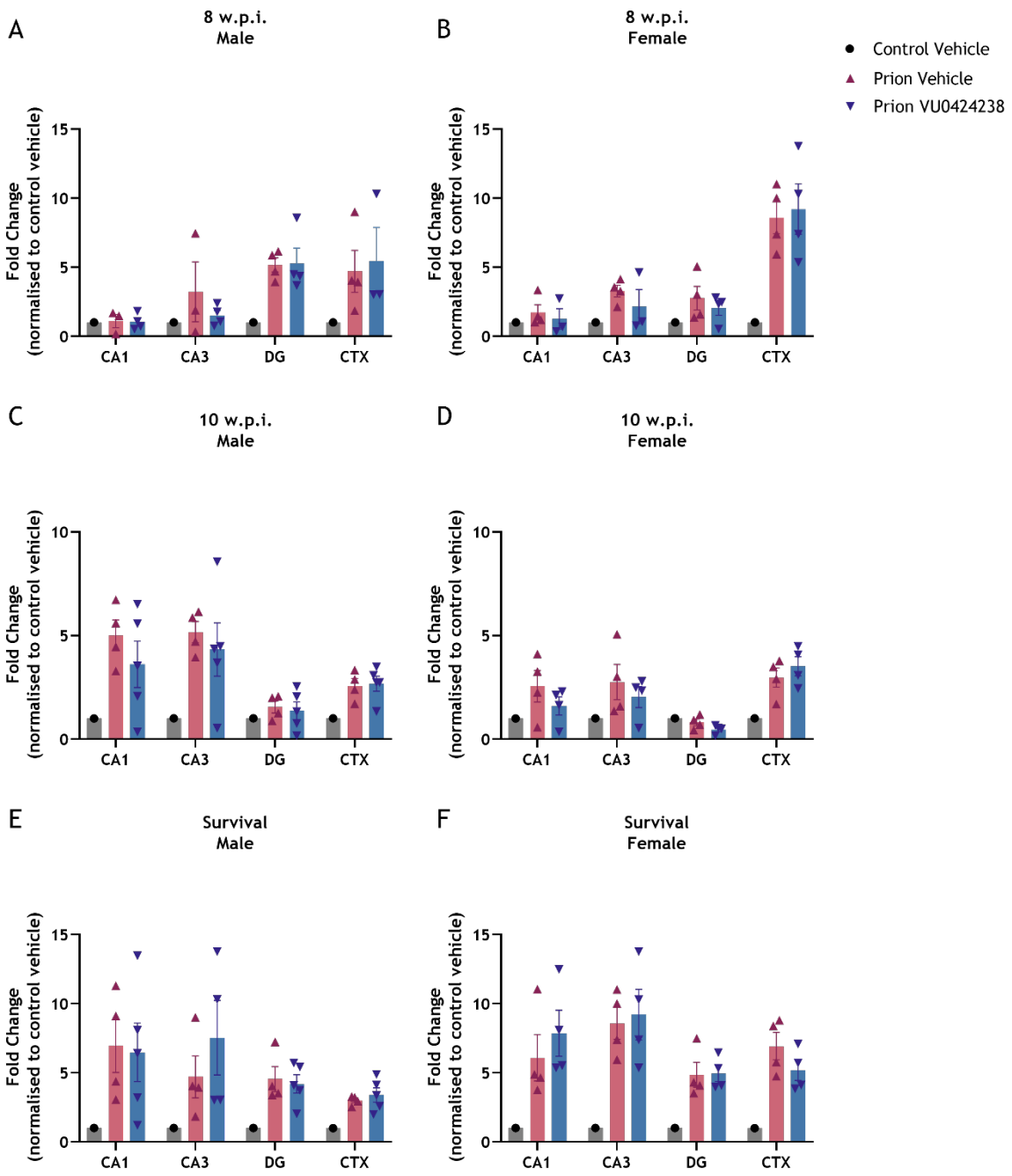

Appendix Figure 4 Comparison of Iba-1 expression in the cortex and hippocampus of male and female prion-diseased mice treated with either vehicle or VU0424238. Quantification of IHC images from Figure 4-23, Appendix Figure 9, and Appendix Figure 10, showing data from male (A, C and E) and female (B, D, and F) mice at 8 w.p.i. (A-B), 10 w.p.i. (C-D) and survival (E-F). Data were normalised to control vehicle and are shown as mean ± S.E.M. with data points representing individual mice (n=3-4). Statistical analysis was a two-way ANOVA (Tukey's multiple comparisons); only differences between prion vehicle and prion VU0424238 are shown.

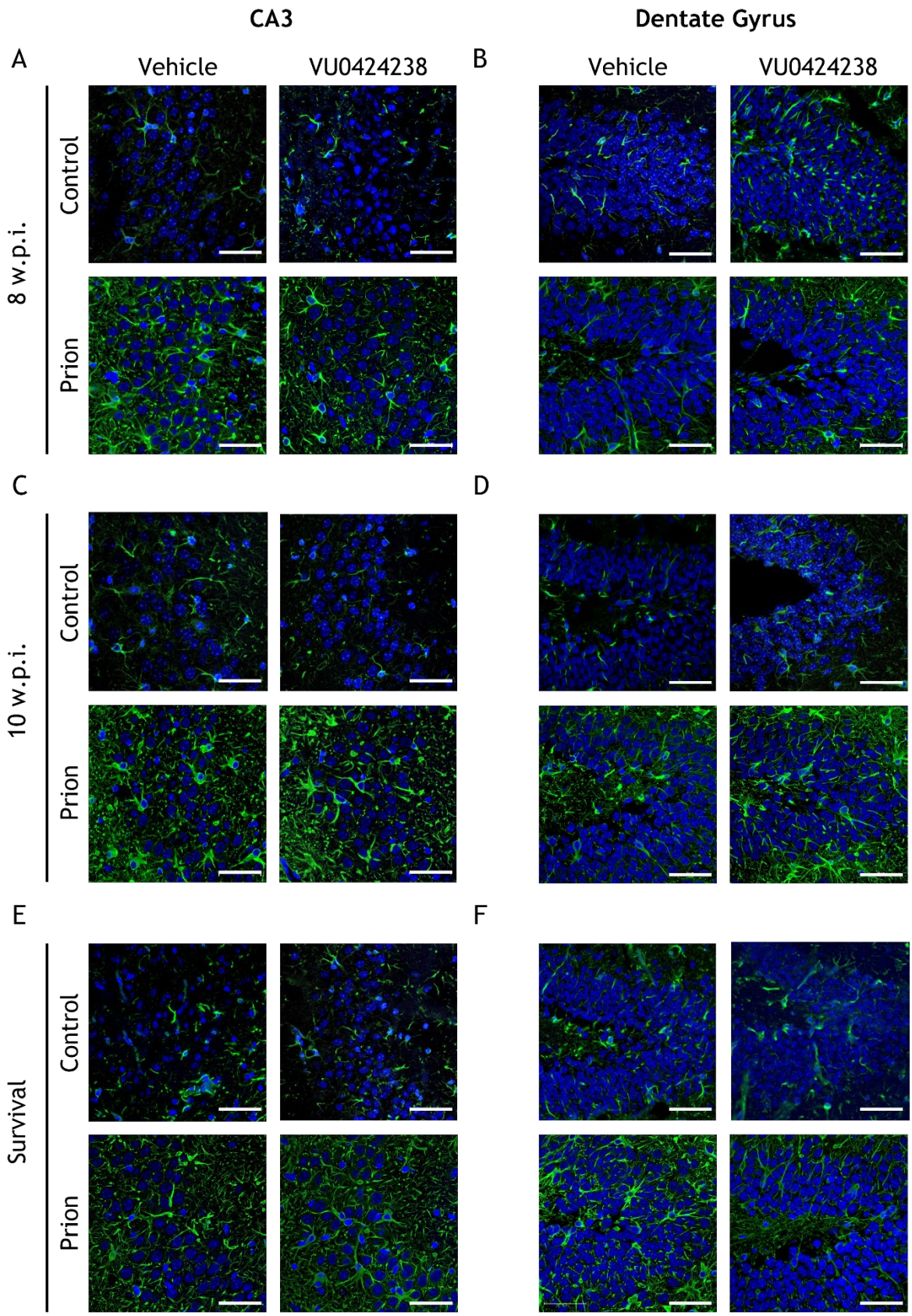

Appendix Figure 5 GFAP staining in the CA3 and dentate gyrus regions of the hippocampus of vehicle and VU0424238 treated control and prion-diseased mice. Representative images of immunohistochemical staining of 5 µm thick coronal sections through the brains of vehicle- and VU0424238-treated control- and prion-infected mice at 8 w.p.i. (A-B), 10 w.p.i. (C-D), and survival (E-F). Images shown are from the CA3 and dentate gyrus regions of the hippocampus with staining for GFAP (green) and DAPI (blue). Images shown are representative of n=3-8 mice per group. Images taken on a Zeiss 880 confocal microscope with 40x objective, scale bar = 50 µm.

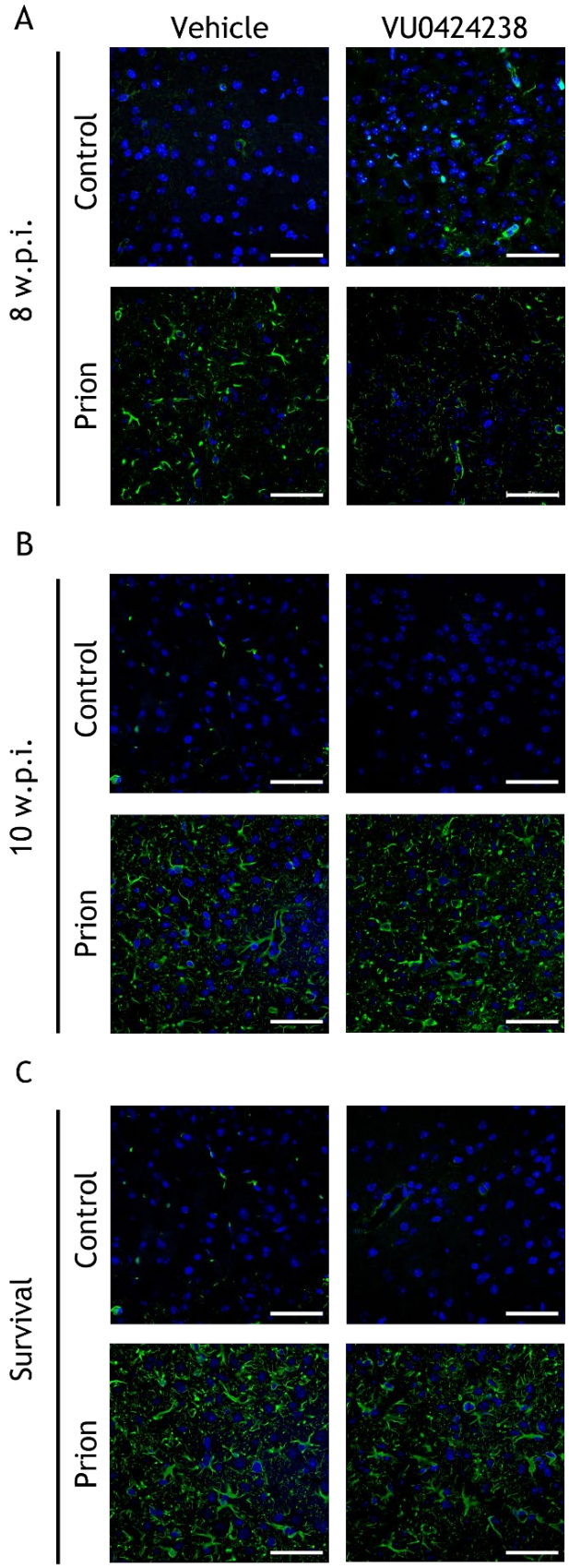

Appendix Figure 6 GFAP staining in the cortex of vehicle and VU0424238 treated control and prion-diseased mice. Representative images of immunohistochemical staining of 5 µm thick coronal sections through the brains of vehicle- and VU0424238-treated control- and prion-infected mice at 8 w.p.i. (A), 10 w.p.i. (B), and survival (C). Images shown are from the cortex, with staining for GFAP (green) and DAPI (blue). Images shown are representative of n=3-8 mice per group. Images taken on a Zeiss 880 confocal microscope with 40x objective, scale bar = 50 µm.

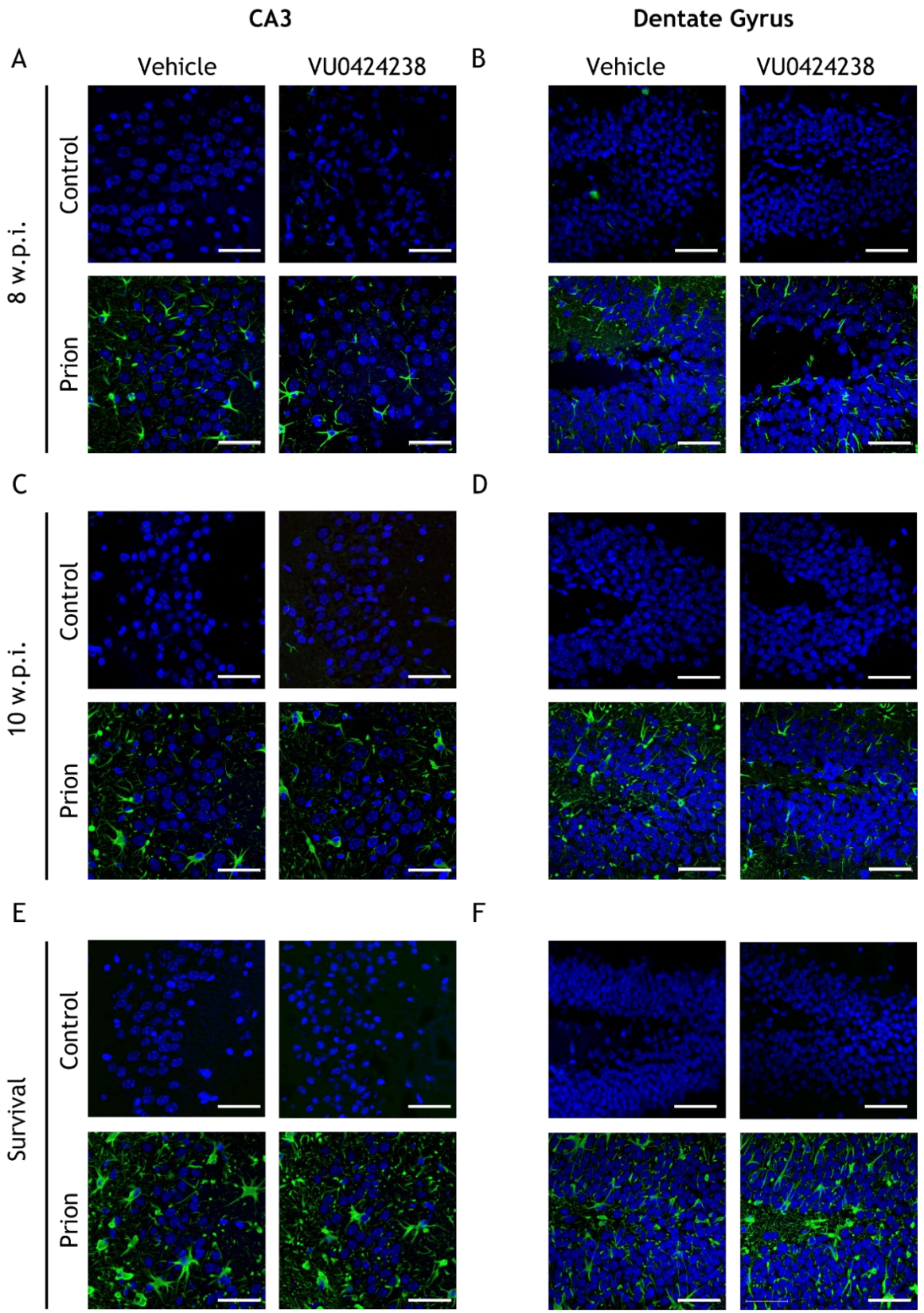

Appendix Figure 7 Vimentin staining in the CA3 and dentate gyrus regions of the hippocampus of vehicle and VU0424238 treated control and prion-diseased mice. Representative images of immunohistochemical staining of 5 µm thick coronal sections through the brains of vehicle- and VU0424238-treated control- and prion-infected mice at 8 w.p.i. (A-B), 10 w.p.i. (C-D), and survival (E-F). Images shown are from the CA3 and dentate gyrus regions of the hippocampus with staining for vimentin (green) and DAPI (blue). Images shown are representative of n=3-8 mice per group. Images taken on a Zeiss 880 confocal microscope with 40x objective, scale bar = 50 µm.

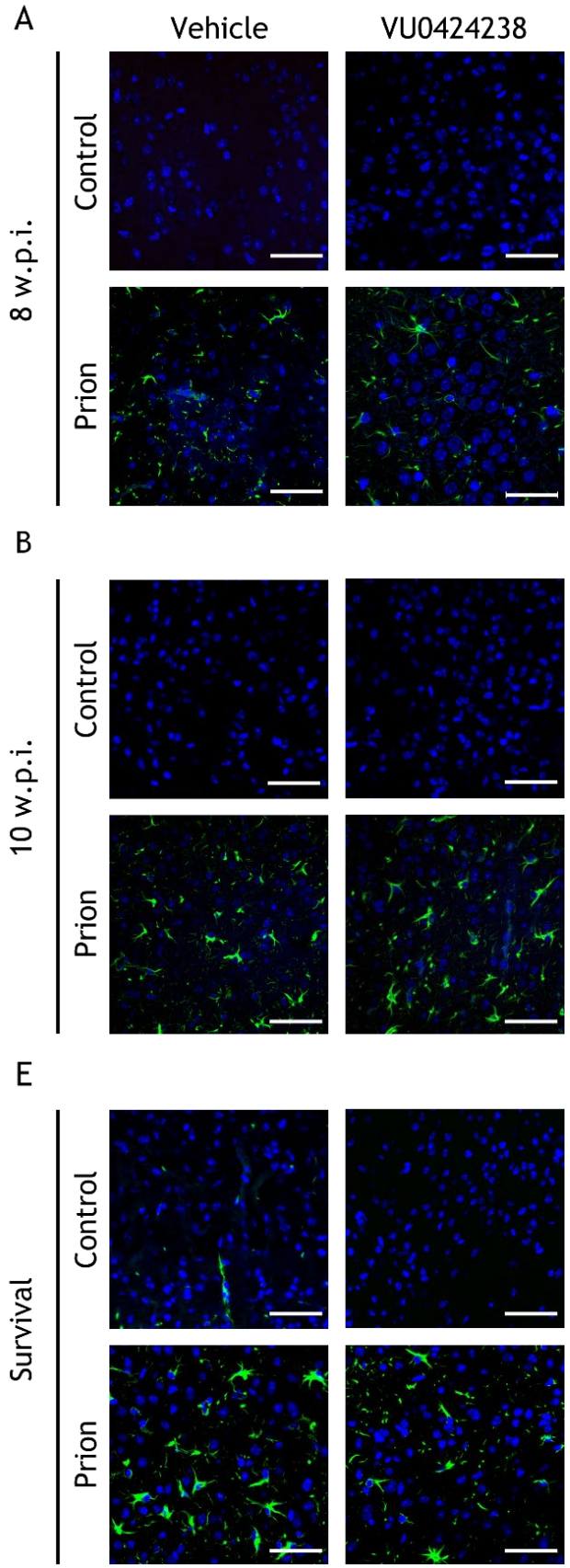

Appendix Figure 8 Vimentin staining in the cortex of vehicle and VU0424238 treated control and prion-diseased mice. Representative images of immunohistochemical staining of 5 µm thick coronal sections through the brains of vehicle- and VU0424238-treated control- and prion-infected mice at 8 w.p.i. (A), 10 w.p.i. (B), and survival (C). Images shown are from the cortex, with staining for vimentin (green) and DAPI (blue). Images shown are representative of n=3-8 mice per group. Images taken on a Zeiss 880 confocal microscope with 40x objective, scale bar = 50 µm.

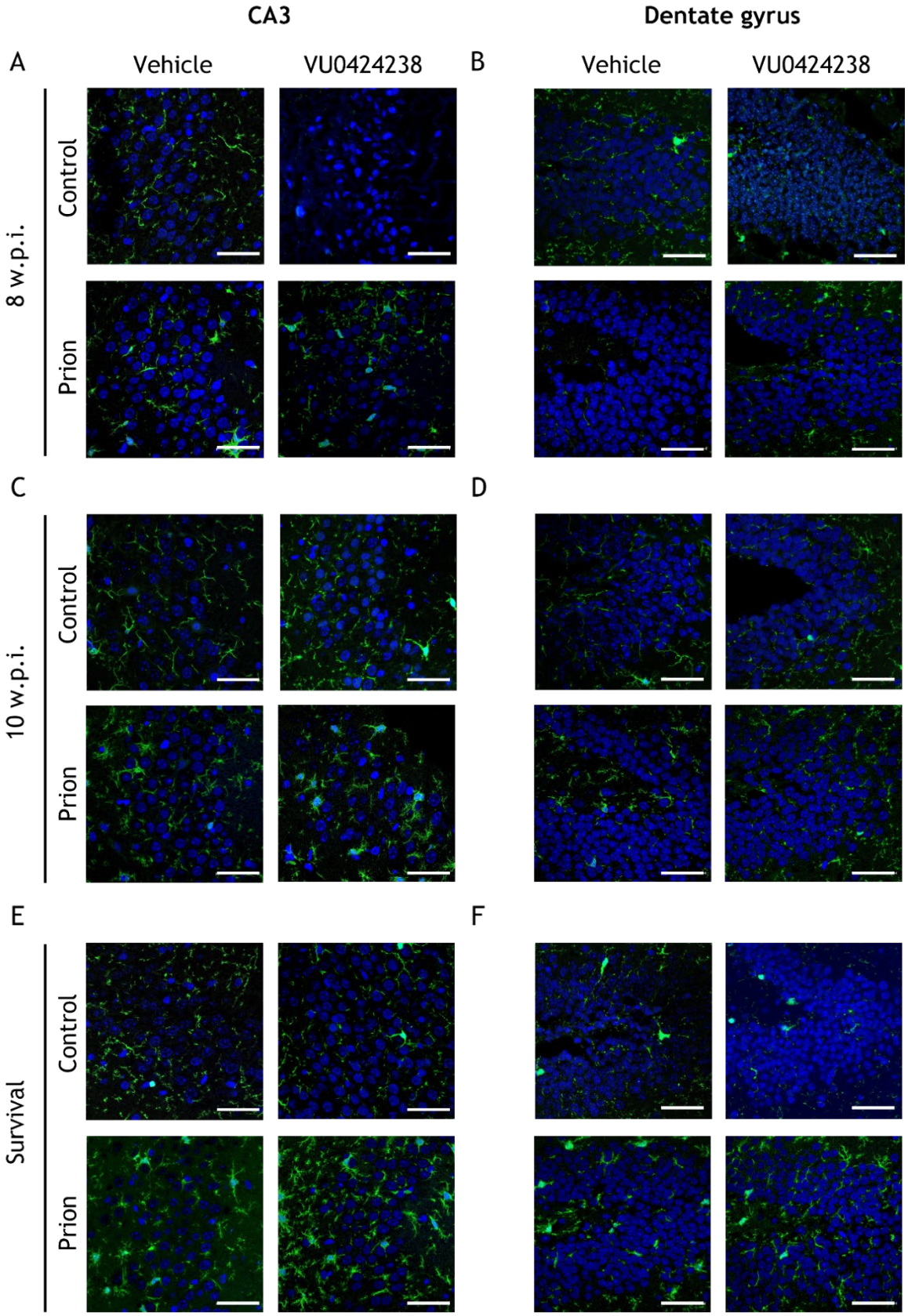

Appendix Figure 9 Iba-1 staining in the CA3 and dentate gyrus regions of the hippocampus of vehicle and VU0424238 treated control and prion-diseased mice. Representative images of immunohistochemical staining of 5 µm thick coronal sections through the brains of vehicle- and VU0424238-treated control- and prion-infected mice at 8 w.p.i. (A-B), 10 w.p.i. (C-D), and survival (E-F). Images shown are from the CA3 and dentate gyrus regions of the hippocampus with staining for Iba-1 (green) and DAPI (blue). Images shown are representative of n=3-8 mice per group. Images taken on a Zeiss 880 confocal microscope with 40x objective, scale bar = 50 µm.

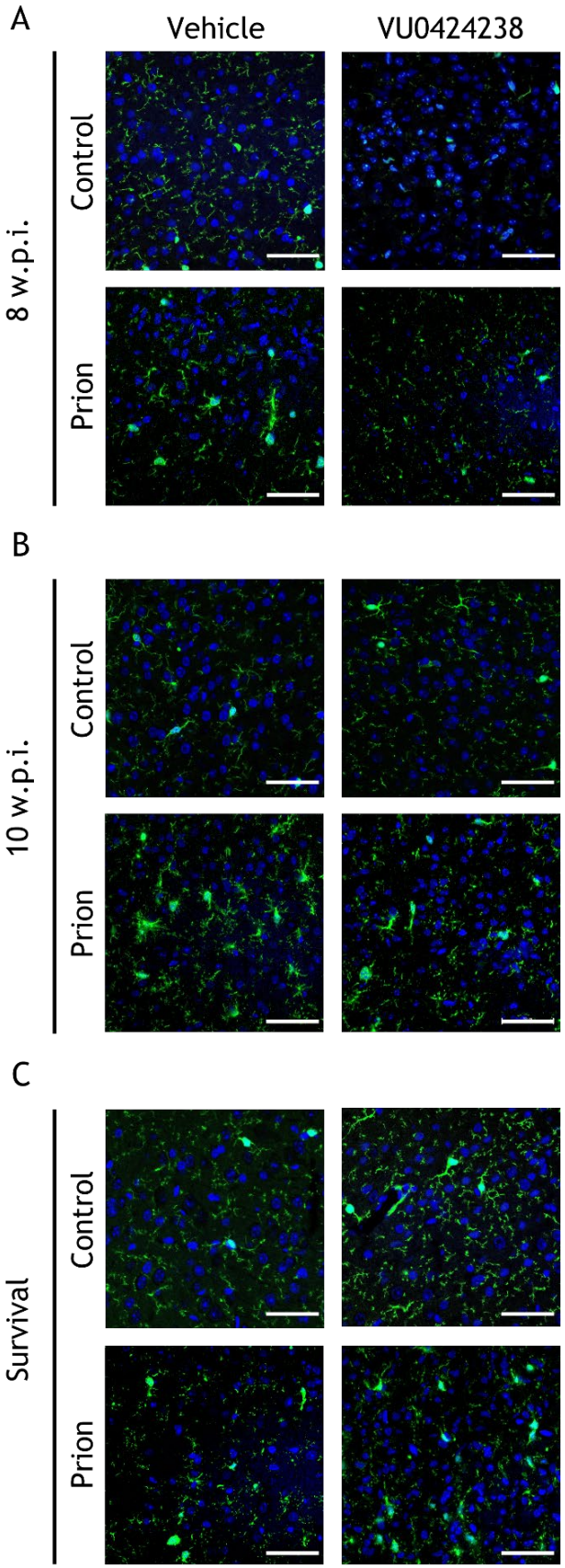

Appendix Figure 10 Iba-1 staining in the cortex of vehicle and VU0424238 treated control and prion-diseased mice. Representative images of immunohistochemical staining of 5 µm thick coronal sections through the brains of vehicle- and VU0424238-treated control- and prion-infected mice at 8 w.p.i. (A), 10 w.p.i. (B), and survival (C). Images shown are from the cortex, with staining for Iba-1 (green) and DAPI (blue). Images shown are representative of n=3-8 mice per group. Images taken on a Zeiss 880 confocal microscope with 40x objective, scale bar = 50 µm.

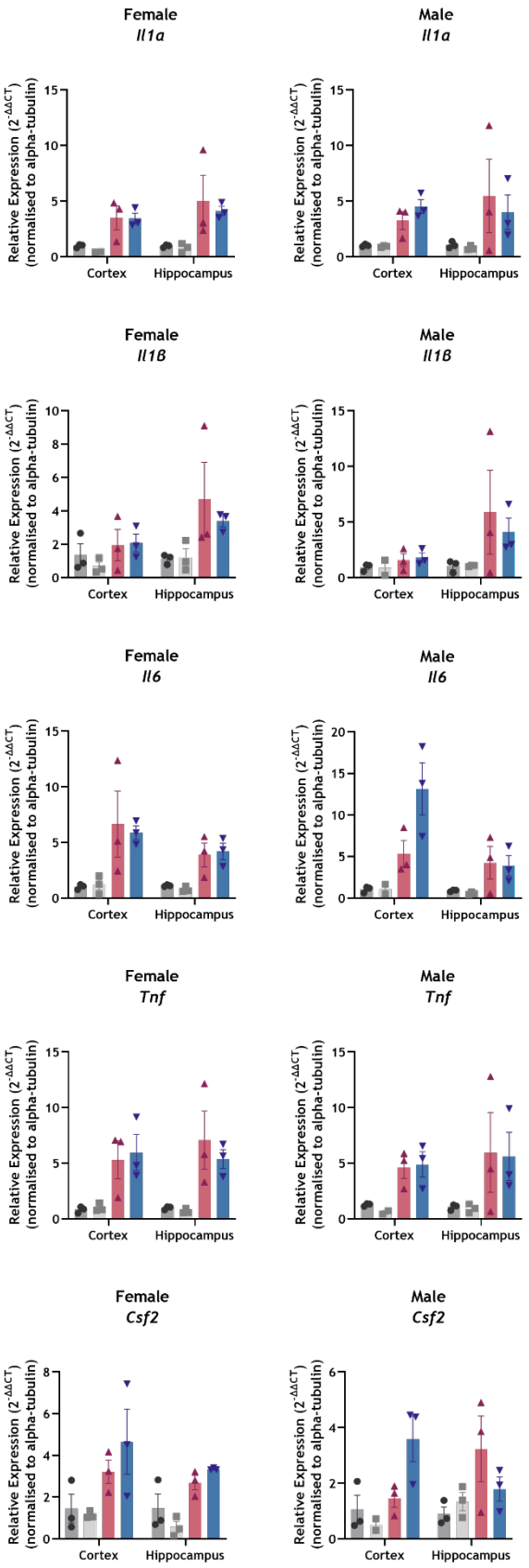

Appendix Figure 11 Comparison of chemokine and cytokine expression in male and female prion-diseased mice after chronic dosing with VU0424238. RT-qPCR showing the expression of pro-inflammatory cytokines and an adaptive immunity cytokine in the cortex and hippocampus of male and female control or prion-diseased mice treated with either vehicle or VU0424238 at 10 weeks post inoculation. Data were normalised to control vehicle and are shown as means ± S.E.M., with data points representing individual mice (n=2-4).

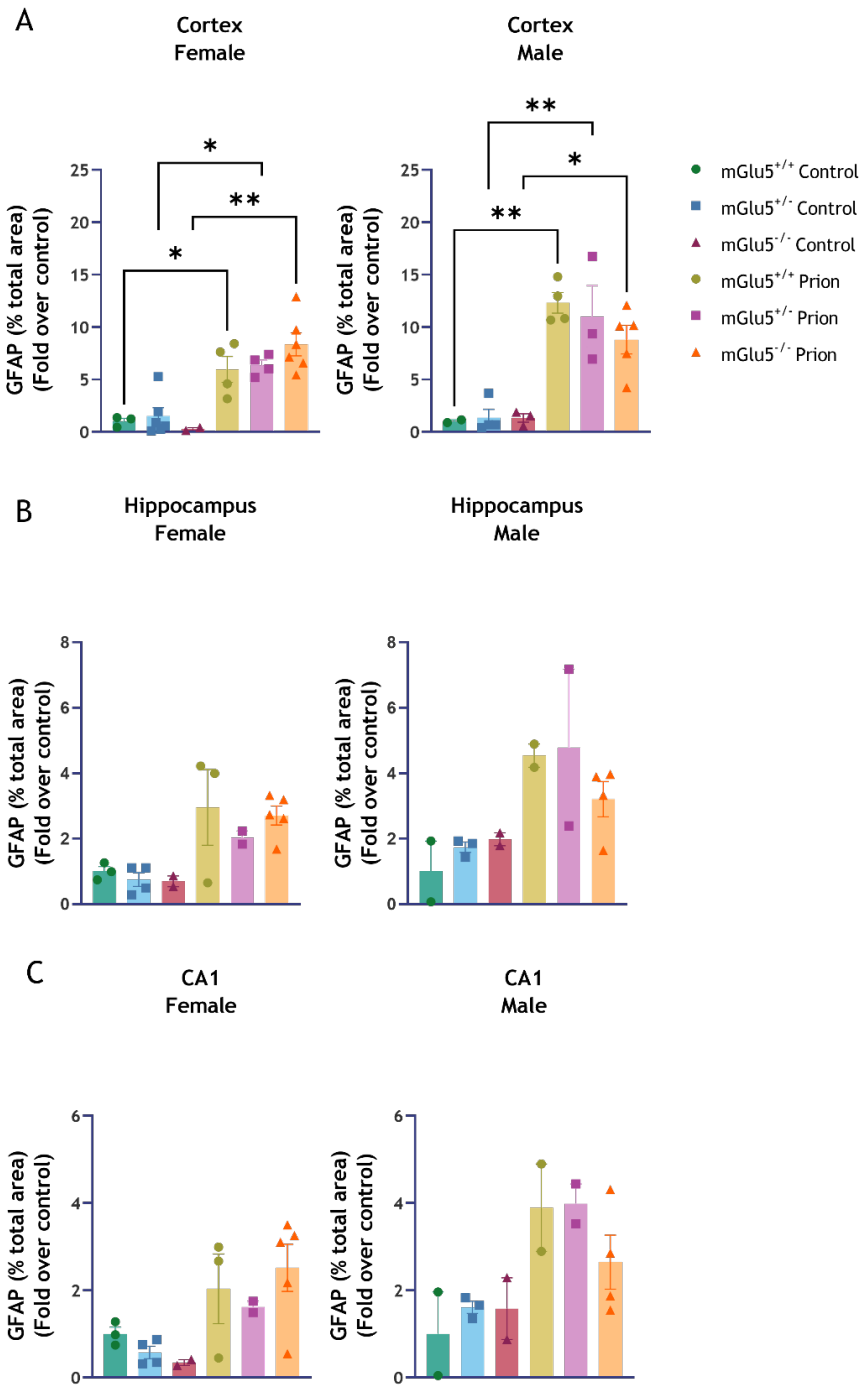

Appendix Figure 12 Comparison of GFAP expression in the cortex and hippocampus of male and female mGlu$_5$ deficient prion-diseased mice. Quantification of IHC images in Figure 5-19, showing data from male and female at survival in the (A) cortex, (B) hippocampus, and (C) CA1 region. Data was normalised to mGlu5$^{+/+}$ control and are shown as means ± S.E.M. with data points representing individual mice (n=2-6). Statistical analysis was a two-way ANOVA (Tukey's multiple comparisons), where * P ≤ 0.05, ** P ≤ 0001, and *** P ≤ 0.001.

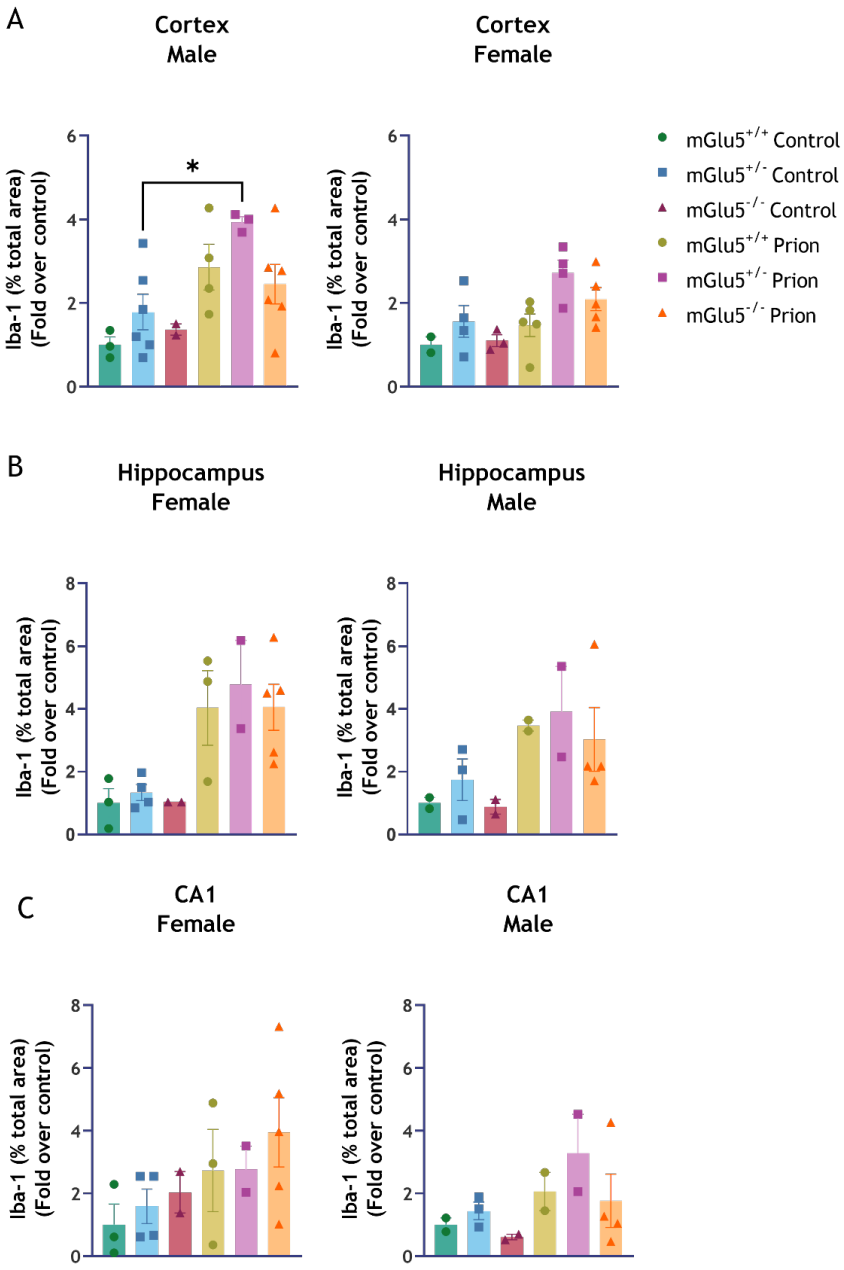

Appendix Figure 13 Comparison of Iba-1 expression in the cortex and hippocampus of male and female mGlu$_5$ deficient prion-diseased mice. Quantification of images in Figure 5-23, showing data from male and female at survival in the (A) cortex, (B) hippocampus, and (C) CA1 region. Data was normalised to mGlu5$^{+/+}$ control and are shown as mean ± S.E.M. with data points representing individual mice (n=2-6). Statistical analysis was a two-way ANOVA (Tukey's multiple comparisons), where * $P \leq 0.05$.

List of References

Abd-Elrahman, K. S., Albaker, A., de Souza, J. M., Ribeiro, F. M., Schlossmacher, M. G., Tiberi, M., Hamilton, A., & Ferguson, S. S. G. (2020a). Aβ oligomers induce pathophysiological mGluR5 signaling in Alzheimer's disease model mice in a sex-selective manner. *Science Signaling*, *13*(662). https://doi.org/10.1126/scisignal.abd2494

Abd-Elrahman, K. S., & Ferguson, S. S. G. (2019). Modulation of mTOR and CREB pathways following mGluR5 blockade contribute to improved Huntington's pathology in zQ175 mice. *Molecular Brain*, *12*(1). https://doi.org/10.1186/S13041-019-0456-1

Abd-Elrahman, K. S., & Ferguson, S. S. G. (2022). Noncanonical Metabotropic Glutamate Receptor 5 Signaling in Alzheimer's Disease. *Https://Doi.Org/10.1146/Annurev-Pharmtox-021821-091747*, *62*, 235–254. https://doi.org/10.1146/ANNUREV-PHARMTOX-021821-091747

Abd-Elrahman, K. S., Hamilton, A., Albaker, A., & Ferguson, S. S. G. (2020b). mGluR5 Contribution to Neuropathology in Alzheimer Mice Is Disease Stage-Dependent. *ACS Pharmacology & Translational Science*, *3*(2), 334–344. https://doi.org/10.1021/acsptsci.0c00013

Abd-Elrahman, K. S., Hamilton, A., Hutchinson, S. R., Liu, F., Russell, R. C., & Ferguson, S. S. G. (2017). mGluR5 antagonism increases autophagy and prevents disease progression in the zQ175 mouse model of Huntington's disease. *Science Signaling*, *10*(510). https://doi.org/10.1126/SCISIGNAL.AAN6387

Abd-Elrahman, K. S., Hamilton, A., Vasefi, M., & Ferguson, S. S. G. (2018). Autophagy is increased following either pharmacological or genetic silencing of mGluR5 signaling in Alzheimer's disease mouse models. *Molecular Brain*, *11*(1). https://doi.org/10.1186/s13041-018-0364-9

Abe, T., Sugihara, H., Nawa, H., Shigemoto, R., Mizuno, N., & Nakanishi, S. (1992). Molecular characterization of a novel metabotropic glutamate receptor mGluR5 coupled to inositol phosphate/Ca2+ signal transduction. *The Journal of Biological Chemistry*, *267*(19), 13361–13368.

Abou Farha, K., Bruggeman, R., & Baljé-Volkers, C. (2014). Metabotropic Glutamate Receptor 5 Negative Modulation in Phase I Clinical Trial: Potential Impact of Circadian Rhythm on the Neuropsychiatric Adverse Reactions—Do Hallucinations Matter? *ISRN Psychiatry*, *2014*, 1–8. https://doi.org/10.1155/2014/652750

Aguilar, D. D., Strecker, R. E., Basheer, R., & McNally, J. M. (2020). Alterations in sleep, sleep spindle, and EEG power in mGluR5 knockout mice. *Journal of Neurophysiology*, *123*(1), 22–33. https://doi.org/10.1152/jn.00532.2019

Aguzzi, A., & Zhu, C. (2017). Microglia in prion diseases. *Journal of Clinical Investigation*, *127*(9), 3230–3239. https://doi.org/10.1172/JCI90605

Ahnaou, A., Raeymaekers, L., Steckler, T., & Drinkenbrug, W. H. I. M. (2015). Relevance of the metabotropic glutamate receptor (mGluR5) in the regulation of NREM-REM sleep cycle and homeostasis: Evidence from mGluR5 (−/−) mice. *Behavioural Brain Research*, *282*, 218–226. https://doi.org/10.1016/j.bbr.2015.01.009

Alaluf, S., Mulvihill, E. R., & McIlhinney, R. A. J. (1995). Rapid agonist mediated phosphorylation of the metabotropic glutamate receptor 1α by protein kinase C in permanently transfected BHK cells. *FEBS Letters*, *367*(3), 301–305. https://doi.org/10.1016/0014-5793(95)00575-T

Alberdi, E., Sánchez-Gómez, M. V., Cavaliere, F., Pérez-Samartín, A., Zugaza, J. L., Trullas, R., Domercq, M., & Matute, C. (2010). Amyloid beta oligomers induce Ca2+ dysregulation and neuronal death through activation of ionotropic

glutamate receptors. *Cell Calcium*, *47*(3), 264–272. https://doi.org/10.1016/J.CECA.2009.12.010

Albin, R. L., & Greenamyre, J. T. (1992). Alternative excitotoxic hypotheses. *Neurology*, *42*(4), 733–738. https://doi.org/10.1212/WNL.42.4.733

Al-Chalabi, A., & Hardiman, O. (2013). The epidemiology of ALS: a conspiracy of genes, environment and time. *Nature Reviews Neurology*, *9*(11), 617–628. https://doi.org/10.1038/nrneurol.2013.203

Alexander, G. M., Deitch, J. S., Seeburger, J. L., Valle, L. Del, & Heiman-Patterson, T. D. (2002). Elevated Cortical Extracellular Fluid Glutamate in Transgenic Mice Expressing Human Mutant (G93A) Cu/Zn Superoxide Dismutase. *Journal of Neurochemistry*, *74*(4), 1666–1673. https://doi.org/10.1046/j.1471-4159.2000.0741666.x

Alexander, S. P. H., Christopoulos, A., Davenport, A. P., Kelly, E., Mathie, A., Peters, J. A., Veale, E. L., Armstrong, J. F., Faccenda, E., Harding, S. D., Pawson, A. J., Sharman, J. L., Southan, C., Davies, J. A., Abbracchio, M. P., Alexander, W., Al-hosaini, K., Bäck, M., Beaulieu, J., … Yao, C. (2019). THE CONCISE GUIDE TO PHARMACOLOGY 2019/20: G protein-coupled receptors. *British Journal of Pharmacology*, *176*(S1). https://doi.org/10.1111/bph.14748

Allan, S.M., Tyrrell, P.J., Rothwell, N.J., 2005. Interleukin-1 and neuronal injury. Nat Rev Immunol 5, 629–640. https://doi.org/10.1038/nri1664

Alzforum. (2023). *Research Models*. Accessed May 15, 2023. Https://Www.Alzforum.Org/Research-Models.

Alzheimer's Association. (2023). 2023 Alzheimer's Disease Facts and Figures. *Alzheimers Dement*, 19(4). Https://doi.ord/10.1002/alz.13016.

Anborgh, P. H., Godin, C., Pampillo, M., Dhami, G. K., Dale, L. B., Cregan, S. P., Truant, R., & Ferguson, S. S. G. (2005). Inhibition of Metabotropic Glutamate Receptor Signaling by the Huntingtin-binding Protein Optineurin. *Journal of Biological Chemistry*, *280*(41), 34840–34848. https://doi.org/10.1074/jbc.M504508200

Anderson, G. D. (2005). Sex and Racial Differences in Pharmacological Response: Where Is the Evidence? Pharmacogenetics, Pharmacokinetics, and Pharmacodynamics. *Journal of Women's Health*, *14*(1), 19–29. https://doi.org/10.1089/jwh.2005.14.19

Anderson, C. M., & Swanson, R. A. (2000). Astrocyte glutamate transport: review of properties, regulation, and physiological functions. *Glia*, *32*(1), 1–14.

Anderson, J. J., Rao, S. P., Rowe, B., Giracello, D. R., Holtz, G., Chapman, D. F., Tehrani, L., Bradbury, M. J., Cosford, N. D. P., & Varney, M. A. (2002). [3 H]Methoxymethyl-3-[(2-methyl-1,3-thiazol-4-yl)ethynyl]pyridine Binding to Metabotropic Glutamate Receptor Subtype 5 in Rodent Brain: In Vitro and in Vivo Characterization. *Journal of Pharmacology and Experimental Therapeutics*, *303*(3), 1044–1051. https://doi.org/10.1124/jpet.102.040618

Angulo, M. C., Kozlov, A. S., Charpak, S., & Audinat, E. (2004). Glutamate Released from Glial Cells Synchronizes Neuronal Activity in the Hippocampus. *The Journal of Neuroscience*, *24*(31), 6920–6927. https://doi.org/10.1523/JNEUROSCI.0473-04.2004

Anneser, J. M. H., Ince, P. G., Shaw, P. J., & Borasio, G. D. (2004). Differential expression of mGluR5 in human lumbosacral motoneurons. *Neuroreport*, *15*(2), 271–273. https://doi.org/10.1097/00001756-200402090-00012

Anne Stephenson, F., Cousins, S. L., & Kenny, A. V. (2008). Assembly and forward trafficking of NMDA receptors (Review). *Molecular Membrane Biology*, *25*(4), 311–320. https://doi.org/10.1080/09687680801971367

Arai, T., Hasegawa, M., Akiyama, H., Ikeda, K., Nonaka, T., Mori, H., Mann, D., Tsuchiya, K., Yoshida, M., Hashizume, Y., & Oda, T. (2006). TDP-43 is a

component of ubiquitin-positive tau-negative inclusions in frontotemporal lobar degeneration and amyotrophic lateral sclerosis. *Biochemical and Biophysical Research Communications*, *351*(3), 602–611. https://doi.org/10.1016/j.bbrc.2006.10.093

Arndt, J. W., Qian, F., Smith, B. A., Quan, C., Kilambi, K. P., Bush, M. W., Walz, T., Pepinsky, R. B., Bussière, T., Hamann, S., Cameron, T. O., & Weinreb, P. H. (2018). Structural and kinetic basis for the selectivity of aducanumab for aggregated forms of amyloid-ß. *Scientific Reports*, *8*(1), 6412. https://doi.org/10.1038/s41598-018-24501-0

Arnold, S. E., Hyman, B. T., Flory, J., Damasio, A. R., & Van Hoesen, G. W. (1991). The topographical and neuroanatomical distribution of neurofibrillary tangles and neuritic plaques in the cerebral cortex of patients with Alzheimer's disease. *Cerebral Cortex (New York, N.Y. : 1991)*, *1*(1), 103–116. https://doi.org/10.1093/CERCOR/1.1.103

Armitage, R. (2007). Sleep and circadian rhythms in mood disorders. *Acta Psychiatrica Scandinavica*, *115*(s433), 104–115. https://doi.org/10.1111/j.1600-0447.2007.00968.x

Aronica, E., Catania, M. v., Geurts, J., Yankaya, B., & Troost, D. (2001). Immunohistochemical localisation of group I and II metabotropic glutamate receptors in control and amyotrophic lateral sclerosis human spinal cord: upregulation in reactive astrocytes. *Neuroscience*, *105*(2), 509–520. https://doi.org/10.1016/S0306-4522(01)00181-6

Arzberger, T., Krampel, K., Leimgruber, S., & Weindl, A. (1997). Changes of NMDA Receptor Subunit (NR1, NR2B) and Glutamate Transporter (GLT1) mRNA Expression in Huntington's Disease—An In Situ Hybridization Study. *Journal of Neuropathology and Experimental Neurology*, *56*(4), 440–454. https://doi.org/10.1097/00005072-199704000-00013

Atwood, B. K., Lopez, J., Wager-Miller, J., Mackie, K., & Straiker, A. (2011). Expression of G protein-coupled receptors and related proteins in HEK293, AtT20, BV2, and N18 cell lines as revealed by microarray analysis. *BMC Genomics*, *12*(1), 14. https://doi.org/10.1186/1471-2164-12-14

Ast, A., Buntru, A., Schindler, F., Hasenkopf, R., Schulz, A., Brusendorf, L., Klockmeier, K., Grelle, G., McMahon, B., Niederlechner, H., Jansen, I., Diez, L., Edel, J., Boeddrich, A., Franklin, S. A., Baldo, B., Schnoegl, S., Kunz, S., Purfürst, B., … Wanker, E. E. (2018). mHTT Seeding Activity: A Marker of Disease Progression and Neurotoxicity in Models of Huntington's Disease. *Molecular Cell*, *71*(5), 675-688.e6. https://doi.org/10.1016/j.molcel.2018.07.032

Awad, H., Hubert, G. W., Smith, Y., Levey, A. I., & Conn, P. J. (2000). Activation of Metabotropic Glutamate Receptor 5 Has Direct Excitatory Effects and Potentiates NMDA Receptor Currents in Neurons of the Subthalamic Nucleus. *The Journal of Neuroscience*, *20*(21), 7871–7879. https://doi.org/10.1523/JNEUROSCI.20-21-07871.2000

Bachiller, S., Jiménez-Ferrer, I., Paulus, A., Yang, Y., Swanberg, M., Deierborg, T., Boza-Serrano, A. (2018). Microglia in neurological diseases: A road map to brain-disease dependent-inflammatory response. *Front Cell Neurosci,* 12(488). https://doi.org/10.3389/FNCEL.2018.00488/BIBTEX

Baker, C. A., Lu, Z. Y., Zaitsev, I., & Manuelidis, L. (1999). Microglial Activation Varies in Different Models of Creutzfeldt-Jakob Disease. *Journal of Virology*, *73*(6), 5089–5097. https://doi.org/10.1128/JVI.73.6.5089-5097.1999

Baker, C. A., & Manuelidis, L. (2003). Unique inflammatory RNA profiles of microglia in Creutzfeldt–Jakob disease. *Proceedings of the National Academy of Sciences*, *100*(2), 675–679. https://doi.org/10.1073/pnas.0237313100

Balázs, R., Miller, S., Romano, C., De Vries, A., Chun, Y., & Cotman, C. W. (1997). Metabotropic Glutamate Receptor mGluR5 in Astrocytes: Pharmacological Properties and Agonist Regulation. *Journal of Neurochemistry*, *69*(1), 151–163. https://doi.org/10.1046/J.1471-4159.1997.69010151.X

Baldwin, J. M., Schertler, G. F. X., & Unger, V. M. (1997). An alpha-carbon template for the transmembrane helices in the rhodopsin family of G-protein-coupled receptors 1 1Edited by R. Huber. *Journal of Molecular Biology*, *272*(1), 144–164. https://doi.org/10.1006/jmbi.1997.1240

Balu, D. T., Li, Y., Takagi, S., Presti, K. T., Ramikie, T. S., Rook, J. M., Jones, C. K., Lindsley, C. W., Conn, P. J., Bolshakov, V. Y., & Coyle, J. T. (2016). An mGlu5-Positive Allosteric Modulator Rescues the Neuroplasticity Deficits in a Genetic Model of NMDA Receptor Hypofunction in Schizophrenia. *Neuropsychopharmacology*, *41*(8), 2052–2061. https://doi.org/10.1038/npp.2016.2

Barbaric, I., Miller, G., Dear, T.N. (2007). Appearances can be deceiving: phenotypes of knockout mice. *Brief Funct Genomic Proteomic*, 6, 91–103. https://doi.org/10.1093/bfgp/elm008

Barcikowska, M., Liberski, P. P., Boellaard, J. W., Brown, P., Gajdusek, D. C., & Budka, H. (1993). Microglia is a component of the prion protein amyloid plaque in the Gerstmann-Strüssler-Scheinker syndrome. *Acta Neuropathologica*, *85*(6), 623–627. https://doi.org/10.1007/BF00334672

Bate, C., Boshuizen, R. S., Langeveld, J. P. M., & Williams, A. (2002). Temporal and spatial relationship between the death of PrP-damaged neurones and microglial activation. *NeuroReport*, *13*(13), 1695–1700. https://doi.org/10.1097/00001756-200209160-00025

Bateman, R. J., Aisen, P. S., De Strooper, B., Fox, N. C., Lemere, C. A., Ringman, J. M., Salloway, S., Sperling, R. A., Windisch, M., & Xiong, C. (2010). Autosomal-dominant Alzheimer's disease: a review and proposal for the prevention of Alzheimer's disease. *Alzheimer's Research & Therapy*, *3*(1), 1. https://doi.org/10.1186/alzrt59

Batista E. M., Doria J. G., Ferreira-Vieira T. H., Alves-Silva J., Ferguson S. S., Moreira F. A., Ribeiro F. M. (2016). Orchestrated activation of mGluR5 and CB1 promotes neuroprotection. *Mol Brain*. 20;9(1):80. doi: 10.1186/s13041-016-0259-6.

Beal, M. F., Kowall, N. W., Ellison, D. W., Mazurek, M. F., Swartz, K. J., & Martin, J. B. (1986). Replication of the neurochemical characteristics of Huntington's disease by quinolinic acid. *Nature*, *321*(6066), 168–171. https://doi.org/10.1038/321168a0

Behl, T., Kaur, I., Sehgal, A., Singh, S., Sharma, N., Makeen, H. A., Albratty, M., Alhazmi, H. A., Felemban, S. G., Alsubayiel, A. M., Bhatia, S., & Bungau, S. (2022). "Aducanumab" making a comeback in Alzheimer's disease: An old wine in a new bottle. *Biomedicine & Pharmacotherapy*, *148*, 112746. https://doi.org/10.1016/j.biopha.2022.112746

Béïque, J., & Andrade, R. (2003). PSD-95 regulates synaptic transmission and plasticity in rat cerebral cortex. *The Journal of Physiology*, *546*(3), 859–867. https://doi.org/10.1113/jphysiol.2002.031369

Bellozi, P. M. Q., Gomes, G. F., da Silva, M. C. M., Lima, I. V. de A., Batista, C. R. Á., Carneiro Junior, W. de O., Dória, J. G., Vieira, É. L. M., Vieira, R. P., de Freitas, R. P., Ferreira, C. N., Candelario-Jalil, E., Wyss-Coray, T., Ribeiro, F. M., & de Oliveira, A. C. P. (2019). A positive allosteric modulator of mGluR5 promotes neuroprotective effects in mouse models of Alzheimer's disease. *Neuropharmacology*, *160*. https://doi.org/10.1016/J.NEUROPHARM.2019.107785

Belozertseva, I., Kos, T., Popik, P., Danysz, W., Bespalov, A. (2007). Antidepressant-like effects of mGluR1 and mGluR5 antagonists in the rat forced swim and the

mouse tail suspension tests. *European Neuropsychopharmacology*, 17, 172–179. https://doi.org/10.1016/j.euroneuro.2006.03.002

Benarroch, E. E. (2018). Glutamatergic synaptic plasticity and dysfunction in Alzheimer disease. *Neurology*, *91*(3), 125–132. https://doi.org/10.1212/WNL.0000000000005807

Ben Haim, L., Carrillo-de Sauvage, M.-A., CeyzÃ©riat, K., & Escartin, C. (2015). Elusive roles for reactive astrocytes in neurodegenerative diseases. *Frontiers in Cellular Neuroscience*, *9*. https://doi.org/10.3389/fncel.2015.00278

Bennett, D. A., Schneider, J. A., Wilson, R. S., Bienias, J. L., & Arnold, S. E. (2004). Neurofibrillary Tangles Mediate the Association of Amyloid Load With Clinical Alzheimer Disease and Level of Cognitive Function. *Archives of Neurology*, *61*(3), 378–384. https://doi.org/10.1001/ARCHNEUR.61.3.378

Bennett, K. A., Doré, A. S., Christopher, J. A., Weiss, D. R., & Marshall, F. H. (2015). Structures of mGluRs shed light on the challenges of drug development of allosteric modulators. *Current Opinion in Pharmacology*, *20*, 1–7. https://doi.org/10.1016/j.coph.2014.09.022

Bennett, K. A., Sergeev, E., MacSweeney, C. P., Bakker, G., & Cooper, A. E. (2021). Understanding Exposure-Receptor Occupancy Relationships for Metabotropic Glutamate Receptor 5 Negative Allosteric Modulators across a Range of Preclinical and Clinical Studies. *Journal of Pharmacology and Experimental Therapeutics*, *377*(1), 157–168. https://doi.org/10.1124/jpet.120.000371

Bensimon, G., Lacomblez, L., & Meininger, V. (1994). A Controlled Trial of Riluzole in Amyotrophic Lateral Sclerosis. *New England Journal of Medicine*, *330*(9), 585–591. https://doi.org/10.1056/NEJM199403033300901

Beraldo, F. H., Ostapchenko, V. G., Caetano, F. A., Guimaraes, A. L. S., Ferretti, G. D. S., Daude, N., Bertram, L., Nogueira, K. O. P. C., Silva, J. L., Westaway, D., Cashman, N. R., Martins, V. R., Prado, V. F., & Prado, M. A. M. (2016). Regulation of Amyloid β Oligomer Binding to Neurons and Neurotoxicity by the Prion Protein-mGluR5 Complex. *Journal of Biological Chemistry*, *291*(42), 21945–21955. https://doi.org/10.1074/jbc.M116.738286

Bernardinelli, Y., Randall, J., Janett, E., Nikonenko, I., König, S., Jones, E. V., Flores, C. E., Murai, K. K., Bochet, C. G., Holtmaat, A., & Muller, D. (2014). Activity-Dependent Structural Plasticity of Perisynaptic Astrocytic Domains Promotes Excitatory Synapse Stability. *Current Biology*, *24*(15), 1679–1688. https://doi.org/10.1016/j.cub.2014.06.025

Berridge, M. J. (1993). Inositol trisphosphate and calcium signalling. *Nature*, *361*(6410), 315–325. https://doi.org/10.1038/361315a0

Bertram, L. (2005). The genetic epidemiology of neurodegenerative disease. *Journal of Clinical Investigation*, *115*(6), 1449–1457. https://doi.org/10.1172/JCI24761

Bertoglio, D., Kosten, L., Verhaeghe, J., Thomae, D., Wyffels, L., Stroobants, S., Wityak, J., Dominguez, C., Mrzljak, L., & Staelens, S. (2018). Longitudinal Characterization of mGluR5 Using 11 C-ABP688 PET Imaging in the Q175 Mouse Model of Huntington Disease. *Journal of Nuclear Medicine : Official Publication, Society of Nuclear Medicine*, *59*(11), 1722–1727. https://doi.org/10.2967/JNUMED.118.210658

Betmouni, S., Perry, V. H., & Gordon, J. L. (1996). Evidence for an early inflammatory response in the central nervous system of mice with scrapie. *Neuroscience*, *74*(1), 1–5. https://doi.org/10.1016/0306-4522(96)00212-6

Bhattacharya, P., Budnick, I., Singh, M., Thiruppathi, M., Alharshawi, K., Elshabrawy, H., Holterman, M. J., & Prabhakar, B. S. (2015). Dual Role of GM-CSF as a Pro-Inflammatory and a Regulatory Cytokine: Implications for Immune Therapy. *Journal of Interferon & Cytokine Research*, *35*(8), 585–599. https://doi.org/10.1089/jir.2014.0149

Bhudia, N., Desai, S., King, N., Ancellin, N., Grillot, D., Barnes, A. A., & Dowell, S. J. (2020). G Protein-Coupling of Adhesion GPCRs ADGRE2/EMR2 and ADGRE5/CD97, and Activation of G Protein Signalling by an Anti-EMR2 Antibody. *Scientific Reports*, *10*(1), 1004. https://doi.org/10.1038/s41598-020-57989-6

Biber, K., Laurie, D. J., Berthele, A., Sommer, B., Tölle, T. R., Gebicke-Härter, P. J., Van Calker, D., & Boddeke, H. W. G. M. (1999). Expression and Signaling of Group I Metabotropic Glutamate Receptors in Astrocytes and Microglia. *Undefined*, *72*(4), 1671–1680. https://doi.org/10.1046/J.1471-4159.1999.721671.X

Bieschke, J., Herbst, M., Wiglenda, T., Friedrich, R. P., Boeddrich, A., Schiele, F., Kleckers, D., Lopez Del Amo, J. M., Grüning, B. A., Wang, Q., Schmidt, M. R., Lurz, R., Anwyl, R., Schnoegl, S., Fändrich, M., Frank, R. F., Reif, B., Günther, S., Walsh, D. M., & Wanker, E. E. (2011). Small-molecule conversion of toxic oligomers to nontoxic β-sheet-rich amyloid fibrils. *Nature Chemical Biology*, *8*(1), 93–101. https://doi.org/10.1038/NCHEMBIO.719

Bikbaev, A., Neyman, S., Ngomba, R. T., Conn, J., Nicoletti, F., & Manahan-Vaughan, D. (2008). MGluR5 Mediates the Interaction between Late-LTP, Network Activity, and Learning. *PLoS ONE*, *3*(5), e2155. https://doi.org/10.1371/journal.pone.0002155

Biogen. (2023, April 25). *Approval for QALSODY™ (tofersen) for SOD1-ALS, a Major Scientific Advancement as the First Treatment to Target a Genetic Cause of ALS*. Https://Investors.Biogen.Com/News-Releases/News-Release-Details/Fda-Grants-Accelerated-Approval-Qalsodytm-Tofersen-Sod1-Als. Accessed: July 31st 2023.

Björkqvist, M., Wild, E. J., Thiele, J., Silvestroni, A., Andre, R., Lahiri, N., Raibon, E., Lee, R. V., Benn, C. L., Soulet, D., Magnusson, A., Woodman, B., Landles, C., Pouladi, M. A., Hayden, M. R., Khalili-Shirazi, A., Lowdell, M. W., Brundin, P., Bates, G. P., … Tabrizi, S. J. (2008). A novel pathogenic pathway of immune activation detectable before clinical onset in Huntington's disease. *Journal of Experimental Medicine*, *205*(8), 1869–1877. https://doi.org/10.1084/jem.20080178

Block, M. L., Zecca, L., & Hong, J.-S. (2007). Microglia-mediated neurotoxicity: uncovering the molecular mechanisms. *Nature Reviews Neuroscience*, *8*(1), 57–69. https://doi.org/10.1038/nrn2038

Blum, S., Moore, A. N., Adams, F., & Dash, P. K. (1999). A Mitogen-Activated Protein Kinase Cascade in the CA1/CA2 Subfield of the Dorsal Hippocampus Is Essential for Long-Term Spatial Memory. *The Journal of Neuroscience*, *19*(9), 3535–3544. https://doi.org/10.1523/JNEUROSCI.19-09-03535.1999

Boese, A. S., Saba, R., Campbell, K., Majer, A., Medina, S., Burton, L., Booth, T. F., Chong, P., Westmacott, G., Dutta, S. M., Saba, J. A., & Booth, S. A. (2016). MicroRNA abundance is altered in synaptoneurosomes during prion disease. *Molecular and Cellular Neuroscience*, *71*, 13–24. https://doi.org/10.1016/j.mcn.2015.12.001

Bohn, L. M., Lefkowitz, R. J., Gainetdinov, R. R., Peppel, K., Caron, M. G., & Lin, F.-T. (1999). Enhanced Morphine Analgesia in Mice Lacking β-Arrestin 2. *Science*, *286*(5449), 2495–2498. https://doi.org/10.1126/science.286.5449.2495

Boissonneault, V., Filali, M., Lessard, M., Relton, J., Wong, G., & Rivest, S. (2008). Powerful beneficial effects of macrophage colony-stimulating factor on -amyloid deposition and cognitive impairment in Alzheimer's disease. *Brain*, *132*(4), 1078–1092. https://doi.org/10.1093/brain/awn331

Bossi, S., Musante, I., Usai, C., Conti, F., Bonanno, G., & Milanese, M. (2017). In-vivo effects of knocking-down metabotropic glutamate receptor 5 in the SOD1 G93A

mouse model of amyotrophic lateral sclerosis. *Neuropharmacology*, *123*, 433–445. https://doi.org/10.1016/J.NEUROPHARM.2017.06.020

Bonifacino, T., Cattaneo, L., Gallia, E., Puliti, A., Melone, M., Provenzano, F., Bossi, S., Musante, I., Usai, C., Conti, F., Bonanno, G., & Milanese, M. (2017). In-vivo effects of knocking-down metabotropic glutamate receptor 5 in the SOD1 G93A mouse model of amyotrophic lateral sclerosis. *Neuropharmacology*, *123*, 433–445. https://doi.org/10.1016/J.NEUROPHARM.2017.06.020

Bonifacino, T., Provenzano, F., Gallia, E., Ravera, S., Torazza, C., Bossi, S., Ferrando, S., Puliti, A., Van Den Bosch, L., Bonanno, G., & Milanese, M. (2019). In-vivo genetic ablation of metabotropic glutamate receptor type 5 slows down disease progression in the SOD1G93A mouse model of amyotrophic lateral sclerosis. *Neurobiology of Disease*, *129*, 79–92. https://doi.org/10.1016/j.nbd.2019.05.007

Bourdenx, M., Koulakiotis, N. S., Sanoudou, D., Bezard, E., Dehay, B., & Tsarbopoulos, A. (2017). Protein aggregation and neurodegeneration in prototypical neurodegenerative diseases: Examples of amyloidopathies, tauopathies and synucleinopathies. *Progress in Neurobiology*, *155*, 171–193. https://doi.org/10.1016/j.pneurobio.2015.07.003

Bourgognon, J.-M., Spiers, J. G., Scheiblich, H., Antonov, A., Bradley, S. J., Tobin, A. B., & Steinert, J. R. (2018). Alterations in neuronal metabolism contribute to the pathogenesis of prion disease. *Cell Death & Differentiation*, *25*(8), 1408–1425. https://doi.org/10.1038/s41418-018-0148-x

Boyd, T. D., Bennett, S. P., Mori, T., Governatori, N., Runfeldt, M., Norden, M., Padmanabhan, J., Neame, P., Wefes, I., Sanchez-Ramos, J., Arendash, G. W., & Potter, H. (2010). GM-CSF Upregulated in Rheumatoid Arthritis Reverses Cognitive Impairment and Amyloidosis in Alzheimer Mice. *Journal of Alzheimer's Disease*, *21*(2), 507–518. https://doi.org/10.3233/JAD-2010-091471

Braak, H., Alafuzoff, I., Arzberger, T., Kretzschmar, H., & del Tredici, K. (2006). Staging of Alzheimer disease-associated neurofibrillary pathology using paraffin sections and immunocytochemistry. *Acta Neuropathologica*, *112*(4), 389–404. https://doi.org/10.1007/s00401-006-0127-z

Braak, H., Brettschneider, J., Ludolph, A. C., Lee, V. M., Trojanowski, J. Q., & Tredici, K. Del. (2013). Amyotrophic lateral sclerosis—a model of corticofugal axonal spread. *Nature Reviews Neurology*, *9*(12), 708–714. https://doi.org/10.1038/nrneurol.2013.221

Bradley, S. J., Bourgognon, J.-M., Sanger, H. E., Verity, N., Mogg, A. J., White, D. J., Butcher, A. J., Moreno, J. A., Molloy, C., Macedo-Hatch, T., Edwards, J. M., Wess, J., Pawlak, R., Read, D. J., Sexton, P. M., Broad, L. M., Steinert, J. R., Mallucci, G. R., Christopoulos, A., … Tobin, A. B. (2016). M1 muscarinic allosteric modulators slow prion neurodegeneration and restore memory loss. *Journal of Clinical Investigation*, *127*(2), 487–499. https://doi.org/10.1172/JCI87526

Bradley, S. J., Langmead, C. J., Watson, J. M., & Challiss, R. A. J. (2011). Quantitative analysis reveals multiple mechanisms of allosteric modulation of the mGlu5 receptor in rat astroglia. *Molecular Pharmacology*, *79*(5), 874–885. https://doi.org/10.1124/MOL.110.068882

Brakeman, P. R., Lanahan, A. A., O'Brien, R., Roche, K., Barnes, C. A., Huganir, R. L., & Worley, P. F. (1997). Homer: a protein that selectively binds metabotropic glutamate receptors. *Nature*, *386*(6622), 284–288. https://doi.org/10.1038/386284a0

Bramham, C. R., & Messaoudi, E. (2005). BDNF function in adult synaptic plasticity: The synaptic consolidation hypothesis. *Progress in Neurobiology*, *76*(2), 99–125. https://doi.org/10.1016/j.pneurobio.2005.06.003

Bramham, C. R., Worley, P. F., Moore, M. J., & Guzowski, J. F. (2008). The Immediate Early Gene *Arc / Arg3.1* : Regulation, Mechanisms, and Function. *The Journal of Neuroscience*, *28*(46), 11760–11767. https://doi.org/10.1523/JNEUROSCI.3864-08.2008

Bridges, T. M., Rook, J. M., Noetzel, M. J., Morrison, R. D., Zhou, Y., Gogliotti, R. D., Vinson, P. N., Xiang, Z., Jones, C. K., Niswender, C. M., Lindsley, C. W., Stauffer, S. R., Conn, P. J., & Daniels, J. S. (2013). Biotransformation of a Novel Positive Allosteric Modulator of Metabotropic Glutamate Receptor Subtype 5 Contributes to Seizure-Like Adverse Events in Rats Involving a Receptor Agonism-Dependent Mechanism. *Drug Metabolism and Disposition*, *41*(9), 1703–1714. https://doi.org/10.1124/dmd.113.052084

Brightwell, J. (2004). Hippocampal CREB1 but not CREB2 is decreased in aged rats with spatial memory impairments. *Neurobiology of Learning and Memory*, *81*(1), 19–26. https://doi.org/10.1016/j.nlm.2003.08.001

Brock, C., Schaefer, M., Reusch, H. P., Czupalla, C., Michalke, M., Spicher, K., Schultz, G., & Nürnberg, B. (2003). Roles of Gβγ in membrane recruitment and activation of p110γ/p101 phosphoinositide 3-kinase γ. *Journal of Cell Biology*, *160*(1), 89–99. https://doi.org/10.1083/jcb.200210115

Brodin, L., & Shupliakov, O. (2006). Giant reticulospinal synapse in lamprey: molecular links between active and periactive zones. *Cell and Tissue Research*, *326*(2), 301–310. https://doi.org/10.1007/s00441-006-0216-2

Brown, J., Iacovelli, L., di Cicco, G., Grayson, B., Rimmer, L., Fletcher, J., Neill, J. C., Wall, M. J., Ngomba, R. T., & Harte, M. (2022). The comparative effects of mGlu5 receptor positive allosteric modulators VU0409551 and VU0360172 on cognitive deficits and signalling in the sub-chronic PCP rat model for schizophrenia. *Neuropharmacology*, *208*, 108982. https://doi.org/10.1016/j.neuropharm.2022.108982

Brosseron, F., Krauthausen, M., Kummer, M., & Heneka, M. T. (2014). Body Fluid Cytokine Levels in Mild Cognitive Impairment and Alzheimer's Disease: a Comparative Overview. *Molecular Neurobiology*, *50*(2), 534–544. https://doi.org/10.1007/s12035-014-8657-1

Brown, A. R., Webb, J., Rebus, S., Walker, R., Williams, A., & Fazakerley, J. K. (2003). Inducible cytokine gene expression in the brain in the ME7/CV mouse model of scrapie is highly restricted, is at a strikingly low level relative to the degree of gliosis and occurs only late in disease. *Journal of General Virology*, *84*(9), 2605–2611. https://doi.org/10.1099/vir.0.19137-0

Brownell, A.-L., Kuruppu, D., Kil, K.-E., Jokivarsi, K., Poutiainen, P., Zhu, A., & Maxwell, M. (2015). PET imaging studies show enhanced expression of mGluR5 and inflammatory response during progressive degeneration in ALS mouse model expressing SOD1-G93A gene. *Journal of Neuroinflammation*, *12*(1), 217. https://doi.org/10.1186/s12974-015-0439-9

Bruijn, L. I., Becher, M. W., Lee, M. K., Anderson, K. L., Jenkins, N. A., Copeland, N. G., Sisodia, S. S., Rothstein, J. D., Borchelt, D. R., Price, D. L., & Cleveland, D. W. (1997). ALS-Linked SOD1 Mutant G85R Mediates Damage to Astrocytes and Promotes Rapidly Progressive Disease with SOD1-Containing Inclusions. *Neuron*, *18*(2), 327–338. https://doi.org/10.1016/S0896-6273(00)80272-X

Bruijn, L. I., Houseweart, M. K., Kato, S., Anderson, K. L., Anderson, S. D., Ohama, E., Reaume, A. G., Scott, R. W., & Cleveland, D. W. (1998). Aggregation and Motor Neuron Toxicity of an ALS-Linked SOD1 Mutant Independent from Wild-Type SOD1. *Science*, *281*(5384), 1851–1854. https://doi.org/10.1126/science.281.5384.1851

Brust, T. F., Conley, J. M., & Watts, V. J. (2015). Gαi/o-coupled receptor-mediated sensitization of adenylyl cyclase: 40 years later. *European Journal of Pharmacology*, *763*, 223–232. https://doi.org/10.1016/j.ejphar.2015.05.014

Buccitelli, C., & Selbach, M. (2020). mRNAs, proteins and the emerging principles of gene expression control. *Nature Reviews Genetics*, *21*(10), 630–644. https://doi.org/10.1038/s41576-020-0258-4

Buckley, R. F., Mormino, E. C., Rabin, J. S., Hohman, T. J., Landau, S., Hanseeuw, B. J., Jacobs, H. I. L., Papp, K. V., Amariglio, R. E., Properzi, M. J., Schultz, A. P., Kirn, D., Scott, M. R., Hedden, T., Farrell, M., Price, J., Chhatwal, J., Rentz, D. M., Villemagne, V. L., … Sperling, R. A. (2019). Sex Differences in the Association of Global Amyloid and Regional Tau Deposition Measured by Positron Emission Tomography in Clinically Normal Older Adults. *JAMA Neurology*, *76*(5), 542. https://doi.org/10.1001/jamaneurol.2018.4693

Budd Haeberlein, S., Aisen, P. S., Barkhof, F., Chalkias, S., Chen, T., Cohen, S., Dent, G., Hansson, O., Harrison, K., von Hehn, C., Iwatsubo, T., Mallinckrodt, C., Mummery, C. J., Muralidharan, K. K., Nestorov, I., Nisenbaum, L., Rajagovindan, R., Skordos, L., Tian, Y., … Sandrock, A. (2022). Two Randomized Phase 3 Studies of Aducanumab in Early Alzheimer's Disease. *The Journal of Prevention of Alzheimer's Disease*. https://doi.org/10.14283/jpad.2022.30

Budgett, R. F., Bakker, G., Sergeev, E., Bennett, K. A., & Bradley, S. J. (2022). Targeting the Type 5 Metabotropic Glutamate Receptor: A Potential Therapeutic Strategy for Neurodegenerative Diseases? *Frontiers in Pharmacology*, *13*. https://doi.org/10.3389/fphar.2022.893422

Budka, H. (2003). Neuropathology of prion diseases. *British Medical Bulletin*, *66*(1), 121–130. https://doi.org/10.1093/bmb/66.1.121

Büeler, H., Fischer, M., Lang, Y., Bluethmann, H., Lipp, H.-P., Dearmond, S. J., Prusiner, S. B., Aguet, M. & Weissman, C. 1992. Normal development and behaviour of mice lacking the neuronal cell-surface PrP protein. *Nature,* 356, 577-582.

Büeler, H., Raeber, A., Sailer, A., Fischer, M., Aguzzi, A., Weissmann, C. (1994). High prion and PrPSc levels but delayed onset of disease in scrapie-inoculated mice heterozygous for a disrupted PrP gene. *Mol Med,* 1, 19–30.

Burke, S. N., & Barnes, C. A. (2010). Senescent synapses and hippocampal circuit dynamics. *Trends in Neurosciences*, *33*(3), 153–161. https://doi.org/10.1016/j.tins.2009.12.003

Burket, J. A., Herndon, A. L., Winebarger, E. E., Jacome, L. F., & Deutsch, S. I. (2011). Complex effects of mGluR5 antagonism on sociability and stereotypic behaviors in mice: Possible implications for the pharmacotherapy of autism spectrum disorders. *Brain Research Bulletin*, *86*(3–4), 152–158. https://doi.org/10.1016/j.brainresbull.2011.08.001

Butcher, A. J., Prihandoko, R., Kong, K. C., McWilliams, P., Edwards, J. M., Bottrill, A., Mistry, S., & Tobin, A. B. (2011). Differential G-protein-coupled Receptor Phosphorylation Provides Evidence for a Signaling Bar Code. *Journal of Biological Chemistry*, *286*(13), 11506–11518. https://doi.org/10.1074/jbc.M110.154526

Butterfield, D. A., & Pocernich, C. B. (2003). The glutamatergic system and Alzheimer's disease: therapeutic implications. *CNS Drugs*, *17*(9), 641–652. https://doi.org/10.2165/00023210-200317090-00004

Byrnes, K. R., Stoica, B., Loane, D. J., Riccio, A., Davis, M. I., & Faden, A. I. (2009). Metabotropic glutamate receptor 5 activation inhibits microglial associated inflammation and neurotoxicity. *Glia*, *57*(5), 550–560. https://doi.org/10.1002/GLIA.20783

Cabrera-Vera, T. M., Vanhauwe, J., Thomas, T. O., Medkova, M., Preininger, A., Mazzoni, M. R., & Hamm, H. E. (2003). Insights into G Protein Structure,

Function, and Regulation. *Endocrine Reviews*, *24*(6), 765–781. https://doi.org/10.1210/er.2000-0026

Cahoy, J. D., Emery, B., Kaushal, A., Foo, L. C., Zamanian, J. L., Christopherson, K. S., Xing, Y., Lubischer, J. L., Krieg, P. A., Krupenko, S. A., Thompson, W. J., & Barres, B. A. (2008). A Transcriptome Database for Astrocytes, Neurons, and Oligodendrocytes: A New Resource for Understanding Brain Development and Function. *Journal of Neuroscience*, *28*(1), 264–278. https://doi.org/10.1523/JNEUROSCI.4178-07.2008

Cai, Z., Schools, G. P., & Kimelberg, H. K. (2000). Metabotropic glutamate receptors in acutely isolated hippocampal astrocytes: developmental changes of mGluR5 mRNA and functional expression. *Glia*, *29*(1), 70–80. https://doi.org/10.1002/(sici)1098-1136(20000101)29:1<70::aid-glia7>3.0.co;2-v

Cai, G., Zhu, Y., Chen, J., Zhao, S., Wang, L., Wang, M., Huang, J., Wu, S. (2020). Analysis of the Gut Microbiota and Inflammatory Factors in mGluR5-Knockout Mice. *Front Psychiatry*, 11. https://doi.org/10.3389/fpsyt.2020.00335

Calebiro, D., Koszegi, Z., Lanoiselée, Y., Miljus, T., & O'Brien, S. (2021). G protein-coupled receptor-G protein interactions: a single-molecule perspective. *Physiological Reviews*, *101*(3), 857–906. https://doi.org/10.1152/physrev.00021.2020

Cali, I., Miller, C.J., Parisi, J.E., Geschwind, M.D., Gambetti, P., Schonberger, L.B. (2015). Distinct pathological phenotypes of Creutzfeldt-Jakob disease in recipients of prion-contaminated growth hormone. *Acta Neuropathol Commun,* 3(37). https://doi.org/10.1186/s40478-015-0214-2

Campbell, I. L., Eddleston, M., Kemper, P., Oldstone, M. B., & Hobbs, M. V. (1994). Activation of cerebral cytokine gene expression and its correlation with onset of reactive astrocyte and acute-phase response gene expression in scrapie. *Journal of Virology*, *68*(4), 2383–2387. https://doi.org/10.1128/jvi.68.4.2383-2387.1994

Canevelli, M., Quarata, F., Remiddi, F., Lucchini, F., Lacorte, E., Vanacore, N., Bruno, G., & Cesari, M. (2017). Sex and gender differences in the treatment of Alzheimer's disease: A systematic review of randomized controlled trials. *Pharmacological Research*, *115*, 218–223. https://doi.org/10.1016/j.phrs.2016.11.035

Cankaya, S., Cankaya, B., Kilic, U., Kilic, E., & Yulug, B. (2019). The therapeutic role of minocycline in Parkinson's disease. *Drugs in Context*, *8*, 1–14. https://doi.org/10.7573/dic.212553

Capecchi, M.R. (2005). Gene targeting in mice: functional analysis of the mammalian genome for the twenty-first century. *Nat Rev Genet,* 6, 507–512. https://doi.org/10.1038/nrg1619

Cardoso-Moreira, M., Halbert, J., Valloton, D., Velten, B., Chen, C., Shao, Y., Liechti, A., Ascenção, K., Rummel, C., Ovchinnikova, S., Mazin, P. V., Xenarios, I., Harshman, K., Mort, M., Cooper, D.N., Sandi, C., Soares, M.J., Ferreira, P.G., Afonso, S., Carneiro, M., Turner, J.M.A., VandeBerg, J.L., Fallahshahroudi, A., Jensen, P., Behr, R., Lisgo, S., Lindsay, S., Khaitovich, P., Huber, W., Baker, J., Anders, S., Zhang, Y.E., Kaessmann, H. (2019). Gene expression across mammalian organ development. *Nature,* 571, 505–509. https://doi.org/10.1038/s41586-019-1338-5

Carman, C. V, & Benovic, J. L. (1998). G-protein-coupled receptors: turn-ons and turn-offs. *Current Opinion in Neurobiology*, *8*(3), 335–344. https://doi.org/10.1016/S0959-4388(98)80058-5

Carmona-Rosas, G., Alcántara-Hernández, R., & Hernández-Espinosa, D. A. (2019). *The role of β-arrestins in G protein-coupled receptor heterologous desensitization: A brief story* (pp. 195–204). https://doi.org/10.1016/bs.mcb.2018.08.004

Carroll, J. A., Race, B., Williams, K., Striebel, J., & Chesebro, B. (2018). Microglia Are Critical in Host Defense against Prion Disease. *Journal of Virology*, *92*(15). https://doi.org/10.1128/JVI.00549-18

Carvalho, T.G., Alves-Silva, J., de Souza, J.M., Real, A.L.C.V., Doria, J.G., Vieira, E.L.M., Gomes, G.F., de Oliveira, A.C., Miranda, A.S., Ribeiro, F.M. (2019). Metabotropic glutamate receptor 5 ablation accelerates age-related neurodegeneration and neuroinflammation. *Neurochem Int*, 126, 218–228. https://doi.org/10.1016/J.NEUINT.2019.03.020

Casley, C. S., Lakics, V., Lee, H. gon, Broad, L. M., Day, T. A., Cluett, T., Smith, M. A., O'Neill, M. J., & Kingston, A. E. (2009). Up-regulation of astrocyte metabotropic glutamate receptor 5 by amyloid-ß peptide. *Brain Research*, *1260*, 65–75. https://doi.org/10.1016/J.BRAINRES.2008.12.082

Castellano, J. M., Kim, J., Stewart, F. R., Jiang, H., DeMattos, R. B., Patterson, B. W., Fagan, A. M., Morris, J. C., Mawuenyega, K. G., Cruchaga, C., Goate, A. M., Bales, K. R., Paul, S. M., Bateman, R. J., & Holtzman, D. M. (2011). Human apoE Isoforms Differentially Regulate Brain Amyloid-ß Peptide Clearance. *Science Translational Medicine*, *3*(89). https://doi.org/10.1126/scitranslmed.3002156

Ceprian, M., & Fulton, D. (2019). Glial Cell AMPA Receptors in Nervous System Health, Injury and Disease. *International Journal of Molecular Sciences*, *20*(10), 2450. https://doi.org/10.3390/ijms20102450

Chakraborty, S., Lennon, J. C., Malkaram, S. A., Zeng, Y., Fisher, D. W., & Dong, H. (2019). Serotonergic system, cognition, and BPSD in Alzheimer's disease. *Neuroscience Letters*, *704*, 36–44. https://doi.org/10.1016/j.neulet.2019.03.050

Chanda D, Neumann D, Glatz JFC. (2019). The endocannabinoid system: Overview of an emerging multi-faceted therapeutic target. *Prostaglandins Leukot Essent Fatty Acids*. 140:51-56. doi: 10.1016/j.plefa.2018.11.016.

Chantong, B., Kratschmar, D. V., Lister, A., & Odermatt, A. (2014). Inhibition of metabotropic glutamate receptor 5 induces cellular stress through pertussis toxinsensitive Gi-proteins in murine BV-2 microglia cells. *Journal of Neuroinflammation*, *11*(1), 1–16. https://doi.org/10.1186/S12974-014-0190-7/FIGURES/8

Chemin, J. (2003). Mechanisms underlying excitatory effects of group I metabotropic glutamate receptors via inhibition of 2P domain K+ channels. *The EMBO Journal*, *22*(20), 5403–5411. https://doi.org/10.1093/emboj/cdg528

Chen, G., Xu, T., Yan, Y., Zhou, Y., Jiang, Y., Melcher, K., & Xu, H. E. (2017). Amyloid beta: structure, biology and structure-based therapeutic development. *Acta Pharmacologica Sinica*, *38*(9), 1205–1235. https://doi.org/10.1038/aps.2017.28

Chen, P.-C., Vargas, M. R., Pani, A. K., Smeyne, R. J., Johnson, D. A., Kan, Y. W., & Johnson, J. A. (2009). Nrf2-mediated neuroprotection in the MPTP mouse model of Parkinson's disease: Critical role for the astrocyte. *Proceedings of the National Academy of Sciences of the United States of America*, *106*(8), 2933–2938. https://doi.org/10.1073/PNAS.0813361106

Chen, Y., Goudet, C., Pin, J.-P., & Conn, P. J. (2008). *N* -{4-Chloro-2-[(1,3-dioxo-1,3-dihydro-2 *H* -isoindol-2-yl)methyl]phenyl}-2-hydroxybenzamide (CPPHA) Acts through a Novel Site as a Positive Allosteric Modulator of Group 1 Metabotropic Glutamate Receptors. *Molecular Pharmacology*, *73*(3), 909–918. https://doi.org/10.1124/mol.107.040097

Chen, Y., Vartiainen, N. E., Ying, W., Chan, P. H., Koistinaho, J., & Swanson, R. A. (2001). Astrocytes protect neurons from nitric oxide toxicity by a glutathione-dependent mechanism. *Journal of Neurochemistry*, *77*(6), 1601–1610. https://doi.org/10.1046/J.1471-4159.2001.00374.X

Cherry, J. D., Olschowka, J. A., & O'Banion, M. K. (2014). Neuroinflammation and M2 microglia: the good, the bad, and the inflamed. *Journal of Neuroinflammation*, *11*(1), 98. https://doi.org/10.1186/1742-2094-11-98

Chiarini, A., Armato, U., Gardenal, E., Gui, L., & Dal Prà, I. (2017). Amyloid ß-Exposed Human Astrocytes Overproduce Phospho-Tau and Overrelease It within Exosomes, Effects Suppressed by Calcilytic NPS 2143-Further Implications for Alzheimer's Therapy. *Frontiers in Neuroscience*, *11*(APR). https://doi.org/10.3389/FNINS.2017.00217

Chipman, P. H., Fung, C. C. A., Pazo Fernandez, A., Sawant, A., Tedoldi, A., Kawai, A., Ghimire Gautam, S., Kurosawa, M., Abe, M., Sakimura, K., Fukai, T., & Goda, Y. (2021). Astrocyte GluN2C NMDA receptors control basal synaptic strengths of hippocampal CA1 pyramidal neurons in the stratum radiatum. *ELife*, *10*. https://doi.org/10.7554/eLife.70818

Choe, E. S., & Wang, J. Q. (2001). Group I metabotropic glutamate receptors control phosphorylation of CREB, Elk-1 and ERK via a CaMKII-dependent pathway in rat striatum. *Neuroscience Letters*, *313*(3), 129–132. https://doi.org/10.1016/S0304-3940(01)02258-3

Choi, D. W. (1987). Ionic dependence of glutamate neurotoxicity. *The Journal of Neuroscience : The Official Journal of the Society for Neuroscience*, *7*(2), 369–379. https://doi.org/10.1523/JNEUROSCI.07-02-00369.1987

Christopher, J. A., Aves, S. J., Bennett, K. A., Doré, A. S., Errey, J. C., Jazayeri, A., Marshall, F. H., Okrasa, K., Serrano-Vega, M. J., Tehan, B. G., Wiggin, G. R., & Congreve, M. (2015). Fragment and Structure-Based Drug Discovery for a Class C GPCR: Discovery of the mGlu5 Negative Allosteric Modulator HTL14242 (3-Chloro-5-[6-(5-fluoropyridin-2-yl)pyrimidin-4-yl]benzonitrile). *Journal of Medicinal Chemistry*, *58*(16), 6653–6664. https://doi.org/10.1021/ACS.JMEDCHEM.5B00892

Christopher, J. A., Orgován, Z., Congreve, M., Doré, A. S., Errey, J. C., Marshall, F. H., Mason, J. S., Okrasa, K., Rucktooa, P., Serrano-Vega, M. J., Ferenczy, G. G., & Keserű, G. M. (2019). Structure-Based Optimization Strategies for G Protein-Coupled Receptor (GPCR) Allosteric Modulators: A Case Study from Analyses of New Metabotropic Glutamate Receptor 5 ($mGlu_5$) X-ray Structures. *Journal of Medicinal Chemistry*, *62*(1), 207–222. https://doi.org/10.1021/acs.jmedchem.7b01722

Christopoulos, A. (2002). G Protein-Coupled Receptor Allosterism and Complexing. *Pharmacological Reviews*, *54*(2), 323–374. https://doi.org/10.1124/pr.54.2.323

Christopoulos, A., Changeux, J.-P., Catterall, W. A., Fabbro, D., Burris, T. P., Cidlowski, J. A., Olsen, R. W., Peters, J. A., Neubig, R. R., Pin, J.-P., Sexton, P. M., Kenakin, T. P., Ehlert, F. J., Spedding, M., & Langmead, C. J. (2014). International Union of Basic and Clinical Pharmacology. XC. Multisite Pharmacology: Recommendations for the Nomenclature of Receptor Allosterism and Allosteric Ligands. *Pharmacological Reviews*, *66*(4), 918–947. https://doi.org/10.1124/pr.114.008862

Chung, G., Shim, H. G., Kim, C. Y., Ryu, H.-H., Jang, D. C., Kim, S. H., Lee, J., Kim, C.-E., Kim, Y. K., Lee, Y.-S., Kim, J., Kim, S. K., Worley, P. F., & Kim, S. J. (2020). Persistent Activity of Metabotropic Glutamate Receptor 5 in the Periaqueductal Gray Constrains Emergence of Chronic Neuropathic Pain. *Current Biology*, *30*(23), 4631-4642.e6. https://doi.org/10.1016/j.cub.2020.09.008

Chung, W., Choi, S. Y., Lee, E., Park, H., Kang, J., Park, H., Choi, Y., Lee, D., Park, S.-G., Kim, R., Cho, Y. S., Choi, J., Kim, M.-H., Lee, J. W., Lee, S., Rhim, I., Jung, M. W., Kim, D., Bae, Y. C., & Kim, E. (2015). Social deficits in IRSp53 mutant mice improved by NMDAR and mGluR5 suppression. *Nature Neuroscience*, *18*(3), 435–443. https://doi.org/10.1038/nn.3927

Clavaguera, F., Bolmont, T., Crowther, R. A., Abramowski, D., Frank, S., Probst, A., Fraser, G., Stalder, A. K., Beibel, M., Staufenbiel, M., Jucker, M., Goedert, M., & Tolnay, M. (2009). Transmission and spreading of tauopathy in transgenic mouse brain. *Nature Cell Biology*, *11*(7), 909–913. https://doi.org/10.1038/ncb1901

Coley, A. A., & Gao, W.-J. (2019). PSD-95 deficiency disrupts PFC-associated function and behavior during neurodevelopment. *Scientific Reports*, *9*(1), 9486. https://doi.org/10.1038/s41598-019-45971-w

Collinge, J., Whittington, M. A., Sidle, K. C., Smith, C. J., Palmer, M. S., Clarke, A. R. & Jeffreys, J. G. (1994). Prion protein is necessary for normal synaptic function. *Nature*, 370, 295-7.

Collinge, J., Sidle, K. C. L., Meads, J., Ironside, J., & Hill, A. F. (1996). Molecular analysis of prion strain variation and the aetiology of 'new variant' CJD. *Nature*, *383*(6602), 685–690. https://doi.org/10.1038/383685a0

Collins, M., Tremblay, M., Chapman, N., Curtiss, M., Rothman, P. B., & Houtman, J. C. D. (2009). The T cell receptor-mediated phosphorylation of Pyk2 tyrosines 402 and 580 occurs via a distinct mechanism than other receptor systems. *Journal of Leukocyte Biology*, *87*(4), 691–701. https://doi.org/10.1189/jlb.0409227

Colonna, M., & Butovsky, O. (2017). Microglia Function in the Central Nervous System During Health and Neurodegeneration. *Annual Review of Immunology*, *35*, 441–468. https://doi.org/10.1146/ANNUREV-IMMUNOL-051116-052358

Conde-Ceide, S., Martínez-Viturro, C. M., Alcázar, J., Garcia-Barrantes, P. M., Lavreysen, H., Mackie, C., Vinson, P. N., Rook, J. M., Bridges, T. M., Daniels, J. S., Megens, A., Langlois, X., Drinkenburg, W. H., Ahnaou, A., Niswender, C. M., Jones, C. K., Macdonald, G. J., Steckler, T., Conn, P. J., … Lindsley, C. W. (2015). Discovery of VU0409551/JNJ-46778212: An mGlu5 Positive Allosteric Modulator Clinical Candidate Targeting Schizophrenia. *ACS Medicinal Chemistry Letters*, *6*(6), 716–720. https://doi.org/10.1021/ACSMEDCHEMLETT.5B00181/SUPPL_FILE/ML5B00181_SI_001.PDF

Condello, C., Lemmin, T., Stöhr, J., Nick, M., Wu, Y., Maxwell, A. M., Watts, J. C., Caro, C. D., Oehler, A., Keene, C. D., Bird, T. D., van Duinen, S. G., Lannfelt, L., Ingelsson, M., Graff, C., Giles, K., DeGrado, W. F., & Prusiner, S. B. (2018). Structural heterogeneity and intersubject variability of Aß in familial and sporadic Alzheimer's disease. *Proceedings of the National Academy of Sciences*, *115*(4). https://doi.org/10.1073/pnas.1714966115

Conn, P. J., Lindsley, C. W., & Jones, C. K. (2009). Activation of metabotropic glutamate receptors as a novel approach for the treatment of schizophrenia. *Trends in Pharmacological Sciences*, *30*(1), 25–31. https://doi.org/10.1016/j.tips.2008.10.006

Conn, P. J., Lindsley, C. W., Meiler, J., & Niswender, C. M. (2014). Opportunities and challenges in the discovery of allosteric modulators of GPCRs for treating CNS disorders. *Nature Reviews Drug Discovery*, *13*(9), 692–708. https://doi.org/10.1038/nrd4308

Conn, P. J., & Pin, J.-P. (1997). Pharmacology and functions of metabotropic glutamate receptors. *Annual Review of Pharmacology and Toxicology*, *37*(1), 205–237. https://doi.org/10.1146/annurev.pharmtox.37.1.205

Connolly, N. M. C., & Prehn, J. H. M. (2015). The metabolic response to excitotoxicity – lessons from single-cell imaging. *Journal of Bioenergetics and Biomembranes*, *47*(1–2), 75–88. https://doi.org/10.1007/s10863-014-9578-4

Constantino, S., Santos, R., Gisselbrecht, S., & Gouilleux, F. (2001). The ecdysone inducible gene expression system: unexpected effects of muristerone A and

ponasterone A on cytokine signaling in mammalian cells. *European Cytokine Network*, *12*(2), 365–367.

Conway, M. E. (2020). Alzheimer's disease: targeting the glutamatergic system. *Biogerontology*, *21*(3), 257–274. https://doi.org/10.1007/s10522-020-09860-4

Conway, M. E., & Hutson, S. M. (2016). BCAA Metabolism and NH3 Homeostasis. *Advances in Neurobiology*, *13*, 99–132. https://doi.org/10.1007/978-3-319-45096-4_5

Cosford, N. D. P., Roppe, J., Tehrani, L., Schweiger, E. J., Seiders, T. J., Chaudary, A., Rao, S., & Varney, M. A. (2003). [3H]-Methoxymethyl-MTEP and [3H]-Methoxy-PEPy: potent and selective radioligands for the metabotropic glutamate subtype 5 (mGlu5) receptor. *Bioorganic & Medicinal Chemistry Letters*, *13*(3), 351–354. https://doi.org/10.1016/S0960-894X(02)00997-6

Costello, D. A., & Herron, C. E. (2004). The role of c-Jun N-terminal kinase in the Aß-mediated impairment of LTP and regulation of synaptic transmission in the hippocampus. *Neuropharmacology*, *46*(5), 655–662. https://doi.org/10.1016/j.neuropharm.2003.11.016

Coyle, J. T., & Schwarz, R. (1976). Lesion of striatal neurons with kainic acid provides a model for Huntington's chorea. *Nature*, *263*(5574), 244–246. https://doi.org/10.1038/263244a0

Craig, N. L. (1988). The Mechanism of Conservative Site-Specific Recombination. *Annual Review of Genetics*, *22*(1), 77–105. https://doi.org/10.1146/annurev.ge.22.120188.000453

Crasto, C. (2010). Hydrophobicity profiles in G protein-coupled receptor transmembrane helical domains. *Journal of Receptor, Ligand and Channel Research*, 123. https://doi.org/10.2147/JRLCR.S14437

Creutzfeldt, H. G. (1989). On a particular focal disease of the central nervous system (preliminary communication), 1920. *Alzheimer Disease and Associated Disorders*, *3*(1–2), 3–25.

Cronier, S., Laude, H., & Peyrin, J.-M. (2004). Prions can infect primary cultured neurons and astrocytes and promote neuronal cell death. *Proceedings of the National Academy of Sciences*, *101*(33), 12271–12276. https://doi.org/10.1073/pnas.0402725101

Crouch, R. D., Blobaum, A. L., Felts, A. S., Conn, P. J., & Lindsley, C. W. (2017). Species-Specific Involvement of Aldehyde Oxidase and Xanthine Oxidase in the Metabolism of the Pyrimidine-Containing mGlu $_5$ -Negative Allosteric Modulator VU0424238 (Auglurant). *Drug Metabolism and Disposition*, *45*(12), 1245–1259. https://doi.org/10.1124/dmd.117.077552

Cummings, J., Lee, G., Nahed, P., Kambar, M. E. Z. N., Zhong, K., Fonseca, J., & Taghva, K. (2022). Alzheimer's disease drug development pipeline: 2022. *Alzheimer's & Dementia: Translational Research & Clinical Interventions*, *8*(1). https://doi.org/10.1002/trc2.12295

Cunningham, C., Boche, D., & Perry, V. H. (2002). Transforming growth factor beta1, the dominant cytokine in murine prion disease: influence on inflammatory cytokine synthesis and alteration of vascular extracellular matrix. *Neuropathology and Applied Neurobiology*, *28*(2), 107–119. https://doi.org/10.1046/j.1365-2990.2002.00383.x

Danielsson, F., Peterson, M., Caldeira Araújo, H., Lautenschläger, F., & Gad, A. (2018). Vimentin Diversity in Health and Disease. *Cells*, *7*(10), 147. https://doi.org/10.3390/cells7100147

David, T. K., Prashanth, N. K., Rajendraswami, M., Pallalu, D., Castelhano, A. L., Kates, M. J., Blobaum, A. L., Jones, C. K., Emmitte, K. A., Conn, P. J., & Lindsley, C. W. (2017). Development and kilogram-scale synthesis of mGlu5

negative allosteric modulator VU0424238 (auglurant). *Tetrahedron Letters*, *58*(36), 3554–3558. https://doi.org/10.1016/j.tetlet.2017.07.100

Davies, S. W., Mark, T., Cozens, B. A., Raza, A. S., Mahal, A., Mangiarini, L., & Bates, G. P. (1999). From neuronal inclusions to neurodegeneration: neuropathological investigation of a transgenic mouse model of Huntington'sdisease. *Philosophical Transactions of the Royal Society of London. Series B: Biological Sciences*, *354*(1386), 971–979. https://doi.org/10.1098/rstb.1999.0448

Deacon, R. M. J. (2006). Burrowing in rodents: a sensitive method for detecting behavioral dysfunction. *Nature Protocols*, *1*(1), 118–121. https://doi.org/10.1038/nprot.2006.19

DeArmond, S. et al., (1997). Selective neuronal targeting in prion disease. Neuron, Volume 19, pp. 1337-1346.

De Felice, F. G., Velasco, P. T., Lambert, M. P., Viola, K., Fernandez, S. J., Ferreira, S. T., & Klein, W. L. (2007). Abeta oligomers induce neuronal oxidative stress through an N-methyl-D-aspartate receptor-dependent mechanism that is blocked by the Alzheimer drug memantine. *The Journal of Biological Chemistry*, *282*(15), 11590–11601. https://doi.org/10.1074/JBC.M607483200

De Giorgio, F., Maduro, C., Fisher, E. M. C., & Acevedo-Arozena, A. (2019). Transgenic and physiological mouse models give insights into different aspects of amyotrophic lateral sclerosis. *Disease Models & Mechanisms*, *12*(1). https://doi.org/10.1242/dmm.037424

Degorce, F. (2009). HTRF: A Technology Tailored for Drug Discovery - A Review of Theoretical Aspects and Recent Applications. *Current Chemical Genomics*, *3*(1), 22–32. https://doi.org/10.2174/1875397300903010022

Desai, M. A., Burnett, J. P., Mayne, N. G., & Schoepp, D. D. (1995). Cloning and expression of a human metabotropic glutamate receptor 1 alpha: enhanced coupling on co-transfection with a glutamate transporter. *Molecular Pharmacology*, *48*(4), 648–657.

De Souza, J. M., Abd-Elrahman, K. S., Ribeiro, F. M., & Ferguson, S. S. G. (2020). mGluR5 regulates REST/NRSF signaling through N-cadherin/ß-catenin complex in Huntington's disease. *Molecular Brain*, *13*(1). https://doi.org/10.1186/S13041-020-00657-7

De Souza, J.M., Ferreira-Vieira, T.H., Maciel, E.M.A., Silva, N.C., Lima, I.B.Q., Doria, J.G., Olmo, I.G., Ribeiro, F.M. (2022). mGluR5 ablation leads to age-related synaptic plasticity impairments and does not improve Huntington's disease phenotype. *Sci Rep*, 12, 8982. https://doi.org/10.1038/s41598-022-13029-z

Deacon, R.M.J. (2006). Burrowing in rodents: a sensitive method for detecting behavioral dysfunction. *Nat Protoc*, 1, 118–121. https://doi.org/10.1038/nprot.2006.19

Deming, Y., Dumitrescu, L., Barnes, L. L., Thambisetty, M., Kunkle, B., Gifford, K. A., Bush, W. S., Chibnik, L. B., Mukherjee, S., De Jager, P. L., Kukull, W., Huentelman, M., Crane, P. K., Resnick, S. M., Keene, C. D., Montine, T. J., Schellenberg, G. D., Haines, J. L., Zetterberg, H., … Hohman, T. J. (2018). Sex-specific genetic predictors of Alzheimer's disease biomarkers. *Acta Neuropathologica*, *136*(6), 857–872. https://doi.org/10.1007/s00401-018-1881-4

Desplats, P., Lee, H.-J., Bae, E.-J., Patrick, C., Rockenstein, E., Crews, L., Spencer, B., Masliah, E., & Lee, S.-J. (2009). Inclusion formation and neuronal cell death through neuron-to-neuron transmission of α-synuclein. *Proceedings of the National Academy of Sciences*, *106*(31), 13010–13015. https://doi.org/10.1073/pnas.0903691106

Devoy, A., Kalmar, B., Stewart, M., Park, H., Burke, B., Noy, S. J., Redhead, Y., Humphrey, J., Lo, K., Jaeger, J., Mejia Maza, A., Sivakumar, P., Bertolin, C.,

Soraru, G., Plagnol, V., Greensmith, L., Acevedo Arozena, A., Isaacs, A. M., Davies, B., … Fisher, E. M. C. (2017). Humanized mutant FUS drives progressive motor neuron degeneration without aggregation in 'FUSDelta14' knockin mice. *Brain*, *140*(11), 2797–2805. https://doi.org/10.1093/brain/awx248

DeWire, S. M., Ahn, S., Lefkowitz, R. J., & Shenoy, S. K. (2007). β-Arrestins and Cell Signaling. *Annual Review of Physiology*, *69*(1), 483–510. https://doi.org/10.1146/annurev.physiol.69.022405.154749

Dhami, G. K., & Ferguson, S. S. G. (2006). Regulation of metabotropic glutamate receptor signaling, desensitization and endocytosis. *Pharmacology & Therapeutics*, *111*(1), 260–271. https://doi.org/10.1016/j.pharmthera.2005.01.008

DiCarlo, G. (2001). Intrahippocampal LPS injections reduce AÎ² load in APP+PS1 transgenic mice. *Neurobiology of Aging*, *22*(6), 1007–1012. https://doi.org/10.1016/S0197-4580(01)00292-5

Diedrich, J. F., Bendheim, P. E., Kim, Y. S., Carp, R. I., & Haase, A. T. (1991). Scrapie-associated prion protein accumulates in astrocytes during scrapie infection. *Proceedings of the National Academy of Sciences*, *88*(2), 375–379. https://doi.org/10.1073/pnas.88.2.375

Dogrul, A., Ossipov, M. H., Lai, J., Malan, T. P., & Porreca, F. (2000). Peripheral and spinal antihyperalgesic activity of SIB-1757, a metabotropic glutamate receptor (mGLUR5) antagonist, in experimental neuropathic pain in rats. *Neuroscience Letters*, *292*(2), 115–118. https://doi.org/10.1016/S0304-3940(00)01458-0

Doherty, A. J., Palmer, M. J., Henley, J. M., Cillingridge, G. L., & Jane, D. E. (1997). (RS)-2-Chloro-5-Hydroxyphenylglycine (CHPG) Activates mGlu5, but not mGlu1, Receptors Expressed in CHO Cells and Potentiates NMDA Responses in the Hippocampus. *Neuropharmacology*, *36*(2), 265–267. https://doi.org/10.1016/S0028-3908(97)00001-4

Domin, H., Szewczyk, B., Woźniak, M., Wawrzak-Wleciał, A., & Śmiałowska, M. (2014). Antidepressant-like effect of the mGluR5 antagonist MTEP in an astroglial degeneration model of depression. *Behavioural Brain Research*, *273*, 23–33. https://doi.org/10.1016/j.bbr.2014.07.019

Doré, A. S., Okrasa, K., Patel, J. C., Serrano-Vega, M., Bennett, K., Cooke, R. M., Errey, J. C., Jazayeri, A., Khan, S., Tehan, B., Weir, M., Wiggin, G. R., & Marshall, F. H. (2014). Structure of class C GPCR metabotropic glutamate receptor 5 transmembrane domain. *Nature*, *511*(7511), 557–562. https://doi.org/10.1038/nature13396

Dore, K., Carrico, Z., Alfonso, S., Marino, M., Koymans, K., Kessels, H. W., & Malinow, R. (2021). PSD-95 protects synapses from β-amyloid. *Cell Reports*, *35*(9), 109194. https://doi.org/10.1016/j.celrep.2021.109194

Doria, J. G., de Souza, J. M., Andrade, J. N., Rodrigues, H. A., Guimaraes, I. M., Carvalho, T. G., Guatimosim, C., Dobransky, T., & Ribeiro, F. M. (2015). The mGluR5 positive allosteric modulator, CDPPB, ameliorates pathology and phenotypic signs of a mouse model of Huntington's disease. *Neurobiology of Disease*, *73*, 163–173. https://doi.org/10.1016/j.nbd.2014.08.021

Doria, J. G., de Souza, J. M., Silva, F. R., Olmo, I. G., Carvalho, T. G., Alves-Silva, J., Ferreira-Vieira, T. H., Santos, J. T., Xavier, C. Q. S., Silva, N. C., Maciel, E. M. A., Conn, P. J., & Ribeiro, F. M. (2018). The mGluR5 positive allosteric modulator VU0409551 improves synaptic plasticity and memory of a mouse model of Huntington's disease. *Journal of Neurochemistry*, *147*(2), 222–239. https://doi.org/10.1111/jnc.14555

Dormann, D., Rodde, R., Edbauer, D., Bentmann, E., Fischer, I., Hruscha, A., Than, M. E., Mackenzie, I. R. A., Capell, A., Schmid, B., Neumann, M., & Haass, C. (2010). ALS-associated fused in sarcoma (FUS) mutations disrupt Transportin-

mediated nuclear import. *The EMBO Journal*, *29*(16), 2841–2857. https://doi.org/10.1038/emboj.2010.143

Downey, Patrick. M., Lozza, G., Petrò, R., Diodato, E., Foglia, C., Bottazzoli, F., Brusa, R., Asquini, T., Reggiani, A., & Grilli, M. (2005). Ecdysone-Based System for Controlled Inducible Expression of Metabotropic Glutamate Receptor Subtypes 2, 5, and 8. *SLAS Discovery*, *10*(8), 841–848. https://doi.org/10.1177/1087057105280285

Dracheva, S., Marras, S. A. E., Elhakem, S. L., Kramer, F. R., Davis, K. L., & Haroutunian, V. (2001). *N* -Methyl- <scp>d</scp> -Aspartic Acid Receptor Expression in the Dorsolateral Prefrontal Cortex of Elderly Patients With Schizophrenia. *American Journal of Psychiatry*, *158*(9), 1400–1410. https://doi.org/10.1176/appi.ajp.158.9.1400

Dror, R. O., Mildorf, T. J., Hilger, D., Manglik, A., Borhani, D. W., Arlow, D. H., Philippsen, A., Villanueva, N., Yang, Z., Lerch, M. T., Hubbell, W. L., Kobilka, B. K., Sunahara, R. K., & Shaw, D. E. (2015). Structural basis for nucleotide exchange in heterotrimeric G proteins. *Science*, *348*(6241), 1361–1365. https://doi.org/10.1126/science.aaa5264

Drouin-Ouellet, J., Brownell, A. L., Saint-Pierre, M., Fasano, C., Emond, V., Trudeau, L. E., Lévesque, D., & Cicchetti, F. (2011). Neuroinflammation is associated with changes in glial mGluR5 expression and the development of neonatal excitotoxic lesions. *Glia*, *59*(2), 188–199. https://doi.org/10.1002/GLIA.21086

Drummond, E., & Wisniewski, T. (2017). Alzheimer's disease: experimental models and reality. *Acta Neuropathologica*, *133*(2), 155–175. https://doi.org/10.1007/s00401-016-1662-x

Du, L.-L. (2020). Resurrection from lethal knockouts: Bypass of gene essentiality. *Biochem Biophys Res Commun*, 528, 405–412. https://doi.org/10.1016/j.bbrc.2020.05.207

Dunlop, J., Lou, Z., & McIlvain, H. B. (1999). Steroid Hormone-Inducible Expression of the GLT-1 Subtype of High-Affinity l-Glutamate Transporter in Human Embryonic Kidney Cells. *Biochemical and Biophysical Research Communications*, *265*(1), 101–105. https://doi.org/10.1006/bbrc.1999.1633

Duprat, F. (1997). TASK, a human background K+ channel to sense external pH variations near physiological pH. *The EMBO Journal*, *16*(17), 5464–5471. https://doi.org/10.1093/emboj/16.17.5464

Dwomoh, L., Rossi, M., Scarpa, M., Khajehali, E., Molloy, C., Herzyk, P., Mistry, S. N., Bottrill, A. R., Sexton, P. M., Christopoulos, A., Conn, J., Lindsley, C. W., Bradley, S. J., & Tobin, A. B. (2022). M1 muscarinic receptor activation reduces the molecular pathology and slows the progression of prion-mediated neurodegenerative disease. *Science Signaling*, *15*(760). https://doi.org/10.1126/scisignal.abm3720

Eftekharzadeh, B., Daigle, J. G., Kapinos, L. E., Coyne, A., Schiantarelli, J., Carlomagno, Y., Cook, C., Miller, S. J., Dujardin, S., Amaral, A. S., Grima, J. C., Bennett, R. E., Tepper, K., DeTure, M., Vanderburgh, C. R., Corjuc, B. T., DeVos, S. L., Gonzalez, J. A., Chew, J., … Hyman, B. T. (2018). Tau Protein Disrupts Nucleocytoplasmic Transport in Alzheimer's Disease. *Neuron*, *99*(5), 925-940.e7. https://doi.org/10.1016/J.NEURON.2018.07.039

Eichel, K., Jullié, D., & von Zastrow, M. (2016). β-Arrestin drives MAP kinase signalling from clathrin-coated structures after GPCR dissociation. *Nature Cell Biology*, *18*(3), 303–310. https://doi.org/10.1038/ncb3307

Eli Lilly and Company. (2023). *Lilly's Donanemab Significantly Slowed Cognitive and Functional Decline in Phase 3 Study of Early Alzheimer's Disease*. Accessed May 3, 2023. https://investor.lilly.com/news-releases/news-release-details/lillys-donanemab-significantly-slowed-cognitive-and-functional

Elmore, S. (2007). Apoptosis: A Review of Programmed Cell Death. *Toxicologic Pathology*, *35*(4), 495–516. https://doi.org/10.1080/01926230701320337

Eng, A. G., Kelver, D. A., Hedrick, T. P., & Swanson, G. T. (2016). Transduction of group I mGluR-mediated synaptic plasticity by β-arrestin2 signalling. *Nature Communications*, *7*(1), 13571. https://doi.org/10.1038/ncomms13571

Eng, L. F., Vanderhaeghen, J. J., Bignami, A., & Gerstl, B. (1971). An acidic protein isolated from fibrous astrocytes. *Brain Research*, *28*(2), 351–354. https://doi.org/10.1016/0006-8993(71)90668-8

Eriksson, C., Van Dam, A.M., Lucassen, P.J., Bol, J.G.J.M., Winblad, B., Schultzberg, M., 1999. Immunohistochemical localization of interleukin-1β, interleukin-1 receptor antagonist and interleukin-1β converting enzyme/caspase-1 in the rat brain after peripheral administration of kainic acid. Neuroscience 93, 915–930. https://doi.org/10.1016/S0306-4522(99)00178-5

Escartin, C., Galea, E., Lakatos, A., O'Callaghan, J. P., Petzold, G. C., Serrano-Pozo, A., Steinhäuser, C., Volterra, A., Carmignoto, G., Agarwal, A., Allen, N. J., Araque, A., Barbeito, L., Barzilai, A., Bergles, D. E., Bonvento, G., Butt, A. M., Chen, W.-T., Cohen-Salmon, M., … Verkhratsky, A. (2021). Reactive astrocyte nomenclature, definitions, and future directions. *Nature Neuroscience*, *24*(3), 312–325. https://doi.org/10.1038/s41593-020-00783-4

Esterlis, I., Holmes, S.E., Sharma, P., Krystal, J.H., DeLorenzo, C. (2018). Metabotropic Glutamatergic Receptor 5 and Stress Disorders: Knowledge Gained From Receptor Imaging Studies. *Biol Psychiatry*, 84, 95–105. https://doi.org/10.1016/j.biopsych.2017.08.025

Evans, S. J., Douglas, I., Rawlins, M. D., Wexler, N. S., Tabrizi, S. J., & Smeeth, L. (2013). Prevalence of adult Huntington's disease in the UK based on diagnoses recorded in general practice records. *Journal of Neurology, Neurosurgery & Psychiatry*, *84*(10), 1156–1160. https://doi.org/10.1136/jnnp-2012-304636

Falsig, J., Julius, C., Margalith, I., Schwarz, P., Heppner, F. L., & Aguzzi, A. (2008). A versatile prion replication assay in organotypic brain slices. *Nature Neuroscience*, *11*(1), 109–117. https://doi.org/10.1038/nn2028

Fang, T., Al Khleifat, A., Meurgey, J.-H., Jones, A., Leigh, P. N., Bensimon, G., & Al-Chalabi, A. (2018). Stage at which riluzole treatment prolongs survival in patients with amyotrophic lateral sclerosis: a retrospective analysis of data from a dose-ranging study. *The Lancet Neurology*, *17*(5), 416–422. https://doi.org/10.1016/S1474-4422(18)30054-1

Fang, F., Ingre, C., Roos, P., Kamel, F., & Piehl, F. (2015). Risk factors for amyotrophic lateral sclerosis. *Clinical Epidemiology*, 181. https://doi.org/10.2147/CLEP.S37505

Fang, X. T., Eriksson, J., Antoni, G., Yngve, U., Cato, L., Lannfelt, L., Sehlin, D., & Syvänen, S. (2017). Brain mGluR5 in mice with amyloid beta pathology studied with in vivo [11C]ABP688 PET imaging and ex vivo immunoblotting. *Neuropharmacology*, *113*, 293–300. https://doi.org/10.1016/j.neuropharm.2016.10.009

Farso, M. C., O'Shea, R. D., & Beart, P. M. (2009). Evidence group I mGluR drugs modulate the activation profile of lipopolysaccharide-exposed microglia in culture. *Neurochemical Research*, *34*(10), 1721–1728. https://doi.org/10.1007/S11064-009-9999-3/FIGURES/2

Feigin, A., Evans, E. E., Fisher, T. L., Leonard, J. E., Smith, E. S., Reader, A., Mishra, V., Manber, R., Walters, K. A., Kowarski, L., Oakes, D., Siemers, E., Kieburtz, K. D., Zauderer, M., Kayson, E., Goldstein, J., Barbano, R., Marder, K., Dayalu, P., … Anderson, K. (2022). Pepinemab antibody blockade of SEMA4D in early Huntington's disease: a randomized, placebo-controlled, phase 2 trial.

Nature Medicine, *28*(10), 2183–2193. https://doi.org/10.1038/s41591-022-01919-8

Fellin, T., Pascual, O., Gobbo, S., Pozzan, T., Haydon, P. G., & Carmignoto, G. (2004). Neuronal Synchrony Mediated by Astrocytic Glutamate through Activation of Extrasynaptic NMDA Receptors. *Neuron*, *43*(5), 729–743. https://doi.org/10.1016/j.neuron.2004.08.011

Felton, L. M., Cunningham, C., Rankine, E. L., Waters, S., Boche, D., & Perry, V. H. (2005). MCP-1 and murine prion disease: Separation of early behavioural dysfunction from overt clinical disease. *Neurobiology of Disease*, *20*(2), 283–295. https://doi.org/10.1016/j.nbd.2005.03.008

Felts, A. S., Bollinger, K. A., Brassard, C. J., Rodriguez, A. L., Morrison, R. D., Scott Daniels, J., Blobaum, A. L., Niswender, C. M., Jones, C. K., Jeffrey Conn, P., Emmitte, K. A., & Lindsley, C. W. (2019). Discovery of 4-alkoxy-6-methylpicolinamide negative allosteric modulators of metabotropic glutamate receptor subtype 5. *Bioorganic & Medicinal Chemistry Letters*, *29*(1), 47–50. https://doi.org/10.1016/j.bmcl.2018.11.017

Felts, A. S., Rodriguez, A. L., Blobaum, A. L., Morrison, R. D., Bates, B. S., Thompson Gray, A., Rook, J. M., Tantawy, M. N., Byers, F. W., Chang, S., Venable, D. F., Luscombe, V. B., Tamagnan, G. D., Niswender, C. M., Daniels, J. S., Jones, C. K., Conn, P. J., Lindsley, C. W., & Emmitte, K. A. (2017). Discovery of N-(5-Fluoropyridin-2-yl)-6-methyl-4-(pyrimidin-5-yloxy)picolinamide (VU0424238): A Novel Negative Allosteric Modulator of Metabotropic Glutamate Receptor Subtype 5 Selected for Clinical Evaluation. *Journal of Medicinal Chemistry*, *60*(12), 5072–5085. https://doi.org/10.1021/ACS.JMEDCHEM.7B00410

Ferguson, M. W., Kennedy, C. J., Palpagama, T. H., Waldvogel, H. J., Faull, R. L. M., & Kwakowsky, A. (2022). Current and Possible Future Therapeutic Options for Huntington's Disease. *Journal of Central Nervous System Disease*, *14*, 117957352210925. https://doi.org/10.1177/11795735221092517

Ferguson, S. S. (2001). Evolving concepts in G protein-coupled receptor endocytosis: the role in receptor desensitization and signaling. *Pharmacological Reviews*, *53*(1), 1–24.

Ferreira, D.G., Temido-Ferreira, M., Vicente Miranda, H., Batalha, V.L., Coelho, J.E., Szegö, É.M., Marques-Morgado, I., Vaz, S.H., Rhee, J.S., Schmitz, M., Zerr, I., Lopes, L. V, Outeiro, T.F. (2017). α-synuclein interacts with PrPC to induce cognitive impairment through mGluR5 and NMDAR2B. *Nat Neurosci,* 20, 1569–1579. https://doi.org/10.1038/nn.4648

Ferreira-Vieira, T., M. Guimaraes, I., R. Silva, F., & M. Ribeiro, F. (2016). Alzheimer's disease: Targeting the Cholinergic System. *Current Neuropharmacology*, *14*(1), 101–115. https://doi.org/10.2174/1570159X13666150716165726

Ferrer, I. (2017). Diversity of astroglial responses across human neurodegenerative disorders and brain aging. *Brain Pathology*, *27*(5), 645–674. https://doi.org/10.1111/bpa.12538

Fink, M. (1998). A neuronal two P domain K+ channel stimulated by arachidonic acid and polyunsaturated fatty acids. *The EMBO Journal*, *17*(12), 3297–3308. https://doi.org/10.1093/emboj/17.12.3297

Finkbeiner, S., Tavazoie, S. F., Maloratsky, A., Jacobs, K. M., Harris, K. M., & Greenberg, M. E. (1997). CREB: A Major Mediator of Neuronal Neurotrophin Responses. *Neuron*, *19*(5), 1031–1047. https://doi.org/10.1016/S0896-6273(00)80395-5

Fisher, K., Lefebvre, C., & Coderre, T. J. (2002). Antinociceptive effects following intrathecal pretreatment with selective metabotropic glutamate receptor

compounds in a rat model of neuropathic pain. *Pharmacology Biochemistry and Behavior*, *73*(2), 411–418. https://doi.org/10.1016/S0091-3057(02)00832-8

Foo, L. C., Allen, N. J., Bushong, E. A., Ventura, P. B., Chung, W.-S., Zhou, L., Cahoy, J. D., Daneman, R., Zong, H., Ellisman, M. H., & Barres, B. A. (2011). Development of a Method for the Purification and Culture of Rodent Astrocytes. *Neuron*, *71*(5), 799–811. https://doi.org/10.1016/j.neuron.2011.07.022

Foster, S. R., Hauser, A. S., Vedel, L., Strachan, R. T., Huang, X.-P., Gavin, A. C., Shah, S. D., Nayak, A. P., Haugaard-Kedström, L. M., Penn, R. B., Roth, B. L., Bräuner-Osborne, H., & Gloriam, D. E. (2019). Discovery of Human Signaling Systems: Pairing Peptides to G Protein-Coupled Receptors. *Cell*, *179*(4), 895-908.e21. https://doi.org/10.1016/j.cell.2019.10.010

Francesconi, A., & Duvoisin, R. M. (1998). Role of the Second and Third Intracellular Loops of Metabotropic Glutamate Receptors in Mediating Dual Signal Transduction Activation. *Journal of Biological Chemistry*, *273*(10), 5615–5624. https://doi.org/10.1074/jbc.273.10.5615

Frankland, P. W., & Bontempi, B. (2005). The organization of recent and remote memories. *Nature Reviews Neuroscience*, *6*(2), 119–130. https://doi.org/10.1038/nrn1607

Fraser, E., McDonagh, A. M., Head, M., Bishop, M., Ironside, J. W., & Mann, D. M. A. (2003). Neuronal and astrocytic responses involving the serotonergic system in human spongiform encephalopathies. *Neuropathology and Applied Neurobiology*, *29*(5), 482–495. https://doi.org/10.1046/j.1365-2990.2003.00486.x

Frau-Méndez, M. A., Fernández-Vega, I., Ansoleaga, B., Blanco Tech, R., Carmona Tech, M., Antonio del Rio, J., Zerr, I., Llorens, F., José Zarranz, J., & Ferrer, I. (2017). Fatal familial insomnia: mitochondrial and protein synthesis machinery decline in the mediodorsal thalamus. *Brain Pathology*, *27*(1), 95–106. https://doi.org/10.1111/bpa.12408

Fredriksson, R., Lagerström, M. C., Lundin, L.-G., & Schiöth, H. B. (2003). The G-Protein-Coupled Receptors in the Human Genome Form Five Main Families. Phylogenetic Analysis, Paralogon Groups, and Fingerprints. *Molecular Pharmacology*, *63*(6), 1256–1272. https://doi.org/10.1124/mol.63.6.1256

Fredriksson, R., & Schiöth, H. B. (2005). The Repertoire of G-Protein–Coupled Receptors in Fully Sequenced Genomes. *Molecular Pharmacology*, *67*(5), 1414–1425. https://doi.org/10.1124/mol.104.009001

Friedel, R.H., Wurst, W., Wefers, B., Kühn, R. (2011). Generating Conditional Knockout Mice. pp. 205–231. https://doi.org/10.1007/978-1-60761-974-1_12

Friedmann, C. T. H., Davis, L. J., Ciccone, P. E., & Rubin, R. T. (1980). Phase II double-blind controlled study of a new anxiolytic, fenobam (McN-3377) vs placebo. *Current Therapeutic Research - Clinical and Experimental*, *27*(2), 144–151.

Frost, B., Jacks, R. L., & Diamond, M. I. (2009). Propagation of Tau Misfolding from the Outside to the Inside of a Cell. *Journal of Biological Chemistry*, *284*(19), 12845–12852. https://doi.org/10.1074/jbc.M808759200

Fukata, Y., Hirano, Y., Miyazaki, Y., Yokoi, N., & Fukata, M. (2021). Trans-synaptic LGI1–ADAM22–MAGUK in AMPA and NMDA receptor regulation. *Neuropharmacology*, *194*, 108628. https://doi.org/10.1016/j.neuropharm.2021.108628

Fulmer, C. G., VonDran, M. W., Stillman, A. A., Huang, Y., Hempstead, B. L., & Dreyfus, C. F. (2014). Astrocyte-Derived BDNF Supports Myelin Protein Synthesis after Cuprizone-Induced Demyelination. *The Journal of Neuroscience*, *34*(24), 8186. https://doi.org/10.1523/JNEUROSCI.4267-13.2014

Furukawa, H., Singh, S. K., Mancusso, R., & Gouaux, E. (2005). Subunit arrangement and function in NMDA receptors. *Nature*, *438*(7065), 185–192. https://doi.org/10.1038/nature04089

Gale, S.A., Acar, D., Daffner, K.R. (2018). Dementia. *Am J Med,* 131, 1161–1169. https://doi.org/10.1016/j.amjmed.2018.01.022

Gallagher, S. M., Daly, C. A., Bear, M. F., & Huber, K. M. (2004). Extracellular Signal-Regulated Protein Kinase Activation Is Required for Metabotropic Glutamate Receptor-Dependent Long-Term Depression in Hippocampal Area CA1. *The Journal of Neuroscience*, *24*(20), 4859–4864. https://doi.org/10.1523/JNEUROSCI.5407-03.2004

Games, D., Adams, D., Alessandrini, R., Barbour, R., Borthelette, P., Blackwell, C., Carr, T., Clemens, J., Donaldson, T., Gillespie, F., Guido, T., Hagopian, S., Johnson-Wood, K., Khan, K., Lee, M., Leibowitz, P., Lieberburg, I., Little, S., Masliah, E., … Zhao, J. (1995). Alzheimer-type neuropathology in transgenic mice overexpressing V717F ß-amyloid precursor protein. *Nature*, *373*(6514), 523–527. https://doi.org/10.1038/373523a0

Garbison, K. E., Heinz, B. A., & Lajiness, M. E. (2012). IP-3/IP-1 Assays. In Markossian S, Grossman A, & Brimacombe K (Eds.), *Assay Guidance Manual [Internet]*. Eli Lilly & Company and the National Center for Advancing Translational Sciences.

Gasparini, F., Lingenhöhl, K., Stoehr, N., Flor, P. J., Heinrich, M., Vranesic, I., Biollaz, M., Allgeier, H., Heckendorn, R., Urwyler, S., Varney, M. A., Johnson, E. C., Hess, S. D., Rao, S. P., Sacaan, A. I., Santori, E. M., Veliçelebi, G., & Kuhn, R. (1999). 2-Methyl-6-(phenylethynyl)-pyridine (MPEP), a potent, selective and systemically active mGlu5 receptor antagonist. *Neuropharmacology*, *38*(10), 1493–1503. https://doi.org/10.1016/S0028-3908(99)00082-9

Gasparini, F., Andres, H., Flor, P. J., Heinrich, M., Inderbitzin, W., Lingenhöhl, K., Müller, H., Munk, V. C., Omilusik, K., Stierlin, C., Stoehr, N., Vranesic, I., & Kuhn, R. (2002). [3H]-M-MPEP, a Potent, Subtype-Selective Radioligand for the Metabotropic Glutamate Receptor Subtype 5. *Bioorganic & Medicinal Chemistry Letters*, *12*(3), 407–409. https://doi.org/10.1016/S0960-894X(01)00767-3

Gautam, N., Downes, G. B., Yan, K., & Kisselev, O. (1998). The G-Protein βγ Complex. *Cellular Signalling*, *10*(7), 447–455. https://doi.org/10.1016/S0898-6568(98)00006-0

Gereau, R. W., & Heinemann, S. F. (1998). Role of Protein Kinase C Phosphorylation in Rapid Desensitization of Metabotropic Glutamate Receptor 5. *Neuron*, *20*(1), 143–151. https://doi.org/10.1016/S0896-6273(00)80442-0

Gerics, B., Szalay, F., & Hajos, F. (2006). Glial fibrillary acidic protein immunoreactivity in the rat suprachiasmatic nucleus: circadian changes and their seasonal dependence. *Journal of Anatomy*, *209*(2), 231–237. https://doi.org/10.1111/j.1469-7580.2006.00593.x

Gether, U. (2000). Uncovering Molecular Mechanisms Involved in Activation of G Protein-Coupled Receptors. *Endocrine Reviews*, *21*(1), 90–113. https://doi.org/10.1210/edrv.21.1.0390

Giese, A., Brown, D. R., Groschup, M. H., Feldmann, C., Haist, I., & Kretzschmar, H. A. (2006). Role of Microglia in Neuronal Cell Death in Prion Disease. *Brain Pathology*, *8*(3), 449–457. https://doi.org/10.1111/j.1750-3639.1998.tb00167.x

Gilman, A. G. (1987). G Proteins: Transducers of Receptor-Generated Signals. *Annual Review of Biochemistry*, *56*(1), 615–649. https://doi.org/10.1146/annurev.bi.56.070187.003151

Giribaldi, F., Milanese, M., Bonifacino, T., Anna Rossi, P. I., Di Prisco, S., Pittaluga, A., Tacchetti, C., Puliti, A., Usai, C., & Bonanno, G. (2013). Group I metabotropic glutamate autoreceptors induce abnormal glutamate exocytosis in

a mouse model of amyotrophic lateral sclerosis. *Neuropharmacology*, *66*, 253–263. https://doi.org/10.1016/J.NEUROPHARM.2012.05.018

Gispert, J. D., Suárez-Calvet, M., Monté, G. C., Tucholka, A., Falcon, C., Rojas, S., Rami, L., Sánchez-Valle, R., Lladó, A., Kleinberger, G., Haass, C., & Molinuevo, J. L. (2016). Cerebrospinal fluid sTREM2 levels are associated with gray matter volume increases and reduced diffusivity in early Alzheimer's disease. *Alzheimer's & Dementia*, *12*(12), 1259–1272. https://doi.org/10.1016/j.jalz.2016.06.005

Giunti, S., Andersen, N., Rayes, D., & De Rosa, M. J. (2021). Drug discovery: Insights from the invertebrate *Caenorhabditis elegans*. *Pharmacology Research & Perspectives*, *9*(2). https://doi.org/10.1002/prp2.721

Gloriam, D. E., Fredriksson, R., & Schiöth, H. B. (2007). The G protein-coupled receptor subset of the rat genome. *BMC Genomics*, *8*(1), 338. https://doi.org/10.1186/1471-2164-8-338

Gogos, A., Langmead, C., Sullivan, J. C., & Lawrence, A. J. (2019). The importance of sex differences in pharmacology research. *British Journal of Pharmacology*, *176*(21), 4087–4089. https://doi.org/10.1111/bph.14819

Gómez-Nicola, D., Fransen, N. L., Suzzi, S., & Perry, V. H. (2013). Regulation of Microglial Proliferation during Chronic Neurodegeneration. *The Journal of Neuroscience*, *33*(6), 2481–2493. https://doi.org/10.1523/JNEUROSCI.4440-12.2013

Gómez-Nicola, D., Schetters, S. T. T., & Perry, V. H. (2014). Differential role of CCR2 in the dynamics of microglia and perivascular macrophages during prion disease. *Glia*, *62*(7), 1041–1052. https://doi.org/10.1002/glia.22660

Gong, Y., Lippa, C. F., Zhu, J., Lin, Q., & Rosso, A. L. (2009). Disruption of glutamate receptors at Shank-postsynaptic platform in Alzheimer's disease. *Brain Research*, *1292*, 191–198. https://doi.org/10.1016/j.brainres.2009.07.056

Goniotaki, D., Lakkaraju, A. K. K., Shrivastava, A. N., Bakirci, P., Sorce, S., Senatore, A., Marpakwar, R., Hornemann, S., Gasparini, F., Triller, A., & Aguzzi, A. (2017). Inhibition of group-I metabotropic glutamate receptors protects against prion toxicity. *PLOS Pathogens*, *13*(11), e1006733. https://doi.org/10.1371/journal.ppat.1006733

Gorman, A. M. (2008). Neuronal cell death in neurodegenerative diseases: recurring themes around protein handling. *Journal of Cellular and Molecular Medicine*, *12*(6a), 2263–2280. https://doi.org/10.1111/j.1582-4934.2008.00402.x

Goodman, O. B., Krupnick, J. G., Santini, F., Gurevich, V. V., Penn, R. B., Gagnon, A. W., Keen, J. H., & Benovic, J. L. (1996). β-Arrestin acts as a clathrin adaptor in endocytosis of the β2-adrenergic receptor. *Nature*, *383*(6599), 447–450. https://doi.org/10.1038/383447a0

Götz, J., Streffer, J. R., David, D., Schild, A., Hoerndli, F., Pennanen, L., Kurosinski, P., & Chen, F. (2004). Transgenic animal models of Alzheimer's disease and related disorders: histopathology, behavior and therapy. *Molecular Psychiatry*, *9*(7), 664–683. https://doi.org/10.1038/sj.mp.4001508

Gray, L., van den Buuse, M., Scarr, E., Dean, B., & Hannan, A. J. (2009). Clozapine reverses schizophrenia-related behaviours in the metabotropic glutamate receptor 5 knockout mouse: association with N-methyl-d-aspartic acid receptor up-regulation. *The International Journal of Neuropsychopharmacology*, *12*(01), 45. https://doi.org/10.1017/S1461145708009085

Gray, M., Shirasaki, D. I., Cepeda, C., Andre, V. M., Wilburn, B., Lu, X.-H., Tao, J., Yamazaki, I., Li, S.-H., Sun, Y. E., Li, X.-J., Levine, M. S., & Yang, X. W. (2008). Full-Length Human Mutant Huntingtin with a Stable Polyglutamine Repeat Can Elicit Progressive and Selective Neuropathogenesis in BACHD Mice. *Journal of*

Neuroscience, *28*(24), 6182–6195. https://doi.org/10.1523/JNEUROSCI.0857-08.2008

Greenamyre, J. T., & Young, A. B. (1989). Excitatory amino acids and Alzheimer's disease. *Neurobiology of Aging*, *10*(5), 593–602. https://doi.org/10.1016/0197-4580(89)90143-7

Gregory, K. J., & Conn, P. J. (2015). Molecular Insights into Metabotropic Glutamate Receptor Allosteric Modulation. *Molecular Pharmacology*, *88*(1), 188–202. https://doi.org/10.1124/mol.114.097220

Gregory, K. J., Nguyen, E. D., Reiff, S. D., Squire, E. F., Stauffer, S. R., Lindsley, C. W., Meiler, J., & Conn, P. J. (2013). Probing the Metabotropic Glutamate Receptor 5 ($mGlu_5$) Positive Allosteric Modulator (PAM) Binding Pocket: Discovery of Point Mutations That Engender a "Molecular Switch" in PAM Pharmacology. *Molecular Pharmacology*, *83*(5), 991–1006. https://doi.org/10.1124/mol.112.083949

Gregory, K. J., Noetzel, M. J., Rook, J. M., Vinson, P. N., Stauffer, S. R., Rodriguez, A. L., Emmitte, K. A., Zhou, Y., Chun, A. C., Felts, A. S., Chauder, B. A., Lindsley, C. W., Niswender, C. M., & Conn, P. J. (2012). Investigating Metabotropic Glutamate Receptor 5 Allosteric Modulator Cooperativity, Affinity, and Agonism: Enriching Structure-Function Studies and Structure-Activity Relationships. *Molecular Pharmacology*, *82*(5), 860–875. https://doi.org/10.1124/mol.112.080531

Grizenkova, J., Akhtar, S., Brandner, S., Collinge, J., & Lloyd, S. E. (2014). Microglial Cx3cr1knockout reduces prion disease incubation time in mice. *BMC Neuroscience*, *15*(1), 44. https://doi.org/10.1186/1471-2202-15-44

Guimaraes, I. M., Carvalho, T. G., Ferguson, S. S., Pereira, G. S., & Ribeiro, F. M. (2015). The metabotropic glutamate receptor 5 role on motor behavior involves specific neural substrates. *Molecular Brain*, *8*(1), 24. https://doi.org/10.1186/s13041-015-0113-2

Guiroy, D. C., Wakayama, I., Liberski, P. P., & Gajdusek, D. C. (1994). Relationship of microglia and scrapie amyloid-immunoreactive plaques in kuru, Creutzfeldt-Jakob disease and Gerstmann-Strüßler syndrome. *Acta Neuropathologica*, *87*(5), 526–530. https://doi.org/10.1007/BF00294180

Gulyás, B., Sovago, J., Gomez-Mancilla, B., Jia, Z., Szigeti, C., Gulya, K., Schumacher, M., Maguire, R. P., Gasparini, F., & Halldin, C. (2015). Decrease of mGluR5 receptor density goes parallel with changes in enkephalin and substance P immunoreactivity in Huntington's disease: a preliminary investigation in the postmortem human brain. *Brain Structure and Function*, *220*(5), 3043–3051. https://doi.org/10.1007/S00429-014-0812-Y/FIGURES/4

Guo, F., Liu, X., Cai, H., & Le, W. (2018). Autophagy in neurodegenerative diseases: pathogenesis and therapy. *Brain Pathology*, *28*(1), 3–13. https://doi.org/10.1111/bpa.12545

Guo, J. P., Arai, T., Miklossy, J., & McGeer, P. L. (2006). Abeta and tau form soluble complexes that may promote self aggregation of both into the insoluble forms observed in Alzheimer's disease. *Proceedings of the National Academy of Sciences of the United States of America*, *103*(6), 1953–1958. https://doi.org/10.1073/PNAS.0509386103

Gurney, M. E., Pu, H., Chiu, A. Y., Dal Canto, M. C., Polchow, C. Y., Alexander, D. D., Caliendo, J., Hentati, A., Kwon, Y. W., Deng, H.-X., Chen, W., Zhai, P., Sufit, R. L., & Siddique, T. (1994). Motor Neuron Degeneration in Mice that Express a Human Cu,Zn Superoxide Dismutase Mutation. *Science*, *264*(5166), 1772–1775. https://doi.org/10.1126/science.8209258

Gustavsson, A., Norton, N., Fast, T., Frölich, L., Georges, J., Holzapfel, D., Kirabali, T., Krolak-Salmon, P., Rossini, P. M., Ferretti, M. T., Lanman, L., Chadha, A. S.,

& van der Flier, W. M. (2023). Global estimates on the number of persons across the Alzheimer's disease continuum. *Alzheimer's & Dementia*, *19*(2), 658–670. https://doi.org/10.1002/alz.12694

Gylys, K. H., Fein, J. A., Yang, F., Wiley, D. J., Miller, C. A., & Cole, G. M. (2004). Synaptic Changes in Alzheimer's Disease. *The American Journal of Pathology*, *165*(5), 1809–1817. https://doi.org/10.1016/S0002-9440(10)63436-0

Haas, L. T., Salazar, S. V., Kostylev, M. A., Um, J. W., Kaufman, A. C., & Strittmatter, S. M. (2016). Metabotropic glutamate receptor 5 couples cellular prion protein to intracellular signalling in Alzheimer's disease. *Brain*, *139*(2), 526–546. https://doi.org/10.1093/brain/awv356

Haas, L. T., Salazar, S. V., Smith, L. M., Zhao, H. R., Cox, T. O., Herber, C. S., Degnan, A. P., Balakrishnan, A., Macor, J. E., Albright, C. F., & Strittmatter, S. M. (2017). Silent Allosteric Modulation of mGluR5 Maintains Glutamate Signaling while Rescuing Alzheimer's Mouse Phenotypes. *Cell Reports*, *20*(1), 76–88. https://doi.org/10.1016/j.celrep.2017.06.023

Haas, L. T., & Strittmatter, S. M. (2016). Oligomers of Amyloid β Prevent Physiological Activation of the Cellular Prion Protein-Metabotropic Glutamate Receptor 5 Complex by Glutamate in Alzheimer Disease. *Journal of Biological Chemistry*, *291*(33), 17112–17121. https://doi.org/10.1074/jbc.M116.720664

Habib, N., McCabe, C., Medina, S., Varshavsky, M., Kitsberg, D., Dvir-Szternfeld, R., Green, G., Dionne, D., Nguyen, L., Marshall, J. L., Chen, F., Zhang, F., Kaplan, T., Regev, A., & Schwartz, M. (2020). Disease-associated astrocytes in Alzheimer's disease and aging. *Nature Neuroscience*, *23*(6), 701–706. https://doi.org/10.1038/s41593-020-0624-8

Hall, B., Mak, E., Cervenka, S., Aigbirhio, F. I., Rowe, J. B., & O'Brien, J. T. (2017). In vivo tau PET imaging in dementia: Pathophysiology, radiotracer quantification, and a systematic review of clinical findings. *Ageing Research Reviews*, *36*, 50–63. https://doi.org/10.1016/j.arr.2017.03.002

Halliday, M., & Mallucci, G. R. (2015). Review: Modulating the unfolded protein response to prevent neurodegeneration and enhance memory. *Neuropathology and Applied Neurobiology*, *41*(4), 414–427. https://doi.org/10.1111/nan.12211

Hamill, T. G., Krause, S., Ryan, C., Bonnefous, C., Govek, S., Seiders, T. J., Cosford, N. D. P., Roppe, J., Kamenecka, T., Patel, S., Gibson, R. E., Sanabria, S., Riffel, K., Eng, W., King, C., Yang, X., Green, M. D., O'malley, S. S., Hargreaves, R., & Burns, H. D. (2005). Synthesis, characterisation, and first successful monkey imaging studies of metabotropic glutamate receptor subtype 5 (mGluR5) PET radiotracers. *Synapse*, *56*(4), 205–216. https://doi.org/10.1002/syn.20147

Hamilton, A., Esseltine, J. L., Devries, R. A., Cregan, S. P., & Ferguson, S. S. G. (2014). Metabotropic glutamate receptor 5 knockout reduces cognitive impairment and pathogenesis in a mouse model of Alzheimer's disease. *Molecular Brain*, *7*(1). https://doi.org/10.1186/1756-6606-7-40

Hamilton, A., Vasefi, M., Vander Tuin, C., McQuaid, R. J., Anisman, H., & Ferguson, S. S. G. (2016). Chronic Pharmacological mGluR5 Inhibition Prevents Cognitive Impairment and Reduces Pathogenesis in an Alzheimer Disease Mouse Model. *Cell Reports*, *15*(9), 1859–1865. https://doi.org/10.1016/J.CELREP.2016.04.077

Hamm, H. E. (1998). The Many Faces of G Protein Signaling. *Journal of Biological Chemistry*, *273*(2), 669–672. https://doi.org/10.1074/jbc.273.2.669

Hampel, H., Hardy, J., Blennow, K., Chen, C., Perry, G., Kim, S. H., Villemagne, V. L., Aisen, P., Vendruscolo, M., Iwatsubo, T., Masters, C. L., Cho, M., Lannfelt, L., Cummings, J. L., & Vergallo, A. (2021). The Amyloid-β Pathway in Alzheimer's Disease. *Molecular Psychiatry 2021 26:10*, *26*(10), 5481–5503. https://doi.org/10.1038/s41380-021-01249-0

Han, J., Chitu, V., Stanley, E. R., Wszolek, Z. K., Karrenbauer, V. D., & Harris, R. A. (2022). Inhibition of colony stimulating factor-1 receptor (CSF-1R) as a potential therapeutic strategy for neurodegenerative diseases: opportunities and challenges. *Cellular and Molecular Life Sciences*, *79*(4), 219. https://doi.org/10.1007/s00018-022-04225-1

Hanisch, U. K., & Kettenmann, H. (2007). Microglia: active sensor and versatile effector cells in the normal and pathologic brain. *Nature Neuroscience*, *10*(11), 1387–1394. https://doi.org/10.1038/NN1997

Hardiman, O., Al-Chalabi, A., Chio, A., Corr, E. M., Logroscino, G., Robberecht, W., Shaw, P. J., Simmons, Z., & van den Berg, L. H. (2017). Amyotrophic lateral sclerosis. *Nature Reviews Disease Primers*, *3*(1), 17071. https://doi.org/10.1038/nrdp.2017.71

Harkany, T., Ábrahám, I., Timmerman, W., Laskay, G., Tóth, B., Sasvári, M., Kónya, C., Sebens, J. B., Korf, J., Nyakas, C., Zarándi, M., Soós, K., Penke, B., & Luiten, P. G. M. (2000). β-Amyloid neurotoxicity is mediated by a glutamate-triggered excitotoxic cascade in rat nucleus basalis. *European Journal of Neuroscience*, *12*(8), 2735–2745. https://doi.org/10.1046/j.1460-9568.2000.00164.x

Harkany, T., O'Mahony, S., Kelly, J. P., Soós, K., Törõ, I., Penke, B., Luiten, P. G. M., Nyakas, C., Gulya, K., & Leonard, B. E. (1998). β-Amyloid(Phe(SO3H)24)25–35 in rat nucleus basalis induces behavioral dysfunctions, impairs learning and memory and disrupts cortical cholinergic innervation. *Behavioural Brain Research*, *90*(2), 133–145. https://doi.org/10.1016/S0166-4328(97)00091-0

Hartigan, J. A., Xiong, W.-C., & Johnson, G. V. W. (2001). Glycogen Synthase Kinase 3β Is Tyrosine Phosphorylated by PYK2. *Biochemical and Biophysical Research Communications*, *284*(2), 485–489. https://doi.org/10.1006/bbrc.2001.4986

Hartmann, K., Sepulveda-Falla, D., Rose, I. V. L., Madore, C., Muth, C., Matschke, J., Butovsky, O., Liddelow, S., Glatzel, M., & Krasemann, S. (2019). Complement 3+-astrocytes are highly abundant in prion diseases, but their abolishment led to an accelerated disease course and early dysregulation of microglia. *Acta Neuropathologica Communications*, *7*(1), 83. https://doi.org/10.1186/s40478-019-0735-1

Hasel, P., & Liddelow, S. A. (2021). Astrocytes. *Current Biology*, *31*(7), R326–R327. https://doi.org/10.1016/J.CUB.2021.01.056

Hauser, A. S., Attwood, M. M., Rask-Andersen, M., Schiöth, H. B., & Gloriam, D. E. (2017). Trends in GPCR drug discovery: new agents, targets and indications. *Nature Reviews Drug Discovery*, *16*(12), 829–842. https://doi.org/10.1038/nrd.2017.178

Heemskerk, A.-W., & Roos, R. A. C. (2011). Dysphagia in Huntington's Disease: A Review. *Dysphagia*, *26*(1), 62–66. https://doi.org/10.1007/s00455-010-9302-4

Heneka, M. T., O'Banion, M. K., Terwel, D., & Kummer, M. P. (2010). Neuroinflammatory processes in Alzheimer's disease. *Journal of Neural Transmission (Vienna, Austria : 1996)*, *117*(8), 919–947. https://doi.org/10.1007/S00702-010-0438-Z

Hentosh, S., Zhu, L., Patino, J., Furr, J. W., Rocha, N. P., & Furr Stimming, E. (2021). Sex Differences in Huntington's Disease: Evaluating the <scp>Enroll-HD</scp> Database. *Movement Disorders Clinical Practice*, *8*(3), 420–426. https://doi.org/10.1002/mdc3.13178

Hermans, E., Young, K. W., Challiss, R. A. J., & Nahorski, S. R. (2002). Effects of Human Type 1α Metabotropic Glutamate Receptor Expression Level on Phosphoinositide and Ca2+ Signalling in an Inducible Cell Expression System. *Journal of Neurochemistry*, *70*(4), 1772–1775. https://doi.org/10.1046/j.1471-4159.1998.70041772.x

Hermans, E. (2003). Biochemical and pharmacological control of the multiplicity of coupling at G-protein-coupled receptors. *Pharmacology & Therapeutics*, *99*(1), 25–44. https://doi.org/10.1016/S0163-7258(03)00051-2

Hermans, E., & Challiss, R. A. J. (2001). Structural, signalling and regulatory properties of the group I metabotropic glutamate receptors: prototypic family C G-protein-coupled receptors. *Biochemical Journal*, *359*(3), 465. https://doi.org/10.1042/0264-6021:3590465

Hernandez, C. M., McQuail, J. A., Schwabe, M. R., Burke, S. N., Setlow, B., & Bizon, J. L. (2018). Age-Related Declines in Prefrontal Cortical Expression of Metabotropic Glutamate Receptors that Support Working Memory. *Eneuro*, *5*(3), ENEURO.0164-18.2018. https://doi.org/10.1523/ENEURO.0164-18.2018

Hewavitharana, T., & Wedegaertner, P. B. (2012). Non-canonical signaling and localizations of heterotrimeric G proteins. *Cellular Signalling*, *24*(1), 25–34. https://doi.org/10.1016/j.cellsig.2011.08.014

Higgins, G.A., Olschowka, J.A. (1991). Induction of interleukin-1β mRNA in adult rat brain. *Molecular Brain Research,* 9, 143–148. https://doi.org/10.1016/0169-328X(91)90139-O

Hill, A. F., Desbruslais, M., Joiner, S., Sidle, K. C. L., Gowland, I., Collinge, J., Doey, L. J., & Lantos, P. (1997). The same prion strain causes vCJD and BSE. *Nature*, *389*(6650), 448–450. https://doi.org/10.1038/38925

Hoffner, G., Island, M.-L., & Djian, P. (2005). Purification of neuronal inclusions of patients with Huntington's disease reveals a broad range of N-terminal fragments of expanded huntingtin and insoluble polymers. *Journal of Neurochemistry*, *95*(1), 125–136. https://doi.org/10.1111/j.1471-4159.2005.03348.x

Hol, E. M., & Pekny, M. (2015). Glial fibrillary acidic protein (GFAP) and the astrocyte intermediate filament system in diseases of the central nervous system. *Current Opinion in Cell Biology*, *32*, 121–130. https://doi.org/10.1016/j.ceb.2015.02.004

Holter, K. M., Lekander, A. D., LaValley, C. M., Bedingham, E. G., Pierce, B. E., Sands, L. P., Lindsley, C. W., Jones, C. K., & Gould, R. W. (2021). Partial mGlu5 Negative Allosteric Modulator M-5MPEP Demonstrates Antidepressant-Like Effects on Sleep Without Affecting Cognition or Quantitative EEG. *Frontiers in Neuroscience*, *15*. https://doi.org/10.3389/fnins.2021.700822

Holst, S. C., Sousek, A., Hefti, K., Saberi-Moghadam, S., Buck, A., Ametamey, S. M., Scheidegger, M., Franken, P., Henning, A., Seifritz, E., Tafti, M., & Landolt, H.-P. (2017). Cerebral mGluR5 availability contributes to elevated sleep need and behavioral adjustment after sleep deprivation. *ELife*, *6*. https://doi.org/10.7554/eLife.28751

Homayoun, H., Stefani, M. R., Adams, B. W., Tamagan, G. D., & Moghaddam, B. (2004). Functional Interaction Between NMDA and mGlu5 Receptors: Effects on Working Memory, Instrumental Learning, Motor Behaviors, and Dopamine Release. *Neuropsychopharmacology*, *29*(7), 1259–1269. https://doi.org/10.1038/sj.npp.1300417

Hopkins, A. L., & Groom, C. R. (2002). The druggable genome. *Nature Reviews Drug Discovery*, *1*(9), 727–730. https://doi.org/10.1038/nrd892

Hou, L., & Klann, E. (2004). Activation of the Phosphoinositide 3-Kinase-Akt-Mammalian Target of Rapamycin Signaling Pathway Is Required for Metabotropic Glutamate Receptor-Dependent Long-Term Depression. *The Journal of Neuroscience*, *24*(28), 6352–6361. https://doi.org/10.1523/JNEUROSCI.0995-04.2004

Hou, X., Hayashi, R., Itoh, M., & Tonoki, A. (2023). Small-molecule screening in aged *Drosophila* identifies mGluR as a regulator of age-related sleep impairment. *Sleep*. https://doi.org/10.1093/sleep/zsad018

Hsia, J. A., Moss, J., Hewlett, E. L., & Vaughan, M. (1984). ADP-ribosylation of adenylate cyclase by pertussis toxin. Effects on inhibitory agonist binding. *The Journal of Biological Chemistry*, *259*(2), 1086–1090.

Hsiao, K., Chapman, P., Nilsen, S., Eckman, C., Harigaya, Y., Younkin, S., Yang, F., & Cole, G. (1996). Correlative Memory Deficits, Aß Elevation, and Amyloid Plaques in Transgenic Mice. *Science*, *274*(5284), 99–103. https://doi.org/10.1126/science.274.5284.99

Hu, C., Chen, C., Xia, Y., Chen, J., Yang, W., Wang, L., Chen, D.-D., Wu, Y.-Z., Fan, Q., Jia, X.-X., Xiao, K., Shi, Q., Chen, Z.-B., & Dong, X.-P. (2022). Different Aberrant Changes of mGluR5 and Its Downstream Signaling Pathways in the Scrapie-Infected Cell Line and the Brains of Scrapie-Infected Experimental Rodents. *Frontiers in Cell and Developmental Biology*, *10*. https://doi.org/10.3389/fcell.2022.844378

Huang, H., Degnan, A. P., Balakrishnan, A., Easton, A., Gulianello, M., Huang, Y., Matchett, M., Mattson, G., Miller, R., Santone, K. S., Senapati, A., Shields, E. E., Sivarao, D. V., Snyder, L. B., Westphal, R., Whiterock, V. J., Yang, F., Bronson, J. J., & Macor, J. E. (2016). Oxazolidinone-based allosteric modulators of mGluR5: Defining molecular switches to create a pharmacological tool box. *Bioorganic & Medicinal Chemistry Letters*, *26*(17), 4165–4169. https://doi.org/10.1016/J.BMCL.2016.07.065

Huang, H., & van den Pol, A. N. (2007). Rapid Direct Excitation and Long-Lasting Enhancement of NMDA Response by Group I Metabotropic Glutamate Receptor Activation of Hypothalamic Melanin-Concentrating Hormone Neurons. *The Journal of Neuroscience*, *27*(43), 11560–11572. https://doi.org/10.1523/JNEUROSCI.2147-07.2007

Hubert, G. W., Paquet, M., & Smith, Y. (2001). Differential Subcellular Localization of mGluR1a and mGluR5 in the Rat and Monkey Substantia Nigra. *The Journal of Neuroscience*, *21*(6), 1838–1847. https://doi.org/10.1523/JNEUROSCI.21-06-01838.2001

Hughes, J., Rees, S., Kalindjian, S., Philpott, K., 2011. Principles of early drug discovery. Br J Pharmacol 162, 1239–1249. https://doi.org/10.1111/j.1476-5381.2010.01127.x

Hughes, M. M., Field, R. H., Perry, V. H., Murray, C. L., & Cunningham, C. (2010). Microglia in the degenerating brain are capable of phagocytosis of beads and of apoptotic cells, but do not efficiently remove PrPSc, even upon LPS stimulation. *Glia*, *58*(16), 2017–2030. https://doi.org/10.1002/glia.21070

Husain, M. (2017). Transdiagnostic neurology: neuropsychiatric symptoms in neurodegenerative diseases. *Brain*, *140*(6), 1535–1536. https://doi.org/10.1093/BRAIN/AWX115

Iaccarino, H. F., Singer, A. C., Martorell, A. J., Rudenko, A., Gao, F., Gillingham, T. Z., Mathys, H., Seo, J., Kritskiy, O., Abdurrob, F., Adaikkan, C., Canter, R. G., Rueda, R., Brown, E. N., Boyden, E. S., & Tsai, L.-H. (2016). Gamma frequency entrainment attenuates amyloid load and modifies microglia. *Nature*, *540*(7632), 230–235. https://doi.org/10.1038/nature20587

Ikeda, K., Akiyama, H., Kondo, H., Haga, C., Tanno, E., Tokuda, T., & Ikeda, S. (1995). Thorn-shaped astrocytes: possibly secondarily induced tau-positive glial fibrillary tangles. *Acta Neuropathologica 1995 90:6*, *90*(6), 620–625. https://doi.org/10.1007/BF00318575

Ikeda, S. R. (1996). Voltage-dependent modulation of N-type calcium channels by G-protein β γsubunits. *Nature*, *380*(6571), 255–258. https://doi.org/10.1038/380255a0

Illenberger, D., Walliser, C., Nürnberg, B., Lorente, M. D., & Gierschik, P. (2003). Specificity and Structural Requirements of Phospholipase C-β Stimulation by Rho GTPases Versus G Protein βγ Dimers. *Journal of Biological Chemistry*, *278*(5), 3006–3014. https://doi.org/10.1074/jbc.M208282200

Imai, Y., Ibata, I., Ito, D., Ohsawa, K., & Kohsaka, S. (1996). A Novel Geneiba1in the Major Histocompatibility Complex Class III Region Encoding an EF Hand Protein Expressed in a Monocytic Lineage. *Biochemical and Biophysical Research Communications*, *224*(3), 855–862. https://doi.org/10.1006/bbrc.1996.1112

Inta, D., Vogt, M.A., Luoni, A., Filipović, D., Lima-Ojeda, J.M., Pfeiffer, N., Gasparini, F., Riva, M.A., Gass, P. (2013). Significant increase in anxiety during aging in mGlu5 receptor knockout mice. *Behavioural Brain Research,* 241, 27–31. https://doi.org/10.1016/j.bbr.2012.11.042

Ishijima, T., & Nakajima, K. (2021). Inflammatory cytokines TNFα, IL-1β, and IL-6 are induced in endotoxin- stimulated microglia through different signaling cascades. *Science Progress*, *104*(4), 003685042110549. https://doi.org/10.1177/00368504211054985

Jacob, C. P., Koutsilieri, E., Bartl, J., Neuen-Jacob, E., Arzberger, T., Zander, N., Ravid, R., Roggendorf, W., Riederer, P., & Grünblatt, E. (2007). Alterations in expression of glutamatergic transporters and receptors in sporadic Alzheimer's disease. *Journal of Alzheimer's Disease: JAD*, *11*(1), 97–116. https://doi.org/10.3233/JAD-2007-11113

Jakob, A. (1989). Concerning a disorder of the central nervous system clinically resembling multiple sclerosis with remarkable anatomic findings (spastic pseudosclerosis). Report of a fourth case. *Alzheimer Disease and Associated Disorders*, *3*(1–2), 26–45.

Jankovska, N., Rusina, R., Bruzova, M., Parobkova, E., Olejar, T., & Matej, R. (2021). Human Prion Disorders: Review of the Current Literature and a Twenty-Year Experience of the National Surveillance Center in the Czech Republic. *Diagnostics*, *11*(10), 1821. https://doi.org/10.3390/diagnostics11101821

Jean, Y. Y., Lercher, L. D., & Dreyfus, C. F. (2008). Glutamate elicits release of BDNF from basal forebrain astrocytes in a process dependent on metabotropic receptors and the PLC pathway. *Neuron Glia Biology*, *4*(1), 35–42. https://doi.org/10.1017/S1740925X09000052

Jerónimo-Santos, A., Vaz, S. H., Parreira, S., Rapaz-Lérias, S., Caetano, A. P., Buée-Scherrer, V., Castrén, E., Valente, C. A., Blum, D., Sebastião, A. M., & Diógenes, M. J. (2015). Dysregulation of TrkB Receptors and BDNF Function by Amyloid-β Peptide is Mediated by Calpain. *Cerebral Cortex*, *25*(9), 3107–3121. https://doi.org/10.1093/cercor/bhu105

Jew, C.P., Wu, C.-S., Sun, H., Zhu, J., Huang, J.-Y., Yu, D., Justice, N.J., Lu, H.-C. (2013). mGluR5 Ablation in Cortical Glutamatergic Neurons Increases Novelty-Induced Locomotion. *PLoS One,* 8, e70415. https://doi.org/10.1371/journal.pone.0070415

Jing, R., Wilhelmsson, U., Goodwill, W., Li, L., Pan, Y., Pekny, M., & Skalli, O. (2007). Synemin is expressed in reactive astrocytes in neurotrauma and interacts differentially with vimentin and GFAP intermediate filament networks. *Journal of Cell Science*, *120*(7), 1267–1277. https://doi.org/10.1242/jcs.03423

Johansen, J., Rosenblad, C., Andsberg, K., Møller, A., Lundberg, C., Björlund, A., & Johansen, T. E. (2002). Evaluation of Tet-on system to avoid transgene down-regulation in ex vivo gene transfer to the CNS. *Gene Therapy*, *9*(19), 1291–1301. https://doi.org/10.1038/sj.gt.3301778

Johnson, J. W., & Ascher, P. (1987). Glycine potentiates the NMDA response in cultured mouse brain neurons. *Nature*, *325*(6104), 529–531. https://doi.org/10.1038/325529a0

Joly, C., Gomeza, J., Brabet, I., Curry, K., Bockaert, J., & Pin, J. (1995). Molecular, functional, and pharmacological characterization of the metabotropic glutamate receptor type 5 splice variants: comparison with mGluR1. *The Journal of Neuroscience*, *15*(5), 3970–3981. https://doi.org/10.1523/JNEUROSCI.15-05-03970.1995

Jones, M. W., Errington, M. L., French, P. J., Fine, A., Bliss, T. V. P., Garel, S., Charnay, P., Bozon, B., Laroche, S., & Davis, S. (2001). A requirement for the immediate early gene Zif268 in the expression of late LTP and long-term memories. *Nature Neuroscience*, *4*(3), 289–296. https://doi.org/10.1038/85138

Jong, Y.-J. I., Kumar, V., Kingston, A. E., Romano, C., & O'Malley, K. L. (2005). Functional Metabotropic Glutamate Receptors on Nuclei from Brain and Primary Cultured Striatal Neurons. *Journal of Biological Chemistry*, *280*(34), 30469–30480. https://doi.org/10.1074/jbc.M501775200

Jong, Y.-J. I., Kumar, V., & O'Malley, K. L. (2009). Intracellular Metabotropic Glutamate Receptor 5 (mGluR5) Activates Signaling Cascades Distinct from Cell Surface Counterparts. *Journal of Biological Chemistry*, *284*(51), 35827–35838. https://doi.org/10.1074/jbc.M109.046276

Jong, Y.-J. I., Sergin, I., Purgert, C. A., & O'Malley, K. L. (2014). Location-Dependent Signaling of the Group 1 Metabotropic Glutamate Receptor mGlu5. *Molecular Pharmacology*, *86*(6), 774–785. https://doi.org/10.1124/mol.114.094763

Jucker, M., & Walker, L. C. (2011). Pathogenic protein seeding in alzheimer disease and other neurodegenerative disorders. *Annals of Neurology*, *70*(4), 532–540. https://doi.org/10.1002/ana.22615

Jung K. M., Astarita G., Zhu C., Wallace M., Mackie K., Piomelli D. (2007). A key role for diacylglycerol lipase-alpha in metabotropic glutamate receptor-dependent endocannabinoid mobilization. *Mol Pharmacol*. Sep;72(3):612-21. doi: 10.1124/mol.107.037796.

Jung K. M., Sepers M., Henstridge C. M., Lassalle O., Neuhofer D., Martin H., Ginger M., Frick A., DiPatrizio N. V., Mackie K., Katona I., Piomelli D., Manzoni O.J. (2012). Uncoupling of the endocannabinoid signalling complex in a mouse model of fragile X syndrome. *Nat Commun*. 3:1080. doi: 10.1038/ncomms2045.

Kågedal, M., Cselényi, Z., Nyberg, S., Raboisson, P., Ståhle, L., Stenkrona, P., Varnäs, K., Halldin, C., Hooker, A. C., & Karlsson, M. O. (2013). A positron emission tomography study in healthy volunteers to estimate mGluR5 receptor occupancy of AZD2066 — Estimating occupancy in the absence of a reference region. *NeuroImage*, *82*, 160–169. https://doi.org/10.1016/j.neuroimage.2013.05.006

Kaltenbach, L. S., Romero, E., Becklin, R. R., Chettier, R., Bell, R., Phansalkar, A., Strand, A., Torcassi, C., Savage, J., Hurlburt, A., Cha, G.-H., Ukani, L., Chepanoske, C. Lou, Zhen, Y., Sahasrabudhe, S., Olson, J., Kurschner, C., Ellerby, L. M., Peltier, J. M., … Hughes, R. E. (2007). Huntingtin Interacting Proteins Are Genetic Modifiers of Neurodegeneration. *PLoS Genetics*, *3*(5), e82. https://doi.org/10.1371/journal.pgen.0030082

Kamato, D., Thach, L., Bernard, R., Chan, V., Zheng, W., Kaur, H., Brimble, M., Osman, N., & Little, P. J. (2015). Structure, Function, Pharmacology, and Therapeutic Potential of the G Protein, GÎ±/q,11. *Frontiers in Cardiovascular Medicine*, *2*. https://doi.org/10.3389/fcvm.2015.00014

Kaminski, B. J., Duke, A. N., & Weerts, E. M. (2012). Effects of naltrexone on alcohol drinking patterns and extinction of alcohol seeking in baboons. *Psychopharmacology*, *223*(1), 55–66. https://doi.org/10.1007/s00213-012-2688-y

Kandel, E. R. (2012). The molecular biology of memory: cAMP, PKA, CRE, CREB-1, CREB-2, and CPEB. *Molecular Brain*, *5*(1), 14. https://doi.org/10.1186/1756-6606-5-14

Kang, K., Lee, S.-W., Han, J. E., Choi, J. W., & Song, M.-R. (2014). The complex morphology of reactive astrocytes controlled by fibroblast growth factor signaling. *Glia*, *62*(8), 1328–1344. https://doi.org/10.1002/glia.22684

Kano M., Ohno-Shosaku T., Hashimotodani Y., Uchigashima M., Watanabe M. (2009). Endocannabinoid-mediated control of synaptic transmission. *Physiol Rev*. 89(1):309-80. doi: 10.1152/physrev.00019.2008.

Karageorgos, V., Venihaki, M., Sakellaris, S., Pardalos, M., Kontakis, G., Matsoukas, M.-T., Gravanis, A., Margioris, A., & Liapakis, G. (2018). Current understanding of the structure and function of family B GPCRs to design novel drugs. *Hormones*, *17*(1), 45–59. https://doi.org/10.1007/s42000-018-0009-5

Karch, C. M., & Goate, A. M. (2015). Alzheimer's disease risk genes and mechanisms of disease pathogenesis. *Biological Psychiatry*, *77*(1), 43. https://doi.org/10.1016/J.BIOPSYCH.2014.05.006

Karp, N. A., & Reavey, N. (2019). Sex bias in preclinical research and an exploration of how to change the status quo. *British Journal of Pharmacology*, *176*(21), 4107–4118. https://doi.org/10.1111/bph.14539

Katona I., Urbán G.M., Wallace M., Ledent C., Jung K.M., Piomelli D., Mackie K., Freund T.F. (2006). Molecular composition of the endocannabinoid system at glutamatergic synapses. *J Neurosci*. 24;26(21):5628-37. doi: 10.1523/JNEUROSCI.0309-06.2006.

Kaushal, A., Wani, W. Y., Anand, R., & Gill, K. D. (2013). Spontaneous and Induced Nontransgenic Animal Models of AD. *American Journal of Alzheimer's Disease & Other Dementiasr*, *28*(4), 318–326. https://doi.org/10.1177/1533317513488914

Kawabata, S., Tsutsumi, R., Kohara, A., Yamaguchi, T., Nakanishi, S., & Okada, M. (1996). Control of calcium oscillations by phosphorylation of metabotropic glutamate receptors. *Nature*, *383*(6595), 89–92. https://doi.org/10.1038/383089a0

Kayed, R., & Lasagna-Reeves, C. A. (2013). Molecular mechanisms of amyloid oligomers toxicity. *Journal of Alzheimer's Disease : JAD*, *33 Suppl 1*(SUPPL. 1). https://doi.org/10.3233/JAD-2012-129001

Kenakin, T. (2002). Efficacy at g-protein-coupled receptors. *Nature Reviews Drug Discovery*, *1*(2), 103–110. https://doi.org/10.1038/nrd722

Kercher, L., Favara, C., Striebel, J. F., LaCasse, R., & Chesebro, B. (2007). Prion Protein Expression Differences in Microglia and Astroglia Influence Scrapie-Induced Neurodegeneration in the Retina and Brain of Transgenic Mice. *Journal of Virology*, *81*(19), 10340–10351. https://doi.org/10.1128/JVI.00865-07

Kilian, J. G., Hsu, H. W., Mata, K., Wolf, F. W., & Kitazawa, M. (2017). Astrocyte transport of glutamate and neuronal activity reciprocally modulate tau pathology in Drosophila. *Neuroscience*, *348*, 191–200. https://doi.org/10.1016/J.NEUROSCIENCE.2017.02.011

Kinney, G.G., Burno, M., Campbell, U.C., Hernandez, L.M., Rodriguez, D., Bristow, L.J., Conn, P.J., 2003. Metabotropic Glutamate Subtype 5 Receptors Modulate Locomotor Activity and Sensorimotor Gating in Rodents. Journal of Pharmacology and Experimental Therapeutics 306, 116–123. https://doi.org/10.1124/jpet.103.048702

Kinney, G. G., O'Brien, J. A., Lemaire, W., Burno, M., Bickel, D. J., Clements, M. K., Chen, T.-B., Wisnoski, D. D., Lindsley, C. W., Tiller, P. R., Smith, S., Jacobson,

M. A., Sur, C., Duggan, M. E., Pettibone, D. J., Conn, P. J., & Williams, D. L. (2005). A Novel Selective Positive Allosteric Modulator of Metabotropic Glutamate Receptor Subtype 5 Has in Vivo Activity and Antipsychotic-Like Effects in Rat Behavioral Models. *Journal of Pharmacology and Experimental Therapeutics*, *313*(1), 199–206. https://doi.org/10.1124/jpet.104.079244

Kino, Y., Washizu, C., Kurosawa, M., Yamada, M., Miyazaki, H., Akagi, T., Hashikawa, T., Doi, H., Takumi, T., Hicks, G. G., Hattori, N., Shimogori, T., & Nukina, N. (2015). FUS/TLS deficiency causes behavioral and pathological abnormalities distinct from amyotrophic lateral sclerosis. *Acta Neuropathologica Communications*, *3*(1), 24. https://doi.org/10.1186/s40478-015-0202-6

Kirby, J., Al Sultan, A., Waller, R., & Heath, P. (2016). The genetics of amyotrophic lateral sclerosis: current insights. *Degenerative Neurological and Neuromuscular Disease*, 49. https://doi.org/10.2147/DNND.S84956

Kistner, A., Gossen, M., Zimmermann, F., Jerecic, J., Ullmer, C., Lübbert, H., & Bujard, H. (1996). Doxycycline-mediated quantitative and tissue-specific control of gene expression in transgenic mice. *Proceedings of the National Academy of Sciences*, *93*(20), 10933–10938. https://doi.org/10.1073/pnas.93.20.10933

Kiyota, T., Machhi, J., Lu, Y., Dyavarshetty, B., Nemati, M., Yokoyama, I., Mosley, R. L., & Gendelman, H. E. (2018). Granulocyte-macrophage colony-stimulating factor neuroprotective activities in Alzheimer's disease mice. *Journal of Neuroimmunology*, *319*, 80–92. https://doi.org/10.1016/j.jneuroim.2018.03.009

Kniazeff, J., Bessis, A.-S., Maurel, D., Ansanay, H., Prézeau, L., & Pin, J.-P. (2004). Closed state of both binding domains of homodimeric mGlu receptors is required for full activity. *Nature Structural & Molecular Biology*, *11*(8), 706–713. https://doi.org/10.1038/nsmb794

Knopman, D. S., Amieva, H., Petersen, R. C., Chételat, G., Holtzman, D. M., Hyman, B. T., Nixon, R. A., & Jones, D. T. (2021). Alzheimer disease. *Nature Reviews Disease Primers*, *7*(1), 33. https://doi.org/10.1038/s41572-021-00269-y

Koehl, A., Hu, H., Feng, D., Sun, B., Zhang, Y., Robertson, M. J., Chu, M., Kobilka, T. S., Laeremans, T., Steyaert, J., Tarrasch, J., Dutta, S., Fonseca, R., Weis, W. I., Mathiesen, J. M., Skiniotis, G., & Kobilka, B. K. (2019). Structural insights into the activation of metabotropic glutamate receptors. *Nature*, *566*(7742), 79–84. https://doi.org/10.1038/s41586-019-0881-4

Koffie, R. M., Meyer-Luehmann, M., Hashimoto, T., Adams, K. W., Mielke, M. L., Garcia-Alloza, M., Micheva, K. D., Smith, S. J., Kim, M. L., Lee, V. M., Hyman, B. T., & Spires-Jones, T. L. (2009). Oligomeric amyloid β associates with postsynaptic densities and correlates with excitatory synapse loss near senile plaques. *Proceedings of the National Academy of Sciences*, *106*(10), 4012–4017. https://doi.org/10.1073/pnas.0811698106

Kofuji, P., & Araque, A. (2021). G-Protein-Coupled Receptors in Astrocyte–Neuron Communication. *Neuroscience*, *456*, 71–84. https://doi.org/10.1016/j.neuroscience.2020.03.025

Kordek, R., Nerurkar, V. R., Liberski, P. P., Isaacson, S., Yanagihara, R., & Gajdusek, D. C. (1996). Heightened expression of tumor necrosis factor alpha, interleukin 1 alpha, and glial fibrillary acidic protein in experimental Creutzfeldt-Jakob disease in mice. *Proceedings of the National Academy of Sciences*, *93*(18), 9754–9758. https://doi.org/10.1073/pnas.93.18.9754

Kranich, J., Krautler, N. J., Falsig, J., Ballmer, B., Li, S., Hutter, G., Schwarz, P., Moos, R., Julius, C., Miele, G., & Aguzzi, A. (2010). Engulfment of cerebral apoptotic bodies controls the course of prion disease in a mouse strain-dependent manner. *Journal of Experimental Medicine*, *207*(10), 2271–2281. https://doi.org/10.1084/jem.20092401

Krejciova, Z., Alibhai, J., Zhao, C., Krencik, R., Rzechorzek, N. M., Ullian, E. M., Manson, J., Ironside, J. W., Head, M. W., & Chandran, S. (2017). Human stem cell–derived astrocytes replicate human prions in a PRNP genotype–dependent manner. *Journal of Experimental Medicine*, *214*(12), 3481–3495. https://doi.org/10.1084/jem.20161547

Kos, C.H. (2004). Cre/loxP System for Generating Tissue-specific Knockout Mouse Models. *Nutr Rev*, 62, 243–246. https://doi.org/10.1301/nr2004.jun243-246

Kuemmerle, S., Gutekunst, C. A., Klein, A. M., Li, X. J., Li, S. H., Beal, M. F., Hersch, S. M., & Ferrante, R. J. (1999). Huntington aggregates may not predict neuronal death in Huntington's disease. *Annals of Neurology*, *46*(6), 842–849.

Kullmann, D. M., & Lamsa, K. P. (2007). Long-term synaptic plasticity in hippocampal interneurons. *Nature Reviews Neuroscience*, *8*(9), 687–699. https://doi.org/10.1038/nrn2207

Kumar, A., Dhull, D. K., & Mishra, P. S. (2015). Therapeutic potential of mGluR5 targeting in Alzheimer's disease. *Frontiers in Neuroscience*, *9*(JUN), 1–9. https://doi.org/10.3389/fnins.2015.00215

Kumar, A., Fontana, I. C., & Nordberg, A. (2023). Reactive astrogliosis: A friend or foe in the pathogenesis of Alzheimer's disease. *Journal of Neurochemistry*, *164*(3), 309–324. https://doi.org/10.1111/JNC.15565

Kumar, V., Fahey, P. G., Jong, Y.-J. I., Ramanan, N., & O'Malley, K. L. (2012). Activation of Intracellular Metabotropic Glutamate Receptor 5 in Striatal Neurons Leads to Up-regulation of Genes Associated with Sustained Synaptic Transmission Including Arc/Arg3.1 Protein. *Journal of Biological Chemistry*, *287*(8), 5412–5425. https://doi.org/10.1074/jbc.M111.301366

Kumar, V., Jong, Y. J. I., & O'Malley, K. L. (2008). Activated nuclear metabotropic glutamate receptor mGlu5 couples to nuclear Gq/11 proteins to generate inositol 1,4,5-trisphosphate-mediated nuclear Ca2+ release. *The Journal of Biological Chemistry*, *283*(20), 14072–14083. https://doi.org/10.1074/JBC.M708551200

Kunishima, N., Shimada, Y., Tsuji, Y., Sato, T., Yamamoto, M., Kumasaka, T., Nakanishi, S., Jingami, H., & Morikawa, K. (2000). Structural basis of glutamate recognition by a dimeric metabotropic glutamate receptor. *Nature*, *407*(6807), 971–977. https://doi.org/10.1038/35039564

Kwiatkowski, T. J., Bosco, D. A., LeClerc, A. L., Tamrazian, E., Vanderburg, C. R., Russ, C., Davis, A., Gilchrist, J., Kasarskis, E. J., Munsat, T., Valdmanis, P., Rouleau, G. A., Hosler, B. A., Cortelli, P., de Jong, P. J., Yoshinaga, Y., Haines, J. L., Pericak-Vance, M. A., Yan, J., … Brown, R. H. (2009). Mutations in the *FUS/TLS* Gene on Chromosome 16 Cause Familial Amyotrophic Lateral Sclerosis. *Science*, *323*(5918), 1205–1208. https://doi.org/10.1126/science.1166066

Lacomblez, L., Bensimon, G., Meininger, V., Leigh, P. N., & Guillet, P. (1996). Dose-ranging study of riluzole in amyotrophic lateral sclerosis. *The Lancet*, *347*(9013), 1425–1431. https://doi.org/10.1016/S0140-6736(96)91680-3

Lacor, P. N., Buniel, M. C., Furlow, P. W., Sanz Clemente, A., Velasco, P. T., Wood, M., Viola, K. L., & Klein, W. L. (2007). Aß Oligomer-Induced Aberrations in Synapse Composition, Shape, and Density Provide a Molecular Basis for Loss of Connectivity in Alzheimer's Disease. *The Journal of Neuroscience*, *27*(4), 796–807. https://doi.org/10.1523/JNEUROSCI.3501-06.2007

LaCrosse, A. L., Burrows, B. T., Angulo, R. M., Conrad, P. R., Himes, S. M., Mathews, N., Wegner, S. A., Taylor, S. B., & Olive, M. F. (2015). mGluR5 positive allosteric modulation and its effects on MK-801 induced set-shifting impairments in a rat operant delayed matching/non-matching-to-sample task. *Psychopharmacology*, *232*(1), 251–258. https://doi.org/10.1007/s00213-014-3653-8

LaFerla, F. M., & Green, K. N. (2012). Animal Models of Alzheimer Disease. *Cold Spring Harbor Perspectives in Medicine*, *2*(11), a006320–a006320. https://doi.org/10.1101/cshperspect.a006320

LaGanke, C., Samkoff, L., Edwards, K., Jung Henson, L., Repovic, P., Lynch, S., Stone, L., Mattson, D., Galluzzi, A., Fisher, T. L., Reilly, C., Winter, L. A., Leonard, J. E., & Zauderer, M. (2017). Safety/tolerability of the anti-semaphorin 4D antibody VX15/2503 in a randomized phase 1 trial. *Neurology - Neuroimmunology Neuroinflammation*, *4*(4), e367. https://doi.org/10.1212/NXI.0000000000000367

Lagerström, M. C., & Schiöth, H. B. (2008). Structural diversity of G protein-coupled receptors and significance for drug discovery. *Nature Reviews Drug Discovery*, *7*(4), 339–357. https://doi.org/10.1038/nrd2518

Lagier-Tourenne, C., Polymenidou, M., & Cleveland, D. W. (2010). TDP-43 and FUS/TLS: emerging roles in RNA processing and neurodegeneration. *Human Molecular Genetics*, *19*(R1), R46–R64. https://doi.org/10.1093/hmg/ddq137

Lajoie, P., & Snapp, E. L. (2010). Formation and Toxicity of Soluble Polyglutamine Oligomers in Living Cells. *PLoS ONE*, *5*(12), e15245. https://doi.org/10.1371/journal.pone.0015245

Lambert, D., & Calo, G. (2020). Approval of oliceridine (TRV130) for intravenous use in moderate to severe pain in adults. *British Journal of Anaesthesia*, *125*(6), e473–e474. https://doi.org/10.1016/j.bja.2020.09.021

Lambright, D. G., Sondek, J., Bohm, A., Skiba, N. P., Hamm, H. E., & Sigler, P. B. (1996). The 2.0 Å crystal structure of a heterotrimeric G protein. *Nature*, *379*(6563), 311–319. https://doi.org/10.1038/379311a0

Lamptey, R. N. L., Chaulagain, B., Trivedi, R., Gothwal, A., Layek, B., & Singh, J. (2022). A Review of the Common Neurodegenerative Disorders: Current Therapeutic Approaches and the Potential Role of Nanotherapeutics. *International Journal of Molecular Sciences*, *23*(3), 1851. https://doi.org/10.3390/ijms23031851

Langmead, C. J., & Christopoulos, A. (2006). Allosteric agonists of 7TM receptors: expanding the pharmacological toolbox. *Trends in Pharmacological Sciences*, *27*(9), 475–481. https://doi.org/10.1016/j.tips.2006.07.009

Lanoiselée, H.-M., Nicolas, G., Wallon, D., Rovelet-Lecrux, A., Lacour, M., Rousseau, S., Richard, A.-C., Pasquier, F., Rollin-Sillaire, A., Martinaud, O., Quillard-Muraine, M., de la Sayette, V., Boutoleau-Bretonniere, C., Etcharry-Bouyx, F., Chauviré, V., Sarazin, M., le Ber, I., Epelbaum, S., Jonveaux, T., … Campion, D. (2017). APP, PSEN1, and PSEN2 mutations in early-onset Alzheimer disease: A genetic screening study of familial and sporadic cases. *PLOS Medicine*, *14*(3), e1002270. https://doi.org/10.1371/journal.pmed.1002270

Larson, M., Sherman, M. A., Amar, F., Nuvolone, M., Schneider, J. A., Bennett, D. A., Aguzzi, A., & Lesné, S. E. (2012). The Complex PrP ^{c} -Fyn Couples Human Oligomeric Aß with Pathological Tau Changes in Alzheimer's Disease. *The Journal of Neuroscience*, *32*(47), 16857–16871. https://doi.org/10.1523/JNEUROSCI.1858-12.2012

Laschet, C., Dupuis, N., & Hanson, J. (2018). The G protein-coupled receptors deorphanization landscape. *Biochemical Pharmacology*, *153*, 62–74. https://doi.org/10.1016/j.bcp.2018.02.016

Lasmezas, C. I., Deslys, J.-P., Demaimay, R., Adjou, K. T., Hauw, J.-J., & Dormont, D. (1996). Strain specific and common pathogenic events in murine models of scrapie and bovine spongiform encephalopathy. *Journal of General Virology*, *77*(7), 1601–1609. https://doi.org/10.1099/0022-1317-77-7-1601

Laurén, J., Gimbel, D. A., Nygaard, H. B., Gilbert, J. W., & Strittmatter, S. M. (2009). Cellular prion protein mediates impairment of synaptic plasticity by

amyloid-β oligomers. *Nature*, *457*(7233), 1128–1132. https://doi.org/10.1038/nature07761

Lauritzen, I., Chemin, J., Honoré, E., Jodar, M., Guy, N., Lazdunski, M., & Jane Patel, A. (2005). Cross-talk between the mechano-gated K_{2P} channel TREK-1 and the actin cytoskeleton. *EMBO Reports*, *6*(7), 642–648. https://doi.org/10.1038/sj.embor.7400449

Leach, K., Sexton, P. M., & Christopoulos, A. (2007). Allosteric GPCR modulators: taking advantage of permissive receptor pharmacology. *Trends in Pharmacological Sciences*, *28*(8), 382–389. https://doi.org/10.1016/j.tips.2007.06.004

Lee, M., Lee, H. J., Park, I. S., Park, J. A., Kwon, Y. J., Ryu, Y. H., Kim, C. H., Kang, J. H., Hyun, I. Y., Lee, K. C., & Choi, J. Y. (2018). Aβ pathology downregulates brain mGluR5 density in a mouse model of Alzheimer. *Neuropharmacology*, *133*, 512–517. https://doi.org/10.1016/J.NEUROPHARM.2018.02.003

Lee, G., Thangavel, R., Sharma, V. M., Litersky, J. M., Bhaskar, K., Fang, S. M., Do, L. H., Andreadis, A., Van Hoesen, G., & Ksiezak-Reding, H. (2004). Phosphorylation of Tau by Fyn: Implications for Alzheimer's Disease. *The Journal of Neuroscience*, *24*(9), 2304–2312. https://doi.org/10.1523/JNEUROSCI.4162-03.2004

Lee, Y.-S., & Silva, A. J. (2009). The molecular and cellular biology of enhanced cognition. *Nature Reviews Neuroscience*, *10*(2), 126–140. https://doi.org/10.1038/nrn2572

Lefkowitz, R. J. (2007). Seven transmembrane receptors: something old, something new. *Acta Physiologica*, *190*(1), 9–19. https://doi.org/10.1111/j.1365-201X.2007.01693.x

Lesage, F., & Lazdunski, M. (2000). Molecular and functional properties of two-pore-domain potassium channels. *American Journal of Physiology-Renal Physiology*, *279*(5), F793–F801. https://doi.org/10.1152/ajprenal.2000.279.5.F793

Leuba, G., Savioz, A., Vernay, A., Carnal, B., Kraftsik, R., Tardif, E., Riederer, I., & Riederer, B. M. (2008). Differential Changes in Synaptic Proteins in the Alzheimer Frontal Cortex with Marked Increase in PSD-95 Postsynaptic Protein. *Journal of Alzheimer's Disease*, *15*(1), 139–151. https://doi.org/10.3233/JAD-2008-15112

Levine, M. S., Klapstein, G. J., Koppel, A., Gruen, E., Cepeda, C., Vargas, M. E., Jokel, E. S., Carpenter, E. M., Zanjani, H., Hurst, R. S., Efstratiadis, A., Zeitlin, S., & Chesselet, M. F. (1999). Enhanced sensitivity to N-methyl-D-aspartate receptor activation in transgenic and knockin mouse models of Huntington's disease. *Journal of Neuroscience Research*, *58*(4), 515–532.

Levitz, J., Habrian, C., Bharill, S., Fu, Z., Vafabakhsh, R., & Isacoff, E. Y. (2016). Mechanism of Assembly and Cooperativity of Homomeric and Heteromeric Metabotropic Glutamate Receptors. *Neuron*, *92*(1), 143–159. https://doi.org/10.1016/j.neuron.2016.08.036

Li, C., Zhao, R., Gao, K., Wei, Z., Yaoyao Yin, M., Ting Lau, L., Chui, D., & Cheung Hoi Yu, A. (2011). Astrocytes: Implications for Neuroinflammatory Pathogenesis of Alzheimers Disease. *Current Alzheimer Research*, *8*(1), 67–80. https://doi.org/10.2174/156720511794604543

Li, J. Y., Popovic, N., & Brundin, P. (2005). The use of the R6 transgenic mouse models of Huntington's disease in attempts to develop novel therapeutic strategies. *NeuroRX*, *2*(3), 447–464. https://doi.org/10.1602/neurorx.2.3.447

Li, S. H., Colson, T.-L. L., Abd-Elrahman, K. S., & Ferguson, S. S. G. (2022). Metabotropic Glutamate Receptor 5 Antagonism Reduces Pathology and Differentially Improves Symptoms in Male and Female Heterozygous zQ175

Huntington's Mice. *Frontiers in Molecular Neuroscience*, *0*, 6. https://doi.org/10.3389/FNMOL.2022.801757

Liao, Y.-H., Wang, Y.-H., Sun, L.-H., Deng, W.-T., Lee, H.-T., & Yu, L. (2018). mGluR5 upregulation and the effects of repeated methamphetamine administration and withdrawal on the rewarding efficacy of ketamine and social interaction. *Toxicology and Applied Pharmacology*, *360*, 58–68. https://doi.org/10.1016/j.taap.2018.09.035

Liddelow, S. A., & Barres, B. A. (2017). Reactive Astrocytes: Production, Function, and Therapeutic Potential. *Immunity*, *46*(6), 957–967. https://doi.org/10.1016/J.IMMUNI.2017.06.006

Liévens, J.-C., Woodman, B., Mahal, A., Spasic-Boscovic, O., Samuel, D., Kerkerian-Le Goff, L., & Bates, G. P. (2001). Impaired Glutamate Uptake in the R6 Huntington's Disease Transgenic Mice. *Neurobiology of Disease*, *8*(5), 807–821. https://doi.org/10.1006/nbdi.2001.0430

Lim, D., Iyer, A., Ronco, V., Grolla, A. A., Canonico, P. L., Aronica, E., & Genazzani, A. A. (2013). Amyloid beta deregulates astroglial mGluR5-mediated calcium signaling via calcineurin and Nf-kB. *Glia*, *61*(7), 1134–1145. https://doi.org/10.1002/GLIA.22502

Lindemann, L., Jaeschke, G., Michalon, A., Vieira, E., Honer, M., Spooren, W., Porter, R., Hartung, T., Kolczewski, S., Büttelmann, B., Flament, C., Diener, C., Fischer, C., Gatti, S., Prinssen, E. P., Parrott, N., Hoffmann, G., & Wettstein, J. G. (2011). CTEP: A Novel, Potent, Long-Acting, and Orally Bioavailable Metabotropic Glutamate Receptor 5 Inhibitor. *Journal of Pharmacology and Experimental Therapeutics*, *339*(2), 474–486. https://doi.org/10.1124/jpet.111.185660

Lipkind, D., Sakov, A., Kafkafi, N., Elmer, G.I., Benjamini, Y., Golani, I. (2004). New replicable anxiety-related measures of wall vs. center behavior of mice in the open field. *J Appl Physiol*, 97, 347–359. https://doi.org/10.1152/japplphysiol.00148.2004

Liu, F., Grauer, S., Kelley, C., Navarra, R., Graf, R., Zhang, G., Atkinson, P. J., Popiolek, M., Wantuch, C., Khawaja, X., Smith, D., Olsen, M., Kouranova, E., Lai, M., Pruthi, F., Pulicicchio, C., Day, M., Gilbert, A., Pausch, M. H., … Marquis, K. L. (2008). ADX47273 [*S* -(4-Fluoro-phenyl)-{3-[3-(4-fluoro-phenyl)-[1,2,4]-oxadiazol-5-yl]-piperidin-1-yl}-methanone]: A Novel Metabotropic Glutamate Receptor 5-Selective Positive Allosteric Modulator with Preclinical Antipsychotic-Like and Procognitive Activities. *Journal of Pharmacology and Experimental Therapeutics*, *327*(3), 827–839. https://doi.org/10.1124/jpet.108.136580

Livingston, G., Huntley, J., Sommerlad, A., Ames, D., Ballard, C., Banerjee, S., Brayne, C., Burns, A., Cohen-Mansfield, J., Cooper, C., Costafreda, S. G., Dias, A., Fox, N., Gitlin, L. N., Howard, R., Kales, H. C., Kivimäki, M., Larson, E. B., Ogunniyi, A., … Mukadam, N. (2020). Dementia prevention, intervention, and care: 2020 report of the Lancet Commission. *The Lancet*, *396*(10248), 413–446. https://doi.org/10.1016/S0140-6736(20)30367-6

Loane, D. J., Stoica, B. A., Byrnes, K. R., Jeong, W., & Faden, A. I. (2013). Activation of mGluR5 and inhibition of NADPH oxidase improves functional recovery after traumatic brain injury. *Journal of Neurotrauma*, *30*(5), 403–412. https://doi.org/10.1089/NEU.2012.2589

Loane, D. J., Stoica, B. A., & Faden, A. I. (2012). Metabotropic glutamate receptor-mediated signaling in neuroglia. *Wiley Interdisciplinary Reviews: Membrane Transport and Signaling*, *1*(2), 136–150. https://doi.org/10.1002/WMTS.30

Loane, D. J., Stoica, B. A., Pajoohesh-Ganji, A., Byrnes, K. R., & Faden, A. I. (2009). Activation of metabotropic glutamate receptor 5 modulates microglial reactivity

and neurotoxicity by inhibiting NADPH oxidase. *The Journal of Biological Chemistry*, *284*(23), 15629–15639. https://doi.org/10.1074/JBC.M806139200

Loane, D. J., Stoica, B. A., Tchantchou, F., Kumar, A., Barrett, J. P., Akintola, T., Xue, F., Conn, P. J., & Faden, A. I. (2014). Novel mGluR5 Positive Allosteric Modulator Improves Functional Recovery, Attenuates Neurodegeneration, and Alters Microglial Polarization after Experimental Traumatic Brain Injury. *Neurotherapeutics*, *11*(4), 857–869. https://doi.org/10.1007/s13311-014-0298-6

Lodge, D. (2009). The history of the pharmacology and cloning of ionotropic glutamate receptors and the development of idiosyncratic nomenclature. *Neuropharmacology*, *56*(1), 6–21. https://doi.org/10.1016/j.neuropharm.2008.08.006

Logothetis, D. E., Kurachi, Y., Galper, J., Neer, E. J., & Clapham, D. E. (1987). The βγ subunits of GTP-binding proteins activate the muscarinic K+ channel in heart. *Nature*, *325*(6102), 321–326. https://doi.org/10.1038/325321a0

Love, S., Siew, L. K., Dawbarn, D., Wilcock, G. K., Ben-Shlomo, Y., & Allen, S. J. (2006). Premorbid effects of APOE on synaptic proteins in human temporal neocortex. *Neurobiology of Aging*, *27*(6), 797–803. https://doi.org/10.1016/j.neurobiolaging.2005.04.008

Lu, Y.-M., Jia, Z., Janus, C., Henderson, J. T., Gerlai, R., Wojtowicz, J. M., & Roder, J. C. (1997). Mice Lacking Metabotropic Glutamate Receptor 5 Show Impaired Learning and Reduced CA1 Long-Term Potentiation (LTP) But Normal CA3 LTP. *The Journal of Neuroscience*, *17*(13), 5196–5205. https://doi.org/10.1523/JNEUROSCI.17-13-05196.1997

Luján, R., Nusser, Z., Roberts, J. D. B., Shigemoto, R., & Somogyi, P. (1996). Perisynaptic Location of Metabotropic Glutamate Receptors mGluR1 and mGluR5 on Dendrites and Dendritic Spines in the Rat Hippocampus. *European Journal of Neuroscience*, *8*(7), 1488–1500. https://doi.org/10.1111/j.1460-9568.1996.tb01611.x

Luk, K. C., Kehm, V., Carroll, J., Zhang, B., O'Brien, P., Trojanowski, J. Q., & Lee, V. M.-Y. (2012). Pathological α-Synuclein Transmission Initiates Parkinson-like Neurodegeneration in Nontransgenic Mice. *Science*, *338*(6109), 949–953. https://doi.org/10.1126/science.1227157

Luttrell, L. M., Rocca, G. J. Della, van Biesen, T., Luttrell, D. K., & Lefkowitz, R. J. (1997). Gβγ Subunits Mediate Src-dependent Phosphorylation of the Epidermal Growth Factor Receptor. *Journal of Biological Chemistry*, *272*(7), 4637–4644. https://doi.org/10.1074/jbc.272.7.4637

Lutz, C. (2018). Mouse models of ALS: Past, present and future. *Brain Research*, *1693*, 1–10. https://doi.org/10.1016/j.brainres.2018.03.024

Lv, M.-M., Cheng, Y.-C., Xiao, Z.-B., Sun, M.-Y., Ren, P.-C., & Sun, X.-D. (2014). Down-regulation of Homer1b/c attenuates group I metabotropic glutamate receptors dependent Ca2+ signaling through regulating endoplasmic reticulum Ca2+ release in PC12 cells. *Biochemical and Biophysical Research Communications*, *450*(4), 1568–1574. https://doi.org/10.1016/j.bbrc.2014.07.044

Macdonald, M. (1993). A novel gene containing a trinucleotide repeat that is expanded and unstable on Huntington's disease chromosomes. *Cell*, *72*(6), 971–983. https://doi.org/10.1016/0092-8674(93)90585-E

Mackenzie, I. R. A., Bigio, E. H., Ince, P. G., Geser, F., Neumann, M., Cairns, N. J., Kwong, L. K., Forman, M. S., Ravits, J., Stewart, H., Eisen, A., McClusky, L., Kretzschmar, H. A., Monoranu, C. M., Highley, J. R., Kirby, J., Siddique, T., Shaw, P. J., Lee, V. M.-Y., & Trojanowski, J. Q. (2007). Pathological TDP-43 distinguishes sporadic amyotrophic lateral sclerosis from amyotrophic lateral

sclerosis withSOD1 mutations. *Annals of Neurology*, *61*(5), 427–434. https://doi.org/10.1002/ana.21147

Magee, J. C., & Grienberger, C. (2020). Synaptic Plasticity Forms and Functions. *Annual Review of Neuroscience*, *43*(1), 95–117. https://doi.org/10.1146/annurev-neuro-090919-022842

Mahanty, N. K., & Sah, P. (1998). Calcium-permeable AMPA receptors mediate long-term potentiation in interneurons in the amygdala. *Nature*, *394*(6694), 683–687. https://doi.org/10.1038/29312

Makarava, N., Chang, J. C.-Y., Kushwaha, R., & Baskakov, I. V. (2019). Region-Specific Response of Astrocytes to Prion Infection. *Frontiers in Neuroscience*, *13*. https://doi.org/10.3389/fnins.2019.01048

Makarava, N., Chang, J. C.-Y., Molesworth, K., & Baskakov, I. V. (2020). Region-specific glial homeostatic signature in prion diseases is replaced by a uniform neuroinflammation signature, common for brain regions and prion strains with different cell tropism. *Neurobiology of Disease*, *137*, 104783. https://doi.org/10.1016/j.nbd.2020.104783

Makarava, N., Kovacs, G. G., Savtchenko, R., Alexeeva, I., Budka, H., Rohwer, R. G., & Baskakov, I. V. (2011). Genesis of Mammalian Prions: From Non-infectious Amyloid Fibrils to a Transmissible Prion Disease. *PLoS Pathogens*, *7*(12), e1002419. https://doi.org/10.1371/journal.ppat.1002419

Makarava, N., Mychko, O., Chang, J. C.-Y., Molesworth, K., & Baskakov, I. V. (2021). The degree of astrocyte activation is predictive of the incubation time to prion disease. *Acta Neuropathologica Communications*, *9*(1), 87. https://doi.org/10.1186/s40478-021-01192-9

Makarava, N., Savtchenko, R., & Baskakov, I. V. (2015). Two alternative pathways for generating transmissible prion disease de novo. *Acta Neuropathologica Communications*, *3*(1), 69. https://doi.org/10.1186/s40478-015-0248-5

Mallucci, G., Dickinson, A., Linehan, J., Klöhn, P.-C., Brandner, S., & Collinge, J. (2003). Depleting Neuronal PrP in Prion Infection Prevents Disease and Reverses Spongiosis. *Science*, *302*(5646), 871–874. https://doi.org/10.1126/science.1090187

Mallucci, G. R. (2009). Prion neurodegeneration. *Prion*, *3*(4), 195–201. https://doi.org/10.4161/pri.3.4.9981

Mallucci, G. R., Ratté, S., Asante, E. A., Linehan, J., Gowland, I., Jefferys, J. G. R., & Collinge, J. (2002). Post-natal knockout of prion protein alters hippocampal CA1 properties, but does not result in neurodegeneration. *The EMBO Journal*, *21*(3), 202–210. https://doi.org/10.1093/emboj/21.3.202

Mallucci, G. R., White, M. D., Farmer, M., Dickinson, A., Khatun, H., Powell, A. D., Brandner, S., Jefferys, J. G. R., & Collinge, J. (2007). Targeting Cellular Prion Protein Reverses Early Cognitive Deficits and Neurophysiological Dysfunction in Prion-Infected Mice. *Neuron*, *53*(3), 325–335. https://doi.org/10.1016/j.neuron.2007.01.005

Manahan-Vaughan, D., & Braunewell, K.-H. (2005). The Metabotropic Glutamate Receptor, mGluR5, is a Key Determinant of Good and Bad Spatial Learning Performance and Hippocampal Synaptic Plasticity. *Cerebral Cortex*, *15*(11), 1703–1713. https://doi.org/10.1093/cercor/bhi047

Manson, J., West, J. D., Thomson, V., Mcbride, P., Kaufman, M. H., & Hope, J. (1992). The prion protein gene: a role in mouse embryogenesis? *Development*, *115*(1), 117–122. https://doi.org/10.1242/dev.115.1.117

Manson, J. C., Clarke, A. R., Hooper, M. L., Aitchison, L., McConnel, I. & Hope, J. (1994). 129/Ola mice carrying a null mutation in PrP that abolishes mRNA production are developmentally normal. *Mol Neurobiol*, 8, 121-7.

Mao, C., Shen, C., Li, C., Shen, D.-D., Xu, C., Zhang, S., Zhou, R., Shen, Q., Chen, L.-N., Jiang, Z., Liu, J., & Zhang, Y. (2020). Cryo-EM structures of inactive and active GABAB receptor. *Cell Research*, *30*(7), 564–573. https://doi.org/10.1038/s41422-020-0350-5

Marin, B., Boumédiene, F., Logroscino, G., Couratier, P., Babron, M.-C., Leutenegger, A. L., Copetti, M., Preux, P.-M., & Beghi, E. (2016). Variation in worldwide incidence of amyotrophic lateral sclerosis: a meta-analysis. *International Journal of Epidemiology*, dyw061. https://doi.org/10.1093/ije/dyw061

Marino, M. J., & Conn, P. J. (2002). Direct and indirect modulation of the N-methyl D-aspartate receptor. *Current Drug Targets. CNS and Neurological Disorders*, *1*(1), 1–16. https://doi.org/10.2174/1568007023339544

Marsicano G., Goodenough S., Monory K., Hermann H., Eder M., Cannich A., Azad S.C., Cascio M.G., Gutiérrez S.O., van der Stelt M., López-Rodriguez M.L., Casanova E., Schütz G., Zieglgänsberger W., Di Marzo V., Behl C., Lutz B. (2003). CB1 cannabinoid receptors and on-demand defense against excitotoxicity. *Science*. 3;302(5642):84-8. doi: 10.1126/science.1088208.

Martín-Belmonte, A., Aguado, C., Alfaro-Ruiz, R., Albasanz, J. L., Martín, M., Moreno-Martínez, A. E., Fukazawa, Y., & Luján, R. (2021). The density of group i mglu5 receptors is reduced along the neuronal surface of hippocampal cells in a mouse model of alzheimer's disease. *International Journal of Molecular Sciences*, *22*(11). https://doi.org/10.3390/IJMS22115867/S1

Martini-Stoica, H., Cole, A. L., Swartzlander, D. B., Chen, F., Wan, Y. W., Bajaj, L., Bader, D. A., Lee, V. M. Y., Trojanowski, J. Q., Liu, Z., Sardiello, M., & Zheng, H. (2018). TFEB enhances astroglial uptake of extracellular tau species and reduces tau spreading. *The Journal of Experimental Medicine*, *215*(9), 2355–2377. https://doi.org/10.1084/JEM.20172158

Masrori, P., & Van Damme, P. (2020). Amyotrophic lateral sclerosis: a clinical review. *European Journal of Neurology*, *27*(10), 1918–1929. https://doi.org/10.1111/ene.14393

Martínez, M., Martínez, N., & Silva, W. (2017). Measurement of the Intracellular Calcium Concentration with Fura-2 AM Using a Fluorescence Plate Reader. *BIO-PROTOCOL*, *7*(14). https://doi.org/10.21769/BioProtoc.2411

Masu, M., Tanabe, Y., Tsuchida, K., Shigemoto, R., & Nakanishi, S. (1991). Sequence and expression of a metabotropic glutamate receptor. *Nature*, *349*(6312), 760–765. https://doi.org/10.1038/349760a0

Matthews, C. C., Zielke, H. R., Wollack, J. B., & Fishman, P. S. (2002). Enzymatic Degradation Protects Neurons from Glutamate Excitotoxicity. *Journal of Neurochemistry*, *75*(3), 1045–1052. https://doi.org/10.1046/j.1471-4159.2000.0751045.x

Mattson, M. R. (2007). Calcium and neurodegeneration. *Aging Cell*, *6*(3), 337–350. https://doi.org/10.1111/J.1474-9726.2007.00275.X

Maudsley, S., A. Patel, S., Park, S.-S., M. Luttrell, L., & Martin, B. (2012). Functional Signaling Biases in G Protein-Coupled Receptors: Game Theory and Receptor Dynamics. *Mini-Reviews in Medicinal Chemistry*, *12*(9), 831–840. https://doi.org/10.2174/138955712800959071

Mayer, M. L., Westbrook, G. L., & Guthrie, P. B. (1984). Voltage-dependent block by Mg2+ of NMDA responses in spinal cord neurones. *Nature*, *309*(5965), 261–263. https://doi.org/10.1038/309261a0

McAlary, L., Aquilina, J. A., & Yerbury, J. J. (2016). Susceptibility of Mutant SOD1 to Form a Destabilized Monomer Predicts Cellular Aggregation and Toxicity but Not In vitro Aggregation Propensity. *Frontiers in Neuroscience*, *10*. https://doi.org/10.3389/fnins.2016.00499

McCarthy, M. M. (2015). Incorporating Sex as a Variable in Preclinical Neuropsychiatric Research: Fig. 1. *Schizophrenia Bulletin*, *41*(5), 1016–1020. https://doi.org/10.1093/schbul/sbv077

McColgan, P., & Tabrizi, S. J. (2018). Huntington's disease: a clinical review. *European Journal of Neurology*, *25*(1), 24–34. https://doi.org/10.1111/ene.13413

McCord, J. M., & Fridovich, I. (1969). Superoxide dismutase. An enzymic function for erythrocuprein (hemocuprein). *The Journal of Biological Chemistry*, *244*(22), 6049–6055.

McCudden, C. R., Hains, M. D., Kimple, R. J., Siderovski, D. P., & Willard, F. S. (2005). G-protein signaling: back to the future. *Cellular and Molecular Life Sciences*, *62*(5), 551–577. https://doi.org/10.1007/s00018-004-4462-3

McCullock, T. W., & Kammermeier, P. J. (2021). The evidence for and consequences of metabotropic glutamate receptor heterodimerization. *Neuropharmacology*, *199*, 108801. https://doi.org/10.1016/j.neuropharm.2021.108801

McGeer, E. G., & McGeer, P. L. (1976). Duplication of biochemical changes of Huntington's chorea by intrastriatal injections of glutamic and kainic acids. *Nature*, *263*(5577), 517–519. https://doi.org/10.1038/263517a0

McShane, R., Westby, M. J., Roberts, E., Minakaran, N., Schneider, L., Farrimond, L. E., Maayan, N., Ware, J., & Debarros, J. (2019). Memantine for dementia. *Cochrane Database of Systematic Reviews*. https://doi.org/10.1002/14651858.CD003154.pub6

Mecca, A. P., McDonald, J. W., Michalak, H. R., Godek, T. A., Harris, J. E., Pugh, E. A., Kemp, E. C., Chen, M. K., Salardini, A., Nabulsi, N. B., Lim, K., Huang, Y., Carson, R. E., Strittmatter, S. M., & Van Dyck, C. H. (2020). PET imaging of mGluR5 in Alzheimer's disease. *Alzheimer's Research & Therapy*, *12*(1). https://doi.org/10.1186/S13195-020-0582-0

Mecca, A. P., Rogers, K., Jacobs, Z., McDonald, J. W., Michalak, H. R., DellaGioia, N., Zhao, W., Hillmer, A. T., Nabulsi, N., Lim, K., Ropchan, J., Huang, Y., Matuskey, D., Esterlis, I., Carson, R. E., & van Dyck, C. H. (2021). Effect of age on brain metabotropic glutamate receptor subtype 5 measured with [18F]FPEB PET. *NeuroImage*, *238*, 118217. https://doi.org/10.1016/J.NEUROIMAGE.2021.118217

Medinas, D. B., Valenzuela, V., & Hetz, C. (2017). Proteostasis disturbance in amyotrophic lateral sclerosis. *Human Molecular Genetics*, *26*(R2), R91–R104. https://doi.org/10.1093/hmg/ddx274

Mejzini, R., Flynn, L. L., Pitout, I. L., Fletcher, S., Wilton, S. D., & Akkari, P. A. (2019). ALS Genetics, Mechanisms, and Therapeutics: Where Are We Now? *Frontiers in Neuroscience*, *13*. https://doi.org/10.3389/fnins.2019.01310

Menalled, L. B. (2005). Knock-in mouse models of Huntington's disease. *NeuroRX*, *2*(3), 465–470. https://doi.org/10.1602/neurorx.2.3.465

Ménard, C., & Quirion, R. (2012). Successful Cognitive Aging in Rats: A Role for mGluR5 Glutamate Receptors, Homer 1 Proteins and Downstream Signaling Pathways. *PLoS ONE*, *7*(1), e28666. https://doi.org/10.1371/journal.pone.0028666

Menting, K. W., & Claassen, J. A. H. R. (2014). Î²-secretase inhibitor; a promising novel therapeutic drug in Alzheimer's disease. *Frontiers in Aging Neuroscience*, *6*. https://doi.org/10.3389/fnagi.2014.00165

Menzies, F. M., Fleming, A., Caricasole, A., Bento, C. F., Andrews, S. P., Ashkenazi, A., Füllgrabe, J., Jackson, A., Jimenez Sanchez, M., Karabiyik, C., Licitra, F., Lopez Ramirez, A., Pavel, M., Puri, C., Renna, M., Ricketts, T., Schlotawa, L., Vicinanza, M., Won, H., … Rubinsztein, D. C. (2017). Autophagy and

Neurodegeneration: Pathogenic Mechanisms and Therapeutic Opportunities. *Neuron*, *93*(5), 1015–1034. https://doi.org/10.1016/j.neuron.2017.01.022

Meyer-Ficca, M. L., Meyer, R. G., Kaiser, H., Brack, A. R., Kandolf, R., & Küpper, J.-H. (2004). Comparative analysis of inducible expression systems in transient transfection studies. *Analytical Biochemistry*, *334*(1), 9–19. https://doi.org/10.1016/j.ab.2004.07.011

Michler-Stuke, A., Wolff, J. R., & Bottenstein, J. E. (1984). Factors influencing astrocyte growth and development in defined media. *International Journal of Developmental Neuroscience*, *2*(6), 575–584. https://doi.org/10.1016/0736-5748(84)90035-2

Middeldorp, J., & Hol, E. M. (2011). GFAP in health and disease. *Progress in Neurobiology*, *93*(3), 421–443. https://doi.org/10.1016/j.pneurobio.2011.01.005

Milanese, M., Bonifacino, T., Torazza, C., Provenzano, F., Kumar, M., Ravera, S., Zerbo, A. R., Frumento, G., Balbi, M., Nguyen, T. P. N., Bertola, N., Ferrando, S., Viale, M., Profumo, A., & Bonanno, G. (2021). Blocking glutamate mGlu5 receptors with the negative allosteric modulator CTEP improves disease course in SOD1G93A mouse model of amyotrophic lateral sclerosis. *British Journal of Pharmacology*, *178*(18), 3747–3764. https://doi.org/10.1111/BPH.15515

Miller, J., Arrasate, M., Brooks, E., Libeu, C. P., Legleiter, J., Hatters, D., Curtis, J., Cheung, K., Krishnan, P., Mitra, S., Widjaja, K., Shaby, B. A., Lotz, G. P., Newhouse, Y., Mitchell, E. J., Osmand, A., Gray, M., Thulasiramin, V., Saudou, F., … Finkbeiner, S. (2011). Identifying polyglutamine protein species in situ that best predict neurodegeneration. *Nature Chemical Biology*, *7*(12), 925–934. https://doi.org/10.1038/nchembio.694

Miller, J., Arrasate, M., Shaby, B. A., Mitra, S., Masliah, E., & Finkbeiner, S. (2010). Quantitative Relationships between Huntingtin Levels, Polyglutamine Length, Inclusion Body Formation, and Neuronal Death Provide Novel Insight into Huntington's Disease Molecular Pathogenesis. *The Journal of Neuroscience*, *30*(31), 10541–10550. https://doi.org/10.1523/JNEUROSCI.0146-10.2010

Miller, Y., Ma, B., & Nussinov, R. (2011). Synergistic interactions between repeats in tau protein and Aß amyloids may be responsible for accelerated aggregation via polymorphic States. *Biochemistry*, *50*(23), 5172–5181. https://doi.org/10.1021/BI200400U/SUPPL_FILE/BI200400U_SI_001.PDF

Minakami, R., Iida, K., Hirakawa, N., & Sugiyama, H. (2002). The Expression of Two Splice Variants of Metabotropic Glutamate Receptor Subtype 5 in the Rat Brain and Neuronal Cells During Development. *Journal of Neurochemistry*, *65*(4), 1536–1542. https://doi.org/10.1046/j.1471-4159.1995.65041536.x

Mincheva-Tasheva, S., & Soler, R. M. (2013). NF-κB Signaling Pathways. *The Neuroscientist*, *19*(2), 175–194. https://doi.org/10.1177/1073858412444007

Miranda, M., Morici, J.F., Zanoni, M.B., Bekinschtein, P., 2019. Brain-Derived Neurotrophic Factor: A Key Molecule for Memory in the Healthy and the Pathological Brain. Front Cell Neurosci 13. https://doi.org/10.3389/fncel.2019.00363

Miyazono, M., Iwaki, T., Kitamoto, T., Kaneko, Y., Doh-ura, K., & Tateishi, J. (1991). A comparative immunohistochemical study of Kuru and senile plaques with a special reference to glial reactions at various stages of amyloid plaque formation. *The American Journal of Pathology*, *139*(3), 589–598.

Mizuguchi, H., & Hayakawa, T. (2001). Characteristics of adenovirus-mediated tetracycline-controllable expression system. *Biochimica et Biophysica Acta (BBA) - General Subjects*, *1568*(1), 21–29. https://doi.org/10.1016/S0304-4165(01)00195-7

Molinari, C., Morsanuto, V., Ruga, S., Notte, F., Farghali, M., Galla, R., Uberti, F., 2020. The Role of BDNF on Aging-Modulation Markers. Brain Sci 10, 285. https://doi.org/10.3390/brainsci10050285

Monti, B., Berteotti, C., & Contestabile, A. (2005). Dysregulation of memory-related proteins in the hippocampus of aged rats and their relation with cognitive impairment. *Hippocampus*, *15*(8), 1041–1049. https://doi.org/10.1002/hipo.20099

Montine, T. J., Phelps, C. H., Beach, T. G., Bigio, E. H., Cairns, N. J., Dickson, D. W., Duyckaerts, C., Frosch, M. P., Masliah, E., Mirra, S. S., Nelson, P. T., Schneider, J. A., Thal, D. R., Trojanowski, J. Q., Vinters, H. V., & Hyman, B. T. (2012). National Institute on Aging-Alzheimer's Association guidelines for the neuropathologic assessment of Alzheimer's disease: a practical approach. *Acta Neuropathologica*, *123*(1), 1. https://doi.org/10.1007/S00401-011-0910-3

Moreels, M., Vandenabeele, F., Dumont, D., Robben, J., & Lambrichts, I. (2008). Alpha-smooth muscle actin (alpha-SMA) and nestin expression in reactive astrocytes in multiple sclerosis lesions: potential regulatory role of transforming growth factor-beta 1 (TGF-beta1). *Neuropathology and Applied Neurobiology*, *34*(5), 532–546. https://doi.org/10.1111/J.1365-2990.2007.00910.X

Moreno, J. A., Radford, H., Peretti, D., Steinert, J. R., Verity, N., Martin, M. G., Halliday, M., Morgan, J., Dinsdale, D., Ortori, C. A., Barrett, D. A., Tsaytler, P., Bertolotti, A., Willis, A. E., Bushell, M., & Mallucci, G. R. (2012). Sustained translational repression by eIF2α-P mediates prion neurodegeneration. *Nature*, *485*(7399), 507–511. https://doi.org/10.1038/nature11058

Morris, R. G. M., Anderson, E., Lynch, G. S., & Baudry, M. (1986). Selective impairment of learning and blockade of long-term potentiation by an N-methyl-D-aspartate receptor antagonist, AP5. *Nature*, *319*(6056), 774–776. https://doi.org/10.1038/319774a0

Movsesyan, V. A., Stoica, B. A., & Faden, A. I. (2004). MGLuR5 activation reduces ß-amyloid-induced cell death in primary neuronal cultures and attenuates translocation of cytochrome *c* and apoptosis-inducing factor. *Journal of Neurochemistry*, *89*(6), 1528–1536. https://doi.org/10.1111/j.1471-4159.2004.02451.x

Müller Herde, A., Schibli, R., Weber, M., & Ametamey, S. M. (2019). Metabotropic glutamate receptor subtype 5 is altered in LPS-induced murine neuroinflammation model and in the brains of AD and ALS patients. *European Journal of Nuclear Medicine and Molecular Imaging*, *46*(2), 407–420. https://doi.org/10.1007/S00259-018-4179-9/FIGURES/6

Murgaš, M., Michenthaler, P., Reed, M. B., Gryglewski, G., & Lanzenberger, R. (2022). Correlation of receptor density and mRNA expression patterns in the human cerebral cortex. *NeuroImage*, *256*, 119214. https://doi.org/10.1016/j.neuroimage.2022.119214

Muth, C., Schröck, K., Madore, C., Hartmann, K., Fanek, Z., Butovsky, O., Glatzel, M., & Krasemann, S. (2017). Activation of microglia by retroviral infection correlates with transient clearance of prions from the brain but does not change incubation time. *Brain Pathology*, *27*(5), 590–602. https://doi.org/10.1111/bpa.12441

Na, Y.-J., Jin, J.-K., Kim, J.-I., Choi, E.-K., Carp, R. I., & Kim, Y.-S. (2007). JAK-STAT signaling pathway mediates astrogliosis in brains of scrapie-infected mice. *Journal of Neurochemistry*, *103*(2), 637–649. https://doi.org/10.1111/j.1471-4159.2007.04769.x

Nakahara, K., Okada, M., & Nakanishi, S. (1997). The Metabotropic Glutamate Receptor mGluR5 Induces Calcium Oscillations in Cultured Astrocytes via Protein

Kinase C Phosphorylation. *Journal of Neurochemistry*, *69*(4), 1467–1475. https://doi.org/10.1046/j.1471-4159.1997.69041467.x

Nakaya, T., & Maragkakis, M. (2018). Amyotrophic Lateral Sclerosis associated FUS mutation shortens mitochondria and induces neurotoxicity. *Scientific Reports*, *8*(1), 15575. https://doi.org/10.1038/s41598-018-33964-0

Näslund, J. (2000). Correlation Between Elevated Levels of Amyloid ß-Peptide in the Brain and Cognitive Decline. *JAMA*, *283*(12), 1571. https://doi.org/10.1001/jama.283.12.1571

Nasrallah, C., Cannone, G., Briot, J., Rottier, K., Berizzi, A. E., Huang, C.-Y., Quast, R. B., Hoh, F., Banères, J.-L., Malhaire, F., Berto, L., Dumazer, A., Font-Ingles, J., Gómez-Santacana, X., Catena, J., Kniazeff, J., Goudet, C., Llebaria, A., Pin, J.-P., … Lebon, G. (2021). Agonists and allosteric modulators promote signaling from different metabotropic glutamate receptor 5 conformations. *Cell Reports*, *36*(9), 109648. https://doi.org/10.1016/j.celrep.2021.109648

Navarro, J. F., Postigo, D., Martín, M., & Burón, E. (2006). Antiaggressive effects of MPEP, a selective antagonist of mGlu5 receptors, in agonistic interactions between male mice. *European Journal of Pharmacology*, *551*(1–3), 67–70. https://doi.org/10.1016/j.ejphar.2006.08.055

Nayak, D., Roth, T. L., & McGavern, D. B. (2014). Microglia development and function. *Annual Review of Immunology*, *32*, 367–402. https://doi.org/10.1146/ANNUREV-IMMUNOL-032713-120240

Neumann, M., Sampathu, D. M., Kwong, L. K., Truax, A. C., Micsenyi, M. C., Chou, T. T., Bruce, J., Schuck, T., Grossman, M., Clark, C. M., McCluskey, L. F., Miller, B. L., Masliah, E., Mackenzie, I. R., Feldman, H., Feiden, W., Kretzschmar, H. A., Trojanowski, J. Q., & Lee, V. M.-Y. (2006). Ubiquitinated TDP-43 in Frontotemporal Lobar Degeneration and Amyotrophic Lateral Sclerosis. *Science*, *314*(5796), 130–133. https://doi.org/10.1126/science.1134108

Newcombe, J., Uddin, A., Dove, R., Patel, B., Turski, L., Nishizawa, Y., & Smith, T. (2008). Glutamate receptor expression in multiple sclerosis lesions. *Brain Pathology*, *18*(1), 52–61. https://doi.org/10.1111/J.1750-3639.2007.00101.X

Newell, K. A. (2013). Metabotropic glutamate receptor 5 in schizophrenia: emerging evidence for the development of antipsychotic drugs. *Future Medicinal Chemistry*, *5*(13), 1471–1474. https://doi.org/10.4155/fmc.13.137

Newman, E. L., Chu, A., Bahamón, B., Takahashi, A., DeBold, J. F., & Miczek, K. A. (2012). NMDA receptor antagonism: escalation of aggressive behavior in alcohol-drinking mice. *Psychopharmacology*, *224*(1), 167–177. https://doi.org/10.1007/s00213-012-2734-9

Nicolas, L. B., Kolb, Y., & Prinssen, E. P. M. (2006). A combined marble burying–locomotor activity test in mice: A practical screening test with sensitivity to different classes of anxiolytics and antidepressants. *European Journal of Pharmacology*, *547*(1–3), 106–115. https://doi.org/10.1016/j.ejphar.2006.07.015

Nicoletti, F., Bockaert, J., Collingridge, G. L., Conn, P. J., Ferraguti, F., Schoepp, D. D., Wroblewski, J. T., & Pin, J. P. (2011). Metabotropic glutamate receptors: From the workbench to the bedside. *Neuropharmacology*, *60*(7–8), 1017–1041. https://doi.org/10.1016/j.neuropharm.2010.10.022

Nicoletti, F., Orlando, R., Di Menna, L., Cannella, M., Notartomaso, S., Mascio, G., Iacovelli, L., Matrisciano, F., Fazio, F., Caraci, F., Copani, A., Battaglia, G., & Bruno, V. (2019). Targeting mGlu Receptors for Optimization of Antipsychotic Activity and Disease-Modifying Effect in Schizophrenia. *Frontiers in Psychiatry*, *10*. https://doi.org/10.3389/fpsyt.2019.00049

Niswender, C. M., & Conn, P. J. (2010). Metabotropic Glutamate Receptors: Physiology, Pharmacology, and Disease. *Annual Review of Pharmacology and*

Toxicology, *50*(1), 295–322. https://doi.org/10.1146/annurev.pharmtox.011008.145533

Niu, Y., Zeng, X., Qin, G., Zhang, D., Zhou, J., & Chen, L. (2021). Downregulation of metabotropic glutamate receptor 5 alleviates central sensitization by activating autophagy via inhibiting mTOR pathway in a rat model of chronic migraine. *Neuroscience Letters*, *743*, 135552. https://doi.org/10.1016/j.neulet.2020.135552

Nixon, R.A., 2013. The role of autophagy in neurodegenerative disease. Nat Med 19, 983–997. https://doi.org/10.1038/nm.3232

Noda, M. (2013). Possible Contribution of Microglial Glutamate Receptors to Inflammatory Response upon Neurodegenerative Diseases. *Journal of Neurological Disorders*, *01*(03). https://doi.org/10.4172/2329-6895.1000131

Noetzel, M. J., Gregory, K. J., Vinson, P. N., Manka, J. T., Stauffer, S. R., Lindsley, C. W., Niswender, C. M., Xiang, Z., & Conn, P. J. (2013). A Novel Metabotropic Glutamate Receptor 5 Positive Allosteric Modulator Acts at a Unique Site and Confers Stimulus Bias to mGlu5 Signaling. *Molecular Pharmacology*, *83*(4), 835–847. https://doi.org/10.1124/mol.112.082891

Nolan, M., Talbot, K., & Ansorge, O. (2016). Pathogenesis of FUS-associated ALS and FTD: insights from rodent models. *Acta Neuropathologica Communications*, *4*(1), 99. https://doi.org/10.1186/s40478-016-0358-8

Nordstrom, K. J. V., Lagerstrom, M. C., Waller, L. M. J., Fredriksson, R., & Schioth, H. B. (2008). The Secretin GPCRs Descended from the Family of Adhesion GPCRs. *Molecular Biology and Evolution*, *26*(1), 71–84. https://doi.org/10.1093/molbev/msn228

Nucifora, L. G., Burke, K. A., Feng, X., Arbez, N., Zhu, S., Miller, J., Yang, G., Ratovitski, T., Delannoy, M., Muchowski, P. J., Finkbeiner, S., Legleiter, J., Ross, C. A., & Poirier, M. A. (2012). Identification of Novel Potentially Toxic Oligomers Formed in Vitro from Mammalian-derived Expanded huntingtin Exon-1 Protein. *Journal of Biological Chemistry*, *287*(19), 16017–16028. https://doi.org/10.1074/jbc.M111.252577

Oblak, A. L., Forner, S., Territo, P. R., Sasner, M., Carter, G. W., Howell, G. R., Sukoff-Rizzo, S. J., Logsdon, B. A., Mangravite, L. M., Mortazavi, A., Baglietto-Vargas, D., Green, K. N., MacGregor, G. R., Wood, M. A., Tenner, A. J., LaFerla, F. M., & Lamb, B. T. (2020). Model organism development and evaluation for late-onset Alzheimer's disease: MODEL-AD. *Alzheimer's & Dementia: Translational Research & Clinical Interventions*, *6*(1). https://doi.org/10.1002/trc2.12110

O'Brien, J. A., Lemaire, W., Chen, T.-B., Chang, R. S. L., Jacobson, M. A., Ha, S. N., Lindsley, C. W., Schaffhauser, H. J., Sur, C., Pettibone, D. J., Conn, P. J., & Williams, D. L. (2003). A Family of Highly Selective Allosteric Modulators of the Metabotropic Glutamate Receptor Subtype 5. *Molecular Pharmacology*, *64*(3), 731–740. https://doi.org/10.1124/mol.64.3.731

O'Brien, J. A., Lemaire, W., Wittmann, M., Jacobson, M. A., Ha, S. N., Wisnoski, D. D., Lindsley, C. W., Schaffhauser, H. J., Rowe, B., Sur, C., Duggan, M. E., Pettibone, D. J., Conn, P. J., & Williams, D. L. (2004). A Novel Selective Allosteric Modulator Potentiates the Activity of Native Metabotropic Glutamate Receptor Subtype 5 in Rat Forebrain. *Journal of Pharmacology and Experimental Therapeutics*, *309*(2), 568–577. https://doi.org/10.1124/jpet.103.061747

Oddo, S., Caccamo, A., Shepherd, J. D., Murphy, M. P., Golde, T. E., Kayed, R., Metherate, R., Mattson, M. P., Akbari, Y., & LaFerla, F. M. (2003). Triple-Transgenic Model of Alzheimer's Disease with Plaques and Tangles. *Neuron*, *39*(3), 409–421. https://doi.org/10.1016/S0896-6273(03)00434-3

Oehme, I., Bösser, S., & Zörnig, M. (2006). Agonists of an ecdysone-inducible mammalian expression system inhibit Fas Ligand- and TRAIL-induced apoptosis in the human colon carcinoma cell line RKO. *Cell Death & Differentiation*, *13*(2), 189–201. https://doi.org/10.1038/sj.cdd.4401730

O'Gorman, S., Fox, D. T., & Wahl, G. M. (1991). Recombinase-Mediated Gene Activation and Site-Specific Integration in Mammalian Cells. *Science*, *251*(4999), 1351–1355. https://doi.org/10.1126/science.1900642

O'Hara, P. J., Sheppard, P. O., Thógersen, H., Venezia, D., Haldeman, B. A., McGrane, V., Houamed, K. M., Thomsen, C., Gilbert, T. L., & Mulvihill, E. R. (1993). The ligand-binding domain in metabotropic glutamate receptors is related to bacterial periplasmic binding proteins. *Neuron*, *11*(1), 41–52. https://doi.org/10.1016/0896-6273(93)90269-W

Ohno-Shosaku T., Maejima T., Kano M. (2001). Endogenous cannabinoids mediate retrograde signals from depolarized postsynaptic neurons to presynaptic terminals. *Neuron*. 29(3):729-38. doi: 10.1016/s0896-6273(01)00247-1.

Ohno-Shosaku T., Shosaku J., Tsubokawa H., Kano M. (2002). Cooperative endocannabinoid production by neuronal depolarization and group I metabotropic glutamate receptor activation. *Eur J Neurosci*. 15(6):953-61. doi: 10.1046/j.1460-9568.2002.01929.x.

Ojeda-Juárez, D., Lawrence, J. A., Soldau, K., Pizzo, D. P., Wheeler, E., Aguilar-Calvo, P., Khuu, H., Chen, J., Malik, A., Funk, G., Nam, P., Sanchez, H., Geschwind, M. D., Wu, C., Yeo, G. W., Chen, X., Patrick, G. N., & Sigurdson, C. J. (2022). Prions induce an early Arc response and a subsequent reduction in mGluR5 in the hippocampus. *Neurobiology of Disease*, *172*, 105834. https://doi.org/10.1016/j.nbd.2022.105834

O'Leary, L. A., Davoli, M. A., Belliveau, C., Tanti, A., Ma, J. C., Farmer, W. T., Turecki, G., Murai, K. K., & Mechawar, N. (2020). Characterization of Vimentin-Immunoreactive Astrocytes in the Human Brain. *Frontiers in Neuroanatomy*, *14*. https://doi.org/10.3389/fnana.2020.00031

Oldham, W. M., & E. Hamm, H. (2006). Structural basis of function in heterotrimeric G proteins. *Quarterly Reviews of Biophysics*, *39*(2), 117–166. https://doi.org/10.1017/S0033583506004306

Oldham, W. M., & Hamm, H. E. (2008). Heterotrimeric G protein activation by G-protein-coupled receptors. *Nature Reviews Molecular Cell Biology*, *9*(1), 60–71. https://doi.org/10.1038/nrm2299

Olsen, C. M., Childs, D. S., Stanwood, G. D., & Winder, D. G. (2010). Operant Sensation Seeking Requires Metabotropic Glutamate Receptor 5 (mGluR5). *PLoS ONE*, *5*(11), e15085. https://doi.org/10.1371/journal.pone.0015085

O'Malley, K. L., Jong, Y.-J. I., Gonchar, Y., Burkhalter, A., & Romano, C. (2003). Activation of Metabotropic Glutamate Receptor mGlu5 on Nuclear Membranes Mediates Intranuclear Ca2+ Changes in Heterologous Cell Types and Neurons. *Journal of Biological Chemistry*, *278*(30), 28210–28219. https://doi.org/10.1074/jbc.M300792200

O'Riordan, K. J., Huang, I.-C., Pizzi, M., Spano, P., Boroni, F., Egli, R., Desai, P., Fitch, O., Malone, L., Jin Ahn, H., Liou, H.-C., Sweatt, J. D., & Levenson, J. M. (2006). Regulation of Nuclear Factor κB in the Hippocampus by Group I Metabotropic Glutamate Receptors. *The Journal of Neuroscience*, *26*(18), 4870–4879. https://doi.org/10.1523/JNEUROSCI.4527-05.2006

O'Shea, M., Maytham, E. G., Linehan, J. M., Brandner, S., Collinge, J., & Lloyd, S. E. (2008). Investigation of *Mcp1* as a Quantitative Trait Gene for Prion Disease Incubation Time in Mouse. *Genetics*, *180*(1), 559–566. https://doi.org/10.1534/genetics.108.090894

Oskarsson, B., Gendron, T. F., & Staff, N. P. (2018). Amyotrophic Lateral Sclerosis: An Update for 2018. *Mayo Clinic Proceedings*, *93*(11), 1617–1628. https://doi.org/10.1016/j.mayocp.2018.04.007

Overk, C. R., Cartier, A., Shaked, G., Rockenstein, E., Ubhi, K., Spencer, B., Price, D. L., Patrick, C., Desplats, P., & Masliah, E. (2014). Hippocampal neuronal cells that accumulate α-synuclein fragments are more vulnerable to Aß oligomer toxicity via mGluR5 – implications for dementia with Lewy bodies. *Molecular Neurodegeneration*, *9*(1), 18. https://doi.org/10.1186/1750-1326-9-18

Pagano, A., Rüegg, D., Litschig, S., Stoehr, N., Stierlin, C., Heinrich, M., Floersheim, P., Prezèau, L., Carroll, F., Pin, J. P., Cambria, A., Vranesic, I., Flor, P. J., Gasparini, F., & Kuhn, R. (2000). The non-competitive antagonists 2-methyl-6-(phenylethynyl)pyridine and 7-hydroxyiminocyclopropan [b]chromen-1a-carboxylic acid ethyl ester interact with overlapping binding pockets in the transmembrane region of group I metabotropic glutamate receptors. *Journal of Biological Chemistry*, *275*(43), 33750–33758. https://doi.org/10.1074/jbc.M006230200

Pal, K., Melcher, K., & Xu, H. E. (2012). Structure and mechanism for recognition of peptide hormones by Class B G-protein-coupled receptors. *Acta Pharmacologica Sinica*, *33*(3), 300–311. https://doi.org/10.1038/aps.2011.170

Pałucha, A., Brański, P., Szewczyk, B., Wierońska, J. M., Kłak, K., & Pilc, A. (2005). Potential antidepressant-like effect of MTEP, a potent and highly selective mGluR5 antagonist. *Pharmacology Biochemistry and Behavior*, *81*(4), 901–906. https://doi.org/10.1016/j.pbb.2005.06.015

Pan, K. M., Baldwin, M., Nguyen, J., Gasset, M., Serban, A., Groth, D., Mehlhorn, I., Huang, Z., Fletterick, R. J., & Cohen, F. E. (1993). Conversion of alpha-helices into beta-sheets features in the formation of the scrapie prion proteins. *Proceedings of the National Academy of Sciences*, *90*(23), 10962–10966. https://doi.org/10.1073/pnas.90.23.10962

Paoletti, P. (2011). Molecular basis of NMDA receptor functional diversity. *European Journal of Neuroscience*, *33*(8), 1351–1365. https://doi.org/10.1111/j.1460-9568.2011.07628.x

Paquet, M., Ribeiro, F. M., Guadagno, J., Esseltine, J. L., Ferguson, S. S., & Cregan, S. P. (2013). Role of metabotropic glutamate receptor 5 signaling and homer in oxygen glucose deprivation-mediated astrocyte apoptosis. *Molecular Brain*, *6*(1), 9. https://doi.org/10.1186/1756-6606-6-9

Park, D., Jhon, D. Y., Lee, C. W., Lee, K. H., & Rhee, S. G. (1993). Activation of phospholipase C isozymes by G protein beta gamma subunits. *The Journal of Biological Chemistry*, *268*(7), 4573–4576.

Park, H.-J., Westin, C.-F., Kubicki, M., Maier, S. E., Niznikiewicz, M., Baer, A., Frumin, M., Kikinis, R., Jolesz, F. A., McCarley, R. W., & Shenton, M. E. (2004). White matter hemisphere asymmetries in healthy subjects and in schizophrenia: a diffusion tensor MRI study. *NeuroImage*, *23*(1), 213–223. https://doi.org/10.1016/j.neuroimage.2004.04.036

Parmentier-Batteur, S., Hutson, P. H., Menzel, K., Uslaner, J. M., Mattson, B. A., O'Brien, J. A., Magliaro, B. C., Forest, T., Stump, C. A., Tynebor, R. M., Anthony, N. J., Tucker, T. J., Zhang, X. F., Gomez, R., Huszar, S. L., Lambeng, N., Fauré, H., Le Poul, E., Poli, S., … Williams, T. M. (2014). Mechanism based neurotoxicity of mGlu5 positive allosteric modulators – Development challenges for a promising novel antipsychotic target. *Neuropharmacology*, *82*, 161–173. https://doi.org/10.1016/J.NEUROPHARM.2012.12.003

Parsons, R. G., Gafford, G. M., & Helmstetter, F. J. (2006). Translational Control via the Mammalian Target of Rapamycin Pathway Is Critical for the Formation and Stability of Long-Term Fear Memory in Amygdala Neurons. *The Journal of*

Neuroscience, *26*(50), 12977–12983. https://doi.org/10.1523/JNEUROSCI.4209-06.2006

Pasti, L., Volterra, A., Pozzan, T., & Carmignoto, G. (1997). Intracellular Calcium Oscillations in Astrocytes: A Highly Plastic, Bidirectional Form of Communication between Neurons and Astrocytes *In Situ*. *The Journal of Neuroscience*, *17*(20), 7817–7830. https://doi.org/10.1523/JNEUROSCI.17-20-07817.1997

Patel, A. J., & Honoré, E. (2001). Properties and modulation of mammalian 2P domain K+ channels. *Trends in Neurosciences*, *24*(6), 339–346. https://doi.org/10.1016/S0166-2236(00)01810-5

Patel, A. J., Honoré, E., Lesage, F., Fink, M., Romey, G., & Lazdunski, M. (1999). Inhalational anesthetics activate two-pore-domain background K+ channels. *Nature Neuroscience*, *2*(5), 422–426. https://doi.org/10.1038/8084

Patriarchi, T., Buonarati, O. R., & Hell, J. W. (2018). Postsynaptic localization and regulation of AMPA receptors and Cav1.2 by ß2 adrenergic receptor/PKA and Ca^{2+} /CaMKII signaling. *The EMBO Journal*, *37*(20). https://doi.org/10.15252/embj.201899771

Paul, S.M., Mytelka, D.S., Dunwiddie, C.T., Persinger, C.C., Munos, B.H., Lindborg, S.R., Schacht, A.L., 2010. How to improve R&D productivity: the pharmaceutical industry's grand challenge. Nat Rev Drug Discov 9, 203–214. https://doi.org/10.1038/nrd3078

Payne, S. H. (2015). The utility of protein and mRNA correlation. *Trends in Biochemical Sciences*, *40*(1), 1–3. https://doi.org/10.1016/j.tibs.2014.10.010

Peggion, C., Stella, R., Lorenzon, P., Spisni, E., Bertoli, A., & Massimino, M. L. (2020). Microglia in Prion Diseases: Angels or Demons? *International Journal of Molecular Sciences*, *21*(20), 7765. https://doi.org/10.3390/ijms21207765

Pekny, M. (2001). *Astrocytic intermediate filaments: lessons from GFAP and vimentin knock-out mice* (pp. 23–30). https://doi.org/10.1016/S0079-6123(01)32062-9

Petkova, A. T., Leapman, R. D., Guo, Z., Yau, W.-M., Mattson, M. P., & Tycko, R. (2005). Self-Propagating, Molecular-Level Polymorphism in Alzheimer's ß-Amyloid Fibrils. *Science*, *307*(5707), 262–265. https://doi.org/10.1126/science.1105850

Philips, T., & Rothstein, J. D. (2015). Rodent Models of Amyotrophic Lateral Sclerosis. *Current Protocols in Pharmacology*, *69*(1). https://doi.org/10.1002/0471141755.ph0567s69

Picher-Martel, V., Valdmanis, P. N., Gould, P. V., Julien, J.-P., & Dupré, N. (2016). From animal models to human disease: a genetic approach for personalized medicine in ALS. *Acta Neuropathologica Communications*, *4*(1), 70. https://doi.org/10.1186/s40478-016-0340-5

Pierce, K. L., & Lefkowitz, R. J. (2001). Classical and new roles of ß-arrestins in the regulation of G-PROTEIN-COUPLED receptors. *Nature Reviews Neuroscience*, *2*(10), 727–733. https://doi.org/10.1038/35094577

Pieri, L., Madiona, K., Bousset, L., & Melki, R. (2012). Fibrillar α-Synuclein and Huntingtin Exon 1 Assemblies Are Toxic to the Cells. *Biophysical Journal*, *102*(12), 2894–2905. https://doi.org/10.1016/j.bpj.2012.04.050

Piers, T. M., Heales, S. J., & Pocock, J. M. (2011). Positive allosteric modulation of metabotropic glutamate receptor 5 down-regulates fibrinogen-activated microglia providing neuronal protection. *Neuroscience Letters*, *505*(2), 140–145. https://doi.org/10.1016/J.NEULET.2011.10.007

Pin, J.-P., & Bettler, B. (2016). Organization and functions of mGlu and GABAB receptor complexes. *Nature*, *540*(7631), 60–68. https://doi.org/10.1038/nature20566

Pin, J.-P., & Duvoisin, R. (1995). The metabotropic glutamate receptors: Structure and functions. *Neuropharmacology*, *34*(1), 1–26. https://doi.org/10.1016/0028-3908(94)00129-G

Pin, J.-P., Galvez, T., & Prézeau, L. (2003). Evolution, structure, and activation mechanism of family 3/C G-protein-coupled receptors. *Pharmacology & Therapeutics*, *98*(3), 325–354. https://doi.org/10.1016/S0163-7258(03)00038-X

Pin, J.-P., Kniazeff, J., Liu, J., Binet, V., Goudet, C., Rondard, P., & Prézeau, L. (2005). Allosteric functioning of dimeric class C G-protein-coupled receptors. *FEBS Journal*, *272*(12), 2947–2955. https://doi.org/10.1111/j.1742-4658.2005.04728.x

Pisani, A., Gubellini, P., Bonsi, P., Conquet, F., Picconi, B., Centonze, D., Bernardi, G., & Calabresi, P. (2001). Metabotropic glutamate receptor 5 mediates the potentiation of N-methyl-D-aspartate responses in medium spiny striatal neurons. *Neuroscience*, *106*(3), 579–587. https://doi.org/10.1016/S0306-4522(01)00297-4

Plath, N., Ohana, O., Dammermann, B., Errington, M.L., Schmitz, D., Gross, C., Mao, X., Engelsberg, A., Mahlke, C., Welzl, H., Kobalz, U., Stawrakakis, A., Fernandez, E., Waltereit, R., Bick-Sander, A., Therstappen, E., Cooke, S.F., Blanquet, V., Wurst, W., Salmen, B., Bösl, M.R., Lipp, H.-P., Grant, S.G.N., Bliss, T.V.P., Wolfer, D.P., Kuhl, D., 2006. Arc/Arg3.1 Is Essential for the Consolidation of Synaptic Plasticity and Memories. Neuron 52, 437–444. https://doi.org/10.1016/j.neuron.2006.08.024

Pooler, A. M., Noble, W., & Hanger, D. P. (2014). A role for tau at the synapse in Alzheimer's disease pathogenesis. *Neuropharmacology*, *76 Pt A*(PART A), 1–8. https://doi.org/10.1016/J.NEUROPHARM.2013.09.018

Porter, R. H. P., Jaeschke, G., Spooren, W., Ballard, T. M., Büttelmann, B., Kolczewski, S., Peters, J.-U., Prinssen, E., Wichmann, J., Vieira, E., Mühlemann, A., Gatti, S., Mutel, V., & Malherbe, P. (2005). Fenobam: A Clinically Validated Nonbenzodiazepine Anxiolytic Is a Potent, Selective, and Noncompetitive mGlu5 Receptor Antagonist with Inverse Agonist Activity. *Journal of Pharmacology and Experimental Therapeutics*, *315*(2), 711–721. https://doi.org/10.1124/jpet.105.089839

Pouladi, M. A., Morton, A. J., & Hayden, M. R. (2013). Choosing an animal model for the study of Huntington's disease. *Nature Reviews Neuroscience*, *14*(10), 708–721. https://doi.org/10.1038/nrn3570

Pound, P., Ritskes-Hoitinga, M., 2018. Is it possible to overcome issues of external validity in preclinical animal research? Why most animal models are bound to fail. J Transl Med 16, 304. https://doi.org/10.1186/s12967-018-1678-1

Price, D. L., Rockenstein, E., Ubhi, K., Phung, V., Maclean-Lewis, N., Askay, D., Cartier, A., Spencer, B., Patrick, C., Desplats, P., Ellisman, M. H., & Masliah, E. (2010). Alterations in mGluR5 expression and signaling in Lewy body disease and in transgenic models of alpha-synucleinopathy--implications for excitotoxicity. *PloS One*, *5*(11). https://doi.org/10.1371/JOURNAL.PONE.0014020

Proctor, D. T., Coulson, E. J., & Dodd, P. R. (2010). Reduction in Post-Synaptic Scaffolding PSD-95 and SAP-102 Protein Levels in the Alzheimer Inferior Temporal Cortex is Correlated with Disease Pathology. *Journal of Alzheimer's Disease*, *21*(3), 795–811. https://doi.org/10.3233/JAD-2010-100090

Prömel, S., Langenhan, T., & Araç, D. (2013). Matching structure with function: the GAIN domain of Adhesion-GPCR and PKD1-like proteins. *Trends in Pharmacological Sciences*, *34*(8), 470–478. https://doi.org/10.1016/j.tips.2013.06.002

Pronin, A. N. (2004). Identification of Ligands for Two Human Bitter T2R Receptors. *Chemical Senses*, *29*(7), 583–593. https://doi.org/10.1093/chemse/bjh064

Prusiner, S. B. (1982). Novel Proteinaceous Infectious Particles Cause Scrapie. *Science*, *216*(4542), 136–144. https://doi.org/10.1126/science.6801762

Prusiner, S. B. (1998). Prions. *Proceedings of the National Academy of Sciences*, *95*(23), 13363–13383. https://doi.org/10.1073/pnas.95.23.13363

Prüßing, K., Voigt, A., & Schulz, J. B. (2013). Drosophila melanogaster as a model organism for Alzheimer's disease. *Molecular Neurodegeneration*, *8*(1), 35. https://doi.org/10.1186/1750-1326-8-35

Purgert, C. A., Izumi, Y., Jong, Y.-J. I., Kumar, V., Zorumski, C. F., & O'Malley, K. L. (2014). Intracellular mGluR5 Can Mediate Synaptic Plasticity in the Hippocampus. *Journal of Neuroscience*, *34*(13), 4589–4598. https://doi.org/10.1523/JNEUROSCI.3451-13.2014

Pupillo, E., Bianchi, E., Chiò, A., Casale, F., Zecca, C., Tortelli, R., & Beghi, E. (2018). Amyotrophic lateral sclerosis and food intake. *Amyotrophic Lateral Sclerosis and Frontotemporal Degeneration*, *19*(3–4), 267–274. https://doi.org/10.1080/21678421.2017.1418002

Quiroz, J. A., Tamburri, P., Deptula, D., Banken, L., Beyer, U., Rabbia, M., Parkar, N., Fontoura, P., & Santarelli, L. (2016). Efficacy and Safety of Basimglurant as Adjunctive Therapy for Major Depression. *JAMA Psychiatry*, *73*(7), 675. https://doi.org/10.1001/jamapsychiatry.2016.0838

Raeber, A. J. (1997). Astrocyte-specific expression of hamster prion protein (PrP) renders PrP knockout mice susceptible to hamster scrapie. *The EMBO Journal*, *16*(20), 6057–6065. https://doi.org/10.1093/emboj/16.20.6057

Rajagopal, S., Rajagopal, K., & Lefkowitz, R. J. (2010). Teaching old receptors new tricks: biasing seven-transmembrane receptors. *Nature Reviews Drug Discovery*, *9*(5), 373–386. https://doi.org/10.1038/nrd3024

Rajagopal, S., & Shenoy, S. K. (2018). GPCR desensitization: Acute and prolonged phases. *Cellular Signalling*, *41*, 9–16. https://doi.org/10.1016/j.cellsig.2017.01.024

Ransohoff, R. M. (2016). How neuroinflammation contributes to neurodegeneration. *Science (New York, N.Y.)*, *353*(6301), 777–783. https://doi.org/10.1126/SCIENCE.AAG2590

Rare Disease Database, 2018. (2018). Fatal Familial Insomnia. Accessed June 12, 2023. https://rarediseases.org/rare-diseases/fatal-familial-insomnia/.

Ray, K., & Hauschild, B. C. (2000). Cys-140 Is Critical for Metabotropic Glutamate Receptor-1 Dimerization. *Journal of Biological Chemistry*, *275*(44), 34245–34251. https://doi.org/10.1074/jbc.M005581200

Reichel, C. M., Schwendt, M., McGinty, J. F., Olive, M. F., & See, R. E. (2011). Loss of Object Recognition Memory Produced by Extended Access to Methamphetamine Self-Administration is Reversed by Positive Allosteric Modulation of Metabotropic Glutamate Receptor 5. *Neuropsychopharmacology*, *36*(4), 782–792. https://doi.org/10.1038/npp.2010.212

Renner, M., Lacor, P. N., Velasco, P. T., Xu, J., Contractor, A., Klein, W. L., & Triller, A. (2010). Deleterious Effects of Amyloid ß Oligomers Acting as an Extracellular Scaffold for mGluR5. *Neuron*, *66*(5), 739–754. https://doi.org/10.1016/j.neuron.2010.04.029

Resenberger, U. K., Harmeier, A., Woerner, A. C., Goodman, J. L., Müller, V., Krishnan, R., Vabulas, R. M., Kretzschmar, H. A., Lindquist, S., Hartl, F. U., Multhaup, G., Winklhofer, K. F., & Tatzelt, J. (2011). The cellular prion protein mediates neurotoxic signalling of ß-sheet-rich conformers independent of prion replication. *The EMBO Journal*, *30*(10), 2057–2070. https://doi.org/10.1038/emboj.2011.86

Ribé, E. M., Pérez, M., Puig, B., Gich, I., Lim, F., Cuadrado, M., Sesma, T., Catena, S., Sánchez, B., Nieto, M., Gómez-Ramos, P., Morán, M. A., Cabodevilla, F.,

Samaranch, L., Ortiz, L., Pérez, A., Ferrer, I., Avila, J., & Gómez-Isla, T. (2005). Accelerated amyloid deposition, neurofibrillary degeneration and neuronal loss in double mutant APP/tau transgenic mice. *Neurobiology of Disease*, *20*(3), 814–822. https://doi.org/10.1016/j.nbd.2005.05.027

Ribeiro, F. M., DeVries, R. A., Hamilton, A., Guimaraes, I. M., Cregan, S. P., Pires, R. G. W., & Ferguson, S. S. G. (2014). Metabotropic glutamate receptor 5 knockout promotes motor and biochemical alterations in a mouse model of Huntington's disease. *Human Molecular Genetics*, *23*(8), 2030–2042. https://doi.org/10.1093/hmg/ddt598

Ribeiro, F. M., Ferreira, L. T., Paquet, M., Cregan, T., Ding, Q., Gros, R., & Ferguson, S. S. G. (2009). Phosphorylation-independent Regulation of Metabotropic Glutamate Receptor 5 Desensitization and Internalization by G Protein-coupled Receptor Kinase 2 in Neurons. *Journal of Biological Chemistry*, *284*(35), 23444–23453. https://doi.org/10.1074/jbc.M109.000778

Ribeiro, F. M., Paquet, M., Ferreira, L. T., Cregan, T., Swan, P., Cregan, S. P., & Ferguson, S. S. G. (2010). Metabotropic Glutamate Receptor-Mediated Cell Signaling Pathways Are Altered in a Mouse Model of Huntington's Disease. *The Journal of Neuroscience*, *30*(1), 316. https://doi.org/10.1523/JNEUROSCI.4974-09.2010

Riek, R., Hornemann, S., Wider, G., Billeter, M., Glockshuber, R., & Wüthrich, K. (1996). NMR structure of the mouse prion protein domain PrP(121–231). *Nature*, *382*(6587), 180–182. https://doi.org/10.1038/382180a0

Riek, R., Hornemann, S., Wider, G., Glockshuber, R. & Wuthrich, K. (1997). NMR characterization of the full-length recombinant murine prion protein, mPrP(23-231). *FEBS Lett*, 413, 282-8.

Ripps, M. E., Huntley, G. W., Hof, P. R., Morrison, J. H., & Gordon, J. W. (1995). Transgenic mice expressing an altered murine superoxide dismutase gene provide an animal model of amyotrophic lateral sclerosis. *Proceedings of the National Academy of Sciences*, *92*(3), 689–693. https://doi.org/10.1073/pnas.92.3.689

Rivera-Milla, E., Stuermer, C. A. O., & Málaga-Trillo, E. (2003). An evolutionary basis for scrapie disease: identification of a fish prion mRNA. *Trends in Genetics*, *19*(2), 72–75. https://doi.org/10.1016/S0168-9525(02)00032-X

Rodriguez, A. L., Grier, M. D., Jones, C. K., Herman, E. J., Kane, A. S., Smith, R. L., Williams, R., Zhou, Y., Marlo, J. E., Days, E. L., Blatt, T. N., Jadhav, S., Menon, U. N., Vinson, P. N., Rook, J. M., Stauffer, S. R., Niswender, C. M., Lindsley, C. W., Weaver, C. D., & Conn, P. J. (2010). Discovery of Novel Allosteric Modulators of Metabotropic Glutamate Receptor Subtype 5 Reveals Chemical and Functional Diversity and In Vivo Activity in Rat Behavioral Models of Anxiolytic and Antipsychotic Activity. *Molecular Pharmacology*, *78*(6), 1105–1123. https://doi.org/10.1124/mol.110.067207

Rodríguez, J. J., Terzieva, S., Olabarria, M., Lanza, R. G., & Verkhratsky, A. (2013). Enriched environment and physical activity reverse astrogliodegeneration in the hippocampus of AD transgenic mice. *Cell Death & Disease*, *4*(6), e678–e678. https://doi.org/10.1038/cddis.2013.194

Rodrigues, S.M., Bauer, E.P., Farb, C.R., Schafe, G.E., LeDoux, J.E., 2002. The Group I Metabotropic Glutamate Receptor mGluR5 Is Required for Fear Memory Formation and Long-Term Potentiation in the Lateral Amygdala. The Journal of Neuroscience 22, 5219–5229. https://doi.org/10.1523/JNEUROSCI.22-12-05219.2002

Rojas, A., & Dingledine, R. (2013). Ionotropic Glutamate Receptors: Regulation by G-Protein-Coupled Receptors. *Molecular Pharmacology*, *83*(4), 746–752. https://doi.org/10.1124/mol.112.083352

Romano, C., Van den Pol, A. N., & O'Malley, K. L. (1996). Enhanced early developmental expression of the metabotropic glutamate receptor mGluR5 in rat brain: Protein, mRNA splice variants, and regional distribution. *The Journal of Comparative Neurology*, *367*(3), 403–412. https://doi.org/10.1002/(SICI)1096-9861(19960408)367:3<403::AID-CNE6>3.0.CO;2-9

Romano, C., Yang, W.-L., & O'Malley, K. L. (1996). Metabotropic Glutamate Receptor 5 Is a Disulfide-linked Dimer. *Journal of Biological Chemistry*, *271*(45), 28612–28616. https://doi.org/10.1074/jbc.271.45.28612

Rondard, P., Liu, J., Huang, S., Malhaire, F., Vol, C., Pinault, A., Labesse, G., & Pin, J.-P. (2006). Coupling of Agonist Binding to Effector Domain Activation in Metabotropic Glutamate-like Receptors. *Journal of Biological Chemistry*, *281*(34), 24653–24661. https://doi.org/10.1074/jbc.M602277200

Ronesi, J. A., & Huber, K. M. (2008). Homer Interactions Are Necessary for Metabotropic Glutamate Receptor-Induced Long-Term Depression and Translational Activation. *The Journal of Neuroscience*, *28*(2), 543–547. https://doi.org/10.1523/JNEUROSCI.5019-07.2008

Rong, R., Ahn, J.-Y., Huang, H., Nagata, E., Kalman, D., Kapp, J. A., Tu, J., Worley, P. F., Snyder, S. H., & Ye, K. (2003). PI3 kinase enhancer–Homer complex couples mGluRI to PI3 kinase, preventing neuronal apoptosis. *Nature Neuroscience*, *6*(11), 1153–1161. https://doi.org/10.1038/nn1134

Rook, J. M., Noetzel, M. J., Pouliot, W. A., Bridges, T. M., Vinson, P. N., Cho, H. P., Zhou, Y., Gogliotti, R. D., Manka, J. T., Gregory, K. J., Stauffer, S. R., Dudek, F. E., Xiang, Z., Niswender, C. M., Daniels, J. S., Jones, C. K., Lindsley, C. W., & Conn, P. J. (2013). Unique Signaling Profiles of Positive Allosteric Modulators of Metabotropic Glutamate Receptor Subtype 5 Determine Differences in In Vivo Activity. *Biological Psychiatry*, *73*(6), 501–509. https://doi.org/10.1016/j.biopsych.2012.09.012

Rook, J. M., Xiang, Z., Lv, X., Ghoshal, A., Dickerson, J. W., Bridges, T. M., Johnson, K. A., Foster, D. J., Gregory, K. J., Vinson, P. N., Thompson, A. D., Byun, N., Collier, R. L., Bubser, M., Nedelcovych, M. T., Gould, R. W., Stauffer, S. R., Daniels, J. S., Niswender, C. M., … Conn, P. J. (2015). Biased mGlu 5 -Positive Allosteric Modulators Provide In Vivo Efficacy without Potentiating mGlu 5 Modulation of NMDAR Currents. *Neuron*, *86*(4), 1029–1040. https://doi.org/10.1016/j.neuron.2015.03.063

Rosen, D. R., Siddique, T., Patterson, D., Figlewicz, D. A., Sapp, P., Hentati, A., Donaldson, D., Goto, J., O'Regan, J. P., Deng, H.-X., Rahmani, Z., Krizus, A., McKenna-Yasek, D., Cayabyab, A., Gaston, S. M., Berger, R., Tanzi, R. E., Halperin, J. J., Herzfeldt, B., … Brown, R. H. (1993). Mutations in Cu/Zn superoxide dismutase gene are associated with familial amyotrophic lateral sclerosis. *Nature*, *362*(6415), 59–62. https://doi.org/10.1038/362059a0

Rosenbaum, D. M., Rasmussen, S. G. F., & Kobilka, B. K. (2009). The structure and function of G-protein-coupled receptors. *Nature*, *459*(7245), 356–363. https://doi.org/10.1038/nature08144

Rosenkilde, M. M., & Schwartz, T. W. (2000). Potency of Ligands Correlates with Affinity Measured against Agonist and Inverse Agonists but Not against Neutral Ligand in Constitutively Active Chemokine Receptor. *Molecular Pharmacology*, *57*(3), 602–609. https://doi.org/10.1124/mol.57.3.602

Ross, C. A., Becher, M. W., Colomer, V., Engelender, S., Wood, J. D., & Sham, A. H. (1997). Huntington's Disease and Dentatorubral-Pallidoluysian Atrophy: Proteins, Pathogenesis and Pathology. *Brain Pathology*, *7*(3), 1003–1016. https://doi.org/10.1111/j.1750-3639.1997.tb00898.x

Ross, E. M., & Gilman, A. G. (1977). Resolution of some components of adenylate cyclase necessary for catalytic activity. *The Journal of Biological Chemistry*, *252*(20), 6966–6969.

Rossi, D., Brambilla, L., Valori, C. F., Roncoroni, C., Crugnola, A., Yokota, T., Bredesen, D. E., & Volterra, A. (2008). Focal degeneration of astrocytes in amyotrophic lateral sclerosis. *Cell Death & Differentiation 2008 15:11*, *15*(11), 1691–1700. https://doi.org/10.1038/cdd.2008.99

Rudd, P. M., Endo, T., Colominas, C., Groth, D., Wheeler, S. F., Harvey, D. J., Wormald, M. R., Serban, H., Prusiner, S. B., Kobata, A., & Dwek, R. A. (1999). Glycosylation differences between the normal and pathogenic prion protein isoforms. *Proceedings of the National Academy of Sciences*, *96*(23), 13044–13049. https://doi.org/10.1073/pnas.96.23.13044

Rush, A. M., Wu, J., Rowan, M. J., & Anwyl, R. (2002). Group I Metabotropic Glutamate Receptor (mGluR)-Dependent Long-Term Depression Mediated via p38 Mitogen-Activated Protein Kinase Is Inhibited by Previous High-Frequency Stimulation and Activation of mGluRs and Protein Kinase C in the Rat Dentate Gyrus *In Vitro*. *The Journal of Neuroscience*, *22*(14), 6121–6128. https://doi.org/10.1523/JNEUROSCI.22-14-06121.2002

Sahl, S. J., Weiss, L. E., Duim, W. C., Frydman, J., & Moerner, W. E. (2012). Cellular Inclusion Bodies of Mutant Huntingtin Exon 1 Obscure Small Fibrillar Aggregate Species. *Scientific Reports*, *2*(1), 895. https://doi.org/10.1038/srep00895

Saito, T., Matsuba, Y., Mihira, N., Takano, J., Nilsson, P., Itohara, S., Iwata, N., & Saido, T. C. (2014). Single App knock-in mouse models of Alzheimer's disease. *Nature Neuroscience*, *17*(5), 661–663. https://doi.org/10.1038/nn.3697

Saito, T., Matsuba, Y., Yamazaki, N., Hashimoto, S., & Saido, T. C. (2016). Calpain Activation in Alzheimer's Model Mice Is an Artifact of APP and Presenilin Overexpression. *The Journal of Neuroscience*, *36*(38), 9933–9936. https://doi.org/10.1523/JNEUROSCI.1907-16.2016

Saleem, S., & Kannan, R. R. (2018). Zebrafish: an emerging real-time model system to study Alzheimer's disease and neurospecific drug discovery. *Cell Death Discovery*, *4*(1), 45. https://doi.org/10.1038/s41420-018-0109-7

Salling, M. C., Grassetti, A., Ferrera, V. P., Martinez, D., & Foltin, R. W. (2021). Negative allosteric modulation of metabotropic glutamate receptor 5 attenuates alcohol self-administration in baboons. *Pharmacology Biochemistry and Behavior*, *208*, 173227. https://doi.org/10.1016/j.pbb.2021.173227

Salter, M. W. (1998). Src, N-methyl-d-aspartate (NMDA) receptors, and synaptic plasticity. *Biochemical Pharmacology*, *56*(7), 789–798. https://doi.org/10.1016/S0006-2952(98)00124-5

Salter, M. W., & Stevens, B. (2017). Microglia emerge as central players in brain disease. *Nature Medicine*, *23*(9), 1018–1027. https://doi.org/10.1038/nm.4397

Sandberg, M. K., Al-Doujaily, H., Sharps, B., De Oliveira, M. W., Schmidt, C., Richard-Londt, A., Lyall, S., Linehan, J. M., Brandner, S., Wadsworth, J. D. F., Clarke, A. R., & Collinge, J. (2014). Prion neuropathology follows the accumulation of alternate prion protein isoforms after infective titre has peaked. *Nature Communications*, *5*(1), 4347. https://doi.org/10.1038/ncomms5347

Sangwan, S., Zhao, A., Adams, K. L., Jayson, C. K., Sawaya, M. R., Guenther, E. L., Pan, A. C., Ngo, J., Moore, D. M., Soriaga, A. B., Do, T. D., Goldschmidt, L., Nelson, R., Bowers, M. T., Koehler, C. M., Shaw, D. E., Novitch, B. G., & Eisenberg, D. S. (2017). Atomic structure of a toxic, oligomeric segment of SOD1 linked to amyotrophic lateral sclerosis (ALS). *Proceedings of the National Academy of Sciences of the United States of America*, *114*(33), 8770–8775. https://doi.org/10.1073/pnas.1705091114

Santos, R., Ursu, O., Gaulton, A., Bento, A. P., Donadi, R. S., Bologa, C. G., Karlsson, A., Al-Lazikani, B., Hersey, A., Oprea, T. I., & Overington, J. P. (2017). A comprehensive map of molecular drug targets. *Nature Reviews Drug Discovery*, *16*(1), 19–34. https://doi.org/10.1038/nrd.2016.230

Sasaki, A., Hirato, J., & Nakazato, Y. (1993). Immunohistochemical study of microglia in the Creutzfeldt-Jakob diseased brain. *Acta Neuropathologica*, *86*(4), 337–344. https://doi.org/10.1007/BF00369445

Satlin, A., Wang, J., Logovinsky, V., Berry, S., Swanson, C., Dhadda, S., & Berry, D. A. (2016). Design of a Bayesian adaptive phase 2 proof-of-concept trial for BAN2401, a putative disease-modifying monoclonal antibody for the treatment of Alzheimer's disease. *Alzheimer's & Dementia: Translational Research & Clinical Interventions*, *2*(1), 1–12. https://doi.org/10.1016/j.trci.2016.01.001

Sattler, R., & Tymianski, M. (2000). Molecular mechanisms of calcium-dependent excitotoxicity. *Journal of Molecular Medicine (Berlin, Germany)*, *78*(1), 3–13. https://doi.org/10.1007/S001090000077

Saudou, F., Finkbeiner, S., Devys, D., & Greenberg, M. E. (1998). Huntingtin Acts in the Nucleus to Induce Apoptosis but Death Does Not Correlate with the Formation of Intranuclear Inclusions. *Cell*, *95*(1), 55–66. https://doi.org/10.1016/S0092-8674(00)81782-1

Sauer, B. (1994). Site-specific recombination: developments and applications. *Current Opinion in Biotechnology*, *5*(5), 521–527. https://doi.org/10.1016/0958-1669(94)90068-X

Savioz, A., Leuba, G., & Vallet, P. G. (2014). A framework to understand the variations of PSD-95 expression in brain aging and in Alzheimer's disease. *Ageing Research Reviews*, *18*, 86–94. https://doi.org/10.1016/j.arr.2014.09.004

Sayas, C. L., Ariaens, A., Ponsioen, B., & Moolenaar, W. H. (2006). GSK-3 Is Activated by the Tyrosine Kinase Pyk2 during LPA_1 -mediated Neurite Retraction. *Molecular Biology of the Cell*, *17*(4), 1834–1844. https://doi.org/10.1091/mbc.e05-07-0688

Scarpa, M., Molloy, C., Jenkins, L., Strellis, B., Budgett, R. F., Hesse, S., Dwomoh, L., Marsango, S., Tejeda, G. S., Rossi, M., Ahmed, Z., Milligan, G., Hudson, B. D., Tobin, A. B., & Bradley, S. J. (2021). Biased M1 muscarinic receptor mutant mice show accelerated progression of prion neurodegenerative disease. *Proceedings of the National Academy of Sciences*, *118*(50). https://doi.org/10.1073/pnas.2107389118

Scekic-Zahirovic, J., Oussini, H. El, Mersmann, S., Drenner, K., Wagner, M., Sun, Y., Allmeroth, K., Dieterlé, S., Sinniger, J., Dirrig-Grosch, S., René, F., Dormann, D., Haass, C., Ludolph, A. C., Lagier-Tourenne, C., Storkebaum, E., & Dupuis, L. (2017). Motor neuron intrinsic and extrinsic mechanisms contribute to the pathogenesis of FUS-associated amyotrophic lateral sclerosis. *Acta Neuropathologica*, *133*(6), 887–906. https://doi.org/10.1007/s00401-017-1687-9

Schafer, D. P., Lehrman, E. K., Kautzman, A. G., Koyama, R., Mardinly, A. R., Yamasaki, R., Ransohoff, R. M., Greenberg, M. E., Barres, B. A., & Stevens, B. (2012). Microglia sculpt postnatal neural circuits in an activity and complement-dependent manner. *Neuron*, *74*(4), 691–705. https://doi.org/10.1016/J.NEURON.2012.03.026

Scheckel, C., Imeri, M., Schwarz, P., & Aguzzi, A. (2020). Ribosomal profiling during prion disease uncovers progressive translational derangement in glia but not in neurons. *ELife*, *9*. https://doi.org/10.7554/eLife.62911

Scheff, S. W., DeKosky, S. T., & Price, D. A. (1990). Quantitative assessment of cortical synaptic density in Alzheimer's disease. *Neurobiology of Aging*, *11*(1), 29–37. https://doi.org/10.1016/0197-4580(90)90059-9

Scheff, S. W., Price, D. A., Schmitt, F. A., & Mufson, E. J. (2006). Hippocampal synaptic loss in early Alzheimer's disease and mild cognitive impairment. *Neurobiology of Aging*, *27*(10), 1372–1384. https://doi.org/10.1016/j.neurobiolaging.2005.09.012

Schiefer, J., Sprünken, A., Puls, C., Lüesse, H.-G., Milkereit, A., Milkereit, E., Johann, V., & Kosinski, C. M. (2004). The metabotropic glutamate receptor 5 antagonist MPEP and the mGluR2 agonist LY379268 modify disease progression in a transgenic mouse model of Huntington's disease. *Brain Research*, *1019*(1–2), 246–254. https://doi.org/10.1016/j.brainres.2004.06.005

Schiöth, H. B., & Fredriksson, R. (2005). The GRAFS classification system of G-protein coupled receptors in comparative perspective. *General and Comparative Endocrinology*, *142*(1–2), 94–101. https://doi.org/10.1016/j.ygcen.2004.12.018

Schiweck, J., Eickholt, B. J., & Murk, K. (2018). Important Shapeshifter: Mechanisms Allowing Astrocytes to Respond to the Changing Nervous System During Development, Injury and Disease. *Frontiers in Cellular Neuroscience*, *12*. https://doi.org/10.3389/FNCEL.2018.00261

Schneider, L. S. (2011). Lack of Evidence for the Efficacy of Memantine in Mild Alzheimer Disease. *Archives of Neurology*, *68*(8), 991. https://doi.org/10.1001/archneurol.2011.69

Schulte, G., & Wright, S. C. (2018). Frizzleds as GPCRs – More Conventional Than We Thought! *Trends in Pharmacological Sciences*, *39*(9), 828–842. https://doi.org/10.1016/j.tips.2018.07.001

Schultz, J., Schwarz, A., Neidhold, S., Burwinkel, M., Riemer, C., Simon, D., Kopf, M., Otto, M., & Baier, M. (2004). Role of Interleukin-1 in Prion Disease-Associated Astrocyte Activation. *The American Journal of Pathology*, *165*(2), 671–678. https://doi.org/10.1016/S0002-9440(10)63331-7

Schwappach, B. (2008). An overview of trafficking and assembly of neurotransmitter receptors and ion channels (Review). *Molecular Membrane Biology*, *25*(4), 270–278. https://doi.org/10.1080/09687680801960998

Scott, H. A., Gebhardt, F. M., Mitrovic, A. D., Vandenberg, R. J., & Dodd, P. R. (2011). Glutamate transporter variants reduce glutamate uptake in Alzheimer's disease. *Neurobiology of Aging*, *32*(3), 553.e1-553.e11. https://doi.org/10.1016/J.NEUROBIOLAGING.2010.03.008

Selkoe, D. J. (2011). Resolving controversies on the path to Alzheimer's therapeutics. *Nature Medicine*, *17*(9), 1060–1065. https://doi.org/10.1038/nm.2460

Selkoe, D. J., & Hardy, J. (2016). The amyloid hypothesis of Alzheimer's disease at 25 years. *EMBO Molecular Medicine*, *8*(6), 595–608. https://doi.org/10.15252/EMMM.201606210

Sengmany, K., & Gregory, K. J. (2016). Metabotropic glutamate receptor subtype 5: molecular pharmacology, allosteric modulation and stimulus bias. *British Journal of Pharmacology*, *173*(20), 3001–3017. https://doi.org/10.1111/bph.13281

Sengmany, K., Singh, J., Stewart, G. D., Conn, P. J., Christopoulos, A., & Gregory, K. J. (2017). Biased allosteric agonism and modulation of metabotropic glutamate receptor 5: Implications for optimising preclinical neuroscience drug discovery. *Neuropharmacology*, *115*, 60–72. https://doi.org/10.1016/j.neuropharm.2016.07.001

Serrano-Pozo, A., Frosch, M. P., Masliah, E., & Hyman, B. T. (2011). Neuropathological alterations in Alzheimer disease. *Cold Spring Harbor Perspectives in Medicine*, *1*(1). https://doi.org/10.1101/CSHPERSPECT.A006189

Sevigny, J., Chiao, P., Bussière, T., Weinreb, P. H., Williams, L., Maier, M., Dunstan, R., Salloway, S., Chen, T., Ling, Y., O'Gorman, J., Qian, F., Arastu, M., Li, M., Chollate, S., Brennan, M. S., Quintero-Monzon, O., Scannevin, R. H., Arnold, H. M., … Sandrock, A. (2016). The antibody aducanumab reduces Aß plaques in

Alzheimer's disease. *Nature*, *537*(7618), 50–56. https://doi.org/10.1038/nature19323

Shaftel, S.S., Griffin, W.S.T., O'Banion, M.K., 2008. The role of interleukin-1 in neuroinflammation and Alzheimer disease: an evolving perspective. J Neuroinflammation 5, 7. https://doi.org/10.1186/1742-2094-5-7

Shah, A., Silverstein, P. S., Singh, D. P., & Kumar, A. (2012). Involvement of metabotropic glutamate receptor 5, AKT/PI3K Signaling and NF-κB pathway in methamphetamine-mediated increase in IL-6 and IL-8 expression in astrocytes. *Journal of Neuroinflammation*, *9*(1), 1–10. https://doi.org/10.1186/1742-2094-9-52/FIGURES/5_547

Shao, C. Y., Mirra, S. S., Sait, H. B. R., Sacktor, T. C., & Sigurdsson, E. M. (2011). Postsynaptic degeneration as revealed by PSD-95 reduction occurs after advanced Aß and tau pathology in transgenic mouse models of Alzheimer's disease. *Acta Neuropathologica*, *122*(3), 285–292. https://doi.org/10.1007/s00401-011-0843-x

Sharief, M. K., Green, A., Dick, J. P. R., Gawler, J., & Thompson, E. J. (1999). Heightened intrathecal release of proinflammatory cytokines in Creutzfeldt-Jakob disease. *Neurology*, *52*(6), 1289–1289. https://doi.org/10.1212/WNL.52.6.1289

Shaw, P. J., Forrest, V., Ince, P. G., Richardson, J. P., & Wastell, H. J. (1995). CSF and Plasma Amino Acid Levels in Motor Neuron Disease: Elevation of CSF Glutamate in a Subset of Patients. *Neurodegeneration*, *4*(2), 209–216. https://doi.org/10.1006/neur.1995.0026

Shen M., Piser T.M., Seybold V.S., Thayer S.A. (1996). Cannabinoid receptor agonists inhibit glutamatergic synaptic transmission in rat hippocampal cultures. *J Neurosci*. 15;16(14):4322-34. doi: 10.1523/JNEUROSCI.16-14-04322.1996.

Sheng, M., & Kim, E. (2011). The Postsynaptic Organization of Synapses. *Cold Spring Harbor Perspectives in Biology*, *3*(12), a005678–a005678. https://doi.org/10.1101/cshperspect.a005678

Shenoy, S. K., Drake, M. T., Nelson, C. D., Houtz, D. A., Xiao, K., Madabushi, S., Reiter, E., Premont, R. T., Lichtarge, O., & Lefkowitz, R. J. (2006). ß-Arrestin-dependent, G Protein-independent ERK1/2 Activation by the ß2 Adrenergic Receptor. *Journal of Biological Chemistry*, *281*(2), 1261–1273. https://doi.org/10.1074/jbc.M506576200

Shepherd, J. D., & Bear, M. F. (2011). New views of Arc, a master regulator of synaptic plasticity. *Nature Neuroscience*, *14*(3), 279–284. https://doi.org/10.1038/nn.2708

Sherman, M. A., Lacroix, M., Amar, F., Larson, M. E., Forster, C., Aguzzi, A., Bennett, D. A., Ramsden, M., & Lesné, S. E. (2016). Soluble Conformers of Aß and Tau Alter Selective Proteins Governing Axonal Transport. *The Journal of Neuroscience*, *36*(37), 9647. https://doi.org/10.1523/JNEUROSCI.1899-16.2016

Shigemoto, R., Nomura, S., Ohishi, H., Sugihara, H., Nakanishi, S., & Mizuno, N. (1993). Immunohistochemical localization of a metabotropic glutamate receptor, mGluR5, in the rat brain. *Neuroscience Letters*, *163*(1), 53–57. https://doi.org/10.1016/0304-3940(93)90227-C

Shih, A. Y., Johnson, D. A., Wong, G., Kraft, A. D., Jiang, L., Erb, H., Johnson, J. A., & Murphy, T. H. (2003). Coordinate Regulation of Glutathione Biosynthesis and Release by Nrf2-Expressing Glia Potently Protects Neurons from Oxidative Stress. *The Journal of Neuroscience*, *23*(8), 3394. https://doi.org/10.1523/JNEUROSCI.23-08-03394.2003

Shin, S., Kwon, O., Kang, J. I., Kwon, S., Oh, S., Choi, J., Kim, C. H., & Kim, D. G. (2015). mGluR5 in the nucleus accumbens is critical for promoting resilience to

chronic stress. *Nature Neuroscience*, *18*(7), 1017–1024. https://doi.org/10.1038/nn.4028

Shinohara, M., Fujioka, S., Murray, M. E., Wojtas, A., Baker, M., Rovelet-Lecrux, A., Rademakers, R., Das, P., Parisi, J. E., Graff-Radford, N. R., Petersen, R. C., Dickson, D. W., & Bu, G. (2014). Regional distribution of synaptic markers and APP correlate with distinct clinicopathological features in sporadic and familial Alzheimer's disease. *Brain*, *137*(5), 1533–1549. https://doi.org/10.1093/brain/awu046

Shrivastava, A. N., Kowalewski, J. M., Renner, M., Bousset, L., Koulakoff, A., Melki, R., Giaume, C., & Triller, A. (2013). ß-amyloid and ATP-induced diffusional trapping of astrocyte and neuronal metabotropic glutamate type-5 receptors. *Glia*, *61*(10), 1673–1686. https://doi.org/10.1002/GLIA.22548

Si, Z.-Z., Zou, C.-J., Mei, X., Li, X.-F., Luo, H., Shen, Y., Hu, J., Li, X.-X., Wu, L., & Liu, Y. (2023). Targeting neuroinflammation in Alzheimer's disease: from mechanisms to clinical applications. *Neural Regeneration Research*, *18*(4), 708. https://doi.org/10.4103/1673-5374.353484

Sidiropoulos, K., Viteri, G., Sevilla, C., Jupe, S., Webber, M., Orlic-Milacic, M., Jassal, B., May, B., Shamovsky, V., Duenas, C., Rothfels, K., Matthews, L., Song, H., Stein, L., Haw, R., D'Eustachio, P., Ping, P., Hermjakob, H., & Fabregat, A. (2017). Reactome enhanced pathway visualization. *Bioinformatics*, *33*(21), 3461–3467. https://doi.org/10.1093/bioinformatics/btx441

Sieradzan, K. A., Mechan, A. O., Jones, L., Wanker, E. E., Nukina, N., & Mann, D. M. A. (1999). Huntington's Disease Intranuclear Inclusions Contain Truncated, Ubiquitinated Huntingtin Protein. *Experimental Neurology*, *156*(1), 92–99. https://doi.org/10.1006/exnr.1998.7005

Silva, A.J., Kogan, J.H., Frankland, P.W., Kida, S., 1998. CREB AND MEMORY. Annu Rev Neurosci 21, 127–148. https://doi.org/10.1146/annurev.neuro.21.1.127

Silva, G. A., Theriault, E., Mills, L. R., Pennefather, P. S., & Feeney, C. J. (1999). Group I and II metabotropic glutamate receptor expression in cultured rat spinal cord astrocytes. *Neuroscience Letters*, *263*(2–3), 117–120. https://doi.org/10.1016/S0304-3940(99)00145-7

Silverman, J. L., Tolu, S. S., Barkan, C. L., & Crawley, J. N. (2010). Repetitive Self-Grooming Behavior in the BTBR Mouse Model of Autism is Blocked by the mGluR5 Antagonist MPEP. *Neuropsychopharmacology*, *35*(4), 976–989. https://doi.org/10.1038/npp.2009.201

Simon, M. I., Strathmann, M. P., & Gautam, N. (1991). Diversity of G Proteins in Signal Transduction. *Science*, *252*(5007), 802–808. https://doi.org/10.1126/science.1902986

Sipos, E., Kurunczi, A., Kasza, Á., Horváth, J., Felszeghy, K., Laroche, S., Toldi, J., Párducz, Á., Penke, B., & Penke, Z. (2007). ß-Amyloid pathology in the entorhinal cortex of rats induces memory deficits: Implications for Alzheimer's disease. *Neuroscience*, *147*(1), 28–36. https://doi.org/10.1016/j.neuroscience.2007.04.011

Sitcheran, R., Comb, W. C., Cogswell, P. C., & Baldwin, A. S. (2008). Essential Role for Epidermal Growth Factor Receptor in Glutamate Receptor Signaling to NF-κB. *Molecular and Cellular Biology*, *28*(16), 5061–5070. https://doi.org/10.1128/MCB.00578-08

Skowrońska, K., Obara-Michlewska, M., Zielińska, M., & Albrecht, J. (2019). NMDA Receptors in Astrocytes: In Search for Roles in Neurotransmission and Astrocytic Homeostasis. *International Journal of Molecular Sciences*, *20*(2), 309. https://doi.org/10.3390/ijms20020309

Slattery, D. A., & Cryan, J. F. (2012). Using the rat forced swim test to assess antidepressant-like activity in rodents. *Nature Protocols*, *7*(6), 1009–1014. https://doi.org/10.1038/nprot.2012.044

Smith, E. S., Jonason, A., Reilly, C., Veeraraghavan, J., Fisher, T., Doherty, M., Klimatcheva, E., Mallow, C., Cornelius, C., Leonard, J. E., Marchi, N., Janigro, D., Argaw, A. T., Pham, T., Seils, J., Bussler, H., Torno, S., Kirk, R., Howell, A., … Zauderer, M. (2015). SEMA4D compromises blood–brain barrier, activates microglia, and inhibits remyelination in neurodegenerative disease. *Neurobiology of Disease*, *73*, 254–268. https://doi.org/10.1016/j.nbd.2014.10.008

Smith, J. A., Das, A., Ray, S. K., & Banik, N. L. (2012). Role of pro-inflammatory cytokines released from microglia in neurodegenerative diseases. *Brain Research Bulletin*, *87*(1), 10–20. https://doi.org/10.1016/j.brainresbull.2011.10.004

Smolders, I., De Klippel, N., Sarre, S., Ebinger, G., & Michotte, Y. (1995). Tonic GABA-ergic modulation of striatal dopamine release studied by in vivo microdialysis in the freely moving rat. *European Journal of Pharmacology*, *284*(1–2), 83–91. https://doi.org/10.1016/0014-2999(95)00369-V

Smrcka, A. V., & Fisher, I. (2019). G-protein βγ subunits as multi-functional scaffolds and transducers in G-protein-coupled receptor signaling. *Cellular and Molecular Life Sciences*, *76*(22), 4447–4459. https://doi.org/10.1007/s00018-019-03275-2

Song, C., Zhang, Y., Parsons, C. G., & Liu, Y. F. (2003). Expression of Polyglutamine-expanded Huntingtin Induces Tyrosine Phosphorylation of N-Methyl-D-aspartate Receptors. *Journal of Biological Chemistry*, *278*(35), 33364–33369. https://doi.org/10.1074/jbc.M304240200

Sorce, S., Nuvolone, M., Keller, A., Falsig, J., Varol, A., Schwarz, P., Bieri, M., Budka, H., & Aguzzi, A. (2014). The Role of the NADPH Oxidase NOX2 in Prion Pathogenesis. *PLoS Pathogens*, *10*(12), e1004531. https://doi.org/10.1371/journal.ppat.1004531

Sorensen, S. D., & Conn, P. J. (2003). G protein-coupled receptor kinases regulate metabotropic glutamate receptor 5 function and expression. *Neuropharmacology*, *44*(6), 699–706. https://doi.org/10.1016/S0028-3908(03)00053-4

Soto, C., Estrada, L., & Castilla, J. (2006). Amyloids, prions and the inherent infectious nature of misfolded protein aggregates. *Trends in Biochemical Sciences*, *31*(3), 150–155. https://doi.org/10.1016/j.tibs.2006.01.002

Southwell, A. L., Franciosi, S., Villanueva, E. B., Xie, Y., Winter, L. A., Veeraraghavan, J., Jonason, A., Felczak, B., Zhang, W., Kovalik, V., Waltl, S., Hall, G., Pouladi, M. A., Smith, E. S., Bowers, W. J., Zauderer, M., & Hayden, M. R. (2015). Anti-semaphorin 4D immunotherapy ameliorates neuropathology and some cognitive impairment in the YAC128 mouse model of Huntington disease. *Neurobiology of Disease*, *76*, 46–56. https://doi.org/10.1016/j.nbd.2015.01.002

Spampinato, S. F., Copani, A., Nicoletti, F., Sortino, M. A., & Caraci, F. (2018). Metabotropic glutamate receptors in glial cells: A new potential target for neuroprotection? *Frontiers in Molecular Neuroscience*, *11*, 414. https://doi.org/10.3389/FNMOL.2018.00414/BIBTEX

Spiering, D., & Hodgson, L. (2011). Dynamics of the Rho-family small GTPases in actin regulation and motility. *Cell Adhesion & Migration*, *5*(2), 170–180. https://doi.org/10.4161/cam.5.2.14403

Spina Purrello, V., Cormaci, G., Denaro, L., Reale, S., Costa, A., Lalicata, C., Sabbatini, M., Marchetti, B., & Avola, R. (2002). Effect of growth factors on nuclear and mitochondrial ADP-ribosylation processes during astroglial cell development and aging in culture. *Mechanisms of Ageing and Development*, *123*(5), 511–520. https://doi.org/10.1016/S0047-6374(01)00354-2

Spires-Jones, T. L., & Hyman, B. T. (2014). The Intersection of Amyloid Beta and Tau at Synapses in Alzheimer's Disease. *Neuron*, *82*(4), 756–771. https://doi.org/10.1016/J.NEURON.2014.05.004

Spurrier, J., Nicholson, L., Fang, X. T., Stoner, A. J., Toyonaga, T., Holden, D., Siegert, T. R., Laird, W., Allnutt, M. A., Chiasseu, M., Brody, A. H., Takahashi, H., Nies, S. H., Cañamás, A. P., Sadasivam, P., Lee, S., Li, S., Zhang, L., Huang, Y. H., … Strittmatter, S. M. (2022). Reversal of synapse loss in Alzheimer mouse models by targeting mGluR5 to prevent synaptic tagging by C1Q. *Science Translational Medicine*, *14*(647). https://doi.org/10.1126/scitranslmed.abi8593

Sriram, K., & Insel, P. A. (2018). G Protein-Coupled Receptors as Targets for Approved Drugs: How Many Targets and How Many Drugs? *Molecular Pharmacology*, *93*(4), 251–258. https://doi.org/10.1124/mol.117.111062

Stahl, N., Borchelt, D. R., Hsiao, K. & Prusiner, S. B. (1987). Scrapie prion protein contains a phosphatidylinositol glycolipid. *Cell,* 51, 229-240.

Steiger, A., & Pawlowski, M. (2019). Depression and Sleep. *International Journal of Molecular Sciences*, *20*(3), 607. https://doi.org/10.3390/ijms20030607

Stimson, E., Hope, J., Chong, A., & Burlingame, A. L. (1999). Site-Specific Characterization of the N-Linked Glycans of Murine Prion Protein by High-Performance Liquid Chromatography/Electrospray Mass Spectrometry and Exoglycosidase Digestions. *Biochemistry*, *38*(15), 4885–4895. https://doi.org/10.1021/bi982330q

Stoeck, K., Bodemer, M., Ciesielczyk, B., Meissner, B., Bartl, M., Heinemann, U., & Zerr, I. (2005). Interleukin 4 and Interleukin 10 Levels Are Elevated in the Cerebrospinal Fluid of Patients With Creutzfeldt-Jakob Disease. *Archives of Neurology*, *62*(10). https://doi.org/10.1001/archneur.62.10.1591

Stoppel, L. J., Auerbach, B. D., Senter, R. K., Preza, A. R., Lefkowitz, R. J., & Bear, M. F. (2017). β-Arrestin2 Couples Metabotropic Glutamate Receptor 5 to Neuronal Protein Synthesis and Is a Potential Target to Treat Fragile X. *Cell Reports*, *18*(12), 2807–2814. https://doi.org/10.1016/j.celrep.2017.02.075

Storto, M., Sallese, M., Salvatore, L., Poulet, R., Condorelli, D., Dell'Albani, P., Marcello, M., Romeo, R., Piomboni, P., Barone, N., Nicoletti, F., Nicoletti, F., De Blasi, A., 2001. Expression of metabotropic glutamate receptors in the rat and human testis. Journal of Endocrinology 170, 71–78. https://doi.org/10.1677/joe.0.1700071

Strumbo, B., Ronchi, S., Bolis, L. C., & Simonic, T. (2001). Molecular cloning of the cDNA coding for *Xenopus laevis* prion protein. *FEBS Letters*, *508*(2), 170–174. https://doi.org/10.1016/S0014-5793(01)03027-7

Sturchler-Pierrat, C., Abramowski, D., Duke, M., Wiederhold, K.-H., Mistl, C., Rothacher, S., Ledermann, B., Bürki, K., Frey, P., Paganetti, P. A., Waridel, C., Calhoun, M. E., Jucker, M., Probst, A., Staufenbiel, M., & Sommer, B. (1997). Two amyloid precursor protein transgenic mouse models with Alzheimer disease-like pathology. *Proceedings of the National Academy of Sciences*, *94*(24), 13287–13292. https://doi.org/10.1073/pnas.94.24.13287

Sullivan, J. M., Lim, K., Labaree, D., Lin, S., McCarthy, T. J., Seibyl, J. P., Tamagnan, G., Huang, Y., Carson, R. E., Ding, Y.-S., & Morris, E. D. (2013). Kinetic Analysis of the Metabotropic Glutamate Subtype 5 Tracer [18 F]FPEB in Bolus and Bolus-Plus-Constant-Infusion Studies in Humans. *Journal of Cerebral Blood Flow & Metabolism*, *33*(4), 532–541. https://doi.org/10.1038/jcbfm.2012.195

Sun, D., Gao, W., Hu, H., Zhou, S., 2022. Why 90% of clinical drug development fails and how to improve it? Acta Pharm Sin B 12, 3049–3062. https://doi.org/10.1016/j.apsb.2022.02.002

Sutherland, E. W. (1972). Studies on the Mechanism of Hormone Action. *Science*, *177*(4047), 401–408. https://doi.org/10.1126/science.177.4047.401

Swanson, C. J., Zhang, Y., Dhadda, S., Wang, J., Kaplow, J., Lai, R. Y. K., Lannfelt, L., Bradley, H., Rabe, M., Koyama, A., Reyderman, L., Berry, D. A., Berry, S., Gordon, R., Kramer, L. D., & Cummings, J. L. (2021). A randomized, double-blind, phase 2b proof-of-concept clinical trial in early Alzheimer's disease with lecanemab, an anti-Aß protofibril antibody. *Alzheimer's Research & Therapy*, *13*(1), 80. https://doi.org/10.1186/s13195-021-00813-8

Syrovatkina, V., Alegre, K. O., Dey, R., & Huang, X.-Y. (2016). Regulation, Signaling, and Physiological Functions of G-Proteins. *Journal of Molecular Biology*, *428*(19), 3850–3868. https://doi.org/10.1016/j.jmb.2016.08.002

Szczepek, M., Beyrière, F., Hofmann, K. P., Elgeti, M., Kazmin, R., Rose, A., Bartl, F. J., von Stetten, D., Heck, M., Sommer, M. E., Hildebrand, P. W., & Scheerer, P. (2014). Crystal structure of a common GPCR-binding interface for G protein and arrestin. *Nature Communications*, *5*(1), 4801. https://doi.org/10.1038/ncomms5801

Szczesny, R. J., Kowalska, K., Klosowska-Kosicka, K., Chlebowski, A., Owczarek, E. P., Warkocki, Z., Kulinski, T. M., Adamska, D., Affek, K., Jedroszkowiak, A., Kotrys, A. v., Tomecki, R., Krawczyk, P. S., Borowski, L. S., & Dziembowski, A. (2018). Versatile approach for functional analysis of human proteins and efficient stable cell line generation using FLP-mediated recombination system. *PLOS ONE*, *13*(3), e0194887. https://doi.org/10.1371/journal.pone.0194887

Tafuri, F., Ronchi, D., Magri, F., Comi, G. P., & Corti, S. (2015). SOD1 misplacing and mitochondrial dysfunction in amyotrophic lateral sclerosis pathogenesis. *Frontiers in Cellular Neuroscience*, *9*. https://doi.org/10.3389/fncel.2015.00336

Tallaksen-Greene, S. J., Kaatz, K. W., Romano, C., & Albin, R. L. (1998). Localization of mGluR1a-like immunoreactivity and mGluR5-like immunoreactivity in identified populations of striatal neurons. *Brain Research*, *780*(2), 210–217. https://doi.org/10.1016/S0006-8993(97)01141-4

Tahir, W., Abdulrahman, B., Abdelaziz, D. H., Thapa, S., Walia, R., & Schätzl, H. M. (2020). An astrocyte cell line that differentially propagates murine prions. *Journal of Biological Chemistry*, *295*(33), 11572–11583. https://doi.org/10.1074/jbc.RA120.012596

Tambini, M. D., Norris, K. A., & D'Adamio, L. (2020). Opposite changes in APP processing and human Aß levels in rats carrying either a protective or a pathogenic APP mutation. *ELife*, *9*. https://doi.org/10.7554/eLife.52612

Tamgüney, G., Giles, K., Glidden, D. V., Lessard, P., Wille, H., Tremblay, P., Groth, D. F., Yehiely, F., Korth, C., Moore, R. C., Tatzelt, J., Rubinstein, E., Boucheix, C., Yang, X., Stanley, P., Lisanti, M. P., Dwek, R. A., Rudd, P. M., Moskovitz, J., … Prusiner, S. B. (2008). Genes contributing to prion pathogenesis. *Journal of General Virology*, *89*(7), 1777–1788. https://doi.org/10.1099/vir.0.2008/001255-0

Tang, S. J., Fesharaki-Zadeh, A., Takahashi, H., Nies, S. H., Smith, L. M., Luo, A., Chyung, A., Chiasseu, M., & Strittmatter, S. M. (2020). Fyn kinase inhibition reduces protein aggregation, increases synapse density and improves memory in transgenic and traumatic Tauopathy. *Acta Neuropathologica Communications*, *8*(1), 96. https://doi.org/10.1186/s40478-020-00976-9

Tang, T.-S., Slow, E., Lupu, V., Stavrovskaya, I. G., Sugimori, M., Llinás, R., Kristal, B. S., Hayden, M. R., & Bezprozvanny, I. (2005). Disturbed Ca^{2+} signaling and apoptosis of medium spiny neurons in Huntington's disease. *Proceedings of the National Academy of Sciences*, *102*(7), 2602–2607. https://doi.org/10.1073/pnas.0409402102

Tang, T.-S., Tu, H., Chan, E. Y. W., Maximov, A., Wang, Z., Wellington, C. L., Hayden, M. R., & Bezprozvanny, I. (2003). Huntingtin and Huntingtin-Associated Protein 1 Influence Neuronal Calcium Signaling Mediated by Inositol-(1,4,5) Triphosphate Receptor Type 1. *Neuron*, *39*(2), 227–239. https://doi.org/10.1016/S0896-6273(03)00366-0

Tang, X., Wang, Y., Li, D., Luo, J., & Liu, M. (2012). Orphan G protein-coupled receptors (GPCRs): biological functions and potential drug targets. *Acta Pharmacologica Sinica*, *33*(3), 363–371. https://doi.org/10.1038/aps.2011.210

Tang, Z., Shao, X., Wu, J., Chen, H., Zhang, A., Xu, F., Ping, H., Li, S., Liu, C., Li, Y., Xue, X., & Yuan, B. (2021). Naloxone Protects against Lipopolysaccharide-Induced Neuroinflammation and Microglial Activation via Inhibiting ATP-Sensitive Potassium Channel. *Computational and Mathematical Methods in Medicine*, *2021*, 1–9. https://doi.org/10.1155/2021/7731528

Tatarczyńska, E., Kłodzińska, A., Chojnacka-Wójcik, E., Pałucha, A., Gasparini, F., Kuhn, R., Pilc, A., 2001. Potential anxiolytic- and antidepressant-like effects of MPEP, a potent, selective and systemically active mGlu5 receptor antagonist. Br J Pharmacol 132, 1423–1430. https://doi.org/10.1038/sj.bjp.0703923

Taylor, J. P., Brown, R. H., & Cleveland, D. W. (2016). Decoding ALS: from genes to mechanism. *Nature*, *539*(7628), 197–206. https://doi.org/10.1038/nature20413

Tcw, J., & Goate, A. M. (2017). Genetics of β-Amyloid Precursor Protein in Alzheimer's Disease. *Cold Spring Harbor Perspectives in Medicine*, *7*(6). https://doi.org/10.1101/CSHPERSPECT.A024539

Terry, R. D., Masliah, E., Salmon, D. P., Butters, N., DeTeresa, R., Hill, R., Hansen, L. A., & Katzman, R. (1991). Physical basis of cognitive alterations in Alzheimer's disease: synapse loss is the major correlate of cognitive impairment. *Annals of Neurology*, *30*(4), 572–580. https://doi.org/10.1002/ANA.410300410

Testa, C., Standaert, D., Young, A., & Penney, J. (1994). Metabotropic glutamate receptor mRNA expression in the basal ganglia of the rat. *The Journal of Neuroscience*, *14*(5), 3005–3018. https://doi.org/10.1523/JNEUROSCI.14-05-03005.1994

Thackray, A. M., McKenzie, A. N., Klein, M. A., Lauder, A., & Bujdoso, R. (2004). Accelerated Prion Disease in the Absence of Interleukin-10. *Journal of Virology*, *78*(24), 13697–13707. https://doi.org/10.1128/JVI.78.24.13697-13707.2004

Thambisetty, M., An, Y., & Tanaka, T. (2013). Alzheimer's disease risk genes and the age-at-onset phenotype. *Neurobiology of Aging*, *34*(11), 2696.e1-2696.e5. https://doi.org/10.1016/J.NEUROBIOLAGING.2013.05.028

Thandi, S., Blank, J. L., & Challiss, R. A. J. (2002). Group-I metabotropic glutamate receptors, mGlu1a and mGlu5a, couple to extracellular signal-regulated kinase (ERK) activation via distinct, but overlapping, signalling pathways. *Journal of Neurochemistry*, *83*(5), 1139–1153. https://doi.org/10.1046/j.1471-4159.2002.01217.x

Thomas, A., Burant, A., Bui, N., Graham, D., Yuva-Paylor, L. A., & Paylor, R. (2009). Marble burying reflects a repetitive and perseverative behavior more than novelty-induced anxiety. *Psychopharmacology*, *204*(2), 361–373. https://doi.org/10.1007/s00213-009-1466-y

Tobin, A. B. (2008). G-protein-coupled receptor phosphorylation: where, when and by whom. *British Journal of Pharmacology*, *153*(S1), S167–S176. https://doi.org/10.1038/sj.bjp.0707662

Traynelis, S. F., Wollmuth, L. P., McBain, C. J., Menniti, F. S., Vance, K. M., Ogden, K. K., Hansen, K. B., Yuan, H., Myers, S. J., & Dingledine, R. (2010). Glutamate Receptor Ion Channels: Structure, Regulation, and Function. *Pharmacological Reviews*, *62*(3), 405–496. https://doi.org/10.1124/pr.109.002451

Treyer, V., Gietl, A. F., Suliman, H., Gruber, E., Meyer, R., Buchmann, A., Johayem, A., Unschuld, P. G., Nitsch, R. M., Buck, A., Ametamey, S. M., & Hock, C. (2020). Reduced uptake of [11C]-ABP688, a PET tracer for metabolic glutamate receptor 5 in hippocampus and amygdala in Alzheimer's dementia. *Brain and Behavior*, *10*(6). https://doi.org/10.1002/BRB3.1632

Tribouillard-Tanvier, D., Striebel, J. F., Peterson, K. E., & Chesebro, B. (2009). Analysis of Protein Levels of 24 Cytokines in Scrapie Agent-Infected Brain and Glial Cell Cultures from Mice Differing in Prion Protein Expression Levels. *Journal of Virology*, *83*(21), 11244–11253. https://doi.org/10.1128/JVI.01413-09

Trinh, P. N. H., May, L. T., Leach, K., & Gregory, K. J. (2018). Biased agonism and allosteric modulation of metabotropic glutamate receptor 5. *Clinical Science*, *132*(21), 2323–2338. https://doi.org/10.1042/CS20180374

Trojsi, F., D'Alvano, G., Bonavita, S., & Tedeschi, G. (2020). Genetics and Sex in the Pathogenesis of Amyotrophic Lateral Sclerosis (ALS): Is There a Link? *International Journal of Molecular Sciences*, *21*(10), 3647. https://doi.org/10.3390/ijms21103647

Tsien, J. Z., Huerta, P. T., & Tonegawa, S. (1996). The Essential Role of Hippocampal CA1 NMDA Receptor–Dependent Synaptic Plasticity in Spatial Memory. *Cell*, *87*(7), 1327–1338. https://doi.org/10.1016/S0092-8674(00)81827-9

Tu, J. C., Xiao, B., Naisbitt, S., Yuan, J. P., Petralia, R. S., Brakeman, P., Doan, A., Aakalu, V. K., Lanahan, A. A., Sheng, M., & Worley, P. F. (1999). Coupling of mGluR/Homer and PSD-95 Complexes by the Shank Family of Postsynaptic Density Proteins. *Neuron*, *23*(3), 583–592. https://doi.org/10.1016/S0896-6273(00)80810-7

Tu, J. C., Xiao, B., Yuan, J. P., Lanahan, A. A., Leoffert, K., Li, M., Linden, D. J., & Worley, P. F. (1998). Homer Binds a Novel Proline-Rich Motif and Links Group 1 Metabotropic Glutamate Receptors with IP3 Receptors. *Neuron*, *21*(4), 717–726. https://doi.org/10.1016/S0896-6273(00)80589-9

Turk, R., 't Hoen, P.A., Sterrenburg, E., de Menezes, R.X., de Meijer, E.J., Boer, J.M., van Ommen, G.-J.B., den Dunnen, J.T., 2004. Gene expression variation between mouse inbred strains. BMC Genomics 5, 57. https://doi.org/10.1186/1471-2164-5-57

Tyndall, J., & Sandilya, R. (2005). GPCR Agonists and Antagonists in the Clinic. *Medicinal Chemistry*, *1*(4), 405–421. https://doi.org/10.2174/1573406054368675

Ugalde-Triviño, L., & Díaz-Guerra, M. (2021). PSD-95: An Effective Target for Stroke Therapy Using Neuroprotective Peptides. *International Journal of Molecular Sciences*, *22*(22), 12585. https://doi.org/10.3390/ijms222212585

Um, J. W., Kaufman, A. C., Kostylev, M., Heiss, J. K., Stagi, M., Takahashi, H., Kerrisk, M. E., Vortmeyer, A., Wisniewski, T., Koleske, A. J., Gunther, E. C., Nygaard, H. B., & Strittmatter, S. M. (2013). Metabotropic Glutamate Receptor 5 Is a Coreceptor for Alzheimer Aß Oligomer Bound to Cellular Prion Protein. *Neuron*, *79*(5), 887–902. https://doi.org/10.1016/j.neuron.2013.06.036

U.S. Food and Drug Administration. (2021) *FDA Grants Accelerated Approval for Alzheimer's Drug*. Accessed June 7, 2023. https://www.fda.gov/news-events/press-announcements/fda-grants-accelerated-approval-alzheimers-drug

Valant, C., Felder, C. C., Sexton, P. M., & Christopoulos, A. (2012). Probe Dependence in the Allosteric Modulation of a G Protein-Coupled Receptor: Implications for Detection and Validation of Allosteric Ligand Effects. *Molecular Pharmacology*, *81*(1), 41–52. https://doi.org/10.1124/mol.111.074872

Valerio, A., Rizzonelli, P., Paterlini, M., Moretto, G., Knöpfel, T., Kühn, R., Memo, M., & Spano, P. F. (1997). mGluR5 metabotropic glutamate receptor distribution

in rat and human spinal cord: a developmental study. *Neuroscience Research*, *28*(1), 49–57. https://doi.org/10.1016/S0168-0102(97)01175-9

Valiukas, Z., Ephraim, R., Tangalakis, K., Davidson, M., Apostolopoulos, V., & Feehan, J. (2022). Immunotherapies for Alzheimer's Disease—A Review. *Vaccines*, *10*(9), 1527. https://doi.org/10.3390/vaccines10091527

Van Dam, D., & De Deyn, P. P. (2011). Animal models in the drug discovery pipeline for Alzheimer's disease. *British Journal of Pharmacology*, *164*(4), 1285–1300. https://doi.org/10.1111/j.1476-5381.2011.01299.x

van der Lee, S. J., Wolters, F. J., Ikram, M. K., Hofman, A., Ikram, M. A., Amin, N., & van Duijn, C. M. (2018). The effect of APOE and other common genetic variants on the onset of Alzheimer's disease and dementia: a community-based cohort study. *The Lancet. Neurology*, *17*(5), 434–444. https://doi.org/10.1016/S1474-4422(18)30053-X

van Dyck, C. H., Tariot, P. N., Meyers, B., & Malca Resnick, E. (2007). A 24-week Randomized, Controlled Trial of Memantine in Patients With Moderate-to-severe Alzheimer Disease. *Alzheimer Disease & Associated Disorders*, *21*(2), 136–143. https://doi.org/10.1097/WAD.0b013e318065c495

van Es, M. A., Hardiman, O., Chio, A., Al-Chalabi, A., Pasterkamp, R. J., Veldink, J. H., & van den Berg, L. H. (2017). Amyotrophic lateral sclerosis. *The Lancet*, *390*(10107), 2084–2098. https://doi.org/10.1016/S0140-6736(17)31287-4

Van Everbroeck, B., Dobbeleir, I., De Waele, M., De Leenheir, E., Lübke, U., Martin, J.-J., & Cras, P. (2004). Extracellular protein deposition correlates with glial activation and oxidative stress in Creutzfeldt-Jakob and Alzheimer's disease. *Acta Neuropathologica*, *108*(3), 194–200. https://doi.org/10.1007/s00401-004-0879-2

Vance, C., Rogelj, B., Hortobágyi, T., De Vos, K. J., Nishimura, A. L., Sreedharan, J., Hu, X., Smith, B., Ruddy, D., Wright, P., Ganesalingam, J., Williams, K. L., Tripathi, V., Al-Saraj, S., Al-Chalabi, A., Leigh, P. N., Blair, I. P., Nicholson, G., de Belleroche, J., … Shaw, C. E. (2009). Mutations in FUS, an RNA Processing Protein, Cause Familial Amyotrophic Lateral Sclerosis Type 6. *Science*, *323*(5918), 1208–1211. https://doi.org/10.1126/science.1165942

Vargas, M. R., Johnson, D. A., Sirkis, D. W., Messing, A., & Johnson, J. A. (2008). Nrf2 activation in astrocytes protects against neurodegeneration in mouse models of familial amyotrophic lateral sclerosis. *The Journal of Neuroscience : The Official Journal of the Society for Neuroscience*, *28*(50), 13574–13581. https://doi.org/10.1523/JNEUROSCI.4099-08.2008

Varney, M. A., Rao, S. P., Jachec, C., Deal, C., Hess, S. D., Daggett, L. P., Lin, F., Johnson, E. C., & Veliçelebi, G. (1998). Pharmacological characterization of the human ionotropic glutamate receptor subtype GluR3 stably expressed in mammalian cells. *The Journal of Pharmacology and Experimental Therapeutics*, *285*(1), 358–370.

Varty, G. B., Grilli, M., Forlani, A., Fredduzzi, S., Grzelak, M. E., Guthrie, D. H., Hodgson, R. A., Lu, S. X., Nicolussi, E., Pond, A. J., Parker, E. M., Hunter, J. C., Higgins, G. A., Reggiani, A., & Bertorelli, R. (2005). The antinociceptive and anxiolytic-like effects of the metabotropic glutamate receptor 5 (mGluR5) antagonists, MPEP and MTEP, and the mGluR1 antagonist, LY456236, in rodents: a comparison of efficacy and side-effect profiles. *Psychopharmacology*, *179*(1), 207–217. https://doi.org/10.1007/s00213-005-2143-4

Vela, J., 2002. Interleukin-1 Regulates Proliferation and Differentiation of Oligodendrocyte Progenitor Cells. Molecular and Cellular Neuroscience 20, 489–502. https://doi.org/10.1006/mcne.2002.1127

Venkatakrishnan, A. J., Deupi, X., Lebon, G., Tate, C. G., Schertler, G. F., & Babu, M. M. (2013). Molecular signatures of G-protein-coupled receptors. *Nature*, *494*(7436), 185–194. https://doi.org/10.1038/nature11896

Verghese, P. B., Castellano, J. M., & Holtzman, D. M. (2011). Apolipoprotein E in Alzheimer's disease and other neurological disorders. *The Lancet. Neurology*, *10*(3), 241–252. https://doi.org/10.1016/S1474-4422(10)70325-2

Vergouts, M., Doyen, P. J., Peeters, M., Opsomer, R., & Hermans, E. (2018). Constitutive downregulation protein kinase C epsilon in hSOD1G93A astrocytes influences mGluR5 signaling and the regulation of glutamate uptake. *Glia*, *66*(4), 749–761. https://doi.org/10.1002/GLIA.23279

Vermeiren, C., De Hemptinne, I., Vanhoutte, N., Tilleux, S., Maloteaux, J. M., & Hermans, E. (2006). Loss of metabotropic glutamate receptor-mediated regulation of glutamate transport in chemically activated astrocytes in a rat model of amyotrophic lateral sclerosis. *Journal of Neurochemistry*, *96*(3), 719–731. https://doi.org/10.1111/J.1471-4159.2005.03577.X

Vermeiren, C., Najimi, M., Vanhoutte, N., Tilleux, S., De Hemptinne, I., Maloteaux, J. M., & Hermans, E. (2005). Acute up-regulation of glutamate uptake mediated by mGluR5a in reactive astrocytes. *Journal of Neurochemistry*, *94*(2), 405–416. https://doi.org/10.1111/J.1471-4159.2005.03216.X

Vey, M., Pilkuhn, S., Wille, H., Nixon, R., DeArmond, S. J., Smart, E. J., Anderson, R. G. W., Taraboulos, A., & Prusiner, S. B. (1996). Subcellular colocalization of the cellular and scrapie prion proteins in caveolae-like membranous domains. *Proceedings of the National Academy of Sciences*, *93*(25), 14945–14949. https://doi.org/10.1073/pnas.93.25.14945

Vezina, P., & Kim, J.-H. (1999). Metabotropic glutamate receptors and the generation of locomotor activity: Interactions with midbrain dopamine. *Neuroscience & Biobehavioral Reviews*, *23*(4), 577–589. https://doi.org/10.1016/S0149-7634(98)00055-4

Vincent, K., Cornea, V. M., Jong, Y.-J. I., Laferrière, A., Kumar, N., Mickeviciute, A., Fung, J. S. T., Bandegi, P., Ribeiro-da-Silva, A., O'Malley, K. L., & Coderre, T. J. (2016). Intracellular mGluR5 plays a critical role in neuropathic pain. *Nature Communications*, *7*(1), 10604. https://doi.org/10.1038/ncomms10604

Vincenti, J. E., Murphy, L., Grabert, K., McColl, B. W., Cancellotti, E., Freeman, T. C., & Manson, J. C. (2016). Defining the Microglia Response during the Time Course of Chronic Neurodegeneration. *Journal of Virology*, *90*(6), 3003–3017. https://doi.org/10.1128/JVI.02613-15

Violin, J. D., Crombie, A. L., Soergel, D. G., & Lark, M. W. (2014). Biased ligands at G-protein-coupled receptors: promise and progress. *Trends in Pharmacological Sciences*, *35*(7), 308–316. https://doi.org/10.1016/j.tips.2014.04.007

Vögler, O., Barceló, J. M., Ribas, C., & Escribá, P. V. (2008). Membrane interactions of G proteins and other related proteins. *Biochimica et Biophysica Acta (BBA) - Biomembranes*, *1778*(7–8), 1640–1652. https://doi.org/10.1016/j.bbamem.2008.03.008

Võikar, V., Stanford, S.C., 2023. The Open Field Test. pp. 9–29. https://doi.org/10.1007/978-1-0716-2748-8_2

Vonsattel, J.-P., Myers, R. H., Stevens, T. J., Ferrante, R. J., Bird, E. D., & Richardson, E. P. (1985). Neuropathological Classification of Huntington's Disease. *Journal of Neuropathology and Experimental Neurology*, *44*(6), 559–577. https://doi.org/10.1097/00005072-198511000-00003

Waard, M. De, Liu, H., Walker, D., Scott, V. E. S., Gurnett, C. A., & Campbell, K. P. (1997). Direct binding of G-protein βλ complex to voltage-dependent calcium channels. *Nature*, *385*(6615), 446–450. https://doi.org/10.1038/385446a0

Wacker, D., Stevens, R. C., & Roth, B. L. (2017). How Ligands Illuminate GPCR Molecular Pharmacology. *Cell*, *170*(3), 414–427. https://doi.org/10.1016/j.cell.2017.07.009

Waldvogel, H. J., Kim, E. H., Tippett, L. J., Vonsattel, J.-P. G., & Faull, R. L. (2014). *The Neuropathology of Huntington's Disease* (pp. 33–80). https://doi.org/10.1007/7854_2014_354

Walker, D. G., & Lue, L.-F. (2015). Immune phenotypes of microglia in human neurodegenerative disease: challenges to detecting microglial polarization in human brains. *Alzheimer's Research & Therapy*, *7*(1), 56. https://doi.org/10.1186/s13195-015-0139-9

Walsh, D. T., Betmouni, S., & Perry, V. H. (2001). Absence of Detectable IL-1ß Production in Murine Prion Disease: A Model of Chronic Neurodegeneration. *Journal of Neuropathology & Experimental Neurology*, *60*(2), 173–182. https://doi.org/10.1093/jnen/60.2.173

Walsh, S., Merrick, R., Milne, R., & Brayne, C. (2021). Aducanumab for Alzheimer's disease? *BMJ*, n1682. https://doi.org/10.1136/bmj.n1682

Wang, D. D., & Bordey, A. (2008). The astrocyte odyssey. *Progress in Neurobiology*, *86*(4), 342–367. https://doi.org/10.1016/J.PNEUROBIO.2008.09.015

Wang, H., & Zhuo, M. (2012). Group I Metabotropic Glutamate Receptor-Mediated Gene Transcription and Implications for Synaptic Plasticity and Diseases. *Frontiers in Pharmacology*, *3*. https://doi.org/10.3389/fphar.2012.00189

Wang, J., Logovinsky, V., Hendrix, S. B., Stanworth, S. H., Perdomo, C., Xu, L., Dhadda, S., Do, I., Rabe, M., Luthman, J., Cummings, J., & Satlin, A. (2016). ADCOMS: a composite clinical outcome for prodromal Alzheimer's disease trials. *Journal of Neurology, Neurosurgery & Psychiatry*, *87*(9), 993–999. https://doi.org/10.1136/jnnp-2015-312383

Wang, J. Q., Fibuch, E. E., & Mao, L. (2007). Regulation of mitogen-activated protein kinases by glutamate receptors. *Journal of Neurochemistry*, *100*(1), 1–11. https://doi.org/10.1111/j.1471-4159.2006.04208.x

Wang, Q., Johnson, J. L., Agar, N. Y. R., & Agar, J. N. (2008). Protein Aggregation and Protein Instability Govern Familial Amyotrophic Lateral Sclerosis Patient Survival. *PLoS Biology*, *6*(7), e170. https://doi.org/10.1371/journal.pbio.0060170

Wang, W. Y., Tan, M. S., Yu, J. T., & Tan, L. (2015). Role of pro-inflammatory cytokines released from microglia in Alzheimer's disease. *Annals of Translational Medicine*, *3*(10), 136. https://doi.org/10.3978/J.ISSN.2305-5839.2015.03.49

Ward, R. J., Alvarez-Curto, E., & Milligan, G. (2011). *Using the Flp-InTM T-RExTM System to Regulate GPCR Expression* (pp. 21–37). https://doi.org/10.1007/978-1-61779-126-0_2

Weatherall, M. (1966). The meaning and importance of drug potency in medicine. *Clinical Pharmacology & Therapeutics*, *7*(5), 577–582. https://doi.org/10.1002/cpt196675577 Weber, E. M., Zidar, J., Ewaldsson, B., Askevik, K., Udén, E., Svensk, E., & Törnqvist, E. (2022). Aggression in Group-Housed Male Mice: A Systematic Review. *Animals*, *13*(1), 143. https://doi.org/10.3390/ani13010143

Weisberg, S. J., Lyakhovetsky, R., Werdiger, A., Gitler, A. D., Soen, Y., & Kaganovich, D. (2012). Compartmentalization of superoxide dismutase 1 (SOD1G93A) aggregates determines their toxicity. *Proceedings of the National Academy of Sciences*, *109*(39), 15811–15816. https://doi.org/10.1073/pnas.1205829109

Weldon, D. T., Rogers, S. D., Ghilardi, J. R., Finke, M. P., Cleary, J. P., O'Hare, E., Esler, W. P., Maggio, J. E., & Mantyh, P. W. (1998). Fibrillar ß-Amyloid Induces Microglial Phagocytosis, Expression of Inducible Nitric Oxide Synthase, and Loss

of a Select Population of Neurons in the Rat CNS *In Vivo*. *The Journal of Neuroscience*, *18*(6), 2161–2173. https://doi.org/10.1523/JNEUROSCI.18-06-02161.1998

West Greenlee, M. H., Lind, M., Kokemuller, R., Mammadova, N., Kondru, N., Manne, S., Smith, J., Kanthasamy, A., & Greenlee, J. (2016). Temporal Resolution of Misfolded Prion Protein Transport, Accumulation, Glial Activation, and Neuronal Death in the Retinas of Mice Inoculated with Scrapie. *The American Journal of Pathology*, *186*(9), 2302–2309. https://doi.org/10.1016/j.ajpath.2016.05.018

Westmark, C.J., Malter, J.S., 2012. The regulation of AβPP expression by RNA-binding proteins. Ageing Res Rev 11, 450–459. https://doi.org/10.1016/j.arr.2012.03.005

Wettschureck, N., & Offermanns, S. (2005). Mammalian G Proteins and Their Cell Type Specific Functions. *Physiological Reviews*, *85*(4), 1159–1204. https://doi.org/10.1152/physrev.00003.2005

Will, R. G., Ironside, J. W., Zeidler, M., Estibeiro, K., Cousens, S. N., Smith, P. G., Alperovitch, A., Poser, S., Pocchiari, M., & Hofman, A. (1996). A new variant of Creutzfeldt-Jakob disease in the UK. *The Lancet*, *347*(9006), 921–925. https://doi.org/10.1016/S0140-6736(96)91412-9

Williams, A. E., Lawson, L. J., Perry, V. H., & Fraser, H. (1994). Characterization of the microglial response in murine scrapie. *Neuropathology and Applied Neurobiology*, *20*(1), 47–55. https://doi.org/10.1111/j.1365-2990.1994.tb00956.x

Williams, A. E., van Dam, A.-M., Man-A-Hing, W. K. H., Berkenbosch, F., Eikelenboom, P., & Fraser, H. (1994). Cytokines, prostaglandins and lipocortin-1 are present in the brains of scrapie-infected mice. *Brain Research*, *654*(2), 200–206. https://doi.org/10.1016/0006-8993(94)90480-4

Williams, A., Lucassen, P. J., Ritchie, D., & Bruce, M. (1997). PrP Deposition, Microglial Activation, and Neuronal Apoptosis in Murine Scrapie. *Experimental Neurology*, *144*(2), 433–438. https://doi.org/10.1006/exnr.1997.6424

Wilson, D. M., Cookson, M. R., Van Den Bosch, L., Zetterberg, H., Holtzman, D. M., & Dewachter, I. (2023). Hallmarks of neurodegenerative diseases. *Cell*, *186*(4), 693–714. https://doi.org/10.1016/j.cell.2022.12.032

Wilson R.I., Nicoll R.A. (2001). Endogenous cannabinoids mediate retrograde signalling at hippocampal synapses. *Nature*. 410(6828):588-92. doi: 10.1038/35069076. Erratum in: Nature 2001 Jun 21;411(6840):974.

Wiśniewski, K., & Car, H. (2006). (S)-3,5-DHPG: A Review. *CNS Drug Reviews*, *8*(1), 101–116. https://doi.org/10.1111/j.1527-3458.2002.tb00218.x

Woerner, A. C., Frottin, F., Hornburg, D., Feng, L. R., Meissner, F., Patra, M., Tatzelt, J., Mann, M., Winklhofer, K. F., Hartl, F. U., & Hipp, M. S. (2016). Cytoplasmic protein aggregates interfere with nucleocytoplasmic transport of protein and RNA. *Science*, *351*(6269), 173–176. https://doi.org/10.1126/science.aad2033

Wong, D. F., Waterhouse, R., Kuwabara, H., Kim, J., Brašić, J. R., Chamroonrat, W., Stabins, M., Holt, D. P., Dannals, R. F., Hamill, T. G., & Mozley, P. D. (2013). ^{18}F-FPEB, a PET Radiopharmaceutical for Quantifying Metabotropic Glutamate 5 Receptors: A First-in-Human Study of Radiochemical Safety, Biokinetics, and Radiation Dosimetry. *Journal of Nuclear Medicine*, *54*(3), 388–396. https://doi.org/10.2967/jnumed.112.107995

Wong, P. C., Pardo, C. A., Borchelt, D. R., Lee, M. K., Copeland, N. G., Jenkins, N. A., Sisodia, S. S., Cleveland, D. W., & Price, D. L. (1995). An adverse property of a familial ALS-linked SOD1 mutation causes motor neuron disease characterized by vacuolar degeneration of mitochondria. *Neuron*, *14*(6), 1105–1116. https://doi.org/10.1016/0896-6273(95)90259-7

Wootten, D., Christopoulos, A., Marti-Solano, M., Babu, M. M., & Sexton, P. M. (2018). Mechanisms of signalling and biased agonism in G protein-coupled receptors. *Nature Reviews Molecular Cell Biology*, *19*(10), 638–653. https://doi.org/10.1038/s41580-018-0049-3

Wootten, D., Christopoulos, A., & Sexton, P. M. (2013). Emerging paradigms in GPCR allostery: implications for drug discovery. *Nature Reviews Drug Discovery*, *12*(8), 630–644. https://doi.org/10.1038/nrd4052

World Health Organisation. (2021). *Global status report on the public health response to dementia*. Accessed February 12, 2023. https://www.who.int/publications/i/item/9789240033245

Wu, H.-Y., & Lynch, D. R. (2006). Calpain and Synaptic Function. *Molecular Neurobiology*, *33*(3), 215–236. https://doi.org/10.1385/MN:33:3:215

Wu, Y., Zhang, J., Peng, B., Tian, D., Zhang, D., Li, Y., Feng, X., Liu, J., Li, J., Zhang, T., Liu, X., Lu, J., Chen, B., Wang, S., 2019. Generating viable mice with heritable embryonically lethal mutations using the CRISPR-Cas9 system in two-cell embryos. Nat Commun 10, 2883. https://doi.org/10.1038/s41467-019-10748-2

Wuolikainen, A., Moritz, T., Marklund, S. L., Antti, H., & Andersen, P. M. (2011). Disease-Related Changes in the Cerebrospinal Fluid Metabolome in Amyotrophic Lateral Sclerosis Detected by GC/TOFMS. *PLoS ONE*, *6*(4), e17947. https://doi.org/10.1371/journal.pone.0017947

Xiao, B., Tu, J. C., Petralia, R. S., Yuan, J. P., Doan, A., Breder, C. D., Ruggiero, A., Lanahan, A. A., Wenthold, R. J., & Worley, P. F. (1998). Homer Regulates the Association of Group 1 Metabotropic Glutamate Receptors with Multivalent Complexes of Homer-Related, Synaptic Proteins. *Neuron*, *21*(4), 707–716. https://doi.org/10.1016/S0896-6273(00)80588-7

Xu, J., Marshall, J. J., Kraniotis, S., Nomura, T., Zhu, Y., & Contractor, A. (2021). Genetic disruption of Grm5 causes complex alterations in motor activity, anxiety and social behaviors. *Behavioural Brain Research*, *411*, 113378. https://doi.org/10.1016/j.bbr.2021.113378

Xu, Y., & Li, Z. (2019). Imaging metabotropic glutamate receptor system: Application of positron emission tomography technology in drug development. *Medicinal Research Reviews*, *39*(5), 1892–1922. https://doi.org/10.1002/med.21566

Xu, J., Zhu, Y., Contractor, A., & Heinemann, S. F. (2009). mGluR5 Has a Critical Role in Inhibitory Learning. *The Journal of Neuroscience*, *29*(12), 3676–3684. https://doi.org/10.1523/JNEUROSCI.5716-08.2009

Yamada, M., Chiba, T., Sasabe, J., Nawa, M., Tajima, H., Niikura, T., Terashita, K., Aiso, S., Kita, Y., Matsuoka, M., & Nishimoto, I. (2005). Implanted cannula-mediated repetitive administration of Aβ25–35 into the mouse cerebral ventricle effectively impairs spatial working memory. *Behavioural Brain Research*, *164*(2), 139–146. https://doi.org/10.1016/j.bbr.2005.03.026

Yamada, T., Kawamata, T., Walker, D. G., & McGeer, P. L. (1992). Vimentin immunoreactivity in normal and pathological human brain tissue. *Acta Neuropathologica*, *84*(2), 157–162. https://doi.org/10.1007/BF00311389

Yang, D., Zhou, Q., Labroska, V., Qin, S., Darbalaei, S., Wu, Y., Yuliantie, E., Xie, L., Tao, H., Cheng, J., Liu, Q., Zhao, S., Shui, W., Jiang, Y., & Wang, M.-W. (2021). G protein-coupled receptors: structure- and function-based drug discovery. *Signal Transduction and Targeted Therapy*, *6*(1), 7. https://doi.org/10.1038/s41392-020-00435-w

Yang, L., Mao, L., Chen, H., Catavsan, M., Kozinn, J., Arora, A., Liu, X., & Wang, J. Q. (2006). A Signaling Mechanism from Gαq-Protein-Coupled Metabotropic Glutamate Receptors to Gene Expression: Role of the c-Jun N-Terminal Kinase

Pathway. *The Journal of Neuroscience*, *26*(3), 971–980. https://doi.org/10.1523/JNEUROSCI.4423-05.2006

Yang, L., Mao, L., Tang, Q., Samdani, S., Liu, Z., & Wang, J. Q. (2004). A Novel Ca^{2+}-Independent Signaling Pathway to Extracellular Signal-Regulated Protein Kinase by Coactivation of NMDA Receptors and Metabotropic Glutamate Receptor 5 in Neurons. *The Journal of Neuroscience*, *24*(48), 10846–10857. https://doi.org/10.1523/JNEUROSCI.2496-04.2004

Yao, F., Svensjö, T., Winkler, T., Lu, M., Eriksson, C., & Eriksson, E. (1998). Tetracycline Repressor, tetR, rather than the tetR-Mammalian Cell Transcription Factor Fusion Derivatives, Regulates Inducible Gene Expression in Mammalian Cells. *Human Gene Therapy*, *9*(13), 1939–1950. https://doi.org/10.1089/hum.1998.9.13-1939

Ye, X., Yu, L., Zuo, D., Zhang, L., Zu, J., Hu, J., Tang, J., Bao, L., Cui, C., Zhang, R., Jin, G., Zan, K., Zhang, Z., Yang, X., Shi, H., Zhang, Z., Xiao, Q., Liu, Y., Xiang, J., … Cui, G. (2017). Activated mGluR5 protects BV2 cells against OGD/R induced cytotoxicity by modulating BDNF-TrkB pathway. *Neuroscience Letters*, *654*, 70–79. https://doi.org/10.1016/J.NEULET.2017.06.029

Yiannopoulou, K. G., & Papageorgiou, S. G. (2013). Current and future treatments for Alzheimer's disease. *Therapeutic Advances in Neurological Disorders*, *6*(1), 19–33. https://doi.org/10.1177/1756285612461679

Yoon, D. Y., Mansukhani, N. A., Stubbs, V. C., Helenowski, I. B., Woodruff, T. K., & Kibbe, M. R. (2014). Sex bias exists in basic science and translational surgical research. *Surgery*, *156*(3), 508–516. https://doi.org/10.1016/j.surg.2014.07.001

Zalewska, T., Pawelec, P., Ziabska, K., & Ziemka-Nalecz, M. (2022). Sexual Dimorphism in Neurodegenerative Diseases and in Brain Ischemia. *Biomolecules*, *13*(1), 26. https://doi.org/10.3390/biom13010026

Zamanian, J. L., Xu, L., Foo, L. C., Nouri, N., Zhou, L., Giffard, R. G., & Barres, B. A. (2012). Genomic Analysis of Reactive Astrogliosis. *Journal of Neuroscience*, *32*(18), 6391–6410. https://doi.org/10.1523/JNEUROSCI.6221-11.2012

Zelenaia, O., Schlag, B. D., Gochenauer, G. E., Ganel, R., Song, W., Beesley, J. S., Grinspan, J. B., Rothstein, J. D., & Robinson, M. B. (2000). Epidermal Growth Factor Receptor Agonists Increase Expression of Glutamate Transporter GLT-1 in Astrocytes through Pathways Dependent on Phosphatidylinositol 3-Kinase and Transcription Factor NF-κB. *Molecular Pharmacology*, *57*(4), 667–678. https://doi.org/10.1124/mol.57.4.667

Zeisel, A., Hochgerner, H., Lönnerberg, P., Johnsson, A., Memic, F., van der Zwan, J., Häring, M., Braun, E., Borm, L. E., La Manno, G., Codeluppi, S., Furlan, A., Lee, K., Skene, N., Harris, K. D., Hjerling-Leffler, J., Arenas, E., Ernfors, P., Marklund, U., & Linnarsson, S. (2018). Molecular Architecture of the Mouse Nervous System. *Cell*, *174*(4), 999-1014.e22. https://doi.org/10.1016/j.cell.2018.06.021

Zhang, T., Dong, K., Liang, W., Xu, D., Xia, H., Geng, J., Najafov, A., Liu, M., Li, Y., Han, X., Xiao, J., Jin, Z., Peng, T., Gao, Y., Cai, Y., Qi, C., Zhang, Q., Sun, A., Lipinski, M., … Yuan, J. (2015). G-protein-coupled receptors regulate autophagy by ZBTB16-mediated ubiquitination and proteasomal degradation of Atg14L. *ELife*, *4*. https://doi.org/10.7554/eLife.06734

Zhang, W., Xiao, D., Mao, Q., & Xia, H. (2023). Role of neuroinflammation in neurodegeneration development. *Signal Transduction and Targeted Therapy*, *8*(1), 267. https://doi.org/10.1038/s41392-023-01486-5

Zhang Y, Rodriguez AL, Conn PJ. (2005). Allosteric potentiators of metabotropic glutamate receptor subtype 5 have differential effects on different signaling pathways in cortical astrocytes. *J Pharmacol Exp Ther*, 315(3), 1212-9. doi: 10.1124/jpet.105.090308.

Zhang, Y., Thompson, R., Zhang, H., Xu, H. (2011). APP processing in Alzheimer's disease. *Mol Brain*, *4*, 3. https://doi.org/10.1186/1756-6606-4-3

Zhang, Y., Wu, K.-M., Yang, L., Dong, Q., & Yu, J.-T. (2022). Tauopathies: new perspectives and challenges. *Molecular Neurodegeneration*, *17*(1), 28. https://doi.org/10.1186/s13024-022-00533-z

Zhang, Y.-N., Fan, J.-K., Gu, L., Yang, H.-M., Zhan, S.-Q., & Zhang, H. (2021). Metabotropic glutamate receptor 5 inhibits α-synuclein-induced microglia inflammation to protect from neurotoxicity in Parkinson's disease. *Journal of Neuroinflammation*, *18*(1). https://doi.org/10.1186/S12974-021-02079-1

Zhang, Z., Zhang, S., Fu, P., Zhang, Z., Lin, K., Ko, J. K. S., & Yung, K. K. L. (2019). Roles of glutamate receptors in Parkinson's disease. *International Journal of Molecular Sciences*, *20*(18), 1–17. https://doi.org/10.3390/ijms20184391

Zhao, L., Mühleisen, T. W., Pelzer, D. I., Burger, B., Beins, E. C., Forstner, A. J., Herms, S., Hoffmann, P., Amunts, K., Palomero-Gallagher, N., & Cichon, S. (2023). Relationships between neurotransmitter receptor densities and expression levels of their corresponding genes in the human hippocampus. *NeuroImage*, *273*, 120095. https://doi.org/10.1016/j.neuroimage.2023.120095

Zhu, C., Beck, M. V., Griffith, J. D., Deshmukh, M., & Dokholyan, N. V. (2018). Large SOD1 aggregates, unlike trimeric SOD1, do not impact cell viability in a model of amyotrophic lateral sclerosis. *Proceedings of the National Academy of Sciences*, *115*(18), 4661–4665. https://doi.org/10.1073/pnas.1800187115

Zhu, C., Herrmann, U. S., Falsig, J., Abakumova, I., Nuvolone, M., Schwarz, P., Frauenknecht, K., Rushing, E. J., & Aguzzi, A. (2016). A neuroprotective role for microglia in prion diseases. *Journal of Experimental Medicine*, *213*(6), 1047–1059. https://doi.org/10.1084/jem.20151000

Zoicas, I., Kornhuber, J., 2019. The Role of Metabotropic Glutamate Receptors in Social Behavior in Rodents. Int J Mol Sci 20, 1412. https://doi.org/10.3390/ijms20061412

Zuberi, A., Lutz, C., 2016. Mouse Models for Drug Discovery. Can New Tools and Technology Improve Translational Power? ILAR J 57, 178–185. https://doi.org/10.1093/ilar/ilw021